Electrochemical Membrane Technology for Water and Wastewater Treatment

Edited by
Zhiwei Wang, Kwang-Ho Choo, Chuyang Y. Tang and T. David Waite

ELSEVIER

ELECTROCHEMICAL MEMBRANE TECHNOLOGY FOR WATER AND WASTEWATER TREATMENT

This book belongs to Badji Mokhtar Annaba University
Central Library

Copyright Elsevier 2025

This page intentionally left blank

This book belongs to Badji Mokhtar Annaba University Central Library

Copyright Elsevier 2025

ELECTROCHEMICAL MEMBRANE TECHNOLOGY FOR WATER AND WASTEWATER TREATMENT

Edited by

ZHIWEI WANG

State Key Laboratory of Pollution Control and Resource Reuse, Shanghai Institute of Pollution Control and Ecological Safety, Tongji Advanced Membrane Technology Center, School of Environmental Science and Engineering, Tongji University, Shanghai, SH, P.R. China

KWANG-HO CHOO

Department of Environmental Engineering, Kyungpook National University, Daegu, South Korea

CHUYANG Y. TANG

Department of Civil Engineering, The University of Hong Kong, Pokfulam, Hong Kong, P.R. China

T. DAVID WAITE

School of Civil and Environmental Engineering, The University of New South Wales, Sydney, NSW, Australia

ELSEVIER

This book belongs to Badji Mokhtar Annaba University Central Library

Copyright Elsevier 2025

Elsevier
Radarweg 29, PO Box 211, 1000 AE Amsterdam, Netherlands
The Boulevard, Langford Lane, Kidlington, Oxford OX5 1GB, United Kingdom
50 Hampshire Street, 5th Floor, Cambridge, MA 02139, United States

Copyright © 2022 Elsevier Inc. All rights reserved.

No part of this publication may be reproduced or transmitted in any form or by any means, electronic or mechanical, including photocopying, recording, or any information storage and retrieval system, without permission in writing from the publisher. Details on how to seek permission, further information about the Publisher's permissions policies and our arrangements with organizations such as the Copyright Clearance Center and the Copyright Licensing Agency, can be found at our website: www.elsevier.com/permissions.

This book and the individual contributions contained in it are protected under copyright by the Publisher (other than as may be noted herein).

Notices

Knowledge and best practice in this field are constantly changing. As new research and experience broaden our understanding, changes in research methods, professional practices, or medical treatment may become necessary.

Practitioners and researchers must always rely on their own experience and knowledge in evaluating and using any information, methods, compounds, or experiments described herein. In using such information or methods they should be mindful of their own safety and the safety of others, including parties for whom they have a professional responsibility.

To the fullest extent of the law, neither the Publisher nor the authors, contributors, or editors, assume any liability for any injury and/or damage to persons or property as a matter of products liability, negligence or otherwise, or from any use or operation of any methods, products, instructions, or ideas contained in the material herein.

ISBN: 978-0-12-824470-8

For Information on all Elsevier publications
visit our website at https://www.elsevier.com/books-and-journals

Publisher: Susan Dennis
Editorial Project Manager: Emerald Li
Production Project Manager: Selvaraj Raviraj
Cover Designer: Greg Harris

Typeset by MPS Limited, Chennai, India

Working together to grow libraries in developing countries
www.elsevier.com • www.bookaid.org

This book belongs to Badji Mokhtar Annaba University Central Library

Copyright Elsevier 2025

Contents

List of contributors *ix*

1. Introduction to electrochemical membrane technology: current status and recent developments 1

Jiayi Li, Yang Li, Mei Chen, Fei Gao, Xuesong Li, Jinxing Ma and Zhiwei Wang

1.1 Introduction 1
1.2 Fundamentals of electrochemical membrane technology 3
1.3 Applications of electrochemical membrane technologies 13
1.4 Conclusions and perspectives 27
Acknowledgments 28
References 28

2. Fundamentals of electrochemical membrane technology 43

Jingqiu Sun, Tianyu Wang, Zhenao Gu, Chenghai Lu, Zhibin Chen, You Wu and Chengzhi Hu

2.1 Introduction 43
2.2 Electrokinetic ions/colloids 45
2.3 Ion transmembrane mass transfer 51
2.4 Electrical double layer on membrane surface 55
2.5 Polarization of organic molecules 63
2.6 Electrochemical reactions on electrode/membrane 68
2.7 Challenges and perspectives 74
Acknowledgment 77
References 77

3. Electrochemical membrane materials and modules 81

Zhouyan Li, Xi Chen, Jia Yuan, Yiwen Qiao, Ruobin Dai, Xueye Wang, Xuesong Li, Jinxing Ma and Zhiwei Wang

3.1 Introduction 81
3.2 Materials for conductive membranes 83
3.3 Materials for ion exchange membranes 97
3.4 Electrochemical membrane modules 100
3.5 Conclusions and perspectives 102
Acknowledgment 103
References 103

This book belongs to Badji Mokhtar Annaba University Central Library

Copyright Elsevier 2025

4. Electrified carbon nanotube membrane technology for water treatment 111

Yanbiao Liu, Yifan Ren and Shijie You

4.1 Introduction 111
4.2 Fabrication of electroactive membranes 112
4.3 Reactor configuration 115
4.4 Environmental applications of electrochemical CNT membranes 116
4.5 Conclusions and perspectives 132
Acknowledgments 133
References 134

5. Electrochemical membrane technology for disinfection 141

Yin-Hu Wu, Zheng-Yang Huo, Hai Liu, Xin-Ye Ni, Hao-Bin Wang, Han Liu and Hong-Ying Hu

5.1 Introduction 141
5.2 Principal mechanisms of electrochemical membrane technology for disinfection 142
5.3 Reactor configuration of electrochemical membrane for disinfection 151
5.4 Limitations and challenges of electrochemical membrane disinfection technology 156
5.5 Conclusions and perspectives 157
Acknowledgment 158
References 158

6. Electrochemical membrane bioreactors for wastewater treatment 163

Mary Vermi Aizza Corpuz, Laura Borea, Florencio Ballesteros Jr, Vincenzo Belgiorno, Shadi W. Hasan and Vincenzo Naddeo

6.1 Introduction 163
6.2 Pollutant removal 164
6.3 Membrane fouling mitigation 175
6.4 Operating conditions, materials, and configurations 181
6.5 Microbiological community 185
6.6 Energy consumption 187
6.7 Challenges and future prospects 189
6.8 Conclusions 190
References 190

7. Electrochemical membrane technology for fouling control 195

Naresh Mameda and Kwang-Ho Choo

7.1 Introduction 195
7.2 Understanding membrane fouling 196
7.3 Electrochemical membrane materials 198
7.4 Electrochemical membrane process configurations 202
7.5 Electrochemical reactions 205

This book belongs to Badji Mokhtar Annaba University Central Library Copyright Elsevier 2025

7.6 Electrical and electrochemical fouling control 207
7.7 Concluding remarks and future research needs 215
Acknowledgment 218
References 219

8. Electrochemical membrane technology for environmental remediation 227
Xiangtong Kong, Lihu Liu, Changyong Zhang, Chia-Hung Hou, Zhong Zhang and Jinxing Ma
8.1 Introduction 227
8.2 Electrodialytic remediation 229
8.3 Electrocatalytic remediation 249
8.4 Conclusions and perspectives 257
References 259

9. Electrodialysis membrane technology for industrial wastewater treatment: recent advances 265
Ying Mei, Chenxiao Jiang, Yang Liu, Yang Zhang, Lei Wang and Chuyang Y. Tang
9.1 Introduction to electrodialysis technology 265
9.2 Basic configuration of electrodialysis and brief historical development 266
9.3 Development of ion exchange membranes for industrial wastewater treatment 268
9.4 Electrodialysis for industrial wastewater treatment 270
9.5 BMED for chemical production from industrial wastewater 281
9.6 Electrodialysis for other special/emerging applications 301
9.7 Conclusion and future perspectives 303
References 305

10. Membrane-based electrochemical technologies: I. Membrane capacitive deionization and flow-electrode capacitive deionization 317
Clare Bales, Changyong Zhang and T. David Waite
10.1 Introduction 317
10.2 Electrode materials and ion exchange membranes 319
10.3 Membrane capacitive deionization 320
10.4 Flow capacitive deionization 337
10.5 Challenges and perspectives 351
References 353

11. Membrane-based electrochemical technologies: II. Microbial desalination cell 361
Kuichang Zuo, Shuai Luo and Xia Huang
11.1 Introduction 361
11.2 Microbial desalination cell principle 362

This book belongs to Badji Mokhtar Annaba University Central Library Copyright Elsevier 2025

11.3 Microbial desalination cell configurations 368
11.4 Optimization of microbial desalination cell devices and operational conditions 374
11.5 Microbial desalination cell application 381
11.6 Integrating microbial desalination cells with existing technologies 387
11.7 Challenges and perspectives 391
11.8 Conclusion 393
References 394

12. Membrane-based electrochemical technologies: III. Selective ion removal and recovery 403

Anaira Román Santiago, Jemin Jeon, Emmanuel Kayiwa, Roland Cusick and Xiao Su
12.1 Introduction 403
12.2 Principles of selective ion removal and recovery 405
12.3 Architectures and fabrication of membrane modules 413
12.4 Applications 418
12.5 Technoeconomic analysis considerations 434
12.6 Conclusions and perspectives 435
Acknowledgments 436
References 436

13. Membrane-based electrochemical technologies for simultaneous water treatment and salinity-gradient energy production 445

Miao Gao and Wen-Wei Li
13.1 Introduction 445
13.2 Fundamentals of membrane-based electricity generation technologies 446
13.3 Future perspectives and outlook 454
Acknowledgments 457
References 457

Index 463

This book belongs to Badji Mokhtar Annaba University Central Library Copyright Elsevier 2025

List of contributors

Clare Bales
School of Civil and Environmental Engineering, University of New South Wales, Sydney, NSW, Australia

Florencio Ballesteros, Jr
Environmental Engineering Program, National Graduate School of Engineering, University of the Philippines, Diliman, Quezon City, Philippines; Department of Chemical Engineering, College of Engineering, University of the Philippines, Diliman, Quezon City, Philippines

Vincenzo Belgiorno
Sanitary Environmental Engineering Division (SEED), Department of Civil Engineering, University of Salerno, Fisciano, Italy

Laura Borea
Sanitary Environmental Engineering Division (SEED), Department of Civil Engineering, University of Salerno, Fisciano, Italy

Mei Chen
State Key Laboratory of Pollution Control and Resource Reuse, Shanghai Institute of Pollution Control and Ecological Safety, Tongji Advanced Membrane Technology Center, School of Environmental Science and Engineering, Tongji University, Shanghai, P.R. China

Xi Chen
State Key Laboratory of Pollution Control and Resource Reuse, Shanghai Institute of Pollution Control and Ecological Safety, Tongji Advanced Membrane Technology Center, School of Environmental Science and Engineering, Tongji University, Shanghai, SH, P.R. China

Zhibin Chen
State Key Laboratory of Environmental Aquatic Chemistry, Research Center for Eco-Environmental Sciences, Chinese Academy of Sciences, Beijing, P.R. China; University of Chinese Academy of Sciences, Beijing, P.R. China

Kwang-Ho Choo
School of Architectural, Civil, Environmental, and Energy Engineering, Kyungpook National University, Daegu, Republic of Korea; Department of Environmental Engineering, Kyungpook National University, Daegu, Republic of Korea; Advanced Institute of Water Industry, Kyungpook National University, Daegu, Republic of Korea

Mary Vermi Aizza Corpuz
Environmental Engineering Program, National Graduate School of Engineering, University of the Philippines, Diliman, Quezon City, Philippines

Roland Cusick
Department of Civil and Environmental Engineering, University of Illinois-Urbana Champaign, Urbana, IL, United States

Ruobin Dai
State Key Laboratory of Pollution Control and Resource Reuse, Shanghai Institute of Pollution Control and Ecological Safety, Tongji Advanced Membrane Technology Center, School of Environmental Science and Engineering, Tongji University, Shanghai, SH, P.R. China

This book belongs to Badji Mokhtar Annaba University Central Library

Copyright Elsevier 2025

Fei Gao
State Key Laboratory of Pollution Control and Resource Reuse, Shanghai Institute of Pollution Control and Ecological Safety, Tongji Advanced Membrane Technology Center, School of Environmental Science and Engineering, Tongji University, Shanghai, P.R. China

Miao Gao
Department of Environmental Science and Engineering, University of Science and Technology of China, Hefei, P.R. China

Zhenao Gu
State Key Laboratory of Environmental Aquatic Chemistry, Research Center for Eco-Environmental Sciences, Chinese Academy of Sciences, Beijing, P.R. China; University of Chinese Academy of Sciences, Beijing, P.R. China

Shadi W. Hasan
Center for Membranes and Advanced Water Technology (CMAT), Department of Chemical Engineering, Khalifa University of Science and Technology, Abu Dhabi, United Arab Emirates

Chia-Hung Hou
Graduate Institute of Environmental Engineering, National Taiwan University, Taipei, Taiwan, ROC

Chengzhi Hu
State Key Laboratory of Environmental Aquatic Chemistry, Research Center for Eco-Environmental Sciences, Chinese Academy of Sciences, Beijing, P.R. China; University of Chinese Academy of Sciences, Beijing, P.R. China

Hong-Ying Hu
Environmental Simulation and Pollution Control State Key Joint Laboratory, State Environmental Protection Key Laboratory of Microorganism Application and Risk Control (SMARC), Beijing Laboratory for Environmental Frontier Technologies, School of Environment, Tsinghua University, Beijing, P.R. China; Shenzhen Environmental Science and New Energy Technology Engineering Laboratory, Tsinghua-Berkeley Shenzhen Institute, Shenzhen, P.R. China

Xia Huang
School of Environment, Tsinghua University, Beijing, P.R. China

Zheng-Yang Huo
School of Environment and Natural Resources, Renmin University of China, Beijing, P.R. China

Jemin Jeon
Department of Chemical and Biomolecular Engineering, University of Illinois-Urbana Champaign, Urbana, IL, United States

Chenxiao Jiang
Department of Civil Engineering, The University of Hong Kong, Pokfulam, Hong Kong, P.R. China; CAS Key Laboratory of Soft Matter Chemistry, Collaborative Innovation Centre of Chemistry for Energy Materials, School of Chemistry and Materials Science, University of Science and Technology of China, Hefei, Anhui, P.R. China

Emmanuel Kayiwa
Department of Civil and Environmental Engineering, University of Illinois-Urbana Champaign, Urbana, IL, United States

This book belongs to Badji Mokhtar Annaba University Central Library Copyright Elsevier 2025

Xiangtong Kong
UNSW Water Research Centre, School of Civil and Environmental Engineering, The University of New South Wales, Sydney, NSW, Australia

Jiayi Li
State Key Laboratory of Pollution Control and Resource Reuse, Shanghai Institute of Pollution Control and Ecological Safety, Tongji Advanced Membrane Technology Center, School of Environmental Science and Engineering, Tongji University, Shanghai, P.R. China

Wen-Wei Li
Department of Environmental Science and Engineering, University of Science and Technology of China, Hefei, P.R. China

Xuesong Li
State Key Laboratory of Pollution Control and Resource Reuse, Shanghai Institute of Pollution Control and Ecological Safety, Tongji Advanced Membrane Technology Center, School of Environmental Science and Engineering, Tongji University, Shanghai, SH, P.R. China

Yang Li
State Key Laboratory of Pollution Control and Resource Reuse, Shanghai Institute of Pollution Control and Ecological Safety, Tongji Advanced Membrane Technology Center, School of Environmental Science and Engineering, Tongji University, Shanghai, P.R. China

Zhouyan Li
State Key Laboratory of Pollution Control and Resource Reuse, Shanghai Institute of Pollution Control and Ecological Safety, Tongji Advanced Membrane Technology Center, School of Environmental Science and Engineering, Tongji University, Shanghai, SH, P.R. China

Hai Liu
School of Environment, Guangzhou Key Laboratory of Environmental Exposure and Health, and Guangdong Key Laboratory of Environmental Pollution and Health, Jinan University, Guangzhou, P.R. China

Han Liu
Environmental Simulation and Pollution Control State Key Joint Laboratory, State Environmental Protection Key Laboratory of Microorganism Application and Risk Control (SMARC), Beijing Laboratory for Environmental Frontier Technologies, School of Environment, Tsinghua University, Beijing, P.R. China

Lihu Liu
College of Resources and Environment, Huazhong Agricultural University, Wuhan, Hubei, P.R. China

Yanbiao Liu
Textile Pollution Controlling Engineering Center of Ministry of Environmental Protection, College of Environmental Science and Engineering, Donghua University, Shanghai, P.R. China

Yang Liu
College of Environment and Safety Engineering, Qingdao University of Science and Technology, Qingdao, Shandong, P.R. China

Chenghai Lu
State Key Laboratory of Environmental Aquatic Chemistry, Research Center for Eco-Environmental Sciences, Chinese Academy of Sciences, Beijing, P.R. China; University of Chinese Academy of Sciences, Beijing, P.R. China

This book belongs to Badji Mokhtar Annaba University Central Library Copyright Elsevier 2025

Shuai Luo
School of Environment, Tsinghua University, Beijing, P.R. China

Jinxing Ma
Key Laboratory for City Cluster Environmental Safety and Green Development of the Ministry of Education, School of Ecology, Environment and Resources, Guangdong University of Technology, Guangzhou, Guangdong, P.R. China; UNSW Water Research Centre, School of Civil and Environmental Engineering, University of New South Wales, Sydney, NSW, Australia

Naresh Mameda
School of Architectural, Civil, Environmental, and Energy Engineering, Kyungpook National University, Daegu, Republic of Korea

Ying Mei
Research and Development Center for Watershed Environmental Eco-Engineering, Advanced Institute of Natural Sciences, Beijing Normal University, Zhuhai, Guangdong, P.R. China; Department of Civil Engineering, The University of Hong Kong, Pokfulam, Hong Kong, P.R. China

Vincenzo Naddeo
Sanitary Environmental Engineering Division (SEED), Department of Civil Engineering, University of Salerno, Fisciano, Italy

Xin-Ye Ni
Environmental Simulation and Pollution Control State Key Joint Laboratory, State Environmental Protection Key Laboratory of Microorganism Application and Risk Control (SMARC), Beijing Laboratory for Environmental Frontier Technologies, School of Environment, Tsinghua University, Beijing, P.R. China

Yiwen Qiao
State Key Laboratory of Pollution Control and Resource Reuse, Shanghai Institute of Pollution Control and Ecological Safety, Tongji Advanced Membrane Technology Center, School of Environmental Science and Engineering, Tongji University, Shanghai, SH, P.R. China

Yifan Ren
Textile Pollution Controlling Engineering Center of Ministry of Environmental Protection, College of Environmental Science and Engineering, Donghua University, Shanghai, P.R. China

Anaira Román Santiago
Department of Chemical and Biomolecular Engineering, University of Illinois-Urbana Champaign, Urbana, IL, United States

Xiao Su
Department of Chemical and Biomolecular Engineering, University of Illinois-Urbana Champaign, Urbana, IL, United States

Jingqiu Sun
State Key Laboratory of Environmental Aquatic Chemistry, Research Center for Eco-Environmental Sciences, Chinese Academy of Sciences, Beijing, P.R. China; University of Chinese Academy of Sciences, Beijing, P.R. China

Chuyang Y. Tang
Department of Civil Engineering, The University of Hong Kong, Pokfulam, Hong Kong, P.R. China

T. David Waite
School of Civil and Environmental Engineering, University of New South Wales, Sydney, NSW, Australia; UNSW Centre for Transformational Environmental Technologies (CTET), Yixing, Jiangsu, P.R. China

This book belongs to Badji Mokhtar Annaba University Central Library Copyright Elsevier 2025

Hao-Bin Wang
Environmental Simulation and Pollution Control State Key Joint Laboratory, State Environmental Protection Key Laboratory of Microorganism Application and Risk Control (SMARC), Beijing Laboratory for Environmental Frontier Technologies, School of Environment, Tsinghua University, Beijing, P.R. China

Lei Wang
Shenzhen Key Laboratory of Polymer Science and Technology, College of Materials Science and Engineering, Shenzhen University, Shenzhen, Guangdong, P.R. China

Tianyu Wang
State Key Laboratory of Environmental Aquatic Chemistry, Research Center for Eco-Environmental Sciences, Chinese Academy of Sciences, Beijing, P.R. China; University of Chinese Academy of Sciences, Beijing, P.R. China

Xueye Wang
State Key Laboratory of Pollution Control and Resource Reuse, Shanghai Institute of Pollution Control and Ecological Safety, Tongji Advanced Membrane Technology Center, School of Environmental Science and Engineering, Tongji University, Shanghai, SH, P.R. China

Zhiwei Wang
State Key Laboratory of Pollution Control and Resource Reuse, Shanghai Institute of Pollution Control and Ecological Safety, Tongji Advanced Membrane Technology Center, School of Environmental Science and Engineering, Tongji University, Shanghai, SH, P.R. China

Yin-Hu Wu
Environmental Simulation and Pollution Control State Key Joint Laboratory, State Environmental Protection Key Laboratory of Microorganism Application and Risk Control (SMARC), Beijing Laboratory for Environmental Frontier Technologies, School of Environment, Tsinghua University, Beijing, P.R. China

You Wu
State Key Laboratory of Environmental Aquatic Chemistry, Research Center for Eco-Environmental Sciences, Chinese Academy of Sciences, Beijing, P.R. China; University of Chinese Academy of Sciences, Beijing, P.R. China

Shijie You
State Key Laboratory of Urban Water Resource and Environment, School of Environment, Harbin Institute of Technology, Harbin, P.R. China

Jia Yuan
State Key Laboratory of Pollution Control and Resource Reuse, Shanghai Institute of Pollution Control and Ecological Safety, Tongji Advanced Membrane Technology Center, School of Environmental Science and Engineering, Tongji University, Shanghai, SH, P.R. China

Changyong Zhang
School of Civil and Environmental Engineering, University of New South Wales, Sydney, NSW, Australia; UNSW Water Research Centre, School of Civil and Environmental Engineering, The University of New South Wales, Sydney, NSW, Australia

Yang Zhang
College of Environment and Safety Engineering, Qingdao University of Science and Technology, Qingdao, Shandong, P.R. China

This book belongs to Badji Mokhtar Annaba University Central Library Copyright Elsevier 2025

Zhong Zhang
Key Laboratory for City Cluster Environmental Safety and Green Development of the Ministry of Education, School of Ecology, Environment and Resources, Guangdong University of Technology, Guangzhou, Guangdong, P.R. China

Kuichang Zuo
The Key Laboratory of Water and Sediment Sciences, Ministry of Education, College of Environment Sciences and Engineering, Peking University, Beijing, P.R. China

This book belongs to Badji Mokhtar Annaba University Central Library Copyright Elsevier 2025

CHAPTER ONE

Introduction to electrochemical membrane technology: current status and recent developments

Jiayi Li[1], Yang Li[1], Mei Chen[1], Fei Gao[1], Xuesong Li[1], Jinxing Ma[2] and Zhiwei Wang[1]
[1]State Key Laboratory of Pollution Control and Resource Reuse, Shanghai Institute of Pollution Control and Ecological Safety, Tongji Advanced Membrane Technology Center, School of Environmental Science and Engineering, Tongji University, Shanghai, P.R. China
[2]UNSW Water Research Centre, School of Civil and Environmental Engineering, University of New South Wales, Sydney, NSW, Australia

1.1 Introduction

Water is essential for all living things to survive on the earth. However, billions of people in the world lack access to clean water [1,2] and this problem is exacerbated by the water contamination and the climate change problem [3–5]. Therefore it is of great significance to effectively treat the living beings-produced wastewaters, thereby ensuring a sufficient fresh water supply to meet the needs of human survival [6]. Moreover, the emerging of recalcitrant pollutants, heavy metals, synthetic materials, and other toxic/nontoxic matters in wastewaters urges more effective wastewater treatment strategies [7,8].

Nowadays, a novel wastewater treatment strategy has emerged, named membrane process, where membrane film is used as a physical barrier to remove pollutants from wastewater [9]. The operation of the membrane does not need phase change, chemicals, or reactions, but after coming in contact with wastewater, it only produces a filtered stream and a rejected stream. Hence, membrane filtration process is widely used as a wastewater separation technology for aqueous mixtures, acting as an affordable alternative to municipal and industrial water/wastewater treatment methods [10]. Nevertheless, the membrane process suffers the drawbacks of membrane fouling and, usually, requires a proper treatment of rejected concentrate/disposal [11,12]. Sometimes the efficacy/cost-effectiveness of the membrane process cannot meet the requirements of wastewater treatment and, therefore efforts must be made to overcome the shortages of the membrane process to spur on ahead its development.

With the emerging of some special membranes (e.g., surface-charged membranes and conductive membranes (CM), it helped develop the electrochemical membrane

Electrochemical Membrane Technology for Water and Wastewater Treatment.
DOI: https://doi.org/10.1016/B978-0-12-824470-8.00003-6
© 2022 Elsevier Inc.
All rights reserved.

This book belongs to Badji Mokhtar Annaba University Central Library
Copyright Elsevier 2025

technology, showing a superior wastewater treatment performance. Surface-charged membranes (ion exchange membranes [IEMs]) could selectively allow/reject ions passage, while conductive membranes (CMs) as electrodes could transfer electrons. Being coupled with an electric field, IEM-based electrochemical process could achieve sophisticated selective ion separation, while CM-based electrochemical process could perform membrane electrode properties, like electrostatic repulsion [13], electrochemical advanced oxidation processes (EAOPs), and electrochemical reduction. These processes can work synergistically to treat watewater and produce clean water.

The electrochemical membrane technology actually has long been studied and applied in practice. The historical development of electrochemical membrane technologies is schematically illustrated in Fig. 1.1. The earliest use of electrochemical membrane technology dates back to 1889 when Maigrot and Sabates proposed the concept of combining the electric field and selective separation materials [14]. This was probably the original prototype of electrodialysis (ED). However, this concept did not get

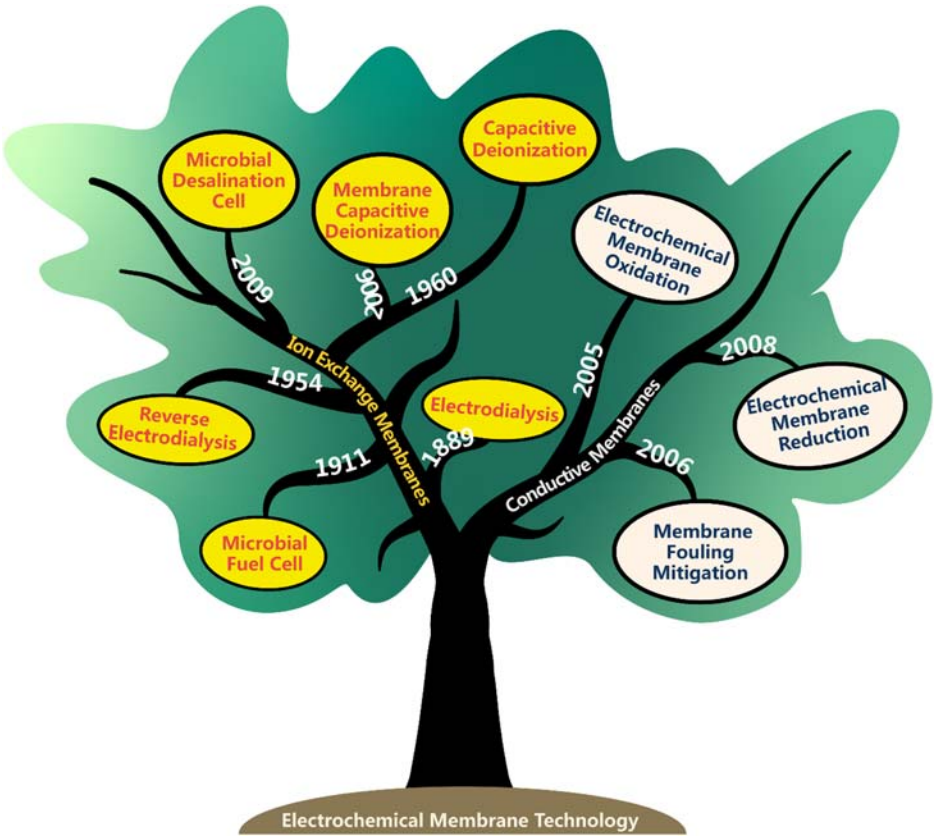

Figure 1.1 Timeline of the development of electrochemical membrane technology.

This book belongs to Badji Mokhtar Annaba University Central Library Copyright Elsevier 2025

much attention until 1939, when the IEM was fabricated and used to substitute the selective separation materials [15]. On the other hand, the concept of producing electricity from microbes, which gained name of the microbial fuel cell (MFC) afterwards, was conceived in 1911 [16] but its rapid development was attained only in the 1980–90s [17,18]. On the basis of MFC, microbial desalination cell (MDC) was designed using IEMs and applied for water desalination and energy production in 2009 [19]. Capacitive deionization (CDI) was proposed in the late 1960s but its development was sluggish until the 2000s [20,21], when IEMs were introduced to the CDI system, with the nomenclature given of membrane capacitive deionization (MCDI) in 2006 [22]. The abovementioned electrochemical membrane technologies share the same type of membranes – IEMs, which are employed for selective ion transport. The electrochemical membrane technologies based on CM emerged in 2005. The major function of CMs is transferring electrons with which purpose CMs are mainly used as electrodes. The combination of EAOP and CMs, namely electrochemical membrane oxidation, was first reported in 2005 [23], while the first study of electrochemical membrane reduction was conducted in 2008 [24]. A study in 2006 found that applying an electrical field to CMs could mitigate membrane fouling [25]. Apparently, the integration of the membrane process with the electrochemical process can be beneficial by improving the performance of each process while also boosting their applications in water/wastewater treatment.

In this chapter, the electrochemical membrane technology is given an introduction, whence the fundamentals of electrochemical membrane technology such as definition, classification, working principles, and preparations are provided. Afterwards, a series of electrochemical membrane technologies, including ED, reverse electrodialysis (RED), MCDI, MFC, MDC, membrane fouling mitigation, electrochemical membrane oxidation, and electrochemical membrane reduction are introduced and reviewed. In the last section, the conclusions are derived and perspectives are given based on the current status and recent advances of the electrochemical membrane technology.

1.2 Fundamentals of electrochemical membrane technology

1.2.1 Definition of electrochemical membrane technology

1.2.1.1 Electrochemical Processes

Electric charge, which is either positive or negative, can cause two objects to attract or repel [26]. Moreover, when an electric field is applied to the objects, charged species can be forced to move directionally, which is the major working principle of many electrochemical processes, such as electromigration (electrophoresis), electro-osmosis

This book belongs to Badji Mokhtar Annaba University Central Library Copyright Elsevier 2025

and electrosorption. In contrast, the transfer of charged species (usually the electron) between two or more substances would cause electrochemical reactions like electrolysis, electrochemical oxidation/reduction, and electro-Fenton (EF). Brief definitions and introductions to these electrochemical phenomena or reactions are listed in Table 1.1. It is noteworthy that a special process called "microbial metabolism" is also included in this table since it is also involved with electron transfer and plays an important role in microbe-based electrochemical technology.

1.2.1.2 Membrane processes

Membrane is denoted as a selective physical barrier which only allows some substances to pass through but rejects others [35]. Therefore the selective separation of pollutants in waters can be achieved by membrane filtration. Again, given the dynamics of the fluid around the membrane would change due to the convection flow effects, the solutes or particles in the thin liquid layer adjacent to the membrane would accumulate and thereby cause concentration polarization phenomenon [36–38], which could further lead to membrane fouling.

1.2.1.3 Electrochemical membrane technology

Electrochemical membrane technology is referred as the membrane-based process coupling with electric field. In the electrochemical membrane process, both electrochemical phenomena (e.g., electromigration/electrophoresis, electro-osmosis, electro-sorption, electrolysis, EF, electro-oxidation, electroreduction, and microbial metabolism) and membrane phenomena (e.g., fouling, filtration) can be observed. Moreover, the coupling of both processes is beneficial for performance enhancement by, for example, facilitating mass transfer, mitigating fouling, and improving charge efficiency.

1.2.2 Classification of electrochemical membrane technologies

According to the characteristics of membranes used in electrochemical membrane technologies, the membranes can be classified into two types: one, nonconductive but surface-charged membranes, allowing certain ions to pass the membrane film while rejecting others (e.g., IEM); and two, CM that can transfer electrons (e.g., metallic membranes). Both membranes can function as selective barriers while each of them also shows unique properties when being coupled with the electric field.

Given the classification of membranes, thus correspondingly, the electrochemical membrane technologies are also classified into two types: one, IEM-based electrochemical membrane technology and, two, CM-based electrochemical membrane technology. Furthermore, the IEM-based electrochemical technology includes ED, RED, MFC, MDC, and MCDI; while CM-based electrochemical technology includes membrane fouling mitigation, electrochemical membrane oxidation, and electrochemical membrane reduction. A brief overview of the main applications of each technology in water and wastewater treatment is summarized in Table 1.2.

This book belongs to Badji Mokhtar Annaba University Central Library Copyright Elsevier 2025

This book belongs to Badji Mokhtar Annaba University Central Library

Table 1.1 Definitions and descriptions of electrochemical phenomena or reactions in electrochemical membrane technologies.

Electrochemical phenomena/reactions	Definitions and descriptions
Electromigration/electrophoresis	Electromigration (or electrophoresis) is the motion of ions (or charged particles) in the aqueous media, which is driven by the electrical field applied between the electrodes. Generally, cations/positively charged particles move toward the cathode, while anions/negatively charged particles move toward the anode [27].
Electro-osmosis	Electro-osmosis is the motion of water induced by the motion of net mobile electric charge in this water. As cations are moving to the cathode, hydrated water of cations is also carried to the cathode. Since H-bonding is the cohesive nature of the hydrated water, it could lead the whole buffer solution being dragged to the cathode and thereby forming the electro-osmosis flow (EOF) [28].
Electro-sorption	Electro-sorption is the migration of ions into electrical double layers (EDLs), which was formed along the pore surfaces of electrode/water interface. Electro-sorption is ubiquitous in electrified systems and the contribution of electro-sorption to ions removal depends on electrode potential (a higher potential over the non-Faradaic reaction window will result in electrolysis) and the electrode properties (e.g., specific surface area) [29,30].
Electrolysis	Electrolysis is known to occur when direct electric potential (potential is required to be higher than non-Faradaic reaction window) is applied to the electrodes immersed in water without external control. Generally, anode generates acid front while cathode produces base front. Notably, the type of electrolysis reactions depends on the availability of the chemical species around the electrodes and the electrochemical potential of these reactions [31].
Electrochemical oxidation/reduction	Electrochemical oxidation and reduction are the redox processes involving electrons transfer from the electrode. These processes can remove target pollutants via direct/indirect effects. In direct electrochemical redox process, pollutants are first adsorbed on the electrode surfaces, and then removed through direct electron transfer from the electrodes. In indirect electrochemical redox process, intermediate reactants (e.g., •OH, H*) are generated and then react with the target species [32].
EF	EF is an electrochemically assisted Fenton's reaction where hydroxyl radicals (•OH) could be produced between H_2O_2 and ferrous iron. In contrast to the need of Fenton's reagent ($H_2O_2 + Fe^{2+}$) in classical Fenton's process, it could in situ electrogenerate H_2O_2 or regenerate Fe^{2+} via electrocatalysis [33].
Microbial metabolism	Microbial metabolism could produce electricity in bioelectrochemical systems. Bacteria could transfer electrons from "fuel" (e.g., organics, nitrate, sulfate, carbon dioxide, etc.). Afterwards, electrons are directly/indirectly transferred from the cell to metal oxides or electrodes [34].

EF, electro-Fenton.

Copyright Elsevier 2025

This book belongs to Badji Mokhtar Annaba University Central Library

Table 1.2 Classification and overview of electrochemical membrane technology.

Category	Technology	Membrane	Main Functions and applications
IEM-based electrochemical technology	Electrodialysis	Cation/anion exchange membranes	*Salt production and ion separation*: ions from the treated solution (the diluent) migrate to another solution (the concentrate) through IEMs, resulting in streams with dilute and concentrated ions.
	Reverse electrodialysis	Cation/anion exchange membranes	*Energy generation*: electricity is captured by mixing two water streams of different salinities, usually sea water and river water.
	Membrane capacitive deionization	Cation/anion exchange membranes	*Ion separation*: ions are electrosorbed at the surface of charged electrodes and the co-ion expulsion of CDI is alleviated by employing IEMs.
	Microbial fuel cell	Proton-exchange membranes	*Energy generation*: electrical current is generated by microorganisms oxidizing the organic matter and releasing electrons outside the cell.
	Microbial desalination cell	Cation/anion exchange membranes	*Energy generation and ion separation*: electricity is generated by biodegradation of organics in wastewater and the electricity produced is used for concurrent wastewater desalination with the assistance of IEMs.
CM-based electrochemical technology	Membrane fouling mitigation	Conductive membranes	*Fouling control*: membrane fouling/scaling is alleviated through hampering the deposition/adsorption of foulants on membrane surface, mainly the result of electrostatic repulsion taking place between the applied electrical potential and the charged foulants.
	Electrochemical membrane oxidation	Conductive membranes	*Organic pollutant/microorganism oxidation*: oxidation of organic pollutants or microorganisms is realized by direct electron transfer or indirect intermediate oxidants (e.g., •OH) of conductive membrane electrodes or EF oxidation. The performance is further improved owing to the mass transfer enhancement by membrane filtration.
	Electrochemical membrane reduction	Conductive membranes	*Denitrification/dehalogenation or electrodeposition*: reduction of nitrate/halide/metal ions is realized via the direct electron transfer or indirect intermediate reductants (e.g., H*) of the conductive membrane electrodes; and the performance is further improved owing to the mass transfer enhancement by membrane filtration.

EF, electro-Fenton.

Copyright Elsevier 2025

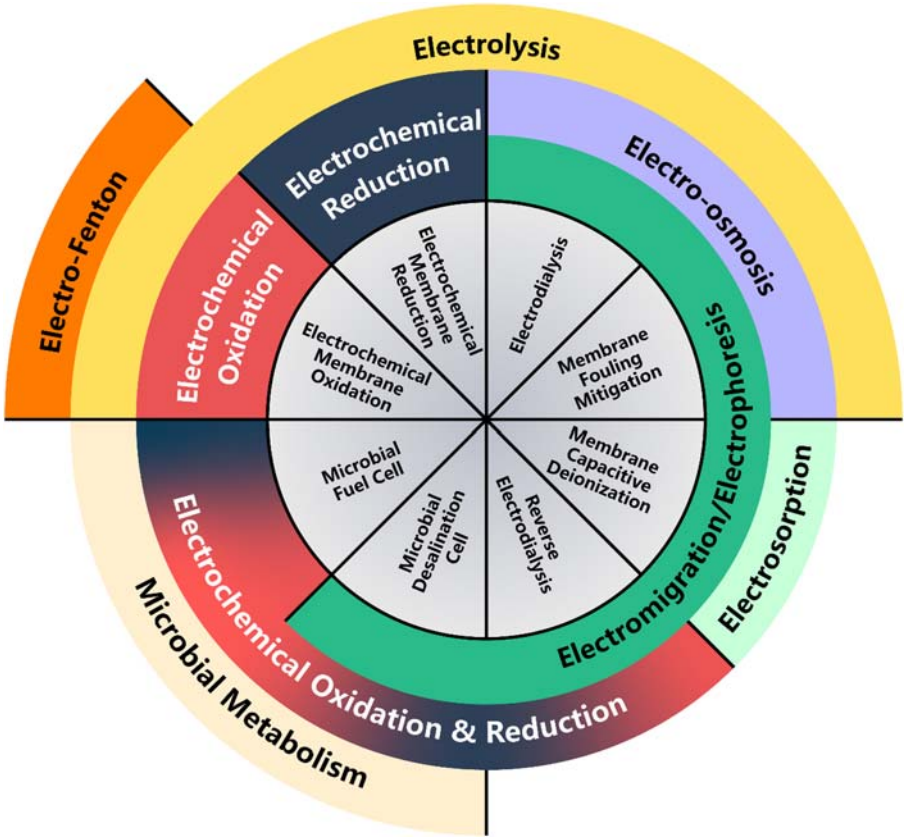

Figure 1.2 Electrochemical phenomena involved in electrochemical membrane technologies.

As already mentioned, both electrochemistry- and membrane-related phenomena can be observed with electrochemical membrane technology at work. Therefore we summarized the electrochemical phenomena that can occur with each technology in Fig. 1.2. As for membrane phenomena, it should be noted that membrane fouling/scaling or selective separation occurs in all the electrochemical membrane technologies, while fluid filtration only occurs in the CM-based electrochemical membrane technology.

1.2.3 Working principles of electrochemical membrane technologies

The reactions occurring between electrochemical processes mainly include Faradaic reactions and non-Faradaic reactions and thus the following discussion on the basic working principles of electrochemical membrane technologies is focused on these two reactions.

In these reactions, the pollutants removal is due to not only the chemical degradation of pollutants, but also some physical processes (e.g., adsorption, diffusion, and transfer) [39]. However, the physical processes may be affected by the presence of electrostatic

This book belongs to Badji Mokhtar Annaba University Central Library Copyright Elsevier 2025

repulsion and limited active sites on the electrode surface [40]. For example, the mass transfer of anion to the active sites on the cathode will be hindered due to the electrostatic repulsion between the anion and the negatively charged cathode [40].

To address these issues, some researches proposed the use of the electrochemical membrane because the membrane can provide unique nanofluidic channels to enhance the mass transfer [41]. As such, the effect of the electrostatic repulsion on the pollutant diffusion process could be alleviated due to the confined space in the nanofluidic channels. For example, two-dimensional (2D) materials (e.g., graphene oxide, MXene, and MoS_2) can be assembled into a membrane via vacuum filtration [42–44]. The nanosized channels in these membranes have the potential to propel the pollutants into the boundaries, resulting in a high concentration of pollutants in the close vicinity of the active sites [45].

Faradaic reaction is the redox process occurring on the electrode, which is accompanied by the process of electron transfer between the solution and the electrode interface. This process refers to the Faraday's law, that is, the amount of chemical reaction caused by the current is proportional to the quantity of electric charge [46]. Faradaic reactions in water and wastewater treatment methods are commonly categorized into oxidation reaction and reduction reaction. Non-Faradaic reaction is a process without charge transfer between the electrode and solution interface, given that this process will be affected by the chemical surface charge of the electrode and ion kinetics [30].

As depicted in Fig. 1.3, non-Faradaic reaction includes MCDI, whereas faradaic reaction includes electrochemical membrane oxidation and reduction. Meanwhile,

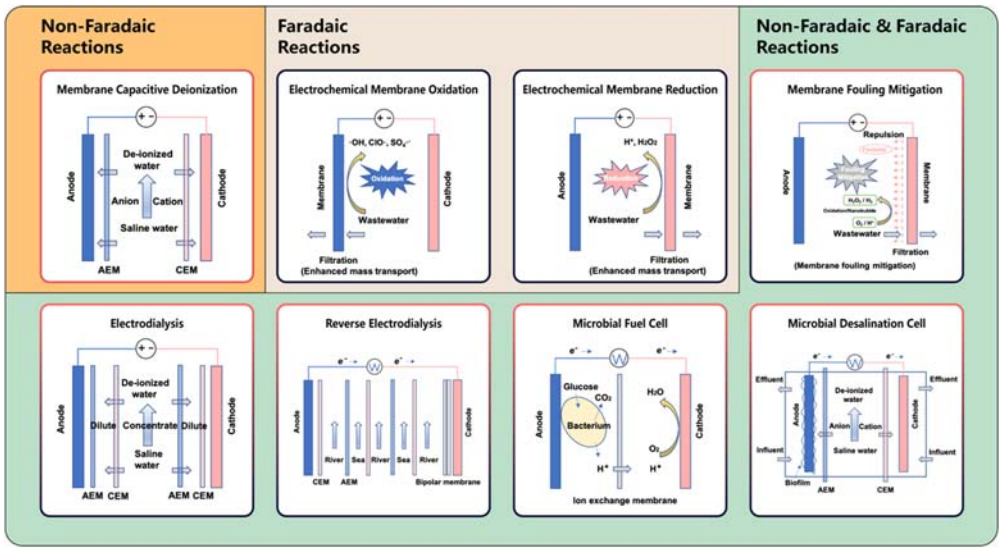

Figure 1.3 Working principles of electrochemical membrane technology.

This book belongs to Badji Mokhtar Annaba University Central Library Copyright Elsevier 2025

there are five technologies involved with both reactions (e.g., membrane fouling mitigation, ED, RED, MFC, and MDC).

During the non-Faradaic electrosorption process in CDI, the electric charge within the porous electrodes is compensated by the concurrent release of co-ions and the immobilization of counterions, thereby reducing the desalination property [47]. To overcome this issue, the IEM are set in front of the electrodes to improve the CDI performance and this system is called MCDI [48].

For MCDI systems, ion adsorption capacity is affected by the effective specific surface area of electrodes, making MCDI suitable only for the treatment of low salinity water [49]. Moreover, the preparation of the electrode is more complex than that of CDI [50]. To overcome these issues, flow-electrode capacitive deionization (FCDI) modified with some carbon materials (e.g., flowing carbon electrode instead of the fixed electrodes) has attracted extensive attention [51]. FCDI possesses a high salt removal efficiency in the treatment of high-salinity wastewater due to the infinite capacity of ion adsorption based on the uncharged carbon materials during the continual inflow [52].

Electrochemical oxidation is a redox process involving the transfer of electrons from the electrode, and it can remove pollutants via direct and indirect electrolysis. The direct electrochemical oxidation requires the adsorption of pollutants on the electrode surface and then degradation of the pollutants via direct electron-transfer [53]. During this process, the pollutants can be degraded at relatively low potentials because the oxidation potential is lower than that of oxygen evolution [54]. However, the rate of electrochemical oxidation is always affected by the slow reaction kinetics caused by a slow diffusion and a decline in catalytic activity of the electrode [32]. Boron-doped diamond (BDD) electrodes have been exploited extensively in the direct electrochemical oxidation processes as BDD possesses a higher O_2 overpotential than the commonly used metal oxide anodes [55–57]. Moreover, the high efficiency of BDD anode towards electrochemical oxidation could be attributed to the presence of adsorbed •OH generated by water oxidation at the anode surface [58]. The reaction is shown as follows:

$$\mathrm{BDD} + \mathrm{H_2O} \rightarrow \mathrm{BDD}(\bullet\mathrm{OH}) + \mathrm{H}^+ + e^- \tag{1.1}$$

The indirect electrochemical oxidation relies on the oxidizing species formed on the electrode (e.g., •OH, ClO^-, and $SO_4^{\bullet-}$), which facilitate the transformation of pollutants [59,60]. The formation of these oxidizing species is affected by the electrode material and applied potential, such as the adsorption property and O_2 overpotential of the electrode [61]. A recent study showed that the TiO_2 nanotube array had a higher electrocatalytic activity than the commercial BDD electrode for producing chlorine and •OH [62]. Thus TiO_2-based materials have a great potential to be the next-generation electrode for wastewater treatment and remediation.

This book belongs to Badji Mokhtar Annaba University Central Library Copyright Elsevier 2025

Similar to electrochemical oxidation, electrochemical reduction also involves direct and indirect reduction processes. Typically, some toxic heavy metal ions [e.g., Cr(VI) and Cu(II)] can be removed by the direct reduction [63,64]. During the reduction process, the heavy metal ions will migrate to the cathode surface by electrosorption and then be reduced via the direct electron-transfer. On the other hand, the indirect reduction process has more complex pathways in the pollutant removal. For example, the Pd based cathode will generate atomic H* in the electroreduction of H_2O/H^+ and then reduce bromate to bromide [65]:

$$\mathrm{Pd} + \mathrm{H_2O} + e^- \rightarrow \mathrm{Pd}\text{-}H^* + \mathrm{OH}^- \tag{1.2}$$

$$6\mathrm{Pd}\text{-}H^* + \mathrm{BrO_3^-} \rightarrow 6\mathrm{Pd} + \mathrm{Br}^- + 3\mathrm{H_2O} \tag{1.3}$$

In addition, the cathodic EF is also a Faradaic reaction widely used for pollutant removal. For example, the electrode (e.g., carbon materials) showing an excellent performance in the oxygen reduction reaction can produce H_2O_2 at a low cell voltage [66].

$$2\mathrm{H}^+_{(aq)} + \mathrm{O}_{2(aq)} + 2e^- \rightarrow \mathrm{H_2O}_{2(aq)} \tag{1.4}$$

Membrane fouling is a matter of great concern during the application of membrane technology in the wastewater treatment. As such, membrane fouling/scaling can be alleviated through hampering the deposition/adsorption of foulants on membrane surface, mainly the result of the electrostatic repulsion taking place between the applied electrical potential and the charged foulants. Besides, the fouling in the membrane surface can be alleviated when the cathode generates hydrogen gas and H_2O_2 [67].

For the ED technology, it is generally called "no phase transition" process [68]. The ED system equipped with selective IEM can be used in the selective recovery of heavy metals (e.g., Ni^{2+}, Cr^{3+}, and Cr^{6+}) and nutrients (e.g., K^+, NH_4^+, and PO_4^{3-}) [68]. During the ED operation, the anions and the cations in the solution will transfer through the IEM and move to the electrodes with opposite charge.

RED can be applied in the recovery of salinity-gradient energy (blue energy) using river water and sea water and directly produces electricity. RED uses IEM for ion transport, but not for water transport, and the electricity is generated by a redox reaction occurring at the electrodes [69].

In terms of RED, the energy produced by the mixture of fresh water and salty water is put to work by using alternatively arranged cation exchange membranes (CEMs) and anion exchange membranes (AEMs), with different solutions flowing through each alternate channel (Fig. 1.3). These membranes only allow selective transport of ions (anions through the AEM and cations through the CEM) from a high concentration solution to a low concentration solution. In this system, the electrochemical potential difference can be attributed to the cation migrating one way and the negative ions moving the other being converted to electrical current at the electrodes [70].

This book belongs to Badji Mokhtar Annaba University Central Library Copyright Elsevier 2025

MFC technologies can be used to generate energy by taking advantage of organic matter in wastewater. In MFC, the electrical current is generated by microorganisms oxidizing the organic matter (e.g., glucose) and releasing electrons outside the cell, which are further exploited for generating electrical power, biofuels, and value-added chemical products [71]. MFCs provide a unique pathway to directly gather the energy in wastewater, potentially changing a sewage treatment plant into a power plant. For example, exoelectrogenic bacteria can release protons into the wastewater and transfer electrons to anodes, while the electrons and protons combine with oxygen to form water at the cathode, generating a voltage for energy supply. MFCs can also be used for environmental remediation and chemical production such as hydrogen, methane and acetate.

MDC is a modified configuration of a MFC. It generates electricity via the biodegradation of organic matters in wastewater. Meanwhile, the captured electricity is used for concurrent seawater desalination and wastewater treatment [72]. In terms of MDCs, salt ions are migrated from the sea or brackish water compartments to the counter compartments through IEMs. MDCs can also be applied to the recovery of value-added substances (e.g., biohydrogen, H_2O_2, humic acid, and fulvic acid) from wastewater.

1.2.4 Preparations of electrochemical membranes

The preparation of IEMs is distinctly different from that of CMs and the typical preparation methods of the electrochemical membranes are briefly introduced below.

1.2.4.1 Preparation of ion exchange membrane

A conventional process for preparing IEMs is casting, in which the membrane is prepared by casting polymer onto a leveling plate followed with an evaporation of solvents. Nowadays, it is still the most widely used method for preparing and modifying IEMs.

Polymer blending: Could combine the superior characteristics of each polymer while overcoming the shortcoming of the membrane made of a single polymer. Therefore this method could not only improve the stability, selectivity and ion conductivity, but also reduce the cost and swelling rate of IEMs [73].

Pore filling: Can not only inhibit swelling of IEMs but also increase the selectivity of IEMs. Nonetheless, an appropriate porous substrate, which is required to be mechanically stable and chemically inert, has to be prepared to restrict the expansion of soft polyelectrolytes in pores when using this method [74].

In situ polymerization: Is a simple, rapid, and environment-friendly method in which the liquid monomers are directly polymerized and fully integrated with the substrate [75–78]. It is solvent-free and does not need any postmodification processing.

Electrospinning: Could produce nanofibers with nanoscale diameters, which possess attractive characteristics like high porosity, large specific surface area, fully interconnected pores, and three dimensional networks [79,80].

This book belongs to Badji Mokhtar Annaba University Central Library Copyright Elsevier 2025

1.2.4.2 Preparation of conductive membrane

The preparation method of CM is subject to conductive membrane's having the membrane types of polymer-, metal-, and carbon-based CM.

Polymer-based CM: Some general preparation methods of polymer-based CM are introduced below. However, in some circumstances, there might be some combinations of these preparation methods to meet specific requirements [81,82].

1. *In situ polymerization*: Is used to form a conductive coating on the membrane substrate. Typically, monomers start polymerizing in the presence of an initiator, which is previously adhered to the membrane substrate surface through soaking [83], spraying [84], or painting [85].
2. *Phase inversion*: Is another typical method of fabricating membrane. The membrane is formed instantly when the precursor is immersed into the inversion phase. The properties of the membrane largely depend on the operation conditions of phase inversion and the polymer dope. CM could be obtained using a casting solution containing the conductive materials [86–91].
3. *Electrospinning*: Is another membrane fabricating method and is operated by an electrospinner and a polymer solution. Therefore a polymer solution blended with conductive materials is used to fabricate the conductive polymer membrane [92,93].

Inorganic CM: Are generally classified into metal membranes and metal oxide membranes. Methods for fabricating these membranes are introduced below.

1. *Dry-wetting spinning* (metal membranes): Is an emerging approach for fabricating metal hollow-fiber membranes. The spinning solution usually contains metals (e.g., stainless steel powder) and casting solutions. The obtained membranes can exhibit more robust mechanical strength than polymeric membranes or ceramic membranes [94].
2. *Electrodeposition* (metal membranes): Can coat a porous metallic layer on the surface of the porous substrate [95,96]. The process is usually performed in a cell and the conductive substrate acts as the cathode.
3. *Sol-gel method* (metal oxide membranes): Needs precursors containing metal ions [97] to form metal-oxo or metal-hydroxo polymers, followed with drying and sintering to coat metal oxide materials on the substrate [98,99].
4. *Sintering method* (metal oxide membranes): This method is usually performed to prepare a metal oxide membrane by using metal-oxide powder and binder [100,101]. Sintering temperature and atmosphere are the key parameters to successful output.
5. *Modified phase inversion* (metal-base composite membranes): This method is used to fabricate a composite membrane comprising metallic support and polymeric membrane. It was realized by introducing metal materials into conventional phase inversion process, and the metallic support and the polymeric membrane act as conductive base and separation barrier, respectively [102,103].

This book belongs to Badji Mokhtar Annaba University Central Library Copyright Elsevier 2025

Carbon-based CM: can be fabricated by self-assembly and chemical vapor deposit.

1. *Self-assembly*: The self-assembly of graphene oxide, reduced graphene oxide, and MXene membrane was realized by filtrating a dispersion solution of nanomaterials onto a substrate due to hydrophobic effect, van der Waals force, or electrostatic interaction [104,105].
2. *Chemical vapor deposit (CVD)*: This fabrication method can produce carbon-based nanomaterials (e.g., carbon nanotubes (CNTs) and graphene) on membrane surface in situ [106,107], in which the substrate is exposed to gaseous compounds or elemental substances containing target elements at high temperature (e.g., acetylene and H_2) to finish the reaction [107].

1.3 Applications of electrochemical membrane technologies

1.3.1 Ion exchange membrane based electrochemical membrane technologies

1.3.1.1 Electrodialysis

Traditional ED process (ED), where a voltage is applied between the anode and cathode electrodes, can selectively separate and concentrate ions. The concept of ED was first proposed by Maigrot and Sabates in 1889 [14]; however, the term "Electrodialysis" was used in 1900 for the first time in Schollmeyer's patent for sugar syrup purification [108]. Afterwards (in 1939), IEM were employed by Manegold and Kalauch in a 3-compartment ED apparatus in the form of perm-selective anion and cation-selective membranes [15]. And then the multisections ED was invented by Meyer and Strauss in 1940 to improve the energy efficiency [108]. Later, significant advancements had been made in the following years such as stability, high selectivity, and low electric resistance, eventually leading to a large-scale ED system for the treatment of industrial wastewater [14,109].

ED is now a widely used electrochemical membrane technology for salt production and ion separation. ED can separate ionic and nonionic species from wastewaters (e.g., industrial, brackish, and municipal wastewaters) or remove charged components in versatile processes (e.g., food and drug industries, chemical processes [110–112], table salt production [113,114], biotechnology, heavy metals, electronics removal [115–117], and acids/bases production). ED has a higher water recovery, easier operation conditions, and longer membrane lifetime compared with reverse osmosis (RO, another membrane-based desalination technology). Moreover, it can selectively separate monovalent ions (e.g., K^+, Na^+, $NH_4{}^+$, Cl^-, $NO_3{}^-$) from multivalent ions (e.g., $PO_4{}^{3-}$, $SO_4{}^{2-}$, Mg^{2+}, Ca^{2+}) with those IEMs perm-selective to monovalent ions [113,118–122]. As summarized in Table 1.3, some ED was used to recover and concentrate ions like potassium ions (K^+)

This book belongs to Badji Mokhtar Annaba University Central Library Copyright Elsevier 2025

This book belongs to Badji Mokhtar Annaba University Central Library

Table 1.3 Summary of typical applications of electrochemical membrane technologies.

Technology	Materials	Operating parameters				Performance evaluation index				Reference
		Cell voltage (V)/ Current density (mA/cm^2)	Pollutant concentration	pH	Membrane/ electrode area (cm^2)	Energy consumption	Charge efficiency (%)	Removal efficiency (%)	Flow rate	
Electrodialysis	Polymer inclusion membrane/ IEM: AEM, CEM	2.3 ~ 10.9 V; 10 mA/cm^2	Cr (VI) (250 mg/L)	n.a.	20	n.a.	n.a.	86.4 ~ 91.2	n.a.	Li et al. [123]
	Polypyrrole membrane/ IEM: AEM, CEM	2 V	K^+ (632.6 mg/L)	7	n.a.	3.80 kWh/ (kg K)	n.a.	n.a.	n.a.	Zhou et al. [124]
	Pt and Ti electrode / IEM: AEM, CEM	0 ~ 12 V	Cobalt (1180 mg/L)	n.a.	17500	1.76 ~ 4.8 kWh/m^3	n.a.	99.5	n.a.	Alkhadra et al. [125]
	TiO_2 electrode/ IEM: AEM, CEM	5 ~ 25 V	NO_3^--N (1000 mg/L)	8	n.a.	0.8 ~ 7.5 kWh/m^3	n.a.	> 94	0.5 ~ 1.17 L/min	Aliaskari et al. [126]
	Ti wire electrode/IEM: AEM, CEM	6 ~ 10 V	$H_2PO_4^-$-P (40 mg/L)	10	n.a.	29.4 ~ 160.1 kWh/kg	2.54%	> 99	n.a.	Ye et al. [127]
	IEM: AEM, CEM	10 ~ 25 mA/cm^2	$ZnSO_4$ (16.1 g/L)	2	16	2.34 ~ 2.93 kWh $(kg\ ZnSO_4)^{-1}$	n.a.	94.6	n.a.	Babilas et al. [128]
	Ti/TiO_2-RuO_2-IrO_2 electrode/IEM: MSAEM, CEM	13 V;30 mA/cm^2	Na_2SO_4 (8.8 g/L)	12.9	50	96 kWh/m^3	70	87	240 ~ 840 mL/h	Selvaraj et al. [129]
Reverse electrodialysis	Pt/ stainless steel electrode/ IEM: AEM, CEM	~1.2 V;0.026 mA/cm^2	NaCl (35.1 g/L)	7.2	19.6	n.a.	22	n.a.	0.8 mL/min	Nam et al. [130]
	IEM: AEM, CEM	n.a.	NaCl (35.1 g/L)	n.a.	n.a.	0.36 kWh/m^3	33 ~ 44	n.a.	n.a.	Yip et al. [131]
	Pt/Ti mesh electrode /IEM: AEM, CEM	1.6 ~ 3.3 V; 0 ~ 1.5 mA/cm^2	Urea (9016 ± 1381 mg/L)	n.a.	19.6	0.018−0.053 kWh/m^3	5 ~ 22	4.4	5 mL/min	Volpin et al. [132]
	RED stack BV electrode /IEM: AEM, CEM	n.a.	NaCl (5.9 ~ 29.3 g/L)	n.a.	36 ~ 1936	n.a.	44.9	n.a.	70 ~ 4096 mL/min	Moreno et al. [133]
	Carbon felt electrode/ IEM: AEM, CEM	1.5 V;0.4 mA/cm^2	$MgCl_2 \cdot 6H_2O$ (4 g/L)	8	190	0.29 W/m^2	n.a.	99.5	n.a.	Jwa et al. [70]
	IEM: AEM, CEM	1 mA/cm^2	NaCl (29.7 g/L)	n.a.	100	<0.7 W/m^2	n.a.	n.a.	60 mL/min	Vermaas et al. [134]
Microbial fuel cell	Carbon veil electrode /IEM: AEM, CEM	n.a.	PO_4^{3-} (950 mg/L)	9.2	2430	n.a.	n.a.	99.7	n.a.	Merino et al. [135]
	Carbon brushes electrode /IEM: CEM	0.2 V	Aniline (260.8 mg/L)	7	7	n.a.	5.1 ~ 11.9	91.2 ± 2.2	n.a.	Cheng et al. [136]
	Carbon felt electrode/ proton exchange membrane	1.1 mA/cm^2	COD (1108 ± 87 mg/L)	7	19.6	n.a.	n.a.	78.9 ± 2.4	1.0 mL/min	Zhang et al. [137]

Copyright Elsevier 2025

This book belongs to Badji Mokhtar Annaba University Central Library

	Graphite/Mn electrode	49.3 mA/cm^2	Ciprofloxacin (200∼600 mg/L)	n.a.	n.a.	n.a.	n.a.	97.8	n.a.	Li et al. [138]
	PPy@NMCF-1000 electrode	1.2 mA/cm^2	NH_4Cl (7.2 g/L) Sodium acetate (25.2 g/L)	7	n.a.	5 W/m^2	2.2∼2.7	n.a.	n.a.	Wang et al. [71]
	Steel plate electrode	0.07∼0.3 mA/cm^2	COD (621.3 mg/L) TN (51.9 mg/L) TP (18.7 mg/L)	6.9∼7.5	100	56∼982 mW/m^2	n.a.	COD 75∼100% TN 57∼86% TP 80∼100%	n.a.	Saeed et al. [139]
Microbial desalination cell	Pt/C electrode/IEM: AEM, CEM	n.a.	NaCl (5∼35 g/L)	n.a.	n.a.	n.a.	n.a.	79.2 ± 4.7	0.06∼0.1 mL/min	Ping et al. [140]
	Activated carbon granules electrode/IEM: AEM, CEM	0.55 mA/cm^2	NaCl (0.5 g/L)	7	675	n.a.	n.a.	> 93	80 mL/min	Zuo et al. [141]
	Ti mesh electrode/IEM: AEM, CEM	0.018∼0.027 mA/cm^2	COD (612.7 ± 90.3 mg/L)	n.a.	140	113.9 $mW/(m^2\ s)$	6.28∼7.71	97.2	4∼20 mL/min	Zuo et al. [142]
	Graphite electrode/ IEM: AEM, CEM	1.54 V	COD (4911 mg/L)	7	n.a.	8.16 W/m^3	n.a.	91.1	n.a.	Ebrahimi et al. [143]
	Carbon paper electrode/ IEM: AEM, CEM	n.a.	COD (500 mg/L)	6.8	28.27	1.1 W/m^3	68	n.a.	n.a.	Kokabian et al. [72]
	IEM: AEM, CEM	n.a.	COD (750 mg/L)	n.a.	150	n.a.	83.6∼90.2	93	n.a.	Yuan et al. [144]
Membrane capacitive deionization	Porous carbon electrode/ IEM: AEM, CEM	0.4 V	NaCl (503.1 mg/L)	7	5900	23.9∼712 kJ/m^3	n.a.	17.9∼90.6	1 L/min	Długołęcki et al. [145]
	Activated carbon electrode/ IEM: AEM, CEM	1.2 V	NaCl (585 mg/L)	n.a.	10	n.a.	86.3%	n.a.	n.a.	Jain et al. [146]
	Flow electrode/ IEM: AEM, CEM	n.a.	NH_4^+-N (40 mg/L)	n.a.	34.9	9.9∼21.1 kWh $(kg\ of\ N)^{-1}$	n.a.	∼90	0.85∼2.55 mL/min.	Zhang et al. [147]
	Granular activated carbon electrode/ IEM: AEM, CEM	1.2 V	NaCl (100 mg/L)	7	7.1	n.a.	n.a.	n.a.	13.5 mL/min	Bian et al. [148]
	Activated carbon electrode/ IEM: AEM, CEM	1.2∼1.5 V	NO_3^--N (10.6 mg/L)	n.a.	100	n.a.	73.3	91	0.5∼2.5 mL/min	Kim et al. [149]
	Ti-Ru electrode/ IEM: AEM, CEM	1.2 V	NH_4^+-N (19.6 mg/L)	n.a.	40	n.a.	>94	>65	14.4 mL/min	Wang et al. [150]

(*continued*)

Copyright Elsevier 2025

This book belongs to Badji Mokhtar Annaba University Central Library

Table 1.3 (Continued)

Technology	Materials	Operating parameters				Performance evaluation index				Reference
		Cell voltage (V)/ Current density (mA/cm^2)	Pollutant concentration	pH	Membrane/ electrode area (cm^2)	Energy consumption	Charge efficiency (%)	Removal efficiency (%)	Flow rate	
Electrochemical membrane oxidation	GO/SnO_2/CFs membrane	3.4 V	SMX (10 mg/L)	n.a.	11.34	n.a.	n.a.	85	n.a.	Yu et al. [151]
	FeOOH-CNT filter	1∼3 V	As (V) (500 μg/L)	2∼6	n.a.	n.a.	n.a.	98.3	1.5∼6 mL/min	Liu et al. [152]
	TiO_x membrane	6∼30 mA/cm^2	Paracetamol (110 mg-TOC/L)	3	27.6	n.a.	n.a.	59	1∼3 L/min	Trellu et al. [153]
	TiO_2 membrane	1∼5 V	Triclosan (10 mg/L)	7	50.24	n.a.	n.a.	99.8	300 mL/min	Qian et al. [154]
	Bi-SnO_2-TiO_x membrane	2.1∼3.5 V	Terephthalic acid (166 mg/L)	n.a.	0.95	<0.53 kWh/m^3	n.a.	72.4	0.2∼1.0 mL/min	Gayen et al. [155]
	Ti_4O_7 membrane	1.7∼3.2 V/0∼3.5 mA/cm^2	p-methoxyphenol (124 mg/L)	n.a.	125.6	n.a.	25.9∼99	59∼99	600 mL/min	Zaky et al. [156]
Electrochemical membrane reduction	Pd-Cu/REM membrane	5 V	NO_3^--N (14 mg-N/L)	8.1	n.a.	1.1 kWh/ m^3	29	43	0.2∼1.8 mL/min	Gayen et al. [157]
	Au-CNT filter	5 V	Tetracycline (17.7 mg/L)	7.8	n.a.	0.25 kWh/m^3	n.a.	76.8	1.5∼4.5 mL/min	Liu et al. [158]
	PANI-CNT filter	5 V	Cr (VI) (1 mg/L)	7	n.a.	0.032 kWh/m^3	n.a.	70.2	1.5∼6 mL/min	Liu et al. [63]
	CNT-$COOFe^{2+}$ filter	2.89 V	Trichloroacetic acid (40.9 mg/L)	7	9.6	45.8 kWh $(kg\ TOC)^{-1}$	45	n.a.	1.6 mL/min	Gao et al. [159]
	MWCNT-Ti_4O_7 membrane	3 V	Dibromoacetic acid (1 mg/L)	n.a.	0.5	0.22 kWh/m^3	n.a.	96	n.a.	Almassi et al. [101]
	PVDF membrane/Ti mesh	3 V	Cu-EDTA (178.1 mg/L)	n.a.	70	93.5 g/ kWh	n.a.	81.5	2.5 mL/min	Li et al. [102]

Note: n.a. is the abbreviation of "not available." *CNT*, carbon nanotubes; *PVDF*, polyvinylidene difluoride; *REM*, reactive electrochemical membrane; *TOC*, total organic carbon.

Copyright Elsevier 2025

[124], nitrate $\left(NO_3^-\right)$ [126], dihydric phosphate $\left(H_2PO_4^-\right)$ [127], and sulfate $\left(SO_4^{2-}\right)$ [129]. Also, some was used to remove heavy metals ions from wastewater such as chromium (Cr^{6+}) [123] and cobalt (Co^{2+}) [125].

In an ED cell, several anion exchange membranes (AEMs) and CEM were set between the anode and cathode electrodes. The IEMs were separated by a spacer gasket to create dilute and concentrate compartments. The electrolyte solution is then circulated in the electrode rinse compartments. Obviously, IEMs are the key component not only in ED configuration but also in ED applications to achieve a high desalination efficiency and high water recovery [160]. However, a main obstacle that restricts the widespread application of ED is IEM fouling (e.g., organic fouling, biofouling are some examples).

Much effort has been focused on the enhancement of antifouling properties of IEMs. A typical strategy to reduce the membrane fouling is to apply external forces such as microwave, magnetic field, ultrasonic, and electric pulse, [161] but it would increase the ED operation costs. An alternative to fouling control is the ED reversal (EDR) operation, which has been proved to be effective in reducing the fouling propensity of IEMs [162]. Moreover, EDR is also beneficial in operation cost control by reducing pH adjustment, pre-treatments, and cleaning procedures. EDR can also be applied in harsh conditions like super-saturated salt solution because the EDR concentrate chamber residence time could influence the salt nucleation kinetics [163]. A much longer lifetime of IEMs (up to 10–15 years) is achieved by employing the EDR operation [162].

Another strategy for fouling control is that of applying the pulsed electrical field (PEF) in ED [164,165]. The deposition of charged molecules on the IEMs surface could be effectively disturbed by the discontinuous electric current. This was verified by Sayadi et al. and Suwal et al. who observed the positive effect of PEF on fouling control [166,167].

1.3.1.2 Reverse electrodialysis

RED is designed for capturing energy from water streams, which was mixed by two water streams of different salinities. In the first prototype of RED invented in 1954, fresh water and seawater were mixed at 39°C in a bench scale "hydroelectric pile" comprising 47 pairs of alternating acidic and basic membranes. It could only gain an electromotive force of 3.1 V and a power output of 0.2 W/m^2 [168]. However, theoretical models of RED were not established until two decades later [169,170]. Although early theoretical studies argued that RED was a competitive technology to harvest energy [171,172], the performance of the early works did not match the predicted levels but showed impractically low power output and density. In 1983, concentration of 250 g/L of NaCl solution paired to a 1 g/L NaCl solution could merely produce 0.4 W/m^2 [173]. Therefore much attention has been focused on the role of

This book belongs to Badji Mokhtar Annaba University Central Library Copyright Elsevier 2025

IEMs [174,175], stack configuration [175–178], and operation conditions to improve the performance of RED thereafter [176,179–182]. In 2012, an energy density of 1.27 W/m^2 was reported by applying a tailor-made IEM for RED [183]. Moreover, the nano/microfluidic RED employing ion-selective nanochannels dramatically increased the energy density to 20 $W/m^2 \sim 2600$ W/m^2 [184,185]. Some recent studies of reverse ED are also summarized in Table 1.3.

RED is also combined with other technologies to produce energy. For instance, thermal-based solution separation process (e.g., distillation process) could be integrated with RED to form a closed-loop RED heat engine, which could convert low-grade heat ($\geq 40°C$) to electricity [186–188]. Moreover, bioelectrochemical fuel cell (i.e., microbial RED cell) could also be combined with RED, which could prevent electrode reactions of high overpotential in RED stack and thereby boosted power output of bioelectrochemical fuel cell [189–191]. Furthermore, the combination of RED with different desalination processes (e.g., RO, ED, or CDI) has also proved feasible in enhancing RED power generation [192–197].

1.3.1.3 Membrane capacitive deionization

The CDI technology was proposed in the late 1960s, followed by its sluggish development between the late 1970s and 2000s [20,21]. The conventional CDI system may be affected by Faradaic reactions on the electrode surface and the effect of co-ions, leading to a sharp decline in the capacitive performance of the carbon electrode [22,198,199]. In 2006, the membrane was first introduced in the CDI system and this modified CDI system was called "MCDI" [22].

Compared with CDI, the technology of MCDI can minimize Faradaic reactions on the electrode surface and prevent the effect of coions [22,198,199]. In this system, the IEM are placed in the front of the electrode. When an electric field is applied in the MCDI system, the anions migrate to the anode, going through an anion exchange membrane (AEM). There are two main IEMs for MCDI, that is, anion exchange membrane and cation exchange membrane. During the salt adsorption, the IEMs govern the ion mass transfer. Specifically, the divalent ions (e.g., Ca^{2+}) show a slower diffusion coefficient than do monovalent ions (e.g., K^+, Na^+) [200]. In the capacitive ion storage process, ions are commonly adsorbed electrostatically and stored capacitively in the intraparticle pores of the carbon electrode [30]. Therefore charged ionic species like sodium ions (Na^+) [145,146,148], nitrate $\left(NO_3^-\right)$ [149], and ammonium ions $\left(NH_4^+\right)$ [147,150] could be removed from aqueous solutions. Some recent MCDI studies are listed in Table 1.3.

The ion storage in the MCDI desalination process includes two main processes, that is, Faradaic and non-Faradaic processes [201]. The Faradaic process can be categorized as oxidation reactions, reduction reactions, and Faradaic ion storage processes. Some of these processes may generate by-products or result in pH fluctuations, leading

This book belongs to Badji Mokhtar Annaba University Central Library Copyright Elsevier 2025

to the decrease of energy efficiency and electrode lifespan [202,203]. The oxidation reactions taking place at the anode that include water oxidation, carbon electrode oxidation, chloride oxidation, and oxidations of other organic matters and inorganic ions. Among these reactions, the carbon electrode oxidation caught the people's attention to an extensive degree because it can impair pore structure in the electrode and thereby cause a decline of the CDI performance of the carbon electrode [204]. The reduction reaction occurs at the cathode and it is mainly involved with the oxygen reduction reaction, which may generate some by-products (e.g., H_2O_2) and accelerate the carbon oxidation reaction at the anode [205].

Unlike Faradaic processes, non-Faradaic processes trap ions by the electrical double layer (EDL) on the carbon electrode surface. To improve the non-Faradaic capacitive ion storage, many protocols have been explored to prepare an electrode with a high electrical conductivity, a large surface area, an appropriate pore distribution, and an excellent chemical stability [21,32,206,207].

Current MCDI technology is mainly applied in the brackish water desalination, disinfection, and selective removal of the specific ion from a multiionic salt solution. For the brackish water desalination, however, the generation of concentrated streams can be an issue. A recovery of specific ions from the concentrated streams (e.g., recovery of ammonium by the gas stripping method, or the recovery of palladium by the electrowinning method) can be a viable approach to overcome this issue, even though the recovery process requires an extremely concentrated solution [147,208].

MCDI has also been applied as a feasible disinfection technology [209]. A relatively high potential can disturb the redox potential of the biomembrane, resulting in an inhibition of bacterial growth. In addition, due to the difference of hydrated radius, diffusion coefficient, and ion charge number, MCDI can achieve a satisfactory removal of specific ions from mixed ions [210]. For example, Cohen et al. demonstrated a selective recovery of Br^- from a mixture of Cl^- and Br^- with MCDI. During this process, Br_2 molecules were generated and physically adsorbed on the anode surface. After the discharging operation, Br_2 molecules were reduced back to Br^- and released to the solution [211].

1.3.1.4 Microbial fuel cell

MFC, an alternative energy harnessing and storage technology, has drawn considerable attention since it could convert chemical energy into electricity via anodic microbial catalytic reactions and cathodic microbial/enzymatic/abiotic reactions [19,212]. In 1911, M.C. Potter first conceived the concept of producing electricity using microbes [16], notwithstanding the idea of "animal electricity" dating back to the 18th century with the frog legs experiments by Galvani [213]. M.C. Potter demonstrated that living cultures of *Escherichia coli* and *Saccharomyces* could produce electrical energy by using platinum electrodes. This important discovery did not arouse much curiosity until the 1980s–90s when electrochemically active bacteria, instead of synthetic mediators, was

This book belongs to Badji Mokhtar Annaba University Central Library Copyright Elsevier 2025

first reported to produce natural shuttle molecules for electron transfer [17,18]. This led to the fast development of the so-called "analytical MFC." Since then, MFCs have been used for harnessing energy from the metabolism of microorganisms and simultaneously to treat wastewater [214,215].

Conventional MFC reactor consists of two chambers, including an anodic chamber and a cathodic chamber, where an IEM was used as chambers separation technique. The IEM used in MFC should have had good insulation, durability, biocompatibility, ion selectivity (e.g., proton-conducting), ionic conduction, chemical stability, fouling resistance as well as a low cost [216]. There are 5 categories of IEMs including mosaic IEMs, bipolar membranes (BPMs), amphoteric IEMs, anion exchange membranes (AEMs) (also called monopolar membranes), and CEMs [216]. CEMs contain negatively charged groups (e.g., $-PO_3H^-$, $-PO_3^{2-}$, $-SO_3^-$, or $-COO^-$) fixed to the membrane backbone, with the proton exchange membrane (PEM) being a typical CEM, which is specially designed to allow the transfer of protons into the cathode chamber [217]. Nafion is one of the most commonly used PEMs in MFCs [218] but the high cost hampers its application in MFCs. Therefore it is important to employ other low-cost membranes (e.g., earthen pot, porous ceramic, nylon and glass fiber filters, and composite and nanocomposite membranes) as replacement for Nafion membranes or use membrane-less MFCs [219,220]. In the anodic chamber, electrons and protons are generated by microorganisms consuming organic matters in the wastewater through metabolism (anaerobic degradation). Electrons migrate from anode through an external circuit to the cathode, while protons pass through the PEM to the cathode chamber to maintain the electroneutrality.

Therefore in comparison with conventional wastewater treatment technologies, MFCs exhibit some distinctive advantages: (1) direct transformation of organic substrates into clean electricity or sustainable energy through biotic electrocatalyst, (2) less sludge production, and (3) absence of energy input for aeration. These unique advantages of the MFC over conventional technologies for wastewater treatment facilitate the development of MFCs for wastewater treatment, power generation, biohydrogen generation, and biosensor manufacturing [221]. The bibliometric analysis of MFC in the Web of Science database retrieved 3514 publications on this scenario for the period from 2011 to 2020 by utilizing keywords "MFC" and "wastewater treatment," among which various pollutants like organics [136–139], nitrogen [71], and phosphorus [135] are effectively removed by the MFCs. Some recent MFC studies are summarized in Table 1.3.

Despite tremendous improvements having been made in the last decade, there are still some big obstacles for the practical applications and scale-up of MFCs. The main bottleneck of MFC application from the practical standpoint concerns the cost of MFC [222,223], due to its requiring the usage of expensive membrane materials/separators and electrode materials. Moreover, the performance of MFC systems is also influenced by several other factors, such as organic loading, membrane stability, and fouling.

This book belongs to Badji Mokhtar Annaba University Central Library Copyright Elsevier 2025

Since the electrode materials are strongly associated with the performance of MFCs, numerous efforts have been conducted to modify electrode materials to acquire higher power output. In recent years, carbon-based materials such as graphite rod/plates/fiber brush and carbon cloth/paper/felt are increasingly used in MFCs [224,225]. Substantial efforts have been made to improve the performance of MFC through optimizing configuration design, microorganisms, membranes, and electrodes.

1.3.1.5 Microbial desalination cell

The MDC is a promising technology which combines MFC process and ED for seawater desalination, wastewater treatment, and the production of renewable energy [226,227]. The pioneering MDCs, with the form of plate stacking with an installed IEM to remove salts from seawater and brackish water, were designed and fabricated by Cao et al. in 2009 [19]. Since then, various configurations of the MDC have been designed to realize different functions [228].

In order to convert an MFC to an MDC, a third chamber, which is used as a desalination chamber, is inserted between the anodic and cathodic chambers using a pair of CEM and AEM (Fig. 1.3). Once the current is generated by the microorganisms on the anode, protons would be released into the solution and negatively charged species will move from the middle chamber to the anode because the positively charged species could not leave the anode by the AEM. While in the cathode chamber, the protons are gradually consumed and result in positively charged species in the middle chamber moving to the cathode chamber. The elimination of ionic species from the middle chamber leads to water desalination without water pressurization or draw solutions. As such, electricity is generated and, in the meantime, the water is desalinated [19,229,230]. Some recent studies of MDC are summarized in Table 1.3.

1.3.2 Conductive membrane based electrochemical membrane technologies

1.3.2.1 Membrane fouling mitigation

In 2006, Madaeni found that CM could obtain higher fluxes in filtration of bovine serum albumin (BSA, charged protein) solution than would a nonconductive membrane, and it was identified that this can be mainly attributed to the electrostatic repulsion between negatively charged BSA and membrane surface [25]. This finding triggered the application of CM in fouling mitigation, with some related studies listed in Table 1.4. Different configurations of CM, including microfiltration/ultrafiltration (MF/UF) [231–236], membrane bioreactor (MBR) [242], forward osmosis (FO) [241], RO [239], and membrane distillation (MD) [237], have been investigated and have been known to achieve fouling/scaling mitigation with the assistance of an electric field.

This book belongs to Badji Mokhtar Annaba University Central Library Copyright Elsevier 2025

This book belongs to Badji Mokhtar Annaba University Central Library

Table 1.4 Summary of electrochemical membrane technologies on membrane fouling mitigation.

Technology	Materials	Operating parameters				Performance evaluation index			Reference
		Cell voltage (V)/Current density (mA/cm^2)	Pollutant concentration	pH	Membrane/ electrode area (cm^2)	Removal efficiency (%)	Flow rate	Performance	
Electrified membrane separation (Membrane Fouling Mitigation)	Graphene nanoplates (GNPs)/PVDF membrane	6 V	Sodium alginate (20 ppm) + NaCl (10000 ppm)	n.a.	10.2	n.a.	n.a.	Approximately 10-fold increase of flux could be achieved by in situ cleaning of membrane surface via periodical electrolysis and gas-bubbles generation.	Abid et al. [231]
	PDA/PVDF/Ag@Ni membrane	0 ~ 20 V	Congo red (CR, 50 mg/L), Methylene blue (MB, 20 mg/L) and Rhodamine B (RB, 20 mg/L)	n.a.	12	CR: 49.83 ~ 97.93 MB: > 30 RB: 5 ~ 30	202.51 ± 9.63 L/m^2/h	Extremely high permeability and high selectivity of Congo red (CR), and an enhancement in antibacterial performance.	Zhang et al. [232]
	MWCNTs/graphene/ PTFE membrane	0.5 ~ 1.5 V/cm	Humic acid (HA, 20 mg/L) + NaCl (3.5 *wt*.%) + NaOH (40 g/L)	n.a.	20	99.5	~ 12 L/m^2/h	Best antifouling performance is achieved using an intermittent electric field with a field strength of 1.0 V/cm (less than 30% flux reduction after filtration of 360 min).	Huang et al. [233]
	Ni/PES membrane	100 mA/cm^2	Yeast (5 g/L) + Na_2SO_4 (100 mM)	n.a.	n.a.	n.a.	300 L/m^2 h	60% of total TMP could be recovered in the last filtration cycle by in situ cleaning of membrane surface via periodic electrolysis and gas-bubbles generation.	Bell et al. [234]
	sSEBS/ PEDOT membrane	n.a.	Pectin (0.1*wt*%) + Tannic acid (0.02*wt*%) + Sodium bitartrate (0.1 M)	n.a.	15.9	n.a.	250 mL/min	The fouling process of conductive sSEBS/ PEDOT microfiltration membrane can be monitored by membrane resistance measurements in real-time.	Li et al. [235]

Copyright Elsevier 2025

This book belongs to Badji Mokhtar Annaba University Central Library

h-CNT/CM	0 ~ 4 V	Sodiumalginate (SA) (4 mg/L) + NaCl (100 mM)	Ambient	12.6	n.a.	500 mL/min	A near complete water flux recovery could be achieved by in situ electro-generation of RCS, following a short (1 min) self-cleaning with an applied voltage and NaCl solution.	Wang et al. [236]
CNT/polymer composite MD membrane	20 mA	Simulated geothermal brines	n.a.	n.a.	n.a.	14 cm/s	Membrane flux is increased due to the enhanced heat transport from the bulk feed to the membrane surface, and electrochemical cleaning of silicate scaling could be achieved by water electrolysis on the electrically conducting membrane surface, negating the need of chemical cleaning.	Tang et al. [237]
CNTs/ceramic membrane	Anodic polarization at +1.0 V, cathodic polarization at -1.0 V, alternating polarization at ±0.5 to ±1.5 V	*Escherichia coli*, 10^7 cfu/mL), HA (10 mg/L), *E. coli* (10^3 cfu/mL) + HA (10 mg/L)	n.a.	10	*E. coli* 100% TOC removal: 35% ~ 90%	0.2 m/s	An 8.1-fold and 1.5-fold enhancements in permeate flux were obtained by electro-polarizing the membrane while filtering bacteria and NOM from water, respectively.	Fan et al. [238]
PA-CNT RO membrane	1.5 V in $CaSO_4$ scaling experiments, and 2.5 V in $CaCO_3$ scaling experiments	Na_2SO_4 (0.0105 M) + $MgSO_4$ (0.0145 M) + $CaCl_2$ (0.0164 M), Na_2CO_3 (0.0094M) + KCl (0.0107M) + $CaCl_2$ (0.0072M) + $MgCl_2$ (0.0047M)	n.a.	20	n.a.	$CaSO_4$ scaling experiments: 3.4 cm/s $CaCO_3$ scaling experiments: 4.5 cm/s	$CaCO_3$ and $CaSO_4$ were efficiently removed from the membrane surface through the intermittent application of a 2.5 V potential and the continuous application of 1.5 V DC to the membrane surface, respectively.	Duan et al. [239]

(*continued*)

Copyright Elsevier 2025

This book belongs to Badji Mokhtar Annaba University Central Library

Table 1.4 (Continued)

Technology	Materials	Operating parameters				Performance evaluation index			Reference
		Cell voltage (V)/Current density (mA/cm^2)	Pollutant concentration	pH	Membrane/ electrode area (cm^2)	Removal efficiency (%)	Flow rate	Performance	
	PPy-DBS membrane	± 1.8 V	HA (20 mg/L), HA (20 mg/L) in various salt solutions	n.a.	6	n.a.	PPy-DBS membrane: 158.02 L/m^2/h bar PPy-DBS membrane with oxidation and reduction: 170.43 and 134.16 L/m^2/h bar	Membrane fouling could be effectively alleviated by adjusting the membrane pore size combined with cleaning. The specific flux of PPy-DBS membrane was increased by 21.91% after applying the voltages and backwashing.	Tan et al. [240]
	Car-PES FO TFC membrane	0, 2.0 V DC	*E. coli* and *Staphylococcus aureus* (10^7 CFU/mL), BSA-FITC solution (0.5 mg/mL PBS solution)	n.a.	9.62	n.a.	0.1 L/min	Good organic and microbial fouling resistances could be achieved by applying a 2.0 V DC voltage and the carbon paper-based FO-TFC membranes possess good mechanical stability for practical use.	Liu et al. [241]
	PVDF hollow fiber ultrafiltration membrane	1 and 3 V/cm	Simulated municipal wastewater	7.12 ± 0.31	470	Orthophosphate (PO_4-P): 96.06% Ammonia nitrogen (NH^4-N): 69.34%	15 LMH	An enhancement of the effluent quality and a reduction of membrane fouling could be achieved by applying 1 and 3 V/cm voltage gradients. The membrane fouling rate was reduced by 15.84% at 1 V/cm and 54.33% at 3 V/cm compared to the control.	Borea et al. [242]

Note: n.a. is the abbreviation of "not available." *CNT*, carbon nanotubes; *PVDF*, polyvinylidene difluoride; *TOC*, total organic carbon.

Copyright Elsevier 2025

The phenomenon of less fouling having occurred on CM is mainly attributed to electrostatic repulsion while there are also some other reasons. For example, organic, inorganic scaling, and biological foulants can be removed by in situ generated gas-bubbles [231,234], hydroxide ion [237], or reactive chlorine species [236]. Moreover, the electrochemical oxidation reaction could further reduce the membrane fouling (discussed in the next section). Other than electrochemical reactions, membrane surface properties such as charge [237], hydrophilicity [239], and interfacial nanostructure [240] can be adjusted under the electric field and will provide an additional means to reduce membrane fouling.

1.3.2.2 Electrochemical membrane oxidation

Advanced oxidation processes (AOPs) refer to those processes involved with the generation of a powerful oxidant agent (e.g., •OH) in solution under near-ambient temperature and pressure [243]. Since •OH could be generated either by anodic electrolysis of water or by Fenton/Fenton-like chemistry with electrogenerated H_2O_2, the electrochemical advanced oxidation processes (EAOPs) are classified into either traditional electrochemical systems or EF systems. EAOP is an effective approach to remove refractory pollutants [244,245]. However, its efficiency was not so high as expected when used for treating real wastewater because the poor mass transfer around the electrodes. Membrane filtration could facilitate the mass transfer in the vicinity of the electrodes and thereby enhance the efficiency of pollutant degradation [102]. Moreover, EAOPs could eliminate membrane fouling via the oxidation of the foulants [10].

The first study of electrochemical membrane oxidation was reported in 2005 in which an activated carbon fiber cathode and EF's reagent were employed to mineralize an azo dye (i.e., Acid Red 14) [23]. Afterwards, this technology has experienced rapid development owing to its superior performance. Nowadays, electrochemical membrane oxidation has gained increasing attention and been applied in wastewater treatment for the removal of organic pollutants [151,153–156] and toxic arsenic (As^{3+}) [152]. Some related studies are given in Table 1.3.

As already mentioned, the membrane configuration could significantly enhance the mass transfer of pollutants towards the membrane electrode surface compared with that achieved with the traditional electrode configuration [246]. The performance of reactive electrochemical membrane (REM) could be further improved by coupling it with an EF system in degrading organic pollutants. For example, about (67% ± 2%) of 55 mg/L of initial total organic carbon (TOC) could be removed and the mineralization current efficiency (MCE) reached as high as (43% ± 1%) in REM/EF process. While, only 47% (MCE = 30%) and 31% (MCE = 20%) removals of TOC were achieved in a standalone REM and an EF process, respectively [153]. Also, membrane filtration could also protect the electrode from the fouling of particulate and colloidal matters existing in wastewaters [247]. Meanwhile, the powerful degradation capability

This book belongs to Badji Mokhtar Annaba University Central Library Copyright Elsevier 2025

of electrochemical process also alleviates membrane fouling [248]. The enhancement effect is also observed in MBR, and it is called electrochemical membrane bioreactors (eMBR) after combining MBR with electrochemical technology. Electrochemical MBR (eMBR) with sacrificial anodes can achieve enhanced removal efficiencies of phosphorus (up to 40%) and micropollutant (5%–60%), which is attributed to the direct/indirect oxidation and electrocoagulation of the electrochemical process. Moreover, membrane fouling is also less severe in eMBR compared with conventional MBR [247].

1.3.2.3 Electrochemical membrane reduction

In the 1990s, Cheng et al. used the electrochemical reduction technology for the dechlorination of organic pollutants for wastewater treatment [249–251]. A carbon fiber/alumina tubular composite membrane had been used to treat Cu-CMP (chemical mechanical polishing) wastewater under the electrofiltration process in 2008 [24]. Since then, electrochemical membrane reduction has been applied to remove heavy metals or reduce nitrate in various wastewaters, which are involved with a couple of novel membrane electrodes such as CNT membrane [63], TiO_2 membrane [100], and Ti_4O_7 membrane [157].

Electrochemical reduction on the membrane is mainly involved with two mechanisms: direct and indirect charge transfer. For the direct charge transfer, the pollutant migrates to the electrode surface and is then reduced [e.g., the reduction of Cr(VI)] [252]. Therefore the removal efficiency achieved by this mechanism depends on the diffusion behavior of the pollutant, though it's the fluidic channels in the membrane that can enhance the mass transfer of pollutants in a flow-through mode. In contrast, the indirect charge transfer process has a more complex pathway in the pollutant removal. In a recent study, the Pd based cathode was used to generate atomic H* in the electroreduction of H_2O/H^+ and then to reduce bromate to bromide [253]. Moreover, the low energy consumption in the cathodic Fenton process is favorable to the application of electrochemical reduction membrane in the removal of organic pollutants [254]. Table 1.3 lists some typical studies including the removal of chromium and copper by direct reduction [63,102], reduction of nitrate to nitrogen gas (N_2) by indirect reduction [157], and degradation of organic pollutants by cathodic Fenton process [101,158,159].

Electrochemical CNT membranes can remove various pollutants via the direct electron-transfer or the cathodic EF process [255]. For example, the conductive CNT/polymer composite ultrafiltration membrane was used to treat the Cr(VI) wastewater (1 ppm) via the direct electron-transfer process [256]. Additionally, the cathodic EF process can oxidize some aromatic compounds such as diuron and oxcarbazepine at a lower potential compared to the anodic oxidation process [257,258]. The CNTs membrane exhibited a high removal efficiency (>98%) of phenol at a hydraulic retention time of only 2 s [259]. The CNT membrane with precious metals has also

This book belongs to Badji Mokhtar Annaba University Central Library Copyright Elsevier 2025

been used for cathodic EF. For example, the CNT membrane modified by the atomically-precise gold nanoclusters had a high catalytic efficiency for the decomposition of H_2O_2 to $HO\cdot$ by the redox cycling of Au^0/Au^+ [158]. The energy consumption for the tetracycline removal by Au-CNT is lower than that by AOP.

Ti_4O_7 REM has also been applied in the electrochemical reduction for removing nitrate, haloacetic acids, and N-Nitrosodimethylamine (NDMA) [100,101,157]. For the nitrate reduction, an optimal performance could be achieved using a $Pd-Cu/$ REM, which exhibited a sharp decline of nitrate concentration in a single flow-through mode (residence time ~ 2 s) at a cathode potential of -2.5 V (vs standard hydrogen electrode, SHE). This reaction was not affected by the dissolved oxygen and carbonate species [157]. Furthermore, this membrane was also employed in the degradation of dibromoacetic acid (DBAA) [101]. The energy consumption for reducing the DBAA was 0.10 ± 0.06 kWh/m^3 when this technology was applied in the dehalogenation treatment of tap water, while the energy consumption of reducing NDMA was 0.12 ± 0.03 kWh/m^3 (10 μM NDMA) for the MWCNT-REM.

A composite membrane made by integrating polyvinylidene difluoride with a steel mesh on the nonwoven substrate was also reported. Due to the oxygen reduction reaction on the Fe^0 sites and enhanced mass transfer, the membrane could achieve a high sulphanilic acid removal [103]. This apart, the electrochemical membrane filtration system was also applied for recovering Cu from the wastewater containing Cu-organic complexes [102]. This system could achieve 81.5% decomplexation of the Cu-EDTA complex and 72.4% recovery of Cu at 3 V cell voltage. The energy consumption was 93.5 g/kWh and 15.0 g/kWh for Cu-EDTA decomplexation and Cu recovery, respectively.

1.4 Conclusions and perspectives

Electrochemical membrane technology is a hybrid process of the electrochemical technology and the membrane technology. Thus the development of both these technologies could undoubtedly promote the advancement of the electrochemical membrane technology. Benefiting from the rapid development of the membrane technology in recent years, the performance of IEM-based electrochemical process and CM-based electrochemical process has been significantly boosted with indicators such as permeability, selectivity, and energy efficiency. However, some obstacles still exist. One of the main obstacles in IEM-based electrochemical technology is membrane fouling/scaling. Another defect that may restrict the development of the electrochemical membrane technology is the electrochemical side-reactions. For example, oxygen evolution reaction may generate oxygen bubbles, which are easily trapped in

This book belongs to Badji Mokhtar Annaba University Central Library Copyright Elsevier 2025

small-sized confined flow channels, thereby affecting the long-term permeability and selectivity of reactive electrochemical membranes [260], despite some measures such as ultrasound, microwave, and light source having been introduced to minimize the effect. Last but not least, most of the electrochemical membrane technologies are still stagnating in the lab-scale studies, and larger-scale studies are urgently needed to promote the practical applications of electrochemical membrane technologies.

Acknowledgments

X. Li and Z. Wang acknowledge the funding support from the Science and Technology Commission of Shanghai Municipality (Grant no. 20230713700).

References

[1] H. Wang, Low-energy desalination, Nat. Nanotechnol. 13 (2018) 273–274. Available from: https://doi.org/10.1038/s41565-018-0118-y.
[2] L. Song, X.-F. Zhang, Z. Wang, T. Zheng, J. Yao, Fe_3O_4/polyvinyl alcohol decorated delignified wood evaporator for continuous solar steam generation, Desalination 507 (2021) 115024. https://doi.org/10/gh6zbz.
[3] C.A. Damalas, I.G. Eleftherohorinos, Pesticide exposure, safety issues, and risk assessment indicators, Int. J. Environ. Res. Public Health 8 (2011) 1402–1419. https://doi.org/10/fk4tf6.
[4] K. Kümmerer, The presence of pharmaceuticals in the environment due to human use – present knowledge and future challenges, J. Environ. Manage. 90 (2009) 2354–2366. https://doi.org/10/c8jcqn.
[5] K.P. Sharma, S. Sharma, S. Sharma, P.K. Singh, S. Kumar, R. Grover, et al., A comparative study on characterization of textile wastewaters (untreated and treated) toxicity by chemical and biological tests, Chemosphere. 69 (2007) 48–54. https://doi.org/10/br6xxr.
[6] D.W. Kolpin, E.T. Furlong, M.T. Meyer, E.M. Thurman, S.D. Zaugg, L.B. Barber, et al., Pharmaceuticals, hormones, and other organic wastewater contaminants in U.S. streams, 1999 – 2000: a national reconnaissance, Environ. Sci. Technol. 36 (2002) 1202–1211. https://doi.org/10/fc5qc5.
[7] M.B. Ahmed, J.L. Zhou, H.H. Ngo, W. Guo, N.S. Thomaidis, J. Xu, Progress in the biological and chemical treatment technologies for emerging contaminant removal from wastewater: A critical review, J. Hazard. Mater. 323 (2017) 274–298. https://doi.org/10/f9hmnn.
[8] P.F. Tee, M.O. Abdullah, I.A.W. Tan, N.K.A. Rashid, M.A.M. Amin, C. Nolasco-Hipolito, et al., Review on hybrid energy systems for wastewater treatment and bio-energy production, Renew. Sustain. Energy Rev. 54 (2016) 235–246. https://doi.org/10/f76q8d.
[9] V.G. Gude, Desalination and sustainability – an appraisal and current perspective, Water Res. 89 (2016) 87–106. https://doi.org/10/gjgxpn.
[10] S.O. Ganiyu, E.D. van Hullebusch, M. Cretin, G. Esposito, M.A. Oturan, Coupling of membrane filtration and advanced oxidation processes for removal of pharmaceutical residues: a critical review, Sep. Purif. Technol. 156 (2015) 891–914. https://doi.org/10/f729ds.
[11] B. Van der Bruggen, M. Mänttäri, M. Nyström, Drawbacks of applying nanofiltration and how to avoid them: a review, Sep. Purif. Technol. 63 (2008) 251–263. https://doi.org/10/fj7hfp.
[12] T. Zhou, T.-T. Lim, S.-S. Chin, A.G. Fane, Treatment of organics in reverse osmosis concentrate from a municipal wastewater reclamation plant: feasibility test of advanced oxidation processes with/without pretreatment, Chem. Eng. J. 166 (2011) 932–939. https://doi.org/10/dnfkxh.
[13] P. Formoso, E. Pantuso, G. De Filpo, F. Nicoletta, Electro-conductive membranes for permeation enhancement and fouling mitigation: a short review, Membranes 7 (2017) 39. https://doi.org/10/ghtcsw.
[14] M. Paidar, V. Fateev, K. Bouzek, Membrane electrolysis—history, current status and perspective, Electrochim. Acta 209 (2016) 737–756. https://doi.org/10/f8vnc2.

This book belongs to Badji Mokhtar Annaba University Central Library Copyright Elsevier 2025

[15] E. Manegold, K. Kalauch, über Kapillarsysteme XXII - Die Wirksamkeit verschiedener Reinigungsmethoden (Filtration, Dialyse, Elektrolyse und ihre Kombinationen), Kolloid-Z 86 (1939) 93–101. https://doi.org/10/cqtpm5.
[16] M.C. Potter, A.D. Waller, Electrical effects accompanying the decomposition of organic compounds, Proc. R. Soc. Lond. Ser. B Contain. Pap. Biol. Character. 84 (1911) 260–276. https://doi.org/10/cwvw43.
[17] W. Habermann, E.H. Pommer, Biological fuel cells with sulphide storage capacity, Appl. Microbiol. Biotechnol. 35 (1991). https://doi.org/10/dqq499.
[18] H.P. Bennetto, Electricity generation by microorganisms, Biotechnol. Educ. 1 (1990) 163–168.
[19] X. Cao, X. Huang, P. Liang, K. Xiao, Y. Zhou, X. Zhang, et al., A new method for water desalination using microbial desalination cells, Environ. Sci. Technol. 43 (2009) 7148–7152. https://doi.org/10/dp4n5v.
[20] A.M. Johnson, J. Newman, Desalting by means of porous carbon electrodes, J. Electrochem. Soc. 118 (1971) 510. Available from: https://doi.org/10.1149/1.2408094.
[21] S. Dahiya, A. Singh, B.K. Mishra, Capacitive deionized hybrid systems for wastewater treatment and desalination: a review on synergistic effects, mechanisms and challenges, Chem. Eng. J. 417 (2021) 128129. https://doi.org/10/gj8xth.
[22] J.-B. Lee, K.-K. Park, H.-M. Eum, C.-W. Lee, Desalination of a thermal power plant wastewater by membrane capacitive deionization, Desalination 196 (2006) 125–134. https://doi.org/10/dgpqmr.
[23] A. Wang, J. Qu, J. Ru, H. Liu, J. Ge, Mineralization of an azo dye Acid Red 14 by electro-Fenton's reagent using an activated carbon fiber cathode, Dye. Pigment. 65 (2005) 227–233. https://doi.org/10/ctxgrf.
[24] G.C.C. Yang, C.-M. Tsai, Preparation of carbon fibers/carbon/alumina tubular composite membranes and their applications in treating Cu-CMP wastewater by a novel electrochemical process, J. Membr. Sci. 321 (2008) 232–239. Available from: https://doi.org/10.1016/j.memsci.2008.04.060.
[25] S.S. Madaeni, Preparation and properties of composite membranes composed of non-conductive membranes and polypyrrole, Indian J. Chem. Technol. 6 (2006).
[26] A. Lim, What Is an Electric Field? Definition, Formula, Example., ThoughtCo. (n.d.). <https://www.thoughtco.com/electric-field-4174366> (accessed 07.04.21).
[27] K.J. Vetter, Electrochemical Kinetics, Elsevier, 1967. Available from: https://doi.org/10.1016/C2013-0-12183-6.
[28] J.W. Jorgenson, K.D. Lukacs, High-resolution separations based on electrophoresis and electroosmosis, J. Chromatogr. A. 218 (1981) 209–216. https://doi.org/10/fvjv77.
[29] M.E. Suss, S. Porada, X. Sun, P.M. Biesheuvel, J. Yoon, V. Presser, Water desalination via capacitive deionization: what is it and what can we expect from it? Energy Environ. Sci. 8 (2015) 2296–2319. https://doi.org/10/gfsxrr.
[30] S. Porada, R. Zhao, A. van der Wal, V. Presser, P.M. Biesheuvel, Review on the science and technology of water desalination by capacitive deionization, Prog. Mater. Sci. 58 (2013) 1388–1442. https://doi.org/10/f5f2rk.
[31] Y.B. Acar, A.N. Alshawabkeh, Principles of electrokinetic remediation, Environ. Sci. Technol. 27 (1993) 2638–2647. https://doi.org/10/cr82xg.
[32] J. Radjenovic, D.L. Sedlak, Challenges and opportunities for electrochemical processes as next-generation technologies for the treatment of contaminated water, Environ. Sci. Technol. 49 (2015) 11292–11302. https://doi.org/10/f7t6jx.
[33] M.A. Rodrigo, N. Oturan, M.A. Oturan, Electrochemically assisted remediation of pesticides in soils and water: a review, Chem. Rev. 114 (2014) 8720–8745. https://doi.org/10/gfw692.
[34] B.E. Logan, K. Rabaey, Conversion of wastes into bioelectricity and chemicals by using microbial electrochemical technologies, Science 337 (2012) 686–690. https://doi.org/10/f35rks.
[35] M. Cheryan, Ultrafiltration and Microfiltration Handbook, CRC Press, 1998.
[36] S. Bhattacharjee, A.S. Kim, M. Elimelech, Concentration polarization of interacting solute particles in cross-flow membrane filtration, J. Colloid Interface Sci. 212 (1999) 81–99. https://doi.org/10/ck8wt6.

This book belongs to Badji Mokhtar Annaba University Central Library Copyright Elsevier 2025

[37] M.C. Porter, Concentration polarization with membrane ultrafiltration, Prod. RD 11 (1972) 234–248. https://doi.org/10/fdrtv4.
[38] Z. Wang, J. Ma, C.Y. Tang, K. Kimura, Q. Wang, X. Han, Membrane cleaning in membrane bioreactors: a review, J. Membr. Sci. 468 (2014) 276–307. https://doi.org/10/f6cp2c.
[39] B.N. Ehrl, K. Kundu, M. Gharasoo, S. Marozava, M. Elsner, Rate-limiting mass transfer in micropollutant degradation revealed by isotope fractionation in chemostat, Environ. Sci. Technol. 53 (2019) 1197–1205. Available from: https://doi.org/10.1021/acs.est.8b05175.
[40] A.C. Forse, J.M. Griffin, C. Merlet, J. Carretero-Gonzalez, A.-R.O. Raji, N.M. Trease, et al., Direct observation of ion dynamics in supercapacitor electrodes using in situ diffusion NMR spectroscopy, Nat. Energy. 2 (2017) 1–7. Available from: https://doi.org/10.1038/nenergy.2016.216.
[41] R. Dai, H. Han, T. Wang, X. Li, Z. Wang, Enhanced removal of hydrophobic endocrine disrupting compounds from wastewater by nanofiltration membranes intercalated with hydrophilic MoS_2 nanosheets: role of surface properties and internal nanochannels, J. Membr. Sci. 628 (2021) 119267. Available from: https://doi.org/10.1016/j.memsci.2021.119267.
[42] F. Pan, H. Ding, W. Li, Y. Song, H. Yang, H. Wu, et al., Constructing facilitated transport pathway in hybrid membranes by incorporating MoS_2 nanosheets, J. Membr. Sci. 545 (2018) 29–37. Available from: https://doi.org/10.1016/j.memsci.2017.09.054.
[43] Y. Sun, D. Xu, S. Li, L. Cui, Y. Zhuang, W. Xing, et al., Assembly of multidimensional MXene-carbon nanotube ultrathin membranes with an enhanced anti-swelling property for water purification, J. Membr. Sci. 623 (2021) 119075. Available from: https://doi.org/10.1016/j.memsci.2021.119075.
[44] H. Lin, Y. Li, J. Zhu, Cross-linked GO membranes assembled with GO nanosheets of differently sized lateral dimensions for organic dye and chromium separation, J. Membr. Sci. 598 (2020) 117789. Available from: https://doi.org/10.1016/j.memsci.2019.117789.
[45] Y. Chen, G. Zhang, H. Liu, J. Qu, Confining free radicals in close vicinity to contaminants enables ultrafast fenton-like processes in the interspacing of MoS_2, Membranes, Angew. Chem. Int. (Ed.) 58 (2019) 8134–8138. Available from: https://doi.org/10.1002/anie.201903531.
[46] R.K. Anand, E.S. Johnson, D.T. Chiu, Negative dielectrophoretic capture and repulsion of single cells at a bipolar electrode: the impact of Faradaic ion enrichment and depletion, J. Am. Chem. Soc. 137 (2015) 776–783. Available from: https://doi.org/10.1021/ja5102689.
[47] K. Luo, Q. Niu, Y. Zhu, B. Song, G. Zeng, W. Tang, et al., Desalination behavior and performance of flow-electrode capacitive deionization under various operational modes, Chem. Eng. J. 389 (2020) 124051. Available from: https://doi.org/10.1016/j.cej.2020.124051.
[48] S. Porada, L. Zhang, J.E. Dykstra, Energy consumption in membrane capacitive deionization and comparison with reverse osmosis, Desalination 488 (2020) 114383. Available from: https://doi.org/10.1016/j.desal.2020.114383.
[49] R. Zhao, S. Porada, P.M. Biesheuvel, A. van der Wal, Energy consumption in membrane capacitive deionization for different water recoveries and flow rates, and comparison with reverse osmosis, Desalination 330 (2013) 35–41. Available from: https://doi.org/10.1016/j.desal.2013.08.017.
[50] S. Wang, G. Wang, T. Wu, C. Li, Y. Wang, X. Pan, et al., Membrane-free hybrid capacitive deionization system based on redox reaction for high-efficiency NaCl removal, Environ. Sci. Technol. 53 (2019) 6292–6301. Available from: https://doi.org/10.1021/acs.est.9b00662.
[51] S. Yang, J. Choi, J. Yeo, S. Jeon, H. Park, D.K. Kim, Flow-electrode capacitive deionization using an aqueous electrolyte with a high salt concentration, Environ. Sci. Technol. 50 (2016) 5892–5899. Available from: https://doi.org/10.1021/acs.est.5b04640.
[52] X. Xu, M. Wang, Y. Liu, T. Lu, L. Pan, Ultrahigh desalinization performance of asymmetric flow-electrode capacitive deionization device with an improved operation voltage of 1.8 V, ACS Sustain. Chem. Eng. 5 (2017) 189–195. Available from: https://doi.org/10.1021/acssuschemeng.6b01212.
[53] L. Shi, Z. Hu, Y. Wang, E. Bei, P.N.L. Lens, O. Thomas, et al., In situ electrochemical oxidation in electrodialysis for antibiotics removal during nutrient recovery from pig manure digestate, Chem. Eng. J. (2020) 127485. Available from: https://doi.org/10.1016/j.cej.2020.127485.

This book belongs to Badji Mokhtar Annaba University Central Library Copyright Elsevier 2025

[54] F.L. Souza, M. Zougagh, C. Sáez, P. Cañizares, A. Ríos, M.A. Rodrigo, Electrochemically-based hybrid oxidative technologies for the treatment of micropollutants in drinking water, Chem. Eng. J. 414 (2021) 128531. Available from: https://doi.org/10.1016/j.cej.2021.128531.
[55] W. Yan, M. Li, H. Li, C. Li, S. Xu, L. Su, et al., Aqueous lithium and sodium ion capacitors with boron-doped graphene/BDD/TiO_2 anode and boron-doped graphene/BDD cathode exhibiting AC line-filtering performance, Chem. Eng. J. 388 (2020) 124265. Available from: https://doi.org/10.1016/j.cej.2020.124265.
[56] H. Olvera-Vargas, N. Gore-Datar, O. Garcia-Rodriguez, S. Mutnuri, O. Lefebvre, Electro-Fenton treatment of real pharmaceutical wastewater paired with a BDD anode: reaction mechanisms and respective contribution of homogeneous and heterogeneous OH, Chem. Eng. J. 404 (2021) 126524. Available from: https://doi.org/10.1016/j.cej.2020.126524.
[57] E. Lacasa, J. Llanos, P. Cañizares, M.A. Rodrigo, Electrochemical denitrificacion with chlorides using DSA and BDD anodes, Chem. Eng. J. 184 (2012) 66–71. Available from: https://doi.org/10.1016/j.cej.2011.12.090.
[58] C. Comninellis, Electrocatalysis in the electrochemical conversion/combustion of organic pollutants for waste water treatment, Electrochim. Acta 39 (1994) 1857–1862. Available from: https://doi.org/10.1016/0013-4686(94)85175-1.
[59] F. Yao, Q. Yang, Y. Zhong, X. Shu, F. Chen, J. Sun, et al., Indirect electrochemical reduction of nitrate in water using zero-valent titanium anode: factors, kinetics, and mechanism, Water Res. 157 (2019) 191–200. Available from: https://doi.org/10.1016/j.watres.2019.03.078.
[60] K. Serrano, P.A. Michaud, C. Comninellis, A. Savall, Electrochemical preparation of peroxodisulfuric acid using boron doped diamond thin film electrodes, Electrochim. Acta 48 (2002) 431–436. Available from: https://doi.org/10.1016/S0013-4686(02)00688-6.
[61] C.R. Costa, F. Montilla, E. Morallón, P. Olivi, Electrochemical oxidation of acid black 210 dye on the boron-doped diamond electrode in the presence of phosphate ions: effect of current density, pH, and chloride ions, Electrochim. Acta 54 (2009) 7048–7055. Available from: https://doi.org/10.1016/j.electacta.2009.07.027.
[62] C. Kim, S. Kim, J. Choi, J. Lee, J.S. Kang, Y.-E. Sung, et al., Blue TiO_2 nanotube array as an oxidant generating novel anode material fabricated by simple cathodic polarization, Electrochim. Acta 141 (2014) 113–119. Available from: https://doi.org/10.1016/j.electacta.2014.07.062.
[63] Y. Liu, F. Liu, N. Ding, C. Shen, F. Li, L. Dong, et al., Boosting Cr (VI) detoxification and sequestration efficiency with carbon nanotube electrochemical filter functionalized with nanoscale polyaniline: performance and mechanism, Sci. Total Environ. 695 (2019) 133926. https://doi.org/10/gj8m7j.
[64] X. Wang, Z. Wang, H. Chen, Z. Wu, Removal of Cu(II) ions from contaminated waters using a conducting microfiltration membrane, J. Hazard. Mater. 339 (2017) 182–190. https://doi.org/10/gbswfb.
[65] R. Mao, X. Zhao, H. Lan, H. Liu, J. Qu, Efficient electrochemical reduction of bromate by a Pd/rGO/CFP electrode with low applied potentials, Appl. Catal. B Environ. 160–161 (2014) 179–187. Available from: https://doi.org/10.1016/j.apcatb.2014.04.040.
[66] Y. Liu, G. Gao, C.D. Vecitis, Prospects of an electroactive carbon nanotube membrane toward environmental applications, Acc. Chem. Res. 53 (2020) 2892–2902. Available from: https://doi.org/10.1021/acs.accounts.0c00544.
[67] M. Zheng, Y. Yang, S. Qiao, J. Zhou, X. Quan, A porous carbon-based electro-Fenton hollow fiber membrane with good antifouling property for microalgae harvesting, J. Membr. Sci. 626 (2021) 119189. Available from: https://doi.org/10.1016/j.memsci.2021.119189.
[68] X.-Y. Nie, S.-Y. Sun, Z. Sun, X. Song, J.-G. Yu, Ion-fractionation of lithium ions from magnesium ions by electrodialysis using monovalent selective ion-exchange membranes, Desalination 403 (2017) 128–135. Available from: https://doi.org/10.1016/j.desal.2016.05.010.
[69] D.A. Vermaas, S. Bajracharya, B.B. Sales, M. Saakes, B. Hamelers, K. Nijmeijer, Clean energy generation using capacitive electrodes in reverse electrodialysis, Energy Environ. Sci. 6 (2013) 643–651. Available from: https://doi.org/10.1039/C2EE23562E.

This book belongs to Badji Mokhtar Annaba University Central Library Copyright Elsevier 2025

[70] E. Jwa, Y.-M. Yun, H. Kim, N. Jeong, K.S. Hwang, S. Yang, et al., Energy-efficient seawater softening and power generation using a microbial electrolysis cell-reverse electrodialysis hybrid system, Chem. Eng. J. 391 (2020) 123480. Available from: https://doi.org/10.1016/j.cej.2019.123480.
[71] Y. Wang, C. He, W. Li, W. Zong, Z. Li, L. Yuan, et al., High power generation in mixed-culture microbial fuel cells with corncob-derived three-dimensional N-doped bioanodes and the impact of N dopant states, Chem. Eng. J. 399 (2020) 125848. Available from: https://doi.org/10.1016/j.cej.2020.125848.
[72] B. Kokabian, V.G. Gude, Sustainable photosynthetic biocathode in microbial desalination cells, Chem. Eng. J. 262 (2015) 958–965. Available from: https://doi.org/10.1016/j.cej.2014.10.048.
[73] J.A. Kerres, Blended and cross-linked ionomer membranes for application in membrane fuel cells, Fuel Cell 5 (2005) 230–247. https://doi.org/10/c5tkf8.
[74] F. Croce, J. Hassoun, C. Tizzani, B. Scrosati, Nanoporous composite, low cost, protonic membranes for direct methanol fuel cells, Electrochem. Commun. 8 (2006) 1125–1131. https://doi.org/10/dvhb7f.
[75] Y. Li, X. Lin, L. Wu, C. Jiang, Md.M. Hossain, T. Xu, Quaternized membranes bearing zwitterionic groups for vanadium redox flow battery through a green route, J. Membr. Sci. 483 (2015) 60–69. https://doi.org/10/f67r8d.
[76] X. Lin, Y. Liu, S.D. Poynton, A.L. Ong, J.R. Varcoe, L. Wu, et al., Cross-linked anion exchange membranes for alkaline fuel cells synthesized using a solvent free strategy, J. Power Sources 233 (2013) 259–268. https://doi.org/10/gjg395.
[77] L. Wu, G. Zhou, X. Liu, Z. Zhang, C. Li, T. Xu, Environmentally friendly synthesis of alkaline anion exchange membrane for fuel cells via a solvent-free strategy, J. Membr. Sci. 371 (2011) 155–162. https://doi.org/10/fsd4xz.
[78] T. Xu, J.-J. Woo, S.-J. Seo, S.-H. Moon, In situ polymerization: a novel route for thermally stable proton-conductive membranes, J. Membr. Sci. 325 (2008) 209–216. https://doi.org/10/bv6z8m.
[79] S. Cavaliere, S. Subianto, I. Savych, D.J. Jones, J. Rozière, Electrospinning: designed architectures for energy conversion and storage devices, Energy Environ. Sci. 4 (2011) 4761–4785. https://doi.org/10/b93psq.
[80] V. Thavasi, G. Singh, S. Ramakrishna, Electrospun nanofibers in energy and environmental applications, Energy Environ. Sci. 1 (2008) 205. https://doi.org/10/csj4xc.
[81] Z. Liu, Y.-E. Miao, M. Liu, Q. Ding, W.W. Tjiu, X. Cui, et al., Flexible polyaniline-coated TiO_2/SiO_2 nanofiber membranes with enhanced visible-light photocatalytic degradation performance, J. Colloid Interface Sci. 424 (2014) 49–55. Available from: https://doi.org/10.1016/j.jcis.2014.03.009.
[82] B. Xu, X. Wang, Y. Huang, J. Liu, D. Wang, S. Feng, et al., Electrospinning preparation of PAN/TiO_2/PANI hybrid fiber membrane with highly selective adsorption and photocatalytic regeneration properties, Chem. Eng. J. 399 (2020) 125749. Available from: https://doi.org/10.1016/j.cej.2020.125749.
[83] L. Liu, J. Liu, B. Gao, F. Yang, S. Chellam, Fouling reductions in a membrane bioreactor using an intermittent electric field and cathodic membrane modified by vapor phase polymerized pyrrole, J. Membr. Sci. 394–395 (2012) 202–208. Available from: https://doi.org/10.1016/j.memsci.2011.12.042.
[84] N. Li, L. Liu, F. Yang, Highly conductive graphene/PANi-phytic acid modified cathodic filter membrane and its antifouling property in EMBR in neutral conditions, Desalination 338 (2014) 10–16. Available from: https://doi.org/10.1016/j.desal.2014.01.019.
[85] J. Liu, Y. Wang, L. Wang, Poly (3, 4-ethylenedioxythiophene) modified polyvinylidene fluoride membrane for visible photoelectrocatalysis and filtration, J. Colloid Interface Sci. 553 (2019) 220–227. Available from: https://doi.org/10.1016/j.jcis.2019.06.024.
[86] M.-L. Liu, L. Li, Y.-X. Sun, Z.-J. Fu, X.-L. Cao, S.-P. Sun, Scalable conductive polymer membranes for ultrafast organic pollutants removal, J. Membr. Sci. 617 (2021) 118644. Available from: https://doi.org/10.1016/j.memsci.2020.118644.
[87] E.L. Subtil, J. Gonçalves, H.G. Lemos, E.C. Venancio, J.C. Mierzwa, J. dos, et al., Preparation and characterization of a new composite conductive polyethersulfone membrane using polyaniline (PANI) and reduced graphene oxide (rGO), Chem. Eng. J. 390 (2020) 124612. Available from: https://doi.org/10.1016/j.cej.2020.124612.

This book belongs to Badji Mokhtar Annaba University Central Library Copyright Elsevier 2025

[88] H. Liu, G. Zhang, C. Zhao, J. Liu, F. Yang, Hydraulic power and electric field combined antifouling effect of a novel conductive poly(aminoanthraquinone)/reduced graphene oxide nanohybrid blended PVDF ultrafiltration membrane, J. Mater. Chem. A. 3 (2015) 20277–20287. Available from: https://doi.org/10.1039/C5TA05306D.

[89] N. Shafaei, M. Peyravi, M. Jahanshahi, Improving surface structure of photocatalytic self-cleaning membrane by WO_3/PANI nanoparticles, Polym. Adv. Technol. 27 (2016) 1325–1337. Available from: https://doi.org/10.1002/pat.3800.

[90] A. Pakdel Mojdehi, M. Pourafshari Chenar, M. Namvar-Mahboub, M. Eftekhari, Development of PES/polyaniline-modified TiO_2 adsorptive membrane for copper removal, Colloids Surf. Physicochem. Eng. Asp. 583 (2019) 123931. Available from: https://doi.org/10.1016/j.colsurfa.2019.123931.

[91] S.B. Teli, S. Molina, A. Sotto, E.G. Calvo, J. de Abajob, Fouling resistant polysulfone–PANI/TiO_2 ultrafiltration nanocomposite membranes, Ind. Eng. Chem. Res. 52 (2013) 9470–9479. Available from: https://doi.org/10.1021/ie401037n.

[92] L. Xie, Y. Shu, Y. Hu, J. Cheng, Y. Chen, SWNTs-PAN/TPU/PANI composite electrospun nanofiber membrane for point-of-use efficient electrochemical disinfection: new strategy of CNT disinfection, Chemosphere. 251 (2020) 126286. Available from: https://doi.org/10.1016/j.chemosphere.2020.126286.

[93] S. Aziz, M. Sabzi, A. Fattahi, E. Arkan, Electrospun silk fibroin/PAN double-layer nanofibrous membranes containing polyaniline/TiO_2 nanoparticles for anionic dye removal, J. Polym. Res. 24 (2017) 1–7. Available from: https://doi.org/10.1007/s10965-017-1298-0.

[94] M.W.J. Luiten-Olieman, L. Winnubst, A. Nijmeijer, M. Wessling, N.E. Benes, Porous stainless steel hollow fiber membranes via dry–wet spinning, J. Membr. Sci. 370 (2011) 124–130. Available from: https://doi.org/10.1016/j.memsci.2011.01.004.

[95] D. Hou, A. Iddya, X. Chen, M. Wang, W. Zhang, Y. Ding, et al., Nickel-based membrane electrodes enable high-rate electrochemical ammonia recovery, Environ. Sci. Technol. 52 (2018) 8930–8938. Available from: https://doi.org/10.1021/acs.est.8b01349.

[96] D. Hou, D. Jassby, R. Nerenberg, Z.J. Ren, Hydrophobic gas transfer membranes for wastewater treatment and resource recovery, Environ. Sci. Technol. 53 (2019) 11618–11635. Available from: https://doi.org/10.1021/acs.est.9b00902.

[97] K. Wetchakun, N. Wetchakun, S. Sakulsermsuk, An overview of solar/visible light-driven heterogeneous photocatalysis for water purification: TiO_2- and ZnO-based photocatalysts used in suspension photoreactors, J. Ind. Eng. Chem. 71 (2019) 19–49. Available from: https://doi.org/10.1016/j.jiec.2018.11.025.

[98] J. Zheng, Z. Wang, J. Ma, S. Xu, Z. Wu, Development of an electrochemical ceramic membrane filtration system for efficient contaminant removal from waters, Environ. Sci. Technol. 52 (2018) 4117–4126. Available from: https://doi.org/10.1021/acs.est.7b06407.

[99] Y. Zhang, Y. Qi, Z. Yin, H. Wang, B. He, X. Liang, et al., Nano-V_2O_5/Ti porous membrane electrode with enhanced electrochemical activity for the high-efficiency oxidation of cyclohexane, Green. Chem. 20 (2018) 3944–3953. Available from: https://doi.org/10.1039/C8GC01259H.

[100] S. Almassi, Z. Li, W. Xu, C. Pu, T. Zeng, B.P. Chaplin, Simultaneous adsorption and electrochemical reduction of N-nitrosodimethylamine using carbon-Ti_4O_7 composite reactive electrochemical membranes, Environ. Sci. Technol. 53 (2019) 928–937. https://doi.org/10/gj8m9p.

[101] S. Almassi, P.R.V. Samonte, Z. Li, W. Xu, B.P. Chaplin, Mechanistic investigation of haloacetic acid reduction using carbon-Ti_4O_7 composite reactive electrochemical membranes, Environ. Sci. Technol. 54 (2020) 1982–1991. https://doi.org/10/gj8m9j.

[102] J. Li, J. Ma, R. Dai, X. Wang, M. Chen, T.D. Waite, et al., Self-enhanced decomplexation of Cu-organic complexes and Cu recovery from wastewaters using an electrochemical membrane filtration system, Environ. Sci. Technol. 55 (2021) 655–664. https://doi.org/10/ghjtqv.

[103] J. Zheng, J. Ma, Z. Wang, S. Xu, T.D. Waite, Z. Wu, Contaminant removal from source waters using cathodic electrochemical membrane filtration: mechanisms and implications, Environ. Sci. Technol. 51 (2017) 2757–2765. https://doi.org/10/f9qz3j.

[104] H. Dou, M. Xu, B. Wang, Z. Zhang, D. Luo, B. Shi, et al., Analogous mixed matrix membranes with self-assembled interface pathways, Angew. Chem. 133 (2021) 5928–5934. https://doi.org/10/gj68rm.

This book belongs to Badji Mokhtar Annaba University Central Library Copyright Elsevier 2025

[105] S. Ali, S.A.U. Rehman, H.-Y. Luan, M.U. Farid, H. Huang, Challenges and opportunities in functional carbon nanotubes for membrane-based water treatment and desalination, Sci. Total Environ. 646 (2019) 1126–1139. https://doi.org/10/gj68vm.
[106] Y. Si, C. Sun, D. Li, F. Yang, C.Y. Tang, X. Quan, et al., Flexible superhydrophobic metal-based carbon nanotube membrane for electrochemically enhanced water treatment, Environ. Sci. Technol. 54 (2020) 9074–9082. Available from: https://doi.org/10.1021/acs.est.0c01084.
[107] C.M. Werner, K.P. Katuri, A.R. Hari, W. Chen, Z. Lai, B.E. Logan, et al., Graphene-coated hollow fiber membrane as the cathode in anaerobic electrochemical membrane bioreactors – effect of configuration and applied voltage on performance and membrane fouling, Environ. Sci. Technol. 50 (2016) 4439–4447. Available from: https://doi.org/10.1021/acs.est.5b02833.
[108] A. Ali, R.A. Tufa, F. Macedonio, E. Curcio, E. Drioli, Membrane technology in renewable-energy-driven desalination, Renew. Sustain. Energy Rev. 81 (2018) 1–21. https://doi.org/10/gcqfrx.
[109] L. Alvarado, A. Chen, Electrodeionization: principles, strategies and applications, Electrochim. Acta 132 (2014) 583–597. https://doi.org/10/f56qms.
[110] E. Vera, J. Ruales, M. Dornier, J. Sandeaux, R. Sandeaux, G. Pourcelly, Deacidification of clarified passion fruit juice using different configurations of electrodialysis, J. Chem. Technol. Biotechnol. 78 (2003) 918–925. https://doi.org/10/dg3w8b.
[111] M. Fidaleo, M. Moresi, Electrodialysis applications in the food industry, in: Advances in Food and Nutrition Research, Academic Press, 2006: pp. 265–360. <https://doi.org/10.1016/S1043-4526(06)51005-8>.
[112] F. Gonçalves, C. Fernandes, P. Cameira dos Santos, M.N. de Pinho, Wine tartaric stabilization by electrodialysis and its assessment by the saturation temperature, J. Food Eng. 59 (2003) 229–235. https://doi.org/10/d3mwc4.
[113] H. Strathmann, Electrodialysis, a mature technology with a multitude of new applications, Desalination 264 (2010) 268–288. https://doi.org/10/fdzq73.
[114] T. Yamabe, Present status of electrodialysis in Japan, Desalination. 23 (1977) 195–202. https://doi.org/10/frdgw3.
[115] F. Fu, Q. Wang, Removal of heavy metal ions from wastewaters: a review, J. Environ. Manage. 92 (2011) 407–418. https://doi.org/10/cpmjqp.
[116] M.A. Acheampong, R.J.W. Meulepas, P.N.L. Lens, Removal of heavy metals and cyanide from gold mine wastewater, J. Chem. Technol. Biotechnol. 85 (2010) 590–613. https://doi.org/10/b8mtv5.
[117] L. Marder, A.M. Bernardes, J. Zoppas Ferreira, Cadmium electroplating wastewater treatment using a laboratory-scale electrodialysis system, Sep. Purif. Technol. 37 (2004) 247–255. https://doi.org/10/c5xk9r.
[118] T. Sata, T. Sata, W. Yang, Studies on cation-exchange membranes having permselectivity between cations in electrodialysis, J. Membr. Sci. 206 (2002) 31–60. https://doi.org/10/d4v2r3.
[119] P. Xu, M. Capito, T.Y. Cath, Selective removal of arsenic and monovalent ions from brackish water reverse osmosis concentrate, J. Hazard. Mater. 260 (2013) 885–891. https://doi.org/10/f5bhfg.
[120] N. Kabay, M. Arda, I. Kurucaovali, E. Ersoz, H. Kahveci, M. Can, et al., Effect of feed characteristics on the separation performances of monovalent and divalent salts by electrodialysis, Desalination 158 (2003) 95–100. https://doi.org/10/dg293n.
[121] N. Kabay, H. Kahveci, Ö. İpek, M. Yüksel, Separation of monovalent and divalent ions from ternary mixtures by electrodialysis, Desalination 198 (2006) 74–83. https://doi.org/10/dd5zj3.
[122] Y. Zhang, S. Paepen, L. Pinoy, B. Meesschaert, B. Van der Bruggen, Selectrodialysis: fractionation of divalent ions from monovalent ions in a novel electrodialysis stack, Sep. Purif. Technol. 88 (2012) 191–201. https://doi.org/10/fx22f2.
[123] Z. Li, Y. Liu, B. Wang, Q. Lang, M. Tan, M. Lee, et al., Insights into the facilitated transport mechanisms of Cr(VI) in ionic liquid-based polymer inclusion membrane – electrodialysis (PIM-ED) process, Chem. Eng. J. 397 (2020) 125324. Available from: https://doi.org/10.1016/j.cej.2020.125324.
[124] Y. Zhou, C. Hu, H. Liu, J. Qu, Potassium-ion recovery with a polypyrrole membrane electrode in novel redox transistor electrodialysis, Environ. Sci. Technol. 54 (2020) 4592–4600. Available from: https://doi.org/10.1021/acs.est.9b06665.

This book belongs to Badji Mokhtar Annaba University Central Library Copyright Elsevier 2025

[125] M.A. Alkhadra, K.M. Conforti, T. Gao, H. Tian, M.Z. Bazant, Continuous separation of radionuclides from contaminated water by shock electrodialysis, Environ. Sci. Technol. 54 (2020) 527−536. Available from: https://doi.org/10.1021/acs.est.9b05380.
[126] M. Aliaskari, A.I. Schäfer, Nitrate, arsenic and fluoride removal by electrodialysis from brackish groundwater, Water Res. 190 (2021) 116683. Available from: https://doi.org/10.1016/j.watres.2020.116683.
[127] Z.-L. Ye, K. Ghyselbrecht, A. Monballiu, L. Pinoy, B. Meesschaert, Fractionating various nutrient ions for resource recovery from swine wastewater using simultaneous anionic and cationic selective-electrodialysis, Water Res. 160 (2019) 424−434. Available from: https://doi.org/10.1016/j.watres.2019.05.085.
[128] D. Babilas, J. Muszyński, A. Milewski, K. Leśniak-Ziółkowska, P. Dydo, Electrodialysis enhanced with disodium EDTA as an innovative method for separating Cu(II) ions from zinc salts in wastewater, Chem. Eng. J. 408 (2021) 127908. Available from: https://doi.org/10.1016/j.cej.2020.127908.
[129] H. Selvaraj, P. Aravind, M. Sundaram, Four compartment mono selective electrodialysis for separation of sodium formate from industry wastewater, Chem. Eng. J. 333 (2018) 162−169. Available from: https://doi.org/10.1016/j.cej.2017.09.150.
[130] J.-Y. Nam, R.D. Cusick, Y. Kim, B.E. Logan, Hydrogen generation in microbial reverse-electrodialysis electrolysis cells using a heat-regenerated salt solution, Environ. Sci. Technol. 46 (2012) 5240−5246. Available from: https://doi.org/10.1021/es300228m.
[131] N.Y. Yip, D.A. Vermaas, K. Nijmeijer, M. Elimelech, Thermodynamic, energy efficiency, and power density analysis of reverse electrodialysis power generation with natural salinity gradients, Environ. Sci. Technol. 48 (2014) 4925−4936. Available from: https://doi.org/10.1021/es5005413.
[132] F. Volpin, Y.C. Woo, H. Kim, S. Freguia, N. Jeong, J.-S. Choi, et al., Energy recovery through reverse electrodialysis: harnessing the salinity gradient from the flushing of human urine, Water Res. 186 (2020) 116320. Available from: https://doi.org/10.1016/j.watres.2020.116320.
[133] J. Moreno, S. Grasman, R. van Engelen, K. Nijmeijer, Upscaling reverse electrodialysis, Environ. Sci. Technol. 52 (2018) 10856−10863. Available from: https://doi.org/10.1021/acs.est.8b01886.
[134] D.A. Vermaas, J. Veerman, M. Saakes, K. Nijmeijer, Influence of multivalent ions on renewable energy generation in reverse electrodialysis, Energy Environ. Sci. 7 (2014) 1434−1445. Available from: https://doi.org/10.1039/C3EE43501F.
[135] I. Merino-Jimenez, V. Celorrio, D.J. Fermin, J. Greenman, I. Ieropoulos, Enhanced MFC power production and struvite recovery by the addition of sea salts to urine, Water Res. 109 (2017) 46−53. Available from: https://doi.org/10.1016/j.watres.2016.11.017.
[136] H.-Y. Cheng, B. Liang, Y. Mu, M.-H. Cui, K. Li, W.-M. Wu, et al., Stimulation of oxygen to bioanode for energy recovery from recalcitrant organic matter aniline in microbial fuel cells (MFCs), Water Res. 81 (2015) 72−83. Available from: https://doi.org/10.1016/j.watres.2015.05.012.
[137] X. Zhang, D. Zhang, Y. Huang, S. Wu, P. Lu, The anodic potential shaped a cryptic sulfur cycling with forming thiosulfate in a microbial fuel cell treating hydraulic fracturing flowback water, Water Res. 185 (2020) 116270. Available from: https://doi.org/10.1016/j.watres.2020.116270.
[138] H. Li, H. Xu, Y.-L. Yang, X.-L. Yang, Y. Wu, S. Zhang, et al., Effects of graphite and Mn ore media on electro-active bacteria enrichment and fate of antibiotic and corresponding resistance gene in up flow microbial fuel cell constructed wetland, Water Res. 165 (2019) 114988. Available from: https://doi.org/10.1016/j.watres.2019.114988.
[139] T. Saeed, M. Jihad Miah, Organic matter and nutrient removal in tidal flow-based microbial fuel cell constructed wetlands: media and flood-dry period ratio, Chem. Eng. J. 411 (2021) 128507. Available from: https://doi.org/10.1016/j.cej.2021.128507.
[140] Q. Ping, O. Porat, C.G. Dosoretz, Z. He, Bioelectricity inhibits back diffusion from the anolyte into the desalinated stream in microbial desalination cells, Water Res. 88 (2016) 266−273. Available from: https://doi.org/10.1016/j.watres.2015.10.018.
[141] K. Zuo, J. Cai, S. Liang, S. Wu, C. Zhang, P. Liang, et al., Liter stacked microbial desalination cell packed with mixed ion-exchange resins for secondary effluent desalination, Environ. Sci. Technol. 48 (2014) 9917−9924. Available from: https://doi.org/10.1021/es502075r.

This book belongs to Badji Mokhtar Annaba University Central Library Copyright Elsevier 2025

[142] K. Zuo, Z. Wang, X. Chen, X. Zhang, J. Zuo, P. Liang, et al., Self-driven desalination and advanced treatment of wastewater in a modularized filtration air cathode microbial desalination cell, Environ. Sci. Technol. 50 (2016) 7254–7262. Available from: https://doi.org/10.1021/acs.est.6b00520.
[143] A. Ebrahimi, D. Yousefi Kebria, G.D. Najafpour, Co-treatment of septage and municipal wastewater in a quadripartite microbial desalination cell, Chem. Eng. J. 354 (2018) 1092–1099. Available from: https://doi.org/10.1016/j.cej.2018.08.107.
[144] H. Yuan, I.M. Abu-Reesh, Z. He, Enhancing desalination and wastewater treatment by coupling microbial desalination cells with forward osmosis, Chem. Eng. J. 270 (2015) 437–443. Available from: https://doi.org/10.1016/j.cej.2015.02.059.
[145] P. Długołęcki, A. van der Wal, Energy recovery in membrane capacitive deionization, Environ. Sci. Technol. 47 (2013) 4904–4910. Available from: https://doi.org/10.1021/es3053202.
[146] A. Jain, J. Kim, O.M. Owoseni, C. Weathers, D. Caña, K. Zuo, et al., Aqueous-processed, high-capacity electrodes for membrane capacitive deionization, Environ. Sci. Technol. 52 (2018) 5859–5867. Available from: https://doi.org/10.1021/acs.est.7b05874.
[147] C. Zhang, J. Ma, D. He, T.D. Waite, Capacitive membrane stripping for ammonia recovery (CapAmm) from dilute wastewaters, Environ. Sci. Technol. Lett. 5 (2018) 43–49. https://doi.org/10/gcv6gk.
[148] Y. Bian, X. Yang, P. Liang, Y. Jiang, C. Zhang, X. Huang, Enhanced desalination performance of membrane capacitive deionization cells by packing the flow chamber with granular activated carbon, Water Res. 85 (2015) 371–376. Available from: https://doi.org/10.1016/j.watres.2015.08.058.
[149] D.I. Kim, P. Dorji, G. Gwak, S. Phuntsho, S. Hong, H. Shon, Reuse of municipal wastewater via membrane capacitive deionization using ion-selective polymer-coated carbon electrodes in pilot-scale, Chem. Eng. J. 372 (2019) 241–250. Available from: https://doi.org/10.1016/j.cej.2019.04.156.
[150] Z. Wang, H. Gong, Y. Zhang, P. Liang, K. Wang, Nitrogen recovery from low-strength wastewater by combined membrane capacitive deionization (MCDI) and ion exchange (IE) process, Chem. Eng. J. 316 (2017) 1–6. https://doi.org/10/f94qbk.
[151] S. Yu, Y. Gao, R. Khan, P. Liang, X. Zhang, X. Huang, Electrospun PAN-based graphene/SnO_2 carbon nanofibers as anodic electrocatalysis microfiltration membrane for sulfamethoxazole degradation, J. Membr. Sci. 614 (2020) 118368. https://doi.org/10/ghdqzq.
[152] Y. Liu, S. Yang, H. Jiang, B. Yang, X. Fang, C. Shen, et al., Sea urchin-like FeOOH functionalized electrochemical CNT filter for one-step arsenite decontamination, J. Hazard. Mater. 407 (2021) 124384. Available from: https://doi.org/10.1016/j.jhazmat.2020.124384.
[153] C. Trellu, M. Rivallin, S. Cerneaux, C. Coetsier, C. Causserand, M.A. Oturan, et al., Integration of sub-stoichiometric titanium oxide reactive electrochemical membrane as anode in the electro-Fenton process, Chem. Eng. J. 400 (2020) 125936. https://doi.org/10/ghdqzn.
[154] X. Qian, L. Xu, Y. Zhu, H. Yu, J. Niu, Removal of aqueous triclosan using TiO_2 nanotube arrays reactive membrane by sequential adsorption and electrochemical degradation, Chem. Eng. J. (2020) 127615. https://doi.org/10/gj8nbg.
[155] P. Gayen, C. Chen, J.T. Abiade, B.P. Chaplin, Electrochemical oxidation of atrazine and clothianidin on Bi-doped SnO_2–$TinO_2n$–1 electrocatalytic reactive electrochemical membranes, Environ. Sci. Technol. 52 (2018) 12675–12684. https://doi.org/10/gfp2bh.
[156] A.M. Zaky, B.P. Chaplin, Mechanism of p-substituted phenol oxidation at a Ti_4O_7 reactive electrochemical membrane, Environ. Sci. Technol. 48 (2014) 5857–5867. https://doi.org/10/f55n5b.
[157] P. Gayen, J. Spataro, S. Avasarala, A.-M. Ali, J.M. Cerrato, B.P. Chaplin, Electrocatalytic reduction of nitrate using magnéli phase TiO_2 reactive electrochemical membranes doped with Pd-based catalysts, Environ. Sci. Technol. 52 (2018) 9370–9379. https://doi.org/10/gd6753.
[158] F. Liu, Y. Liu, Q. Yao, Y. Wang, X. Fang, C. Shen, et al., Supported atomically-precise gold nanoclusters for enhanced flow-through electro-fenton, Environ. Sci. Technol. 54 (2020) 5913–5921. https://doi.org/10/gj8m9g.
[159] G. Gao, Q. Zhang, Z. Hao, C.D. Vecitis, Carbon nanotube membrane stack for flow-through sequential regenerative electro-fenton, Environ. Sci. Technol. 49 (2015) 2375–2383. https://doi.org/10/f64fk6.

This book belongs to Badji Mokhtar Annaba University Central Library Copyright Elsevier 2025

[160] S. Al-Amshawee, M.Y.B.M. Yunus, A.A.M. Azoddein, D.G. Hassell, I.H. Dakhil, H.A. Hasan, Electrodialysis desalination for water and wastewater: a review, Chem. Eng. J. 380 (2020) 122231. https://doi.org/10/gg88ww.
[161] J. Ran, L. Wu, Y. He, Z. Yang, Y. Wang, C. Jiang, et al., Ion exchange membranes: New developments and applications, J. Membr. Sci. 522 (2017) 267–291. https://doi.org/10/gfsztr.
[162] A. Campione, L. Gurreri, M. Ciofalo, G. Micale, A. Tamburini, A. Cipollina, Electrodialysis for water desalination: a critical assessment of recent developments on process fundamentals, models and applications, Desalination 434 (2018) 121–160. https://doi.org/10/gdffm5.
[163] M. Turek, P. Dydo, J. Waś, Electrodialysis reversal in high $CaSO_4$ supersaturation mode, Desalination 198 (2006) 288–294. https://doi.org/10/dgkj25.
[164] N. Cifuentes-Araya, G. Pourcelly, L. Bazinet, Impact of pulsed electric field on electrodialysis process performance and membrane fouling during consecutive demineralization of a model salt solution containing a high magnesium/calcium ratio, J. Colloid Interface Sci. 361 (2011) 79–89. https://doi.org/10/cgwhvm.
[165] H.-J. Lee, S.-H. Moon, S.-P. Tsai, Effects of pulsed electric fields on membrane fouling in electrodialysis of NaCl solution containing humate, Sep. Purif. Technol. 27 (2002) 89–95. https://doi.org/10/fh5dns.
[166] I. Ben Salah Sayadi, P. Sistat, M.M. Tlili, Assess of physical antiscale-treatments on conventional electrodialysis pilot unit during brackish water desalination, Chem. Eng. Process. Process Intensif. 88 (2015) 47–57. https://doi.org/10/f6xtmj.
[167] S. Suwal, J. Amiot, L. Beaulieu, L. Bazinet, Effect of pulsed electric field and polarity reversal on peptide/amino acid migration, selectivity and fouling mitigation, J. Membr. Sci. 510 (2016) 405–416. https://doi.org/10/gjgjp5.
[168] R.E. Pattle, Production of electric power by mixing fresh and salt water in the hydroelectric pile, Nature 174 (1954) 660. https://doi.org/10/cjrs3k.
[169] J.C. Fair, J.F. Osterle, Reverse electrodialysis in charged capillary membranes, J. Chem. Phys. 54 (1971) 3307–3316. https://doi.org/10/c4rmc7.
[170] J.N. Weinstein, F.B. Leitz, Electric power from differences in salinity: the dialytic battery, Science 191 (1976) 557–559. https://doi.org/10/czfxw3.
[171] F.E. Kiviat, Energy recovery from saline water by means of electrochemical cells, Science 194 (1976) 719–720. https://doi.org/10/fqtn3g.
[172] G.L. Wick, Power from salinity gradients, Energy 3 (1978) 95–100. https://doi.org/10/fdv4d2.
[173] R. Audinos, Electrodialyse inverse. Etude de l'energie electrique obtenue a partir de deux solutions de salinites differentes, J. Power Sources 10 (1983) 203–217. https://doi.org/10/fjzxsm.
[174] P. Dlugolecki, K. Nymeijer, S. Metz, M. Wessling, Current status of ion exchange membranes for power generation from salinity gradients, J. Membr. Sci. 319 (2008) 214–222. https://doi.org/10/cf2wjd.
[175] J. Veerman, R.M. de Jong, M. Saakes, S.J. Metz, G.J. Harmsen, Reverse electrodialysis: comparison of six commercial membrane pairs on the thermodynamic efficiency and power density, J. Membr. Sci. 343 (2009) 7–15. https://doi.org/10/c74gtv.
[176] P. Długołęcki, A. Gambier, K. Nijmeijer, M. Wessling, Practical potential of reverse electrodialysis as process for sustainable energy generation, Environ. Sci. Technol. 43 (2009) 6888–6894. https://doi.org/10/bswwmj.
[177] J.W. Post, H.V.M. Hamelers, C.J.N. Buisman, Energy recovery from controlled mixing salt and fresh water with a reverse electrodialysis system, Environ. Sci. Technol. 42 (2008) 5785–5790. https://doi.org/10/bjm8s9.
[178] J. Veerman, J.W. Post, M. Saakes, S.J. Metz, G.J. Harmsen, Reducing power losses caused by ionic shortcut currents in reverse electrodialysis stacks by a validated model, J. Membr. Sci. 310 (2008) 418–430. https://doi.org/10/fs86dc.
[179] E. Brauns, Salinity gradient power by reverse electrodialysis: effect of model parameters on electrical power output, Desalination 237 (2009) 378–391. https://doi.org/10/dzp8hk.
[180] M. Turek, B. Bandura, P. Dydo, Power production from coal-mine brine utilizing reversed electrodialysis, Desalination 221 (2008) 462–466. https://doi.org/10/fhjfr8.

This book belongs to Badji Mokhtar Annaba University Central Library Copyright Elsevier 2025

[181] M. Turek, B. Bandura, Renewable energy by reverse electrodialysis, Desalination 205 (2007) 67–74. https://doi.org/10/d6856m.
[182] J. Veerman, M. Saakes, S.J. Metz, G.J. Harmsen, Reverse electrodialysis: performance of a stack with 50 cells on the mixing of sea and river water, J. Membr. Sci. 327 (2009) 136–144. https://doi.org/10/fm765m.
[183] E. Guler, Y. Zhang, M. Saakes, K. Nijmeijer, Tailor-made anion-exchange membranes for salinity gradient power generation using reverse electrodialysis, ChemSusChem 5 (2012) 2262–2270. https://doi.org/10/fz89vf.
[184] L. Cao, W. Guo, W. Ma, L. Wang, F. Xia, S. Wang, et al., Towards understanding the nanofluidic reverse electrodialysis system: well matched charge selectivity and ionic composition, Energy Environ. Sci. 4 (2011) 2259–2266. https://doi.org/10/dsdtcr.
[185] W. Guo, L. Cao, J. Xia, F.-Q. Nie, W. Ma, J. Xue, et al., Energy harvesting with single-ion-selective nanopores: a concentration-gradient-driven nanofluidic power source, Adv. Funct. Mater. 20 (2010) 1339–1344. https://doi.org/10/c5djbc.
[186] G.M. Geise, M.A. Hickner, B.E. Logan, Ammonium bicarbonate transport in anion exchange membranes for salinity gradient energy, ACS Macro Lett. 2 (2013) 814–817. https://doi.org/10/f5pwfv.
[187] K. Kwon, B.H. Park, D.H. Kim, D. Kim, Parametric study of reverse electrodialysis using ammonium bicarbonate solution for low-grade waste heat recovery, Energy Convers. Manag. 103 (2015) 104–110. https://doi.org/10/gjgvdx.
[188] X. Luo, X. Cao, Y. Mo, K. Xiao, X. Zhang, P. Liang, et al., Power generation by coupling reverse electrodialysis and ammonium bicarbonate: implication for recovery of waste heat, Electrochem. Commun. 19 (2012) 25–28. https://doi.org/10/f34g7c.
[189] R.D. Cusick, Y. Kim, B.E. Logan, Energy capture from thermolytic solutions in microbial reverse-electrodialysis cells, Science 335 (2012) 1474–1477. https://doi.org/10/gfc4q6.
[190] Y. Kim, B.E. Logan, Hydrogen production from inexhaustible supplies of fresh and salt water using microbial reverse-electrodialysis electrolysis cells, Proc. Natl. Acad. Sci. 108 (2011) 16176–16181. https://doi.org/10/dps484.
[191] Y. Kim, B.E. Logan, Microbial reverse electrodialysis cells for synergistically enhanced power production, Environ. Sci. Technol. 45 (2011) 5834–5839. https://doi.org/10/b4ftkq.
[192] Q. Chen, Y.-Y. Liu, C. Xue, Y.-L. Yang, W.-M. Zhang, Energy self-sufficient desalination stack as a potential fresh water supply on small islands, Desalination 359 (2015) 52–58. https://doi.org/10/f62x82.
[193] Y.A.C. Jande, W.S. Kim, Integrating reverse electrodialysis with constant current operating capacitive deionization, J. Environ. Manage. 146 (2014) 463–469. https://doi.org/10/f6mk2b.
[194] W. Li, W.B. Krantz, E.R. Cornelissen, J.W. Post, A.R.D. Verliefde, C.Y. Tang, A novel hybrid process of reverse electrodialysis and reverse osmosis for low energy seawater desalination and brine management, Appl. Energy 104 (2013) 592–602. https://doi.org/10/f4tm5d.
[195] F. Luo, Y. Wang, C. Jiang, B. Wu, H. Feng, T. Xu, A power free electrodialysis (PFED) for desalination, Desalination 404 (2017) 138–146. https://doi.org/10/f9nfxg.
[196] Y. Mei, C.Y. Tang, Co-locating reverse electrodialysis with reverse osmosis desalination: synergies and implications, J. Membr. Sci. 539 (2017) 305–312. https://doi.org/10/gbspq2.
[197] Q.-W. Wang, G.-P. Yang, Z.-M. Zhang, S. Jian, Perfluoroalkyl acids in surface sediments of the East China Sea, Environ. Pollut. 231 (2017) 59–67. https://doi.org/10/gck7pp.
[198] C. Zhang, D. He, J. Ma, W. Tang, T.D. Waite, Faradaic reactions in capacitive deionization (CDI) - problems and possibilities: a review, Water Res. 128 (2018) 314–330. Available from: https://doi.org/10.1016/j.watres.2017.10.024.
[199] J. Ma, J. Ma, C. Zhang, J. Song, W. Dong, T.D. Waite, Flow-electrode capacitive deionization (FCDI) scale-up using a membrane stack configuration, Water Res. 168 (2020) 115186. Available from: https://doi.org/10.1016/j.watres.2019.115186.
[200] A. Hassanvand, G.Q. Chen, P.A. Webley, S.E. Kentish, A comparison of multicomponent electrosorption in capacitive deionization and membrane capacitive deionization, Water Res. 131 (2018) 100–109. Available from: https://doi.org/10.1016/j.watres.2017.12.015.

This book belongs to Badji Mokhtar Annaba University Central Library Copyright Elsevier 2025

[201] X. Su, T.A. Hatton, Redox-electrodes for selective electrochemical separations, Adv. Colloid Interface Sci. 244 (2017) 6–20. Available from: https://doi.org/10.1016/j.cis.2016.09.001.
[202] I. Cohen, E. Avraham, Y. Bouhadana, A. Soffer, D. Aurbach, Long term stability of capacitive de-ionization processes for water desalination: The challenge of positive electrodes corrosion, Electrochim. Acta 106 (2013) 91–100. Available from: https://doi.org/10.1016/j.electacta.2013.05.029.
[203] I. Cohen, E. Avraham, Y. Bouhadana, A. Soffer, D. Aurbach, The effect of the flow-regime, reversal of polarization, and oxygen on the long term stability in capacitive de-ionization processes, Electrochim. Acta 153 (2015) 106–114. Available from: https://doi.org/10.1016/j.electacta.2014.12.007.
[204] J.J. Wouters, J.J. Lado, M.I. Tejedor-Tejedor, R. Perez-Roa, M.A. Anderson, Carbon fiber sheets coated with thin-films of SiO_2 and γ-Al_2O_3 as electrodes in capacitive deionization: relationship between properties of the oxide films and electrode performance, Electrochim. Acta 112 (2013) 763–773. Available from: https://doi.org/10.1016/j.electacta.2013.08.170.
[205] D. He, C.E. Wong, W. Tang, P. Kovalsky, T.D. Waite, Faradaic reactions in water desalination by batch-mode capacitive deionization, Environ. Sci. Technol. Lett. 3 (2016) 222–226. Available from: https://doi.org/10.1021/acs.estlett.6b00124.
[206] L. Xu, C. Yu, Y. Mao, Y. Zong, B. Zhang, H. Chu, et al., Can flow-electrode capacitive deionization become a new in-situ soil remediation technology for heavy metal removal? J. Hazard. Mater. 402 (2021) 123568. https://doi.org/10/gj8m7c.
[207] D.-J. Yoon, J.-H. Choi, A new standard metric describing the adsorption capacity of carbon electrode used in membrane capacitive deionization, Water Res. 148 (2019) 126–132. https://doi.org/10/gfzw99.
[208] D.I. Kim, G. Gwak, P. Dorji, D. He, S. Phuntsho, S. Hong, et al., Palladium recovery through membrane capacitive deionization from metal plating wastewater, ACS Sustain. Chem. Eng. 6 (2018) 1692–1701. Available from: https://doi.org/10.1021/acssuschemeng.7b02923.
[209] K. Laxman, M.T.Z. Myint, M. Al Abri, P. Sathe, S. Dobretsov, J. Dutta, Desalination and disinfection of inland brackish ground water in a capacitive deionization cell using nanoporous activated carbon cloth electrodes, Desalination 362 (2015) 126–132. Available from: https://doi.org/10.1016/j.desal.2015.02.010.
[210] J.E. Dykstra, J. Dijkstra, A. van der Wal, H.V.M. Hamelers, S. Porada, On-line method to study dynamics of ion adsorption from mixtures of salts in capacitive deionization, Desalination 390 (2016) 47–52. Available from: https://doi.org/10.1016/j.desal.2016.04.001.
[211] I. Cohen, B. Shapira, E. Avraham, A. Soffer, D. Aurbach, Bromide ions specific removal and recovery by electrochemical desalination, Environ. Sci. Technol. 52 (2018) 6275–6281. Available from: https://doi.org/10.1021/acs.est.8b00282.
[212] B.E. Logan, B. Hamelers, R. Rozendal, U. Schröder, J. Keller, S. Freguia, et al., Microbial fuel cells: methodology and technology †, Environ. Sci. Technol. 40 (2006) 5181–5192. https://doi.org/10/frd3hn.
[213] C. Santoro, C. Arbizzani, B. Erable, I. Ieropoulos, Microbial fuel cells: from fundamentals to applications. A review, J. Power Sources 356 (2017) 225–244. https://doi.org/10/gbgxvb.
[214] T. Kim, J. Yeo, Y. Yang, S. Kang, Y. Paek, J.K. Kwon, et al., Boosting voltage without electrochemical degradation using energy-harvesting circuits and power management system-coupled multiple microbial fuel cells, J. Power Sources 410–411 (2019) 171–178. https://doi.org/10/gfzxcm.
[215] X. Long, H. Wang, C. Wang, X. Cao, X. Li, Enhancement of azo dye degradation and power generation in a photoelectrocatalytic microbial fuel cell by simple cathodic reduction on titania nanotube arrays electrode, J. Power Sources 415 (2019) 145–153. https://doi.org/10/ggqw7m.
[216] J.X. Leong, W.R.W. Daud, M. Ghasemi, K.B. Liew, M. Ismail, Ion exchange membranes as separators in microbial fuel cells for bioenergy conversion: a comprehensive review, Renew. Sustain. Energy Rev. 28 (2013) 575–587. https://doi.org/10/f5mqf2.
[217] M. Oliot, S. Galier, H. Roux de Balmann, A. Bergel, Ion transport in microbial fuel cells: key roles, theory and critical review, Appl. Energy 183 (2016) 1682–1704. https://doi.org/10/f933bm.
[218] K.J. Chae, M. Choi, F.F. Ajayi, W. Park, I.S. Chang, I.S. Kim, Mass transport through a proton exchange membrane (Nafion) in microbial fuel cells†, Energy Fuels 22 (2008) 169–176. https://doi.org/10/fhvkf5.

This book belongs to Badji Mokhtar Annaba University Central Library Copyright Elsevier 2025

[219] M. Shabani, H. Younesi, M. Pontié, A. Rahimpour, M. Rahimnejad, A.A. Zinatizadeh, A critical review on recent proton exchange membranes applied in microbial fuel cells for renewable energy recovery, J. Clean. Prod. 264 (2020) 121446. https://doi.org/10/gjgkm7.
[220] S.M. Daud, B.H. Kim, M. Ghasemi, W.R.W. Daud, Separators used in microbial electrochemical technologies: current status and future prospects, Bioresour. Technol. 195 (2015) 170–179. https://doi.org/10/gjgkm2.
[221] M.H. Do, H.H. Ngo, W.S. Guo, Y. Liu, S.W. Chang, D.D. Nguyen, et al., Challenges in the application of microbial fuel cells to wastewater treatment and energy production: a mini review, Sci. Total Environ. 639 (2018) 910–920. https://doi.org/10/gjjgqc.
[222] V.G. Gude, Wastewater treatment in microbial fuel cells – an overview, J. Clean. Prod. 122 (2016) 287–307. https://doi.org/10/f8jwt5.
[223] G. Palanisamy, H.-Y. Jung, T. Sadhasivam, M.D. Kurkuri, S.C. Kim, S.-H. Roh, A comprehensive review on microbial fuel cell technologies: processes, utilization, and advanced developments in electrodes and membranes, J. Clean. Prod. 221 (2019) 598–621. https://doi.org/10/ggdmvt.
[224] B. Logan, S. Cheng, V. Watson, G. Estadt, Graphite fiber brush anodes for increased power production in air-cathode microbial fuel cells, Environ. Sci. Technol. 41 (2007) 3341–3346. https://doi.org/10/d3jckx.
[225] E. Zhang, F. Wang, Q. Yu, K. Scott, X. Wang, G. Diao, Durability and regeneration of activated carbon air-cathodes in long-term operated microbial fuel cells, J. Power Sources 360 (2017) 21–27. https://doi.org/10/gbr25p.
[226] H.M. Saeed, G.A. Husseini, S. Yousef, J. Saif, S. Al-Asheh, A. Abu Fara, et al., Microbial desalination cell technology: a review and a case study, Desalination 359 (2015) 1–13. https://doi.org/10/gjgkmz.
[227] M. Tawalbeh, A. Al-Othman, K. Singh, I. Douba, D. Kabakebji, M. Alkasrawi, Microbial desalination cells for water purification and power generation: a critical review, Energy 209 (2020) 118493. https://doi.org/10/gjgkm9.
[228] M.N.I. Salehmin, S.S. Lim, I. Satar, W.R.W. Daud, Pushing microbial desalination cells towards field application: prevailing challenges, potential mitigation strategies, and future prospects, Sci. Total Environ. 759 (2021) 143485. https://doi.org/10/gjjgrc.
[229] S. Rahman, T. Jafary, A. Al-Mamun, M.S. Baawain, M.R. Choudhury, H. Alhaimali, et al., Towards upscaling microbial desalination cell technology: A comprehensive review on current challenges and future prospects, J. Clean. Prod. 288 (2021) 125597. https://doi.org/10/gjgkm6.
[230] S. Sevda, H. Yuan, Z. He, I.M. Abu-Reesh, Microbial desalination cells as a versatile technology: functions, optimization and prospective, Desalination 371 (2015) 9–17. https://doi.org/10/f7k4gf.
[231] H.S. Abid, B.S. Lalia, P. Bertoncello, R. Hashaikeh, B. Clifford, D.T. Gethin, et al., Electrically conductive spacers for self-cleaning membrane surfaces via periodic electrolysis, Desalination 416 (2017) 16–23. https://doi.org/10/b7f7.
[232] Y. Zhang, W. Yu, R. Li, Y. Xu, L. Shen, H. Lin, et al., Novel conductive membranes breaking through the selectivity-permeability trade-off for Congo red removal, Sep. Purif. Technol. 211 (2019) 368–376. https://doi.org/10/ghtcs7.
[233] Q. Huang, H. Liu, Y. Wang, C. Xiao, A hybrid electric field assisted vacuum membrane distillation method to mitigate membrane fouling, RSC Adv. 8 (2018) 18084–18092. https://doi.org/10/ghtf2t.
[234] D. Bell, R. Sengpiel, M. Wessling, Metallized hollow fiber membranes for electrochemical fouling control, J. Membr. Sci. 594 (2020) 117397. https://doi.org/10/ghtg54.
[235] S.-Y. Li, B.S. Schon, J. Travas-Sejdic, A conductive microfiltration membrane for in situ fouling detection: proof-of-concept using model wine solutions, Macromol. Rapid Commun. 41 (2020) 2000303. https://doi.org/10/ghtc34.
[236] X. Wang, M. Sun, Y. Zhao, C. Wang, W. Ma, M.S. Wong, et al., In situ electrochemical generation of reactive chlorine species for efficient ultrafiltration membrane self-cleaning, Environ. Sci. Technol. 54 (2020) 6997–7007. https://doi.org/10/gh7vbs.
[237] L. Tang, A. Iddya, X. Zhu, A.V. Dudchenko, W. Duan, C. Turchi, et al., Enhanced flux and electrochemical cleaning of silicate scaling on carbon nanotube-coated membrane distillation membranes treating geothermal brines, ACS Appl. Mater. Interfaces 9 (2017) 38594–38605. https://doi.org/10/gjpghz.

This book belongs to Badji Mokhtar Annaba University Central Library Copyright Elsevier 2025

[238] X. Fan, H. Zhao, X. Quan, Y. Liu, S. Chen, Nanocarbon-based membrane filtration integrated with electric field driving for effective membrane fouling mitigation, Water Res. 88 (2016) 285–292. https://doi.org/10/f75fc8.
[239] W. Duan, A. Dudchenko, E. Mende, C. Flyer, X. Zhu, D. Jassby, Electrochemical mineral scale prevention and removal on electrically conducting carbon nanotube – polyamide reverse osmosis membranes, Environ. Sci. Process. Impacts. 16 (2014) 1300–1308. https://doi.org/10/f59kq6.
[240] X. Tan, C. Hu, Z. Zhu, H. Liu, J. Qu, Electrically pore-size-tunable polypyrrole membrane for antifouling and selective separation, Adv. Funct. Mater. 29 (2019) 1903081. https://doi.org/10/gjpgh4.
[241] Q. Liu, G. Qiu, Z. Zhou, J. Li, G.L. Amy, J. Xie, et al., An effective design of electrically conducting thin-film composite (TFC) membranes for bio and organic fouling control in forward osmosis (FO), Environ. Sci. Technol. 50 (2016) 10596–10605. https://doi.org/10/f869gj.
[242] L. Borea, V. Naddeo, V. Belgiorno, Application of electrochemical processes to membrane bioreactors for improving nutrient removal and fouling control, Environ. Sci. Pollut. Res. 24 (2017) 321–333. https://doi.org/10/f9msf7.
[243] W.H. Glaze, J.-W. Kang, D.H. Chapin, The chemistry of water treatment processes involving ozone, hydrogen peroxide and ultraviolet radiation, Ozone Sci. Eng. 9 (1987) 335–352. https://doi.org/10/fk9q96.
[244] S. Meng, H. Fang, D. Yu, Fractal characteristics, multiple bubbles, and jump anomalies in the chinese stock market, Complexity 2020 (2020) 1–12. https://doi.org/10/gh53p7.
[245] F.C. Moreira, R.A.R. Boaventura, E. Brillas, V.J.P. Vilar, Electrochemical advanced oxidation processes: a review on their application to synthetic and real wastewaters, Appl. Catal. B Environ. 202 (2017) 217–261. https://doi.org/10/ghp3jb.
[246] A.M. Zaky, B.P. Chaplin, Porous substoichiometric TiO_2 anodes as reactive electrochemical membranes for water treatment, Environ. Sci. Technol. 47 (2013) 6554–6563. https://doi.org/10/f45bk7.
[247] M.B. Asif, T. Maqbool, Z. Zhang, Electrochemical membrane bioreactors: State-of-the-art and future prospects, Sci. Total Environ. 741 (2020) 140233. https://doi.org/10/ghdqzv.
[248] J. Zheng, S. Xu, Z. Wu, Z. Wang, Removal of p-chloroaniline from polluted waters using a cathodic electrochemical ceramic membrane reactor, Sep. Purif. Technol. 211 (2019) 753–763. https://doi.org/10/ggfcwd.
[249] I.F. Cheng, Q. Fernando, N. Korte, Electrochemical dechlorination of 4-chlorophenol to phenol, Environ. Sci. Technol. 31 (1997) 1074–1078. Available from: https://doi.org/10.1021/es960602b.
[250] P. Dabo, A. Cyr, F. Laplante, F. Jean, H. Ménard, J. Lessard, Electrocatalytic dehydrochlorination of pentachlorophenol to phenol or cyclohexanol, Environ. Sci. Technol. 34 (2000) 1265–1268. Available from: https://doi.org/10.1021/es9911465.
[251] S.G. Merica, C.E. Banceu, W. Jędral, J. Lipkowski, N.J. Bunce, Electroreduction of hexachlorobenzene in micellar aqueous solutions of Triton-SP 175, Environ. Sci. Technol. 32 (1998) 1509–1514. Available from: https://doi.org/10.1021/es970969w.
[252] Q. Ji, D. Yu, G. Zhang, H. Lan, H. Liu, J. Qu, Microfluidic flow through polyaniline supported by lamellar-structured graphene for mass-transfer-enhanced electrocatalytic reduction of hexavalent chromium, Environ. Sci. Technol. 49 (2015) 13534–13541. Available from: https://doi.org/10.1021/acs.est.5b03314.
[253] X. Zhao, H. Liu, A. Li, Y. Shen, J. Qu, Bromate removal by electrochemical reduction at boron-doped diamond electrode, Electrochim. Acta 62 (2012) 181–184. Available from: https://doi.org/10.1016/j.electacta.2011.12.013.
[254] D. Yu, J. He, Z. Wang, H. Pang, L. Li, Y. Zheng, et al., Mineralization of norfloxacin in a CoFe–LDH/CF cathode-based heterogeneous electro-fenton system: Preparation parameter optimization of the cathode and conversion mechanisms of H_2O_2 to OH, Chem. Eng. J. 417 (2021) 129240. Available from: https://doi.org/10.1016/j.cej.2021.129240.
[255] Y. Liu, F. Liu, N. Ding, X. Hu, C. Shen, F. Li, et al., Recent advances on electroactive CNT-based membranes for environmental applications: the perfect match of electrochemistry and membrane separation, Chin. Chem. Lett. 31 (2020) 2539–2548. Available from: https://doi.org/10.1016/j.cclet.2020.03.011.

This book belongs to Badji Mokhtar Annaba University Central Library Copyright Elsevier 2025

[256] W. Duan, G. Chen, C. Chen, R. Sanghvi, A. Iddya, S. Walker, et al., Electrochemical removal of hexavalent chromium using electrically conducting carbon nanotube/polymer composite ultrafiltration membranes, J. Membr. Sci. 531 (2017) 160–171. Available from: https://doi.org/10.1016/j.memsci.2017.02.050.

[257] H. Qi, X. Sun, Z. Sun, Porous graphite felt electrode with catalytic defects for enhanced degradation of pollutants by electro-Fenton process, Chem. Eng. J. 403 (2021) 126270. Available from: https://doi.org/10.1016/j.cej.2020.126270.

[258] D. Zhang, T. Liu, K. Yin, C. Liu, Y. Wei, Selective H_2O_2 production on N-doped porous carbon from direct carbonization of metal organic frameworks for electro-Fenton mineralization of antibiotics, Chem. Eng. J. 383 (2020) 123184. Available from: https://doi.org/10.1016/j.cej.2019.123184.

[259] Y. Liu, J. Xie, C.N. Ong, C.D. Vecitis, Z. Zhou, Electrochemical wastewater treatment with carbon nanotube filters coupled with in situ generated H_2O_2, Environ. Sci. Water Res. Technol. 1 (2015) 769–778. Available from: https://doi.org/10.1039/C5EW00128E.

[260] J. Teng, S. You, F. Ma, X. Chen, N. Ren, Enhanced electrochemical decontamination and water permeation of titanium suboxide reactive electrochemical membrane based on sonoelectrochemistry, Ultrason. Sonochem. 69 (2020) 105248. https://doi.org/10/ghdjtr.

This book belongs to Badji Mokhtar Annaba University Central Library Copyright Elsevier 2025

CHAPTER TWO

Fundamentals of electrochemical membrane technology

Jingqiu Sun[1,2], Tianyu Wang[1,2], Zhenao Gu[1,2], Chenghai Lu[1,2], Zhibin Chen[1,2], You Wu[1,2] and Chengzhi Hu[1,2]

[1]State Key Laboratory of Environmental Aquatic Chemistry, Research Center for Eco-Environmental Sciences, Chinese Academy of Sciences, Beijing, P.R. China
[2]University of Chinese Academy of Sciences, Beijing, P.R. China

2.1 Introduction

Nowadays, membrane technologies for drinking water purification and wastewater treatment play key roles in coping with the severe challenges of global water shortages, especially clean water for ensuring human health and economic development. However, due to the limited selective separation performance based on size- and charge-exclusion mechanisms, it is exceedingly difficult to separate the species with similar size or charges, which is urgently needed in resource recovery process. Besides, membrane fouling is another key point that restrains the application of the membrane in practical water treatment events, which increases the operation and maintenance costs. The electrochemical membrane technology (EMT) is a promising method to overcome these challenges as it is based on electrochemical processes (e.g., electrochemical reactions) [1–3]. EMT can be used to effectively degrade and/or repulse pollutants by electrooxidation enhanced electrostatic force, which is beneficial for membrane fouling control and long-term operational stability. Correspondingly, due to the combination of membrane sieving with a variety of electrochemical processes, a series of scientific mechanisms needs to be reviewed as the fundamentals in EMT.

Charged species in aqueous solutions can be induced to move directionally by an electric field (EF), which can be described by the Nernst–Planck (NP) equation in an electrical system. The NP equation covers three important aspects of the transport mechanism: convection, diffusion, and electromigration. The regulation of mass transport based on the NP equation is of great significance for the membrane separation process for, according to the NP equation, the application of an external EF is an effective method for regulating ion transport in membrane nanopores [4,5], given ions

Electrochemical Membrane Technology for Water and Wastewater Treatment.
DOI: https://doi.org/10.1016/B978-0-12-824470-8.00001-2
© 2022 Elsevier Inc.
All rights reserved.

This book belongs to Badji Mokhtar Annaba University Central Library
Copyright Elsevier 2025

can electromigrate through the nanopores in membranes using EF forces. In addition, the valence, type, and size of ions considerably influence ion transport through membranes under an EF, which indicates that EFs have the potential to promote ion-selective separation performance of the membranes.

The electrical double layer (EDL) is composed of an inner compact layer and an outer diffusion layer, and the type and concentration of ions, the forces between ions and membranes, and the charge density of the membrane are closely related to the structure of the EDL. Correspondingly, electrified membranes (EMs) can significantly electrically adsorb counterions to form a thick EDL, and a large number of capacitive ions can accumulate on the membrane surface. EMs with high specific capacitances have an excellent ability to allow ion accumulation on the membrane surface; as a result, ions in the bulk solution must overcome strong repulsive forces to permeate the membranes, which is beneficial for realizing ion rejection. In addition, changes in the EDL structure of the inner walls of the nanopores generally influence the ion distribution in the nanopores, which controls the ion transport behavior. Therefore, the development of the EDL theory along with a characterization method for solid—liquid interfaces can provide a fundamental understanding of ion transmembrane transport, which will be conducive to research on ion-selective separation.

EF-induced polarization phenomena are widely observed in electrochemical water treatment systems. When an EF is applied in the direction perpendicular to the membrane surface, the pollutants in water are polarized by the EF and form a regularly arranged filter cake layer on the membrane surface. These loose, hydrophilic, and porous filter cake layers formed under an EF can inhibit membrane fouling and maintain water permeability. However, when the EF strength is too high, more pollutants accumulate on the membrane surface, forming a dense cake layer with high hydraulic resistance and causing serious membrane fouling. Therefore, the polarization of charged pollutants induced by the EF to form a cake layer needs to be controlled to achieve low fouling resistance and high water permeability.

In addition to the pollutant filtration process regulated by a physical EF application, the electrochemical reaction occurring when an EM is employed as an electrode is another important process that may realize membrane fouling mitigation and foulant removal. When the membrane is used as an anode, the foulants on the membrane surface or in the membrane pores can be degraded by direct oxidation. In addition, the foulants are oxidized by the indirect oxidation of the oxidative species (such as H_2O_2, HO•, and Cl•) generated from the electrochemical reactions occurring on the EMs. The electroactive layer, characterized by a large specific surface area and the presence of small pores, enables the EMs to efficiently remove contaminants in a flow-through filtration mode owing to the synergistic effects of the convection-enhanced mass transport, nanoconfinement, and electro-adsorption. Moreover, the spatial confinement in a nanopore increases the local concentrations of oxidative species, which considerably

This book belongs to Badji Mokhtar Annaba University Central Library Copyright Elsevier 2025

improves the degradation rate of foulants blocked in the nanopores. The diffusion pathway between the contaminants and the electroactive surface shrinks (to the pore radius) in the nanoscale environment, which increases the mass transfer rates and accelerates electrochemical reactions. However, the generated oxidative species damages the membranes as well; therefore, further optimization is needed for practical applications.

Based on fundamental mechanisms and theories, various EMT-based systems have been developed and implemented for environmental remediation. This chapter discusses the fundamentals of and the principles associated with the membrane filtration process, including the electrokinetic effect in the transmembrane process, the presence of EDLs on the membrane surface and inner pores, the formation of dynamic membranes due to the polarization effect, and the electrochemical reactions on the EMs. Finally, further challenges to be overcome in EMT research are summarized. These include the development of an advanced in situ characterization methodology for the EM filtration process in fundamental studies, the modification of the basic theory that describes the EDL structure on the EM surface and the nanoconfinement effects, and the design principle of sustainable EMs for practical applications.

2.2 Electrokinetic ions/colloids

2.2.1 Electromigration

2.2.1.1 Ion electromigration

The directional movement of ions under an EF is referred to as ion electromigration. When the electrolyte solution is energized, the anions and cations in the solution that are responsible for conducting electricity move to the anode and cathode, respectively, and the oxidation or the reduction occurs at the corresponding interface of the two electrodes; thus, the concentration of the solution near the electrode also changes.

It is assumed that the bulk solution contains 5 mol each of the positive and negative ions, both of which are monovalent. When 4 mol of electrons have passed through, 4 mol of negative ions are oxidized on the anode, 4 mol of positive ions are reduced on the cathode, and the ions in the solution migrate at the same time. The charge of 4 mol electrons is shared by the positive and negative ions, and the charge transferred by each ion varies with their migration rate. Therefore, there are two cases: in the first case, when the mobilities of the positive and negative ions are equal, the task of conducting electricity is shared by half (2 mol of positive and negative ions passed through each other). In the second case, the mobility of positive ions is three times that of negative ions; thus, 3 mol of positive ions and 1 mol of negative

This book belongs to Badji Mokhtar Annaba University Central Library Copyright Elsevier 2025

ions will penetrate each other in any plane. After energizing, the concentration of the bulk solution remains unchanged; however, the concentrations of the positive and negative ions at the cathode and the anode are lower than the concentrations of those of the original solution because of the different degree of reduction.

2.2.1.2 Electric mobility and migration number of ions

Under the EF force, the positive and negative ions cause directional movement. Although positive and negative ions move in opposite directions, the direction of charge transport is the same. If the total amount of charge is q under an EF, the amount of charge through any cross-section will also be q. The task of delivered electricity q is shared by the positive and negative ions. The amount of charge transferred by the ions varies with the migration rate. The following factors affect the rate of ion movement:

1. *Ionic nature*: The larger the radius (mainly of hydrated ions), the higher the resistance when moving through the solution, and therefore, the lower the ion movement rate. Again, the higher the valency of ions, the stronger the effect of the external EF, and thus, the higher the ion movement rate. Therefore, under the action of the same EF, different ions move at different rates. It is particularly noteworthy that H^+ ions in aqueous solution have a special migration mode and that their ion movement rate is considerably higher than that of ordinary ions. H^+ ions are 5–8 times larger than other ions and exist in the form of H_3O^+ in aqueous solution. In addition to the directional motion under an EF, similar to other ions, H_3O^+ adopts a faster migration mode, in which H^+ is transferred from H_3O^+ to neighboring H_2O molecules, forming a new H_3O^+. The proton on the newly formed H_3O^+ follows the same process. Thus, the protons travel rapidly in a relay.
2. *Total concentration of solution*: In the electrolyte solution, there is an interaction among ions. When the concentration is increased, the distance between ions decreases, the interaction strengthens, and the resistance to ion movement increases.
3. *Temperature*: As the temperature increases, the ion movement rate increases.
4. *Solvent viscosity*: An increase in solvent viscosity also increases the ion movement resistance which leads to a decrease in the ion movement rate.

The rate of ion movement under an EF is related not only to the nature of the ion and the solvent (including ion radius, ion hydration degree, ion charge, solvent viscosity, etc.) but also to the potential gradient of the EF. Obviously, the larger the potential gradient, the higher the driving force of ion movement.

Because the positive and negative ions move at different rates and carry different charges, they perform different tasks when transferring the amount of charge. The most commonly used methods for determining the migration number include the Hittorf method and the interface movement method.

This book belongs to Badji Mokhtar Annaba University Central Library Copyright Elsevier 2025

When ions pass through the membrane, the ion flux (J_{di}) changes according to the concentration gradient. Under an EF, the ions move toward the oppositely charged electrode. For example, when a negative EF is applied, the migration of cations ($J_{mig,ca}$) will be prevented and the migration of anions ($J_{mig,a}$) will be promoted, resulting in a decrease in the cation flux and an increase in the anion flux. When the applied EF is sufficiently strong and the induced flux $J_{mig,ca}$ is larger than J_{di}, the ions will be unable to transport across the membrane, as shown in Fig. 2.1A. Considering the TiO_2 channels as an example, the transport rates through the membrane of Na^+ and Mg^{2+} decrease under the action of a negative EF, as shown in Fig. 2.1B and C [4].

2.2.2 Electrophoresis

Electrophoresis, also called cataphoresis, originally referred to the phenomenon of charged colloidal particles moving under a direct-current EF. However, low-molecular-charged

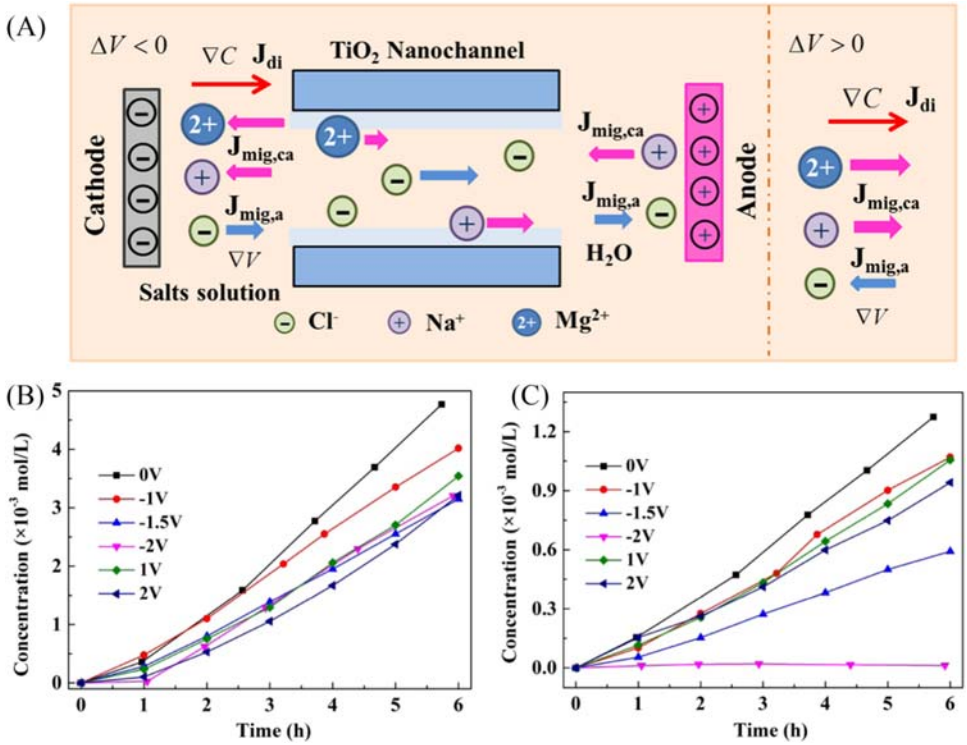

Figure 2.1 (A) Schematic diagram of the effect of an electric field on ion transport behavior in negatively charged channels. Concentrations of (B) Na^+ and (C) Mg^{2+} at different working voltages. *Adapted with permission from D. Li, W.H. Jing, S.Q. Li, H. Shen, W.H. Xing, Electric field-controlled ion transport in TiO_2 nanochannel, ACS Appl. Mater. Interfaces 7 (2015) 11294–11300 [4]. Copyright 2015, American Chemical Society.*

This book belongs to Badji Mokhtar Annaba University Central Library Copyright Elsevier 2025

substances also exhibit movement phenomena. To distinguish between the two, the latter is referred to as ion electrophoresis. Owing to the rapid development of this technology, it has been used to separate various substances, such as proteins [6,7], DNA [8], nucleic acids [9], purines, pyrimidines, other organic compounds [10,11], and even inorganic ions [12]. Using the same instruments and operating methods, the name "electrophoresis" is uniformly used. Electrophoresis is also used to separate and identify charged particles—including ions, polymer polyelectrolytes, colloidal particles, virus particles, and even living cells such as bacteria and red blood cells—in a mixture. Although electrophoresis was discovered more than 150 years ago, it's not until 1937 when Tiselius established the "moving boundary EP" method, which successfully divided serum proteins into five main components, that electrophoresis got worldwide recognition.

Electrophoretic mobility refers to the migration rate of particles per unit EF strength (1 V/cm), which can be determined by calculating the driving force and resistance in the equilibrium state.

The force (F) that drives the motion of the particle is equal to the product of the net charge (Q) of the particle and the EF strength (E), that is,

$$F = QE \tag{2.1}$$

The particle is subject to a certain resistance (F') when it moves. For spherical particles, this resistance obeys Stoker's law:

$$F' = 6\pi r\eta v \tag{2.2}$$

where r is the particle diameter, η is the viscosity of the medium, and v is the migration rate. When the particle moves in a steady state, the electromotive force is equal to the resistance; hence,

$$QE = 6\pi r\eta v \tag{2.3}$$

Electrophoretic mobility (μ) refers to the swimming rate per unit EF strength (1 V/cm), as follows:

$$\mu = \frac{v}{E} \tag{2.4}$$

$$\mu = \frac{Q}{6\pi r\eta} \tag{2.5}$$

In fact, such an ideal situation is difficult to achieve, especially in the case of zone electrophoresis, and there are many deviations.

From Eq. (2.4), the unit of mobility can be derived as follows:

$$\mu = \frac{v}{E} = \frac{d}{t \cdot E} = \frac{\text{cm}}{\text{s} \cdot \frac{\text{V}}{\text{cm}}} = \frac{\text{cm}^2}{\text{V} \cdot \text{s}} \tag{2.6}$$

This book belongs to Badji Mokhtar Annaba University Central Library Copyright Elsevier 2025

where d is the particle movement distance (cm), t is time (s), and E is the potential gradient (V/cm).

Because the mobility value is extremely low, it is usually expressed in mobility units:

$$1 \text{ Migration rate unit} = 10^{-5}\left(\frac{\text{cm}^2}{\text{V}\cdot\text{s}}\right) \tag{2.7}$$

Under certain conditions, the mobility of a substance is constant, which is determined by the physical and chemical properties of the substance.

2.2.3 Electroosmosis

When a solid is in contact with a liquid, the solid surface carries an electric charge, while the liquid around it possesses the opposite charge due to electrostatic attraction. In this event, an EDL is formed at the solid–liquid interface, resulting in a potential difference. When a voltage is applied at both ends of the liquid, the liquid moves relative to the solid surface (Fig. 2.2), a phenomenon called electroosmosis [13,14]. The movement of the entire liquid during this phenomenon is called electroosmotic flow [15].

An important characteristic of the electroosmotic flow is its plane flow pattern, where the electroosmotic driving force is uniformly distributed along the microchannel, and the radial distribution of electroosmotic velocity is almost uniform. Another feature of electroosmosis is that almost all components in the fluid, whether charged/neutral or negatively/positively charged, move in the same direction. The outflow time (migration time) of each component in the capillary depends on the vector sum of the electroosmotic flow velocity and the component electrophoresis velocity.

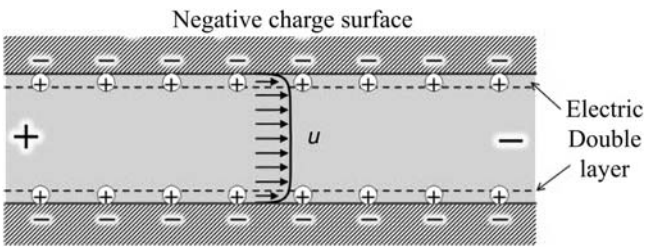

Figure 2.2 Working principle of electroosmosis. *Adapted with permission from K.W. Oh, 6 - Lab-on-chip (LOC) devices and microfluidics for biomedical applications, in: S. Bhansali, A. Vasudev (Eds.), MEMS for Biomedical Applications, Woodhead Publishing, 2012, pp. 150–171 [16]. Copyright 2012, Elsevier.*

This book belongs to Badji Mokhtar Annaba University Central Library Copyright Elsevier 2025

Electroosmotic flow is mainly affected by solid materials, temperature, EF strength, and additives.

1. Solid materials

   For the microchannels of different materials, when the pH of the solution is increased, the number of ionized ions on the microchannel surface increases as do the charge density and zeta potential of the channels; therefore, the electroosmotic mobility increases. In general, the electroosmotic mobility reaches a maximum when the solution pH is 7, at which point the silicon hydroxyl groups on the pipe surface are completely dissociated, and the electroosmotic mobility is almost unchanged. With a decrease in the solution pH, the concentration of hydrogen ions in the solution increases, and the ionized anions in the tube wall are neutralized by the hydrogen ions. In addition, at low pH, the silicon hydroxyl groups on the surface of the microchannels undergo low dissociation, resulting in a decrease in the surface charge density and zeta potential and, thus, a decrease in electroosmotic mobility. Therefore, it is typically necessary to use a buffer solution in the experiment to maintain the stability of the solution pH.

2. Temperature

   The effect of temperature is usually reflected in the variability of the viscosity and dielectric constant of the fluid. When the fluid moves relative to the solid, a tangential force arises because the direction of the tangential force is always opposite to the direction of the fluid movement, resulting in friction resistance. This friction-producing property is called the fluid viscosity, which is one of the physical properties of the fluid. When the temperature in the microchannel is increased, the viscosity of the solution decreases and the electroosmotic flow increases. When the temperature is increased by 1°C, the viscosity of the solution decreases by 2% or 3%.

3. Field strength and zeta potential

   With an increase in the external EF strength, the flow pattern of the electroosmotic fluid does not change, but the velocity increases because the electroosmotic flow is driven by the EF. With an increase in the EF strength, the force of the charged ions in the solution increases, which leads to an increase in the electroosmotic velocity. When the zeta potential of the wall increases, the surface charge and ion concentration in the wall also increase, thereby increasing the driving force of the electroosmotic flow.

4. Additive

The addition of high concentrations of salt, such as K_2SO_4, can induce an increase in the ionic strength and lead to a decrease in the electroosmotic flow. The addition of anionic surfactants, such as sodium dodecyl sulfate, can increase the negative charge on the wall surface and the electroosmotic flow. The addition of polar organic solvents, such as methanol and acetonitrile, can increase the zeta potential of the wall, thus increasing the electroosmotic flow.

This book belongs to Badji Mokhtar Annaba University Central Library Copyright Elsevier 2025

2.3 Ion transmembrane mass transfer

2.3.1 Nernst–Planck equation

There are three types of mass transfer in solution: convection, diffusion, and migration.

1. Convection

   Convection, including natural convection and forced convection, refers to the component flowing within the fluid. Natural convection is caused by a density gradient and forced convection, by an external mechanism. The convection of component i in the solution can be described by Eq. (2.8):

$$J_i = V_x C_i \tag{2.8}$$

where J_i and C_i are the flux and concentration of component i, respectively, and V_x is the velocity of the liquid in the x direction.

2. Diffusion

   Diffusion refers to the movement of a component in a gradient of its concentration. The diffusion of component i in the solution can be described by Eq. (2.9):

$$J_i = -D_i \frac{\partial C_i}{\partial x} \tag{2.9}$$

where J_i, D_i, and C_i are the flux, diffusion coefficient, and concentration of component i [17], respectively.

3. Migration

   Migration is the movement of a component along the gradient of its electrochemical potential. The migration of component i in solution can be described by Eq. (2.10):

$$J_i = -\frac{z_i F}{RT} D_i C_i \frac{\partial \varphi_i}{\partial x} \tag{2.10}$$

where J_i, z_i, D_i, C_i, and φ_i are the flux, charge number, diffusion coefficient, concentration, and electrical potential of component i, respectively. F, R, and T are the Faraday constant, gas constant, and temperature, respectively [18].

Considering the above-mentioned three types of mass transfer, the flux in the solution can be described by Eq. (2.11):

$$J_i = -D_i \frac{\partial C_i}{\partial x} - \frac{z_i F}{RT} D_i C_i \frac{\partial \varphi_i}{\partial x} + V_x C_i \tag{2.11}$$

This book belongs to Badji Mokhtar Annaba University Central Library Copyright Elsevier 2025

Eq. (2.11) is the basic form of the NP equation, which describes liquid mass transfer in a solution [19]. It can also be used to explain the transmembrane transport behavior of ions. The original equation variables, such as the diffusion coefficient and ion concentration in the solution, should be replaced by the corresponding variables in the membrane. Moreover, the effect of mass transfer resistance must be considered because the mass transfer space changes from a solution to a confined pore. The extended NP equation is then proposed (Eq. 2.12):

$$J_i = -D_{i,m}\frac{\partial C_{i,m}}{\partial x} - \frac{z_i F}{RT} D_{i,m} C_{i,m} \frac{\partial \varphi_i}{\partial x} + K_{i,c} V_x C_{i,m} \tag{2.12}$$

where $D_{i,m}$ and $C_{i,m}$ are the diffusion coefficient and concentration of component i in the membrane, respectively. $K_{i,c}$ is the convection steric hindrance factor of component i. In particular, $D_{i,m}$ takes into account the diffusion hindrance factor.

Bowen et al. reported the Donnan steric pore model (DSPM) theory based on Eq. (2.12) to further describe the ion transport in the membrane. The model regarded the membrane as charged porous layers, which are characterized by average pore size, volume charge density, and effective membrane thickness. In addition, steric hindrance and the Donnan effect are considered as the mechanisms of ion rejection [20].

Sun et al. studied the response of partially reduced graphene oxide (GO) membrane rejection to an EF under different conditions by using the DSPM model and concluded that the response of ion rejection to the EF was determined by the effective charge density of the membrane. The homemade filtration setup is shown in Fig. 2.3A. In the experiment, the electrodes consisted of a stainless-steel plate positioned on top of the filtration setup and a porous stainless-steel mesh under the membrane; the membrane was placed in an EF without direct connection to the power supply (Fig. 2.3B). The rejection of Na_2SO_4 was controlled by the EF; the rejection rate decreased when the applied potential was negative and increased when the applied potential was positive, indicating that Na^+ was the crucial component controlling the response of ion rejection to the EF (Fig. 2.3C). The rejection rates of both NaCl and Na_2SO_4 also increased under an external EF. When the voltage increased from 0 to 1.0 V, the rejection of NaCl and Na_2SO_4 increased by 6.89% and 16.84%, respectively (Fig. 2.3D), indicating that the EF has the potential to selectively separate ions owing to the different response of the membrane [21].

Although the DSPM model can explain some of the experimental results, it has shortcomings in predicting membrane performance. First, a single ratio of membrane thickness to membrane porosity does not support the experimental rejection of various electrolytes. In addition, DSPM cannot successfully predict the high rejection of divalent counterions in nanofiltration (NF) membranes, indicating that more factors must be considered in order to better understand and predict the membrane performance.

This book belongs to Badji Mokhtar Annaba University Central Library Copyright Elsevier 2025

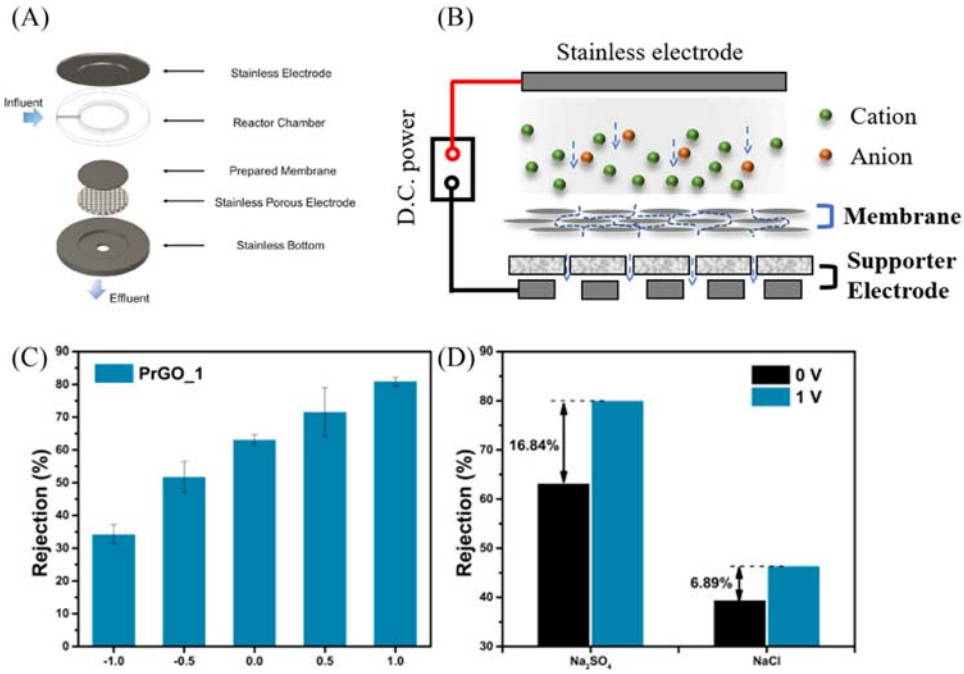

Figure 2.3 (A) Schematic diagram of the homemade filtration setup. (B) schematic diagram of the cell. (C) influence of the electric field (EF) direction and strength on the rejection rate of Na_2SO_4 solution. (D) rejection rates of different salts under different EF strengths. *Adapted with permission from J. Sun, C. Hu, B. Wu, H. Liu, J. Qu, Improving ion rejection of graphene oxide conductive membranes by applying electric field, J. Membr. Sci. 604 (2020) [21]. Copyright 2020, Elsevier.*

In addition, ion transport in nanoconfinement is different from that in the bulk. Because the fluid is confined to the nano- or even sub-nano scale, the mass transfer equation is seriously challenged. In fact, the solvent molecules in the confined membrane pores show a stronger spatial and orientation order, resulting in a decrease in the dielectric constant of the solvent [22]. Ion diffusion is affected by the local EF generated by the surface charge or applied potential, especially the interface EDL caused by the surface potential. Li et al. prepared a layered nanoporous gel membrane containing nanochannels via the supramolecular assembly of chemically converted graphene with interlayer spacing tunable in the nanometer range. The diffusion rate of ions affected by the potential, the combination of ion pairs, and the concentration could be enhanced by up to sevenfold in the nanoconfinement. It was considered that the increase in the ion diffusion rate was related to the strong ion−ion correlations and could not be explained by the traditional theory [23].

It should always be noted that the main limitation of membrane modeling is the requirement of characteristic model parameters such as pore size and membrane charge, which are difficult to accurately measure at the nanometer scale. Therefore,

This book belongs to Badji Mokhtar Annaba University Central Library Copyright Elsevier 2025

the development of models should be synchronized with the progress of in situ characterization methods and technologies.

2.3.2 Donnan effect

The ions migrate between the solution and membrane phases until their ion concentrations reach equilibrium. The fixed charge on the membrane adsorbs counterions (ions with charges opposite to the fixed charges on the membrane) owing to the electrostatic effect, leading to a higher concentration of counterions in the membrane than in the solution and a lower concentration of coions in the membrane than in the solution. The resultant Donnan potential difference prevents the migration of coions from the solution to the membrane, and the migration of counterions is also prevented owing to the principle of solution electric neutrality [24].

The Donnan potential is expressed by the following equation (Eq. 2.13):

$$\varphi_{Don} = \varphi^m - \varphi^s = \frac{RT}{z_i F} ln \frac{a_i^s}{a_i^m} \tag{2.13}$$

where φ_{Don}, φ^m, and φ^s are the Donnan potential, membrane potential, and solution potential, respectively. Parameters a_i^s and a_i^m are the activities in the solution and the membrane of component i, respectively.

The ion concentration in the membrane at the Donnan equilibrium was calculated using Eq. (2.14):

$$\left(\frac{c_{co}^s}{c_{co}^m}\right)^{\frac{1}{z_{co}}} \left(\frac{c_{cou}^m}{c_{cou}^s}\right)^{\frac{1}{z_{cou}}} = \left(\frac{\gamma_{co}^m}{\gamma_{co}^s}\right)^{\frac{1}{z_{co}}} \left(\frac{\gamma_{cou}^s}{\gamma_{cou}^m}\right)^{\frac{1}{z_{cou}}} e^{-\frac{(p^s - p^m)\overline{V}_s}{RT\nu_c z_c}} \tag{2.14}$$

where c, z, γ, p, V, and ν are the concentration, charge number, activity coefficient, osmotic pressure, partial molar volume, and stoichiometric coefficient, respectively; superscripts s and m represent the salt and membrane, respectively; and subscripts co, cou, s, and c denote the coions, counterions, salt, and cation, respectively [25].

In previous studies, the ion activity coefficients in the membrane and salt solution were not of concern, and usually assumed to be equal in order to simplify the calculation [26]. However, the ion activity coefficient in the membrane is typically lower than that in the solution because of the strong electrostatic interaction between the fixed charge group and the ions in the membrane. The agreement between the model and experiment was unsatisfactory, especially when the salt concentration in the solution was considerably low. In addition, the ion activity coefficient in the solution was related to the concentration of the salt solution. In a recent study, Kamcev et al. used Manning's counterion condensation theory to predict the ion activity coefficients in charged membranes, which revealed the important role of the counterion condensation theory in ion transmembrane transport [27].

This book belongs to Badji Mokhtar Annaba University Central Library Copyright Elsevier 2025

Calculating the concentration of coions in the membrane is extremely complicated. In practical applications, the coion concentration in the membrane of a monovalent salt can be estimated using Eq. (2.15):

$$C_{co}^{m} = \frac{C_{salt}^{s2}}{C_{fix}} \tag{2.15}$$

where C_{salt}^{s} and C_{fix} are the salt concentration in the solution and the fixed ion concentration of the membrane, respectively. Eq. (2.15) indicates that the co-ion concentration in the membrane (C_{co}^{m}) increases with increasing salt concentration in the solution [28].

The Donnan effect is crucial for membrane separation. The direct enhancement of the Donnan effect by the EMT can improve the selectivity of the membrane and is expected to break the "trade-off" effect between the flux and selectivity. Hu et al. prepared a 3D GO−carbon nanotube (CNT) membrane (GCM) that contained numerous water transport channels. When a bias voltage was applied to the GCM, the number of capacitive counterions on the membrane increased, which produced strong electrostatic repulsion with the counterions in the solution, resulting in the Donnan effect and salt rejection enhancement (Fig. 2.4A). The rejection rates of all three salts could be improved by applying −1.0 V to the GCM, with the following order of salt rejection ability: $CaCl_2 > Na_2SO_4 > NaCl$ (Fig. 2.4B). With an increase in the applied voltage, the rejection rate of NaCl increased significantly, while the flux of the membrane decreased slightly (Fig. 2.4C) [29].

2.4 Electrical double layer on membrane surface

2.4.1 Electrical double layer structure

2.4.1.1 Formation mechanism and configuration of electrical double layer

Two reactions usually occur at the solid/solution interface. One is the exchange reaction between the charged particles and the solid. The transfer of these charged particles generally occurs when the solid is in contact with the solution. If charges flow through this interface through an external circuit, an electrochemical reaction will occur at the interface (i.e., the faradaic reaction). In contrast, for a given solid/solution interface and within a certain potential range, no charge transfer reaction occurs due to unfavorable thermodynamic or kinetic factors. However, processes such as adsorption and desorption can occur. The ions in the solution form an EDL between the solid/solution interface, where the configuration of the EDL changes with the changes in the electric potential or in the composition of the solution. A high field strength can be generated because the distance between the two charged layers in the EDL is

This book belongs to Badji Mokhtar Annaba University Central Library Copyright Elsevier 2025

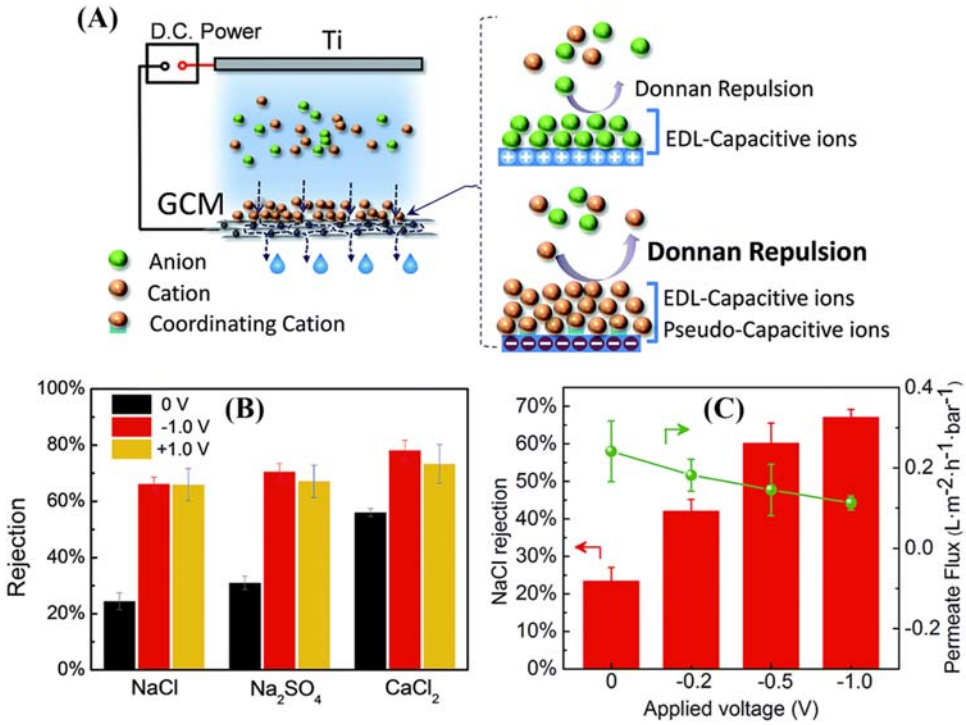

Figure 2.4 (A) Schematic diagram of the GO−carbon nanotube (CNT) membrane salt rejection mechanism under applied voltage. (B) Rejection of NaCl, Na_2SO_4, and $CaCl_2$ by the GO−CNT membrane under applied voltages of 1.0, −1.0, and 0 V. (C) NaCl rejection and permeate flux of the GO−CNT membrane as a function of the applied voltage. *Adapted with permission from C. Hu, Z. Liu, X. Lu, J. Sun, H. Liu, J. Qu, Enhancement of the Donnan effect through capacitive ion increase using an electroconductive rGO-CNT nanofiltration membrane, J. Mater. Chem. A 6 (2018) 4737−4745 [29]. Copyright 2018, Royal Society of Chemistry.*

exceedingly small, reaching 10^8 V/cm. Given the faradaic reaction is the process of gaining and losing electrons, it's thus under such a large interfacial EF that the charge transfer reaction between phases is bound to change significantly. Therefore, it becomes necessary to study the solid−solution interface structure.

There are two interactions at the electrode−solution interface: one, the electrostatic effect, and two, the short-range interaction between the solid and the various particles (such as characteristic adsorption) [30,31] (Fig. 2.5). The electrostatic effect is a long-distance interaction in which the remaining charges with opposite signs try to approach each other, tending to align closely to the solid surface to form a compact layer (i.e., the outer Stern layer). Under short-range interaction (hydrogen bonding, specific-ion effects, etc.), ions are specifically adsorbed on the electrode surface, forming the inner Stern layer. However, the charged particles are not stationary but exhibit constant thermal motion as

This book belongs to Badji Mokhtar Annaba University Central Library Copyright Elsevier 2025

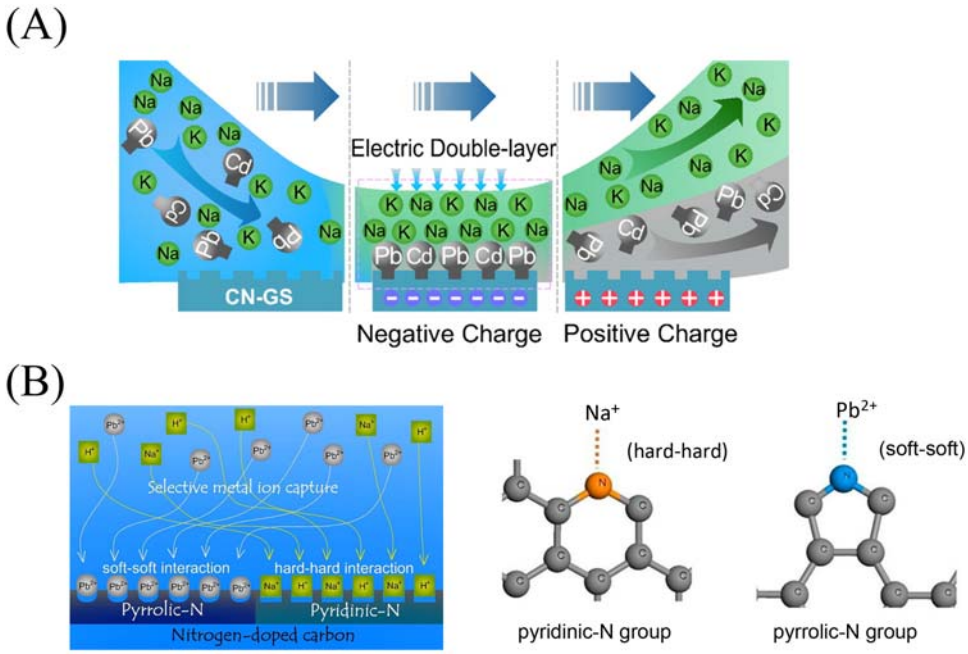

Figure 2.5 Short-range interaction between the ion and electrode: (A) Transformation of the electrical double layer (EDL) in an aqueous solution with Na^+ and Pb^{2+}. (B) Acid-based interactions in the EDL. *Adapted with permission from (A) Q. Ji, X. An, H. Liu, L. Guo, J. Qu, Electric double-layer effects induce separation of aqueous metal ions, ACS Nano 9 (2015) 10922–10930 [31]. Copyright 2015, American Chemical Society. (B) Q. Ji, C. Hu, H. Liu, J. Qu, Development of nitrogen-doped carbon for selective metal ion capture, Chem. Eng. J. 350 (2018) 608–615 [30]. Copyright 2018, Elsevier.*

these are experiencing a short range interaction with the solid surface. The thermal motion promotes the uniform distribution of the charged particles such that the remaining charge is not entirely distributed near the solid surface, thus forming a diffusion layer. In this way, under the action of short/long-range interactions and thermal ion movement, the electrode/solution interface forms an EDL.

2.4.1.2 Existing forms of ions

The dispersibility of the EDL is different depending on the solid system. In a system composed of a metal and an electrolyte, it's because the density of free electrons in the metal phase is exceptionally high that the concentration of a small amount of residual charge at the interface will not significantly damage the uniform distribution of free electrons. Therefore, all the remaining charges in the metal are closely arranged, and the potentials of the metal points are equal. In the solution phase, when the electrolyte concentration and charge density of the solid surface are high, the electrostatic effect between the solid and solution plays a main role in the distribution of the residual

This book belongs to Badji Mokhtar Annaba University Central Library Copyright Elsevier 2025

charge; therefore, the residual charge tends to be arranged closely. If the electrolyte concentration is low or the solid surface charge density is low, the thermal movement of the ions increases, and the residual charge tends to be dispersed. However, for semiconductor materials in the solid phase, owing to the low concentration of the carrier, the residual charge will also be dispersed to a certain extent.

In the Stern layer of the EDL (Fig. 2.6), in addition to the electrostatic effect, a short-range force exists between the solid and the ions. Therefore, the composition of the Stern layer in the solution also changes with the electrolyte. Water molecules are highly polar and can be adsorbed and aligned on the surface of a charged solid to form a dipole layer. The adsorption coverage of water molecules on a solid surface can exceed 70%; therefore, under normal circumstances, the layer closest to the solid surface is a dipole layer of aligned water molecules, and the second layer is a residual charge layer composed of hydrated ions. In addition to being enriched at the solid–solution interface due to static electricity, the ions in the solution may be adsorbed owing to their physical or chemical characteristics. This adsorption is related to the electrode material, the nature of the ions, and the degree of hydration. Most inorganic cations do not undergo characteristic adsorption, and only a few cations with lower hydration energy, such as Tl^+ and Cs^+ ions, can undergo characteristic adsorption. On the other hand, except for fluoride ions, almost all inorganic anions exhibit characteristic adsorption and the characteristic adsorption changes the Stern layer structure. When the solid surface is negatively charged, the residual charge on one side of the EDL solution is composed of cations. As most of the cations do not undergo the characteristic adsorption on the solid surface and have a high degree of hydration, it is difficult for the cations to escape the hydration film and enter the water

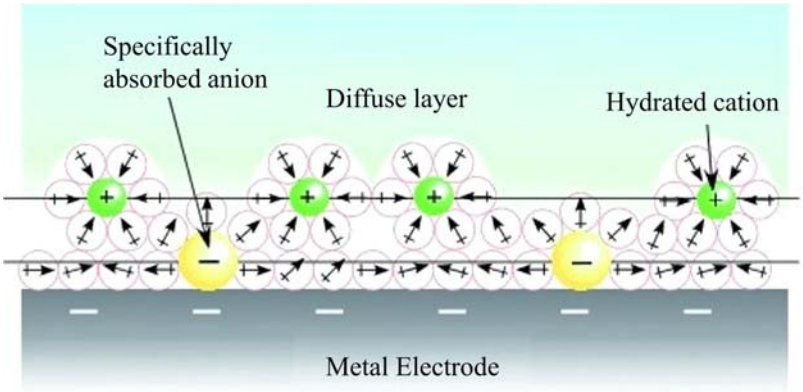

Figure 2.6 Schematic diagram of the Stern layer structure. *Adapted with permission from M. Nakamura, N. Sato, N. Hoshi, O. Sakata, Outer helmholtz plane of the electrical double layer formed at the solid electrode–liquid interface, ChemPhysChem 12 (2011) 1430–1434 [32]. Copyright 2011, Wiley.*

This book belongs to Badji Mokhtar Annaba University Central Library Copyright Elsevier 2025

dipole layer. The Stern layer is composed of a water dipole layer and a hydrated cation layer in series. However, when the solid surface is positively charged, the ions constituting the EDL solution are anions, so that when the anions and the solid surface undergo the characteristic adsorption and, when at the same time, the degree of hydration is low, therefore, it's the anions that can replace the water molecules in the dipole layer and be directly adsorbed on the solid surface.

2.4.2 Electrical double layer model

2.4.2.1 Helmholtz model

The concept of the EDL was first proposed in the 19th century by Helmholtz, who believed that the charge on the electrode surface could be offset by adsorbing a layer of oppositely charged ions (Fig. 2.7) [33]. The charge distribution in the EDL is similar to that in a parallel capacitor. When each electron is transferred from one electrode to the other, a cation is transferred to the negative electrode to compensate for the negative charge on the negative electrode (assuming the ion is monovalent). The anion transfers to the positive electrode to compensate for the positive charge on the positive electrode, thereby removing salt ions from the flow channel. At this moment, the charge efficiency of the entire system reaches 100%. The Helmholtz model (Eq. 2.16) assumes that the capacitance of the system is constant and does not change with the electric potential [34]:

$$C_H = \varepsilon_0 \varepsilon_r \frac{A}{d} \tag{2.16}$$

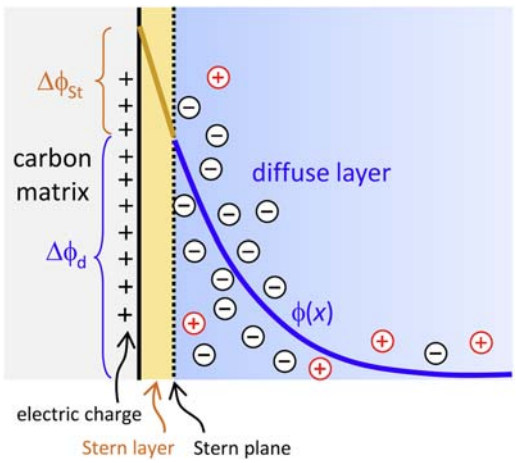

Figure 2.7 Gouy–Chapman–Stern model. *Adapted with permission from S. Porada, R. Zhao, A. van der Wal, V. Presser, P.M. Biesheuvel, Review on the science and technology of water desalination by capacitive deionization, Prog. Mater. Sci. 58 (2013) 1388–1442 [40]. Copyright 2013, Elsevier.*

This book belongs to Badji Mokhtar Annaba University Central Library Copyright Elsevier 2025

where C_H is the Helmholtz capacitance (F), ε_0 *is* the dielectric constant in a vacuum (8.85×10^{-12} F/m), ε_r is the relative permittivity, A is the effective area of the electrode (m^2), and d is the thickness of the EDL (m).

However, the Helmholtz model cannot describe the structure of the EDL in the electrode aperture. Here, it is believed that ions will only accumulate in the plane next to the electrode, and the model does not account for the diffusion and distribution of ions between the electrode and the electrolyte. This model only considers the electrostatic interaction between the electrode and the ion, and ignores the thermal movement of the ion itself, rendering it unsuitable for describing solutions with low salt concentrations.

2.4.2.2 Gouy–Chapman model

Gouy and Chapman considered the combined effects of electrostatic interaction and thermal ion movement, introducing the electron density gradient and thermal effect factors into the Helmholtz model to develop a diffusion layer model (i.e., the Gouy–Chapman model) [35,36]. In this model, the ions are not adsorbed on the electrode surface as they are in the Helmholtz model, but are distributed in the solution owing to their thermal movement. In the equilibrium state, the distribution of the ion concentration can be calculated using the Boltzmann first-order approximate distribution which is based on the Poisson–Boltzmann equation. In the Gouy–Chapman model, the surface charge is compensated in two ways: the adsorption of the counterions in the diffusion layer, and the desorption of the coions. In this case, for each electron transferred, it is estimated that only 0.6–0.8 ions are stored. Moreover, only 0.6–0.8 salt molecules will be removed. Therefore, the charge efficiency drops to 60%–80%. The capacitance is affected by the potential difference and the temperature, which is factored in by the Boltzmann constant. In addition, the electron density gradient is used to eliminate the discreteness of the parallel-plate analogy. The electron density changes with the charge interface distance according to the Thomas–Fermi shielding distance [34]. Therefore, in the Gouy–Chapman model, the capacitance is calculated as

$$C_{GC} = \left(cos\ h \frac{z e_0 \Psi_M}{2kT} \right) \sqrt{\frac{2\varepsilon_r \varepsilon_0 z^2 e_0^2 c_0}{kT}} \tag{2.17}$$

where C_{GC} is the Gouy–Chapman capacitance (F), z is the magnitude of the charges, e_0 is the charge on the electron, Ψ_M is the potential difference (V), k is the Boltzmann constant (1.38×10^{-23} J/K), T is the temperature (K), and c_0 is the initial concentration of the salt solution (mg/L).

However, in practical application, the Gouy–Chapman model is only suitable for highly diluted systems, and the calculated capacitance value is much higher than the

This book belongs to Badji Mokhtar Annaba University Central Library Copyright Elsevier 2025

actual capacitance under other conditions. This is mainly due to the assumption of point charge in the Gouy–Chapman model, which ignores the interaction between the ions; the interaction between the ions is evident in a high-concentration solution, causing the distribution of the electrode surface potential to deviate from the actual situation.

2.4.2.3 Gouy–Chapman–Stern model

Based on this shortcoming, Stern proposed the Gouy–Chapman–Stern model by adding an additional Stern layer between the diffusion layer and the electrode [37]. In this model, the solid–liquid interface is mainly composed of two layers: the Stern layer is close to the electrode and the diffusion layer is close to the solution (Fig. 2.7). The Stern layer, located between the starting point of the electrode and the diffusion layer, is a thin dielectric layer. The starting plane of the diffusion layer is the plane closest to the ion center on the surface of the charged electrode; thus, the thickness of the Stern layer corresponds to the hydration radius of the ion. The voltage drop in the Stern layer is extremely high. Given that this layer contains neither electric charges nor adsorbed ions, it thus only represents the shortest distance for the ions to reach the electrode, and acts as a dielectric layer that separates opposite charges and as a capacitor for charging and discharging. In the Gouy–Chapman–Stern model, the total capacitance can be regarded as the series connection of the Helmholtz capacitance and the Gouy–Chapman capacitance. On the side closest to the electrode (higher ion concentration), the Helmholtz capacitor is the main body, while the Gouy–Chapman capacitor plays a leading role in the electrolyte (lower ion concentration). Therefore, the total capacitance can be calculated using Eq. (2.18):

$$\frac{1}{C_{GCS}} = \frac{1}{C_H} + \frac{1}{C_{GC}} \tag{2.18}$$

where C_{GCS} represents the Gouy–Chapman–Stern capacitance (F).

The Gouy–Chapman–Stern model assumes that there is enough space on the electrode surface to form a diffusion layer, which can be stretched freely without overlapping the EDL. Although the thickness of the diffusion layer cannot be accurately measured, it is empirically observed that the thickness of the diffusion layer is approximately 2–3 times the Debye length. For example, when the Debye length of a 10 mM NaCl solution is approximately 3.1 nm at 20 degrees, a diffusion layer that is approximately 6.2–9.3 nm thick is formed. However, the pore diameter of the micropores is smaller than the thickness of the diffusion layer, which leads to an overlap of the EDL [38]. Under practical conditions, the Gouy–Chapman–Stern model has a large deviation when describing the microporous electrode. At high voltage, the number of the co-ions in the EDL predicted by this theory exceeds that in actuality [39].

This book belongs to Badji Mokhtar Annaba University Central Library Copyright Elsevier 2025

The Gouy–Chapman–Stern model is not applicable to micropores with apertures smaller than or equal to the Debye length.

2.4.2.4 Modified Donnan model

Accordingly, a modified Donnan model was proposed to describe the EDL structure in the micropores. The modified Donnan model was derived from the Donnan model after two modifications [40]. The first modification was to add a Stern layer between the ions in the micropores and to apply an electronic charge on the carbon electrode to account for the fact that the electrons and ions are not in contact. This is mainly due to the change in the ionic size (upon hydration or dehydration) and the inaccuracy of the electronic charge at the edges of the carbon material. The second correction addresses the fact that the ions are transferred from the electrolyte to the interior of the electrode. In addition to the electrostatic force, there is a chemical attraction to the ions to be considered, which is expressed as μ_{att} in the model. The modified Donnan model proved able at accurately describing the adsorption of salt ions and the storage of charge when the EDL is severely overlapped [41–43]. In the modified Donnan model, the concentration of ion j in the electrode micropore, $C_{j,mic}$ (mg/L), can be calculated using Eq. (2.19):

$$C_{j,mic} = C_{salt,mac} \times \exp\left(-Z_j \times \Delta\varnothing_d + \mu_{att}\right) \tag{2.19}$$

where $C_{j,mic}$ is the concentration of ion j in the micropore of the electrode (mg/L); $C_{salt,mac}$ is the salt ion concentration in the macropores of the electrode (assuming only univalent ions exist and the concentrations of anions and cations are equal, mg/L); Z_j is the cationic or anionic charge of $+1$ or -1, respectively; and $\Delta\varnothing_d$ is the Donnan potential difference between the micropores and macropores of the electrodes (V).

The total ion concentration, $C_{ions,mic}$ (mg/L), in the micropores can be calculated by Eq. (2.20):

$$C_{ions,mic} = C_{anion,mic} + C_{cation,mic} = 2C_{salt,mac} \times \exp\left(\mu_{att}\right) \times \cosh\left(\Delta\varnothing_d\right) \tag{2.20}$$

where $C_{cation,mic}$ and $C_{anion,mic}$ are the concentrations of the cations and anions, respectively, in the micropores of the electrode (mg/L).

The local ion charge density, σ_{mic}, in the micropores is calculated by Eq. (2.21):

$$\sigma_{mic} = C_{cation,mic} - C_{anion,mic} = -2C_{salt,mac} \times \exp\left(\mu_{att}\right) \times \sinh\left(\Delta\varnothing_d\right) \tag{2.21}$$

Therefore, charge efficiency Λ of the EDL can be calculated using Eq. (2.22):

$$\Lambda = \frac{C_{ions,mic} - C^0_{ions,mic}}{\sigma_{mic}} = tanh\frac{\Delta\varnothing_d}{2} \tag{2.22}$$

where $C^0{}_{ions,mic}$ is the total ion concentration in the micropores when the voltage is 0 mg/L.

This book belongs to Badji Mokhtar Annaba University Central Library Copyright Elsevier 2025

2.4.3 Regulation mechanism of electrical double layer on conductive membrane surface

The filter membrane mainly achieves pollutant interception through the sieving and electrostatic repulsion effects. The electrostatic repulsion is mainly determined by the charge density on the membrane surface. During filtration, the ions gather on the surface of the membrane, thus forming an EDL at the interface between the membrane and solution. If electrochemistry is combined with membrane separation, the electrostatic repulsion on the membrane surface can be enhanced by increasing the surface charge density of the membrane to enhance ion removal. Recently, various EMs have been developed that exploit the electrokinetic effect to regulate the EDL structure and enhance the separation effect of the membrane. Increasing the voltage can cause the surface of the membrane to absorb more ions and increase the thickness of the EDL [29]. Ions are subjected to stronger electrostatic repulsion during transmembrane transport, which enhances ion removal. At the same time, the EM is placed in the EF but is not connected to the power supply. When the EF direction is opposite to the flow direction, the induced charge on the membrane surface will increase, the EDL on the membrane surface will expand, and the salt removal efficiency will increase. In contrast, when the EF direction is identical to the current direction, the interfacial EDL is compressed, and the salt removal efficiency is reduced [21].

EDL formation is the result of both short- and long-range forces. Therefore, the configuration of the EDL can be regulated by strengthening the short-range forces to achieve selective removal of ions. In a previous study, based on the hard and soft (Lewis) acid–base theory, graphene film electrodes doped with pyrrole nitrogen and pyridine nitrogen were designed and used as working membrane electrodes. Raw graphene film electrodes were used as the reference and counter electrodes. In a through-membrane electrode reactor, the selective separation and recovery of heavy metals and alkali metal ions were successfully realized by regulating the ion interception/release process by the electrode potential [30,31].

Therefore, the EDL structure of the membrane–water interface can be regulated by the electrokinetic effect to enhance ion removal and selective recovery.

2.5 Polarization of organic molecules

2.5.1 Polarity and dipole moment of molecules

A molecule consists of a positively charged nucleus and negatively charged electrons, which as a whole are electrically neutral. The distributions of the positive and negative charges differ depending on the molecule. A molecule whose positive and negative

This book belongs to Badji Mokhtar Annaba University Central Library Copyright Elsevier 2025

charge centers do not overlap, forming a pair of dipoles between the charges, thus becomes a polar molecule; alternatively, a molecule with a coincident positive and negative charge center is nonpolar. The dipoles that exist in polar molecules are called inherent dipoles or permanent dipoles.

The polarity of a polar molecule can be described by the dipole moment (μ), as proposed by Debye in 1912 [44]. Dipole moment μ (measured in C · m) is defined as the product of charge δ (C) on the charge center (positive charge δ^+ or negative charge δ^-) and distance d (m) between the positively charged center and the negatively charge center in a molecule (Fig. 2.8):

$$\mu = \delta \times d \tag{2.23}$$

Dipole moment μ is a vector quantity and moves from the positively charged center to the negatively charged center.

2.5.2 Deformability and polarization of molecule

Under the interaction of an external EF, the internal charge distribution of a molecule changes in the same way as an ion, which is called the molecular deformability [45,46]. For a nonpolar molecule, the external EF will force the positively charged nucleus to shift along the negative direction of the EF, while the negatively charged extranuclear electron clouds move in the opposite direction, resulting in a pair of dipole moments in the nonpolar molecule. This process is referred to as molecular polarization [47,48]. The external-EF-induced dipole moment is defined as the induced dipole moment ($\mu_{induced}$), which is proportional to the EF strength (E):

$$\mu_{induced} = \alpha \times E \tag{2.24}$$

where α is a proportionality constant called the polarizability. If the external EF disappears, the induced dipole moment will be zero ($\mu_{induced} = 0$), and the induced-polarized molecule reverts to a nonpolar molecule. In fact, this phenomenon is not only observed in nonpolar molecules but also in polar molecules, which will also deform to produce an induced dipole moment under an external EF.

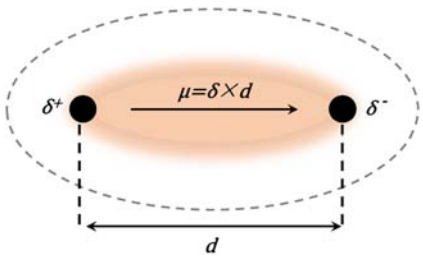

Figure 2.8 Schematic diagram of dipole moments in a polar molecule.

This book belongs to Badji Mokhtar Annaba University Central Library Copyright Elsevier 2025

Polarizability α of a molecule reflects the mobility or variability of the outer-layer electron clouds; therefore, it determines the deformability of a molecule. The experimentally determined polarizability (α) values of some molecules are listed in Table 2.1. For molecules that share the same main group elements (e.g., from HCl to HI), the finding is that α increases with an increase in the relative molecular mass and electron cloud dispersion.

Molecular polarization comprises two types: orientation and displacement polarization. Polar molecules typically move around randomly in space, and their dipoles arrange irregularly. The external EF provides an electrostatic torque to these randomly oriented dipoles, forcing them toward an oriented arrangement; this process is termed orientation polarization (Fig. 2.9A) [45,47–50]. Low-temperature conditions are favorable for the occurrence of orientation polarization. For nonpolar molecules, the attainment of the EF-induced dipole moment is called displacement polarization (Fig. 2.9B) [49,50]. In general, when molecules produce displacement polarization, they simultaneously undergo orientation polarization. It's also usual that the effect of orientation polarization is much stronger than that of displacement polarization; therefore, orientation polarization is usually the main polarization mechanism for polar molecules.

Table 2.1 Polarizability (α) values of some molecules [46].

Molecule	$\alpha/10^{-30}$ m^3	Molecule	$\alpha/10^{-30}$ m^3
HCl	2.56	H_2	0.81
HBr	3.49	O_2	1.55
HI	5.20	N_2	1.72
H_2O	1.59	Cl_2	4.50
H_2S	3.64	Br_2	6.43

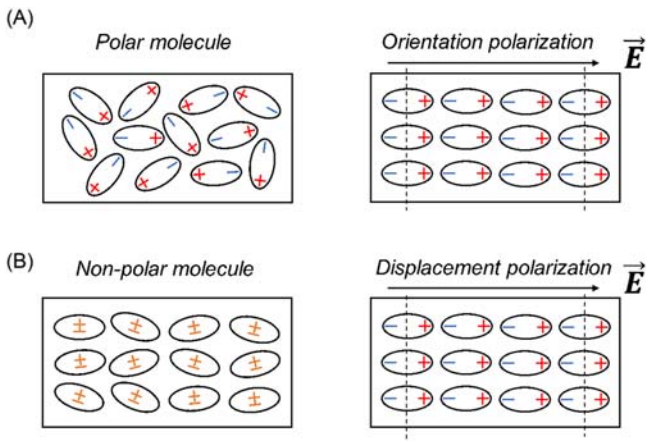

Figure 2.9 External-electric field-induced molecule polarization. (A) Orientation polarization for polar molecule. (B) Displacement polarization for nonpolar molecule.

This book belongs to Badji Mokhtar Annaba University Central Library Copyright Elsevier 2025

2.5.3 Molecular polarization in electrochemical membrane separation

EF-induced polarization phenomena occur widely in electrochemical water treatment systems, such as electrochemical membrane separation and electro-flocculation. During EF application, the interactions between the EF and the dipole moments of pollutants will cause an increase or decrease in molecular polarity [51–53]. EF-induced polarization leads to directional rearrangement of the dipole moment, resulting in structural/conformational changes of some organic pollutants, such as humic acid and protein [54]. Contaminant molecules/particles bounded by electrostatic forces (such as hydrated heavy-metal ions) are also susceptible to EFs and tend to transform into various forms with EF interaction [55]. For a solvent, which is usually an aqueous solution composed of a large number of polar water molecules with different spatial orientations, the EF will rearrange and polarize the water molecules, changing the hydrogen bond structure, and affecting the phase variation process of aqueous solutions [56–59]. This has significant implications for the solute transport behavior [60]. In conclusion, EF-induced polarization has a significant impact on the properties of pollutants, and it is very important for electrochemical water treatment systems to harness the polarization mechanism of pollutant molecules and particles.

Membrane separation technology is intrinsically hampered by membrane fouling, which is related to the deposition of dissolved organic substances (e.g., humic acid, polysaccharides, and proteins) on the membrane's surface [61,62]. Membrane fouling deteriorates membrane permeability and effluent quality, increasing the energy consumption and therefore the cost of membrane separation systems. Electrochemical membrane separation involves the application of the EF during the membrane separation process, which has been reported as an effective technique to alleviate membrane fouling and improve the performance of membrane systems [63–67]. In a typical electrochemical membrane separation system, membrane modules are placed between the electrodes of different materials, such as aluminum, titanium, iron, and ruthenium. The EF is applied perpendicularly to the surface of the membrane; thus, a synergistic effect of electrocoagulation (EC), electrooxidation, and other physicochemical processes (e.g., EF-induced polarization and electrostatic repulsion) is expected to occur to enhance the performance in an electrically driven membrane separation system.

It has been reported that the dipole moment of a pollutant determines the polarity of the molecule, and thus affects the occurrence of membrane fouling. Therefore, EF-induced polarization is considered to be closely related to membrane fouling in electrochemical membrane separation systems. Sun et al. [64] developed a novel integrated electrocoagulation membrane reactor (ECMR) by placing ultrafiltration membrane modules in the EF region of the electrochemical system (Fig. 2.10A). The synergistic effect of flocculation and EF occurs to not only reduce membrane fouling but also improve the effluent quality. In the ECMR system, the structure of the

This book belongs to Badji Mokhtar Annaba University Central Library Copyright Elsevier 2025

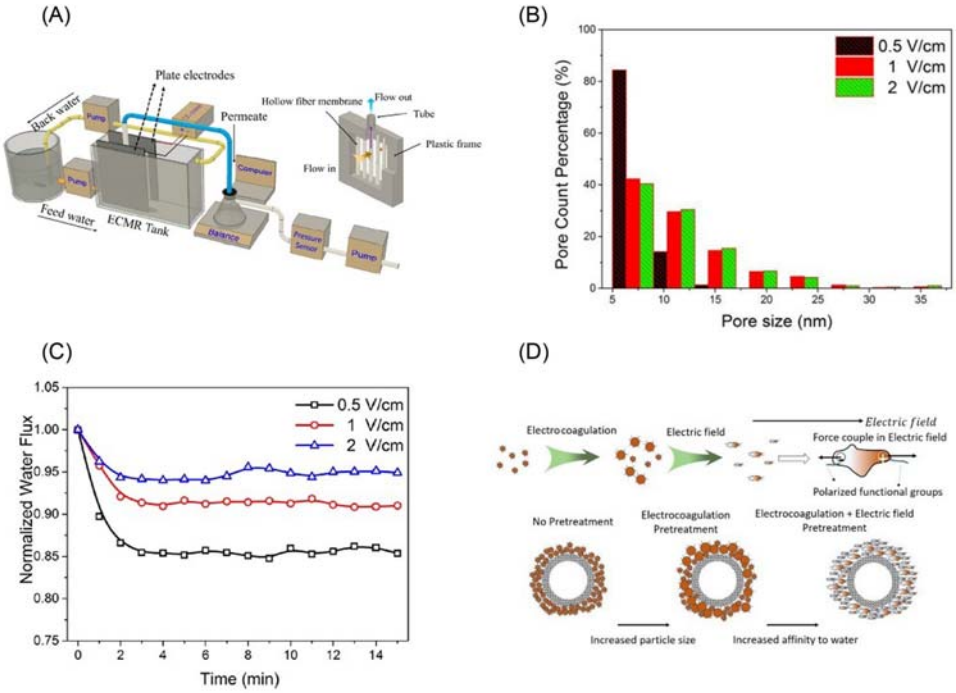

Figure 2.10 Electric field (EF) polarization in ECMR. (A) Integrated electrocoagulation membrane reactor (ECMR). (B) Pore size distributions of a cake layer at various EF strengths. (C) Normalized water flux decline curves at different initial EF strengths. (D) Schematic description of the proposed mechanisms for membrane fouling mitigation in ECMR. *Adapted with permission from J. Sun, C. Hu, T. Tong, K. Zhao, J. Qu, H. Liu, et al., Performance and mechanisms of ultrafiltration membrane fouling mitigation by coupling coagulation and applied electric field in a novel electrocoagulation membrane reactor, Environ. Sci. Technol. 51 (2017) 8544–8551 [64]. Copyright 2017, American Chemical Society.*

formed cake layers is dynamically regulated by the EF strength. As the EF increases, the orientation polarization is reinforced, forcing the negatively charged functional groups to orient to the anode and the positively charged functional groups to orient to the cathode, causing more functional groups to tend to be parallel to the direction of the EF, which leads to more charged functional groups in the cake layers that are aligned along the EF. In addition, the surface charge distribution of the cake layers can also be regulated by displacement polarization. The induced dipole moment of the foulant molecules cause a concentration of charges at the end of the functional groups, resulting in a more highly charged cake layer. Consequently, the interaction inside the cake layers along the direction of the EF is stronger than that in the direction perpendicular to the EF. This orthotropic interaction due to the orthotropy in the charge distribution result in an increased pore size of the cake layers (Fig. 2.10B). Based on this mechanism, the charged pollutants inside the cake layers are more prone to stretch

This book belongs to Badji Mokhtar Annaba University Central Library Copyright Elsevier 2025

along the EF and attach to the membrane surface under higher EF strength, increasing the thickness and stability of the cake layers [68].

EF-induced polarization can also regulate the hydrophilicity of the cake layers by changing the dipole moments of the pollutant molecules. Higher EF strength favors the formation of more hydrophilic cake layers. Many functional groups of dissolved organic substances, such as hydroxyl, amine, and carboxyl groups, are prone to polarization by an EF, especially the hydroxyl and amide groups, because of their higher electric dipole moments. Polarized functional groups are typically more hydrophilic. Furthermore, the polarized pollutants inside the cake layers lead to more charge accumulation at the ends of the molecules parallel to the EF direction, resulting in the attachment of more pollutants to the membrane surface under a higher EF because of the stronger electrostatic interaction. Therefore, this cake layer with higher polarity is more hydrophilic and shows a higher affinity for water molecules, consequently improving water permeability (Fig. 2.10C).

In summary, the EF-induced polarization (i.e., orientation polarization and displacement polarization) can dynamically regulate the structure and polarity of the cake layers of the membrane, which is beneficial for the formation of porous and hydrophilic cake layers in electrochemical membrane separation systems. The charged pollutants inside the cake layers are more likely to be ordered along the direction of the applied EF. The loose and hydrophilic cake layer induced by both coagulation and EF further improves water permeability. This mechanism, based on EF-induced polarization, is proposed in Fig. 2.10D.

It is also suggested that organic pollutants with higher polarity are prone to polarization under the EF. A blindly increasing EF strength is not always beneficial for reducing membrane fouling. When the EF strength is higher than the critical value, the over-polarizing organic pollutants will coagulate more favorably, forming a dense cake layer on the membrane surface, which aggravates membrane fouling [63].

2.6 Electrochemical reactions on electrode/membrane

2.6.1 Fundamentals of electrochemical reactions

In the electrochemical processes, the relationship between charge transport and chemical reactions across the electrode–solution interfaces is of primary concern. Although one electrochemical cell is experimentally composed of at least two electrodes and one electrolyte phase (i.e., two electrode–solution interfaces), it is both rational and useful to consider a single interface for the sake of clarity [69]. The chemical reaction occurring at one of the interfaces is called a half-reaction, which describes the actual chemical change

This book belongs to Badji Mokhtar Annaba University Central Library Copyright Elsevier 2025

at the electrode. According to the International Union of Pure and Applied Chemistry recommendations, a half-reaction equation is always written in the form of a reduction reaction, with a given substance on the left side of the equation and its reduced form on the right, as follows:

$$O + ne^- \rightleftarrows R \tag{2.25}$$

where O is the oxidized form of the standard system and R is the reduced form.

The overall reaction in an electrochemical cell is usually a manifestation of two half-reactions. Generally, one is interested in only one of these half-reactions, and the electrode at which it occurs is called the working electrode. To quantitatively compare different electrodes, a reference electrode with a stable interface structure is essential as a standard. One of the internationally accepted primary references is the standard hydrogen electrode (SHE), which is composed of a platinum electrode dipped in an ideal acidic solution containing 1 M (effective concentration) protons and bubbling pure hydrogen gas at 100 kPa [69,70]. The reversible hydrogen electrode is another reference electrode that is more commonly used than SHE because it does not require the effective proton concentration to be unity. However, from an experimental standpoint, it is more convenient to use other reference electrodes, such as saturated calomel electrode or silver–silver chloride (Ag/AgCl) electrode. The potentials (measured in volts, V) of these reference electrodes are relatively fixed and can be calculated using Eqs. (2.26)–(2.28) [69,70]:

$$E_{RHE} = E_{SHE} - 0.059 \times pH \tag{2.26}$$

$$E_{SCE} = E_{SHE} + 0.242 \tag{2.27}$$

$$E_{Ag/AgCl} = E_{SHE} + 0.197 \tag{2.28}$$

As the electrode potential is a direct indicator of the electron energy, the energy of the electrons within the working electrode can be easily regulated by controlling its potential with respect to the reference. The energy of the electrons increases when the electrode potential is driven to a more negative value, as schematically illustrated in Fig. 2.11. If the electron energy is higher than the vacant electronic states of the oxidized species (O) in the half-reaction, there is a possibility that the electrons will transfer from the electrode to the oxidized species, causing a reduction reaction. In this case, the electrode is called the cathode, and the current is the cathodic current. Similarly, the electron energy is lowered by applying a more positive potential to the electrode. When electrons in the reduced species (R) find a lower electronic state in the electrode, there is a possibility that the electrons will transfer from the reduced species to the electrode, inciting an oxidation reaction. The current induced by the electron flow in this direction is called the anodic current, and the electrode is the anode.

In general, a half-reaction involves three steps: (1) mass transfer of the reactant molecules from the bulk solution to the electrode surface, (2) heterogeneous electron transfer at the electrode–solution interface, and (3) mass transfer of the product

This book belongs to Badji Mokhtar Annaba University Central Library Copyright Elsevier 2025

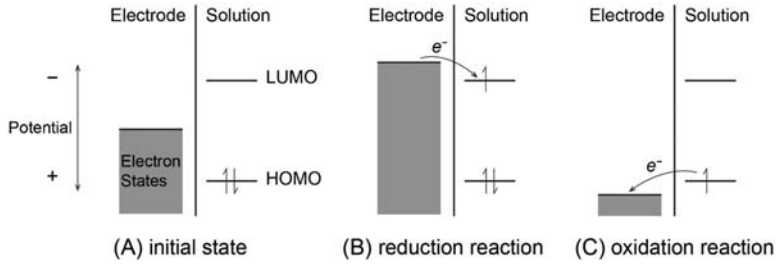

Figure 2.11 Schematic representation of the electron transfer processes in electrochemical reactions: (A) initial state. (B) reduction reaction. (C) oxidation reaction. The highest occupied molecular orbital (HOMO) and lowest unoccupied molecular orbital (LUMO) of the reactants are also shown.

molecules from the electrode surface to the bulk solution. As the half-reaction is composed of a series of pathways, it is often limited by the inherent sluggishness of a certain step, which is called the rate-determining step.

For most electrochemical reactions, mass transfer is a limiting factor. Taking the reduction reaction $O + ne^- \rightleftarrows R$ as an example, the concentration of O at the electrode surface would decrease once the cathodic current passes through. A concentration gradient is established between the bulk solution and cathode surface, which is the driving force for O diffusion. As the potential moves to a more negative value, the surface concentration of the O species drops to nearly zero, and the concentration gradient is maximized. However, if the potential is shifted more negatively, the diffusion layer of O grows thicker, and its mass transfer declines. This phenomenon gives rise to the so-called "reduction peak," which is generally observed in current–potential curves. In a similar manner, when a constant potential is applied to the cathode, there is usually a current decay with time as a consequence of surface reactant depletion.

When the relationship between the number of reacted species and transferred charges follows Faraday's law, this reaction is called a faradaic process.

$$N = \frac{Q}{nF} \tag{2.29}$$

where N is the number of reactants or products in moles, and Q is the number of transferred electrons in coulombs.

In practice, however, two or more faradaic reactions can occur simultaneously on the same electrode, together with non-faradaic processes such as adsorption and desorption. The current efficiency (CE) for a specific reaction, or faradaic efficiency, can be calculated as

$$CE = \frac{nFN_i}{Q} \times 100\% \tag{2.30}$$

where N_i is the number of reactants or products (in moles) that are of our interest.

This book belongs to Badji Mokhtar Annaba University Central Library Copyright Elsevier 2025

2.6.2 Reactive species in electrochemical process

Electrochemical technologies offer attractive approaches for the remediation of aqueous pollution owing to several promising characteristics. (1) Versatility, or the electrochemical techniques that can deal with various pollutants in different quantities; (2) environmental compatibility, or the electrochemical methods use electrons which are clean and effective reagents; and (3) amenability to automation, or the parameters involved in electrochemical reactions (voltage and current) are particularly suited for data acquisition, process automation, and control [71]. The main electrochemical techniques for the remediation of wastewater include electrochemical oxidation, electrochemical reduction, EC, electroflotation, and electrodialysis [72]. Other electrochemical-related techniques, such as electro-Fenton and photoelectrocatalysis, have also received considerable attention.

Electrochemical oxidation, also known as anodic oxidation, is a promising alternative for treating refractory organic wastewater and counted among the most commonly used electrochemical processes. The oxidation of pollutants can occur directly at the electrode through electron transfer from molecules to the anode and indirectly through the generation of oxidative species on the anode surface. The hydroxyl radical (•OH) is a representative of and the most efficient species in electrochemical oxidation reactions. The generation of •OH can be attributed to the loss of protons and electrons from H_2O molecules (Eq. 2.31), where S[•OH] and S[ ] represent the surface sites with and without adsorbed •OH species, respectively [72]. The subsequent oxidation of organic pollutants can be triggered by surface-adsorbed or dissociated •OH (Eq. 2.32). Moreover, the oxygen evolution reaction can occur concomitantly (Eq. 2.33), which inevitably leads to the wasting of the •OH species.

$$S[\,] + H_2O \rightarrow S[\bullet OH] + H^+ + e^- \tag{2.31}$$

$$S[\bullet OH] + R \rightarrow S[\,] + RO + H^+ + e^- \tag{2.32}$$

$$S[\bullet OH] + H_2O \rightarrow S[\,] + O_2 + 3H^+ + 3e^- \tag{2.33}$$

In addition to anodic oxidation, cathodic reduction also plays an important role in the generation of active species and the removal of pollutants. Atomic hydrogen (•H) generated on the cathode via proton/water reduction Volmer reactions (Eqs. 2.34 and 2.35) is one of the strongest reductants [73]. The most well-known application of •H is probably the thermodynamically unfavorable dehalogenation reaction, where the cleavage of the C − X bond is the key step (Eq. 2.36) [72].

$$S[\,] + H^+ + e^- \rightarrow S[\bullet H] \quad \text{(acidic media)}, \tag{2.34}$$

$$S[\,] + H_2O + e^- \rightarrow S[\bullet H] + OH^- \quad \text{(neutral or basic media)}, \tag{2.35}$$

$$S[C - X] + 2S[\bullet H] \rightarrow S[C - H] + HX \tag{2.36}$$

This book belongs to Badji Mokhtar Annaba University Central Library Copyright Elsevier 2025

The cathodic generation of H_2O_2 has also received considerable attention, since on-site H_2O_2 production can entail a considerable reduction of the costs associated with H_2O_2 transportation, storage, and handling. In general, H_2O_2 can be generated via a two-electron reduction reaction of oxygen (Eq. 2.37) [72]. Alternatively, the superoxide radical ($O_2^{\bullet-}$) can be produced by a one-electron reduction of oxygen (Eq. 2.38) [74]. Additionally, the hydroperoxyl radical ($HO_2^{\bullet}$) can be produced through the oxidation of H_2O_2 at the anode surface (Eq. 2.39) [72]. The formation of singlet oxygen ($^1O_2$) may be triggered by the recombination of $O_2^{\bullet-}/HO_2^{\bullet}$ (Eq. 2.40) [74,75].

$$O_2 + 2H^+ + 2e^- \rightarrow H_2O_2 \tag{2.37}$$

$$O_2 + e^- \rightarrow O_2^{\bullet-} \tag{2.38}$$

$$H_2O_2 \rightarrow HO_2^{\bullet} + H^+ + e^- \tag{2.39}$$

$$O_2^{\bullet-}/HO_2^{\bullet} \rightarrow {}^1O_2 \tag{2.40}$$

In addition to the above-mentioned radicals, other inorganic radicals such as •Cl, ClO•, and $SO_4^{\bullet-}$ are also active species commonly involved in electrochemical processes. The oxidative or reductive abilities of these radicals can be roughly evaluated by their standard potentials, because the thermodynamic properties often serve as good indicators of the reaction kinetics [76]. The standard potentials of common radicals are presented in Table 2.2, where a more positive potential indicates a higher oxidative ability. It can be observed that hydrated electrons (e_{aq}^-) and •H show relatively high reductive ability, while •OH, •Cl, and $SO_4^{\bullet-}$ exhibit high oxidative ability.

2.6.3 Membrane electrode process

For electrochemical reactions in environment-related areas, the mass transfer of reactants is particularly important because most environmental pollutants exist at relatively

Table 2.2 Standard potentials of radicals in water [76].

Half-reaction of radicals	Standard potential (V versus SHE)
$e^- + H_2O \rightleftarrows e_{aq}^-$	-2.89 ± 0.03
$H^+ + e^- \rightleftarrows \bullet H$	-2.32 ± 0.03
$O_2 + e^- \rightleftarrows O_2^{\bullet-}$	$+0.64 \pm 0.02$
$O_3 + e^- \rightleftarrows O_3^{\bullet-}$	$+1.03 \pm 0.02$
$ClO\bullet + e^- \rightleftarrows ClO^-$	$+1.39 \pm 0.03$
$HO_2^{\bullet} + H^+ + e^- \rightleftarrows H_2O_2$	$+1.46 \pm 0.01$
$Cl_2\bullet^- + e^- \rightleftarrows 2Cl^-$	$+2.126 \pm 0.017$
$\bullet Cl + e^- \rightleftarrows Cl^-$	$+2.432 \pm 0.018$
$SO_4^{\bullet-} + e^- \rightleftarrows SO_4^{2-}$	$+2.437 \pm 0.019$
$\bullet OH + H^+ + e^- \rightleftarrows H_2O$	$+2.73 \pm 0.017$

This book belongs to Badji Mokhtar Annaba University Central Library Copyright Elsevier 2025

low levels. Compared to conventional plate electrodes with inferior mass transfer efficiency, membrane electrodes with micro/nano channels enable the compression of the diffusion layer and accelerate the mass transport owing to forced convection by flow-through filtration. Consequently, the optimal exposure and utilization of the active sites and high CE on the membrane electrode are achievable. Furthermore, the nano-confinement effect in the membrane electrode changes the EF near the electrocatalyst surface, thus contributing to the formation of temperature gradients and additional mass transport for the electrocatalytic transformation of dilute species [77].

Ji et al. utilized a three-dimensional (3D) graphene-based framework as the skeleton of a membrane electrode, which possessed a large surface area and interconnected macropores [78]. Polyaniline (PANI) nanodots were assembled on the graphene surface as an electrocatalyst, contributing to the formation of nanoconfined spaces for electrocatalytic reactions. Benefiting from the interconnected network comprising numerous slit-shaped pores, the inlet water homogeneously flowed through the microchannels of the membrane electrode (Fig. 2.12A). The pollutant molecules, Cr (VI) species, were quickly driven to the surface of the PANI nanodots by microflow.

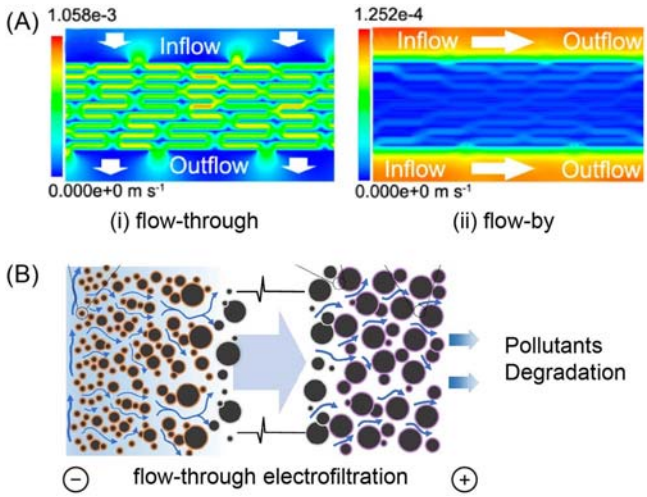

Figure 2.12 (A) Velocity magnitude contour of water in the membrane electrode obtained from computational fluid dynamics calculations: (i) flow-through mode and (ii) flow-by mode. (B) Schematic describing pollutant degradation in a membrane electrode. The arrows represent the flow direction. *Adapted with permission from (A) Q. Ji, D. Yu, G. Zhang, H. Lan, H. Liu, J. Qu, Microfluidic flow through polyaniline supported by lamellar-structured graphene for mass-transfer-enhanced electrocatalytic reduction of hexavalent chromium, Environ. Sci. Technol., 49 (2015) 13534–13541 [78]. Copyright 2015, American Chemical Society. (B) Y. Zhao, M. Sun, X. Wang, C. Wang, D. Lu, W. Ma, S.A. Kube, J. Ma, M. Elimelech, Janus electrocatalytic flow-through membrane enables highly selective singlet oxygen production, Nat. Commun., 11 (2020) 6228 [75]. Copyright 2020, Springer Nature.*

This book belongs to Badji Mokhtar Annaba University Central Library Copyright Elsevier 2025

Consequently, the mass transfer of the reactants and their subsequent reactions were significantly accelerated in the confined spaces. In this regard, the electrochemical reaction efficiency was considerably increased because of the accelerated reactant diffusion and nanoconfinement effect.

Zhao et al. fabricated a Janus electrocatalytic membrane based on a ceramic membrane substrate by depositing Pd and Pt nanoparticles on their corresponding sides [75]. The double-sided conductive surfaces endowed the membrane electrode with electrochemically reactive features. The nanochannels in the membrane electrode spatially confined the reactants and the active sites at the nanoscale, contributing to minimized diffusion distance and enhanced mass transfer, as shown in Fig. 2.12B. Therefore, high rates for the reaction of reactants with electrons could be achieved. In addition, the membrane electrode operated in a flow-through mode and allowed for sequential reduction−oxidation reactions on different sides for efficient $^1O_2$ synthesis. As a result, rapid degradation of the model organic pollutant (sulfamethoxazole) was achieved.

In the recent years, hybrid systems have been intensively developed by combining the principles of electrochemistry, EMT, and biology. Su et al. fabricated an integrated electro-membrane bioreactor (eMBR) by introducing two electrodes in the MBR reactors [79]. The synergistic effect of the EF and EC reactions not only alleviated membrane fouling but also enriched the microbial diversity. By utilizing CNT hollow-fiber membranes as the cathode, Yang et al. achieved a much lower transmembrane pressure increasing the rate in an anaerobic eMBR system [80]. In the presence of an EF, electrostatic repulsion can be established between the membrane surface and extracellular polymeric substances (EPS). Consequently, membrane pore blockage was considerably mitigated because the EPS was pushed away from the membrane surface.

In conclusion, the versatility, mild operating conditions, and ease of automation of electrochemical methods make them attractive for water treatment. The combination of such methods with membrane filtration systems incurs high mass transportation efficiency and nearly full utilization of electrons. Therefore, the design principle of membrane electrodes appears to be promising for the degradation of recalcitrant pollutants in wastewater.

2.7 Challenges and perspectives

The EMT expands the scope of size-based physical separation and can be effectively utilized to remove numerous pollutants through various electrical phenomena

This book belongs to Badji Mokhtar Annaba University Central Library Copyright Elsevier 2025

(including electrical repulsion, electrooxidation, polarization, and electromigration). The movement of charged colloids under the EF is beneficial for forming a porous cake layer and alleviating membrane fouling. The foulants can be kept away from the membrane surface due to electrical repulsion or degradation by in situ electrooxidation. In addition, the foulants under the EF are polarized and form porous, hydrophilic cake layers on the membrane surface, which is beneficial for water permeability. Moreover, ion transport can be regulated by an external EF, leading to the promotion of ion separation performance. The EDL structure on the membrane surface is crucial for understanding the interactions between charged pollutants and the membrane, which is conducive to selective membrane separation performance. The separation of ions can be promoted by the enhanced Donnan effect when a membrane is applied as an electrode.

Although the EMT has demonstrated various advantages in membrane applications, some limitations must be overcome for broadening the scope of practical applications, which will also be facilitated by research toward the in-depth understanding of the fundamental mechanisms. As mentioned in this chapter, three challenges and expectations are proposed as important focal points for future research: (1) advanced characterization technologies for fundamental study, (2) theoretical model development of the EDL and ion selectivity, and (3) design principles of membrane modules for the improvement of basic properties. Theories about nanoconfinement are also discussed in the last part, which are expected to provide new insights for the development of EMT.

First, many deficiencies persist in the in situ characterization methodology during the membrane filtration process, which contain many important parameters needed for theoretical research. The structure of NF membranes, especially the inner structure, is at the nanometer or subnanometer scale, which is beyond the resolution ability of currently available instruments. For example, the scanning electron microscopy has been employed by many researchers to measure the thickness of the polyamide (PA) layer in membranes. However, the resolution ability of these instruments is on the order of only tens of nanometers. Therefore, the thickness of the PA layer cannot be accurately measured, especially for a thin layer with a thickness of <20 nm. This ambiguity of the membrane structure hinders further exploration and analysis of the internal relationship between the membrane pore size and EM retention performance. Similarly, owing to the limitations of experimental methods, to date, extensive research has not been conducted on the polarization of a single anisotropic particle under an EF, particularly for nonuniformly charged particles, which is critical for membrane fouling mechanism analysis. In addition, it is still challenging to achieve accurate tracking of ion transport through a long subnanometer channel by computational simulation over large time-scales, which is essential for establishing an accurate model for the prediction of the ion transport behavior and membrane retention performance. Overall, in

This book belongs to Badji Mokhtar Annaba University Central Library Copyright Elsevier 2025

situ detection methods for elucidating the ion transport behavior and EM characterization are urgently needed to achieve a deeper understanding of the ion-selective transport mechanisms in membrane pores.

Selective separation is another challenge for the EMT practical applications, especially for the recovery of specific ions in wastewater. So far, the separation of ions mainly relies on the size-sieving and electrostatic effects. The formation of the EDL on the EM surface improves the electrical repulsion of foulants in solutions. In addition, the EDL on the EM surface regulates the distribution of ions around the nanopores, which influences the ion migration. However, for the separation of ions with similar sizes and charges, which is difficult but considerably in demand in the resource recycling process, the investigation of the interactions between the membranes (including the surface and inner wall of membrane pores) and ions is more crucial. However, the currently established EDL models inevitably simplify the actual situation, leading to some incorrectly predicted results. Therefore, a universal and comprehensive EDL model that explains the ion distributions in nanopores is required to address the critical principles for explaining ion/molecule transportation through nanopore/nanochannels. In particular, the dehydration of hydrated ions significantly promotes ion migration in confined nanopores. Therefore, further investigation of the EDL structure in nanopores is of considerable significance for understanding the selective separation mechanisms.

Third, oxidative species generated by electrochemical reactions can not only alleviate membrane fouling by degrading organic pollutants but also oxidize susceptible membrane materials and damage the reliability of the filtration system. The design of EMs with high stability and antioxidative ability is crucial for operational stability. Moreover, the design of the EM module requires further investigation to optimize the configuration of connections between the power supply and EMs by wires in a membrane module. Further efforts are needed to develop cost-effective EMs with excellent porosity, conductivity, reactivity, and stability for further application in practical water treatment projects.

In addition, with the advancement of the detection technology, more insights on the nature and behavior of substances have been elucidated at the microscopic scale, especially the discovery of nanoconfinement effects. Confined water at the nanoscale has distinct structures and behaves differently in nanopores and in bulk water. The physicochemical properties of confined water have been proven to vary widely depending on the features of the confinement (e.g., size, structure, and type of functional groups). Moreover, the dehydration of ions may occur under confined conditions, which will radically change the ion transport behavior. The investigation of the confinement effect may provide a foundational understanding of the EM filtration process.

In summary, the fundamentals in EMTs provide potentials to meet the challenges in membrane fouling and selective separation. In order to further develop the

This book belongs to Badji Mokhtar Annaba University Central Library Copyright Elsevier 2025

fundamental theories and mechanisms of the EMT, appropriate characterization methods are urgently needed, which will help achieve the selective separation of targeted species in a complicated practical solution. The EMT is expected to meet the challenges encountered in membrane processes with further investigation and development of fundamental theories.

Acknowledgment

The authors declare no competing financial interest.

References

[1] W. Duan, A. Ronen, S. Walker, D. Jassby, Polyaniline-coated carbon nanotube ultrafiltration membranes: enhanced anodic stability for in situ cleaning and electro-oxidation processes, ACS Appl. Mater. Interfaces 8 (2016) 22574–22584.
[2] J.J. Patil, A. Jana, B.A. Getachew, D.S. Bergsman, Z. Gariepy, B.D. Smith, et al., Conductive carbonaceous membranes: recent progress and future opportunities, J. Mater. Chem. A 9 (2021) 3270–3289.
[3] B. Kang, H.J. Kim, D.K. Kim, Membrane electrode assembly for energy harvesting from salinity gradient by reverse electrodialysis, J. Membr. Sci. 550 (2018) 286–295.
[4] D. Li, W.H. Jing, S.Q. Li, H. Shen, W.H. Xing, Electric field-controlled ion transport in TiO_2 nanochannel, ACS Appl. Mater. Interfaces 7 (2015) 11294–11300.
[5] P.Y. Chen, C.W. Hong, Nanoscale transport dynamics inside a hydrated nafion membrane with electric field effects, Fuel Cell 10 (2010) 17–25.
[6] L. Hajba, A. Guttman, Recent advances in column coatings for capillary electrophoresis of proteins, TrAC Trends Anal. Chem. 90 (2017) 38–44.
[7] T. Rabilloud, M. Chevallet, S. Luche, C. Lelong, Two-dimensional gel electrophoresis in proteomics: past, present and future, J. Proteom. 73 (2010) 2064–2077.
[8] R.V. Goering, Pulsed field gel electrophoresis: a review of application and interpretation in the molecular epidemiology of infectious disease, Infect. Genet. Evol. 10 (2010) 866–875.
[9] P.Y. Lee, J. Costumbrado, C.-Y. Hsu, Y.H. Kim, Agarose gel electrophoresis for the separation of DNA fragments, JoVE (2012) e3923.
[10] W. Lu, X. Wang, X. Wu, D. Liu, J. Li, L. Chen, et al., Multi-template imprinted polymers for simultaneous selective solid-phase extraction of six phenolic compounds in water samples followed by determination using capillary electrophoresis, J. Chromatogr. A 1483 (2017) 30–39.
[11] N. Yan, L. Zhou, Z. Zhu, X. Chen, Determination of melamine in dairy products, fish feed, and fish by capillary zone electrophoresis with diode array detection, J. Agric. Food Chem. 57 (2009) 807–811.
[12] R.L.C. Voeten, I.K. Ventouri, R. Haselberg, G.W. Somsen, Capillary electrophoresis: trends and recent advances, Anal. Chem. 90 (2018) 1464–1481.
[13] J. Prakash, A. Sharma, D. Tripathi, Thermal radiation effects on electroosmosis modulated peristaltic transport of ionic nanoliquids in biomicrofluidics channel, J. Mol. Liq. 249 (2018) 843–855.
[14] J. Prakash, K. Ramesh, D. Tripathi, R. Kumar, Numerical simulation of heat transfer in blood flow altered by electroosmosis through tapered micro-vessels, Microvasc. Res. 118 (2018) 162–172.
[15] S. Bhattacharyya, S. Bera, Combined electroosmosis-pressure driven flow and mixing in a microchannel with surface heterogeneity, Appl. Math. Model. 39 (2015) 4337–4350.
[16] K.W. Oh, 6 - Lab-on-chip (LOC) devices and microfluidics for biomedical applications, in: S. Bhansali, A. Vasudev (Eds.), MEMS for Biomedical Applications, Woodhead Publishing, 2012, pp. 150–171.
[17] J.N. Agar, Diffusion and convection at electrodes, Discuss. Faraday Soc. 1 (1947) 26–37.
[18] K.S. Spiegler, Transport processes in ionic membranes, Trans. Faraday Soc. 54 (1958) 1408–1428.

This book belongs to Badji Mokhtar Annaba University Central Library Copyright Elsevier 2025

[19] M. Planck, Ueber die erregung vol electricitat und warme in electrolyten, Annalen der Phys. 275 (1890) 161–186.
[20] W.R. Bowen, J.S. Welfoot, Modelling of membrane nanofiltration - pore size distribution effects, Chem. Eng. Sci. 57 (2002) 1393–1407.
[21] J. Sun, C. Hu, B. Wu, H. Liu, J. Qu, Improving ion rejection of graphene oxide conductive membranes by applying electric field, J. Membr. Sci. 604 (2020).
[22] T. Mouterde, A. Keerthi, A.R. Poggioli, S.A. Dar, A. Siria, A.K. Geim, et al., Molecular streaming and its voltage control in angstrom-scale channels, Nature 567 (2019) 87.
[23] C. Cheng, G. Jiang, G.P. Simon, J.Z. Liu, D. Li, Low-voltage electrostatic modulation of ion diffusion through layered graphene-based nanoporous membranes, Nat. Nanotechnol. 13 (2018) 685.
[24] F.G. Donnan, The theory of membrane equilibria, Chem. Rev. 1 (1924) 73–90.
[25] H. Strathmann, 2.12: Electromembrane processes: basic aspects and applications, in: E. Drioli, L. Giorno, E. Fontananova (Eds.), Comprehensive Membrane Science and Engineering, second ed., Elsevier, Oxford, 2017, pp. 355–392.
[26] F.G. Helfferich, Ion Exchange, Courier Corporation, 1995.
[27] J. Kamcev, D.R. Paul, B.D. Freeman, Ion activity coefficients in ion exchange polymers: applicability of Manning's counterion condensation theory, Macromolecules 48 (2015) 8011–8024.
[28] E. Drioli, L. Giorno, Comprehensive Membrane Science and Engineering, Newnes, 2010.
[29] C. Hu, Z. Liu, X. Lu, J. Sun, H. Liu, J. Qu, Enhancement of the Donnan effect through capacitive ion increase using an electroconductive rGO-CNT nanofiltration membrane, J. Mater. Chem. A 6 (2018) 4737–4745.
[30] Q. Ji, C. Hu, H. Liu, J. Qu, Development of nitrogen-doped carbon for selective metal ion capture, Chem. Eng. J. 350 (2018) 608–615.
[31] Q. Ji, X. An, H. Liu, L. Guo, J. Qu, Electric double-layer effects induce separation of aqueous metal ions, ACS Nano 9 (2015) 10922–10930.
[32] M. Nakamura, N. Sato, N. Hoshi, O. Sakata, Outer helmholtz plane of the electrical double layer formed at the solid electrode–liquid interface, ChemPhysChem 12 (2011) 1430–1434.
[33] H. Helmholtz, Ueber einige Gesetze der Vertheilung elektrischer Ströme in körperlichen Leitern mit Anwendung auf die thierisch-elektrischen Versuche, Annalen der Phys. 165 (1853) 211–233.
[34] F.A. AlMarzooqi, A.A. Al Ghaferi, I. Saadat, N. Hilal, Application of capacitive deionisation in water desalination: a review, Desalination 342 (2014) 3–15.
[35] D.L. Chapman, LI. A contribution to the theory of electrocapillarity, London, Edinburgh, Dublin Philos. Mag. J. Sci. 25 (1913) 475–481.
[36] M. Gouy, Sur la constitution de la charge électrique à la surface d'un électrolyte, J. Phys. Theor. Appl. 9 (1910) 457–468.
[37] O. Stern, Zur theorie der elektrolytischen doppelschicht, Zeitschrift für Elektrochemie und Angewandte Physikalische Chemie 30 (1924) 508–516.
[38] M.E. Suss, S. Porada, X. Sun, P.M. Biesheuvel, J. Yoon, V. Presser, Water desalination via capacitive deionization: what is it and what can we expect from it? Energy Environ. Sci. 8 (2015) 2296–2319.
[39] R. Zhao, P.M. Biesheuvel, H. Miedema, H. Bruning, A. van der Wal, Charge efficiency: a functional tool to probe the double-layer structure inside of porous electrodes and application in the modeling of capacitive deionization, J. Phys. Chem. Lett. 1 (2010) 205–210.
[40] S. Porada, R. Zhao, A. van der Wal, V. Presser, P.M. Biesheuvel, Review on the science and technology of water desalination by capacitive deionization, Prog. Mater. Sci. 58 (2013) 1388–1442.
[41] R. Zhao, P.M. Biesheuvel, A. van der Wal, Energy consumption and constant current operation in membrane capacitive deionization, Energy Environ. Sci. 5 (2012) 9520–9527.
[42] S. Porada, M. Bryjak, A. van der Wal, P.M. Biesheuvel, Effect of electrode thickness variation on operation of capacitive deionization, Electrochim. Acta 75 (2012) 148–156.
[43] P.M. Biesheuvel, Y. Fu, M.Z. Bazant, Electrochemistry and capacitive charging of porous electrodes in asymmetric multicomponent electrolytes, Russian J. Electrochem. 48 (2012) 580–592.
[44] R.B. King, Encyclopedia of Inorganic Chemistry, first ed., John Wiley & Sons, Ltd, 2006.
[45] Y. Wang, J. Lei, L. Wang, Inorganic Chemistry, second ed., Beijing Science Press, 2013.

This book belongs to Badji Mokhtar Annaba University Central Library Copyright Elsevier 2025

[46] F.A. Cotton, G. Wilkinson, P.L. Gaus, Basic Inorganic Chemistry, third ed., Wiley & Sons Ltd, 1995.
[47] S. Roth, D. Carroll, Foundations of Solid State Physics: Dimensionality and Symmetry, first ed., Wiley-VCH Verlag GmbH & Co. KGaA, 2019.
[48] V.I. Minkin, O.A. Osipov, Y.A. Zhdanov, Dipole Moments in Organic Chemistry, Plenum Press, 1970.
[49] B. Quan, X. Liang, G. Ji, Y. Cheng, W. Liu, J. Ma, et al., Dielectric polarization in electromagnetic wave absorption: review and perspective, J. Alloy. Compd. 728 (2017) 1065–1075.
[50] Z. Yin, Dielectric Physics, second ed., Science press, 2003.
[51] V. Machado de Menezes, R. Mota, I. Zanella, S.B. Fagan, Pristine and functionalized capped carbon nanotubes under electric fields, Phys. Status Solidi (b) 251 (2014) 649–654.
[52] K. Tiwari, P. Arora, N. Pandey, P. Pandey, H.C. Joshi, S. Pant, Experimental and computational approaches on dipole moment of 5-aminoisoquinoline, J. Mol. Liq. 200 (2014) 460–464.
[53] I. Bekard, D.E. Dunstan, Electric field induced changes in protein conformation, Soft Matter 10 (2014) 431–437.
[54] X. Fan, H. Zhao, X. Quan, Y. Liu, S. Chen, Nanocarbon-based membrane filtration integrated with electric field driving for effective membrane fouling mitigation, Water Res. 88 (2016) 285–292.
[55] T. Megyes, S. Balint, T. Grosz, T. Radnai, I. Bako, P. Sipos, The structure of aqueous sodium hydroxide solutions: a combined solution X-ray diffraction and simulation study, J. Chem. Phys. 128 (2008) 044501.
[56] I.M. Svishchev, P.G. Kusalik, Electrofreezing of liquid water: a microscopic perspective, J. Am. Chem. Soc. 118 (1996) 649–654.
[57] D.H. Jung, J.H. Yang, M.S. Jhon, The effect of an external electric field on the structure of liquid water using molecular dynamics simulations, Chem. Phys. 244 (1999) 331–337.
[58] Z. Qian, G. Wei, Electric-field-induced phase transition of confined water nanofilms between two graphene sheets, J. Phys. Chem. A 118 (2014) 8922–8928.
[59] E.M. Choi, Y.H. Yoon, S. Lee, H. Kang, Freezing transition of interfacial water at room temperature under electric fields, Phys. Rev. Lett. 95 (2005) 085701.
[60] P. Marracino, M. Liberti, G. d'Inzeo, F. Apollonio, Water response to intense electric fields: a molecular dynamics study, Bioelectromagnetics 36 (2015) 377–385.
[61] D. Jermann, W. Pronk, S. Meylan, M. Boller, Interplay of different NOM fouling mechanisms during ultrafiltration for drinking water production, Water Res. 41 (2007) 1713–1722.
[62] F. Saravia, C. Zwiener, F.H. Frimmel, Interactions between membrane surface, dissolved organic substances and ions in submerged membrane filtration, Desalination 192 (2006) 280–287.
[63] C. Hu, M. Li, J. Sun, R. Liu, H. Liu, J. Qu, NOM fouling resistance in response to electric field during electro-ultrafiltration: significance of molecular polarity and weight, J. Colloid Interface Sci. 539 (2019) 11–18.
[64] J. Sun, C. Hu, T. Tong, K. Zhao, J. Qu, H. Liu, et al., Performance and mechanisms of ultrafiltration membrane fouling mitigation by coupling coagulation and applied electric field in a novel electrocoagulation membrane reactor, Environ. Sci. Technol. 51 (2017) 8544–8551.
[65] J. Sun, C. Hu, K. Zhao, M. Li, J. Qu, H. Liu, Enhanced membrane fouling mitigation by modulating cake layer porosity and hydrophilicity in an electro-coagulation/oxidation membrane reactor (ECOMR), J. Membr. Sci. 550 (2018) 72–79.
[66] L. Liu, J. Liu, B. Gao, F. Yang, S. Chellam, Fouling reductions in a membrane bioreactor using an intermittent electric field and cathodic membrane modified by vapor phase polymerized pyrrole, J. Membr. Sci. 394–395 (2012) 202–208.
[67] K. Bani-Melhem, M. Elektorowicz, Development of a novel Submerged Membrane Electro-Bioreactor (SMEBR): performance for fouling reduction, Environ. Sci. Technol. 44 (2010) 3298–3304.
[68] K. Zhao, J. Sun, C. Hu, J. Qu, Membrane fouling reduction through electrochemically regulating flocs aggregation in an electro-coagulation membrane reactor, J. Env. Sci. (China) 83 (2019) 144–151.

This book belongs to Badji Mokhtar Annaba University Central Library Copyright Elsevier 2025

[69] A.J. Bard, L.R. Faulkner, Electrochemical Methods: Fundamentals and Applications, second ed., 2000.
[70] G. Jerkiewicz, Standard and reversible hydrogen electrodes: theory, design, operation, and applications, ACS Catal. 10 (2020) 8409–8417.
[71] C.A. Martínez-Huitle, S. Ferro, Electrochemical oxidation of organic pollutants for the wastewater treatment: direct and indirect processes, Chem. Soc. Rev. 35 (2006) 1324–1340.
[72] C.A. Martínez-Huitle, M.A. Rodrigo, I. Sirés, O. Scialdone, Single and coupled electrochemical processes and reactors for the abatement of organic water pollutants: a critical review, Chem. Rev. (2015).
[73] Y.P. Wijaya, K.J. Smith, C.S. Kim, E.L. Gyenge, Electrocatalytic hydrogenation and depolymerization pathways for lignin valorization: toward mild synthesis of chemicals and fuels from biomass, Green Chem. 22 (2020) 7233–7264.
[74] H. Zhou, D. Lu, S. Fang, C. Liu, Y. Chen, Y. Hu, et al., Prompting direct single electron transfer to produce non-radical 1O2/H* by electro-activating peroxydisulfate process with core-shell cathode, J. Environ. Manage. 287 (2021) 112294.
[75] Y. Zhao, M. Sun, X. Wang, C. Wang, D. Lu, W. Ma, et al., Janus electrocatalytic flow-through membrane enables highly selective singlet oxygen production, Nat. Commun. 11 (2020) 6228.
[76] D.A. Armstrong, R.E. Huie, S. Lymar, W.H. Koppenol, G. Merényi, P. Neta, et al., Standard electrode potentials involving radicals in aqueous solution: inorganic radicals, BioInorganic React. Mech. 9 (2013) 59–61.
[77] Q. Ji, G. Zhang, H. Liu, R. Liu, J. Qu, Field-enhanced nanoconvection accelerated electrocatalytic conversion of water contaminants and electricity generation, Environ. Sci. Technol. 53 (2019) 2713–2719.
[78] Q. Ji, D. Yu, G. Zhang, H. Lan, H. Liu, J. Qu, Microfluidic flow through polyaniline supported by lamellar-structured graphene for mass-transfer-enhanced electrocatalytic reduction of hexavalent chromium, Environ. Sci. Technol. 49 (2015) 13534–13541.
[79] F. Su, Y. Liang, G. Liu, C.R. Mota Filho, C. Hu, J. Qu, Enhancement of anti-fouling and contaminant removal in an electro-membrane bioreactor: significance of electrocoagulation and electric field, Sep. Purif. Technol. 248 (2020) 117077.
[80] Y. Yang, S. Qiao, R. Jin, J. Zhou, X. Quan, Novel anaerobic electrochemical membrane bioreactor with a CNTs hollow fiber membrane cathode to mitigate membrane fouling and enhance energy recovery, Environ. Sci. Technol. 53 (2019) 1014–1021.

This book belongs to Badji Mokhtar Annaba University Central Library Copyright Elsevier 2025

CHAPTER THREE

Electrochemical membrane materials and modules

Zhouyan Li[1], Xi Chen[1], Jia Yuan[1], Yiwen Qiao[1], Ruobin Dai[1], Xueye Wang[1], Xuesong Li[1], Jinxing Ma[2] and Zhiwei Wang[1]

[1]State Key Laboratory of Pollution Control and Resource Reuse, Shanghai Institute of Pollution Control and Ecological Safety, Tongji Advanced Membrane Technology Center, School of Environmental Science and Engineering, Tongji University, Shanghai, SH, P.R. China

[2]UNSW Water Research Centre, School of Civil and Environmental Engineering, University of New South Wales, Sydney, NSW, Australia

3.1 Introduction

Electrochemical membrane materials are pivotal for electrochemical membrane technology (EMT) because the properties of electrochemical membranes largely determine the permeability, selectivity, electron or ion conductivity, and other functionalities of the electrochemical membrane materials (e.g., catalytic performance, antifouling property, etc.). As introduced in Chapter 1, the electrochemical membrane can be mainly classified into either conductive membranes or ion exchange membranes (IEMs). Conductive membranes are used as barriers in the membrane separation process, as well as acting the part of electrodes in the electrochemical process to achieve the functionalities of antifouling, disinfection, and degradation of contaminants (as illustrated in Fig. 3.1) [1]. On the other hand, IEMs can partially or totally preclude the passage of ions with the same charge as the membrane (as illustrated in Fig. 3.2) [2]. In practice, these electrochemical membranes are always delicately designed or tailored by various approaches to meet specific requirements [1].

The conductive membranes are commonly applied for their use in flow-through oxidation, enhanced membrane separation, as an electrochemical membrane bioreactor (eMBR), and for membrane distillation (MD), given that conductive membrane materials are supposed to possess good electron conductivity, decent stability, and antifouling properties. The materials mainly used for the preparation of conductive membranes include conductive polymers (CPM) [3] and inorganic materials [4–6]. On the other hand, the IEMs are mainly used in electrodialysis (ED), membrane capacitive deionization (MCDI), microbial fuel cells (MFCs), and microbial desalination cells (MDCs), given that IEMs are expected to have high mechanical strength, selectivity, and ionic conductivity with a low manufacturing cost [7]. IEMs are mainly

Electrochemical Membrane Technology for Water and Wastewater Treatment.
DOI: https://doi.org/10.1016/B978-0-12-824470-8.00006-1
© 2022 Elsevier Inc.
All rights reserved.

This book belongs to Badji Mokhtar Annaba University Central Library
Copyright Elsevier 2025

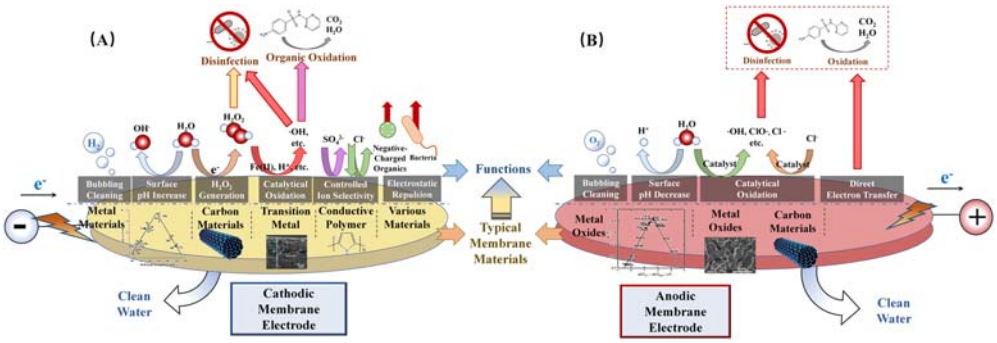

Figure 3.1 Schematic diagrams of some typical membrane materials used for electrochemical membrane technologies. (A) Cathodic membrane electrode. (B) Anodic membrane electrode.

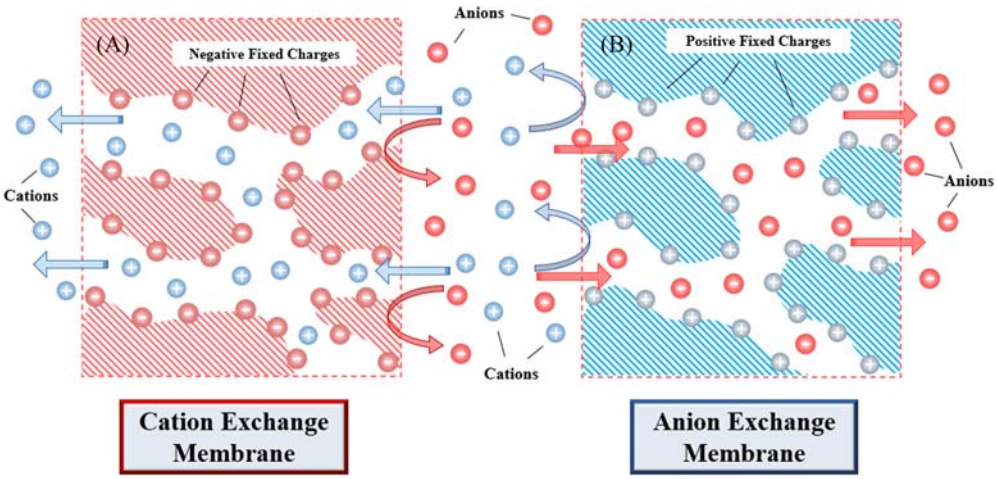

Figure 3.2 Schematic diagram of the structures and working principles of ion exchange membranes: (A) cation exchange membrane and (B) anion exchange membrane.

made of polymers produced through polymerization of tetrafluoroethylene and sulfonyl fluoride vinyl-ether, sulfonated styrene, etc. The electrochemical membrane material preparation method also matters because it determines the structure of the resultant membrane that also significantly affects the membrane performance [8]. In addition, the fabricated membranes need to be installed or assembled in membrane modules for these to function, whereas the configuration of the membrane module also plays an important role in the entire electrochemical membrane separation process.

In this chapter, materials for conductive membranes are categorized into polymer-based membrane materials, metal and metal-oxide membrane materials, and carbon-based membrane materials in terms of material composition. IEM materials are categorized into

This book belongs to Badji Mokhtar Annaba University Central Library Copyright Elsevier 2025

homogeneous IEMs, heterogeneous IEMs, pseudohomogeneous IEMs, and mixed matrix IEMs in terms of the membrane structure. An overview of the recent development of these membranes is provided. Last but not the least, the development of electrochemical membrane modules is also discussed.

3.2 Materials for conductive membranes

3.2.1 Polymer-based membrane materials

CPM are a group of polymeric materials with electrical conductivity. The conductivity is originated from the intrinsic characteristic of the polymer itself or the synergistic effect of the polymer with dopants. The conductive polymer usually has conjugated long chains in its molecular structure, in which the p-orbitals in the series of π-bonds overlap each other, enabling the electrons to be more easily delocalized and transfer freely between atoms. It was first reported by Alan J. Heeger and his coworkers in 1977 [9] that exposing polyacetylene films to iodine vapor could remarkably increase their conductivity sevenfold, or even more. Since then, the boundary between polymers and conductors has been broken, and doping has become a popular method to fabricate CPM. As shown in Fig. 3.3, CPM can undergo both *p*-type doping and *n*-type doping through the oxidation and the reduction process, which generates positive or negative polarons/bipolarons, respectively. The basic principle is explained by electrons having been either extracted from the highest occupied molecular orbital (HOMO) of the valance band (oxidation) or transferred to the lowest occupied molecular orbital (LOMO) of the conduction band (reduction) [10]. The directional migration of delocalized π electrons under the electric field forms electric current, thereby endowing the conductive polymer with electrical conductivity. Apart from conductivity, other properties subject to different external stimuli (such as light, electricity, heat, pressure) including photoelectric anisotropy and reversible redox characteristics make CPM suitable to being applied in various fields such as sensing and charge storage.

The best studied CPM include polyacetylene (PA), polypyrrole (PPy), polythiophene (PT), polyphenylene (PPP), polyaniline (PANI), polyphenylene vinylene (PPV), and poly (3,4-ethylene dioxythiophene) (PEDOT). Among these polymers, PPy, PANI, and their derivatives are relatively easier to be modified using additives and more environmentally sustainable, which makes them the most prevalent CPM used in electrochemical membrane technologies (Table 3.1).

CPM combine the advantages of both metal and polymeric materials and thus show superior conductivity and processability. With a certain electric field applied, CPMs can exhibit excellent selectivity and antifouling properties owing to their conductivity as well as some unique functionalities related to their sensitive responses to

This book belongs to Badji Mokhtar Annaba University Central Library Copyright Elsevier 2025

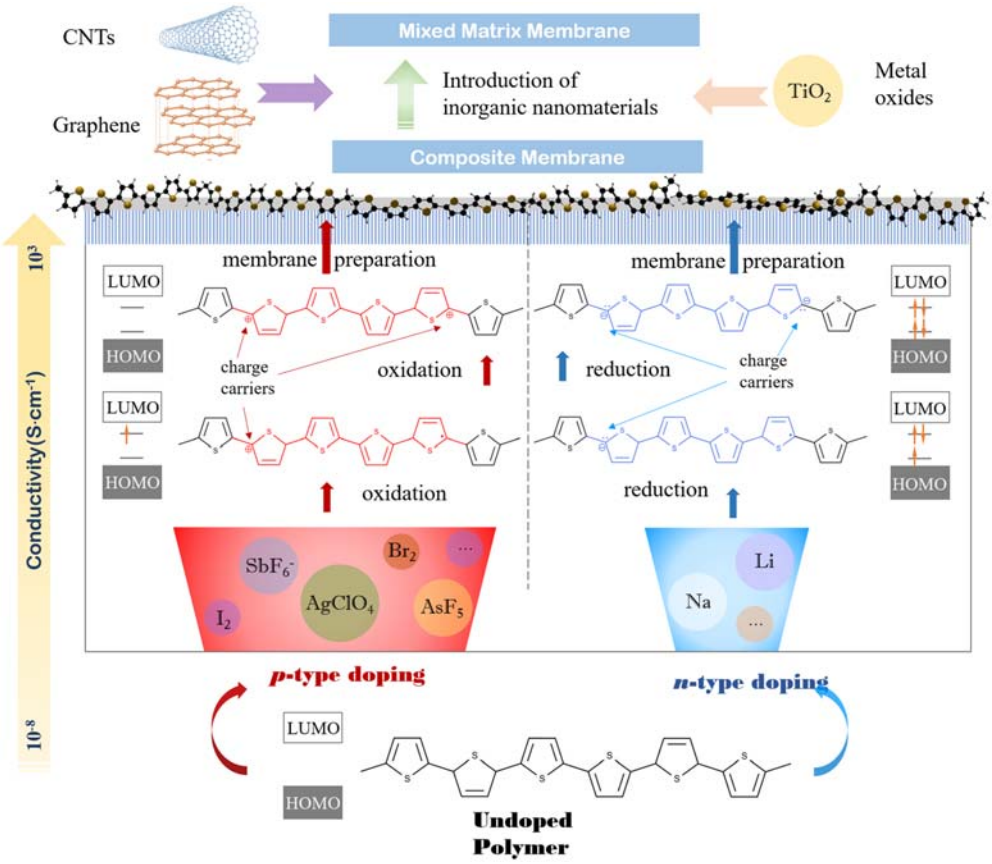

Figure 3.3 The schematic diagram of electrically conductive mechanism of conductive polymers in composite membrane and mixed matrix membrane (HOMO: highest occupied molecular orbital; LUMO: lowest unoccupied molecular orbital).

electrical stimulation. Based on membrane structure, CPMs herein are classified into either composite membranes or mixed matrix membranes. The composite membranes are typically made by blending conductive polymer with other polymers or inorganic additives, and they have only one phase (polymer phase) because of the excellent compatibility between polymers. In contrast, mixed matrix membranes are made by mixing polymers with inorganic nanomaterials (e.g., graphene) and thereby heterogeneous phases are formed in the polymer matrix.

3.2.1.1 Composite membranes

Generally, in order to enhance electrochemical performance (e.g., conductivity, ion selectivity) of CPMs, modification by introducing additives is always a sensible approach widely adopted by most researchers. For example, the inherent stability of

This book belongs to Badji Mokhtar Annaba University Central Library Copyright Elsevier 2025

Table 3.1 Typical conductive polymers.

Polymer	Structure	Conductivity (S/cm)	References
Polyacetylene	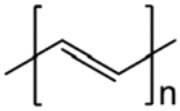	$10^{-10} \sim 10^{5}$	[9]
Polypyrrole	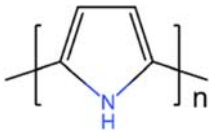	$10^{-8} \sim 7.5 \times 10^{3}$	[11]
Polythiophene	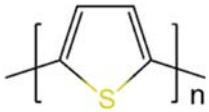	$10^{-8} \sim 10^{3}$	[12]
Polyphenylene		$10^{-12} \sim 10^{2}$	[13,14]
Polyaniline	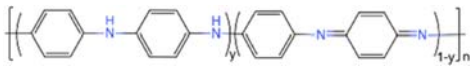	$10^{-10} \sim 10^{2}$	[15,16]
Polyphenylene vinylene	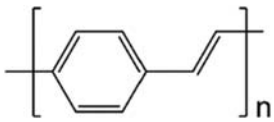	$10^{-12} \sim 10^{4}$	[17]
Poly (3,4-ethylene dioxythiophene)	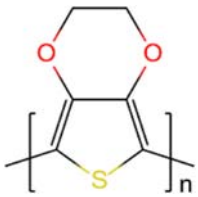	$10^{-1} \sim 5 \times 10^{3}$	[18]

composite membranes can be enhanced by sulfonated additives, of which sodium dodecyl benzene sulfonate (SDBS) is the most commonly used additive to neutralize the positive charge of CPM (e.g., PPy), increase the conductivity, and inhibit the

This book belongs to Badji Mokhtar Annaba University Central Library
Copyright Elsevier 2025

adsorption of negatively charged particles on the membrane surface [19]. Also, SDBS can increase the surface area as well as the number of active sites by forming more branched chains during the polymerization process of pyrrole, and thus can promote its catalytic performance [20]. Chlorosulfonic acid (CSA) and *para*-toluene sulfonic acid (PTS) have also been used to modify PPy to prolong its lifetime under different aging conditions [21]. Similarly, sulfosalicylic acid was added into PANI during membrane fabrication to enhance the stability of the membrane over a wide range of pH.

Of all the scenarios using composite conductive membranes known to have explicit practical benefits, the most important one is the scenario harnessing the property of membrane fouling control using conductive membranes in electrochemical membrane reactors. Liu et al. [22] first internalized the CPM as a cathode in an MBR for wastewater treatment, and the results showed that the membrane modified by pyrrole had a less fouling rate than the unmodified membrane even without an electric field, and that applying a 0.2 V/cm electric field further alleviated the membrane fouling and increased the average flux. In addition, some composite conductive membranes showed tunable wettability under oxidized/reduced states and achieved efficient oil–water separation [23] as well as of ions [24], even those ions carrying same charge and with similar hydrated radius (e.g., K^+ and Na^+) [25].

The special structural properties of CPM are mainly determined by the facilely deposited conductive polymer layer on the surface or inside the pores of supporting membranes. Thus introducing conductive polymer into insulating membranes to form a homogeneous layer becomes a convenient and cost-effective method to increase membrane conductivity, permeability, scalability, or even catalytic ability. PVDF-PPy composite membrane was fabricated via depositing conductive PPy layer on the nonconductive PVDF membrane. This composite conductive membrane was used in the treatment of raw wastewater from the brewery under an electrical field. The electrical field force and the Coulomb force were exerted on the sludge particle or an EPS colloid, thereby inhibiting the compression of the filter cake layer. As a result, the membrane fouling of the composite conductive membrane was largely alleviated, compared with that in the conventional PVDF membranes [21]. At the same time, a higher conductivity can lead to significantly improved permeability recovery rate and electro-oxidative pollutant removal during the electrochemical membrane process [26]. Moreover, PEDOT, a type of conductive polymer with outstanding photoelectric activity, can act as a photogenerated electrons segregator and leave more generated holes for pollutant oxidation when applied with the electric field [27].

3.2.1.2 Mixed matrix membranes

In mixed matrix membranes, the inorganic materials (e.g., graphene and its derivatives, carbon nanotubes, TiO_2) introduced into conductive membranes to be fabricated can

This book belongs to Badji Mokhtar Annaba University Central Library Copyright Elsevier 2025

further improve the conductivity, hydrophilicity, and catalytic performance of conductive membranes, achieving better treating performance. More interestingly, the conjugated structure of the CPM, in turn, assists these nanomaterials in showing enhanced performance [28–30]. Thereby, various mixed matrix membranes which combine conductive polymer and inorganic nanomaterials have attracted extensive research interest in the recent years.

Graphene (Gr) and its derivatives, such as graphene oxide (GO) and reduced graphene oxide (rGO), have been widely used to fabricate mixed matrix membranes because of their outstanding electrical and mechanical properties. The introduction of these carbon materials into CPM during membrane fabrication can significantly increase the conductivity, hydrophilicity, and porosity of the conductive membrane, which are highly favorable for permeability enhancement and fouling control [31,32]. In addition, the combination of membrane separation and catalytic oxidation can be achieved in one integrated system through the incorporating of carbon nanomaterials into conductive polymeric membrane [33]. The porous structure of the membrane can ensure a high conversion rate of the chemical catalysis reaction and long catalyst life, while the reactive oxygen species generated during catalytic reaction helps achieve an ultra-fast pollutant removal and thereby an enhanced antifouling efficiency. In some cases, the sharp-edged graphene nanosheets have been capable of inducing a stress and physical damage to the cell membranes, endowing the membrane with exceptional antibacterial performance capability [34].

Carbon nanotube (CNT) is another major material ideal for the preparation of mixed matrix conductive membrane due to its high strength and flexibility, with excellent electrical conductivity [28]. However, its heightened tendency to agglomerate due to the strong van der Waals force during dispersion as well as poor membrane mechanical strength hinders its wider application. Some studies have revealed that membranes based on CNT-conjugated polymers show improved stability compared to CNT-modified membranes without conjugated polymers because the compatibility of nanoparticle-polymer hybrids with membrane matrix is usually better than that of nanoparticles alone [29]. It can ensure a uniformly dispersed CNT in casting solution and an improved stability of the CNT-modified membranes while maintaining a good conductivity. Following this methodology, PPy-CNT and PANI-CNT membranes were fabricated via chemical polymerization [30] or electropolymerization process [29], which showed excellent antifouling properties and an effective removal of water pollutants. In addition, the mechanical strength of polyacrylonitrile (PAN) and polyurethane (TPU), the disinfection effect of CNTs, and the conductivity of PANI can be reasonably introduced into a novel composite membrane by the coelectrospinning process for effectively inactivating bacteria under an extremely low voltage (< 3.0 V) [35].

Other than carbon materials, TiO_2 is also used to fabricate the mixed matrix conductive membrane, mainly owing to its outstanding photocatalytic activity, high

This book belongs to Badji Mokhtar Annaba University Central Library Copyright Elsevier 2025

hydrophilicity, self-cleaning properties, and excellent chemical stability [36,37]. For instance, both water permeability and organic pollutants rejection can be significantly enhanced by incorporating TiO_2 into a selective layer of PPy. The possible mechanism was that the in situ synthesized TiO_2 prevented the excessive entanglement of PPy chains while PPy helped form a more integrated layer due to the special electronic effect between TiO_2 and PPy [38].

The conductive-polymer based membranes show a great potential in the application of wastewater treatment. Nevertheless, the large-scale application of conductive polymer membranes still faces several challenges. First, the nonrotating conjugated bonds determine the rigidity of polymer chains, resulting in a noticeable trade-off between membrane flexibility and conductivity. Second, the poor solubility of CPM in common solvents as well as their low thermal stability, especially PPy, PANI and PT, is also the main constraint that hinders their widespread application. Third, for mixed matrix membranes, the introduction of inorganic nanomaterials may create defects in the polymer matrix though it enhances conductivity. Last, the prohibitively high cost of some CPM or inorganic materials is also a big concern for their practical application.

3.2.1.3 Summary of preparation methods

In situ polymerization is the most commonly used preparation protocol for composite conductive polymeric membranes, which is categorized into vapor phase polymerization (VPM) and liquid phase polymerization (LPM) (shown in Fig. 3.4A and B). Both methods share the similar preparation procedure. Typically, the solution containing initiator ($FeCl_3$, $(NH_4)_2S_2O_8$ etc.) is firstly cast on the support by means of soaking [22], spraying [39], or painting [27]. Polymerization is then started by depositing monomers (monomer vapor in VPM or monomer solution in LPM) on the surface of the membrane in the presence of the initiator.

When other dopants and additives are needed in the formulation, the simplest way is to blend these materials with polymer to form a homogeneous casting solution (sonication might be needed) prior to the membrane fabrication through phase inversion (shown in Fig. 3.4D) [26,31,32,37,40,41] or electrospinning [35,42] (Fig. 3.4C).

Alternatively, the solution with nanomaterials can be first deposited on the pristine membrane by external force, followed by in situ polymerization of the conductive polymer to form a thin conductive layer on the surface [29,30]. This protocol can minimize the agglomeration of nanomaterials. It was also reported that the nanomaterials were firstly dispersed in the polymer dope before preparing electrospun nanofiber membranes. Afterwards, a conductive polymer coating was carried out via in situ polymerization on the surface of the nanofiber [43,44].

Obviously, the preparation protocol of polymer-based conductive membranes (including composite membranes and mixed matrix membranes) is highly dependent

This book belongs to Badji Mokhtar Annaba University Central Library Copyright Elsevier 2025

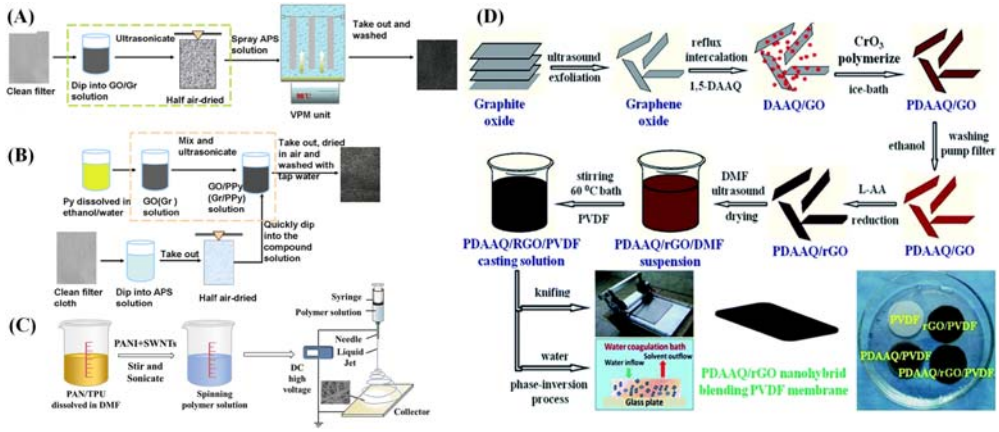

Figure 3.4 In situ polymerization for composite conductive polymeric membranes (A) vapor phase polymerization method process for GO(Gr)/PPy membrane preparation [3], (B) liquid phase polymerization method process for GO(Gr)/PPy membrane preparation [3], (C) a WCNTs/PANI modified membrane preparation process based on electrospinning [35] and (D) a PDAAQ/rGO membrane preparation process which combined PDAAQ modification of rGO and phase-inversion process [32]. *All reproduced with permission from Elsevier and The Royal Society of Chemistry, the UK.*

on the characteristics of conductive polymer as well as the membrane type. Moreover, the properties of nanomaterials also have a significant impact on the selection of the preparation protocol.

3.2.2 Metal and metal-oxide membrane materials

As a family of inorganic membranes which appeared early, metallic or metal-oxide membranes showed the advantages of high mechanical strength (especially resistance to pressure), good electrical/thermal conductivity, high tolerance to harsh cleaning condition, and ease of processing. Above properties enable the widespread application of metal and metal oxide in electrochemistry. With more available selections of materials and with the development of preparation methods, the related research on membrane electrodes based on metal and metal oxide will be further promoted on a bigger scale. This section will summarize the applications of these inorganic materials and provide some examples of recent developments in relevant fields.

3.2.2.1 Metallic membrane

Compared with organic or ceramic materials, metal exhibits excellent electrical conductivity, which can be favorable to its use in EMT. So far, the major materials of metal membrane include nickel, iron, and titanium while their inherent catalytic capability also makes them good candidates for electrocatalytic oxidation. Additionally, the

This book belongs to Badji Mokhtar Annaba University Central Library Copyright Elsevier 2025

high compliance with welding process of metal materials allows the preparation of the metallic membrane with a complicated structure.

Due to its low cost as well as heightened durability, stainless steel is the most widely used metal material for EMT, which has been applied in various fields like cathodic flow-through, catalytic oxidation toward organic degradation, and MD. For instance, micropollutants in water were removed through cathodic electrochemical membranes made with stainless steel mesh. Its effectiveness in the degradation of sulphanilic acid (SA) was further verified by Zheng, et al. [5]. Increasing the charging voltage could enhance the degradation rate, and the underlying mechanism was explained by the heterogenous Fenton reaction triggered by the H_2O_2 produced from O_2 reduction and surface-bound Fe^{2+} generated from corrosion of steel mesh.

The utilization of stainless steel in overcoming the brittleness of inorganic materials can be found in the research on electroconductive stainless steel-carbon nanotube (SS-CNT) membrane. This novel conductive membrane based on stainless steel was used in MD to treat high saline wastewaters. Different from the conventional MD, the electroconductive SS-CNT membrane applied with a microelectrical field could enhance antifouling and anticorrosion while maintaining a stable flux and rejection. The significantly alleviated membrane corrosion under the microelectrical field should be attributed to the cathodic protection effect [45].

Other metal materials, such as nickel and titanium, are also used in preparation of membrane electrode and shows excellent separation performance in water treatment. Ni-based membrane was employed to recover ammonium from wastewater. In this recovery process, NH_4^+ moved toward the cathode under the influence of the electric field and acquired electrons from the surface of cathode to form NH_3, which was subsequently extracted by an acid solution through a membrane contactor. A 40% higher recovery and a 20% lower energy consumption were achieved by this EMT in comparison with that achieved by the conventional gas stripping reactor using hydrophobic membrane [46].

However, although metallic membranes have long been applied in the EMT, its poor corrosion resistance is a big obstacle for its widespread application in this field. Moreover, the pore size of most metal membranes is larger than 1 μm because of the limitation of the fabrication technique, which compromises the membrane's treating efficiency for those pollutants, far smaller than its mean pore size. As such, it is unusual to use the metallic membrane without any modification for electrochemical membrane processes.

3.2.2.2 Metal oxide-metal composite membrane

In order to further enhance the separation efficiency and reduce cost, the composite membrane with metal (normally, these are stainless steel fiber mat, porous stainless steel, nickel, and titanium) as substrate and metal oxide as the selective layer

This book belongs to Badji Mokhtar Annaba University Central Library Copyright Elsevier 2025

gradually gained attention. The active components of the metal oxide can be utilized as a catalyst in advanced oxidation process (AOP) while the metallic particles provide huge specific surface area for adsorbing contaminants. Therefore the composite structure offers more options to design efficient electrochemical membrane technologies.

Titanium oxide materials (e.g., TiO_2, Ti_4O_7) are dominant metal oxides for such composite membranes and have extensively piqued research interests, whereas some other metal oxides (e.g., SnO_2, MnO_x, V_2O_5, Al_2O_3) have also been investigated. Titanium dioxide is well known for its outstanding photoelectrocatalysis ability and has been frequently used for removing contaminants in wastewater. For instance, N-doped TiO_2/NaY zeolite membrane could achieve 89% removal efficiency of phenol in water through photoelectrocatalysis initiated by simulated solar-light radiation [47]. However, more possibilities of direct electrocatalytic oxidation have been explored to overcome the limitations of photoelectrocatalysis in high-turbidity wastewater. An electrocatalytic membrane reactor (ECMR) with Nano-TiO_2/Ti composite membrane electrodes was designed to remove phenol and had achieved a removal efficiency of 93.13% when applied with an electric field of 8 V, which demonstrated the excellent performance of metal oxide-metal composite membrane in the electrochemical process [48].

Apart from TiO_2, magneli phase titanium oxides (which can be described as substoichiometric titanium oxides with the formula represented as Ti_nO_{2n-1}), especially Ti_4O_7, also gained a competitive edge over other metal oxides because of its high electrical conductivity and chemical stability and thus are promising candidates for electrochemical oxidation. Strong oxidants, such as OH• radicals, can be efficiently produced on the surface of Ti_4O_7 out of high oxygen evolution potential (from $+2.0$ to $+2.5$ V vs standard SCE) on electrodes, which had been employed to oxidize dye and herbicide in wastewaters and had achieved very high removal efficiencies ($>$ 90%) [49,50].

Ti_4O_7 also demonstrates superiority in purifying water containing ammonia since oxidants generated on the Ti_4O_7 surface can selectively oxidize ammonia to N_2. In the electroactive filtration system, Ti_4O_7 based membrane was installed as the anode while Pd-Cu co-modified nickel foam was used as the cathode. It was confirmed that ClO• was generated in the anode and played the dominant role in ammonia oxidation, which could achieve 100% of the conversion efficiency under the optimal condition [51].

A recent study showed that electron transfer of Ti_4O_7 can be significantly facilitated after a minor amount of carbon was introduced in the Ti_4O_7 electrodes because the electrochemical activities had been changed. A strengthened understanding of the relationship between oxidation performance and properties of the electrode can be beneficial to a better design of the membrane electrode and the selection of optimal operation conditions [52].

This book belongs to Badji Mokhtar Annaba University Central Library Copyright Elsevier 2025

Another group of widely used electrode is the dimensionally stable anode (DSA) while RuO_2, IrO_2, and SnO_2 are commonly used metal oxides for preparing DSA. Although the conductivity of some oxides like SnO_2 is not sufficiently high, it can be enhanced with doping metals. The semiconductive property and the superb stability of DSA materials endow the DSA electrode with high electrocatalytic capacity and low electrode wear. A TiO_2@SnO_2-Sb anodic membrane which was integrated in an electrochemical ceramic membrane filtration system was developed to remove low-molecular-weight pollutants from water. When using p-chloroaniline (PCA) as model contaminant, a high removal (97.9%) of PCA was achieved in a flow-through mode [53].

Some other metal oxides have also been explored in recent years. Nano-V_2O_5/Ti membrane was prepared by Zhang and it was used in an electrocatalytic membrane reactor (ECMR) to oxidize cyclohexane (CHA). An excellent selectivity (99.9%) of cyclohexanone and cyclohexanol (oxidation products) was observed in the electrochemical reaction. Additionally, the conversion of CHA was also higher than that of most noble metal-based catalysts [54]. Through doping Ce in manganese oxide by the sol-gel method and coating the mixture on a porous Ti membrane, Liang et al. prepared an electrocatalytic membrane electrode which was assembled in the ECMR for treating phenolic wastewater. The study showed that the ratio of Ce—MnO_x and Ti had a significant effect on the degradation of phenolic wastewater and the highest removal was 99.6% at the optimal ratio [55].

While the treating efficiency of wastewater has been improved by using metal-oxide membranes, mainly via electrocatalytic oxidation, the cost of these metal-oxide materials and the tedious preparation process are still big issues in practical application. Enhancing the performance of membrane with low-cost materials and exploring more mature and effective preparation methods will lead the direction of future research.

3.2.2.3 Summary of preparation methods

The methods of preparing metal-based composite membrane generally include electrodeposition and dry-wetting spinning. Electrodeposition is already well-developed as a mature technology for preparing metal membrane electrode in recent years. The coating of the metal layer can be realized in an electrochemical cell where membrane substrate and the metal are used as the cathode and the anode, respectively. The electrolyte solution contains the cation of the metal, the same as the anode, and the metal layer is formed after the reduction on the cathodic membrane substrate. For example, nickel-coated CNT/PP membrane was prepared through this process (as shown in Fig. 3.5A), in which Ni was deposited on the surface of the CNT/PP membrane through reduction under a constant DC current [46].

Dry-wetting spinning process is another emerging approach designed to fabricate metal-based hollow fiber (HF) membranes, which exhibit much higher mechanical strength than do polymeric and ceramic membranes. During the dry-wetting spinning

This book belongs to Badji Mokhtar Annaba University Central Library Copyright Elsevier 2025

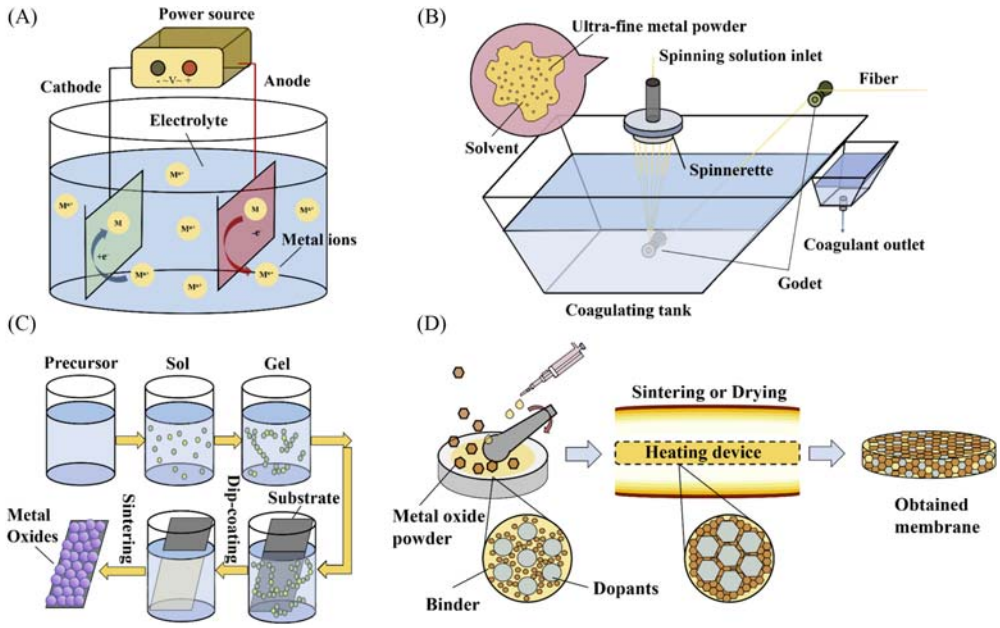

Figure 3.5 The schematic diagram illustrating the preparation method of metal membranes including (A) electrodeposition, (B) dry-wetting spinning process; and the preparation method of metal-oxide membranes including (C) sol–gel method and (D) sintering method.

process, metal powder is added to the polymer dope prior to spinning. The asymmetric HF can be subsequently produced through a sequential dry-wetting spinning (as shown in Fig. 3.5B) [45].

The preparation of metal-oxide membrane mainly relies on the sol-gel method and the sintering method. Metal oxides are mostly integrated with a substrate (e.g., titanium mesh and titanium foam) to improve the mechanical strength and processability. In a wet chemical process, the compounds containing metal ions are usually selected as precursors. As shown in Fig. 3.5C, precursors react with water or alcohol in solution and then form a transparent sol after undergoing hydrolysis and polymerization. A gelling substance will be slowly generated in the solution via polymerization of the aged colloidal particles and, gradually, form a gel with a three-dimensional network. After the drying and sintering, a porous electroactive layer of membrane electrodes is obtained on the substrate [47,54].

The sintering process is illustrated in Fig. 3.5D. To prepare a Ti_4O_7 membrane electrode, during the metal membrane preparation process, the powder of titanium oxide is usually synthesized via reduction in the presence of flowing H_2 gas at high temperature in a tube furnace. The powder and binder (e.g., paraffin oil) are mixed using mortar and pestle, which are subsequently placed in a die with an applied

This book belongs to Badji Mokhtar Annaba University Central Library Copyright Elsevier 2025

pressure followed by sintering in a tube furnace in the presence of inert gas (e.g., Ar) at high temperature [56,57].

3.2.3 Carbon-based membrane materials and MXene

Carbon-based membrane materials, including activated carbon, charcoal, natural graphite, etc., are widely used conventional electrochemical processes for water and wastewater treatment. In the recent years, some novel carbon-based materials [e.g., carbon nanotubes (CNTs), graphene, GO, and rGO] have also attracted much attention and have been intensively studied in the EMT [58]. They exhibit excellent performance in terms of antifouling, filtration-electrocatalytic oxidation.

MXene is a new type of two-dimensional layered inorganic compound which is prepared from its three-dimensional structure MAX by chemical etching. The MAX phase indicates the general formula $M_{n+1}AX_n$ ($n = 1, 2, 3$) where M represents early *d*-block transition metals, A is main group *sp* elements (specifically groups 13 and 14), and X stands for either C or N. It contains transition metal carbides, nitrides, or carbonitrides with a thickness of several atomic layers. Because of the combination of the metallic conductivity of transition metal carbides and the hydrophilic property conferred by their hydroxyl or oxygen terminated surfaces, they have good electrochemical properties and these properties make MXene show great potential in many applications such as energy storage, sensors, and catalysis [59].

3.2.3.1 Carbon nanotube-based membranes

In the EMT, carbon material was mainly used as catalyst supporters, electrodes, and filters. Among the most commonly investigated carbon materials, CNT have caught a lot of attention for its usefulness in electrochemical oxidation process to degrade the refractory pollutants in the wastewater [29,60,61]. CNTs are a type of one-dimensional quantum material, with a special structure, that is, the radial dimension is to the order of nanometers while the axial dimension is to the order of micrometers. The unique structure gives CNTs many excellent properties, such as large specific surface area, robust mechanical strength, good electrical conductivity, and equally good thermal stability. For example, the surface area and the conductivity of CNT material could be up to 30–500 m^2/g and 10^4–10^6 S/m, respectively [47]. When applied in the EMT, these excellent properties endow the CNTs materials with good performance in antifouling and pollutant degradation technologies [45,62]. CNT HF membranes are applied in an aerobic activated sludge system to serve as anode which enabled the system to put on a superior performance in reducing COD and NH_4^+-N in wastewater to that achieved by the conventional MBRs [45]. The high removal efficiency of COD and NH_4^+-N demonstrated the applicability of the CNT-based EMT for wastewater treatment. CNTs have also been used in fouling control and self-cleaning of electrochemical membranes. In an electrified cross-flow membrane

This book belongs to Badji Mokhtar Annaba University Central Library Copyright Elsevier 2025

filtration system, the CNT membrane displayed a good fouling resistance toward the target pollutant sodium alginate in the process and almost recovered the water flux to its original state by applying a relatively low voltage (3 V) [62]. Due to the large specific surface area (30−500 m^2/g) it possessed [47], the CNTs were found to put on a great performance in absorbing diverse organic compounds, mainly due to the hydrophobic inter-force and π-π interactions between contaminants and CNT. Such a good adsorption capability helps organic matter to be adsorbed on the electrode surface and facilitates the degradation of pollutants in the electrochemical membrane process [63].

3.2.3.2 Graphene-based membranes

Graphene has drawn extensive attention in various fields since its discovery in 2004. Due to its outstanding electrochemical and mechanical properties, graphene and its derivatives GO and reduced GO have also been applied in the EMT for water and wastewater treatment. To retain a robust mechanical strength, the two-dimensional materials are typically deposited on a porous support to construct a selective membrane. Graphene can be coated on HF porous membranes via chemical vapor deposition (CVD) and this composite membrane serves as cathodes in an anaerobic electrochemical membrane bioreactor (AnEMBR). It was found that the maximum transmembrane pressure for the reactor was much lower after a long-term continuous operation, implying an enhanced membrane fouling resistance [52].

GO is more active and hydrophilic than graphene due to the presence of abundant oxygen-containing functional groups on its surface. The properties of GO can be tailored through various reactions with oxygen-containing functional groups. The presence of oxygen-containing functional groups on the surface makes GO easily dispersed in the water phase, enabling a facile way to prepare a GO-based membrane. For instance, a conductive membrane was prepared by carbon material-laser-induced graphene and graphene oxide (LIG-GO) through vacuum assisted filtration (VAF), which served as the anode and exhibited extraordinary electrical conductivity and high fouling resistance when treating synthetic waters containing organic pollutants and bacteria [64]. Due to the hydrophilic and negative-charged surface of GO nanosheets, the incorporation of GO into the conductive membrane could largely enhance the antifouling property against microbes and organics. Furthermore, the use of an electrical field in conductive membrane process further improves the antifouling performance via electrostatic repulsion and (or) in situ generation of oxidant species [65].

rGO is prepared from GO through reduction (e.g., chemical reduction, electrochemical reduction, thermal reduction, etc.), which can be used as the substitute of graphene. Compared to GO, there is almost no oxidizing groups on the surface of reduced GO, which makes its structure more stable and ensures a membrane product without unwanted chemical reactions due to excessive activity. At the same time, the

This book belongs to Badji Mokhtar Annaba University Central Library Copyright Elsevier 2025

electrical conductivity of rGO is significantly improved compared to GO. Therefore rGO materials have also been extensively used in water and wastewater treatment in recent years. rGO can be loaded onto some organic substrates by blending rGO into casting solution followed by a phase inversion and the resultant electro-membrane shows good antifouling property [31]. Humic acid (HA) and bovine serum albumin (BSA) were used as model contaminants in the experiments, and the results showed that the flux recovery rate was 48%–68% higher than that of unmodified PES membranes.

3.2.3.3 MXene-based membranes

Recently, MXene materials have also been applied in EMT for the purpose of water treatment. By using VAF method, a new membrane electrode based on MXene material was successfully prepared and used in enhanced desalination. When a voltage was applied to the membrane electrode, the repellency of MXene membrane to methylene blue dye molecules was higher than $97.9 \pm 1.0\%$ and the high water-flux could reach up to 10498 L/(m^2•bar•h), demonstrating a good antifouling ability [66].

Carbon-based and MXene-based membranes generally have good electrical conductivity, which is highly desirable for its application in electrochemical processes such as electrochemical oxidation, electrochemical reduction, electroadsorption, and fouling control in water and wastewater treatment. However, these materials have some common shortcomings also, such as the complex preparation process, high cost of materials, and poor mechanical properties.

3.2.3.4 Summary of preparation methods

The vacuum-assisted filtration (VAF) is the commonly used method to prepare carbon-based and Mxene-based membranes (as shown in Fig. 3.6A), in which the nanosheets (GO, rGO, and MXene) or CNTs are self-assembled horizontally on a substrate to form a selective layer. This approach is a two-step process which is involved with the dispersion of nanomaterials and vacuum filtration of the solution to construct a membrane structure [6]. In the first step, nanomaterials are dispersed in water or other solvents, mainly assisted by sonication. In the second step, the dispersion is filtrated through a substrate driven by hydraulic pressure or vacuum. Last, the resultant membrane is dried in an oven to remove the solvent. The VAF method is widely used in membrane preparation, plaudits to its ease of operation. However, the agglomeration of nanomaterials that may take place in the dispersion in the first step can affect the homogeneity and the stability of the membranes obtained.

Another approach to preparing these membranes is chemical vapor deposition (CVD), mainly for the preparation of carbon-based membranes (as shown in Fig. 3.6B) [45,67]. For instance, graphene layers could be synthesized directly on an Ni-based HF membrane (Ni-HFMs) through CVD by exposing Ni-HFMs to a

This book belongs to Badji Mokhtar Annaba University Central Library Copyright Elsevier 2025

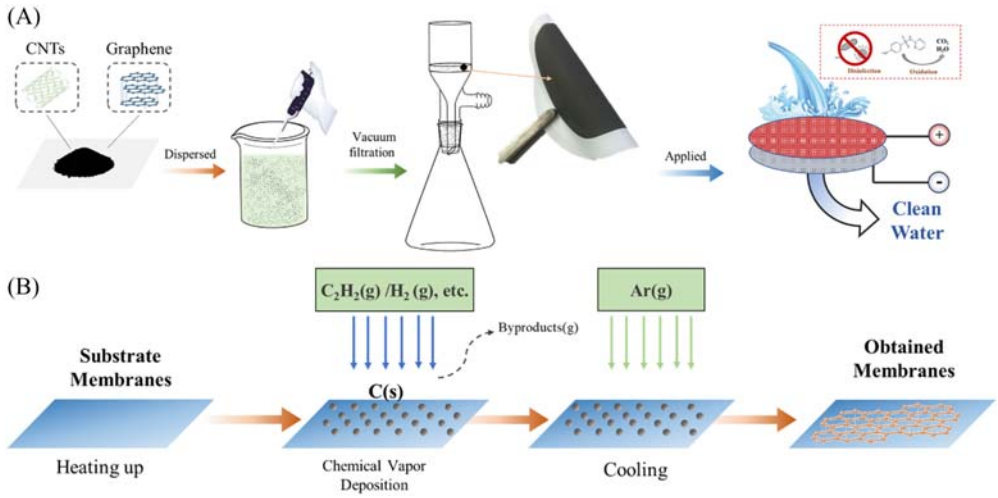

Figure 3.6 Schematic diagram of preparation of carbon-based membranes via (A) vacuum-assisted filtration and (B) chemical vapor deposition.

mixture of acetylene and H_2 gases at 1000°C and then cooled in a tube furnace in argon gas [67]. Compared with the VAF method, CVD is much more complicated due to the need of harsh preparation conditions, though the coating of carbon nanomaterials on membrane surface is more uniform.

3.3 Materials for ion exchange membranes

IEM are a very important category of membrane materials with ionic conductivity, which are essential in electrochemical membrane technologies including ED, MCDI, microbial fuel cells (MFCs), microbial desalination cells (MDCs), and others [68]. IEMs are usually polymeric membranes containing charged groups, which partially or totally preclude the passage of ions with the same charge through the membrane.

In this section, IEMs are introduced in order of their membrane structure and discussed accordingly, including homogeneous IEMs, heterogenous IEMs, pseudohomogenous IEMs, and mixed matrix IEMs. Homogeneous IEMs have a uniform selective layer, while the separation layer of heterogeneous IEMs is discontinuous which is made of ion-exchange resin powder with binder polymer. The selective layer of pseudohomogenous IEMs is uniform at a microscopic scale, however, showing discontinuous at the macroscopic scale. In addition, the mixed matrix membranes which incorporate inorganic nanomaterials into polymeric matrix are also an important

This book belongs to Badji Mokhtar Annaba University Central Library Copyright Elsevier 2025

category of IEMs. Due to the introduction of inorganic materials, they exhibit different properties compared with the substrates. Furthermore, according to the selectivity, IEMs can also be classified into cation exchange membranes (CEMs) containing negatively charged groups, and anion exchange membranes (AEMs) containing positively charged groups. CEMs can be more specifically classified into strong acid IEMs containing sulfonic acid group, and weak acid IEMs containing carboxylic acid group, whilst AEMs can also be classified into strong and weak base IEMs containing quaternary and tertiary amines, respectively. Apart from AEMs and CEMs, bipolar membranes are another type of IEMs, which contain two opposite-charged layers, that is, cation-exchange and anion-exchange layers.

3.3.1 Homogeneous ion exchange membranes

The homogeneous IEMs are prepared by introducing ion-exchange groups into the polymer matrix. This category of membranes usually stand out from the crowd for their electrochemical properties, however, a disadvantage being that these membranes are more expensive than the heterogenous and the pseudo-homogeneous IEMs [7]. The most well-known homogeneous IEM is the perfluorosulfonic acid membranes of the Nafion type. Nafion is a kind of proton exchange membrane made of random copolymer of tetrafluoroethylene and sulfonyl fluoride vinyl-ether [69,70]. It is widely utilized in various electrochemical membrane technologies, and is one of the typical benchmark membrane materials.

However, the swelling of IEMs is a serious problem which may result in the decrease in selectivity and the mechanical properties [62]. To solve this problem, the cross-linking of polymer chains has been used to reduce the degree of swelling of IEMs [71]. This method while significantly improving the selectivity and mechanical properties of IEMs also increases the manufacturing cost of IEMs. In a cross-linking process, the cross-linked agents, for example, divinylbenzene (DVB) or bis-(vinylphenyl)-ethane (BVPE), can be added to the ionomer during the polymerization [72,73]. The obtained IEMs are always highly selective, such as the Neosepta CMX membrane based on sulfonated styrene-DVB copolymer [74]. However, there is no suitable way to simultaneously conduct the cross-linking in a traditional IEMs manufacturing process, which means that the cross-linking method needs additional processing steps. In addition, the cross-linking method can also be used to improve the performances of the heterogeneous and the pseudo-homogeneous IEMs as well.

3.3.2 Heterogeneous ion exchange membranes

The heterogenous IEMs are conventionally prepared by hot rolling or mixing ion-exchange resin powder with binder polymer followed by a posttreatment processing. Due to the preparation method, large macropores exist between the ion-exchange resin and binder polymer [75,76]. According to the results of pore size distribution, heterogeneous

This book belongs to Badji Mokhtar Annaba University Central Library Copyright Elsevier 2025

IEMs have pores ranging from several nm to 1 μm. Therefore the selectivity of heterogenous IEMs is usually lower than that of the homogeneous ones [77].

For the heterogenous IEMs, their surface properties largely determine their selectivity and conductivity. Hence, the surface modification has always been regarded as one of the most effective approaches to improve the heterogeneous IEMs' performance [78]. For instance, the surface of heterogenous IEMs is usually predominately covered with plasticizer (or binder), for example, polyethylene, which makes the surface bare of ion transport channels. Thus coating the IEM with a thin layer of polyelectrolytes with high conductivity could endow the heterogenous IEMs with significantly improved performance [79]. Surface coating by a layer with fixed groups of opposite charge is also an effective approach to improve the selectivity. For example, polyaniline or polyethyleneimine had been used to modify the surface of CEMs [80,81]. It is worth noting that such membranes differ in diffusion permeability and asymmetry of ion transport from the unmodified IEMs. Furthermore, the layer-by-layer (LBL) modification is also an effective way to increase the selectivity of IEMs [82,83]. However, LBL modification also drastically increases the membrane resistance [84]. Plasma treatment is another approach to modify the surface layer of IEMs. Plasma carbon deposition on the membrane surface results in a reduction of the wettability of the membrane surface and an increase of selectivity [85], and through which surface the aluminosilicate nanotubes introduced onto the surface layers of IEMs provide the IEMs with an extra ability for ion exchange capacity [86].

3.3.3 Pseudohomogeneous ion exchange membranes

The pseudohomogeneous IEMs are a type of IEMs which is conventionally prepared by conducting polymerization followed by its functionalization in a porous substrate. As already mentioned, the homogenous IEMs have superior electrochemical properties to heterogenous IEMs, though they are relatively more expensive. The poorer electrochemical property of heterogenous IEMs is mainly due to the macropores formed during the preparation of IEMs using ion-exchange resin powder and binder polymer [77,87]. The strategy of directly using the homogeneous polymer of heterogenous IEMs, for example, sulfonated polystyrene (PS), rather than using the powder of PS, may eliminate the defects caused by macropores. However, in practice, it is challenging to prepare robust IEMs from PS without binder.

To break this bottleneck, pseudohomogenous IEMs can be obtained by conducing polymerization and followed by its functionalization in substrate, which avoids the formation of macropores and acquires a good mechanical strength at the same time. For example, the pseudohomogenous IEMs can be made by preparing the functionalized PS inside the hydrophobic substrate [88,89]. An example is the Neosepta IEMs which are prepared through the polymerization of styrene in a paste with polyvinyl chloride [90].

This book belongs to Badji Mokhtar Annaba University Central Library Copyright Elsevier 2025

Another type of pseudohomogenous IEMs is based on the radical polymerization of styrene inside the hydrophobic substrate followed by sulfonation [91–93]. The manufacturer can vary the radiation dose and irradiation time to adjust the polystyrene content in the hydrophobic substrate, for example, dense polyethylene films, to obtain IEMs without pores. Adequate grafting and sulfonation are always required but an excessive degree of grafting and sulfonation would make IEMs swell severely in water, leading to the loss of selectivity and mechanical strength [94,95].

3.3.4 Mixed matrix ion exchange membranes

The mixed matrix IEMs are those IEMs doped with inorganic nanoparticles that form a discrete phase in the continuous polymer phase [96]. This modification approach is the most frequently utilized way to increase the ionic conductivity of IEMs since the late 1980s [97]. Some inorganic nanomaterials could enhance the mechanical properties of IEMs at the same time [98]. Most of employed nanoparticles are hydrophilic nanomaterials, for example, silica and other oxides [99,100], while graphene is also receiving much attention in the recent years [101–103].

The introduction of hydrophilic nanomaterials into IEMs often leads to an increase of water uptake, which is believed to the main reason for the enhancement of ionic conductivity. However, there are also some exceptions. Some mixed matrix IEMs have higher ionic conductivity but lower water uptake. Moreover, a number of studies showed that a doping content of inorganic nanoparticles higher than 2 vol % often resulted in decreased conductivity [104–106].

3.4 Electrochemical membrane modules

The electrochemical membranes are designed and manufactured in various configurations, including flat-sheet (FS), HF, and tubular membranes (also termed multitube or multichannel membrane) [107]. These membranes can be packed in pressure vessels. For FS membranes packed in pressure vessels, they are usually known as spiral-wound membranes. The HF membranes have the advantage of large specific surface area but they usually suffer from more severe fouling caused by the limited space among neighboring fibers [108].

The design of electrochemical membrane modules is subject to membrane configuration and the application scenarios. For electrochemical membrane modules used in the enhanced contaminant removal and water disinfection process, to maximize the contacts between the target contaminants in stream and membrane electrodes is always a membrane module design prerequisite. For instance, the FS electrochemical

This book belongs to Badji Mokhtar Annaba University Central Library Copyright Elsevier 2025

membranes and perforated counter-electrode (e.g., titanium mesh) can be tightly assembled at the opposite sides of an insulating separator (as shown in Fig. 3.7A) [60]. The stream successively flows through the membrane FS electrochemical membranes and perforated counter-electrode, or in reverse order. The membrane electrodes and counter-electrodes can also be assembled with a bracket and submerged in a reactor. For example, the FS membrane electrodes can be placed on both sides of a bracket to construct a membrane module and the counter-electrodes are assembled in the middle of membrane module to form an integrated cell or placed opposite to the membrane electrode in the reactor (as shown in Fig. 3.7B) [5,53,109]. For the above-mentioned modules, the pressure-driven permeation can help achieve much higher reaction rates, in comparison with the conventional reactor configuration needed for electrolysis [6].

For electrochemical membrane modules designed for fouling control, to modify these modules is the usual practice compared with that followed for conventional modules. In a typical module (as shown in Fig. 3.7C), the electrodes can also be directly assembled with membranes in a compact cross-flow device. After applying a proper electric field, this type

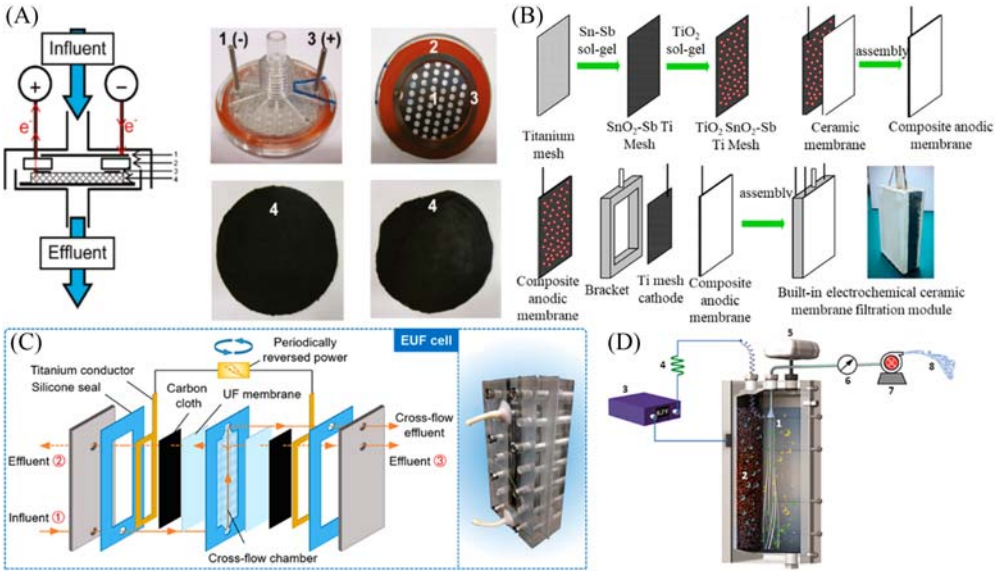

Figure 3.7 (A) The polycarbonate filtration casing for carbon nanotube (CNT) membrane electrode consisting of (1) a perforated stainless steel cathode, (2) an insulating silicone rubber separator and seal, (3) a titanium anodic ring that is pressed into the carbon nanotube anodic filter, and (4) the CNT anodic filter supported by a PTFE membrane; [60] (B) schematic illustration of built-in electrochemical ceramic membrane filtration module with TiO2@SnO_2−Sb coated composite anodic membrane; [53] (C) configuration diagram and photograph of the electrically tuning ultrafiltration cross-flow cell; [110] (D) schematic diagram of the anaerobic electrochemical membrane bioreactors consisting of a graphene-coated hollow fiber membrane and a bioanode [111]. *All reproduced with permission from the American Chemical Society.*

This book belongs to Badji Mokhtar Annaba University Central Library Copyright Elsevier 2025

of device can achieve an enhanced desalination performance and fouling resistance [110]. For the modules used in bioreactors, their configuration is similar to the conventional membrane modules, in which the conductive membrane is connected to the power supply and the (perforated or not-perforated, abiotic or biotic) counter-electrodes are installed in bioreactors (as shown in Fig. 3.7D) [8,67].

In the modules of ED, bioelectrochemical system (including microbial fuel cell, microbial electrolysis cell, microbial desalination cell), and capacitive deionization (including MCDI and flow-electrode capacitive deionization), the IEMs are placed between the anode and cathode in the devices [112]. For ED, CEM, and AEM are of vital importance and are placed between the anode and the cathode with the CEM in front of the anode and the AEM in front of the cathode [113]. Under the electrical field, the cations and the anions in the influent, which enters the chamber between CEM and AEM in ED cell, migrate toward the cathode and the anode, respectively. The CEM and the AEM reject the anions and cations, respectively, to desalinate the feed. For some bioelectrochemical systems, the usage of IEMs is also essential in conducting ions to form a current and thereby preventing the anolyte and the catholyte from mixing because the reactions at the anode and the cathode usually need different circumstances. For mCDI, the IEMs are used to further improve the efficiency of capacitive deionization by allowing the usage of reversed electrical field in regeneration and avoiding the adsorption of coion [114]. As for the FCDI, the IEM can also act as a barrier to prevent the suspended activated carbon from leakage, apart from the benefits mentioned above in mCDI [115].

3.5 Conclusions and perspectives

The membrane materials and modules for electrochemical membrane technologies have been reviewed in this chapter, including the conductive polymeric membranes, metal and metal-oxide membranes, carbon-based membranes, IEM, and electrochemical membrane modules. Examples of these membrane materials are cited and their advantages and disadvantages are given a thorough discussion as well. Although some novel membrane materials exhibit outstanding performance in lab-scale studies, their applications in full-scale are still hindered by several obstacles. For instance, some materials (e.g., Ti_4O_7 and CNTs) still suffer from passivation, corrosion, harsh preparation conditions, and high cost. As for IEMs, the trade-off between selectivity and permeability is a persistent issue. Although various approaches such as cross-linking, surface modification, and preparation of mixed matrix membranes with embedded nanoparticles are used to overcome the trade-off between selectivity and permeability, the increased cost and more complicated preparation procedure become major concerns for scale-up.

This book belongs to Badji Mokhtar Annaba University Central Library Copyright Elsevier 2025

To fill the gap between lab studies and industrial needs, more efforts are still required to seek sustainable and low-cost electrochemical membrane materials as well as further simplify the preparation processes of electrochemical membranes. In addition, there is a critical need to verify the long-term stability and durability of membrane materials under real operation conditions. Finally, the novel configurations of electrochemical membrane modules are also required to ensure an optimal treating efficiency. With increasing attention being focused on this field, it can be expected that more and more novel materials and module designs will be emerging in the near future, further promoting the development and application of electrochemical membrane technologies in water and wastewater treatment.

Acknowledgment

X.Li and Z.Wang acknowledge the funding support from the Science and Technology Commission of Shanghai Municipality (Grant no. 20230713700).

References

[1] M.B. Asif, T. Maqbool, Z. Zhang, Electrochemical membrane bioreactors: State-of-the-art and future prospects, Sci. Total Environ. 741 (2020) 140233. Available from: https://doi.org/10.1016/j.scitotenv.2020.140233.

[2] A. Alabi, A. AlHajaj, L. Cseri, G. Szekely, P. Budd, L. Zou, Review of nanomaterials-assisted ion exchange membranes for electromembrane desalination, NPJ Clean Water 1 (2018) 1–22. Available from: https://doi.org/10.1038/s41545-018-0009-7.

[3] L. Liu, F. Zhao, J. Liu, F. Yang, Preparation of highly conductive cathodic membrane with graphene (oxide)/PPy and the membrane antifouling property in filtrating yeast suspensions in EMBR, J. Membr. Sci. 437 (2013) 99–107. Available from: https://doi.org/10.1016/j.memsci.2013.02.045.

[4] A.M. Zaky, B.P. Chaplin, Porous substoichiometric TiO_2 anodes as reactive electrochemical membranes for water treatment, Environ. Sci. Technol. 47 (2013) 6554–6563. Available from: https://doi.org/10.1021/es401287e.

[5] J. Zheng, J. Ma, Z. Wang, S. Xu, T.D. Waite, Z. Wu, Contaminant removal from source waters using cathodic electrochemical membrane filtration: mechanisms and implications, Environ. Sci. Technol. 51 (2017) 2757–2765. Available from: https://doi.org/10.1021/acs.est.6b05625.

[6] S. Ali, S.A.U. Rehman, H.-Y. Luan, M.U. Farid, H. Huang, Challenges and opportunities in functional carbon nanotubes for membrane-based water treatment and desalination, Sci. Total Environ. 646 (2019) 1126–1139. Available from: https://doi.org/10.1016/j.scitotenv.2018.07.348.

[7] I. Stenina, D. Golubenko, V. Nikonenko, A. Yaroslavtsev, Selectivity of transport processes in ion-exchange membranes: relationship with the structure and methods for its improvement, Int. J. Mol. Sci. 21 (2020) 5517. Available from: https://doi.org/10.3390/ijms21155517.

[8] M. Sun, X. Wang, L.R. Winter, Y. Zhao, W. Ma, T. Hedtke, J.-H. Kim, M. Elimelech, Electrified membranes for water treatment applications, ACS EST. Eng. (2021). Available from: https://doi.org/10.1021/acsestengg.1c00015.

[9] H. Shirakawa, E.J. Louis, A.G. MacDiarmid, C.K. Chiang, A.J. Heeger, Synthesis of electrically conducting organic polymers: halogen derivatives of polyacetylene, (CH)x, J. Chem. Soc., Chem. Commun. (1977) 578–580. Available from: https://doi.org/10.1039/C39770000578.

[10] T.-H. Le, Y. Kim, H. Yoon, Electrical and electrochemical properties of conducting polymers, Polymers 9 (2017) 150. Available from: https://doi.org/10.3390/polym9040150.

[11] E. Eskandari, M. Kosari, M.H. Davood Abadi Farahani, N.D. Khiavi, M. Saeedikhani, R. Katal, M. Zarinejad, A review on polyaniline-based materials applications in heavy metals removal and

This book belongs to Badji Mokhtar Annaba University Central Library Copyright Elsevier 2025

catalytic processes, Sep. Purif. Technol. 231 (2020) 115901. Available from: https://doi.org/10.1016/j.seppur.2019.115901.
[12] R.L. Elsenbaumer, K.Y. Jen, G.G. Miller, L.W. Shacklette, Processible, environmentally stable, highly conductive forms of polythiophene, Synth. Met. 18 (1987) 277–282. Available from: https://doi.org/10.1016/0379-6779(87)90892-7.
[13] D. Pavlović, S. Cohen, Controlled synthesis of unsubstituted high molecular weight poly(para-phenylene) via Suzuki polycondensation-thermal aromatization methodology, Polym. Chem. 11 (2020) 2550–2558. Available from: https://doi.org/10.1039/D0PY00001A.
[14] I. Rabias, C. Langlois, A. Provata, B.J. Howlin, D.N. Theodorou, Linking the atomistic scale and the mesoscale: molecular orbital and solid state packing calculations on poly(p-phenylene), Polymer 43 (2002) 185–193. Available from: https://doi.org/10.1016/S0032-3861(01)00587-0.
[15] N.V. Blinova, J. Stejskal, M. Trchová, J. Prokeš, Control of polyaniline conductivity and contact angles by partial protonation, Polym. Int. 57 (2008) 66–69. Available from: https://doi.org/10.1002/pi.2312.
[16] W.E. Price, C.O. Too, G.G. Wallace, D. Zhou, Development of membrane systems based on conducting polymers, Synth. Met. 102 (1999) 1338–1341. Available from: https://doi.org/10.1016/S0379-6779(98)90212-0.
[17] D. Kumar, R.C. Sharma, Advances in conductive polymers, Eur. Polym. J. 34 (1998) 1053–1060. Available from: https://doi.org/10.1016/S0014-3057(97)00204-8.
[18] M.N. Gueye, A. Carella, J. Faure-Vincent, R. Demadrille, J.-P. Simonato, Progress in understanding structure and transport properties of PEDOT-based materials: a critical review, Prog. Mater. Sci. 108 (2020) 100616. Available from: https://doi.org/10.1016/j.pmatsci.2019.100616.
[19] L. Liu, J. Liu, G. Bo, F. Yang, J. Crittenden, Y. Chen, Conductive and hydrophilic polypyrrole modified membrane cathodes and fouling reduction in MBR, J. Membr. Sci. 429 (2013) 252–258. Available from: https://doi.org/10.1016/j.memsci.2012.11.066.
[20] J. Liu, C. Tian, J. Xiong, B. Gao, S. Dong, L. Wang, Polypyrrole vapor phase polymerization on PVDF membrane surface for conductive membrane preparation and fouling mitigation, J. Chem. Technol. Biotechnol. 93 (2018) 683–689. Available from: https://doi.org/10.1002/jctb.5416.
[21] J. Mansouri, R.P. Burford, Characterization of PVDF-PPy composite membranes, Polymer 38 (1997) 6055–6069. Available from: https://doi.org/10.1016/S0032-3861(97)00169-9.
[22] L. Liu, J. Liu, B. Gao, F. Yang, S. Chellam, Fouling reductions in a membrane bioreactor using an intermittent electric field and cathodic membrane modified by vapor phase polymerized pyrrole, J. Membr. Science 394–395 (2012) 202–208. Available from: https://doi.org/10.1016/j.memsci.2011.12.042.
[23] X. Tan, C. Hu, X. Li, H. Liu, J. Qu, Reversible superwettability switching of a conductive polymer membrane for oil-water separation and self-cleaning, J. Membr. Sci. 605 (2020) 118088. Available from: https://doi.org/10.1016/j.memsci.2020.118088.
[24] A. Bhattacharya, D.C. Mukherjee, J.M. Gohil, Y. Kumar, S. Kundu, Preparation, characterization and performance of conducting polypyrrole composites based on polysulfone, Desalination 225 (2008) 366–372. Available from: https://doi.org/10.1016/j.desal.2006.07.018.
[25] Y. Zhou, C. Hu, H. Liu, J. Qu, Potassium-ion recovery with a polypyrrole membrane electrode in novel redox transistor electrodialysis, Environ. Sci. Technol. 54 (2020) 4592–4600. Available from: https://doi.org/10.1021/acs.est.9b06665.
[26] M.-L. Liu, L. Li, Y.-X. Sun, Z.-J. Fu, X.-L. Cao, S.-P. Sun, Scalable conductive polymer membranes for ultrafast organic pollutants removal, J. Membr. Sci. 617 (2021) 118644. Available from: https://doi.org/10.1016/j.memsci.2020.118644.
[27] J. Liu, Y. Wang, L. Wang, Poly (3, 4-ethylenedioxythiophene) modified polyvinylidene fluoride membrane for visible photoelectrocatalysis and filtration, J. Colloid Interface Sci. 553 (2019) 220–227. Available from: https://doi.org/10.1016/j.jcis.2019.06.024.
[28] I. Chajanovsky, R.Y. Suckeveriene, Preparation of hybrid polyaniline/nanoparticle membranes for water treatment using an inverse emulsion polymerization technique under sonication, Processes 8 (2020) 1503. Available from: https://doi.org/10.3390/pr8111503.

This book belongs to Badji Mokhtar Annaba University Central Library Copyright Elsevier 2025

[29] W. Duan, A. Ronen, S. Walker, D. Jassby, Polyaniline-coated carbon nanotube ultrafiltration membranes: enhanced anodic stability for in situ cleaning and electro-oxidation processes, ACS Appl. Mater. Interfaces 8 (2016) 22574–22584. Available from: https://doi.org/10.1021/acsami.6b07196.

[30] Z.-Y. Guo, X.-S. Yuan, H.-Z. Geng, L.-D. Wang, L.-C. Jing, Z.-Z. Gu, High conductive PPy–CNT surface-modified PES membrane with anti-fouling property, Appl. Nanosci. 8 (2018) 1597–1606. Available from: https://doi.org/10.1007/s13204-018-0826-5.

[31] E.L. Subtil, J. Gonçalves, H.G. Lemos, E.C. Venancio, J.C. Mierzwa, J. dos, S. de Souza, W. Alves, P. Le-Clech, Preparation and characterization of a new composite conductive polyethersulfone membrane using polyaniline (PANI) and reduced graphene oxide (rGO), Chem. Eng. J. 390 (2020) 124612. Available from: https://doi.org/10.1016/j.cej.2020.124612.

[32] H. Liu, G. Zhang, C. Zhao, J. Liu, F. Yang, Hydraulic power and electric field combined antifouling effect of a novel conductive poly(aminoanthraquinone)/reduced graphene oxide nanohybrid blended PVDF ultrafiltration membrane, J. Mater. Chem. A 3 (2015) 20277–20287. Available from: https://doi.org/10.1039/C5TA05306D.

[33] F. Zhao, L. Liu, F. Yang, N. Ren, E-Fenton degradation of MB during filtration with Gr/PPy modified membrane cathode, Chem. Eng. J. 230 (2013) 491–498. Available from: https://doi.org/10.1016/j.cej.2013.06.117.

[34] B. Jiang, Q. Zeng, Y. Hou, J. Liu, J. Xu, H. Li, C. Du, S. Shi, F. Ma, Quorum quenching bacteria bioaugmented GO/PPy modified membrane in EMBR for membrane antifouling, Sci. Total Environ. 718 (2020) 137412. Available from: https://doi.org/10.1016/j.scitotenv.2020.137412.

[35] L. Xie, Y. Shu, Y. Hu, J. Cheng, Y. Chen, SWNTs-PAN/TPU/PANI composite electrospun nanofiber membrane for point-of-use efficient electrochemical disinfection: New strategy of CNT disinfection, Chemosphere 251 (2020) 126286. Available from: https://doi.org/10.1016/j.chemosphere.2020.126286.

[36] K. Venkatesh, G. Arthanareeswaran, A.C. Bose, PVDF mixed matrix nano-filtration membranes integrated with 1D-PANI/TiO2 NFs for oil–water emulsion separation, RSC Adv. 6 (2016) 18899–18908. Available from: https://doi.org/10.1039/C5RA27022G.

[37] S.B. Teli, S. Molina, A. Sotto, E.G. Calvo, J. de Abajob, Fouling resistant polysulfone–PANI/TiO_2 ultrafiltration nanocomposite membranes, Ind. Eng. Chem. Res. 52 (2013) 9470–9479. Available from: https://doi.org/10.1021/ie401037n.

[38] X. Cheng, S. Ding, J. Guo, C. Zhang, Z. Guo, L. Shao, In-situ interfacial formation of TiO2/polypyrrole selective layer for improving the separation efficiency towards molecular separation, J. Membr. Sci. 536 (2017) 19–27. Available from: https://doi.org/10.1016/j.memsci.2017.04.057.

[39] N. Li, L. Liu, F. Yang, Highly conductive graphene/PANi-phytic acid modified cathodic filter membrane and its antifouling property in EMBR in neutral conditions, Desalination 338 (2014) 10–16. Available from: https://doi.org/10.1016/j.desal.2014.01.019.

[40] N. Shafaei, M. Peyravi, M. Jahanshahi, Improving surface structure of photocatalytic self-cleaning membrane by WO_3/PANI nanoparticles, Polym. Adv. Technol. 27 (2016) 1325–1337. Available from: https://doi.org/10.1002/pat.3800.

[41] A. Pakdel Mojdehi, M. Pourafshari Chenar, M. Namvar-Mahboub, M. Eftekhari, Development of PES/polyaniline-modified TiO_2 adsorptive membrane for copper removal, Colloids Surf. A Physicochem. Eng. Asp. 583 (2019) 123931. Available from: https://doi.org/10.1016/j.colsurfa.2019.123931.

[42] S. Aziz, M. Sabzi, A. Fattahi, E. Arkan, Electrospun silk fibroin/PAN double-layer nanofibrous membranes containing polyaniline/TiO2 nanoparticles for anionic dye removal, J. Polym. Res. 24 (2017) 1–7. Available from: https://doi.org/10.1007/s10965-017-1298-0.

[43] Z. Liu, Y.-E. Miao, M. Liu, Q. Ding, W.W. Tjiu, X. Cui, T. Liu, Flexible polyaniline-coated TiO_2/SiO_2 nanofiber membranes with enhanced visible-light photocatalytic degradation performance, J. Colloid Interface Sci. 424 (2014) 49–55. Available from: https://doi.org/10.1016/j.jcis.2014.03.009.

[44] B. Xu, X. Wang, Y. Huang, J. Liu, D. Wang, S. Feng, X. Huang, H. Wang, Electrospinning preparation of PAN/TiO_2/PANI hybrid fiber membrane with highly selective adsorption and photocatalytic regeneration properties, Chem. Eng. J. 399 (2020) 125749. Available from: https://doi.org/10.1016/j.cej.2020.125749.

This book belongs to Badji Mokhtar Annaba University Central Library Copyright Elsevier 2025

[45] Y. Si, C. Sun, D. Li, F. Yang, C.Y. Tang, X. Quan, Y. Dong, M.D. Guiver, Flexible superhydrophobic metal-based carbon nanotube membrane for electrochemically enhanced water treatment, Environ. Sci. Technol. 54 (2020) 9074–9082. Available from: https://doi.org/10.1021/acs.est.0c01084.
[46] D. Hou, A. Iddya, X. Chen, M. Wang, W. Zhang, Y. Ding, D. Jassby, Z.J. Ren, Nickel-based membrane electrodes enable high-rate electrochemical ammonia recovery, Environ. Sci. Technol. 52 (2018) 8930–8938. Available from: https://doi.org/10.1021/acs.est.8b01349.
[47] Z.-L. Cheng, S. Han, Preparation and photoelectrocatalytic performance of N-doped TiO_2/NaY zeolite membrane composite electrode material, Water Sci. Technol. 73 (2015) 486–492. Available from: https://doi.org/10.2166/wst.2015.505.
[48] J. Xu, X. Liang, X. Fan, Y. Song, Z. Zhao, J. Hua, C. Liu, J. Li, Highly enhanced electrocatalytic activity of nano-TiO_2/Ti membrane electrode for phenol wastewater treatment, J. Mater. Sci. Mater Electron. 31 (2020) 13511–13520. Available from: https://doi.org/10.1007/s10854-020-03907-5.
[49] G. Wang, Y. Liu, J. Ye, Z. Lin, X. Yang, Electrochemical oxidation of methyl orange by a Magnéli phase Ti_4O_7 anode, Chemosphere 241 (2020) 125084. Available from: https://doi.org/10.1016/j.chemosphere.2019.125084.
[50] M.F. Silva Barni, L.I. Doumic, R.A. Procaccini, M.A. Ayude, H.E. Romeo, Layered platforms of Ti_4O_7 as flow-through anodes for intensifying the electro-oxidation of bentazon, J. Environ. Manage. 263 (2020) 110403. Available from: https://doi.org/10.1016/j.jenvman.2020.110403.
[51] W. Zhao, J. Mei, Y. Liu, B. Yang, F. Li, X. Fang, M. Huang, W. Sand, A Bifunctional electroactive Ti_4O_7-based membrane system for highly efficient ammonia decontamination, Catalysts 10 (2020) 383. Available from: https://doi.org/10.3390/catal10040383.
[52] J. Xie, J. Ma, C. Zhang, X. Kong, Z. Wang, T.D. Waite, Effect of the presence of carbon in Ti_4O7 electrodes on anodic oxidation of contaminants, Environ. Sci. Technol. 54 (2020) 5227–5236. Available from: https://doi.org/10.1021/acs.est.9b07398.
[53] J. Zheng, Z. Wang, J. Ma, S. Xu, Z. Wu, Development of an electrochemical ceramic membrane filtration system for efficient contaminant removal from waters, Environ. Sci. Technol. 52 (2018) 4117–4126. Available from: https://doi.org/10.1021/acs.est.7b06407.
[54] Y. Zhang, Y. Qi, Z. Yin, H. Wang, B. He, X. Liang, J. Li, Z. Li, Nano-V_2O_5/Ti porous membrane electrode with enhanced electrochemical activity for the high-efficiency oxidation of cyclohexane, Green Chem. 20 (2018) 3944–3953. Available from: https://doi.org/10.1039/C8GC01259H.
[55] D. Zhang, X. Liang, S. Yang, Z. Chen, H. Wang, Y. Feng, H. Wang, J. Li, Investigation of electrocatalytic activity of nanostructure Ce-doped MnOxsol–gel coating deposited on porous Ti membrane electrode, J. Sol-Gel Sci. Technol. 86 (2018) 468–478. Available from: https://doi.org/10.1007/s10971-018-4620-3.
[56] S. Almassi, Z. Li, W. Xu, C. Pu, T. Zeng, B.P. Chaplin, Simultaneous adsorption and electrochemical reduction of N-nitrosodimethylamine using carbon-Ti_4O_7 composite reactive electrochemical membranes, Environ. Sci. Technol. 53 (2019) 928–937. Available from: https://doi.org/10.1021/acs.est.8b05933.
[57] S. Almassi, P.R. Samonte, Z. Li, W. Xu, B.P. Chaplin, Mechanistic investigation of haloacetic acid reduction using carbon-Ti_4O_7 composite reactive electrochemical membranes, Environ. Sci. Technol. 54 (2020) 1982–1991. Available from: https://doi.org/10.1021/acs.est.9b06744.
[58] Y. Yang, J. Li, H. Wang, X. Song, T. Wang, B. He, X. Liang, H.H. Ngo, An electrocatalytic membrane reactor with self-cleaning function for industrial wastewater treatment, Angew. Chem. Int. (Ed.) 50 (2011) 2148–2150. Available from: https://doi.org/10.1002/anie.201005941.
[59] M. Naguib, V.N. Mochalin, M.W. Barsoum, Y. Gogotsi, 25th anniversary article: MXenes: a new family of two-dimensional materials, Adv. Mater. 26 (2014) 992–1005. Available from: https://doi.org/10.1002/adma.201304138.
[60] C.D. Vecitis, G. Gao, H. Liu, Electrochemical carbon nanotube filter for adsorption, desorption, and oxidation of aqueous dyes and anions, J. Phys. Chem. C 115 (2011) 3621–3629. Available from: https://doi.org/10.1021/jp111844j.
[61] X. Zhao, L. Cheng, R. Wang, N. Jia, L. Liu, C. Gao, Bioinspired synthesis of polyzwitterion/titania functionalized carbon nanotube membrane with superwetting property for efficient oil-in-water

This book belongs to Badji Mokhtar Annaba University Central Library Copyright Elsevier 2025

emulsion separation, J. Membr. Sci. 589 (2019) 117257. Available from: https://doi.org/10.1016/j.memsci.2019.117257.

[62] M.S. Cha, J.Y. Lee, T.-H. Kim, H.Y. Jeong, H.Y. Shin, S.-G. Oh, Y.T. Hong, Preparation and characterization of crosslinked anion exchange membrane (AEM) materials with poly(phenylene ether)-based short hydrophilic block for use in electrochemical applications, J. Membr. Sci. 530 (2017) 73–83. Available from: https://doi.org/10.1016/j.memsci.2017.02.015.

[63] G. Gao, Q. Zhang, C.D. Vecitis, CNT–PVDF composite flow-through electrode for single-pass sequential reduction–oxidation, J. Mater. Chem. A 2 (2014) 6185. Available from: https://doi.org/10.1039/c3ta14080f.

[64] A.K. Thakur, S.P. Singh, C. Thamaraiselvan, M.N. Kleinberg, C.J. Arnusch, Graphene oxide on laser-induced graphene filters for antifouling, electrically conductive ultrafiltration membranes, J. Membr. Sci. 591 (2019) 117322. Available from: https://doi.org/10.1016/j.memsci.2019.117322.

[65] I. Alam, L.M. Guiney, M.C. Hersam, I. Chowdhury, Application of external voltage for fouling mitigation from graphene oxide, reduced graphene oxide and molybdenum disulfide functionalized surfaces, Environ. Sci. Nano 6 (2019) 925–936. Available from: https://doi.org/10.1039/C8EN01222A.

[66] C.E. Ren, M. Alhabeb, B.W. Byles, M.-Q. Zhao, B. Anasori, E. Pomerantseva, K.A. Mahmoud, Y. Gogotsi, Voltage-gated ions sieving through 2D MXene Ti3C2Tx membranes, ACS Appl. Nano Mater. 1 (2018) 3644–3652. Available from: https://doi.org/10.1021/acsanm.8b00762.

[67] C.M. Werner, K.P. Katuri, A.R. Hari, W. Chen, Z. Lai, B.E. Logan, G.L. Amy, P.E. Saikaly, Graphene-coated hollow fiber membrane as the cathode in anaerobic electrochemical membrane bioreactors – effect of configuration and applied voltage on performance and membrane fouling, Environ. Sci. Technol. 50 (2016) 4439–4447. Available from: https://doi.org/10.1021/acs.est.5b02833.

[68] R.K. Nagarale, G.S. Gohil, V.K. Shahi, Recent developments on ion-exchange membranes and electro-membrane processes, Adv. Colloid Interface Sci. 119 (2006) 97–130. Available from: https://doi.org/10.1016/j.cis.2005.09.005.

[69] K.A. Mauritz, R.B. Moore, State of understanding of nafion, Chem. Rev. 104 (2004) 4535–4586. Available from: https://doi.org/10.1021/cr0207123.

[70] A. Kusoglu, A.Z. Weber, New insights into perfluorinated sulfonic-acid ionomers, Chem. Rev. 117 (2017) 987–1104. Available from: https://doi.org/10.1021/acs.chemrev.6b00159.

[71] Md.M. Hossain, L. Wu, X. Liang, Z. Yang, J. Hou, T. Xu, Anion exchange membrane crosslinked in the easiest way stands out for fuel cells, J. Power Sources 390 (2018) 234–241. Available from: https://doi.org/10.1016/j.jpowsour.2018.04.064.

[72] T. Yamaki, J. Tsukada, M. Asano, R. Katakai, M. Yoshida, Preparation of highly stable ion exchange membranes by radiation-induced graft copolymerization of styrene and bis(vinyl phenyl) ethane into crosslinked polytetrafluoroethylene films, J. Fuel Cell Sci. Technol. 4 (2006) 56–64. Available from: https://doi.org/10.1115/1.2393305.

[73] J. Chen, M. Asano, T. Yamaki, M. Yoshida, Chemical and radiation crosslinked polymer electrolyte membranes prepared from radiation-grafted ETFE films for DMFC applications, J. Power Sources 158 (2006) 69–77. Available from: https://doi.org/10.1016/j.jpowsour.2005.09.024.

[74] E. Güler, R. Elizen, D.A. Vermaas, M. Saakes, K. Nijmeijer, Performance-determining membrane properties in reverse electrodialysis, J. Membr. Sci. 446 (2013) 266–276. Available from: https://doi.org/10.1016/j.memsci.2013.06.045.

[75] M. Svoboda, J. Beneš, L. Vobecká, Z. Slouka, Swelling induced structural changes of a heterogeneous cation-exchange membrane analyzed by micro-computed tomography, J. Membr. Sci. 525 (2017) 195–201. Available from: https://doi.org/10.1016/j.memsci.2016.10.046.

[76] A.E. Kozmai, V.V. Nikonenko, S. Zyryanova, N.D. Pismenskaya, L. Dammak, L. Baklouti, Modelling of anion-exchange membrane transport properties with taking into account the change in exchange capacity and swelling when varying bathing solution concentration and pH, J. Membr. Sci. 590 (2019) 117291. Available from: https://doi.org/10.1016/j.memsci.2019.117291.

[77] N. Kononenko, V. Nikonenko, D. Grande, C. Larchet, L. Dammak, M. Fomenko, Y. Volfkovich, Porous structure of ion exchange membranes investigated by various techniques, Adv. Colloid Interface Sci. 246 (2017) 196–216. Available from: https://doi.org/10.1016/j.cis.2017.05.007.

This book belongs to Badji Mokhtar Annaba University Central Library Copyright Elsevier 2025

[78] Khoiruddin, D. Ariono, Subagjo, I.G. Wenten, Surface modification of ion-exchange membranes: methods, characteristics, and performance, J. Appl. Polym. Sci. 134 (2017) 45540. Available from: https://doi.org/10.1002/app.45540.
[79] V.I. Zabolotskii, R.K. Chermit, M.V. Sharafan, Mass transfer mechanism and chemical stability of strongly basic anion-exchange membranes under overlimiting current conditions, Russ. J. Electrochem. 50 (2014) 38–45. Available from: https://doi.org/10.1134/S102319351401011X.
[80] X.T. Le, P. Viel, P. Jégou, A. Garcia, T. Berthelot, T.H. Bui, S. Palacin, Diazonium-induced anchoring process: an application to improve the monovalent selectivity of cation exchange membranes, J. Mater. Chem. 20 (2010) 3750–3757. Available from: https://doi.org/10.1039/B918915G.
[81] M. Amara, H. Kerdjoudj, Modification of cation-exchange membrane properties by electro-adsorption of polyethyleneimine, Desalination 155 (2003) 79–87. Available from: https://doi.org/10.1016/S0011-9164(03)00241-8.
[82] L. Ge, B. Wu, D. Yu, A.N. Mondal, L. Hou, N.U. Afsar, Q. Li, T. Xu, J. Miao, T. Xu, Monovalent cation perm-selective membranes (MCPMs): new developments and perspectives, Chin. J. Chem. Eng. 25 (2017) 1606–1615. Available from: https://doi.org/10.1016/j.cjche.2017.06.002.
[83] T. Luo, S. Abdu, M. Wessling, Selectivity of ion exchange membranes: a review, J. Membr. Sci. 555 (2018) 429–454. Available from: https://doi.org/10.1016/j.memsci.2018.03.051.
[84] Y. Zhao, J. Zhu, J. Ding, B. Van der Bruggen, J. Shen, C. Gao, Electric-pulse layer-by-layer assembled of anion exchange membrane with enhanced monovalent selectivity, J. Membr. Sci. 548 (2018) 81–90. Available from: https://doi.org/10.1016/j.memsci.2017.11.007.
[85] E.F. Abdrashitov, V.C. Bokun, Y.A. Dobrovolsky, D.A. Kritskaya, E.A. Sanginov, A.N. Ponomarev, Modification of the proton conducting membranes of MF-4SC with a carbon phase via gamma-initiated graft polymerization of vinyliden chloride, Solid. State Ion 188 (2011) 140–143. Available from: https://doi.org/10.1016/j.ssi.2010.09.026.
[86] A. Filippov, D. Afonin, N. Kononenko, S. Shkirskaya, Characterization of perfluorinated cation-exchange membranes MF-4SC surface modified with halloysite nanotubes, in: AIP Conference Proceedings. 1684 (2015) 030004. <https://doi.org/10.1063/1.4934288>.
[87] N.P. Berezina, N.A. Kononenko, O.A. Dyomina, N.P. Gnusin, Characterization of ion-exchange membrane materials: properties vs structure, Adv. Colloid Interface Sci. 139 (2008) 3–28. Available from: https://doi.org/10.1016/j.cis.2008.01.002.
[88] H.Y. Hwang, H.C. Koh, J.W. Rhim, S.Y. Nam, Preparation of sulfonated SEBS block copolymer membranes and their permeation properties, Desalination 233 (2008) 173–182. Available from: https://doi.org/10.1016/j.desal.2007.09.040.
[89] Y.A. Elabd, M.A. Hickner, Block copolymers for fuel cells, Macromolecules 44 (2011) 1–11. Available from: https://doi.org/10.1021/ma101247c.
[90] M. Nishimura, Y. Mizutani, Correlation between structure and properties of cation-exchange membranes prepared by the paste method, J. Appl. Electrochem. 11 (1981) 165–171. <https://doi.org/10.1007/BF00610976>.
[91] D.V. Golubenko, A.B. Yaroslavtsev, New approach to the preparation of grafted ion exchange membranes based on UV-oxidized polymer films and sulfonated polystyrene, Mendeleev Commun. 27 (2017) 572–573. Available from: https://doi.org/10.1016/j.mencom.2017.11.011.
[92] M.M. Nasef, S.A. Gürsel, D. Karabelli, O. Güven, Radiation-grafted materials for energy conversion and energy storage applications, Prog. Polym. Sci. 63 (2016) 1–41. Available from: https://doi.org/10.1016/j.progpolymsci.2016.05.002.
[93] M.M. Nasef, E.-S.A. Hegazy, Preparation and applications of ion exchange membranes by radiation-induced graft copolymerization of polar monomers onto non-polar films, Prog. Polym. Sci. 29 (2004) 499–561. Available from: https://doi.org/10.1016/j.progpolymsci.2004.01.003.
[94] S. Sadeghi, L. Işıkel Şanlı, E. Güler, S. Alkan Gürsel, Enhancing proton conductivity via sub-micron structures in proton conducting membranes originating from sulfonated PVDF powder by radiation-induced grafting, Solid State Ion 314 (2018) 66–73. Available from: https://doi.org/10.1016/j.ssi.2017.11.017.

This book belongs to Badji Mokhtar Annaba University Central Library Copyright Elsevier 2025

[95] S. Hasegawa, A. Hiroki, Y. Ohta, N. Iimura, A. Fukaya, Y. Maekawa, Thermally stable graft-type polymer electrolyte membranes consisting based on poly (ether ether ketone) and crosslinked graft-polymers for fuel cell applications, Radiat. Phys. Chem. 171 (2020) 108647. Available from: https://doi.org/10.1016/j.radphyschem.2019.108647.
[96] A.B. Yaroslavtsev, Y.P. Yampolskii, Hybrid membranes containing inorganic nanoparticles, Mendeleev Commun. 24 (2014) 319–326. Available from: https://doi.org/10.1016/j.mencom.2014.11.001.
[97] T. Xu, Ion exchange membranes: state of their development and perspective, J. Membr. Sci. 263 (2005) 1–29. Available from: https://doi.org/10.1016/j.memsci.2005.05.002.
[98] S. Subianto, M. Pica, M. Casciola, P. Cojocaru, L. Merlo, G. Hards, D.J. Jones, Physical and chemical modification routes leading to improved mechanical properties of perfluorosulfonic acid membranes for PEM fuel cells, J. Power Sources 233 (2013) 216–230. Available from: https://doi.org/10.1016/j.jpowsour.2012.12.121.
[99] H. Wang, X. Li, X. Zhuang, B. Cheng, W. Wang, W. Kang, L. Shi, H. Li, Modification of nafion membrane with biofunctional SiO_2 nanofiber for proton exchange membrane fuel cells, J. Power Sources 340 (2017) 201–209. Available from: https://doi.org/10.1016/j.jpowsour.2016.11.072.
[100] Y. Patil, K.A. Mauritz, Durability enhancement of Nafion® fuel cell membranes via in situ sol-gel-derived titanium dioxide reinforcement, J. Appl. Polym. Sci. 113 (2009) 3269–3278. Available from: https://doi.org/10.1002/app.30195.
[101] C.W. Lin, Y.S. Lu, Highly ordered graphene oxide paper laminated with a Nafion membrane for direct methanol fuel cells, J. Power Sources 237 (2013) 187–194. Available from: https://doi.org/10.1016/j.jpowsour.2013.03.005.
[102] L. Wang, J. Kang, J.-D. Nam, J. Suhr, A.K. Prasad, S.G. Advani, Composite membrane based on graphene oxide sheets and nafion for polymer electrolyte membrane fuel cells, ECS Electrochem. Lett. 4 (2015) F1. Available from: https://doi.org/10.1149/2.0021501eel.
[103] R. Asmatulu, A. Khan, V.K. Adigoppula, G. Hwang, Enhanced transport properties of graphene-based, thin Nafion® membrane for polymer electrolyte membrane fuel cells, Int. J. Energy Res. 42 (2018) 508–519. Available from: https://doi.org/10.1002/er.3834.
[104] E.Y. Voropaeva, E.A. Sanginov, V.I. Volkov, A.A. Pavlov, A.S. Shalimov, I.A. Stenina, A.B. Yaroslavtsev, Transport properties of MF-4SK membranes modified with inorganic dopants, Russ. J. Inorg. Chem. 53 (2008) 1536–1541. Available from: https://doi.org/10.1134/S0036023608100021.
[105] C.Y. Wong, W.Y. Wong, K. Ramya, M. Khalid, K.S. Loh, W.R.W. Daud, K.L. Lim, R. Walvekar, A.A.H. Kadhum, Additives in proton exchange membranes for low- and high-temperature fuel cell applications: a review, Int. J. Hydrog. Energy 44 (2019) 6116–6135. Available from: https://doi.org/10.1016/j.ijhydene.2019.01.084.
[106] N. Shaari, S.K. Kamarudin, Recent advances in additive-enhanced polymer electrolyte membrane properties in fuel cell applications: an overview, Int. J. Energy Res. 43 (2019) 2756–2794. Available from: https://doi.org/10.1002/er.4348.
[107] Z. Wang, J. Ma, C.Y. Tang, K. Kimura, Q. Wang, X. Han, Membrane cleaning in membrane bioreactors: a review, J. Membr. Sci. 468 (2014) 276–307. Available from: https://doi.org/10.1016/j.memsci.2014.05.060.
[108] D. Hou, D. Jassby, R. Nerenberg, Z.J. Ren, Hydrophobic gas transfer membranes for wastewater treatment and resource recovery, Environ. Sci. Technol. 53 (2019) 11618–11635. Available from: https://doi.org/10.1021/acs.est.9b00902.
[109] J. Sun, Q. Wang, J. Zhang, Z. Wang, Z. Wu, Degradation of sulfadiazine in drinking water by a cathodic electrochemical membrane filtration process, Electrochim. Acta 277 (2018) 77–87. Available from: https://doi.org/10.1016/j.electacta.2018.05.005.
[110] M. Li, K. Zuo, S. Liang, K. Xiao, P. Liang, X. Wang, X. Huang, Electrically Tuning Ultrafiltration Behavior for Efficient Water Purification, Environ. Sci. Technol. 54 (2020) 11536–11545. Available from: https://doi.org/10.1021/acs.est.0c02441.
[111] C. He, J. Ma, C. Zhang, J. Song, T.D. Waite, Short-circuited closed-cycle operation of flow-electrode CDI for Brackish water softening, Environ. Sci. Technol. 52 (2018) 9350–9360. Available from: https://doi.org/10.1021/acs.est.8b02807.
[112] M.A. Ahmed, S. Tewari, Capacitive deionization: processes, materials and state of the technology, J. Electroanalytical Chem. 813 (2018) 178–192. Available from: https://doi.org/10.1016/j.jelechem.2018.02.024.

This book belongs to Badji Mokhtar Annaba University Central Library Copyright Elsevier 2025

[113] H. Strathmann, Electrodialysis, a mature technology with a multitude of new applications, Desalination 264 (2010) 268–288. Available from: https://doi.org/10.1016/j.desal.2010.04.069.
[114] A. Hassanvand, K. Wei, S. Talebi, G. Chen, S. Kentish, The role of ion exchange membranes in membrane capacitive deionisation, Membranes 7 (2017) 54. Available from: https://doi.org/10.3390/membranes7030054.
[115] J. Ma, C. He, D. He, C. Zhang, T.D. Waite, Analysis of capacitive and electrodialytic contributions to water desalination by flow-electrode CDI, Water Res. 144 (2018) 296–303. Available from: https://doi.org/10.1016/j.watres.2018.07.049.

This book belongs to Badji Mokhtar Annaba University Central Library Copyright Elsevier 2025

CHAPTER FOUR

Electrified carbon nanotube membrane technology for water treatment

Yanbiao Liu[1], Yifan Ren[1] and Shijie You[2]
[1]Textile Pollution Controlling Engineering Center of Ministry of Environmental Protection, College of Environmental Science and Engineering, Donghua University, Shanghai, P.R. China
[2]State Key Laboratory of Urban Water Resource and Environment, School of Environment, Harbin Institute of Technology, Harbin, P.R. China

4.1 Introduction

There is an urgent demand for developing advanced water and wastewater treatment technologies toward their practical environmental applications to alleviate the challenge of the water pollution crisis [1,2]. The situation may be aggravated if no sustainable and innovative solutions can be provided. Extensive researches suggest that membrane technology may serve as a viable solution for providing clean and safe water, reducing the adverse environmental impacts of industrial and everyday activities, and securing a clean water supply [3]. However, the removal of emerging toxic contaminants with low molecular weight and given theirs being neutrally charged, it is still challenging to combat the water pollution crisis with the current membrane materials, due to the limitations of conventional size- and charge-exclusion separation mechanisms [4]. In addition, interactions of organic molecules, inorganic salts, and microorganisms with the membrane surface inevitably lead to membrane fouling, which deteriorates the process performance and shortens the membrane lifetime [5,6]. These challenges have spurred on ahead the development of membrane technology with strengthened multifunctionality including the antifouling property.

Recently, the electrochemical membrane (EM) technology, integrating electrochemistry and membrane separation processes, has attracted much interest from the scientific community [7–10]. Compared with the traditional membrane delivering the solute separation via the steric hindrance and the charge exclusion, EM adds additional functionalities by exploiting a variety of electrochemical phenomena, including oxidation and reduction as well as electrostatic adsorption and rejection, etc. [11–13]. EM entails the fabrication of the membrane's active layers with high electrical conductivity and porosity. Among electrically conductive materials (e.g., boron-doped diamond, BDD [14], and substoichiometry titanium oxide, Ti_4O_7 [15], and CNT [16]), CNT has gained the utmost attention due to their intriguing attributes. For example, these

Electrochemical Membrane Technology for Water and Wastewater Treatment.
DOI: https://doi.org/10.1016/B978-0-12-824470-8.00013-9
© 2022 Elsevier Inc.
All rights reserved.

This book belongs to Badji Mokhtar Annaba University Central Library
Copyright Elsevier 2025

1D CNT can form conductive and robust 3D network by vacuum filtration, which enables a flow-through operation by serving as both active electrode and filtration media simultaneously [17,18]. Liu et al. [19] developed a flow-through electro-Fenton system based on the electrochemical CNT filter functionalized with atomically precise Au nanoclusters for the efficient degradation of the antibiotic tetracycline. The integration of electrochemistry in membranes combines separation and electrochemical processes into a single operational unit [20]. Such hybrid designs show a unique synergism between two cleaning processes of different mechanisms. The flow-through electrode can boost electrochemical reaction kinetics via the convection-enhanced mass transport and direct electrolysis degrading of foulants [21,22]. Overall, the EM is expected to reduce the process footprint with increased processing kinetics and decreased energy consumption.

This chapter aims to highlight the synergistic effects of membrane separation and electrochemistry on environmental applications using CNT as a model EM material. The intriguing physicochemical characteristics of CNT-based EM materials coupled with advanced reactor design offer promising solutions for the existing electrochemical water treatment strategies. We first summarize the fabrication protocols of CNT-based EM. We then focus on the delicate design of several different electrochemical filtration systems based on anodic oxidation or cathodic reduction reactions. The underlying working mechanism of each system is systematically reviewed. The technological limitations and future perspectives of this novel technology toward the practical applications in water treatment are also discussed.

4.2 Fabrication of electroactive membranes

Various organic and/or inorganic conductive materials, such as conductive polymers, metals and their oxides, and/or carbon-based materials [12,23], can be used to fabricate EM. The performance of an EM is closely correlated to the structure and physicochemical properties of the active components. This chapter mainly discusses the fabrication of CNT-based EM.

CNT can be visualized as nanoscale cylinders formed by rolled-up graphene sheets [24]. Structurally, CNT has the perfect crystal structure with all carbons bonded in a hexagonal lattice except at their ends, where structural defects can be found. Defects, such as pentagons, heptagons, and other imperfections in the sidewalls, cause less desired physicochemical properties [25]. The CNT is adopted as the most common conductive materials for EM fabrication due to their well-defined 1D morphology, good chemical stability, good mechanical strength, and the capability to form an intertwined compact network with high electric

This book belongs to Badji Mokhtar Annaba University Central Library Copyright Elsevier 2025

conductance and porosity [22,26]. As regards its physicochemical properties, the combination of large specific surface area (30–500 m^2/g) and high electric conductivity (10^4–10^6 S/m) of the EM enables simultaneous adsorption and electrochemical degradation of organic pollutants on-site [27,28]. Concerning design, both single-walled CNT (SWCNT) and multiwalled CNT (MWCNT) can be used for the electro-filtration purpose. SWCNT is characterized by the small diameter, tunable electric properties (from semiconducting to metallic, relying on chirality), and superior thermal and mechanical properties [29]. On the other hand, MWCNT is composed of a series of co-axial SWCNT. MWCNT exhibits unique electronic properties determined by the chirality of SWCNT [30]. Moreover, the SWCNT revealed the highest conductance of water molecules due to its lowest hydrophobic characteristics on the nanotubular walls [31]. In addition, the higher specific surface area of SWCNT helps to adsorb more pollutants. Kim et al. [32] reported that SWCNT had a greater efficiency than the MWCNT had for antibiotics degradation.

The CNT EM can be produced from either the vertically aligned CNT array or the nonwoven matrix membrane [33]. The primary objective to the goal of facilitating antifouling in membranes using CNT is to increase membrane conductivity. This will be able to facilitate fouling prevention or membrane remediation/recovery through applying a constant or intermittent voltage bias. In addition to this, the CNT-based EM can also increase the liquid flux and the ion-selectivity with additional chemical functionality and improved mechanical properties while maintaining high efficiency. To prepare the CNT-based EM, for the aligned CNT membrane, nanotubes are arranged perpendicularly to the substrate (Fig. 4.1A) [34], conducting "superfast water transport" through the inside channels of the CNT. However, it's usually more expensive with its being associated with the delicate fabrication process. Alternatively, a nonwoven matrix CNT membrane can be facilely fabricated by dispersing the CNT into a membrane casting solution to prepare a hybrid membrane with irregular CNT distributions (Fig. 4.1B). As far as mixed matrix membranes are concerned, these can be prepared by either a classical phase inversion process or a simple solution casting process. The rich surface chemistry of CNT also enables further surface chemical modifications (Fig. 4.1C). Vacuum filtration is another commonly adopted low-cost, but reliable, method for depositing a thin CNT layer onto the polytetrafluoroethylene (PTFE) or polyvinylidene fluoride substrates. For example, Wu et al. [35] produced a thin film composite nanofiltration membrane by incorporating a thin hydrophilic MWCNT interlayer between the microfiltration membrane support and the dense polyamide layer created by interfacial polymerization. The MWCNT interlayer can absorb and store the aqueous amino solution to facilitate the subsequent interfacial polymerization. It also provides robust mechanical support for the thin skin layer on the microporous substrate to facilitate the nanofiltration (Fig. 4.1D). The nanostructured interlayer is important for the membrane structure and performance. Moreover,

This book belongs to Badji Mokhtar Annaba University Central Library Copyright Elsevier 2025

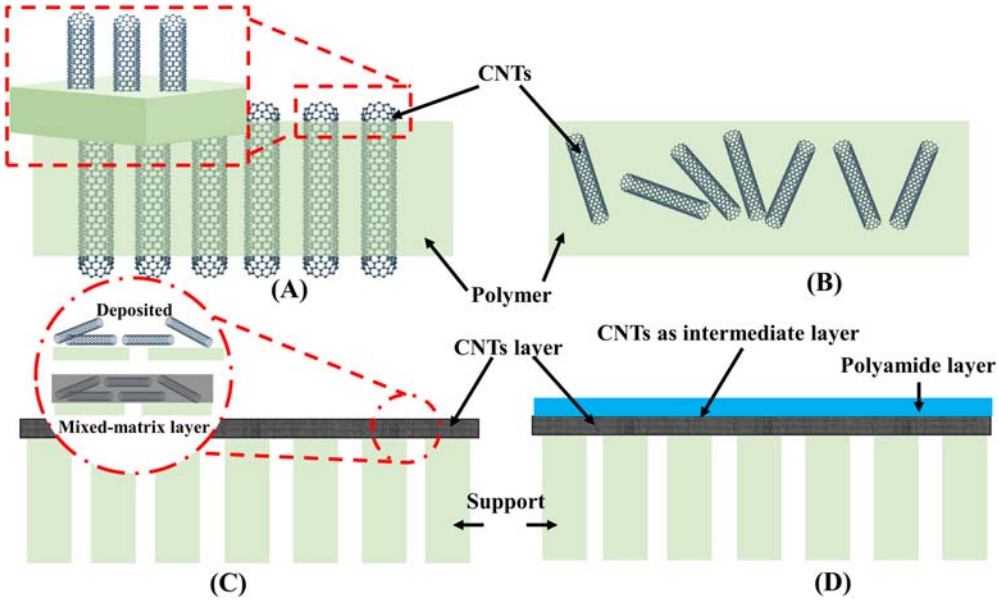

Figure 4.1 Carbon nanotube (CNT) membranes with various structures. (A) Vertically aligned CNT membrane, (B) mixed-matrix CNT membrane, (C) CNT are coated on membrane surface or support, (D) CNT are coated on membrane surface (support) as intermediate layer. *Reprinted (adapted) with permission from M. Sianipar, S.H. Kim, K. Khoiruddin, F. Iskandar, I.G. Wenten, Functionalized carbon nanotube (CNT) membrane: progress and challenges, RSC Adv. 7 (2017) 51175–51198. Copyright 2017 Royal Society of Chemistry.*

water permeation flux is greatly improved without a decrease in salt rejection performance.

To modify CNT-based EM, chemical treatment introduces extra functional groups onto the CNT surface. For example, various hydroxyl and carboxylic functional groups are grafted onto the CNT surface after the treatment with concentrated HNO_3 at 70 °C for 12 h [36]. These oxygen-containing groups have a high affinity to metal ions, which improves the anchoring of various metal ions and/or metal oxides. Liu et al. [37] employed a simple steam hydrolysis approach to coat a thin layer of nanoscale TiO_2 on the preformed CNT filter. The 3D CNT networks maintained superior electric conductivity while providing more active sites to anchor the TiO_2 nanoparticles. For the decontamination of arsenic (As) in water, this TiO_2 modified, hybrid CNT filter showed an increased As(V) and As(III) sorption efficiency by 63% and 12.5%, respectively, with a bias of 2 V with respect to that at 0 V. The observation quantitatively demonstrated the advantages of integration of electrochemistry with membrane filtration functionality. Meanwhile, Zheng et al. [38] developed the CNT filter modified with nanoscale zero-valent copper by reducing the adsorbed Cu^{2+} with $NaBH_4$. The metallic copper-CNT hybrid filter was applied for the in situ

This book belongs to Badji Mokhtar Annaba University Central Library Copyright Elsevier 2025

electrochemical peroxymonosulfate (PMS) activation, achieving excellent degradation kinetics for Congo red due to the boosted redox cyclic kinetics of Cu^{2+}/Cu^{+} controlled by an external electric field. In addition, the multifunctionality of metal oxides can be readily explored in a variety of environmental applications, such as selective chemical sensing for environmental pollutants and catalytic decomposition of pollutants [39,40]. In addition, the delicately designed functional hybrid membranes offer fine control of the chemistry involved since the physicochemical properties of hybrid membranes can be precisely controlled by tailoring these to the attributes of CNT and metal oxides in terms of size, structure, shape, composition, and surface chemistry [41,42].

4.3 Reactor configuration

Currently, most of the electrodes used are conventional plate implemented in parallel plate reactors, for which mass transport of water is severely limited by the diffusion through a thick (10–100 mm) stagnant boundary layer [22]. The possibility to reach high current efficiency depends mainly on the implementation of a preconcentration step by adsorption or filtration [43]. It has been shown that the most promising way to avoid diffusion/mass transfer limitations and to increase the electroactive surface area is to adapt porous electrodes in a flow-through configuration [44,45]. Recent work has also transformed traditional separation membranes into reactive membranes, known as EM, which further expand the application of electrochemical technologies with combined functions of filtration, adsorption, and electrochemical degradation of contaminants [46].

The CNT-based membrane is one of the best investigated EM. A general organic degradation mechanism from an electroactive CNT membrane usually involves four primary steps: (1) mass transfer of organic molecules to the CNT membrane, (2) adsorption and desorption on the CNT membrane, (3) direct electron transfer under electric field, and (4) bulk chemical reactions preceding the subsequent electron transfer [22]. Although direct or indirect electron transfer in steps (3) and (4) is immediately responsible for electrochemical reactions, mass transfer to the CNT membrane surface in step (1) is often identified to be the overall rate-limiting step [47,48].

Electrochemical filtration, combining membrane filtration with electrooxidation, offers an alternative technology for a flow-through mode. In this case, the boundary layer thickness could be significantly minimized to less than 1 μm, due to convection-enhanced mass transport of liquid with the target compounds toward the active sites on the membrane surface. The benefits of the flow-through configuration (Fig. 4.2) on both kinetics and efficiencies can be attributed to the convective enhancement of mass transport to and from the electrode surface. The rapid convective replenishment also promotes direct electron transfer to the target species that can result in enhanced current and energy efficiencies. For example, the flow-through design outperformed

This book belongs to Badji Mokhtar Annaba University Central Library Copyright Elsevier 2025

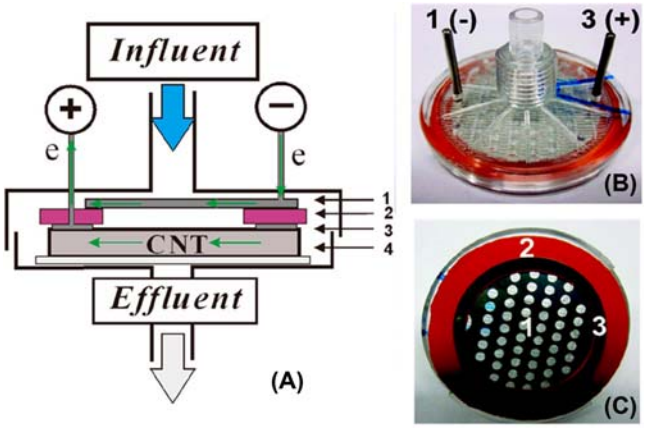

Figure 4.2 Depiction and images of the electrochemical filtration apparatus. (A) Design of the modified commercial polycarbonate filtration casing consisting of (1) a perforated stainless steel cathode, (2) an insulating silicone rubber separator and seal, (3) a titanium anodic ring that is pressed into the carbon nanotube anodic filter, and (4) the carbon nanotube anodic filter supported by a polytetrafluoroethylene membrane. (B), (C) Images of the modified filtration casing. *Reprinted (adapted) with permission from C.D. Vecitis, G.D. Gao, H. Liu, Electrochemical carbon nanotube filter for adsorption, desorption, and oxidation of aqueous dyes and anions, J. Phys. Chem. C. 115 (2011) 3621–3629. Copyright 2011, American Chemical Society.*

the conventional batch system, indicated by an increase of threefold and twofold in the tetracycline removal kinetics and degradation efficiency, respectively [19].

4.4 Environmental applications of electrochemical CNT membranes

The EM has been demonstrated a promising technology through the integration of electrochemistry, membrane separation, and advanced oxidation processes (Fig. 4.3A and B) [16]. An exhaustively large number of studies suggest that the EM is capable of degrading and transforming an array of organic pollutants into nontoxic substances achieving complete mineralization. Thus the need for posttreating of the waste streams is minimized. In the following section, we will exemplify a few successful environmental applications such as the degradation of organic compounds, the decontamination of toxic inorganic contaminants, and the mitigation of membrane fouling.

4.4.1 Degradation of organic contaminants

Decontamination mechanisms by a CNT-based EM mainly involve electrochemical oxidation, while electro-sorption and electro-repulsion may also contribute to the pollutant

This book belongs to Badji Mokhtar Annaba University Central Library Copyright Elsevier 2025

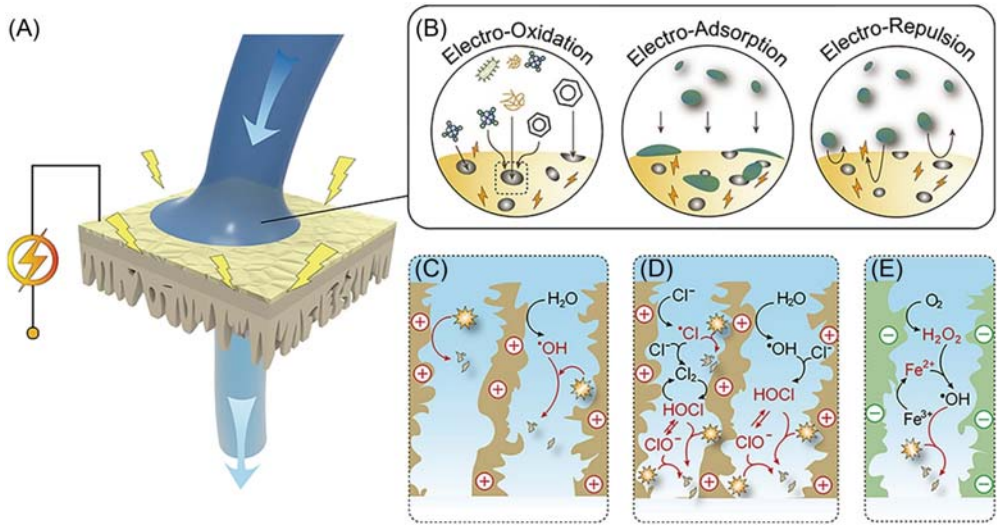

Figure 4.3 Electrified membrane (EM) filtration for water decontamination and purification. (A) Schematic diagram illustrating decontamination by EM filtration. (B) When voltage is applied, EM interacts with contaminants via electro-oxidation, electrostatic adsorption, and electrostatic repulsion, among which electro-oxidation is predominantly responsible for water decontamination. The indirect electro-oxidation process is categorized according to the main oxidation mechanisms: (C)•OH-mediated anodic oxidation, (D) active-chlorine-mediated oxidation, and (E) electro-Fenton process. *Reprinted (adapted) with permission from M. Sun, X.H. Wang, L.R. Winter, Y.M. Zhao, W. Ma, T. Hedtke, et al., Electrified membranes for water treatment applications, ACS EST. Eng. 1 (2021) 725–752. Copyright 2021 American Chemical Society.*

removal (Fig. 4.3B) [49,50]. For the physical adsorption, the CNT with a high-aspect-ratio can easily form the free-standing or porous 3D networks. The electrochemical CNT membranes have demonstrated the capability of degrading several refractory compounds (e.g., azo dyes like methylene blue and methyl orange) and emerging biochemical contaminants (e.g., antibiotics like tetracycline, 4-epianhydrochlortetracycline [51,52], and amoxicillin [53]; phenolic compounds like phenol and bisphenol A [54,55]) involving direct electron-transfer (direct electro-oxidation) or indirect generation of reactive species (e.g., •OH, $HO_2^{\bullet-}$, $Cl^{\bullet}$, $SO_4^{\bullet-}$) (indirect electro-oxidation) [44,56].

4.4.1.1 Direct electro-oxidation of contaminants

Direct electro-oxidation, that is, electrons transferring directly from the micropollutant to the anode surface, is effective for the selective degradation of organics that are readily donating electrons [57,58]. For example, in Fig. 4.4A, the primary oxidation mechanism for methyl orange over a range of low anode potentials (0.4–1 V vs SCE) was determined to be direct oxidation. When the anode potential was greater than 1.0 V versus SCE, indirect oxidation was observed the predominant method instead.

This book belongs to Badji Mokhtar Annaba University Central Library Copyright Elsevier 2025

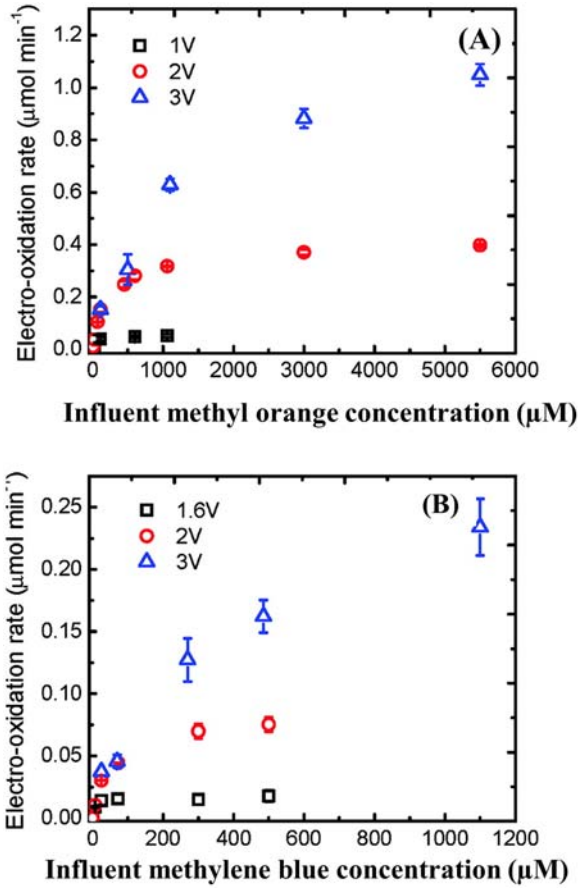

Figure 4.4 Concentration dependent oxidation of methyl orange and methylene blue during electrochemical filtration. (A) Methyl orange and (B) Methylene blue. *Reprinted (adapted) with permission from H. Liu, C.D. Vecitis, Reactive transport mechanism for organic oxidation during electrochemical filtration: mass-transfer, physical adsorption, and electron-transfer, J. Phys. Chem. C. 116 (2011) 374–383. Copyright 2012 American Chemical Society.*

The mechanism switch indicates the change from the mass transfer limiting regime to the electron transfer limiting regime. Interestingly, under similar experimental conditions, the maximum electro-oxidation rates for different contaminants with similar oxidation potentials but opposite charges were significantly different. The degradation rates for positively charged methylene blue were threefold to fivefold less than that for negatively charged methyl orange (Fig. 4.4B). The different oxidation behaviors could be the result of the electromigration effect. With a positive potential, the CNT anodic filter becomes positively charged, which selectively attracts those negatively-charged

This book belongs to Badji Mokhtar Annaba University Central Library Copyright Elsevier 2025

molecules rather than those positively charged ones. This explains why electro-sorption and electrorepulsion can strongly affect the direct electron transfer rates.

4.4.1.2 Indirect electro-oxidation of contaminants

Another major mechanism for contaminant degradation by EM is via indirect generation of oxidizing free radicals (e.g., •OH, $HO_2^{\bullet-}$, $Cl^{\bullet}$, $SO_4^{\bullet-}$) that usually allows non-selective pollutant degradation under an electric field (Fig. 4.3C-E) [59].

4.4.1.2.1 Anodic •OH-mediated decontamination

Hydroxyl radical (•OH) mediated oxidation is the most widely explored pathway for water decontamination by EM filtration. Anodic membrane filtration directly oxidizes water molecules to produce •OH electrochemically without the addition of chemicals (Fig. 4.3C). •OH, the most potent reactive oxygen species has a high standard potential (2.80 V vs SHE) [60], which enables the nonselective and complete oxidation of most organic contaminants. Performance-wise, the water decontamination efficiency of such an EM filtration system depends on the type of anodic membrane material used and the applied voltage. However, the CNT electrode suffers from a low oxygen evolution potential (OEP) [61], which may lead to poor current efficiency at the elevated anode potentials. To further improve the electrochemical property of the CNT EM, it is important to perform surface modification with other nanomaterials with elevated OEP. Yanez et al. [42] reported the zero-valent iron nanoparticle modified CNT membrane electrode, which offered an enhanced electro-oxidation performance with decontamination efficiency of 97% with respect to 74% from the pristine CNT at an applied potential of 1.0 V. Likewise, other nanoparticles with higher OEP can also be used for the modification of CNT to improve the current efficiency and electrode stability. A facile electro-sorption-hydrothermal strategy was developed to deposit a nanometer-thin layer of SnO_2 or doped-SnO_2 nanoparticles onto the CNT membrane [61]. Electrochemical characterizations of the modified electrode material confirmed that the stability of the composite membrane was indeed improved after the modification, with an increase in oxygen evolution potential from 1.27 V (vs Ag/AgCl) of CNT to 1.71 V (vs Ag/AgCl) of Bi-SnO_2-CNT. In addition, doping of boron or nitrogen into CNT could also change their electronic structures, which in turn affect the electrochemical activity of the CNT, as well as changing the conductivity and specific capacitance of the CNT, which are directly related to their electrochemical performances.

In addition to focusing on the anodic oxidation of organic contaminants, the role of a cathode in an electrochemical filter beyond a counter electrode also has been investigated. For example, Yang et al. [51] reported that the electrochemical CNT filter could rapidly decontaminate 4-epianhydrochlortetracycline in water. Under the optimal experimental conditions (e.g., $[\text{4-epianhydrochlortetracycline}]_0 = 10\ \mu\text{mol/L}$, $E_{cell} = 2.5$ V, and flow rate = 1.5 mL/min), an electrochemical 4-epianhydrochlortetracycline oxidative flux of

This book belongs to Badji Mokhtar Annaba University Central Library Copyright Elsevier 2025

1251 ± 28 μmol/(h · m^2) was achieved with >98% degradation efficiency (Fig. 4.5A). The current density with a solid Ti cathode or a porous CNT cathode was 0.85 or 1.27 mA/cm^2, respectively. The study suggested that a CNT network cathode, with an increased specific surface area and a cathodic catalytic capability, improves cell performance compared with the conventional counterpart of titanium (Fig. 4.5B). These promising results suggest that the electroactive CNT membrane technology may provide an effective strategy for the rapid degradation of organic contaminants by integrating electrochemistry, nanofiltration, and advanced oxidation processes.

4.4.1.2.2 Active-chlorine-mediated decontamination

Due to the ubiquity of chloride ions (Cl^-) in natural waters and wastewater effluents, anodic membrane filtration can oxidize chloride into active chlorine, thus enabling water decontamination. Active chlorine includes the potent reactive chlorine species, such as Cl• (2.40 V vs SHE), and free chlorine, namely Cl_2 (1.36 V vs SHE), HClO (1.49 V vs SHE), and ClO^- (0.89 V vs SHE) [44,62]. The formation of active chlorine can occur with or without the involvement of •OH. Specifically, Cl^- first undergoes oxidation at the anodic membrane surface to form the Cl•, which are combined to form Cl_2. The subsequent disproportionation of Cl_2 generates HClO and ClO^- (Fig. 4.3D, left pathway). Alternatively, anodically generated •OH can directly react with Cl^- to form HClO, ClO^-, and other reactive chlorine species (Fig. 4.3D, right pathway) [43,63]. Both "active" and "nonactive" anodes can be used for active-chlorine-mediated decontamination. In Fig. 4.3D, the"active" anodes mostly perform the left pathway due

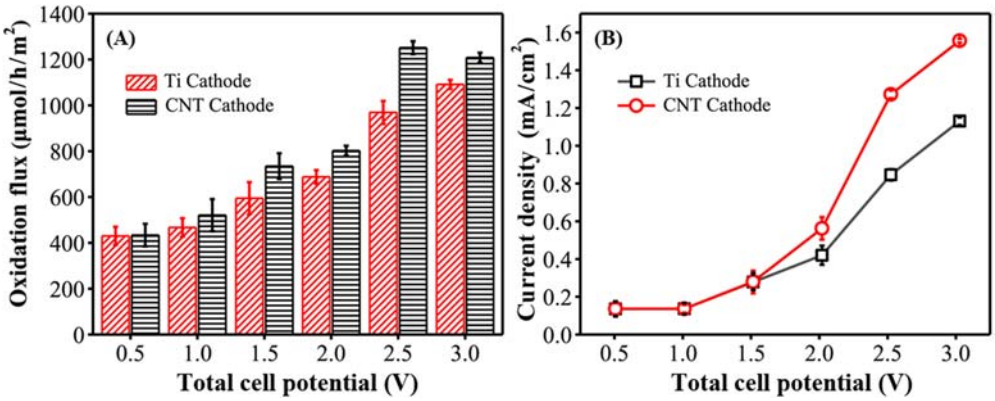

Figure 4.5 Comparative performance of CNT network cathode to conventional Titanium cathode (A) 4-epianhydrochlortetracycline electro-oxidative flux as a function of overall cell potential, and (B) current density as a function of total cell potential and cathode material. *Reprinted (adapted) with permission from S.N. Yang, Y.B. Liu, C.S. Shen, F. Li, B. Yang, M.H. Huang, et al., Rapid decontamination of tetracycline hydrolysis product using electrochemical CNT filter: mechanism, impacting factors and pathways, Chemosphere 244 (2020) 125525. Copyright 2020, Elsevier.*

This book belongs to Badji Mokhtar Annaba University Central Library Copyright Elsevier 2025

to the absence of •OH, while for the "nonactive" anodes, both pathways take place. In addition to the material used for the anode, other factors such as the side reactions, solution pH, and water flux also influence the active-chlorine formation in the EM. Water oxidation is the main side reaction competing with chloride oxidation. Additionally, the formation of weak oxidants, that is, oxychlorides in higher oxidation states (e.g., ClO_3^- and ClO_4^-), reduces the amount of the effective active chlorine [64,65]. Wang et al. [66] utilized an electrochemical approach with in situ generations of reactive chlorine species through the anodization of chloride ions for carbamazepine degradation. A hybridized, CNT-functionalized ceramic membrane with high hydrophilicity, permeability, and conductivity was fabricated. The rapid and complete degradation of carbamazepine in single-pass ultrafiltration indicates a highly localized concentration of reactive chlorine species existed within the three-dimensional porous CNT interwoven layer. The fouled membrane exhibited a nearly complete water flux recovery following a short (1 min) self-cleaning process with an applied voltage of 3 or 4 V and the feed solutions of 100 or 10 mmol/L sodium chloride, respectively.

4.4.1.2.3 Electro-Fenton driven decontamination

Besides anodic oxidation of water contaminants, the cathodic reduction is another important mechanism for the degradation of pollutants. However, it is often overlooked within an electrochemical system. Because the cathode provides electrons for the reduction reaction, it cannot be directly used to oxidize hydrocarbon pollutants. The CNT can serve as an excellent catalyst for the oxygen reduction reaction, which supports a two-electron oxygen reduction reaction to produce H_2O_2 by reducing dissolved O_2 [see Eq. (4.1)].

$$O_2 + 2H^+ + 2e^- \rightarrow H_2O_2 \quad E = 0.695V \text{ vs SHE} \tag{4.1}$$

With moderate oxidation potential ($E_0 = 1.76$ V vs SHE), H_2O_2 can directly oxidize some organic pollutants. For example, phenol can be effectively degraded (>98%) through a single-pass mode of the electrochemical CNT membrane ($\tau = 2$ s) at a cathode potential of -0.4 V versus Ag/AgCl. Its oxidation rate could be directly correlated with the H_2O_2 flux [28]. In contrast, in a conventional batch reactor, an inappreciable decrease in the phenol concentration was observed after 2 h using H_2O_2 alone, indicating the inability of H_2O_2 to oxidize phenol efficiently in a conventional batch system. Additionally, the removal of 0.53 mmol/L phenol by adsorption was achieved in less than 30 min in a filtration system with only CNT. However, the adsorbed phenol could occupy all the reactive surface sites. Therefore physisorption alone with the CNT filters has limited capacity and is not sustainable for wastewater treatment. The H_2O_2 reactivity was increased in a flow-through system, which is hypothesized to be the result of the local regions of high [H_2O_2] or extreme pH/pE fluctuations accessed by passing through phenol.

To boost the oxidation strength of H_2O_2 further, the functionalization of CNT cathode with Fenton catalysts has been explored. Under the cathodic potential, modified

This book belongs to Badji Mokhtar Annaba University Central Library Copyright Elsevier 2025

CNT EM can generate •OH indirectly through an electro-Fenton reaction, featuring in situ electrogenerated Fenton reagents of H_2O_2 and Fe^{2+} for water purification. For example, Gao et al. developed a ferrous ion chelated CNT functional cathode. In this system, the dissolved O_2 was effectively reduced to H_2O_2 at the CNT cathode surface, while the presence of Fe^{2+} decomposed H_2O_2 to •OH [Eq. (4.2); Fig. 4.6) [21]. The applied electric field facilitated the in situ regeneration from Fe^{3+} to Fe^{2+} [Eq. (4.3)] and avoided the unfavorable reaction of Fe^{3+} with H_2O_2 to yield the weaker hydroperoxyl radical [Eq. (4.4)]. However, one evident drawback of this design is the inevitable loss of Fe^{2+}, which deteriorates the filter's long-term performance. This could be mitigated by developing a novel heterogeneous Fenton catalyst with enhanced reactivity and stability.

$$H_2O_2 + Fe^{2+} \rightarrow \bullet OH + Fe^{3+} + OH^- \tag{4.2}$$

$$Fe^{3+} + e^- \rightarrow Fe^{2+} \tag{4.3}$$

$$Fe^{3+} + H_2O_2 \rightarrow Fe^{2+} + HO_2^{\bullet} + H^+ \tag{4.4}$$

For example, Li et al. [67] developed a robust and affordable flow-through electro-Fenton process to degrade antibiotic tetracycline. The key component of this technology is an electroactive CNT filter functionalized with FeOCl. Within this system, the dissolved

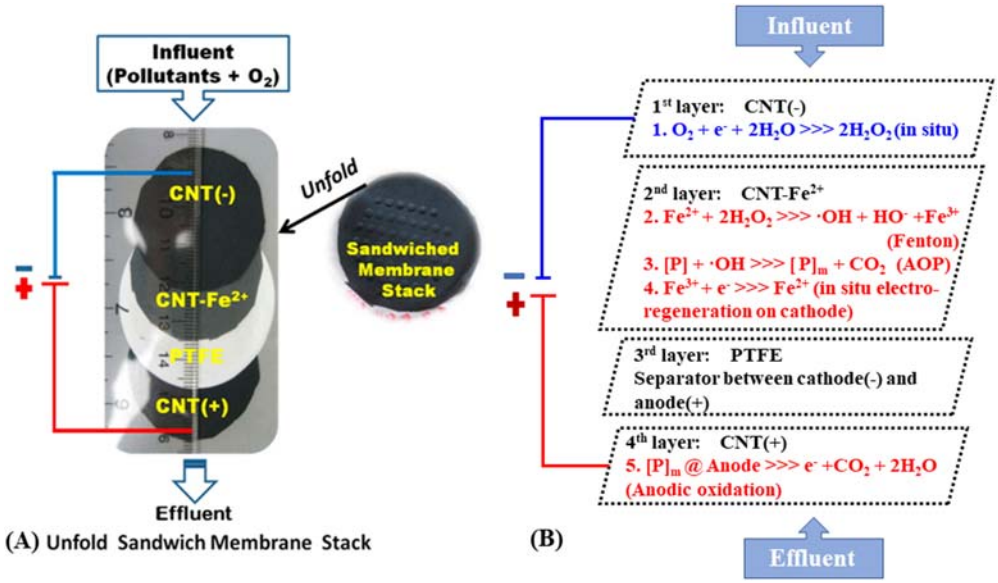

Figure 4.6 Sandwiched electro-Fenton system based on carbon nanotube membrane stacks. (A) Images of the unfolded sandwich membrane stacks including four layers. (B) Schematic of main roles of every layer in membrane stacks, and [P] and $[P]_m$ are pollutants and their oxidation intermediates, respectively. *Reprinted (adapted) with permission from G.D. Gao, Q.Y. Zhang, Z.W. Hao, C. D. Vecitis, Carbon nanotube membrane stack for flow-through sequential regenerative electro-Fenton, Environ. Sci. Technol. 49 (2015) 2375–2383. Copyright 2015 American Chemical Society.*

This book belongs to Badji Mokhtar Annaba University Central Library Copyright Elsevier 2025

O_2 in the influent can be in situ reduced to H_2O_2 by the application of an appropriate negative potential. The effectiveness of FeOCl toward H_2O_2 decomposition had been well documented [67]. Performance-wise, the nanoscale FeOCl can significantly promote the generation of •OH by facilitating the efficient cycling of Fe^{3+}/Fe^{2+}. Compared with a conventional batch reactor, the proposed system showed the enhanced tetracycline degradation kinetics because of the convection-enhanced mass transport. In terms of results achieved, an electrochemical filtration of 0.04 mmol/L tetracycline at -0.8 V versus Ag/AgCl and a flow rate of 1.5 mL/min had resulted in an oxidative flux of 5.32 ± 0.41 mmol/(h · m^2). In addition, the feasibility of using ultrasmall (<2 nm in diameter) and atomically precise Au nanoclusters (25 Au atoms) as the novel Fenton catalysts had also been addressed [17]. Experimental data revealed that these Au nanoclusters reduced the conversion of the in situ generated H_2O_2 to •OH and HO^-, similar to Eq. (4.2). The cycling of Au^+/Au^0 can be readily achieved by the applied electric field.

The CNT-based EM has also been developed for the electrochemical reduction of several refractory and toxic nitro-organic compounds, such as 4-nitrophenol and N-nitrosodimethylamine based on a flow-through electrofiltration [68–70]. Compared with the conventional catalytic reduction methods, CNT membrane filtration minimizes the use of reductants (e.g., $NaBH_4$ and H_2) by electrochemical conversion under the single-pass electro-filtration configuration. For instance, Liu et al. [70] designed a high-performance catalytic membrane composed of ultrasmall gold nanoclusters and high aspect-ratio CNT for the continuous-flow catalytic reactions. The catalytic activity of the designed catalytic membrane was evaluated for the 4-nitrophenol hydrogenation. The results suggested that the continuous flow catalytic reactor could achieve the complete hydrogenation of 4-nitrophenol at a hydraulic residence time of 3.0 s. A CNT EM functionalized with Co − Pt alloy catalysts was also demonstrated with the fast conversion of 4-nitrophenol to 4-aminophenol at a cathodic potential of -0.35 V, realizing the efficient conversion of 4-nitrophenol industrial effluent to the more biodegradable species [71]. The mechanism responsible for the electrochemical-reduction of 4-nitrophenol by the CNT EM coupled with metal catalysts involves the electrochemical generation of atomic hydrogen, which is particularly effective in the hydrogenation of the N − O bonds to form N − H bonds and H_2O [72]. In addition to the metal nanoparticles, metal oxides have also been deposited on the CNT EM for reducing nitro-organic compounds. A Ti_4O_7-CNT composite EM was developed for the simultaneous adsorption and electrochemical reduction of N-nitrosodimethylamine, a carcinogenic disinfection byproduct [69]. The Ti_4O_7-CNT membrane achieved 99.99% conversion of 10 μmol/L N-nitrosodimethylamine in a single-pass electro-filtration at -1.1 V versus SHE. The almost complete hydrogenation suggested the fast kinetics of N-nitrosodimethylamine reduction by the Ti_4O_7-CNT membrane. Density functional theory calculations revealed a probable mechanism for the N-nitrosodimethylamine reduction, where the rate-limiting step was the direct electron transfer reaction. Overall, electrochemical reduction using a CNT-based membrane may provide an alternative approach to

This book belongs to Badji Mokhtar Annaba University Central Library Copyright Elsevier 2025

conventional electrochemical methods for the remediation of wastewater contaminated by nitro-organic compounds.

Halogenated organic contaminants, including perfluorinated or partially fluorinated chemicals, chlorinated organic compounds, and brominated organic compounds, show the characteristics of persistent organic pollutants once they are discharged into the environment. Perfluorooctane sulfonate is a particularly persistent polyfluoroalkyl substance due to its immunity to biological remediation and radical-based oxidation. Su et al. [73] presented a heterogeneous reductive degradation process that coupled direct electron transfer from the surface-modified CNT electrodes (under low potential conditions) to the adsorbed perfluorooctane sulfonate molecules using UV-generated hydrated electrons without any further chemical addition (Fig. 4.7A). The efficient electron transfer dramatically increased the defluorination rate while yielding shorter chain (C_3-C_7) perfluorinated acids.

4.4.1.3 Energy consumption

The electrical energy consumption of decontamination oxidation can be evaluated as the energy consumption per order (EC_{EO}) [74]:

$$EC_{EO} = \frac{U_{cell} I}{Q \log\left[\frac{C_f}{C_p}\right]} \tag{4.5}$$

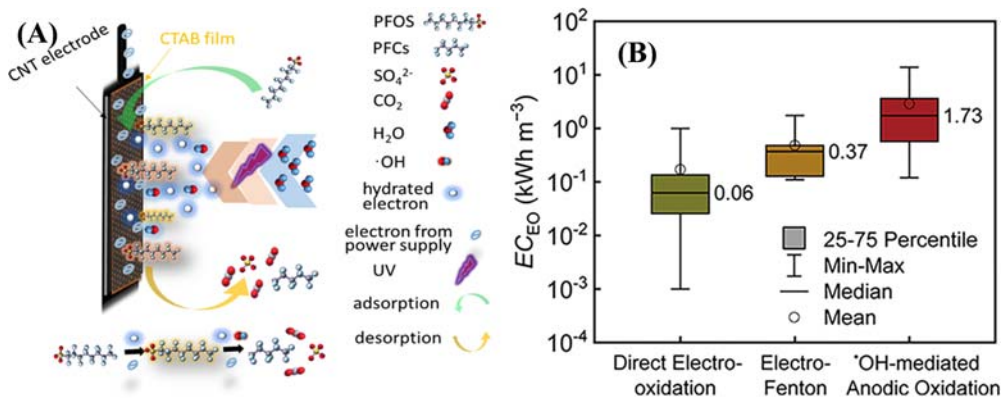

Figure 4.7 Decontamination of water with carbon nanotube (CNT) electrode for electrochemical membrane: (A) Schematic diagram of defluorination of perfluorooctane sulfonate with CNT electrode. (B) Electrical energy consumption during electrified membrane operation. *Reprinted (adapted) with permission from (A) Y.M. Su, U. Rao, C.M. Khor, M.G. Jensen, L.M. Teesch, B.M. Wong, et al., Potential-driven electron transfer lowers the dissociation energy of the C—F bond and facilitates reductive defluorination of perfluorooctane sulfonate (PFOS), ACS Appl. Mater. Inter. 11 (2019) 33913—33922. Copyright 2019 American Chemical Society. (B) Electrical energy consumption during electrified membrane operation; M. Sun, X.H. Wang, L.R. Winter, Y.M. Zhao, W. Ma, T. Hedtke, et al., Electrified membranes for water treatment applications, ACS EST. Eng. 1 (2021) 725—752. Copyright 2021 American Chemical Society.#*

This book belongs to Badji Mokhtar Annaba University Central Library Copyright Elsevier 2025

where I is the current (amperes), U_{cell} is the cell potential (volts), Q is the permeate flow rate, and C_f and C_p are the contaminant concentrations in the feed and permeate, respectively. EC_{EO} represents the electrical energy needed to degrade a contaminant by 1 order of magnitude, equivalent to 90% removal efficiency. Considering the various initial concentrations and removal efficiencies among the different EM processes, EC_{EO} is considered to be the most representative figure of merit for EM energy consumption [23]. The median EC_{EO} for EM-based oxidation is 0.4 kWh/m^3 (Fig. 4.7B), which is lower than the energy consumption in conventional wastewater treatment (~0.6 kWh/m^3) [75] and comparable to the advanced oxidation processes for organics removal [76,77]. According to a previous report [49], direct oxidation processes are energy-efficient with a median EC_{EO} of 0.06 kWh/m^3. The median EC_{EO} for electro-Fenton processes is 0.37 kWh/m^3 due to the regeneration of Fe^{2+} together with the electro-generated H_2O_2. A relatively high EC_{EO} (1.73 kWh/m^3) is inevitable for the •OH-mediated anodic oxidation processes due to the high thermodynamic anodic potential required for generating the •OH through the water oxidation (2.38 V vs SHE) [46]. Table 4.1 shows a summary of exemplary energy consumption of the electrochemical CNT membranes.

Normally, a relatively high electrical energy consumption in the EM processes is necessary for treating wastewaters with complex components and recalcitrant contaminants. Many EM-based oxidation processes cannot completely remove contaminants due to the short residence time and limited current efficiency at low contaminant concentrations. Energy consumption will increase exponentially with the current density. High current density is needed for achieving low residual concentration. Hence, future work should focus on optimizing the EM process to achieve efficient removal of pollutants with overall high current efficiency and low energy consumption.

4.4.2 Decontamination of toxic inorganic contaminants

Toxic inorganic contaminants [e.g., arsenic (As), chromium (Cr), and antimony (Sb)] represent another category of hazardous pollutants that readily permeate the

Table 4.1 Comparison of the energy consumption of different systems.

Materials	Target pollutant	Energy consumption	Reference
CNT/rGO/polyacrylonitrile (A)	Methylene blue (10 mg/L)	6 Wh/m	[78]
CNT-polycinylalcohol (A)	Cr(VI) (1 mg/L)	1.48 kWh/m^3	[79]
TiO_2-CNT (A)	As(III); As(V) (0.9 mg/L)	0.03 kWh/m^3	[80]
CNT/rFeOOH (C)	Sulfamethoxazole (25 mg/L)	300.32 mW/m^2	[81]
Polyaniline-CNT (C)	Cr(VI) (1 mg/L)	0.032 kWh/m^3	[82]
CNT (A)	Phenol (1.0 mmol/L)	0.05 kWh/g TOC	[83]
CNT-COOFe^{3+} (C)	Trichloroacetic acid (0.25 mmol/L)	45.8 kWh/kg TOC	[21]

Notes: A: anode, C: cathode.

This book belongs to Badji Mokhtar Annaba University Central Library
Copyright Elsevier 2025

conventional ultrafilter membranes in water and wastewater treatment [84]. Adsorption by carbon-based materials is an effective technology for heavy metal decontamination due to advantages of operation and low cost [85]. Compared with previous adsorbents, CNT composite materials have the advantages of their scale effect, large specific surface area, strong interface interaction, and unique physical and chemical properties [86,87]. Functionalization of the surface chemistry is an effective way to improve the CNT adsorptive behavior [88]. However, the direct use of nanomaterials in water treatment suffers from the difficulty of collecting used nanoadsorbents and sluggish kinetics. To overcome this application problem, the nanoadsorbent materials have been attached to a porous substrate [89] or blended into a membrane [90]. On the other hand, the valence states of toxic inorganic contaminants are closely related to their physical and chemical properties. For example, compared with Sb(V), Sb(III) is 10 times more toxic, and its removal efficacy by sorption is generally low due to a predominant charge-neutral state across a broad pH range (e.g., 3–9) [91]. Hence, transforming high-valence toxic inorganic contaminants into low-valence-state metal species in the forms of metal oxides, ions, and elemental metals by the means of electrochemical reduction is an effective strategy for removing toxic inorganic contaminants [92].

Despite successes in the efforts at increasing the sorption capacity for toxic inorganic contaminants, the sluggish sorption kinetics is still far from satisfactory. For example, the time needed to achieve As(III) sorption equilibrium for a zero-valent iron-biochar composite was as long as 48 h [93]. On the other hand, a common two-step treatment strategy was adopted to achieve highly efficient detoxification and sequestration simultaneously, which inevitably adds the operation complexity with excessive consumption of chemicals [94]. To overcome these problems, Liu et al. employed an electroactive CNT filter functionalized with electrodeposited sea urchin-like FeOOH to achieve one-step As(III) decontamination [95]. Operation-wise, with the assistance of the electric field, CNT-FeOOH anodic filter can transform As(III) to less toxic As(V) in situ. The electric field accelerates the electromigration kinetics of the negatively-charged As(V) toward the surface of the positively-charged functional filter, achieving enhanced total As removal efficiency. Performance-wise, the CNT-FeOOH membrane showed increased sorption kinetics in comparison with the unmodified CNT membrane because the porous structure improves the accessibility of the active sites. The CNT-FeOOH sorption sites could be regenerated by chemical washing with diluted NaOH solution. The process is similar to the operation of an ion exchange membrane. The system efficacy can be maintained across a wide pH range with different environmental matrixes. Liu et al. [96] recently developed an electrochemical system composed of a TiO_2-CNT membrane anode and a Ti cathode to remove Sb(III) (Fig. 4.8A). With an applied external electric field, the transformation of Sb(III) to less toxic Sb(V) can be achieved in situ, which is further sequestered

This book belongs to Badji Mokhtar Annaba University Central Library Copyright Elsevier 2025

by TiO_2. At 2 V, 100 μg/L Sb(III)-spiked tap water generated ~1600 bed volumes of effluent with >90% removal efficiency over 8 h continuous filtration. The residual Sb were in the dominant form of Sb(V) rather than Sb(III), indicating that the oxidation reaction was active during the filtration process. Both Sb(III) sorption kinetics and capacity were positively related to the applied voltage, indicated by the increase in the sorption capacity from 3.3 mg/g at 0 V to 4.2 mg/g at 2 V. Meanwhile, the time required to achieve equilibrium was also decreased from >8 h at 0 V to 3 h at 2 V. Additionally, the system can be operated over a wide pH range. The system performance could also be enhanced by coupling with some photoresponsive nanomaterials, such as metal-organic frameworks, onto the CNT membrane. For example, Li et al. [97] fabricated a photoelectrical-responsive CNT filter functionalized with MIL-88B (Fe) photocatalysts, which showed excellent "one-step" Sb(III) detoxification performance (Fig. 4.8B). Ren et al. [98] designed a Ti/CeO_x-CNT hybrid membrane as the functional cathode. Under an electric field, in situ generated H_2O_2 reacted with the Ti-Ce binary oxide to produce the hydroperoxide complexes, which enabled the efficient transformation of Sb(III) to the less toxic Sb(V) at neutral pH. In summary, the electroactive CNT membrane surmounts many issues with nanoscale adsorbent materials such as blockage of surface sorption site, sluggish absorption kinetics, and difficulty of separation.

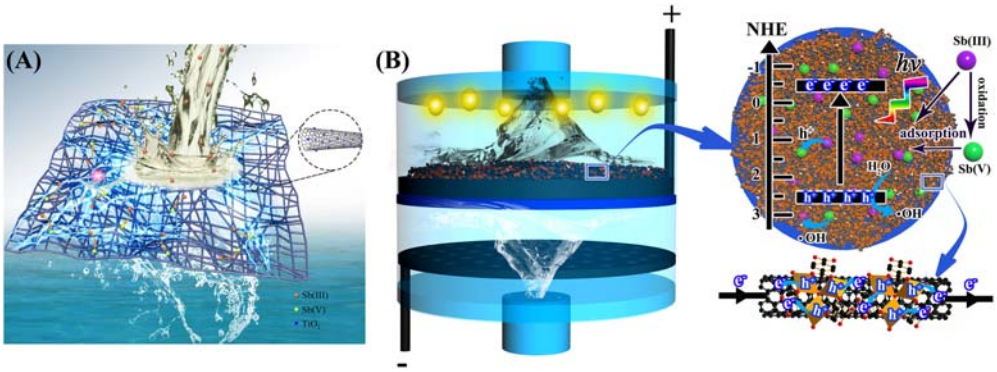

Figure 4.8 Decontamination of water of toxic inorganic pollutants (A) Electroactive modified CNT filter for simultaneous detoxification and sequestration of Sb(III). Reprinted (adapted) with permission from [96]. (B) Photoelectrical-responsive CNT filter functionalized with nanoscale MIL-88B(Fe) photocatalysts for Sb(III) detoxification. *Reprinted (adapted) with permission from (A) Y.B. Liu, P. Wu, F.Q. Liu, F. Li, X. An, J.S. Liu, et al., Electroactive modified carbon nanotube filter for simultaneous detoxification and sequestration of Sb(III), Environ. Sci. Technol. 53 (2019) 1527–1535; (B) Photoelectrical-responsive CNT filter functionalized with nanoscale MIL-88B(Fe) photocatalysts for Sb(III) detoxification; M.H. Li, Y.B. Liu, C.S. Shen, F. Li, C.C. Wang, M.H. Huang, et al., One-step Sb(III) decontamination using a bifunctional photoelectrochemical filter, J. Hazard. Mater. 389 (2020) 121840. Copyright 2020, Elsevier.*

This book belongs to Badji Mokhtar Annaba University Central Library Copyright Elsevier 2025

A similar concept could also be applied for the "reduction-sorption" applications once the functional membrane serves as a cathode. The highly carcinogenic Cr(VI) is 500–1000 times more toxic than Cr(III). We have recently developed an electroactive filter consisting of nanoscale polyaniline modified CNT for the Cr(VI) detoxification and sequestration [82]. Operation-wise, the amine and imine moieties on the polyaniline could chelate the toxic metal ions, although the high removal efficacy was usually restricted to the condition of pH 1–3. Performance-wise, both the reduction kinetics for the Cr(VI) and the sorption capacity of the Cr(III) were enhanced by increasing the flow rate and the applied voltage. For example, at pH 7, Cr(VI) removal efficiency was increased from 29.3% at 0 V to 70.2% at 2.5 V. Efficiency-wise, the energy consumption of this system was 0.032 kWh/m^3, a value much lower than most state-of-the-art technologies. Both the rapid kinetics and excellent performance indicated that the electrochemical CNT membrane may provide an affordable and promising solution for the reductive removal of toxic inorganic contaminants in water.

4.4.3 Construction of electroactive antifouling membranes

4.4.3.1 Antifouling membrane

The performance of the traditional membrane processes is largely constrained by membrane fouling and scaling. The main pollutants in natural water sources and wastewater are bacteria, organic molecules, and inorganic scales formed by low solubility salts [99]. These pollutants will accumulate on the membrane surface to block pores, resulting in temporary or permanent fouling with reduced flux [100,101]. The development of antifouling membranes is essential for addressing these challenges.

Recent studies demonstrated that introducing the electroactive property with conventional membranes through the implementation of EM can be effective for mitigating fouling and scaling [102]. Membrane filtration assisted by an electric field involves the applying of direct current to the membrane. Hence, the surface potential of the membrane can be either negatively or positively adjusted [103]. The introduction of a conductive layer on the membrane surface converts it to an EM, which is essential for improved robustness toward fouling and scaling control. The voltage applied on the conductive layer also helps to improve the separation selectivity. The electrostatic adsorption/rejection or electrochemical reactions can take place directly on the membrane surface [104,105] and the energy consumption can be minimized relative to the use of additional electrodes separated from the membrane [106]. The conductive membrane offers the most efficient technology for antifouling in an electric field-assisted process, given the membranes with good conductivity and stability are the premise to realize antifouling performance. Compared with other conductors, CNT offers a class of carbon-based conductive materials for constructing advanced electroactive antifouling membranes. The electroactive CNT membrane has high porosity and an abundantly interconnected porous structure, which lead to a higher water flux

This book belongs to Badji Mokhtar Annaba University Central Library Copyright Elsevier 2025

even under low working pressure [107]. In addition, CNT has excellent electrochemical properties for fast electron transfer. Therefore the application of an external electric field (direct or alternating current) to a CNT membrane has been demonstrated effective for reducing fouling and increasing the permeate flux rates [108,109]. As regards the problem of scaling, the strategies for electrochemically controlling scaling mainly focus on the increasing electrostatic repulsion between membrane surface and foulants, plus the change of local pH value within the film [110,111].

Electrostatic repulsion represents the most important mechanism to prevent the accumulation of foulants on the membrane surface. Foulant degradation by electrochemical oxidation is an alternative and perhaps more effective practical method for mitigating fouling in EM. Reactive oxygen species such as H_2O_2 and •OH have been confirmed responsible for the degrading and decomposing of refractory foulants [112,113]. Generally, these active species are generated in situ by electron-Fenton and oxygen reduction reactions in the cathodic EM [114,115]. Zhang et al. [116] deposited a CNT-polyvinylidene fluoride composite on top of the ultrafiltration membrane for the capacitive organic fouling reduction. Since the natural organic matter is negatively charged, the modified membrane was used as a cathode to repel the negatively charged organic foulants. The resulting EM with negatively charged surfaces mitigated the membrane fouling by flowing through a sodium alginate solution with an applied voltage of 2 V. In another example reported by Fan et al. [117], a silver nanoparticle modified CNT (Ag-CNT)/ceramic membrane was produced with enhanced antifouling and antimicrobial properties under electrochemical assistance. The steady-state flux in filtering bacterial suspension was 1.9-fold higher than that by an unmodified membrane. H_2O_2 could be produced through the electroreduction of oxygen under a low electrical potential of 2.0 V, which is sufficient for suppressing bacterial attachment and promoting bacterial detachment by reducing microbial cell viability and increasing cellular permeability. Meanwhile, the flux loss was decreased from $>35\%$ without voltage bias to $<10\%$ with a 2 V bias for the feedwater containing both bacteria and organic matter.

Altering localized pH on the membrane surface through electrochemical water splitting reactions can also be used to control the pH-sensitive scaling [12]. $CaCO_3$ scale was efficiently removed from the membrane surface through the intermittent application of a 2.5 V bias to the polyamide membrane, functionalized with CNT, to act as an anode. A porous composite polypropylene membrane coated with a CNT/poly(vinyl alcohol) layer had binary surface properties that combine the hydrophobic property with the hydrophilic and conductive properties of the CNT [118]. In this approach, a local high-pH environment (pH = 12) was formed by the application of an intermittent direct current of 20 mA. It prevented the formation of scale due to the increased silica solubility at high pH. To date, membrane fouling and scaling together with the corresponding control strategies have been studied extensively for conventional membrane processes. The introduction of a conductive layer on the membrane substrate improves the stability of the membrane performance by

This book belongs to Badji Mokhtar Annaba University Central Library Copyright Elsevier 2025

controlling fouling and scaling. Overall, CNT offers a promising carbon material for the fabrication of antifouling membranes.

4.4.3.2 Biofouling mitigation

Biofouling originates from the growth of bacteria and the deposition of their produced extracellular polymeric substances on the porous membrane surface [119]. The biofouling may significantly deteriorate the membrane performance and increase energy consumption. Numerous strategies have been proposed to alleviate this issue by developing novel antibiofouling membranes. However, most strategies, such as that of altering the surface physicochemical properties, only delay the biofilm formation or minimize the impacts of biofilms on membrane performance [120]. EM provides a chemical-free approach that can alleviate bacteria deposition and biofilm formation. Direct oxidation is a contact-mediated bacteria inactivation process with a required anodic potential below that of water electrolysis, thereby minimizing side reactions and toxic byproduct formation [4,5]. For example, Vecitis et al. [18] reported that an electrochemical CNT membrane enables rejection and inactivation of bacteria (*Escherichia coli*) and virus (*bacteriophage* Ms_2). Anodic CNT membrane served as an electron acceptor under an electric field while adsorbing negatively charged bacterial cells on the CNT membrane. Bacteria on CNT membrane or in solution were inactivated during anodic filtration by either direct or indirect electrooxidation. The direct oxidation transferred electrons from the bacteria to anodic EM, leading to the cell inactivation by triggering cellular oxidative stress. At applied potentials of 2 and 3 V, the electrochemically active CNT filter reduced the number of bacteria and viruses in the effluent to a level below the limit of detection. Applying 2 and 3 V for 30 s of postfiltration could inactivate $>75\%$.

However, bacteria inactivation by direct oxidation is limited (60%–90%) [20,121], indicating that a direct oxidation pathway alone is not adequate for biofouling control in long-term membrane operation. Indirect oxidation depends on electrogeneration of highly reactive species (e.g., •OH and Cl•) on anodic membranes through electrooxidation of water molecules. Compared to direct oxidation, indirect oxidation exhibits superior bacteria inactivation. Another approach for biofouling control is to use metal nanomaterial-assisted cathodic filtration. Cathodic membrane suppresses the bacterial deposition by the electrorepulsion of negatively charged microbes away from the membrane surface. Moreover, the gene expressions related to cell respiration and energy metabolism, when influenced by the cathodically generated H_2O_2 [121,122], decreased the density and viability of bacteria on the EM. However, compared with •OH, H_2O_2 has a much lower oxidation potential that is insufficient to achieve the desired level of bacterial inactivation. To overcome this shortage, metal nanoparticles have been used to modify the surface of the cathodic membranes. The electrons released from the oxidation of metal nanoparticles will facilitate the generation of the reduced reactive oxygen species to inhibit the proliferation of the surface attached bacteria. However, metal nanoparticle functionalized membranes have relatively short life

This book belongs to Badji Mokhtar Annaba University Central Library Copyright Elsevier 2025

spans since the surface biocidal metal nanoparticles dissolve over time. This problem can be alleviated by tethering metal nanoparticles to a cathodic membrane, which also serves as an electron donor. For example, Wang et al. [123] fabricated an antibiofouling membrane by introducing copper nanoparticle/CNT on a ceramic substrate. Fan et al. [89] demonstrated a silver nanoparticle modified carbon nanotube (Ag-CNT) deposited on a ceramic membrane with enhanced antifouling and antimicrobial properties under electrochemical conditions. The dissolved metal ions, Ag^{+}/Cu^{2+}, near the membrane surface, when redeposited back on the membrane cathode, it led to the density of the metal nanoparticles being recovered and their associated biocidal activity to continue. Such an electrochemical-assisted metal nanoparticles regeneration process prevents the massive metal leaching, which in turn prolongs the service life of the antimicrobial metal nanoparticle modified cathodic EM.

4.4.4 Nanoconfinement effects in carbon nanotube-based membrane technologies

It has been reported that the well-defined nanochannels inside a CNT with unique electronic tuning properties can provide an intriguing confined environment [124]. Significantly enhanced catalytic activities have been observed from CNT-confined catalysts, that resulted from the tuning of the properties of the active species (e.g., fullerenes and its derivatives, water, alkali metals, and halides) [125,126]. In addition, inside the CNT, the interactions of reactant and product molecules with the CNT inside walls become increasingly important, which eventually become stronger than the intermolecular interaction [127]. Furthermore, if metal catalysts are introduced inside the CNT, a unique metal-support interaction can be observed because of the deformed sp^2 hybridization electron structure of the graphene walls [124]. Deviation from planarity causes π-electron density to shift from the concave inner to the convex outer surface, leading to an electron potential difference between inside and outside of a CNT [128,129]. Thus the metal-support interaction inside CNT must be different from that on the outside of CNT [130,131]. In addition, the theoretical simulation showed that transition metal atoms interact with CNT walls differently from how they react with flat graphite layers with regard to the bonding sites, magnetic moments, and charge-transfer directions [132]. This opens up an opportunity to tune the catalytic performance via the confinement inside CNT. Currently, experimental studies of the reaction over CNT-confined catalysts are essentially limited to MWCNT because they are easier to produce in large quantities than are SWCNT. In addition, techniques for filling metal nanoparticles into MWCNT are more mature due to their relatively larger internal diameters. For example, Guo et al. [133] designed a silicate-enhanced flow-through electro-Fenton system with a Fe_2O_3 nanoparticle filled CNT filter (Fe_2O_3-in-CNT) (Fig. 4.9). The filter was demonstrated for the highly efficient, rapid, and selective degradation of antibiotic tetracycline with the degradation efficiency $>97.5\%$. Under an electric field, this composite

This book belongs to Badji Mokhtar Annaba University Central Library Copyright Elsevier 2025

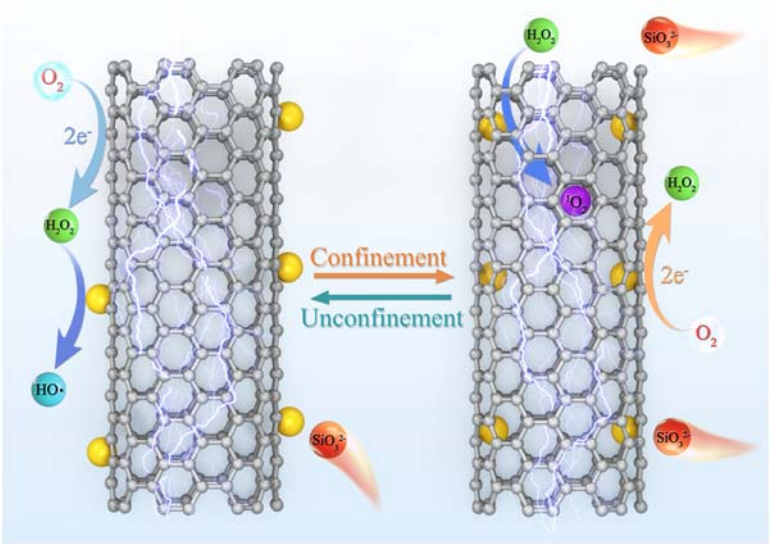

Figure 4.9 Schematic diagram of tetracycline degradation in the Fe_2O_3-in/out-CNT system. *Reprinted (adapted) with permission from D.L. Guo, Y.B. Liu, H.D. Ji, C.C. Wang, B. Chen, C.S. Shen, et al., Silicate-enhanced heterogeneous flow-through electro-Fenton system using iron oxides under nanoconfinement, Environ. Sci. Technol. 55 (2021) 4045–4053. Copyright 2021 American Chemical Society.*

filter also enabled in situ H_2O_2 generation, which was converted to reactive oxygen species accompanied by the redox cycling of Fe^{3+}/Fe^{2+}. Compared with the surface-coated Fe_2O_3 on the CNT (Fe_2O_3-out-CNT) filter, the Fe_2O_3-in-CNT filter demonstrated a 1.65 times higher k_L value toward the degradation of the antibiotic tetracycline. Electron paramagnetic resonance and radical quenching tests consistently verified that the dominant radical species was the $^1O_2$ or •OH in the confined Fe_2O_3-in-CNT or unconfined Fe_2O_3-out-CNT system, respectively. This provides a novel approach to tune the catalytic behavior of supported metal catalysts for specific reactions and efficient remediation of organic contaminants from water.

4.5 Conclusions and perspectives

In this chapter, we systematically reviewed recent advances in the fundamental understanding, rational designs, and applications of the CNT-based EM technology. Several strategies (e.g., chemical treatment, functional group chelation) have been presented for the CNT surface modifications to produce multifunctional composites. Moreover, various potential environmental applications of the EM technology were

This book belongs to Badji Mokhtar Annaba University Central Library Copyright Elsevier 2025

explored including the degradation of organic contaminants, detoxification of toxic inorganic contaminants, and construction of electroactive antifouling membranes.

Overall, EM is suitable for advanced, fit-for-purpose water and wastewater treatment applications. The EM provides a scalable platform for electrochemical processes with enhanced mass transportation, conversion efficiency, and excellent stability. EM expands the functioning of the conventional membrane by transcending simple separation with the capability of effective removal of various pollutants through various electrochemical mechanisms (e.g., direct and free radical-mediated electro-oxidation, electroreduction, and electrostatic interaction), which can provide multifunctional, modular treatment systems. The electroactive layer with high specific surface area and limited pore dimensions offers convection-enhanced mass transport and electrodynamic effects, which allows the highly efficient removal of pollutants in a single-pass flow-through filtration process. Compared with other technologies, EM flow-through filtration can achieve much higher current efficiencies with lower energy consumption. In addition, by introducing the electroactive layer, membrane antifouling can be significantly improved by in situ foulant destruction and/or organic degradation, which in turn improves the membrane performance and lifespan. Given these advantages, EM can be viable for various water treatment applications. Another promising field for EM application is to recover valuable metal ions from water with spontaneous redox reactions. For example, we recently found that a MoS_2-CNT hybrid filter could adsorb Au^{3+} and spontaneously reduce Au^{3+} to Au^0 due to the essential role of the MoS_2 and its high affinity to Au^{3+}.

Although electroactive membrane materials have broad application prospects, the development of more sustainable and affordable electroactive membrane materials still deserves further investigation. Besides developing simpler fabrication protocols, it is also important to find more robust, cheaper, and effective materials beyond CNT. Although CNT production has witnessed significant improvement in the past decade, the cost of these membranes is still high compared with other carbon materials such as activated carbon. Further, improving the CNT mass-production technology could help to decrease the overall operational cost of the water and wastewater treatment systems. Also, future research efforts should be dedicated to scaling up CNT filter and filtration device to facilitate practical engineering applications. Most reported results were obtained in a laboratory and/or at a bench scale on representative contaminants in synthetic waters. Hence, the reported superior performance and efficiency may fail when dealing with real wastewater with complex compositions and high concentrations. The process may also generate more toxic byproducts, leading to secondary environmental pollution.

Acknowledgments

Project was supported by the Open Project of State Key Laboratory of Urban Water Resource and Environment, Harbin Institute of Technology (No. QAK202108) and the National Natural Science Foundation of China (Grant No. 52170068 and U21A20161).

This book belongs to Badji Mokhtar Annaba University Central Library Copyright Elsevier 2025

References

[1] J. Eliasson, The rising pressure of global water shortages, Nature 517 (2015) 6.
[2] Y.L. Luo, W.S. Guo, H.H. Ngo, L.D. Nghiem, F.L. Hai, J. Zhang, et al., A review on the occurrence of micropollutants in the aquatic environment and their fate and removal during wastewater treatment, Sci. Total Environ. 473–474 (2014) 619–641.
[3] B.E. Logan, M. Elimelech, Membrane-based processes for sustainable power generation using water, Nature 488 (2012) 313–319.
[4] K.J. Godri Pollitt, J.-H. Kim, J. Peccia, M. Elimelech, Y. Zhang, G. Charkoftaki, et al., 1,4-Dioxane as an emerging water contaminant: state of the science and evaluation of research needs, Sci. Total Environ. 690 (2019) 853–866.
[5] D.J. Miller, D.R. Dreyer, C.W. Bielawski, D.R. Paul, B.D. Freeman, Surface modification of water purification membranes, Angew. Chem. Int. Ed. 56 (2017) 4662–4711.
[6] Y.-H. Wang, Y.-H. Wu, X. Tong, T. Yu, L. Peng, Y. Bai, et al., Chlorine disinfection significantly aggravated the biofouling of reverse osmosis membrane used for municipal wastewater reclamation, Water Res. 154 (2019) 246–257.
[7] J. Radjenovic, D.L. Sedlak, Challenges and opportunities for electrochemical processes as next-generation technologies for the treatment of contaminated water, Environ. Sci. Technol. 49 (2015) 11292–11302.
[8] I. Sirés, E. Brillas, M.A. Oturan, M.A. Rodrigo, M. Panizza, Electrochemical advanced oxidation processes: today and tomorrow. A review, Environ. Sci. Pollut. Res. 21 (2014) 8336–8367.
[9] F. Zhao, X. Zhao, B. Peng, F. Gan, M. Yao, W. Tan, et al., Polyimide-derived carbon nanofiber membranes as anodes for high-performance flexible lithium ion batteries, Chin. Chem. Lett. 29 (2018) 1692–1697.
[10] B.P. Chaplin, Critical review of electrochemical advanced oxidation processes for water treatment applications, Environ. Sci.: Process. Impacts 16 (2014) 1182–1203.
[11] L. Tang, A. Iddya, X. Zhu, A.V. Dudchenko, W. Duan, C. Turchi, et al., Membrane distillation membranes treating geothermal brines, ACS Appl. Mater. Inter. 9 (2017) 38594–38605.
[12] W. Duan, A. Ronen, S. Walker, D. Jassby, Polyaniline-coated carbon nanotube ultrafiltration membranes: enhanced anodic stability for in situ clean electro-oxidation processes, ACS Appl. Mater. Inter. 8 (2016) 22574–22584.
[13] X. Zhu, D. Jassby, Electroactive membranes for water treatment: enhanced treatment functionalities, energy considerations, and future challenges, Acc. Chem. Res. 52 (2019) 1177–1186.
[14] A. Fernandes, D. Santos, M.J. Pacheco, L. Ciriaco, R. Simoes, A.C. Gomes, et al., Electrochemical treatment of cork boiling wastewater with a boron-doped diamond anode, Environ. Technol. 36 (2015) 26–35.
[15] H.H. Shi, Y.Y. Wang, C.G. Li, R. Pierce, S.X. Gao, Q.G. Huang, Degradation of perfluorooctanesulfonate by reactive electrochemical membrane composed of Magnéli phase titanium suboxide, Environ. Sci. Technol. 53 (2019) 14528–14537.
[16] Y.B. Liu, G.D. Gao, C.D. Vecitis, Prospects of an electroactive carbon nanotube membrane toward environmental applications, Acc. Chem. Res. (2020) 2892–2902.
[17] A. Srivastava, O.N. Srivastava, S. Talapatra, R. Vajtai, P.M. Ajayan, Carbon nanotube filters, Nat. Mater. 3 (2004) 610–614.
[18] A.S. Brady-Estevez, M.H. Schnoor, C.D. Vecitis, N.B. Saleh, M. Elimelech, Multiwalled carbon nanotube filter: improving viral removal at low pressure, Langmuir 26 (2010) 14975–14982.
[19] F.Q. Liu, Y.B. Liu, Q.F. Yao, Y.X. Wang, X.F. Fang, C.S. Shen, et al., Supported atomically-precise gold nanoclusters for enhanced flow-through electro-Fenton, Environ. Sci. Technol. 54 (2020) 5913–5921.
[20] C.D. Vecitis, M.H. Schnoor, M.S. Rahaman, J.D. Schiffman, M. Elimelech, Electrochemical multiwalled carbon nanotube filter for viral and bacterial removal and inactivation, Environ. Sci. Technol. 45 (2011) 3672–3679.
[21] G.D. Gao, Q.Y. Zhang, Z.W. Hao, C.D. Vecitis, Carbon nanotube membrane stack for flow-through sequential regenerative electro-Fenton, Environ. Sci. Technol. 49 (2015) 2375–2383.

This book belongs to Badji Mokhtar Annaba University Central Library Copyright Elsevier 2025

[22] H. Liu, C.D. Vecitis, Reactive transport mechanism for organic oxidation during electrochemical filtration: mass-transfer, physical adsorption, and electron-transfer, J. Phys. Chem. C 116 (2011) 374–383.
[23] B.P. Chaplin, The prospect of electrochemical technologies advancing worldwide water treatment, Acc. Chem. Res. 52 (2019) 596–604.
[24] Y. Zhu, L. Li, C. Zhang, G. Casillas, Z. Sun, Z. Yan, et al., A seamless three-dimensional carbon nanotube graphene hybrid material, Nat. Comm. 3 (2012).
[25] M.F.L. De Volder, S.H. Tawfick, R.H. Baughman, A.J. Hart, Carbon nanotubes: present and future commercial applications, Science 339 (2013) 535–539.
[26] G. Wei, S. Chen, X. Fan, X. Quan, H. Yu, Carbon nanotube hollow fiber membranes: high-throughput fabrication, structural control and electrochemically improved selectivity, J. Membr. Sci. 493 (2015) 97–105.
[27] V.K.K. Upadhyayula, S. Deng, M.C. Mitchell, G.B. Smith, Application of carbon nanotube technology for removal of contaminants in drinking water: a review, Sci. Total Environ. 408 (2009) 1–13.
[28] Y.B. Liu, J.P. Xie, C.N. Ong, C.D. Vecitis, Z. Zhou, Electrochemical wastewater treatment with carbon nanotube filters coupled with: *in situ* generated H_2O_2, Environ. Sci. Water Res. Technol. 1 (2015) 769–778.
[29] J.W.G. Wilder, L. Venema, A. Rinzler, R. Smalley, C. Dekker, Electronic structure of atomically resolved carbon nanotubes, Nature 391 (1998) 59–62.
[30] J. Prásek, J. Drbohlavová, J. Chomoucka, J. Hubálek, O. Jasek, V. Adam, et al., Methods for carbon nanotubes synthesis review, J. Mater. Chem. 21 (2011) 15872–15884.
[31] C. Rizzuto, G. Pugliese, M.A. Bahattab, S.A. Aljlil, E. Drioli, E. Tocci, Multiwalled carbon nanotube membranes for water purification, Sep. Purif. Technol. 193 (2018) 378–385.
[32] H. Kim, Y.S. Hwang, V.K. Sharma, Adsorption of antibiotics and iopromide onto single-walled and multi-walled carbon nanotubes, Chem. Eng. J. 255 (2014) 23–27.
[33] R. Das, M.E. Ali, S.B.A. Hamid, S. Ramakrishna, Z.Z. Chowdhury, Carbon nanotube membranes for water purification: a bright future in water desalination, Desalination 336 (2014) 97–109.
[34] M. Sianipar, S.H. Kim, K. Khoiruddin, F. Iskandar, I.G. Wenten, Functionalized carbon nanotube (CNT) membrane: progress and challenges, RSC Adv. 7 (2017) 51175–51198.
[35] M.-B. Wu, Y. Lv, H.-C. Yang, L.-F. Liu, X. Zhang, Z.-K. Xu, Thin film composite membranes combining carbon nanotube intermediate layer and microfiltration support for high nanofiltration performances, J. Membr. Sci. 515 (2016) 238–244.
[36] G.D. Gao, C.D. Vecitis, Electrochemical carbon nanotube filter oxidative performance as a function of surface chemistry, Environ. Sci. Technol. 45 (2011) 9726–9734.
[37] H. Liu, K.C. Zuo, C.D. Vecitis, Titanium dioxide-coated carbon nanotube network filter for rapid and effective arsenic sorption, Environ. Sci. Technol. 48 (2014) 13871–13879.
[38] W.T. Zheng, Y.B. Liu, W. Liu, H.D. Ji, F. Li, C. Shen, et al., A novel electrocatalytic filtration system with carbon nanotube supported nanoscale zerovalent copper toward ultrafast oxidation of organic pollutants, Water Res. 194 (2021) 116961.
[39] S. Das, V.C. Srivastava, An overview of the synthesis of CuO-ZnO nanocomposite for environmental and other applications, Nanotechnol. Rev. 7 (2018) 267–282.
[40] M. Gaidi, Nanostructured SnO_2 thin films: effects of porosity and catalytic metals on gas-sensing sensitivity, Appl. Phys. A Mater. Sci. Process. 124 (2018) 725–738.
[41] X.T. Zhao, L.J. Cheng, R.X. Wang, N. Jia, L.F. Liu, C.J. Gao, Bioinspired synthesis of polyzwitterion/titania functionalized carbon nanotube membrane with superwetting property for efficient oil-in-water emulsion separation, J. Membr. Sci. 589 (2019) 117257.
[42] J.E.H. Yanez, Z. Wang, S. Lege, M. Obst, S. Roehler, C.J. Burkhardt, et al., Application and characterization of electroactive membranes based on carbon nanotubes and zerovalent iron nanoparticles, Water Res. 108 (2017) 78–85.
[43] S.O. Ganiyu, E.D. Van Hullebusch, M. Cretin, G. Esposito, M.A. Oturan, Coupling of membrane filtration and advanced oxidation processes for removal of pharmaceutical residues: a critical review, Sep. Purif. Technol. 156 (2015) 891–914.

This book belongs to Badji Mokhtar Annaba University Central Library Copyright Elsevier 2025

[44] C.D. Vecitis, G.D. Gao, H. Liu, Electrochemical carbon nanotube filter for adsorption, desorption, and oxidation of aqueous dyes and anions, J. Phys. Chem. C. 115 (2011) 3621–3629.
[45] L. Guo, Y. Jing, B.P. Chaplin, Development and characterization of ultrafiltration TiO_2 Magnéli phase reactive electrochemical membranes, Environ. Sci. Technol. 50 (2016) 1428–1436.
[46] C. Trellu, B.P. Chaplin, C. Coetsier, R. Esmilaire, S. Cerneaux, C. Causserand, et al., Electro-oxidation of organic pollutants by reactive electrochemical membranes, Chemosphere 208 (2018) 159–175.
[47] M.A. Rodrigo, P. Cañizares, A. Sánchez-Carretero, C. Sáez, Use of conductive-diamond electrochemical oxidation for wastewater treatment, Catal. Today 151 (2010) 173–177.
[48] M. Panizza, G. Cerisola, Removal of colour and COD from wastewater containing acid blue 22 by electrochemical oxidation, J. Hazard. Mater. 153 (2008) 83–88.
[49] M. Sun, X.H. Wang, L.R. Winter, Y.M. Zhao, W. Ma, T. Hedtke, et al., Electrified membranes for water treatment applications, ACS EST. Eng. 1 (2021) 725–752.
[50] X. Fan, H. Zhao, Y. Liu, X. Quan, H. Yu, S. Chen, Enhanced permeability, selectivity, and antifouling ability of CNTs/Al_2O_3 membrane under electrochemical assistance, Environ. Sci. Technol. 49 (2015) 2293–2300.
[51] S.N. Yang, Y.B. Liu, C.S. Shen, F. Li, B. Yang, M.H. Huang, et al., Rapid decontamination of tetracycline hydrolysis product using electrochemical CNT filter: mechanism, impacting factors and pathways, Chemosphere 244 (2020) 125525.
[52] Y.B. Liu, H. Liu, Z. Zhou, T. Wang, C.N. Ong, C.D. Vecitis, Degradation of the common aqueous antibiotic tetracycline using a carbon nanotube electrochemical filter, Environ. Sci. Technol. 49 (2015) 7974–7980.
[53] Y. Yang, Z. Xiong, Z. Wang, Y. Liu, Z.J. He, A.K. Cao, et al., Super-adsorptive and photo-regenerable carbon nanotube based membrane for highly efficient water purification, J. Membr. Sci. 621 (2021) 12.
[54] A.R. Bakr, M.S. Rahaman, Removal of bisphenol A by electrochemical carbon-nanotube filter: influential factors and degradation pathway, Chemosphere 185 (2017) 879–887.
[55] G.D. Gao, C.D. Vecitis, Doped carbon nanotube networks for electrochemical filtration of aqueous phenol: electrolyte precipitation and phenol polymerization, ACS Appl. Mater. Inter. 4 (2012) 1478–1489.
[56] M.S. Rahaman, C.D. Vecitis, M. Elimelech, Electrochemical carbon-nanotube filter performance toward virus removal and inactivation in the presence of natural organic matter, Environ. Sci. Technol. 46 (2012) 1556–1564.
[57] B.B. Wang, H.H. Shi, M.Y. Habteselassie, X.Y. Deng, Y. Teng, Y.Y. Wang, et al., Simultaneous removal of multidrug-resistant *Salmonella enterica* serotype typhimurium, antibiotics and antibiotic resistance genes from water by electrooxidation on a Magneli phase Ti_4O_7 anode, Chem. Eng. J. 407 (2021) 8.
[58] X. Tang, L. Wang, B. Yang, C. Fei, T.Y. Yao, W. Liu, et al., Direct oxidation of methane to oxygenates on supported single Cu atom catalyst, Appl. Catal. B Environ. 285 (2021) 119827.
[59] J.J. Patil, A. Jana, B.A. Getachew, D.S. Bergsman, Z. Gariepy, B.D. Smith, et al., Conductive carbonaceous membranes: recent progress and future opportunities, J. Mater. Chem. A 9 (2021) 3270–3289.
[60] S. Gligorovski, R. Strekowski, S. Barbati, D. Vione, Environmental implications of hydroxyl radicals (•OH), Chem. Rev. 115 (2015) 13051–13092.
[61] H. Liu, A. Vajpayee, C.D. Vecitis, Bismuth-doped tin oxide-coated carbon nanotube network: improved anode stability and efficiency for flow-through organic electrooxidation, ACS Appl. Mater. Inter. 5 (2013) 10054–10066.
[62] D. Rajkumar, J.G. Kim, Oxidation of various reactive dyes with *in situ* electro-generated active chlorine for textile dyeing industry wastewater treatment, J. Hazard. Mater. 136 (2006) 203–212.
[63] M. Panizza, G. Cerisola, Direct and mediated anodic oxidation of organic pollutants, Chem. Rev. 109 (2009) 6541–6569.
[64] H. Dodgen, H. Taube, The exchange of chlorine dioxide with chlorite ion and with chlorine in other oxidation states, J. Am. Chem. Soc. 71 (1949) 2501–2504.

This book belongs to Badji Mokhtar Annaba University Central Library Copyright Elsevier 2025

[65] S. Neodo, D. Rosestolato, S. Ferro, A. De, Battisti, On the electrolysis of dilute chloride solutions: influence of the electrode material on faradaic efficiency for active chlorine, chlorate and perchlorate, Electrochim. Acta 80 (2012) 282–291.
[66] X.X. Wang, M. Sun, Y.M. Zhao, C. Wang, W. Ma, M.S. Wong, et al., *In situ* electrochemical generation of reactive chlorine species for efficient ultrafiltration membrane self-cleaning, Environ. Sci. Technol. 54 (2020) 6997–7007.
[67] Z.Z. Li, C.S. Shen, Y.B. Liu, C.Y. Ma, F. Li, B. Yang, et al., Carbon nanotube filter functionalized with iron oxychloride for flow-through electro-Fenton, Appl. Catal. B Environ. 260 (2020) 118204.
[68] Q. Zhang, X. Fan, H. Wang, S. Chen, X. Quan, Fabrication of Au/CNT hollow fiber membrane for 4-nitrophenol reduction, RSC Adv. 6 (2016) 41114–41121.
[69] S. Almassi, Z. Li, W. Xu, C. Pu, T. Zeng, B.P. Chaplin, Simultaneous adsorption and electrochemical reduction of N-nitrosodimethylamine using carbon-Ti_4O_7 composite reactive electrochemical membranes, Environ. Sci. Technol. 53 (2019) 928–937.
[70] Y.B. Liu, Y.Y. Zheng, B.W. Du, R.R. Nasaruddin, T.K. Chen, J.P. Xie, Golden carbon nanotube membrane for continuous flow catalysis, Ind. Eng. Chem. Res. 56 (2017) 2999–3007.
[71] A. Serrà, X. Alcobé, J. Sort, J. Nogués, E. Vallés, Highly efficient electrochemical and chemical hydrogenation of 4-nitrophenol using recyclable narrow mesoporous magnetic CoPt nanowires, J. Mater. Chem. A 4 (2016) 15676–15687.
[72] Y. Bai, M. Mavrikakis, Mechanistic study of nitric oxide reduction by hydrogen on Pt(100) (I): a DFT analysis of the reaction network, J. Phys. Chem. B 122 (2018) 432–443.
[73] Y.M. Su, U. Rao, C.M. Khor, M.G. Jensen, L.M. Teesch, B.M. Wong, et al., Potential-driven electron transfer lowers the dissociation energy of the C–F bond and facilitates reductive defluorination of perfluorooctane sulfonate (PFOS), ACS Appl. Mater. Inter. 11 (2019) 33913–33922.
[74] T.X.H. Le, H. Haflich, A.D. Shah, B.P. Chaplin, Energy-efficient electrochemical oxidation of perfluoroalkyl substances using a Ti_4O_7 reactive electrochemical membrane anode, Environ. Sci. Technol. Lett. 6 (2019) 504–510.
[75] P.L. McCarty, J. Bae, J. Kim, Domestic wastewater treatment as a net energy producer-Can this be achieved? Environ. Sci. Technol. 45 (2011) 7100–7106.
[76] Y. Lee, D. Gerrity, M. Lee, S. Gamage, A. Pisarenko, R.A. Trenholm, et al., Organic contaminant abatement in reclaimed water by UV/H_2O_2 and a combined process consisting of O_3/H_2O_2 followed by UV/H_2O_2: prediction of abatement efficiency, energy consumption, and byproduct formation, Environ. Sci. Technol. 50 (2016) 3809–3819.
[77] I.A. Katsoyiannis, S. Canonica, U. von Gunten, Efficiency and energy requirements for the transformation of organic micropollutants by ozone, O_3/H_2O_2 and UV/H_2O_2, Water Res. 45 (2011) 3811–3822.
[78] G.L. Wei, J. Dong, J. Bai, Y.S. Zhao, Y. Li, Structurally stable, antifouling, and easily renewable reduced graphene oxide membrane with a carbon nanotube protective layer, Environ. Sci. Technol. 53 (2019) 11896–11903.
[79] W.Y. Duan, G.D. Chen, C.X. Chen, R. Sanghvi, A. Iddya, S. Walker, et al., Electrochemical removal of hexavalent chromium using electrically conducting carbon nanotube/polymer composite ultrafiltration membranes, J. Membr. Sci. 531 (2017) 160–171.
[80] B. Zhao, C.X. Zhao, R.S. Li, S.M. Hamidinejad, C.B. Park, Flexible, ultrathin, and high-efficiency electromagnetic shielding properties of poly(vinylidene fluoride)/carbon composite films, ACS Appl. Mater. Inter. 9 (2017) 20873–20884.
[81] S.N. Li, T. Hua, C.S. Yuan, B.K. Li, X.Y. Zhu, F.X. Li, Degradation pathways, microbial community and electricity properties analysis of antibiotic sulfamethoxazole by bio-electro-Fenton system, Bioresour. Technol. 298 (2020) 122501.
[82] Y.B. Liu, F.Q. Liu, N. Ding, C.S. Shen, F. Li, L. Dong, et al., Boosting Cr(VI) detoxification and sequestration efficiency with carbon nanotube electrochemical filter functionalized with nanoscale polyaniline: performance and mechanism, Sci. Total Environ. 695 (2019) 133926.
[83] B.M. Souza-Chaves, M. Dezotti, C.D. Vecitis, Synergism of ozonation and electrochemical filtration during advanced organic oxidation, J. Hazard. Mater. 382 (2020).

This book belongs to Badji Mokhtar Annaba University Central Library Copyright Elsevier 2025

[84] Y. Wu, H. Pang, Y. Liu, X. Wang, S. Yu, D. Fu, et al., Environmental remediation of heavy metal ions by novel-nanomaterials: a review, Environ. Pollut. 246 (2019) 608–620.
[85] F. Fu, Q. Wang, Removal of heavy metal ions from wastewaters: a review, J. Environ. Manage. 92 (2011) 407–418.
[86] X.N. Zhao, K. Ma, T.F. Jiao, R.R. Xing, X.L. Ma, J. Hu, et al., Fabrication of hierarchical layer-by-layer assembled diamond-based core-shell nanocomposites as highly efficient dye absorbents for wastewater treatment, Sci. Rep. 7 (2017) 44076.
[87] L. Huang, J. Li, Z. Wang, Y. Li, X. He, Y. Yuan, Microwave absorption enhancement of porous C@$CoFe_2O_4$ nanocomposites derived from eggshell membrane, Carbon 143 (2019) 507–516.
[88] O.A. Oyetade, A.A. Skelton, V.O. Nyamori, S.B. Jonnalagadda, B.S. Martincigh, Experimental and DFT studies on the selective adsorption of Pb^{2+} and Zn^{2+} from aqueous solution by nitrogen-functionalized multiwalled carbon nanotubes, Sep. Purif. Technol. 188 (2017) 174–187.
[89] H.P. Zhang, F.F. Xu, J.Y. Xue, S.Y. Chen, J.J. Wang, Y.J. Yang, Enhanced removal of heavy metal ions from aqueous solution using manganese dioxide-loaded biochar: behavior and mechanism, Sci. Rep. 10 (2020) 6067.
[90] K.C. Khulbe, T. Matsuura, Removal of heavy metals and pollutants by membrane adsorption techniques, Appl. Water Sci. 8 (2018) 19.
[91] B. He, Z.J. Yun, J.B. Shi, G.B. Jiang, Research progress of heavy metal pollution in China: sources, analytical methods, status, and toxicity, Chin. Sci. Bull. 58 (2013) 134–140.
[92] Q. Ji, D. Yu, G. Zhang, H. Lan, H. Liu, J. Qu, Microfluidic flow through polyaniline supported by lamellar-structured graphene for mass-transfer-enhanced electrocatalytic reduction of hexavalent chromium, Environ. Sci. Technol. 49 (2015) 13534–13541.
[93] S. Bakshi, C. Banik, S.J. Rathke, D.A. Laird, Arsenic sorption on zero-valent iron-biochar complexes, Water Res. 137 (2018) 153–163.
[94] M.A. Ferguson, M.R. Hoffmann, J.G. Hering, TiO_2-photocatalyzed As(III) oxidation in aqueous suspensions: reaction kinetics and effects of adsorption, Environ. Sci. Technol. 39 (2005) 1880–1886.
[95] Y.B. Liu, S.N. Yang, H.L. Jiang, B. Yang, X.F. Fang, C.S. Shen, et al., Sea urchin-like FeOOH functionalized electrochemical CNT filter for one-step arsenite decontamination, J. Hazard. Mater. 407 (2021).
[96] Y.B. Liu, P. Wu, F.Q. Liu, F. Li, X. An, J.S. Liu, et al., Electroactive modified carbon nanotube filter for simultaneous detoxification and sequestration of Sb(III), Environ. Sci. Technol. 53 (2019) 1527–1535.
[97] M.H. Li, Y.B. Liu, C.S. Shen, F. Li, C.C. Wang, M.H. Huang, et al., One-step Sb(III) decontamination using a bifunctional photoelectrochemical filter, J. Hazard. Mater. 389 (2020) 121840.
[98] Y.F. Ren, Y.B. Liu, F.Q. Liu, F. Li, C.S. Shen, Z.C. Wu, Extremely efficient electro-Fenton-like Sb(III) detoxification using nanoscale Ti-Ce binary oxide: an effective design to boost catalytic activity *via* non-radical pathway, Chin. Chem. Lett. 32 (8) (2021) 2519–2523.
[99] A. Matilainen, E.T. Gjessing, T. Lahtinen, L. Hed, A. Bhatnagar, M. Sillanpää, An overview of the methods used in the characterisation of natural organic matter (NOM) in relation to drinking water treatment, Chemosphere 83 (2011) 1431–1442.
[100] W. Yuan, A. Kocic, A.L. Zydney, Analysis of humic acid fouling during microfiltration using a pore blockage-cake filtration model, J. Membr. Sci. 198 (2002) 51–62.
[101] Y.J. Won, J. Lee, D.C. Choi, H.R. Chae, I. Kim, C.H. Lee, et al., Preparation and application of patterned membranes for wastewater treatment, Environ. Sci. Technol. 46 (2012) 11021–11027.
[102] Q. Zhang, C.D. Vecitis, Conductive CNT-PVDF membrane for capacitive organic fouling reduction, J. Membr. Sci. 459 (2014) 143–156.
[103] C.F. de Lannoy, D. Jassby, D.D. Davis, M.R. Wiesner, A highly electrically conductive polymer-multiwalled carbon nanotube nanocomposite membrane, J. Membr. Sci. 415–416 (2012) 718–724.
[104] X. Fan, H. Zhao, X. Quan, Y. Liu, S. Chen, Nanocarbon-based membrane filtration integrated with electric field driving for effective membrane fouling mitigation, Water Res. 88 (2016) 285–292.

This book belongs to Badji Mokhtar Annaba University Central Library Copyright Elsevier 2025

[105] Y. Yang, J. Li, H. Wang, X. Song, T. Wang, B. He, et al., An electrocatalytic membrane reactor with self-cleaning function for industrial wastewater treatment, Angew. Chem. Int. Edit. 50 (2011) 2148–2150.
[106] A. Holder, J. Weik, J. Hinrichs, A study of fouling during long-term fractionation of functional peptides by means of cross-flow ultrafiltration and cross-flow electro membrane filtration, J. Membr. Sci. 446 (2013) 440–448.
[107] J.X. Zhang, W.P. Maddison, Molecular phylogeny, divergence times and biogeography of spiders of the subfamily Euophryinae (Araneae: Salticidae), Mol. Phylogenet. Evol. 68 (2013) 81–92.
[108] X.F. Fan, Y.M. Liu, X.C. Wang, X. Quan, S. Chen, Improvement of antifouling and antimicrobial abilities on silver-carbon nanotube based membranes under electrochemical assistance, Environ. Sci. Technol. 53 (2019) 5292–5300.
[109] C. Thamaraiselvan, A. Ronen, S. Lerman, M. Balaish, Y. Ein-Eli, C.G. Dosoretz, Low voltage electric potential as a driving force to hinder biofouling in self-supporting carbon nanotube membranes, Water Res. 129 (2018) 143–153.
[110] S. Chen, G. Wang, S. Li, X. Li, H. Yu, X. Quan, Porous carbon membrane with enhanced selectivity and antifouling capability for water treatment under electrochemical assistance, J. Colloid Interface Sci. 560 (2020) 59–68.
[111] A.V. Dudchenko, J. Rolf, K. Russell, W. Duan, D. Jassby, Organic fouling inhibition on electrically conducting carbon nanotube-polyvinyl alcohol composite ultrafiltration membranes, J. Membr. Sci. 468 (2014) 1–10.
[112] D.L. Guo, Y.B. Liu, Singlet oxygen-mediated electrochemical filter for selective and rapid degradation of organic compounds, Ind. Eng. Chem. Res. 59 (2020) 14180–14187.
[113] Y. Zhao, M. Sun, X. Wang, C. Wang, D. Lu, W. Ma, et al., Janus electrocatalytic flow-through membrane enables highly selective singlet oxygen production, Nat. Comm. 11 (2020) 6228.
[114] R.D. Webster, S.V.V. Chilukuri, J.A. Levesley, B.J. Webster, Electrochemical cleaning of microporous metallic filters fouled with bovine serum albumin and phosphate under low cross-flow velocities, J. Appl. Electrochem. 30 (2000) 915–924.
[115] H.S. Abid, B.S. Lalia, P. Bertoncello, R. Hashaikeh, B. Clifford, D.T. Gethin, et al., Electrically conductive spacers for self-cleaning membrane surfaces *via* periodic electrolysis, Desalination 416 (2017) 16–23.
[116] Q. Zhang, J. Nghiem, G.J. Silverberg, C.D. Vecitis, Semiquantitative performance and mechanism evaluation of carbon nanomaterials as cathode coatings for microbial fouling reduction, Appl. Environ. Microbiol. 81 (2015) 4744–4755.
[117] X. Fan, Y. Liu, X. Wang, X. Quan, S. Chen, Improvement of antifouling and antimicrobial abilities on silver-carbon nanotube based membranes under electrochemical assistance, Environ. Sci. Technol. 53 (2019) 5292–5300.
[118] L. Tang, A. Iddya, X. Zhu, A.V. Dudchenko, W. Duan, C. Turchi, et al., Enhanced flux and electrochemical cleaning of silicate ccaling on carbon nanotube-coated membrane distillation membranes treating geothermal brines, ACS Appl. Mater. Inter. 9 (2017) 38594–38605.
[119] A. Bogler, S. Lin, E. Bar-Zeev, Biofouling of membrane distillation, forward osmosis and pressure retarded osmosis: principles, impacts and future directions, J. Membr. Sci. 542 (2017) 378–398.
[120] P.S. Goh, A.K. Zulhairun, A.F. Ismail, N. Hilal, Contemporary antibiofouling modifications of reverse osmosis desalination membrane: a review, Desalination 468 (2019) 114072.
[121] A. Ronen, W. Duan, I. Wheeldon, S. Walker, D. Jassby, Microbial attachment inhibition through low-voltage electrochemical reactions on electrically conducting membranes, Environ. Sci. Technol. 49 (2015) 12741–12750.
[122] H. Li, A.K. Singh, L.M. McIntyre, L.A. Sherman, Differential gene expression in response to hydrogen peroxide and the putative PerR regulon of *Synechocystis* sp. strain PCC 6803, J. Bacteriol. 186 (2004) 3331–3345.
[123] X.C. Wang, X.F. Fan, X. Quan, Preparation of Cu-CNT/ceramic hollow fiber membranes and investigation of their antibiofouling performance under electrochemical assistance, Adv. Eng. Res. 170 (2018) 499–502.

This book belongs to Badji Mokhtar Annaba University Central Library Copyright Elsevier 2025

[124] X. Pan, X. Bao, Reactions over catalysts confined in carbon nanotubes, Chem. Commun. (2008) 6271–6281.
[125] W. Chen, Z.L. Fan, X.L. Pan, X.H. Bao, Effect of confinement in carbon nanotubes on the activity of fischer-tropsch iron catalyst, J. Am. Chem. Soc. 130 (2008) 9414–9419.
[126] H.B. Zhang, X.L. Pan, J.Y. Liu, W.Z. Qian, F. Wei, Y.Y. Huang, et al., Enhanced catalytic activity of sub-nanometer titania clusters confined inside double-wall carbon nanotubes, Chemsuschem 4 (2011) 975–980.
[127] E.E. Santiso, A.M. George, C.H. Turner, M.K. Kostov, K.E. Gubbins, M. Buongiorno-Nardelli, et al., Adsorption and catalysis: the effect of confinement on chemical reactions, Appl. Surf. Sci. 252 (2005) 766–777.
[128] D. Ugarte, A. Chatelain, W.Ad Heer, Nanocapillarity and chemistry in carbon nanotubes, Science 274 (1996) 1897–1899.
[129] B. Shan, K. Cho, First-principles study of work functions of double-wall carbon nanotubes, Phys. Rev. B 73 (2006) 081401.
[130] W. Chen, X.L. Pan, M.G. Willinger, D.S. Su, X.H. Bao, Facile autoreduction of iron oxide/carbon nanotube encapsulates, J. Am. Chem. Soc. 128 (2006) 3136–3137.
[131] T.T. Cui, J.H. Dong, X.L. Pan, T. Yu, Q. Fu, X.H. Bao, Enhanced hydrogen evolution reaction over molybdenum carbide nanoparticles confined inside single-walled carbon nanotubes, J. Energy Chem. 28 (2019) 123–127.
[132] M. Menon, A.N. Andriotis, G.E. Froudakis, Curvature dependence of the metal catalyst atom interaction with carbon nanotubes walls, Chem. Phys. Lett. 320 (2000) 425–434.
[133] D.L. Guo, Y.B. Liu, H.D. Ji, C.C. Wang, B. Chen, C.S. Shen, et al., Silicate-enhanced heterogeneous flow-through electro-Fenton system using iron oxides under nanoconfinement, Environ. Sci. Technol. 55 (2021) 4045–4053.

This book belongs to Badji Mokhtar Annaba University Central Library Copyright Elsevier 2025

CHAPTER FIVE

Electrochemical membrane technology for disinfection

Yin-Hu Wu[1], Zheng-Yang Huo[2], Hai Liu[3], Xin-Ye Ni[1], Hao-Bin Wang[1], Han Liu[1] and Hong-Ying Hu[1,4]

[1]Environmental Simulation and Pollution Control State Key Joint Laboratory, State Environmental Protection Key Laboratory of Microorganism Application and Risk Control (SMARC), Beijing Laboratory for Environmental Frontier Technologies, School of Environment, Tsinghua University, Beijing, P.R. China
[2]School of Environment and Natural Resources, Renmin University of China, Beijing, P.R. China
[3]School of Environment, Guangzhou Key Laboratory of Environmental Exposure and Health, and Guangdong Key Laboratory of Environmental Pollution and Health, Jinan University, Guangzhou, P.R. China
[4]Shenzhen Environmental Science and New Energy Technology Engineering Laboratory, Tsinghua-Berkeley Shenzhen Institute, Shenzhen, P.R. China

5.1 Introduction

Water is one of the most important necessities of human existence, if not of any kind of life, for the proliferation and sustenance of life and human society. Disinfection is an essential process to inactivate harmful and undesirable microbes during the utilization of conventional and nonconventional water resources. Conventional disinfection technologies, such as chlorination, ozonation, and ultraviolet (UV) disinfection, have been developed and applied extensively worldwide for several decades [1,2]. However, these disinfection technologies have intrinsic disadvantages, such as the formation of harmful byproducts (DBPs) and microbial reactivation/regrowth [3–5]. Membrane filtration (namely microfiltration and ultrafiltration) occurs through pores smaller than microbial cells and can remove microbes but also suffer from low throughput and intensive energy consumption [6,7]. In addition, the aforementioned disinfection methods are commonly feasible for centralized systems but not easily applicable in less developed or still developing areas on the earth where sanitation facilities and power supplies are unavailable [8]. Therefore the developing of highly efficient, reliable, low-energy-consuming, and easily applicable disinfection technologies for centralized and decentralized water treatment systems is necessary.

Electrochemical membrane technology is an emerging way to effective disinfection that involves novel microbial inactivation mechanisms, such as free radical generation and cell structure decomposition. In contrast to the conventional membranes, the electrochemical membranes consist of conductive materials, including metals and carbon-based materials with mesh- or membrane-like structures. The electrochemical membranes serve as electrodes in the reactor during disinfection. In many recent

Electrochemical Membrane Technology for Water and Wastewater Treatment.
DOI: https://doi.org/10.1016/B978-0-12-824470-8.00009-7
© 2022 Elsevier Inc.
All rights reserved.

This book belongs to Badji Mokhtar Annaba University Central Library
Copyright Elsevier 2025

studies, the membranes or electrodes are modified with nanostructures. Electrochemical membranes have specific biological, electronic, and/or catalytic properties that are capable of achieving microbial disinfection with low DBP formation and without microbial regrowth [9–11]. The suitability of this disinfection technology is also useful for decentralized applications to be deployed because of its flexible reactor design, low energy consumption, and superior disinfection performance at a small scale [12,13].

Developing a high-performance electrochemical membrane disinfection system requires exploiting the unique disinfection mechanisms enabled by electrochemical membranes and improving the treatment efficiency and lifespan of the system. Therefore the three essential factors that need to be considered in the development of electrochemical membrane technology for disinfection are: (1) principal disinfection mechanisms achieved by electrochemical membranes with different materials and structures, (2) feasible reactor configuration designs to improve disinfection efficiency, and (3) suitable strategies to improve the stability of electrochemical membranes.

Various electrochemical membrane disinfection processes have already achieved high treatment performance with conventional or novel mechanisms [14,15]. Multiple studies and proposed processes pose an enormous challenge for the critical assessment of electrochemical membrane disinfection technology. Enabling a comparison between different electrochemical membrane disinfection processes based on disinfection performance, operational costs, and general feasibility is essential.

Therefore in this chapter, we review established and emerging electrochemical membrane technologies for water disinfection by summarily outlining the principal mechanisms and reactor configurations of these technologies. The critical assessment indexes for different disinfection processes are proposed, including the disinfection performance (the shortest contact time required for complete disinfection) and the operation cost (the amount of electrical energy needed to reduce the microbial concentration by one order of magnitude; E_{EO}). Furthermore, the limitations to and challenges of current electrochemical membrane disinfection technologies are also analyzed.

5.2 Principal mechanisms of electrochemical membrane technology for disinfection

5.2.1 Principal mechanisms involved in the disinfection process to be achieved by electrochemical membranes

The pore size of the membranes or the filters used in the electrochemical membrane technology for disinfection are usually much bigger than the microbial cells. Therefore the rejection effects of these membranes are usually not as significant as microfiltration or ultrafiltration, leading to much smaller filtration resistance.

This book belongs to Badji Mokhtar Annaba University Central Library Copyright Elsevier 2025

The principal mechanisms involved in disinfection by electrochemical membranes include direct oxidation, indirect oxidation, and nanowire-assisted electroporation (Fig. 5.1). Direct oxidation refers to the electron transfer between the anode and the cell membrane, which is primarily affected by mass diffusion, electrode surface area, and anode potential [16,17]. Indirect oxidation involves the production of reactive species from electrolyte redox reactions, such as hydroxyl radicals (•OH) and hydrogen peroxide (H_2O_2), which subsequently mediate microbe inactivation in solution [17,18].

Nanowire-assisted electroporation relies on local electric field enhancement attributed to the unique physical properties (high conductivity and sharp structure) of the electrodes or the electrochemical membranes [19–21]. Local electric field enhancement relies on the "lightning rod effect," which occurs when a metallic rod is inserted into a region with a uniform electric field [22]. The electric field strength near the tip of the metallic rod can be enhanced to have a positive correlation with the aspect ratio of the metallic rod [22]. Based on these unique mechanisms, electrochemical membrane technology for disinfection is categorized into electrochemical and nonelectrochemical processes and has been confirmed as feasible for high-performance water disinfection.

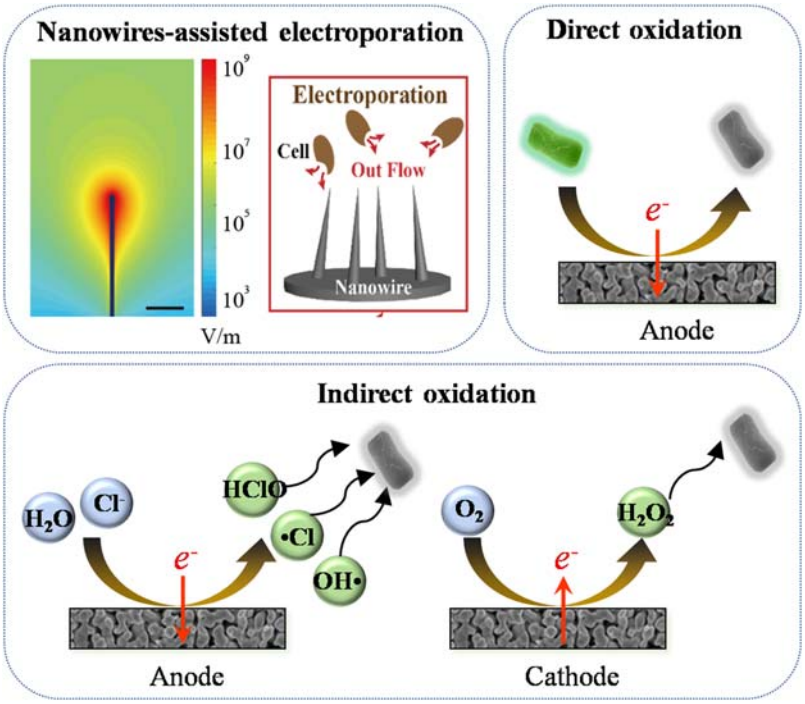

Figure 5.1 Principal mechanisms involved in disinfection by electrochemical membranes.

This book belongs to Badji Mokhtar Annaba University Central Library Copyright Elsevier 2025

5.2.2 Direct oxidation

Direct and indirect oxidation are electrochemical disinfection processes that offer a direct and an effective method to transfer energy to microbes in water [12]. Electrochemical oxidation of microbes is the dominant disinfection mechanism that can occur directly through a charge transfer at the electrode surface (i.e., direct oxidation) and indirectly through reactions with electrochemically generated reactive species (i.e., indirect oxidation) [17,20,23].

The direct oxidation disinfection process is postulated as a two-step process: (1) deposition or adsorption of the microbes onto electrodes, and (2) oxidation of the microbes by electron transfer, which interrupts transmembrane electron transfer and triggers cellular oxidative stress [20,24]. During the direct oxidation disinfection process, the microbe-electrode contact is a speed-limited step, whereas the conventional panel electrode cannot offer a sufficient surface area for highly efficient microbe deposition. Thus nanomaterial-modified electrochemical membranes (e.g., Ag nanowire-modified and CNT) have been studied to improve the treatment rates [25,26]. However, the formation of harmful Cl_2-DBPs in complex water matrices, the high fabrication cost, and the performance stability require further investigation. To solve these problems, low-cost and high-stability materials, such as graphitized carbon fiber membranes, are used in direct oxidation disinfection process with low voltage ($\leq$3 V) [24].

Graphitized carbon fiber membranes showed superior disinfection performance under low voltage, especially powered by alternating pulse voltage with low-frequency [27]. Due to the low voltage used, no free chlorine was detected in the system avoiding the problem of Cl_2-DBPs formation. The stability of graphitized carbon fiber membranes was tested in a continuous flowing experiment for at least 7 days, and the disinfection performance was kept stable with no culturable bacteria in the effluent [24].

5.2.3 Indirect oxidation

In an indirect oxidation disinfection process, specific electrochemical membranes (including boron-doped diamond (BDD), SnO_2, PbO_2, RuO_2, and substoichiometric and doped-TiO_2 membranes) are used as anode materials to generate highly reactive in situ reactive oxygen species (ROS) (e.g., •OH and •Cl) for water disinfection [28–30].

Besides the indirect oxidation at the anode, the dissolved O_2 molecules in the microbe-containing solution can be reduced to H_2O_2 species at the cathode, forming the H_2O_2-concentrated interface on cathode and also releasing H_2O_2 species into the bulk solution. The H_2O_2-concentrated interface can quickly inactivate the nearby microbes, and the H_2O_2 in bulk solution can also cause the microbe inactivation, achieving the disinfection mechanism of indirect oxidation at the cathode.

This book belongs to Badji Mokhtar Annaba University Central Library Copyright Elsevier 2025

One major challenge, however, is the transferring of the generated radicals into the bulk water solution to react with the target microbes. Additionally, the application of indirect electrochemical oxidation is limited by the high membrane production cost, the intensive energy consumption, and the formation of harmful DBPs due to reactions between the generated Cl_2 or other reactive species and organic matter in the wastewater [12]. Furthermore, electrochemical oxidation only occurs at the anode surface, whereas the potential for cathodic reactions is mostly unused.

5.2.4 Electroporation

Electroporation is a physical process that relies on a strong electric field to damage microbial surface structures (membranes for bacteria and capsids for viruses), offers new opportunities for water disinfection, and represents a promising substitute for reducing the chemical demand of conventional water disinfection methods [31,32]. Because nanowires (such as Ag, CuO, and ZnO) can significantly enhance the local electric field (10^7 V/m) with voltages as low as 1 V, a nanowire-assisted electroporation disinfection is feasible for effective water disinfection [33–35].

Nanowire-assisted electroporation disinfection benefits from the physical disinfection mechanism and shows high microbial inactivation efficiency and broad-spectrum effectiveness for most microbes, including bacteria (model bacteria and real wastewater) and viruses (Ms2) without any chemical consumption [32,35]. Additionally, no microbes regrow during the storage process [21]. Furthermore, because of the low operation voltage (1 V), no Cl_2 was generated, ensuring the low formation potential of harmful DBPs. However, nanostructure degradation, including hydraulic detachment and electrochemical dissolution, reduces electrode lifetime and releases hazardous materials (such as heavy metals) into the effluent, posing a great obstacle to practical applications [32,36].

5.2.5 Other mechanisms

In addition to the principal aforementioned mechanisms, other mechanisms may also be involved in the disinfection process due to the special structures of some electrochemical membranes (especially nanomaterial-modified membranes). Nanomaterial-modified membranes can achieve microbial inactivation by relying solely on the physical contact of antimicrobial nanomaterials with microbes (e.g., bacteria and viruses) [37–39]. During the disinfection process, using electrochemical membranes with specific nanostructures, the disinfection performance should be the synergistic effect of these mechanisms.

Antimicrobial nanomaterials directly interact with microbes, enabling cell inactivation by interrupting transmembrane electron transfer, disrupting or penetrating the cell envelope, or oxidizing cell components [40–42]. Additionally, some nanomaterials also generate secondary

This book belongs to Badji Mokhtar Annaba University Central Library Copyright Elsevier 2025

products (e.g., dissolved heavy metal ions and ROSs) that cause cell damage without any other input (e.g., chemical, photo, or electric) [43,44]. Because of the specific disinfection mechanism of physical contact and lack of demand for other inputs, this type of disinfection mechanism is a physical-based category of the process of water disinfection.

Two types of membrane materials are generally involved in this mechanism: (1) carbon-based antimicrobial nanomaterials and (2) metal-based antimicrobial nanomaterials. The antibacterial activities of the carbon-based nanomaterials involved in the physical-based disinfection process [carbon nanotubes (CNTs), graphene, and MXene] are primarily attributed to their unique sharp structures (tips or edges) [37,45]. CNTs can be either single-walled (SWNTs)—a single pipe with a diameter of 1−5 nm—or multiwalled (MWNTs)—a nested tube structure with lengths from 100 nm to 100 μm [46].

SWNTs contact microbes first, resulting in membrane perturbation and the release of intracellular contents. Another disinfection mechanism of SWNTs is the cellular oxidative stress due to the contact between SWNTs and the cytoplasm, where the cellular oxidative stress tends to be affected by the electronic structure of SWNTs (i.e., more toxic SWNTs with a higher percentage of metals) [46]. Membrane stress, a major disinfection mechanism for MWNTs, is caused by direct MWNT-microbe contact [47,48]. Additionally, the MWNT structure can also contribute to microbial removal. The removal of bacteria by SWCNT-MWCNT membranes was confirmed by microbial inactivation by the top layer of SWCNTs, followed by depth filtration by the MWCNT layer [47]. Furthermore, the adsorption of microbes (bacteria and viruses) onto CNTs, attributed to hydrophobicity, is another crucial factor influencing the antimicrobial properties of CNTs [25]. CNTs can be immobilized on the membrane as a CNT membrane, which enables microbial removal by adsorption [49]. The CNT membrane extends the application potential of the CNT-based disinfection process.

Graphene [including graphene oxide (GO); reduced graphene oxide (rGO)], a one-atom-thick two-dimensional (2D) carbon layer; and MXene, a family of two-dimensional materials consisting of transition metal carbides and nitrides, show antibacterial mechanisms similar to those of CNTs [50−52]. The sharp edges of graphene/GO/rGO and MXene ($<$ 10 nm) are capable of piercing the cell membrane, which damages the membrane structure and triggers oxidative stress in the cell [45,53,54]. Additionally, the smaller sheet sizes of graphene, GO, and rGO further increase the antimicrobial activity of the material [52].

Silver nanoparticles (AgNPs) are the most commonly used metal-based antimicrobial nanomaterials and have broad applications in water disinfection [55,56]. To date, several mechanisms have been proposed for the antimicrobial properties of AgNPs: (1) adhesion of nanoparticles to the cell surface, altering the membrane properties (for bacteria); (2) AgNPs penetration inside microbes, resulting in DNA/RNA and/or protein damage (for both bacteria and viruses); and (3) AgNP performance as a vehicle to more effectively deliver released Ag^+ to the cellular cytoplasm (for bacteria) [42,57]. Additionally, copper-based nanomaterials have been widely applied in water

This book belongs to Badji Mokhtar Annaba University Central Library Copyright Elsevier 2025

disinfection. The released copper ions (Cu^{2+}) show obvious toxicity toward both bacteria and viruses, enabling highly efficient disinfection [58,59].

Nanoscale zerovalent iron (NZVI) or iron nanoparticles (FeNPs) show strong redox activity that is attributed to their special valence (Fe^0) and have been investigated as tools for the treatment of contaminated water and soil [60]. Because of the strong reducing conditions at the NZVI surface and the oxidative damage from intracellular ROS produced by Fenton's chemistry, NZVI enables the decomposition of microbial surface structures (membranes for bacteria and capsids for viruses) and of protein and DNA/RNA in microbes (bacteria and viruses) [43,44,61].

5.2.6 Performance comparison of different disinfection mechanisms

After a brief overview of established electrochemical membrane disinfection technologies, a deeper look is warranted by making assessments and comparisons between different disinfection mechanisms based on (1) disinfection performance, and (2) energy consumption to create general guidelines for future research. The shortest contact time or hydraulic retention time (HRT) needed to achieve complete disinfection (i.e., no live microbes in the effluent) can be used to evaluate disinfection capability and upper limitation [15,32,62,63]. To analyze the treatment efficiency of disinfection processes in laboratories, researchers often apply cultivable model microbes (e.g., *Escherichia coli* and *Bacillus subtilis*) to represent bacteria, and Ms2 to represent viruses.

To investigate the treatment capacity, researchers commonly disperse model microbes in water at relatively high concentrations ($\sim 10^7 - 10^9$ colony-forming units/mL or plaque-forming units/mL; CFU or PFU/mL) as the tested microbial solution and will test the shortest contact time for complete disinfection. Because the kinetics of microbial inactivation achieved by electrochemical membranes are often described as a pseudo-first-order model, the contact time required for each microbial log removal is similar. If the initial concentration varies from 10^7 to 10^9 CFU or PFU/mL, the theoretical contact time for removing 10^9 microbes is $[1 - (9/7)] \times 100\% = 28\%$ higher than the contact time for removing 10^7 microbes. Thus the difference in microbial concentration may contribute to the variability of the overviewed contact time for each disinfection process but is unlikely to induce significant differences among the mechanisms of different disinfection processes.

To further investigate the impact of microbial types (bacteria and viruses) on disinfection efficiency, we separately analyzed the contact time needed for virus inactivation and compared it with the contact time for overall microbial (bacteria plus viruses) inactivation. Contact times required for virus inactivation did not introduce significant variability into the disinfection mechanisms (Fig. 5.2). Bacteria and viruses may, therefore share similar inactivation mechanisms for each disinfection process. Bacteria and viruses have different microbial structures, but their biological structures are very

This book belongs to Badji Mokhtar Annaba University Central Library Copyright Elsevier 2025

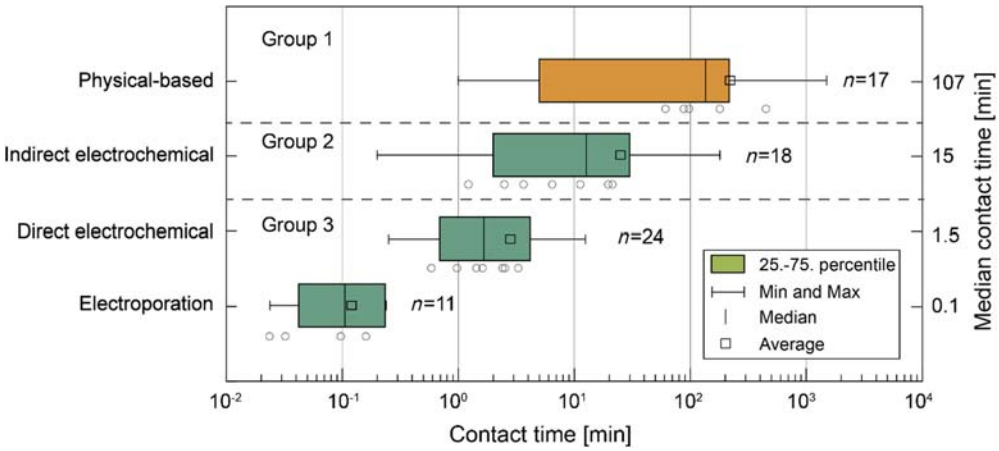

Figure 5.2 The shortest contact time or hydraulic retention time required for complete disinfection of electrochemical membranes; *n* refers to the number of data points for each boxplot and the median values shown on the second *y*-axis. The *light grey* circle (○) is the data point of contact times for virus disinfection. Although different types of microbes (i.e., bacteria and viruses) were applied in different studies, the viruses will not induce significant differences between disinfection processes.

simple and share similar basic and essential substances for living organisms, such as protein and DNA/RNA. Thus the disinfection efficiency of viral mechanisms may not differ significantly from the overall microbial disinfection efficiency (Fig. 5.2); a comparison of the disinfection efficiency among processes is reasonable and feasible.

The impact of different types of model microbial strains on the distinction efficiency was also investigated. *E. coli* is the most commonly used model bacteria in research on electrochemical membrane disinfection technology. Other bacterial strains, such as *Enterococcus faecalis*, *Salmonella enterica*, and *B. subtilis*, have also been tested [32,62,64]. The major difference among these model bacteria is their membrane structure, which can be evaluated by the gram-positive or gram-negative features. Gram-positive bacteria have a thicker peptidoglycan layer than gram-negative bacteria, which leads to a higher resistance to disinfection [32]. However, different bacterial strains do not introduce significant data variability or impact the comparison between different disinfection processes.

For virus disinfection, the bacteriophage Ms2 is the most commonly used model virus; the bacteriophage f2 has been applied in some studies [44]. Because of the similar structure of Ms2 and f2, the type of virus did not introduce significant data variability or impact the comparison among disinfection mechanisms.

To compare the disinfection mechanisms of electrochemical membranes, the data variability introduced by different water quality parameters was also investigated. Many researchers have investigated the impact of water quality on electrochemical

This book belongs to Badji Mokhtar Annaba University Central Library Copyright Elsevier 2025

membrane technology using synthetic water samples. The water quality parameters were controlled within a reasonable range (pH of 6−8, temperature of approximately 15 °C, and ionic strength of 10−100 mM) to simulate the water quality of drinking water and/or wastewater. The impacts of pH and ionic strength were confirmed to be nonsignificant for electro-based disinfection processes [25,65]. Whereas some results show that changing water quality parameters may impact disinfection efficiency, these impacts are less significant than that introduced by different disinfection mechanisms [10]. Thus the impacts of pH, temperature, and ionic strength were not significant and did not affect the comparison between disinfection mechanisms. We did not include studies involving the impact of organic matter in the comparison of different disinfection mechanisms due to the lack of standardized experimental protocols for simulating organic matter in real water/wastewater conditions.

Electrochemical membrane disinfection technology commonly requires electrical energy input during the treatment process, which often represents a major fraction of energy consumption and operation cost. Because the kinetics of microbial inactivation assessed by electrochemical membranes are often described as a pseudo-first-order model, electrical energy consumption scaled with the volume and treatment goals [described as electrical energy per order (E_{EO})] can be calculated and applied to the assessment of energy consumption [66]. E_{EO} represents the amount of electrical energy required to reduce the microbial concentration by one order of magnitude; the E_{EO} calculation method for different disinfection processes is illustrated as follows [10,67].

$$E_{EO} = \frac{U \times I}{\text{Flux} \times \text{order}} \times 6 \times 10^4$$

The unit of the E_{EO} value is kWh/m^3 per order. U is the applied voltage between two electrodes (V); I is current (A); flux is the speed of water flow passing through the reactor (mL/min); and order is the microbial log removal rate by disinfection.

5.2.6.1 Performance comparison of disinfection mechanisms based on shortest contact time

The shortest contact time required for the complete disinfection of different electrochemical membrane technology mechanisms from literature data is summarized in Fig. 5.2 as box plots and sorted by median value. The reported contact times of each disinfection mechanism varied by several orders of magnitude. Such data variability is likely due to the different membrane materials and types of reactors applied in each type of disinfection process. Furthermore, the complex water matrix may also affect the ROS generation efficiency, which affects the disinfection performance and aggravates data variability. Additionally, the difference in the type and concentration of treated microbes induced data variability. However, the variability introduced by microbial types and water quality is not significant for each disinfection mechanism and does not impact the assessment.

This book belongs to Badji Mokhtar Annaba University Central Library Copyright Elsevier 2025

Significant differences among disinfection processes are observed in the literature. Based on the median contact time, electrochemical membrane technology for disinfection can be classified into three groups: (1) mechanisms with median contact time > 100 min (physical-based only, or group 1 mechanisms); (2) contact time between 20 and 100 min (indirect electrochemical-based, or group 2 mechanisms); and (3) contact time < 10 min (direct electrochemical- and electroporation-based, or group 3 mechanisms).

The significant contact time differences for each group were partly caused by the different disinfection mechanisms. In group 1, the relatively long contact time (107 min) required for complete disinfection indicated the low disinfection efficiency of the physical-based process. Physical-based disinfection is highly dependent on the microbe-nanostructure direct contact and on the reaction between microbes and nanomaterials, which requires a specific period for sufficient cytotoxicity. These two steps lead to relatively low disinfection efficiency and long contact time for complete disinfection [37,46].

Because of the feasible design of disinfection reactors (e.g., flow-through reactor), the treatment efficiency of the physical-based disinfection process can be significantly improved; and the shortest contact time for complete disinfection was 1 min [38,55]. Thus the important impact of reactor configuration is discussed systematically later in this chapter.

Disinfection processes in group 2 commonly rely on ROS production to achieve microbial inactivation. Because of the relatively high reactivity of ROS, the disinfection processes in group 2 had higher disinfection efficiencies than that demonstrated by the disinfection processes in group 1 (Fig. 5.2). The difference in disinfection efficiency among the various processes was likely due to ROS generation efficiency.

The disinfection processes in group 3 (i.e., direct electrochemical- and electroporation-based) showed the highest disinfection efficiency with a significantly lower contact time (1.5 and 0.1 min, respectively) than that required by the other mechanisms. Owing to unique disinfection mechanisms (electron transfer or membrane damage caused by the strong electric field), microbes are inactivated immediately after making contact with the electrode or upon entering the area with a sufficiently strong electric field; thus this results in high disinfection efficiency [20,21]. Additionally, with the help of the feasible design of disinfection reactors (e.g., flow-through reactor), the microbes are effectively transferred from the bulk solution to the electrode surface. This leads to a significantly improved disinfection efficiency compared with that displayed by the physical-based process (group 1) or that of the ROS-based disinfection process (group 2) [17,68].

5.2.6.2 Performance comparison of different disinfection mechanisms based on E_{EO}

The E_{EO} values for the different mechanisms of electrochemical membranes from the literature data are summarized in Fig. 5.3 as box plots and sorted by median value.

This book belongs to Badji Mokhtar Annaba University Central Library Copyright Elsevier 2025

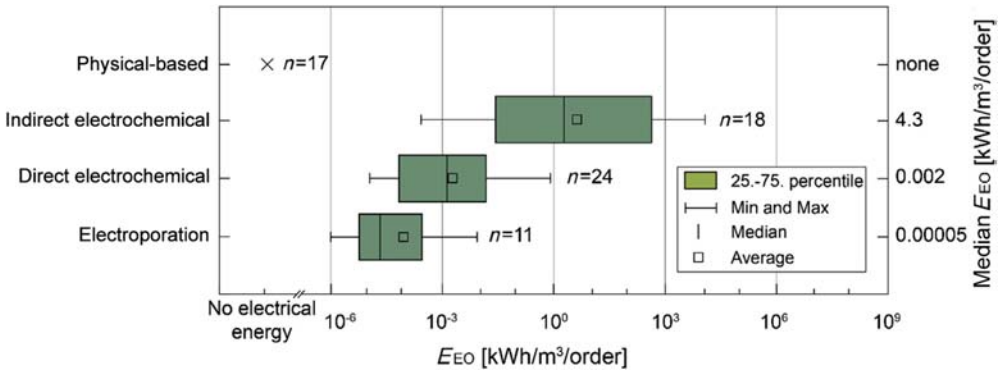

Figure 5.3 The E_{EO} values of electrochemical membranes with different mechanisms; *n* refers to the number of data points for each boxplot and the median values shown on the second *y*-axis.

Except for the additional energy demand for chemicals or catalysts, it's only electric energy consumption that is reflected within the E_{EO}. Direct electrochemical- and electroporation-based disinfection rely on electron transfer or membrane damage by a strong electric field and showed a lower E_{EO} (0.002 and 0.00005 kWh/m^3 per order, respectively) than that of indirect electrochemical-based disinfection (4.3 kWh/m^3 per order), whose disinfection mechanism is ROS-dependent.

Additionally, the E_{EO} values of direct electrochemical- and electroporation-based disinfection were also significantly lower than those of conventional energy-efficient disinfection methods—such as low-pressure UV disinfection ($\sim$0.005 kWh/m^3 per order; *E. coli* for 3-log inactivation) [67,69]. Such low energy consumption increases the potential value of decentralized water treatments for water disinfection in regions without developed infrastructure.

5.3 Reactor configuration of electrochemical membrane for disinfection

This section summarizes and compares the reactor configuration of the electrochemical membrane. The advantages and limitations of the different reactor configurations are briefly discussed. Furthermore, comprehensive assessments of various electrochemical membrane reactors are performed based on disinfection performance and energy efficiency.

5.3.1 Development progress of the reactor configuration

Fig. 5.4 shows the general development progress of the reactor configuration of the electrochemical membrane disinfection technology. Because the basic disinfection

This book belongs to Badji Mokhtar Annaba University Central Library Copyright Elsevier 2025

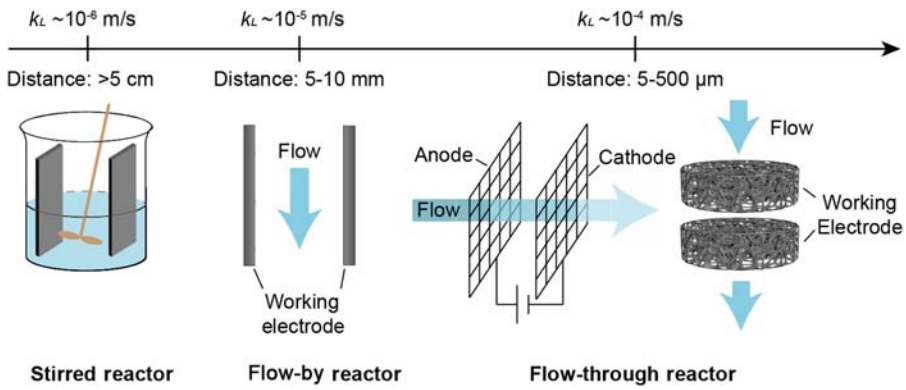

Figure 5.4 Development progress of the reactor configurations. (1) stirred reactor, (2) flow-by reactor, and (3) flow-through reactor. Mass transfer coefficients and the distance for microbes transferring to the electrode surface in each device are summarized. k_L is the mass transfer coefficient.

mechanism of this technology is the contact between microbial cells and the membrane (electrode) materials or the oxidizing species, the key factor for improving the efficiency of this technology is to increase the mass transfer coefficient within the reactor by developing a reactor configuration.

5.3.2 Stirred reactor applied in electrochemical membrane for disinfection

The stirred reactor uses a pair of panel electrodes or electrochemical membranes with specific immobilized or grown nanostructures (Fig. 5.4). Microbial cells are mixed completely in the reactor to provide an opportunity for contact with the electrodes or the oxidizing species. Owing to its easily applicable features, the electrode-stirred reactor is feasible for most disinfection processes and is one of the most widely applied types of reactors. However, because of the required space between two electrodes for stirring the microbial solution using paddles or rotors, a relatively long distance is required (commonly > 5 cm) for microbes to approach the electrodes, which reduces disinfection efficiency and enlarges the area footprint for device construction [70,71]. Additionally, the mass transfer rate for the electrode-stirred reactor is relatively low, with a coefficient of $\sim 10^{-6}$ m/s, leading to a lower disinfection efficiency and an increased E_{EO} value [72].

5.3.3 Flow-by reactor applied in electrochemical membrane for disinfection

The flow-by reactor applied in the electrochemical membrane disinfection technology commonly includes two panel electrodes, to which the microbial solution flows continuously parallel (Fig. 5.4). Microbial inactivation occurs directly, on one hand, through microbe-electrode contact, charge transfer, or a strong electric field at the electrode surface and indirectly, on the other, through ROS reactions. Thus the

This book belongs to Badji Mokhtar Annaba University Central Library Copyright Elsevier 2025

flow-by reactor is feasible for most disinfection processes and is the predominant choice for achieving indirect electrochemical-based disinfection.

The distance between two electrodes in a flow-by reactor is relatively short (5−10 mm), guaranteeing a higher mass transfer efficiency ($\sim 10^{-5}$ m/s) than that of the stirred reactor ($\sim 10^{-6}$ m/s) and leading to better disinfection performance [72−75]. Furthermore, the suitability of the flow-by reactor for practical applications has been attributed to its feasibility for long-term operation without maintenance and the potential for automated control by adjusting the operating conditions according to water quality. However, the short distance between electrodes leads to a huge demand for electrode materials for device construction and results in high electrode fabrication costs. Additionally, the upper limit of mass transfer in the flow-by reactor further hinders the practical application of high-performance disinfection.

5.3.4 Flow-through reactor applied in electrochemical membrane for disinfection

Owing to the heterogeneous nature of the disinfection process achieved by electrochemical membrane technology, the design of reactors with sufficient treatment rates is an impending challenge in the face of mass transfer limitations. A simple stirred and flow-by reactor cannot provide sufficient contact area between the microbial cells and the membrane materials. Thus flow-through reactors with membranes or porous electrodes (Fig. 5.4) have been developed to improve treatment rates. The types of materials used in this type of reactor include mesh-based electrodes or membranes (including Ti mesh and CNT-membrane) and 3-dimensional (3D) porous electrodes, including carbon-based and metal foam-based porous materials [17,76,77]. In flow-through reactors, the microbial solution flows perpendicular to and through the membrane or porous electrodes with a mass transfer rate ($\sim 10^{-4}$ m/s) superior to that of stirred and flow-by reactors, which overcome mass transfer limitations [72].

Flow-through electrodes with microchannels (5−500 μm) acting as microreactors are widely applied in electrochemical membrane technology for disinfection processes [21,78]. Mesh electrodes and thin ($<$ 5 mm) carbon-based membrane electrodes (e.g., carbon cloth) achieved significantly improved ROS generation efficiency compared with those of stirred and flow-by reactors [77]. Gu reported a rational strategy using flow-through photoanodes (ZnO nanorod-modified carbon cloth) to affect ROS generation during the photoelectrocatalytic process. ROS generation performance was evaluated using the degradation kinetics of specific organic matter. Compared to traditional planar photoanodes, flow-through photoanodes exhibited four times (for Rhodamine B) and three times (for bisphenol A) higher degradation kinetics, indicating significantly improved ROS generation efficiency [77].

The highly porous networks of 3D porous electrodes offer a large surface area with numerous active sites, increasing the opportunity for microbes to approach the

This book belongs to Badji Mokhtar Annaba University Central Library Copyright Elsevier 2025

electrode surface and to react with the electrodes; and, this improves the disinfection performance [17,20,24]. Owing to their high disinfection efficiency and high throughput, 3D porous electrodes applied in flow-through disinfection reactors have great potential for practical applications. However, problematic electrode degradation due to hydraulic erosion and electrode clogging caused by microbes or other substances in real water require more attention and research to sharpen the potential of the technology to practical application.

5.3.5 Evaluation and comparison of different configurations

The different reactor configurations must be comprehensively evaluated and compared to guide reactor configuration design in future studies and for practical applications. The shortest contact time required for complete disinfection and the E_{EO} value of electrochemical membrane technology for disinfection are summarized and categorized based on the type of reactor (i.e., stirred, flow-by, and flow-through). The two performance parameters of electrochemical membrane technology with different reactor configurations are summarized in Fig. 5.5, according to data from the literature. The disinfection technologies are separated into three groups (Fig. 5.5) and are almost consistent with the type of reactor.

Figs. 5.6 and 5.7 compare the shortest contact time required for complete disinfection and the E_{EO} values of different reactors, respectively. The flow-through reactor showed the shortest contact time for complete disinfection (median value of 0.1 min), indicating the highest disinfection efficiency (Fig. 5.6). The flow-by and stirred reactors showed longer contact times of 13 and 62 min, respectively (Fig. 5.6), confirming

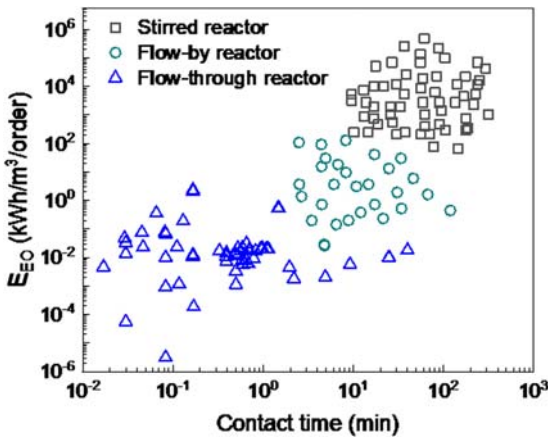

Figure 5.5 The shortest contact time required for complete disinfection and the E_{EO} value of each electrochemical membrane disinfection technology classified by the type of reactor (i.e., stirred, flow-by, and flow-through).

This book belongs to Badji Mokhtar Annaba University Central Library Copyright Elsevier 2025

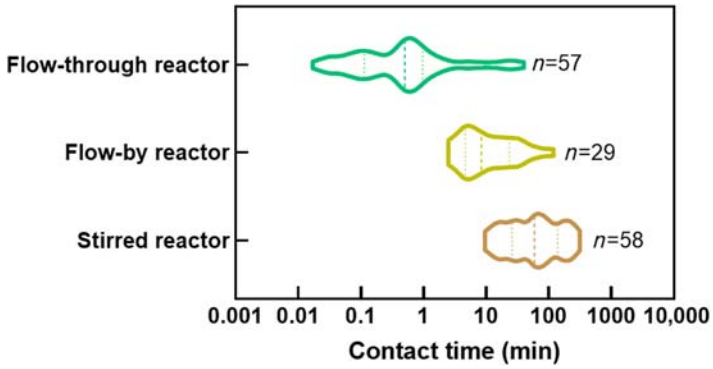

Figure 5.6 The shortest contact time required for complete disinfection of electrochemical membrane reactors; *n* refers to the number of data points for each boxplot and the median values shown next to the 50th percentile line.

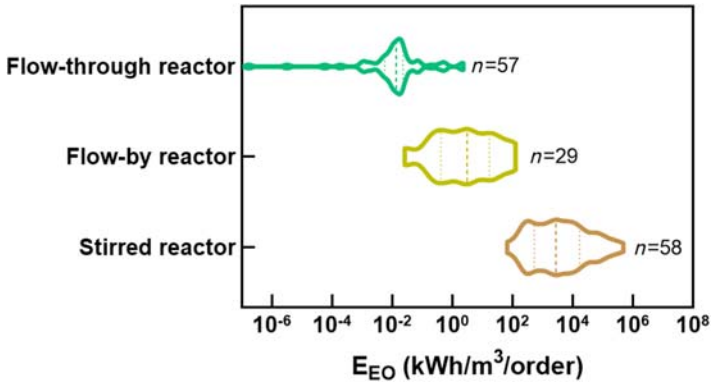

Figure 5.7 E_{EO} value of electrochemical membrane reactors for disinfection; *n* refers to the number of data points for each boxplot and the median values shown next to the 50th percentile line.

a lower disinfection efficiency. Furthermore, the flow-through reactor showed the lowest E_{EO} value (0.002 kWh/m^3 per order), indicating the highest energy efficiency; whereas the flow-by and stirred reactor showed higher E_{EO} values of 76 and 1123 kWh/m^3 per order, respectively, indicating intensive energy consumption (Fig. 5.7).

The flow-through reactor had the highest mass transfer rate for microbes approaching the membrane surface and, therefore showed the highest disinfection efficiency (contact time of 0.1 min) and the lowest energy consumption (E_{EO} value of 0.002 kWh/m^3 per order) among the reactor configurations. The flow-through reactor applied in electrochemical membrane technology for disinfection showed a comparable or even superior disinfection performance and energy efficiency to the conventional low-pressure UV technology, which is a conventional fast and energy-efficient

This book belongs to Badji Mokhtar Annaba University Central Library Copyright Elsevier 2025

disinfection technology with contact time of ~1.3 min and E_{EO} value ~0.005 kWh/m^3 per order (3-log inactivation of *E. coli*) [67,69]. Thus the flow-through configuration showed great potential for practical applications.

5.4 Limitations and challenges of electrochemical membrane disinfection technology

Emerging electrochemical membrane technology has achieved efficient disinfection performance on a laboratory scale; however, significant obstacles must be overcome before this technology can be applied to practical water treatment in centralized and decentralized systems. Most difficulties originate from the unique properties of the electrochemical membranes, including low disinfection efficiency and energy intensiveness, and membrane strengthening/optimization [12,79]. Many novel electrochemical membranes for disinfection are modified with nanostructures, which are relatively fragile during long-term operation. Degradation of these nanostructures can reduce the lifetime of electrochemical membranes and release hazardous materials into the effluent. Thus the membrane strengthening/optimization strategies (including anchoring and coating) are promising approaches to improve the stability of electrochemical membranes.

On the one hand, solving these challenges for practical applications requires the assessment of electrochemical membrane technology for disinfection to guide process selection and reactor design based on disinfection performance, energy efficiency, and operating stability. On the other hand, the rapid development of material science offers new opportunities for the development of specific functional materials and approaches to membrane strengthening/optimization.

The most commonly used immobilization method for electrochemical membranes modified with nanostructures is based on the physical junctions between nanomaterials and the membrane surface, and is unsuitable for practical applications because of its insufficient stability. Additionally, these nanostructures commonly have high aspect ratios or fragile structures, resulting in easy detachment from the membrane surface, especially in the presence of fast-flowing water-carrying microbes. One promising approach to improve the stability of electrochemical membranes modified with nanostructures is to apply robust immobilization strategies, including anchoring and coating.

Anchoring methods are feasible for strengthening electrochemical membranes with nanostructures in water disinfection and include the application of molecular linkers to connect nanostructures and membranes and of anchor materials, on one hand, to fill junctions between nanostructures and membranes, on the other [80,81]. For coating methods, a nanoscale thin film is commonly applied to protect the nanostructures on

This book belongs to Badji Mokhtar Annaba University Central Library Copyright Elsevier 2025

the membranes by encapsulating the entire nanostructure or only covering the nanostructure surface while maintaining the morphology [23,82,83]. As the degradation caused by chemical corrosion mostly occurs at the solution-membrane interface, the thin film covering the entire nanostructure surface can effectively reduce electrochemical corrosion and improve the stability of the electrochemical membranes.

Another major challenge for the practical application of electrochemical membranes for disinfection is the mass transfer limitation. Although flow-through systems enable fast mass transfer, most studies only report microbial disinfection with novel materials that have not enabled the optimization method of the flow-through system with the specific objective of microbial disinfection [84–86]. Little information is available on understanding the impact of pore structure and the size effects of flow-through systems on disinfection, which are critical for the design and utilization of flow-through systems. Computational fluid dynamics (CFD), a finite element simulation method, is a promising approach to optimize the flow-through system by describing electrochemical membrane properties and fluid conditions [87]. Furthermore, CFD simulation is capable of simulating a larger-scale reactor by clarifying the device boundary, the treatment rate, and the operation load and has great potential value for transforming the laboratory-scale disinfection process to water treatment in practice [77].

In addition to the stability of the electrochemical membranes, another critical issue in practical applications is the lowered disinfection performance under real water/wastewater conditions, which is commonly neglected in the development of novel materials. Natural organic matter from surface water and dissolved organic matter from wastewater commonly exist in considerable quantities (~mg/L) [88]. For the ROS-dependent mechanisms, the disinfection efficiency decreases because of the ROS-scavenging effect of organic matter [89]. For physical-based and direct oxidation disinfection mechanisms, the disinfection efficiency may be hindered by the organic matter due to competitive adsorption onto membrane surfaces [89,90]. A CNT membrane achieved virus log removal rates of 1.52 and > 7.2 in the presence of 1 mg/ L of alginate and no organic matter, respectively [25]. Although the impact of water quality parameters has been investigated at the lab scale, the lack of standardized experimental protocols for simulating real water/wastewater conditions (especially for organic matter) presents challenges for quantitative assessments of disinfection performance [25,65,91].

5.5 Conclusions and perspectives

Electrochemical membrane technology, as an emerging efficient disinfection technology, has been investigated extensively in the last decade. Various disinfection mechanisms, membrane materials, membrane structures as well as reactor configurations are

This book belongs to Badji Mokhtar Annaba University Central Library Copyright Elsevier 2025

investigated in the current studies. Specific disinfection mechanism (i.e., direct oxidation and electroporation by the electrochemical membranes) and reactor configuration (i.e., flow-through reactor) showed superior disinfection efficiency in the aspects of contact time and energy consumption, which indicated the future direction for the development of this technology.

However, most of the current results and evaluations are based on the model microbes (i.e., *Escherichia coli*) in the water samples with simple water quality (i.e., NaCl solution) under short-term operation (i.e., less than 1 day). The feasibility of these technologies should be validated in the practical water conditions (i.e., complex microbial community and complex water qualities) under long-term operation. Compared with the investigation or exploration on novel disinfection mechanisms achieved by novel materials, the technologies adapted to the nature of water treatment in the real world are rather in need. The development direction of electrochemical membrane technology should be to change from enhancing the disinfection efficiency to enhancing the performance stability under the actual operational conditions of water treatment.

Acknowledgment

The authors declare no competing financial interests. This chapter is supported by the National Natural Science Foundation of China (No. 52000114) and the Key Program of the National Natural Science Foundation of China (No. 51738005).

References

[1] W.A. Rutala, D.J. Weber, Disinfection and sterilization in health care facilities: an overview and current issues, Infect. Dis. Clin. 30 (2016) 609–637.
[2] M.A. Shannon, P.W. Bohn, M. Elimelech, J.G. Georgiadis, B.J. Marinas, A.M. Mayes, Science and technology for water purification in the coming decades, Nature 452 (2008) 301–310.
[3] X.-F. Li, W.A. Mitch, Drinking water disinfection byproducts (DBPs) and human health effects: multidisciplinary challenges and opportunities, Environ. Sci. Technol. 52 (2018) 1681–1689.
[4] D.L. Sedlak, U. von Gunten, The chlorine dilemma, Science 331 (2011) 42–43.
[5] M.-T. Guo, Q.-B. Yuan, J. Yang, Distinguishing effects of ultraviolet exposure and chlorination on the horizontal transfer of antibiotic resistance genes in municipal wastewater, Environ. Sci. Technol. 49 (2015) 5771–5778.
[6] D.B. Miklos, C. Remy, M. Jekel, K.G. Linden, J.E. Drewes, U. Huebner, Evaluation of advanced oxidation processes for water and wastewater treatment - a critical review, Water Res. 139 (2018) 118–131.
[7] A. Al-Karaghouli, L.L. Kazmerski, Energy consumption and water production cost of conventional and renewable-energy-powered desalination processes, Renew. Sustain. Energy Rev. 24 (2013) 343–356.
[8] Y. Liu, H. Cui, Q. Ge, Classification of wind use level and required investment for countries below average to upgrade, J. Clean. Prod. 211 (2019) 1427–1433.
[9] X. Qu, P.J.J. Alvarez, Q. Li, Applications of nanotechnology in water and wastewater treatment, Water Res. 47 (2013) 3931–3946.
[10] C. Zhang, Y. Li, D. Shuai, Y. Shen, D. Wang, Progress and challenges in photocatalytic disinfection of waterborne Viruses: a review to fill current knowledge gaps, Chem. Eng. J. 355 (2019) 399–415.

This book belongs to Badji Mokhtar Annaba University Central Library Copyright Elsevier 2025

[11] Q. Li, S. Mahendra, D.Y. Lyon, L. Brunet, M.V. Liga, D. Li, et al., Antimicrobial nanomaterials for water disinfection and microbial control: potential applications and implications, Water Res. 42 (2008) 4591–4602.
[12] B.C., Hodges, E.L. Cates, J.-H. Kim, Challenges and prospects of advanced oxidation water treatment processes using catalytic nanomaterials, Nat. Nanotech. 13 (2018) 642–650.
[13] J. Lee, S. Mahendra, P.J.J. Alvarez, Nanomaterials in the construction industry: a review of their applications and environmental health and safety considerations, ACS Nano 4 (2010) 3580–3590.
[14] M. Pelaez, N.T. Nolan, S.C. Pillai, M.K. Seery, P. Falaras, A.G. Kontos, et al., A review on the visible light active titanium dioxide photocatalysts for environmental applications, Appl. Catal. B 125 (2012) 331–349.
[15] C.A. Martinez-Huitle, E. Brillas, Electrochemical alternatives for drinking water disinfection, Angew. Chem. Int. (Ed.) 47 (2008) 1998–2005.
[16] M. Okochi, N. Nakamura, T. Matsunaga, Electrochemical killing of microorganisms using the oxidized form of ferrocenemonocarboxylic acid, Electrochim. Acta 44 (1999) 3795–3799.
[17] H. Liu, X.-Y. Ni, Z.-Y. Huo, L. Peng, G.-Q. Li, C. Wang, et al., Carbon fiber-based flow-through electrode system (FES) for water disinfection via direct oxidation mechanism with a sequential reduction–oxidation process, Environ. Sci. Technol. 53 (2019) 3238–3249.
[18] S. Monasterio, M. Mascia, M. Di Lorenzo, Electrochemical removal of microalgae with an integrated electrolysis-microbial fuel cell closed-loop system, Sep. Purif. Technol. 183 (2017) 373–381.
[19] S. Ghasemian, B. Asadishad, S. Omanovic, N. Tufenkji, Electrochemical disinfection of bacteria-laden water using antimony-doped tin-tungsten-oxide electrodes, Water Res. 126 (2017) 299–307.
[20] C.D. Vecitis, M.H. Schnoor, M.S. Rahaman, J.D. Schiffman, M. Elimelech, Electrochemical multiwalled carbon nanotube filter for viral and bacterial removal and inactivation, Environ. Sci. Technol. 45 (2011) 3672–3679.
[21] Z.-Y. Huo, X. Xie, T. Yu, Y. Lu, C. Feng, H.-Y. Hu, Nanowire-modified three-dimensional electrode enabling low-voltage electroporation for water disinfection, Environ. Sci. Technol. 50 (2016) 7641–7649.
[22] J.A. Rojas-Chapana, M.A. Correa-Duarte, Z. Ren, K. Kempa, M. Giersig, Enhanced introduction of gold nanoparticles into vital acidothiobacillus ferrooxidans by carbon nanotube-based microwave electroporation, Nano Lett. 4 (2004) 985–988.
[23] Y. Yang, M.R. Hoffmann, Synthesis and stabilization of blue-black TiO_2 nanotube arrays for electrochemical oxidant generation and wastewater treatment, Environ. Sci. Technol. 50 (2016) 11888–11894.
[24] X.Y. Ni, H. Liu, C. Wang, W.L. Wang, Z.B. Xu, Z. Chen, et al., Comparison of carbonized and graphitized carbon fiber electrodes under flow-through electrode system (FES) for high-efficiency bacterial inactivation, Water Res. 168 (2020) 115150.
[25] M.S. Rahaman, C.D. Vecitis, M. Elimelech, Electrochemical carbon-nanotube filter performance toward virus removal and inactivation in the presence of natural organic matter, Environ. Sci. Technol. 46 (2012) 1556–1564.
[26] W. Chen, J. Jiang, W. Zhang, T. Wang, J. Zhou, C.-H. Huang, et al., Silver nanowire-modified filter with controllable silver ion release for point-of-use disinfection, Environ. Sci. Technol. 53 (2019) 7504–7512.
[27] X.-Y. Ni, Y.-H. Wu, H. Liu, X.-J. Zhang, Z.-B. Xu, L. Peng, et al., Enhancing disinfection performance of the carbon fiber-based flow-through electrode system (FES) by alternating pulse current (APC) with low-frequency square wave, Chem. Eng. J. 410 (2021) 128399.
[28] J. Jeong, C. Kim, J. Yoon, The effect of electrode material on the generation of oxidants and microbial inactivation in the electrochemical disinfection processes, Water Res. 43 (2009) 895–901.
[29] M. Kerwick, S. Reddy, A. Chamberlain, D. Holt, Electrochemical disinfection, an environmentally acceptable method of drinking water disinfection? Electrochim. Acta 50 (2005) 5270–5277.
[30] J. Moreno-Andrés, N. Ambauen, O. Vadstein, C. Hallé, A. Acevedo-Merino, E. Nebot, et al., Inactivation of marine heterotrophic bacteria in ballast water by an Electrochemical Advanced Oxidation Process, Water Res. 140 (2018) 377–386.
[31] T. Kotnik, W. Frey, M. Sack, S.H. Meglic, M. Peterka, D. Miklavcic, Electroporation-based applications in biotechnology, Trends Biotechnol. 33 (2015) 480–488.

This book belongs to Badji Mokhtar Annaba University Central Library Copyright Elsevier 2025

[32] C. Liu, X. Xie, W. Zhao, J. Yao, D. Kong, A.B. Boehm, et al., Static electricity powered copper oxide nanowire microbicidal electroporation for water disinfection, Nano Lett. 14 (2014) 5603–5608.
[33] D.T. Schoen, A.P. Schoen, L. Hu, H.S. Kim, S.C. Heilshorn, Y. Cui, High speed water sterilization using one-dimensional nanostructures, Nano Lett. 10 (2010) 3628–3632.
[34] J. Tian, H. Feng, L. Yan, M. Yu, H. Ouyang, H. Li, et al., A self-powered sterilization system with both instant and sustainable anti-bacterial ability, Nano Energy 36 (2017) 241–249.
[35] Z.-Y. Huo, Y. Luo, X. Xie, C. Feng, K. Jiang, J. Wang, et al., Carbon-nanotube sponges enabling highly efficient and reliable cell inactivation by low-voltage electroporation, Environ. Sci. Nano 4 (2017) 2010–2017.
[36] Z.-Y. Huo, H. Liu, W.-L. Wang, Y.-H. Wang, Y.-H. Wu, X. Xie, et al., Low-voltage alternating current powered polydopamine-protected copper phosphide nanowire for electroporation-disinfection in water, J. Mater. Chem. A 7 (2019) 7347–7354.
[37] S. Kang, M. Pinault, L.D. Pfefferle, M. Elimelech, Single-walled carbon nanotubes exhibit strong antimicrobial activity, Langmuir 23 (2007) 8670–8673.
[38] S.-L. Loo, A.G. Fane, T.-T. Lim, W.B. Krantz, Y.-N. Liang, X. Liu, et al., Superabsorbent cryogels decorated with silver nanoparticles as a novel water technology for point-of-use disinfection, Environ. Sci. Technol. 47 (2013) 9363–9371.
[39] C. Lee, J.Y. Kim, W.I. Lee, K.L. Nelson, J. Yoon, D.L. Sedlak, Bactericidal effect of zero-valent iron nanoparticles on *Escherichia coli*, Environ. Sci. Technol. 42 (2008) 4927–4933.
[40] S.-L. Loo, W.B. Krantz, A.G. Fane, Y. Gao, T.-T. Lim, X. Hu, Bactericidal mechanisms revealed for rapid water disinfection by superabsorbent cryogels decorated with silver nanoparticles, Environ. Sci. Technol. 49 (2015) 2310–2318.
[41] D.Y. Lyon, P.J.J. Alvarez, Fullerene water suspension (nC(60)) exerts antibacterial effects via ROS-independent protein oxidation, Environ. Sci. Technol. 42 (2008) 8127–8132.
[42] Z.-m Xiu, Q.-b Zhang, H.L. Puppala, V.L. Colvin, P.J.J. Alvarez, Negligible particle-specific antibacterial activity of silver nanoparticles, Nano Lett. 12 (2012) 4271–4275.
[43] Z. Li, K. Greden, P.J.J. Alvarez, K.B. Gregory, G.V. Lowry, Adsorbed Polymer and NOM limits adhesion and toxicity of nano scale zerovalent iron to E. coli, Environ. Sci. Technol. 44 (2010) 3462–3467.
[44] R. Cheng, G. Li, C. Cheng, P. Liu, L. Shi, Z. Ma, et al., Removal of bacteriophage f2 in water by nanoscale zero-valent iron and parameters optimization using response surface methodology, Chem. Eng. J. 252 (2014) 150–158.
[45] F. Alimohammadi, M.G. Sharifian, N.H. Attanayake, A.C. Thenuwara, Y. Gogotsi, B. Anasori, et al., Antimicrobial properties of 2D MnO_2 and MoS_2 nanomaterials vertically aligned on graphene materials and Ti_3C_2 MXene, Langmuir 34 (2018) 7192–7200.
[46] C.D. Vecitis, K.R. Zodrow, S. Kang, M. Elimelech, Electronic-structure-dependent bacterial cytotoxicity of single-walled carbon nanotubes, ACS Nano 4 (2010) 5471–5479.
[47] A.S. Brady-Estévez, M.H. Schnoor, S. Kang, M. Elimelech, SWNT – MWNT hybrid filter attains high viral removal and bacterial inactivation, Langmuir 26 (2010) 19153–19158.
[48] S. Kang, M.S. Mauter, M. Elimelech, Physicochemical determinants of multiwalled carbon nanotube bacterial cytotoxicity, Environ. Sci. Technol. 42 (2008) 7528–7534.
[49] S.C. Smith, D.F. Rodrigues, Carbon-based nanomaterials for removal of chemical and biological contaminants from water: a review of mechanisms and applications, Carbon 91 (2015) 122–143.
[50] A.H. Castro Neto, F. Guinea, N.M.R. Peres, K.S. Novoselov, A.K. Geim, The electronic properties of graphene, Rev. Mod. Phys. 81 (2009) 109–162.
[51] M. Naguib, V.N. Mochalin, M.W. Barsoum, Y. Gogotsi, 25th anniversary article: MXenes: a new family of two-dimensional materials, Adv. Mater. 26 (2014) 992–1005.
[52] F. Perreault, A.F. De Faria, S. Nejati, M. Elimelech, Antimicrobial properties of graphene oxide nanosheets: why size matters, ACS Nano 9 (2015) 7226–7236.
[53] K. Rasool, M. Helal, A. Ali, C.E. Ren, Y. Gogotsi, K.A. Mahmoud, Antibacterial activity of Ti_3C_2Tx MXene, ACS Nano 10 (2016) 3674–3684.
[54] K. Rasool, K.A. Mahmoud, D.J. Johnson, M. Helal, G.R. Berdiyorov, Y. Gogotsi, Efficient antibacterial membrane based on two-dimensional Ti_3 C_2 Tx (MXene) nanosheets, Sci. Rep. 7 (2017) 1598.

This book belongs to Badji Mokhtar Annaba University Central Library Copyright Elsevier 2025

[55] X. Zeng, D.T. McCarthy, A. Deletic, X. Zhang, Silver/reduced graphene oxide hydrogel as novel bactericidal filter for point-of-use water disinfection, Adv. Funct. Mater. 25 (2015) 4344–4351.
[56] P. Gunawan, C. Guan, X. Song, Q. Zhang, S.S.J. Leong, C. Tang, et al., Hollow fiber membrane decorated with Ag/MWNTs: toward effective water disinfection and biofouling control, ACS Nano 5 (2011) 10033–10040.
[57] M. Rai, A. Yadav, A. Gade, Silver nanoparticles as a new generation of antimicrobials, Biotechnol. Adv. 27 (2009) 76–83.
[58] E.L. Yu-sen, R.D. Vidic, J.E. Stout, C.A. McCartney, L.Y. Victor, Inactivation of mycobacterium avium by copper and silver ions, Water Res. 32 (1998) 1997–2000.
[59] F.M. Aarestrup, H. Hasman, Susceptibility of different bacterial species isolated from food animals to copper sulphate, zinc chloride and antimicrobial substances used for disinfection, Veterinary Microbiol. 100 (2004) 83–89.
[60] R. Crane, T. Scott, Nanoscale zero-valent iron: future prospects for an emerging water treatment technology, J. Hazard. Mater. 211 (2012) 112–125.
[61] Y. Hu, J. Wang, H. Sun, S. Wang, X. Liao, J. Wang, et al., Roles of extracellular polymeric substances in the bactericidal effect of nanoscale zero-valent iron: trade-offs between physical disruption and oxidative damage, Environ. Sci. Nano 6 (2019) 2061–2073.
[62] C. Liu, X. Xie, W. Zhao, N. Liu, P.A. Maraccini, L.M. Sassoubre, et al., Conducting nanosponge electroporation for affordable and high-efficiency disinfection of bacteria and viruses in water, Nano Lett. 13 (2013) 4288–4293.
[63] H. Miao, Z. Teng, S. Wang, L. Xu, C. Wang, H. Chong, Recent advances in the disinfection of water using nanoscale antimicrobial materials, Adv. Mater. Technol. 4 (2019) 1800213.
[64] Z.-Y. Huo, J.-F. Zhou, Y. Wu, Y.-H. Wu, H. Liu, N. Liu, et al., A Cu_3 P nanowire enabling high-efficiency, reliable, and energy-efficient low-voltage electroporation-inactivation of pathogens in water, J. Mater. Chem. A 6 (2018) 18813–18820.
[65] Z.-Y. Huo, G.-Q. Li, T. Yu, Y. Lu, H. Sun, Y.-H. Wu, et al., Impact of water quality parameters on bacteria inactivation by low-voltage electroporation: mechanism and control, Environ. Sci. Water Res. Technol. 4 (2018) 872–881.
[66] J.R. Bolton, K.G. Bircher, W. Tumas, C.A. Tolman, Figures-of-merit for the technical development and application of advanced oxidation processes, J. Adv. Oxid. Technol. 1 (1996) 13–17.
[67] K. Sholtes, K.G. Linden, Pulsed and continuous light UV LED: microbial inactivation, electrical, and time efficiency, Water Res. 165 (2019) 114965.
[68] J. Radjenovic, D.L. Sedlak, Challenges and opportunities for electrochemical processes as next-generation technologies for the treatment of contaminated water, Environ. Sci. Technol. 49 (2015) 11292–11302.
[69] G.-Q. Li, W.-L. Wang, Z.-Y. Huo, Y. Lu, H.-Y. Hu, Comparison of UV-LED and low pressure UV for water disinfection: photoreactivation and dark repair of *Escherichia coli*, Water Res. 126 (2017) 134–143.
[70] X. Xie, C. Mao, X. Liu, L. Tan, Z. Cui, X. Yang, et al., Tuning the bandgap of photo-sensitive polydopamine/Ag_3PO_4/graphene oxide coating for rapid, noninvasive disinfection of implants, ACS Cent. Sci. 4 (2018) 724–738.
[71] O. Baghriche, S. Rtimi, A. Zertal, C. Pulgarin, R. Sanjines, J. Kiwi, Accelerated bacterial reduction on Ag-TaN compared with Ag-ZrN and Ag-TiN surfaces, Appl. Catal. B 174 (2015) 376–382.
[72] A. Anglada, A.M. Urtiaga, I. Ortiz, Laboratory and pilot plant scale study on the electrochemical oxidation of landfill leachate, J. Hazard. Mater. 181 (2010) 729–735.
[73] C.P. Feng, K. Suzuki, S.Y. Zhao, N. Sugiura, S. Shimada, T. Maekawa, Water disinfection by electrochemical treatment, Bioresour. Technol. 94 (2004) 21–25.
[74] C. Pablos, J. Marugan, C. Adan, M. Osuna, R. van Grieken, Performance of TiO_2 photoanodes toward oxidation of methanol and E. coli inactivation in water in a scaled-up photoelectrocatalytic reactor, Electrochim. Acta 258 (2017) 599–606.
[75] A. Cano, C. Barrera, S. Cotillas, J. Llanos, P. Cañizares, M.A. Rodrigo, Use of DiaCell modules for the electro-disinfection of secondary-treated wastewater with diamond anodes, Chem. Eng. J. 306 (2016) 433–440.

This book belongs to Badji Mokhtar Annaba University Central Library Copyright Elsevier 2025

[76] L. Guo, K. Ding, K. Rockne, M. Duran, B.P. Chaplin, Bacteria inactivation at a sub-stoichiometric titanium dioxide reactive electrochemical membrane, J. Hazard. Mater. 319 (2016) 137–146.
[77] Z. Gu, X. An, H. Lan, Y. Tian, J. Zhang, R. Liu, et al., Microfluidic-enhanced 3-D photoanodes with free interfacial energy barrier for photoelectrochemical applications, Appl. Catal. B 244 (2019) 740–747.
[78] C. Wang, L. Yue, S. Wang, Y. Pu, X. Zhang, X. Hao, et al., Role of electric field and reactive oxygen species in enhancing antibacterial activity: a case study of 3D Cu foam electrode with branched CuO–ZnO NWs, J. Phys. Chem. C 122 (2018) 26454–26463.
[79] X. Qu, J. Brame, Q. Li, P.J.J. Alvarez, Nanotechnology for a safe and sustainable water supply: enabling integrated water treatment and reuse, Acc. Chem. Res. 46 (2013) 834–843.
[80] J. Lee, Y. Mackeyev, M. Cho, L.J. Wilson, J.-H. Kim, P.J. Alvarez, C60 aminofullerene immobilized on silica as a visible-light-activated photocatalyst, Environ. Sci. Technol. 44 (2010) 9488–9495.
[81] A. Moncayo-Lasso, R.A. Torres-Palma, J. Kiwi, N. Benítez, C. Pulgarin, Bacterial inactivation and organic oxidation via immobilized photo-Fenton reagent on structured silica surfaces, Appl. Catal. B 84 (2008) 577–583.
[82] Z.-Y. Huo, H. Liu, C. Yu, Y.-H. Wu, H.-Y. Hu, X. Xie, Elevating the stability of nanowire electrodes by thin polydopamine coating for low-voltage electroporation-disinfection of pathogens in water, Chem. Eng. J. 369 (2019) 1005–1013.
[83] Z. Yang, Y. Wu, J. Wang, B. Cap, C.Y. Tang, In situ reduction of silver by polydopamine: a novel antimicrobial modification of a thin-film composite polyamide membrane, Environ. Sci. Technol. 50 (2016) 9543–9550.
[84] S. Luo, Y. Luo, H. Wu, M. Li, L. Yan, K. Jiang, et al., Self-assembly of 3D carbon nanotube sponges: a simple and controllable way to build macroscopic and ultralight porous architectures, Adv. Mater. 29 (2017).
[85] L. Zhang, K. Zhou, Q. Wei, L. Ma, W. Ye, H. Li, et al., Thermal conductivity enhancement of phase change materials with 3D porous diamond foam for thermal energy storage, Appl. Energy 233 (2019) 208–219.
[86] J. Liu, H.-B. Zhang, R. Sun, Y. Liu, Z. Liu, A. Zhou, et al., Hydrophobic, flexible, and lightweight MXene foams for high-performance electromagnetic-interference shielding, Adv. Mater. 29 (2017).
[87] Y. Zhou, Q. Ji, H. Liu, J. Qu, Pore structure-dependent mass transport in flow-through electrodes for water remediation, Environ. Sci. Technol. 52 (2018) 7477–7485.
[88] H.-Y. Hu, Y. Du, Q.-Y. Wu, X. Zhao, X. Tang, Z. Chen, Differences in dissolved organic matter between reclaimed water source and drinking water source, Sci. Total Environ. 551 (2016) 133–142.
[89] J. Brame, M. Long, Q. Li, P. Alvarez, Inhibitory effect of natural organic matter or other background constituents on photocatalytic advanced oxidation processes: mechanistic model development and validation, Water Res. 84 (2015) 362–371.
[90] J. Brame, M. Long, Q. Li, P. Alvarez, Trading oxidation power for efficiency: differential inhibition of photo-generated hydroxyl radicals vs singlet oxygen, Water Res. 60 (2014) 259–266.
[91] J. Chen, Z. Xiu, G.V. Lowry, P.J.J. Alvarez, Effect of natural organic matter on toxicity and reactivity of nano-scale zero-valent iron, Water Res. 45 (2011) 1995–2001.

This book belongs to Badji Mokhtar Annaba University Central Library Copyright Elsevier 2025

CHAPTER SIX

Electrochemical membrane bioreactors for wastewater treatment

Mary Vermi Aizza Corpuz[1], Laura Borea[2], Florencio Ballesteros, Jr[1,3], Vincenzo Belgiorno[2], Shadi W. Hasan[4] and Vincenzo Naddeo[2]

[1]Environmental Engineering Program, National Graduate School of Engineering, University of the Philippines, Diliman, Quezon City, Philippines
[2]Sanitary Environmental Engineering Division (SEED), Department of Civil Engineering, University of Salerno, Fisciano, Italy
[3]Department of Chemical Engineering, College of Engineering, University of the Philippines, Diliman, Quezon City, Philippines
[4]Center for Membranes and Advanced Water Technology (CMAT), Department of Chemical Engineering, Khalifa University of Science and Technology, Abu Dhabi, United Arab Emirates

6.1 Introduction

Membrane bioreactors (MBRs) have been widely studied and applied in wastewater treatment for their use of biodegradation and membrane filtration for the removal of contaminants [1]. They have been shown to be efficient in removal of pollutants, particularly of organic matter from wastewater [2].

However, enhanced removal of nutrients and nonconventional pollutants, and membrane fouling mitigation continue to be challenges for the application of conventional MBRs. Previous studies have aimed to modify MBRs and thereby to improve their performance through integration with other processes. The combination of electrochemical processes with biological processes, and membrane filtration, in electrochemical membrane bioreactors (eMBRs) has been shown to aid in the reduction of fouling rate and thereby enhanced the reduction of pollutants concentration in the effluent [3–7]. The integration of MBRs with electrochemical processes is achieved through addition of electrodes, that may be in an external unit or may be in the same vessel as the MBR tank (as will be discussed further in Section 6.4.3). The application of electric field and the resulting electrochemical processes, which involve electron transfer between the electrodes and components of wastewater, provide additional mechanisms to enhance the reduction of pollutants' concentrations in wastewater and to alleviate the membrane fouling rate [8].

This book chapter presents an overview of the dominant mechanisms of wastewater pollutant degradation/removal and membrane fouling mitigation in eMBRs. Progress on the laboratory-scale and pilot-scale applications are also discussed. This chapter also

Electrochemical Membrane Technology for Water and Wastewater Treatment.
DOI: https://doi.org/10.1016/B978-0-12-824470-8.00010-3
© 2022 Elsevier Inc.
All rights reserved.

This book belongs to Badji Mokhtar Annaba University Central Library
Copyright Elsevier 2025

aims to present findings related to the effect of the electric field application to the microbiological community in the eMBRs.

6.2 Pollutant removal

Electrochemical MBR makes use of biotic and abiotic processes to remove pollutants from wastewater. It utilizes the following main mechanisms: (1) biodegradation of pollutants by microorganisms present in the sludge used, (2) membrane filtration, and (3) electrochemical processes.

6.2.1 Removal of organic pollutants in the electrochemical membrane bioreactor

Previous studies revealed that the % chemical oxygen demand (COD) removal efficiency in eMBRs treating domestic/municipal wastewater in the range of 86% to >99%, compared to that obtained in MBRs without electrochemical assistance (65% to >99%) (Table 6.1). On the other hand, in recent applications on treatment of high-strength wastewater, notably landfill leachates and industrial wastewaters, the % COD removal efficiencies obtained in eMBRs are reported in the range of 71.55%–97% (Table 6.1). The relatively lower COD removal efficiencies of eMBRs treating high-strength wastewater compared to those obtained in low or medium strength wastewater may be attributed to the nature of some pollutants, which are difficult to degrade or may inhibit biodegradation (see Section 6.2.4).

Application of an electric field in the eMBR enhances the biodegradation of organic pollutants in various ways. For example, the presence of an electric field could potentially enhance the activity of microorganisms responsible for degradation of organic pollutants in the wastewater (see Section 6.5). On the other hand, the production of H_2 gas through reduction of water at the cathode provides additional mechanisms for suspending the pollutants [31], making them more available for microorganisms. Different electrochemical processes also contribute to the enhanced removal of organic contaminants in wastewater. One of the electrochemical processes in the eMBR that contributes to the removal of organic pollutants in wastewater is electrocoagulation. When sacrificial electrodes (e.g., Al or Fe) are used in the eMBR, electrochemical dissolution of these electrode materials leads to in situ generation of coagulants such as Al^{3+}, Fe^{3+}, and Fe^{2+}. These ions react with the hydroxide ion (OH^-) formed at the cathode to produce aluminum hydroxides or iron hydroxides, as shown in Eqs. (6.1)–(6.3) [21,31–33]. Organic pollutants are adsorbed into the insoluble hydroxides [18]. The large flocs formed are then separated from the wastewater

This book belongs to Badji Mokhtar Annaba University Central Library Copyright Elsevier 2025

This book belongs to Badji Mokhtar Annaba University Central Library

Table 6.1 Electrochemical membrane bioreactors (eMBRs) for wastewater treatment in recent studies.

Type of wastewater	COD (mg/L)	Configuration/scale	Biological condition	Membrane module	Anode	Cathode	Applied voltage/ current density; mode of electric field application	Pollutant removal efficiency	Reference
Real coal chemical industry wastewater	1486.4 ± 102.4	Submerged eMBR/ Laboratory	Aerobic	Hollow fireber 0.04 μm	Stainless steel plate	Graphite plate	0.5−1.33 mA/cm^2; Intermittent: Ratio of time without current to time with current is at a range of 2−5	COD: 83.53% Total phenol: 93.28%	[9]
High concentration phenol wastewater	Reported as 0.2−5 g/L phenol	Submerged eMBR/ Laboratory	Aerobic	Not reported	Ti/PbO_2	Stainless steel	Current Density not reported Intermittent: 8 min ON/ 2 min OFF	COD: 86.55% Total phenol: ∼99%	[10]
Young landfill leachate	65,000	Submerged eMBR/ Laboratory	Aerobic	Hollow fiber 0.04 μm	Aluminum	Aluminum	24 mA/cm^2; Intermittent: Stage I: 180 s/ day during 5 days of HRTStage II: 360 s/day for 5 days of HRT	COD: 87% NH_3-N: 86% Color: 88%−92%	[11]
Textile wastewater	836−922	Submerged eMBR/ Laboratory	Aerobic	Hollow fiber	Aluminum	Stainless steel	1.0 and 1.5 mA/ cm^2; Intermittent: 6 min ON/ 18 min OFF	COD: 75%−77% NH_3-N: >90% TP: 68%−77% Color: 50%−70%	[12]
Landfill leachate	860−1200	Submerged eMBR/ Laboratory	Aerobic	Hollow fiber 0.04 μm	Iron	Ti/Pt andGraphite	Current density: 0, 0.23, 0.45, and 0.91 mA/cm^2 Continuous	TOC: 38% NH_3-N: 99.8% TP: 99.0%	[13]
Coking wastewater	2565.2	Submerged eMBR/ Laboratory	Aerobic	Flat sheet effective filtration area: 0.004 m^2	Stainless steel net	Stainless steel net (acted as membrane)	Applied voltage: 0.05−0.3 V/cm Intermittent: 5 min ON/ 1 min OFF	COD: 84.8% Phenol: 97.9% Pyridine: 94.7% Quinone: 94.1%	[14]

(continued)

Copyright Elsevier 2025

This book belongs to Badji Mokhtar Annaba University Central Library

Table 6.1 (Continued)

Type of wastewater	COD (mg/L)	Configuration/scale	Biological condition	Membrane module	Anode	Cathode	Applied voltage/ current density; mode of electric field application	Pollutant removal efficiency	Reference
Synthetic hypersaline produced water (waste from oil and natural gas production)	1600–1800	External electrochemical cell + submerged MBR in series/ Laboratory	Aerobic	Hollow fiber 0.035 μm	1. Aluminum 2. Stainless steel	1. Aluminum 2. Stainless steel	Current Density: 5, 10, and 30 mA/ cm^2 Continuous: Contact Times at 5, 15, 30, 60, 90, and 120 min	COD: 91%–97% Oil and Grease: 80%–95%	[15]
Pre-treated oil Shale Wastewater (in different proportions with synthetic municipal wastewater)	391.24–1797.32	Submerged eMBR/ Laboratory Scale	Anoxic/ oxic	Hollow fiber curtain-type 0.1 μm	Iron	Carbon	Current: 0.01 A Intermittent: 5 min ON/ 5 min OFF	COD: 71.55%–93.11% NH_3-N: 59.09%–95.37%	[16]
Concentrated synthetic wastewater	496–508	Submerged eMBR (Operated as Sequencing Batch Reactor)/Laboratory	Anoxic/ Anaerobic, followed by Aerobic	Hollow fiber ultrafiltra-tion module	Aluminum	Stainless Steel	Current Density: 1.0 mA/cm^2 Intermittent: 6 min ON/ 30 min OFF (applied only during aeration/ filtration phase)	COD: > 99% NH_3-N: >99% TP: 89%	[17]
Real municipal wastewater	495–894	Submerged eMBR/ Pilot	Aerobic	PES (Polyethersulfone) flat ultrafiltration module	Aluminum	Stainless Steel	Current Density: 0.5, 1.0, and 1.5 mA/cm^2 Intermittent: 5 min ON/ 10 min OFF	COD: 92%–96% TP: 92.4%–97.9% Acetaminophen: 19%Clarithromycin: 43%Carbamazepine: 28%	[18]
Synthetic domestic wastewater	400	Submerged eMBR/ Laboratory	Aerobic	Hollow fiber PVDF	Iron	Iron	Current Density: 0.2 mA/cm^2 Intermittent: 30 min ON/ 30 min OFF	COD: ~85% TP: ~99%	[19]

Copyright Elsevier 2025

This book belongs to Badji Mokhtar Annaba University Central Library

Municipal wastewater	628.5 ± 102.2	Submerged eMBR/ Laboratory	Aerobic	Hollow Fiber Polyetherimide (PeI) 0.3 μm	Aluminum	Stainless steel	Current Density: 1.0 mA/cm^2 Intermittent: 6 min ON/ 18 min OFF	COD: 98.5% NH3-N: 99.8% TP: 99.2%	[20]
Synthetic municipal wastewater	556.16 ± 33.53	SubmergedeMBR/ Laboratory	Aerobic	Hollow Fiber PVDF 0.04 μm	Aluminum	Stainless steel	Voltage Gradient: 1 V/cm and 3 V/ cm Intermittent: 5 min ON/ 20 min OFF	COD: 97.50% and 98.24% NH3-N: 69.34% PO4-P: 96.06%	[21]
Synthetic municipal wastewater with added pharmaceuti-cals	556.16 ± 33.53	Submerged eMBR/ Laboratory	Aerobic	Hollow Fiber PVDF 0.04 μm	Aluminum	Stainless steel	Current Density: 0.3, 0.5, and 1.15 mA/cm^2 Intermittent: 5 min ON/ 20 min OFF	COD: ∼100% NH3-N: ∼60%–72%PO4-P: ∼100% Amoxicillin: 60.92%–76.47% Diclofenac: 65.79%–79.04% Carbamazepine: 65.23%–77.21%	[22]
Synthetic municipal wastewater	350 ± 27	Submerged eMBR/ Laboratory	Aerobic	Hollow fiber PVDF 0.1 μm	Stainless steel	Stainless steel	Current Density: 0.5, 1.25, 2.0, and 2.3 mA/ cm^2 Intermittent	COD: 85%–90% NH3-N: ∼70% PO4-P: 38%–85%	[23]
Filtered real municipal wastewater added with pharmaceuti-cals and personal care products	not reported	Submerged eMBR/ Laboratory	Aerobic	Composite flatsheet membrane module (steel mesh coated with polymer film (polyvinylidene difluoride and polyvinylpyrro-lidone))	IrO_2-Ta_2O_5@Ti	Stainless steel mesh (also acted as membrane)	Voltage Gradient: 2.0 V/cm Continuous	COD: 92.18 ± 4.35% NH3-N: 97.44 ± 6.79% Ketoprofen: >95% Acetaminophen: >95% Caffeine: >95%	[24]
Synthetic wastewater with sulfametho-xazole (SMX)	Reported as 320 mg/L Sodium acetate	Moving bed eMBR (submerged eMBR with suspended conductive carriers)/ Laboratory	Aerobic	Composite conductive membrane module (titanium mesh coated with solution of polyvinylpyrro-lidone and polyvinylidene difluoride in dimethyl sulfoxide)	Graphite	Titanium mesh (also acted as membrane)	Voltage Gradient: 2.0 V/cm Continuous	COD: 93.7 ± 2.6% NH3-N: > 95%S MX: 88.9%	[25]

(continued)

Copyright Elsevier 2025

This book belongs to Badji Mokhtar Annaba University Central Library

Table 6.1 (Continued)

Type of wastewater	COD (mg/L)	Configuration/scale	Biological condition	Membrane module	Anode	Cathode	Applied voltage/ current density; mode of electric field application	Pollutant removal efficiency	Reference
Synthetic wastewater	Reported as 192.06 ± 30.58 mg/L TOC	Submerged eMBR, baffled tank with 3 cells (each cell with electrodes, membrane at 3rd cell)/Laboratory	Cell I: Anaerobic Cell II: Anoxic Cell III: Aerobic	Hollow fiber membrane module;0.1 μm	Iron	Iron	1 V, 3 V, 5 V, 0.15 A, and undulated voltage of 18 V/ 10 W solar panel Continuous	NH3-N: > 80% PO4-P: 35.91%–92.45%	[26]
Synthetic municipal wastewater	~500	Submerged eMBR/ Laboratory	Aerobic	Carbon nanotube hollow-fiber membrane (CNT-HFM)	CNT-HFM (also used as membrane)	Titanium mesh	0, 0.5, 1.0, 1.5 V Continuous	COD: >92% NH3-N: >88%	[27]
Synthetic municipal wastewater	~500 to ~6000	Submerged eMBR/ Laboratory	Anaerobic	Carbon nanotube hollow-fiber membrane (CNT-HFM)	Titanium mesh	CNT-HFM (also used as membrane)	1.2 V Continuous	COD: > 95%	[28]
Synthetic wastewater	2000	Submerged An-eMBR/ Laboratory	Anaerobic	Silicon carbide (SiC) ceramic membrane	Graphite	SiC (also used as membrane)	0.5 V, 1.0 V, 2.0 V Continuous	COD: 90.3% (at 2 V)	[29]
Real municipal wastewater (pre-screened and de-gritted)	316 ± 146	Submerged eMBR/ Pilot	Aerobic	Hollow fiber PVDF 0.1 μm	Aluminum	Stainless steel	Current Density: 1.2 mA/cm^2 Intermittent: 5 min ON/ 10 min OFF	COD: 92% NH3-N: 99% PO4-P: 99%	[30]

COD, Chemical oxygen demand; *PVDF*, polyvinylidene difluoride.

Copyright Elsevier 2025

by sedimentation and membrane filtration. This increases the retention time of the contaminants in the reactor and provides longer contact time with microorganisms for further biodegradation.

$$Al^{3+}{}_{(aq)} + 3H_2O_{(l)} \rightarrow Al(OH)_{3(s)} + 3H^{+}{}_{(aq)} \tag{6.1}$$

$$Fe^{2+}{}_{(aq)} + 2H_2O_{(l)} \rightarrow Fe(OH)_{2(s)} + 2H^{+}{}_{(aq)} \tag{6.2}$$

$$4Fe^{2+}{}_{(aq)} + 10H_2O_{(l)} + O_{2(g)} \rightarrow 4Fe(OH)_{3(s)} + 8H^{+}{}_{(aq)} \tag{6.3}$$

Electrooxidation is also a potential mechanism to reduce the organic pollutants in the wastewater using the eMBR. Hasan et al. suggested that organic pollutants could undergo oxidation in the eMBR, allowing them to be more available for further degradation by microorganisms [30]. This is important for the degradation of recalcitrant organic compounds, which will be further discussed in Section 6.2.4. Electrooxidation may occur via direct oxidation or indirect oxidation of the organic contaminants [34]. The direct electrooxidation involves electron transfer at the electrodes without participation of other substances. On the other hand, indirect electrooxidation involves oxidation of the organic pollutants through electroactive species that are generated in situ. The indirect electrooxidation may be classified as (1) anodic oxidation, and (2) cathodic oxidation. Anodic electrooxidation involves the degradation of pollutants by oxidation with the hydroxyl radical ($^{\bullet}OH$), which is generated in situ by the oxidation of water at the anode [35]. The $^{\bullet}OH$, a strong oxidant, attacks organic substances to produce dehydrogenated or hydroxylated intermediates and to mineralize these substances to CO_2 and H_2O. Eq. (6.4) shows the oxidation of water by anode (M) to produce $^{\bullet}OH$. The adsorbed $^{\bullet}OH$ on the anode (M ($^{\bullet}OH$)) reacts with the organic pollutant (R) to produce the oxidized organic substance (RO) [34,35].

$$H_2O + M \rightarrow M(^{\bullet}OH) + H^{+} + e^{-} \tag{6.4}$$

$$M(^{\bullet}OH) + R \rightarrow M + RO + H^{+} + e^{-} \tag{6.5}$$

On the other hand, cathodic oxidation in eMBRs commonly involves the production of H_2O_2 through the reduction of oxygen in the cathode, as shown in Eq. (6.6) [34,36].

$$O_2 + 2H^{+} + 2e^{-} \rightarrow H_2O_2 \tag{6.6}$$

A few studies have measured the concentration of H_2O_2 produced with the presence of an electric field in eMBRs. Wang et al. showed that in a submerged eMBR utilizing stainless steel mesh cathode, H_2O_2 ($0.3\ mg/L < concentration < 0.9\ mg/L$) was detected even at a low average output voltage of 0.04–0.52 V (from bioanode derived electricity) [37]. Less than 0.3 mg/L of H_2O_2 was also detected when 1 V external voltage was applied in the eMBR used in this study. The study of Jiang et al.

This book belongs to Badji Mokhtar Annaba University Central Library Copyright Elsevier 2025

also detected 0.12–0.40 mg/L of H_2O_2 in another submerged eMBR with stainless steel mesh as anode and cathode, at an applied voltage of 0.1–0.8 V/cm [36]. The H_2O_2 generated in situ can be reduced at the cathode to form $^{\cdot}OH$, which is an oxidant that exhibits fast and non-selective reactions with organic pollutants. Medel et al. examined the cathodic reduction of H_2O_2 to form $^{\cdot}OH$ using various cathode materials including stainless steel, through the reaction described in Eq. (6.7) [38]. However, it is to be noted that very low concentrations of $^{\cdot}OH$ are produced with stainless steel as cathode as compared to that produced using Pt or graphite.

$$H_2O_2 + H^+ + e^- \rightarrow {}^{\cdot}OH + H_2O \tag{6.7}$$

6.2.2 Removal of nitrogen in the electrochemical membrane bioreactor

Nitrogen-containing compounds are commonly removed from wastewater through processes such as nitrification and denitrification by bacteria present in activated sludge matrix [39]. In the conventional activated sludge process and in the conventional MBRs, ammonium oxidizing bacteria convert NH_4^+ to NO_2^-, which is converted to NO_3^- by nitrite-oxidizing bacteria [40]. NO_3^- is then converted to N_2 gas by the denitrification process [41]. The removal of nitrogen in the eMBRs occurs through biodegradation and through electrochemical processes. NH_3-N removal efficiency in eMBR, from low-strength and high-strength wastewaters, has been reported to be in the range of ~60% to >99% (see Table 6.1). Generally, the combined biological and electrochemical processes in the eMBRs increase nitrogen removal efficiency. In most studies, the application of an electric field in the eMBRs has been shown to increase NH_3-N removal efficiencies compared to that obtained in MBRs without the electric field. Borea et al. showed that an eMBR increased NH_3-N removal efficiency from synthetic municipal wastewater by 10.52% (at 1 V/cm) and by 26.96% (at 3 V/cm), compared to that obtained from an MBR without applied voltage [21]. Kurtoğlu Akkaya and Bilgili also found that NH_3-N removal efficiency from young landfill leachate was higher by 8% in an eMBR compared to that observed in an MBR without applied electric field [11]. The study of Li et al. revealed that the application of an electric field to Fe electrodes in an eMBR increased the specific ammonia oxidation rate and specific nitrate reduction rate (SNRR) by 20.62% and 25.58%, respectively, as compared to the rates in the conventional MBR [42]. However, the specific nitrite oxidation rate (SNOR) was lower by 4.7% in the eMBR than that obtained in the conventional MBR. These findings by Li et al. implied that ammonium oxidation and nitrate reduction were enhanced by the electric field application [42]. The growth of nitrogen-removing microorganisms may also be enhanced by the application of an electric field in the eMBR, as will be discussed further in Section 6.5. The process of electrocoagulation may also contribute to the increase in

This book belongs to Badji Mokhtar Annaba University Central Library Copyright Elsevier 2025

removal efficiency of total nitrogen in eMBRs. Nitrates from water have been previously reported to adsorb into aluminum hydroxides, which were formed by electrocoagulation [43].

However, a few studies have reported lower NH_3-N removal efficiency when using an eMBR instead of the conventional MBR. Bani-Melhem and Smith observed a reduction of 19.6% in the NH_3-N removal efficiency in an eMBR compared to that obtained in an MBR [32]. In this study, the reduction in removal efficiency was attributed to the effect of the intermittently applied 12 V to the microbiological community in the electro bioreactor [32]. Tafti et al. found that at low current densities (0.5–1.25 mA/cm^2), % NH_3-N removal efficiency generally increased as the time of electric field exposure increased, while the reverse trend was observed at higher current densities [23]. In this study, current density greater than 2.0 mA/cm^2 reduced the removal of NH_3-N from synthetic municipal wastewater compared to that observed in an conventional MBR without the application of the current density [23]. The study of Borea et al. also demonstrated that increasing the current density in an eMBR from 0.5 to 1.15 mA/cm^2 decreased the %NH_3^-N removal efficiency by 12% [22]. Tafti et al. suggested that the excessive iron ions released at higher current densities may inhibit the activities of nitrifying bacteria, leading to lower NH_3-N removal [23]. Roy et al. also demonstrated that NH_3-N removal through nitrification could be lowered when using high hydrogen overpotential (HOP) materials, such as graphite [13]. Using HOP materials favor the reduction of NO_3^- to NH_3 at the cathode, as shown in Eqs. (6.8) and (6.9) [13]. This study also showed that using Ti/Pt as cathode can address this problem since it favors the reduction of H_2O to H_2 gas instead of the reduction of NO_3^- to NH_3.

$$NO_3^- + H_2O + 2e^- \rightarrow NO_2^- + 2OH^- \tag{6.8}$$

$$NO_2^- + 5H_2O + 6e^- \rightarrow NH_3 + 7OH^- \tag{6.9}$$

6.2.3 Removal of phosphorus in the electrochemical membrane bioreactor

The potential of the eMBR to increase the removal of phosphorus from wastewater has been demonstrated in previous studies. The range of Total Phosphorus (TP) removal from wastewaters is 68% to >99% in eMBRs (see Table 6.1). Su et al. reported that the TP removal efficiency in an eMBR increased by 39% compared to that obtained in an MBR without electrochemical assistance [19]. The study of Battistelli et al. demonstrated similar results where an eMBR achieved 99.2% ± 1.2% TP removal efficiency compared to the 25.4% ± 11.7% TP removal efficiency by a conventional MBR without the application of the electrochemical assistance [20]. A sequencing batch eMBR also achieved an increase in the TP removal efficiency by 27%, compared to that achieved by the reactor without applied electric field [17].

This book belongs to Badji Mokhtar Annaba University Central Library Copyright Elsevier 2025

In the previous studies, the increase in phosphorus removal efficiency was attributed to different mechanisms. Aside from the biological processes, the additional phosphorus removal mechanisms provided by the application of electric field in the eMBRs are: (1) chemical precipitation, and (2) adsorption to hydroxides. The first involves precipitation with ions generated from electrochemical dissolution of sacrificial anodes such as aluminum and iron. Al^{3+} from the anode and PO_4^{3-} from the wastewater react to form the precipitate aluminum phosphate ($AlPO_4$) according to Eq. (6.10) [17,20,32] or to form $(AlOH)_3(PO4)_2$ according to Eq. (6.11) [44]. $AlPO_4$ is known to have a broad surface area, allowing easier rejection of the precipitate by the membrane filter [20].

$$Al^{3+}_{(aq)} + PO^{3-}_{4(aq)} \rightarrow AlPO_{4(s)} \tag{6.10}$$

$$3Al^{3+}_{(aq)} + 2PO^{3-}_{4(aq)} + 3H_2O_{(l)} \rightarrow (AlOH)_3(PO4)_{2(s)} + 3H^{+}_{(aq)} \tag{6.11}$$

On the other hand, if the anode used is iron, Fe^{2+} and Fe^{3+} are released and form precipitates with PO_4^{3-} according to the reactions shown in Eqs. (6.12) and (6.13) [31].

$$Fe^{2+}_{(aq)} + PO^{3-}_{4(aq)} \rightarrow Fe_3(PO_4)_{2(s)} \tag{6.12}$$

$$Fe^{3+}_{(aq)} + PO^{3-}_{4(aq)} \rightarrow FePO_{4(s)} \tag{6.13}$$

The other main mechanism of phosphorus removal from wastewater is the adsorption of soluble phosphorus to hydroxides [26]. A less examined fate of phosphorus in the eMBRs is the deposition of phosphorus on the electrodes. Wei et al. found that the precipitate deposited on the aluminum anode contained 9.63% (w/w) of phosphorus [44]. A study on the treatment of medium strength raw municipal wastewater using an eMBR showed through X-ray diffusion analysis that phosphates were deposited on the electrodes and on the sludge in the form of aluminum phosphate, calcium phosphate, chromium phosphate, and calcium hydrogen phosphate [41]. Tafti et al. also compared the amount of deposited phosphorus on the stainless steel anode and cathode in an eMBR [23]. Results showed that deposited material on the cathode surface had higher TP than that of the material that attached to the anode [23].

6.2.4 Removal of nonconventional pollutants in the electrochemical membrane bioreactor

6.2.4.1 Removal of phenols

Recent studies on the application of the eMBR have also examined its performance in the treatment of industrial wastewaters, which are characterized by high COD concentrations. Most of these previous studies examined industrial wastewaters that are high in phenol concentrations. Wang et al. evaluated the performance of a submerged eMBR, with Ti/PbO_2 as anode, in the degradation of phenols found in wastewater with high concentration of organics [10]. The % phenol removal efficiency was

This book belongs to Badji Mokhtar Annaba University Central Library Copyright Elsevier 2025

increased by 11.1% in the eMBR compared to that of the sum of % removal obtained by MBR and by stand-alone electrocatalytic process. High % phenol removal efficiency (~99%) was attributed to the combined effects of the enhanced biodegradation and the electrocatalytic process. The authors in the latter study suggested that the intermittent application of an electric field enhanced the microbial metabolism and improved production of enzymes for phenol degradation. The production of $^{\cdot}OH$ helped degrade the intermediate product during the degradation of phenol and resulted in further conversion to smaller organic compounds such as malic acid. However, this study also revealed that despite the high total phenol removal, the % COD removal efficiency achieved was only at 86.55%. This was due to the conversion of phenol to some intermediate products, which are difficult to degrade further into smaller molecules. The latter eMBR study by Wang et al. utilized catalytic electrodes to achieve optimum phenol removal [10]. On the other hand, Hou et al. utilized stainless steel as anode and graphite as cathode in an eMBR to treat coal chemical industry wastewater containing phenols [9]. In this study, the % removal efficiency of phenols was increased from 82.43% in an MBR to 93.28% in a submerged eMBR. Jiang et al. also evaluated the performance of a submerged eMBR, which utilized stainless steel nets as anode and cathode, in the removal of phenols from synthetic coking wastewater [14]. The application of an electric field in the range of 0.05−0.1 V/cm in the eMBR resulted in the higher phenol hydroxylase activity of *Comamonas* sp. JB compared to that observed in the reactor without applied voltage. This result was favorable for wastewater treatment since phenol hydroxylase is an important enzyme for phenol degradation. The retention of biomass inside the eMBRs also enhanced the biodegradation of phenol as the microorganisms had longer contact time with the contaminant.

6.2.4.2 Removal of trace organic pollutants

In previous studies, the potential of MBRs to remove trace organic pollutants from wastewaters had also been investigated. However, due to the nature of the pollutants, there is still a need to improve the efficiency of MBRs in the removal of these contaminants of low concentrations from wastewaters. Recent studies have examined the application of eMBRs for enhanced removal of this kind of pollutants. These studies have proposed that the following are the main mechanisms that enhance the removal of trace organic pollutants: (1) charge neutralization leading to formation of flocs with ions generated by electrocoagulation (2) electrooxidation by reactive oxygen species (ROS) generated in situ, and (3) enrichment of microorganisms capable of degrading trace organic pollutants.

Borea et al. showed that application of an electric field with current densities in the range of 0.3−1.15 mA/cm^2 in an eMBR using cheap electrodes (aluminum and stainless steel) increased the removal of pharmaceutical products compared to that observed in a conventional MBR [22]. Mendes Predolin et al. also used the same type

This book belongs to Badji Mokhtar Annaba University Central Library Copyright Elsevier 2025

of electrodes (aluminum and stainless steel) in an eMBR to remove pharmaceuticals and pesticides from real municipal wastewater. The enhanced removal efficiencies were attributed to charge neutralization between negatively charged pharmaceutical compounds and the Al^{3+}, leading to formation of larger flocs, which were then easily rejected by the membrane [18].

Chen et al. studied the removal of low concentration sulfomethoxazole (SMX), an antibacterial compound, from municipal wastewater using a moving bed eMBR (MMEMBR) [25]. The % SMX removal efficiency was higher by 45% in the MMEMBR compared to that obtained in the similar reactor without the presence of electric field. It was suggested in the latter study that the generated $^{\cdot}OH$, from the electrolysis of H_2O at the graphite anode, oxidized SMX and made it more available for biodegradation. The presence of conductive carbon felt carriers also increased the generation of ROS. The electric field application also enriched the growth of *Actinobacteria* and *Gemmatimonadete*, which have the potential to degrade SMX. Similar results were observed by Chen et al. in a submerged eMBR treating real municipal wastewater added with micropollutants [24]. Removal of residual pharmaceutical compounds and personal care products was improved by the application of an electric field due to the oxidation by ROS ($^{\cdot}OH$ and Fe (IV)O^{2+}), generated by dissolution of the stainless steel net and by electro-Fenton processes.

6.2.4.3 Removal of pathogenic viruses

The MBR technology has been considered to have a potential for water reuse applications [45–47]. Regulations for reuse of wastewater effluent include the sufficient reduction of viruses. Thus, the performance of MBRs in terms of virus removal and the mechanisms of removal have also been studied. Aside from the requirement for water reuse, another reason to study MBRs for virus removal is to determine its potential to remove viruses that cause disease outbreaks from people drinking contaminated water. Lv et al. evaluated the performance of a submerged MBR in the removal of T4, a phage with similar size as the Severe Acute Respiratory Syndrome Coronavirus (SARS-CoV-1) [48]. The results of the study showed that the MBR could remove $\sim$100% of the T4 phage during stable operation. The prevailing pathogenic virus removal mechanisms in conventional MBRs have been identified as the following: (1) attachment/adsorption of viruses to mixed liquor solids, (2) retention of viruses by clean membrane filter, (3) retention of viruses by biological cake layer, and (4) inactivation of viruses by predation and enzymatic breakdown in the mixed liquor [45–47]. Previous studies on removal of different viruses (Ms2, T4, norovirus, and adenovirus among others) using MBRs reported virus removal, in terms of log removal value (LRV), in the range of 0.2 $\log_{10}$ to 7.1 $\log_{10}$ [45,49,50]. The range of virus reduction obtained in previous studies show that there is still a need to improve virus removal in MBRs.

This book belongs to Badji Mokhtar Annaba University Central Library Copyright Elsevier 2025

Chen et al. utilized an eMBR, with IrO_2-Ta_2O_5@Ti as anode and stainless steel as cathode and membrane filter, to enhance the removal of viruses from wastewater [46]. The results of the latter study showed that application of an electric field of 2.0 V to the eMBR (80 days of operation) achieved ~100% removal efficiency of Ms2 bacteriophage, compared to the low removal of 19.8% in a conventional MBR. The high removal efficiency in the eMBR was attributed to the additional removal mechanism of inactivation due to the oxidants generated in situ [46]. Additional mechanisms of inactivation of Ms2 in the eMBR occurred due to the presence of H_2O_2 (generated on the cathodic membrane), $^{\cdot}OH$ (produced at the anode surface), and other Fenton oxidants. As far as the authors have knowledge, the study by Chen et al. is the only one that has so far examined the removal of virus by eMBR [46]. This study used IrO_2-Ta_2O_5@Ti as anode, which allowed the production of the oxidant H_2O_2. Future studies may also examine the performance of virus removal in eMBRs with other electrodes such as aluminum or iron. The removal and inactivation of other types of viruses by the eMBR may also be investigated in future studies.

6.3 Membrane fouling mitigation

Membrane fouling is the unwanted deposition and accumulation of foulants including extracellular polymeric substances (EPS), colloids, soluble organics, microorganisms, and dissolved inorganic compounds on the surface or within the pores of a membrane [2,51]. This phenomenon results in the decrease of permeate flux and increase of transmembrane pressure (TMP). Membrane fouling mitigation measures are geared towards the reduction of concentration of foulants or the degradation of fouling substances, and the prevention of their excessive deposition on the membrane. The main fouling substances that are commonly examined and targeted by the antifouling strategies in previous studies are the EPS, which are biopolymers excreted by microorganisms in the reactor [52]. EPS may be classified as loose or bound EPS. Loose EPS are referred to as soluble microbial products (SMP), which are found at the outer layer surrounding a bacterial cell and are dispersible. On the other hand, bound EPS (referred to as EPS) are in the inner layer surrounding the surface of the cell [53]. This section aims to discuss the mechanisms of reduction of membrane fouling in eMBRs, considering their effects on the fouling substances, including EPS and SMP.

6.3.1 Mechanisms of fouling mitigation

eMBRs reduce fouling through the following main mechanisms: (1) electrocoagulation, (2) electroosmosis, and (3) electrophoresis [6,54], (4) electrooxidation [8,37,55], and (5) regulation of quorum sensing (QS) [4,36] (see Fig. 6.1).

This book belongs to Badji Mokhtar Annaba University Central Library Copyright Elsevier 2025

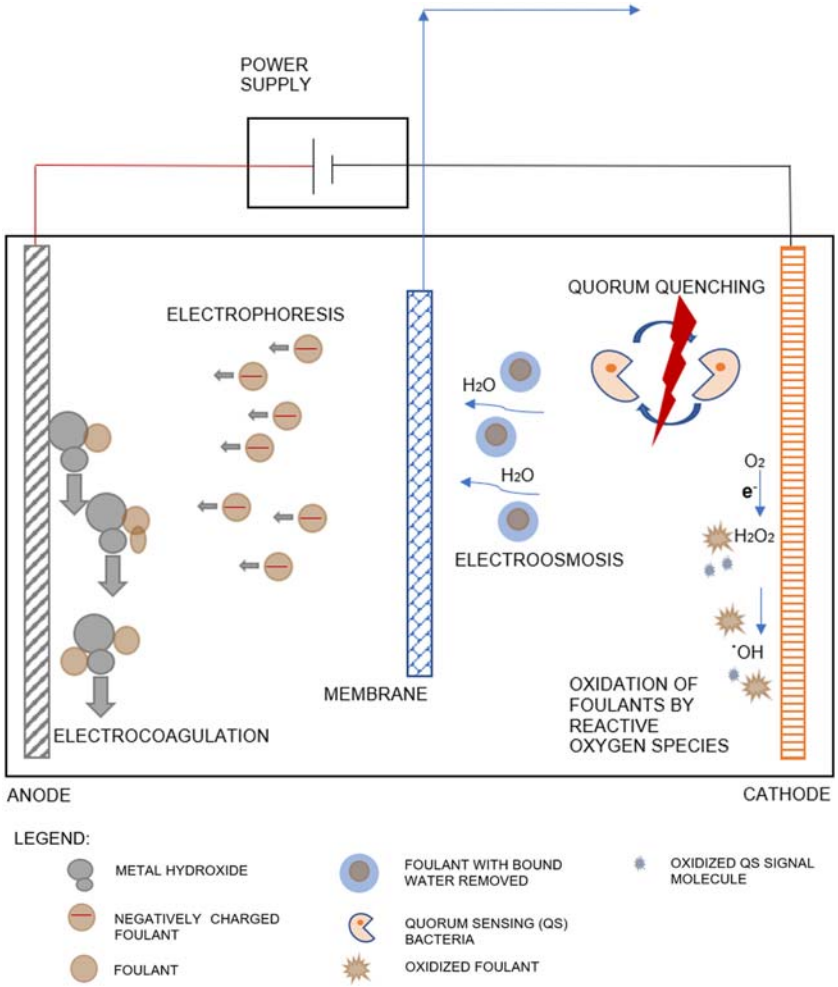

Figure 6.1 Main membrane fouling mitigation mechanisms due to the application of electric field in electrochemical membrane bioreactors including (1) electrocoagulation, (2) electrophoresis, (3) electroosmosis, (4) quorum quenching, and (5) indirect oxidation of foulants and quorum sensing signal molecules by reactive oxygen species generated in situ.

Electrocoagulation involves the electrochemical dissolution of sacrificial electrodes to produce coagulants such as Al^{3+} and Fe^{3+} [56]. The produced ions destabilize particles in the solution and allows them to aggregate to form flocs [8,57]. Fouling substances may form into flocs or may be trapped by hydroxides formed during the electrocoagulation process. This results in a higher tendency of the foulants to settle by gravity instead of adhering to the membrane surface. Qian et al. showed that the SMP and EPS concentrations in the mixed liquor in an eMBR treating oil shale wastewater were reduced

This book belongs to Badji Mokhtar Annaba University Central Library Copyright Elsevier 2025

compared to those obtained in a conventional MBR [16]. In this study, electrocoagulation of suspended EPS and SMP in the bulk liquid led to less foulants that could adhere to the membrane surface.

Electroosmosis is a process that results in the removal of bound water from sludge flocs, leading to change in sludge morphology [7]. In a previous study, the application of current density at 1.5 mA/cm^2 decreased the amount of bound water in wastewater sludge in an eMBR [7,58]. Electroosmosis was also observed by Borea et al. in an eMBR through the increase in relative hydrophobicity (71.72% ± 6.01%) of sludge compared to that of the sludge in a conventional MBR (45.12% ± 1.36%) [21] with no electric field applied. In these previous studies, the removal of bound water from the sludge contributed to the lower membrane fouling rates in the eMBRs compared to the MBRs without electrochemical assistance.

Electrophoresis in the eMBR is the phenomenon where charged particles move towards the electrode with opposite charge. The negatively charged foulants will move towards the anode (positive electrode) and not deposit on the membrane surface. In the study by Bayar et al., foulants deposited on the membrane surface were removed by electrophoresis during the filtration, resulting in an increase in permeate flux [59]. However, in this study, it was found that the effect of electrophoresis was more pronounced at higher applied voltage (30 V and above), which may not be economical and may have adverse effects on the microbial activity in the reactor.

Aside from the three mechanisms mentioned above, Karimi et al. also suggested that the EPS present in wastewater could be reduced by electrochemical oxidation [8]. As discussed in Section 6.2.1, concentration of organic substances may be reduced by electrooxidation. This process may also reduce fouling substances in the eMBRs. Wang et al. observed that higher concentrations of generated H_2O_2, which can potentially oxidize fouling substances, coincided with lower membrane fouling frequency in an eMBR [37]. Yang et al. developed a novel eMBR, which integrated MBR and the electro-Fenton process [55]. In this type of eMBR, H_2O_2 was generated by the reduction of O_2, as previously shown in Eq. (6.6). This induced the generation of $^{\cdot}OH$ with the Fe^{2+} on the surface of the membrane module. Results of the study showed that $^{\cdot}OH$ had the capability to oxidize EPS, and subsequently to reduce the TMP in the electro-Fenton MBR.

The regulation of QS has been recently explored as a means of mitigating membrane fouling in MBRs. QS is a means of communication among bacteria to coordinate their behaviors through signal molecules that they produce [60]. Among these behaviors that the QS coordinates is the formation of biofilms. Previous studies revealed that the concentration of QS signals is strongly correlated with membrane biofilm formation. Regulation of these QS signals is a new approach to mitigate membrane fouling and is referred to as quorum quenching (QQ). Recent studies investigated the addition QQ bacteria [61,62] or QQ enzymes [63]. On the other hand, the

This book belongs to Badji Mokhtar Annaba University Central Library Copyright Elsevier 2025

application of an electric field has been explored as a QQ strategy in eMBRs. Borea et al. showed that the application of an electric field in an eMBR inhibited the production of *N*-octanoyl-L-homoserine lactone (C8-HSL) signal molecules [4]. The reduction in C8-HSL corresponded with lower concentrations of the protein fraction of extracellular polymeric substances (EPSp) and transparent exopolymeric particles (TEP), which resulted in reduced membrane fouling rate.

Jiang et al. also demonstrated the role of electric field in QS regulation as a membrane fouling reduction strategy in an eMBR [36]. In this work, the degradation of *N*-acyl homoserine lactone (AHL) molecules was attributed to two mechanisms: (1) oxidation of carbon chains in AHL molecules by the H_2O_2 generated at the cathode, and (2) enrichment of QQ bacteria and decrease of QS bacteria due to the applied voltage. The results of the study of Khan et al. also suggested that the application of an electric field activated the QQ bacteria that have been added to a submerged eMBR, resulting in reduced membrane fouling rate [64].

6.3.2 Mixed liquor properties and fouling in electrochemical membrane bioreactors

Membrane fouling in eMBRs is a phenomenon that results from the interaction between the mixed liquor and the membrane [2,53]. The following discussion shows the effect of the application of electric field in eMBRs on different mixed liquor properties and, subsequently, on the membrane fouling reduction in eMBRs.

6.3.2.1 Concentration of fouling substances

As seen in Section 6.3.1, the concentration of fouling substances EPS and SMP in mixed liquor has been reported to decrease in the presence of an electric field in eMBRs [21,23]. Excessive SMPs result in the blockage of voids between particles in a cake layer formed on membrane surfaces [8]. Thus, reduced SMP concentrations may contribute to lower membrane fouling rate. The study of Hou et al. showed that a lower SMP concentration was achieved in a submerged eMBR compared to that measured in an MBR after 50 days of operation [9].

EPS and SMP components are mainly classified as proteins (PN) and carbohydrates/polysaccharides (PS) [53]. Previous studies have shown that application of electric field decreased PN/PS ratio in eMBRs [28,36,65]. This is favorable for the prevention of membrane fouling since a lower PN/PS ratio implies the decrease of positively charged amino acids found in proteins. Since carboxylic and phosphoric acid groups in polysaccharides are negatively charged, the lower PN/PS ratio means net surface charge of sludge particles becomes increasingly negative. This increases the absolute zeta potential of the sludge particles and increases the repulsion between particles and negatively charged membranes [28,36]. Proteins have also been reported to chelate with metal ions, forming stable flocs and gel layer, and eventually contribute to

This book belongs to Badji Mokhtar Annaba University Central Library Copyright Elsevier 2025

membrane fouling [19,27]. The inhibition of EPS or SMP protein content production by the application of an electric field can therefore contribute to the reduction of membrane fouling rate [65].

TEPs are polysaccharides of gel-like nature that have high viscosity [66,67]. Because of their nature, TEPs tend to attach easily to the membrane and are difficult to remove from MBRs [66]. Only a few studies have investigated the effect of an electric field on the concentration of TEPs in MBRs. Borea et al. observed that the TEP concentration in an eMBR decreased by 71%–75% compared to those observed in a conventional MBR with no electric field applied. This reduction in the TEP concentration coincided with the lower membrane fouling rate in the eMBR [21]. Belli et al. also found that TEP concentrations in an eMBR positively correlated with the membrane filtration resistance (MFR) [12]. It was revealed that the presence of electric field led to the lower TEP concentrations, and subsequently to lower MFR. Although the mechanisms of their removal or degradation by electrochemical processes have not been specifically examined, TEP concentrations may have been reduced in eMBRs by the same mechanism as the polysaccharide content of EPS.

6.3.2.2 Properties of sludge/foulant particles

Previous studies have investigated the effect of the application of electric field in eMBRs on the particle size distribution (PSD) in the sludge at the mixed liquor [23,29,30,64], and in the cake layer [19]. Lower particle size may result into greater tendency of particles to block pores of the membrane and lead to higher filtration resistance [23]. On the other hand, larger flocs that deposit on the membrane surface could contribute to the formation of a more porous cake layer and lead to lower filtration resistance [19].

Hasan et al. revealed that the mean particle size of freshly activated sludge samples decreased over a 50 day-operation period of a pilot-scale eMBR [30]. The authors in this study suggested that electroosmosis, a phenomenon that reduces bound water in the flocs, reduced the particle size.

On the other hand, Ying et al. observed the increased particle sizes of foulant particles in the supernatant in an anaerobic eMBR (An-eMBR) compared to that obtained in an anerobic MBR (AnMBR) [29]. The increase in particle size implied that the applied voltages in the An-eMBR favored the formation of larger flocs. Similar results were obtained by Li et al. and Qian et al. in submerged eMBRs, where particle sizes of flocs were increased (compared to those of particles in MBRs without electric field) because of the formation of flocs by the generated Fe ions [16,42].

Khan et al. observed an increase in the sludge particle size in the first 15 days of operation of a submerged eMBR, and a decrease of the same parameter after 50 days of operation. The initial increase was attributed to electrocoagulation which resulted in the formation of large flocs [64]. And the subsequent decrease implied the occurrence of electroosmosis. Tafti et al. also observed an increase in particle size in an eMBR

This book belongs to Badji Mokhtar Annaba University Central Library Copyright Elsevier 2025

compared to an MBR without applied electric field. However, reduction in the particle size was observed in the latter study as current density was increased, which favored the electroosmosis process [23]. Su et al. recently examined the effect of PSD in the cake layer formed in an eMBR [19]. It was found that the particle sizes in the cake layers increased as the electric field intensity was increased from 1 to 2 to 4 V/cm. This trend also corresponded with the increase in permeate flux. Although the last study did not examine the size of the particles in the mixed liquor, it has demonstrated that larger flocs that could be deposited on the membrane surface could reduce filtration resistance of the cake layer.

A property of the sludge/foulant particles that is related to the size is the absolute zeta potential, which characterizes the surface charge of the sludge particles [23] and determines their tendency to form aggregates [9]. Lower absolute zeta potential means lower repulsion among flocs and higher tendency to aggregate [68]. Hasan et al. reported a decrease in the absolute zeta potential value of particles from −26.2 mV in an MBR to −14.2 mV in a submerged eMBR [30]. The production of sufficient Al^{3+} in this study was proposed to be able to neutralize and destabilize the negatively charged colloids, allowing them to form large flocs. Tafti et al. and Hou et al. obtained similar results where absolute zeta potential was reduced in eMBRs compared to MBRs due to the Fe ions that neutralized the negative charge on the sludge particles [9,23]. In an eMBR which utilized graphite as anode instead of the sacrificial electrodes Al or Fe, a decrease in absolute zeta potential of the particles was still observed [29]. However, the mechanism behind the reduction in absolute zeta potential was not elaborated further in the latter study.

The application of the electric field in the eMBRs was also reported to affect the sludge surface hydrophobicity. Hydrophobicity of surfaces describes the tendency of nonpolar molecules forming aggregates in order to reduce the surface of contact with polar water molecules [53]. Previous studies have associated hydrophobicity of bulk sludge with the EPS, which are composed of hydrophobic and hydrophilic groups [65]. The protein content of EPS is mainly hydrophobic due to the presence of hydrophobic amino acids. The application of an electric field in eMBRs has been reported to reduce the protein content of EPS, as discussed in Section 6.3.2.1. The reduction of PN/PS ratio of EPS has been considered as an indicator of reduction of hydrophobicity [36,65]. Lower sludge hydrophobicity results in lower tendency of their adsorption on hydrophobic membrane surfaces [36]. In addition, reduction of hydrophobicity may also lead to weakened capabilities of microbial cells to adhere to water surfaces, which may be favorable for membrane fouling mitigation [65,69].

There are a few studies that reported increased hydrophobicity of flocs by the application of electric field in eMBRs. Battistelli et al. obtained an increase in PN/PS ratio of the EPS (although the concentration in EPS decreased) in an eMBR operated at current densities of 1.0 mA/cm^2 compared to that obtained in reactor without

This book belongs to Badji Mokhtar Annaba University Central Library Copyright Elsevier 2025

applied electric field [70]. In this study, the increased PN/PS ratio was also used as an indicator of increased hydrophobicity. Borea et al. measured an increase of sludge relative hydrophobicity from 45.12% in a conventional MBR to 71.72% in an eMBR with applied voltage of 3 V/cm [21]. The observed increase in the relative hydrophobicity was associated with the phenomenon of electroosmosis in the eMBR. In both of the studies, by Battistelli et al. and Borea et al., the increase in hydrophobicity was considered favorable for membrane fouling mitigation due to the reduced interaction between the hydrophobic flocs and the hydrophilic membranes used (polyetherimide and polyvinylidene difluoride (PVDF) membranes, respectively) [21,70].

It is noted that most of the previous studies only determined the EPS PN/PS ratio and not the actual relative sludge hydrophobicity in eMBRs. Future research work may further investigate the effect of the electric field application on sludge or foulants' hydrophobicity by the actual determination of correlation between sludge hydrophobicity and measured EPS PN/PS ratio.

6.4 Operating conditions, materials, and configurations

6.4.1 Current density and duration of application of electric field

Some of the main operating conditions that affect the performance of eMBRs are the intensity of electric field applied and the duration of its application. These conditions highly influence the performance of eMBRs in terms of pollutant removal capability and membrane fouling reduction capacity. In addition, these operating conditions also contribute to the total energy consumption of the reactor. Previous studies on eMBRs have utilized different magnitudes of electric field and different modes of application (see Table 6.1).

The study of Tafti et al. revealed that lower COD removal efficiencies were observed in an eMBR when the applied current density was $>2.0\ mA/cm^2$ [23]. At this value of current density, the pH of the mixed liquor turned alkaline, which might have affected bacterial activity. The authors also proposed that at higher current densities, excessive amount of ferric ions might have affected the microorganisms responsible for organic pollutant degradation/removal. At higher current densities, the phosphorus and ammonium removal efficiencies are also decreased. Similar results were obtained by Borea et al. where COD and NH_3-N removal efficiencies decreased when current density was increased from 0.5 to $1.5\ mA/cm^2$ [22]. In this study, the lower COD and NH_3-N removal efficiencies at higher current density were attributed to the generation of excessive Al^{3+} ions. The very high concentration of aluminum hydroxide complexes were suggested to have affected the transfer of enzymes and of

This book belongs to Badji Mokhtar Annaba University Central Library Copyright Elsevier 2025

nutrients to the cell membranes of the microorganisms. Tafti et al. also found that the duration of application of the electric field influenced the removal of pollutants, where an optimum OFF/ON ratio of the applied magnitude of current density was determined for optimum pollutant removal [23].

In terms of membrane fouling, the effect of varying the magnitude of the electric field was also investigated. The study of Borea et al. showed that membrane fouling rate decreased from 6.80 to 3.69 kPa/day when the applied voltage gradient was increased from 1 to 3 V/cm [21]. Hua et al. also found that increasing the current density (0, 1.0, 2.0, 3.0, and 4.0 mA/cm^2) applied in an eMBR decreased the absolute zeta potential of the sludge [68]. As discussed in Section 6.3.2.2, lower absolute zeta potential may lead to lower tendency for membrane fouling [68]. However, it was also found that at the higher current densities of 3.0 and 4.0 mA/cm^2, the concentrations of polysaccharides and proteins were increased. Hua et al. attributed this increase to the occurrence of cell lysis due to the high current densities [68]. In this study, the current density of 2.0 mA/cm^2 was found to correspond to optimum membrane fouling mitigation [68]. Yang et al. also investigated the effects of different voltages (0, 0.5, 1.0, and 1.5 V) to be used for an eMBR [28]. The study showed that at a lower voltage of 0.5 V, adhesion of protein to the membrane surface was more evident since the degradation of the foulant was not sufficient [28]. On the other hand, the membrane flux was observed to be lower at 1.5 V than in 1.0 V. Mendes Predolin et al. found that TMP increased in an eMBR when the current density was increased from 0.5 mA/cm^2 to 1.0 and 1.5 mA/cm^2 [18]. In this study, this increase in TMP at higher current densities suggested that higher Al^{3+} concentrations could contribute to increase in membrane fouling. The excessive amount of Al^{3+} ions could lead to restabilization of colloids, preventing them from aggregating, and allowing the colloids to contribute to membrane fouling [18,71]. These previous studies highlight the need for determination of optimum current density or voltage to be applied, considering the eMBR's performance in pollutant removal and membrane fouling mitigation, and considering the energy consumption.

6.4.2 Electrode materials

As seen in the preceding sections and in Table 6.1, several materials have been used as electrodes in eMBRs. The choice of electrodes significantly influences the performance of the eMBR, particularly affecting the electrochemical processes that could occur, and having impacts on the cost of the reactor.

Most eMBR studies have used aluminum and/or iron-based electrodes (see Table 6.1). When used as the anodes, their electrochemical dissolution releases ions that can neutralize charges of particles found in the mixed liquor and can initiate electrocoagulation [57]. As discussed in Section 6.2, these ions can form hydroxides and

This book belongs to Badji Mokhtar Annaba University Central Library Copyright Elsevier 2025

precipitates to remove organic pollutants and nutrients from wastewater. The in situ generation of iron ions may also be beneficial to the microorganisms as they are important in the formation of components of enzymes related to bacterial metabolism [3]. However, as discussed in Section 6.4.1, the excessive concentration of these ions may also lead to inhibition of some bacterial activities. Nonsacrificial electrodes have also been used such as titanium and graphite (Table 6.1) in many studies.

Ozbey Unal et al. examined the difference in the eMBR performance between a sacrificial (iron) and nonsacrificial electrode (Ti) used as anodes in an eMBR [72]. Scanning electron microscopy showed that the use of Ti anode resulted in a cleaner membrane surface, resulting in higher membrane flux in an eMBR. The use of Ti as anode led to the occurrence of electrochemical oxidation, which may have reduced the fouling substances that may adhere to the membrane. However, this study also showed that COD removal was higher when using the iron anode. A few studies have utilized Ti-based anodes in eMBRs with the aim to treat wastewater with high COD [10,28] or with recalcitrant compounds such as pharmaceutical products [10,24]. The eMBR in the study of Wang et al. utilized catalytic electrodes (Ti/PbO_2 as anode) to produce $^{\cdot}OH$ that can contribute to the degradation of phenols and their intermediate products [10]. Chen et al. used titanium coated with IrO_2-Ta_2O_5 as the anode [24]. The IrO_2-Ta_2O_5 was determined to have high oxygen evolution potential, which is suitable for the electrooxidation of the low-concentration pharmaceutical compound and personal care products in the wastewater. It was proposed in this study that $^{\cdot}OH$ is also electrogenerated on the surface of the titanium coated with IrO_2-Ta_2O_5. In this study by Chen et al., the cathode used was stainless steel mesh, which was also postulated to produce more $^{\cdot}OH$ and $Fe(IV)O^{2+}$ due to the release of iron ions and the electro-Fenton processes [24].

Karimi et al. investigated the effect of different types of cathodes (aluminum, stainless steel, copper, and iron) to the performance of an eMBR using aluminum as anode [8]. It was found that using iron as cathode resulted in higher production of aluminum ions and hydroxides. This led to the lower membrane fouling rate in the eMBR. However, the reason behind this was not further examined.

6.4.3 Configurations and membrane materials

The configurations of the eMBRs also affect the performance of the electro bioreactors. The differences in configurations influence the strength of electric field needed, the distribution of current density, and the hydrodynamics in the reactor.

One of the configurations used in the previous studies consisted of an electrocoagulation unit and a submerged MBR in series [15,32]. In this configuration (Fig. 6.2A), the electrocoagulation unit serves as a pre-treatment stage before the wastewater goes into the MBR tank. This also prevents direct application of the

This book belongs to Badji Mokhtar Annaba University Central Library Copyright Elsevier 2025

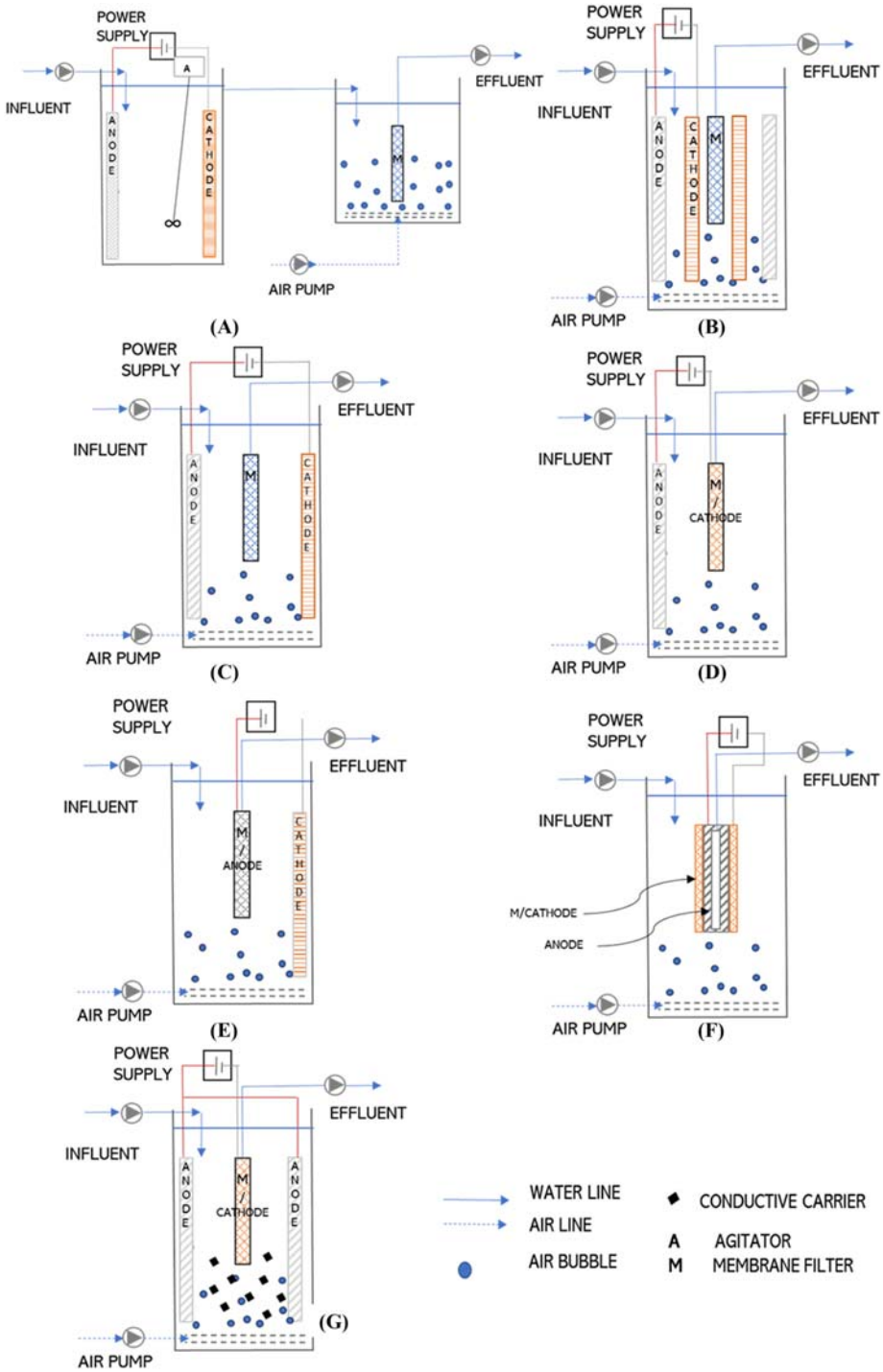

Figure 6.2 Common configurations of electrochemical membrane bioreactors (eMBRs) in previous studies: (A) electrocoagulation system and submerged MBR in series, (B) submerged eMBR with cylindrical electrodes, (C) submerged eMBR with rectangular electrodes/plate electrodes, (D) submerged eMBR with cathode as membrane, (E) submerged eMBR with membrane as anode, (F) submerged eMBR with built-in electrodes in membrane, and (G) moving bed eMBR.

This book belongs to Badji Mokhtar Annaba University Central Library Copyright Elsevier 2025

electric field to the microorganisms in the activated sludge since the electrodes are not submerged in the bioreactor (MBR) [32].

The submerged eMBR configuration, where the electrodes and the membrane module are in a single vessel, has been widely used in previous laboratory and pilot-scale studies (Table 6.1). The configuration developed by Bani-Melhem and Elektorowicz [3], where cylindrical anodes and cathodes were placed concentrically (5 cm apart) around a polymeric membrane module (Fig. 6.2B), was adapted by several studies [11,12,17,18,20–22]. As proposed by Bani-Melhem and Elektorowicz [3], this configuration takes into account the following: (1) optimum distribution of current density, (2) minimum oxidation effect of electric field to the membrane module, and (3) unhindered flow of wastewater into reactor and membrane module. One of the key considerations in the operation of the submerged eMBRs is finding the optimum current density that will not have an adverse effect on the microorganims since they are in the same vessel as the electrodes. Other submerged eMBR configurations used rectangular plates as electrodes (commonly 10 cm apart) where the anode is located at a distance from one side of the membrane and the cathode at a distance from the other side (Fig. 6.2C) [9,10,13,16]. Some studies have utilized conductive membranes as cathodes (Fig. 6.2D), which may be beneficial since lower electric field magnitudes are needed to mitigate fouling [28]. In previous studies, the cathodic membranes are composed of stainless steel mesh [14,24], titanium mesh [25], or carbon nanotubes hollow fiber membranes (CNT-HFMs) [28]. In some studies, eMBRs utilized anode-based membranes [27] (Fig. 6.2E).

Chen et al. developed a submerged eMBR that utilized a membrane with built-in electrodes (Fig. 6.2F) [24]. The anode was a titanium plate coated in IrO_2-Ta_2O_5 and was used as the membrane support frame. The cathode was a stainless steel mesh coated with a polymer film and was used as the membrane. The researchers in this study suggested that this configuration protected the electrodes from risk of fouling.

A recent study has also utilized a modified configuration where the submerged eMBR was added with conductive carbon felt particles as carriers (Fig. 6.2G). The addition of the conductive carriers made it a moving bed eMBR. The conductive carriers increased the generation of ROS by 34.5% compared to that observed in eMBR without the carbon felt particles. This increase in ROS corresponded with an additional removal of SMX, a micropollutant in wastewater.

6.5 Microbiological community

Asif et al. has noted that electric field applied at current densities >2.5 mA/cm^2 has a negative effect on the growth and activity of microorganisms in an eMBR [54].

This book belongs to Badji Mokhtar Annaba University Central Library Copyright Elsevier 2025

However, it has also been shown that intermittent application of low current density could enhance the growth rate of microorganisms in an electro bioreactor used for wastewater treatment. Battistelli et al. showed that the application of 1.0 mA/cm^2 current density in an eMBR increased the oxygen uptake rates (OUR) for ammonium and nitrite oxidation, and their specific oxygen uptake rates (SOUR), compared to those observed in an MBR [20] without electric field applied. In this study, it was proposed that the increase in the microbial activities was due to the presence of electron donors or acceptors, brought about by the action of the electric current. Similar results were obtained by Chen et al. and Hou et al. where the values of SOUR in eMBRs were higher than those obtained in the corresponding MBRs without electric field application [9,25]. The study of Tafti et al. also revealed that at lower densities (<2.0 mA/cm^2), the SOUR of the microorganisms increased as the current density was increased, implying the stimulation of microbial metabolism [23]. A similar trend was observed by Belli et al. in an eMBR where the OUR for ammonium oxidation and the SOUR increased as the electric current density was also increased from 1.0 to 1.5 mA/cm^2 [12].

A few studies have examined further the effect of the application of electric field to the abundance, structure, and diversity of microbial communities in eMBRs. The effect of the application of electric field to the microbial richness (total number of species) and diversity (total number of species, relative abundance of species, or combination of both) [73] in eMBRs has also been investigated by previous studies [19,26,36,74]. Most of the studies revealed that the microbial community's richness and diversity are increased in the eMBRs compared to MBRs without electric field applied [14,19,25,27,28,42]. Su et al. suggested that the electrogenerated ferric ions in an eMBR contributed to the increase in microbial communities [19]. The higher number of species may enhance the stability of the microbial community [27].

In contrast, Liu et al. observed that the application of electric field to an MBR reduced the microbial community richness [26]. In particular, Liu et al. showed that increasing the voltage or the current applied decreased the microbial richness of the activated sludge in an eMBR [26]. However, it was noted in this study that although the microbial richness was decreased, the microbial diversity was maintained in the eMBR. This trend was attributed to the possibility that growth of some species was inhibited by the electric field, while growth of other selected species was stimulated.

A commonly observed effect of the application of an electric field in eMBRs is the increase in relative abundance of nitrifying and denitrifying microorganisms compared to those in conventional MBRs [9,13,42]. This increase has been attributed to the formation of larger and more compact flocs in the eMBRs. The larger and more compact flocs led to anoxic/aerobic micro-environments, which favored the promotion of growth of the nitrogen-removing microorganisms [9]. Larger flocs could lead to anoxic zones in the inner particle due to the longer distance for diffusion of oxygen

This book belongs to Badji Mokhtar Annaba University Central Library Copyright Elsevier 2025

[42,75]. Roy et al. observed the increase of the relative abundance of *Nitrosomonas*, a bacteria that oxidizes ammonia into nitrite, in an eMBR upon applying current at 400 mAh/L, compared to that observed in a conventional MBR without applied current [13]. In the latter study, the increase in relative abundance of *Nitrosomonas* was attributed to the increase in available NH_4 substrate, due to the reduction of nitrate at the Ti/Pt cathode. The study of Li et al. also revealed that electrocoagulation enhanced the growth of *Nitrosomonas* in an eMBR [42].

The previous studies discussed in this section highlight that the presence of electric field, applied at a certain magnitude, may result in stimulation of microbial activity, in changes in microbial richness, and in shifts in microbial structure and diversity (see Table 6.2). These changes and their relationships to membrane fouling mitigation and pollutant removal in eMBRs are important to understand.

6.6 Energy consumption

The energy consumed in the operation of eMBRs is an important aspect to be considered for their use in full-scale applications. A few studies have determined the specific energy consumption of eMBRs, expressed in kWh per m^3 of treated wastewater (see Table 6.3). Yang et al. reported an average specific energy consumption of

Table 6.2 Effects of the applied electric field to the microbial community in the eMBR.

Parameter	Effect of application of electric field to microbial community	References
Bacterial growth (population)	Bacterial count generally increased (less than 2.0 mA/cm^2)	[76,77]
Oxygen uptake rate (OUR) for ammonium and nitrite oxidation	Increased OUR compared to that obtained in MBRs without electrochemical assistance (for CDs less than 2.0 mA/cm^2)	[12,20]
Specific oxygen uptake rate (SOUR)	Increased SOUR compared to that obtained in MBRs without electrochemical assistance (for CDs less than 2.0 mA/cm^2)	[12,20,23]
Microbial richness	Application of electric field generally increased microbial richness Decreased microbial richness at increasing applied voltage	[14,25,26,42]
Microbial diversity	Application of electric field generally increased microbial diversity	[14,25,42]
Relative abundance of nitrifying and denitrifying microorganisms	Increased relative abundance of nitrogen-removing microorganisms	[9,13,42]

This book belongs to Badji Mokhtar Annaba University Central Library Copyright Elsevier 2025

Table 6.3 Energy consumption in previously reported eMBRs.

Applied voltage or current density/mode of application	Specific energy consumption (kWh/m^3 of treated wastewater)	References
1.0 V/continuous	2.1	[27]
0.2 mA/cm^2 Intermittent: 30 min ON/ 30 min OFF	0.02[a]	[19]
1.2 mA/cm^2 Intermittent: 5 min ON/ 10 min OFF	1.1−1.6	[30]
0.5, 1.0, and 1.5 mA/cm^2 Intermittent: 5 min ON/ 10 min OFF	0.26−1.87[a]	[18]
0.8 V/continuous 15 min for each cycle	8.64×10^{-5}	[55]

[a]Note: Values represent the energy applied to electrodes only.

2.1 kWh/m^3 for a laboratory-scale aerobic submerged eMBR, operating at 1.0 V (continuous application) [28]. The energy for aeration was 59.52% of this reported consumption. Only 2.38% of this specific energy consumption was utilized to drive the electrochemical reactions (0.05 kWh/m^3) in the latter study. Su et al. also reported an energy consumption equal to 0.02 kWh/m^3 only for driving the electrochemical reactions using the electric field applied to the electrodes of another laboratory-scale eMBR [19]. Zhang et al. estimated that 10% of additional electricity consumption was needed in a laboratory-scale eMBR compared to that needed in an MBR to have 30% TMP reduction [78].

The specific energy consumption of a pilot-scale eMBR (applying 1.2 mA/cm^2 current density, 5 min ON/10 min OFF cycle) was estimated to be in a range of 1.1−1.6 kWh/m^3 within 7 weeks of operation [30]. This is comparable to the specific energy consumption of MBRs which was reported to be in the range of 0.6−2.4 kWh/m^3 [2]. However, the specific energy consumption reported by Hasan et al. was only determined during the start-up period, leading to the use of rough estimates in the calculations [30]. Mendes Predolin et al. also determined the specific energy consumption of a pilot-scale eMBR that operated for approximately 24 weeks [18]. Specific energy consumption of 0.26, 0.86, and 1.87 kWh/m^3 vis-à-vis 0.5, 1.0, and 1.5 mA/cm^2 current densities applied, respectively, were reported for the pilot-scale eMBR. However, the values obtained represent only the energy consumed to drive the electrochemical processes in the eMBR. Yang et al. found that greater than 50% of the overall specific energy consumption of an aerobic eMBR was utilized for aeration and only 2.38% was used to drive the electrochemical processes [27]. These studies show the potential of the eMBRs to be an alternative technology that utilizes energy comparable to that used in conventional MBRs. The reported specific energy consumptions can be further reduced by determining the minimum strength of electric field applied, and the duration of application, that will still give the optimum pollutant

This book belongs to Badji Mokhtar Annaba University Central Library Copyright Elsevier 2025

removal and membrane fouling reduction capability. Further studies are also needed to reduce the energy requirements for aeration in aerobic MBRs.

6.7 Challenges and future prospects

The eMBR is continuously being studied for its potential to deliver enhanced conventional and nonconventional pollutant removals, and to reduce membrane fouling rate. However, only a few studies have yet studied the eMBR in pilot-scale applications. Pilot-scale eMBR plants should also be examined over longer periods of operation to provide better data on pollutant removal, membrane fouling rate reduction, and energy consumption. These data and detailed cost-analysis (including costs of materials, labor, cleaning, and maintenance) of eMBR operation will be important for future full-scale applications [18]. To date, most of the previous studies focused on the performance of eMBRs employing the aerobic process. Effect of the application of electric field to fouling mitigation in anaerobic eMBRs still need further investigation.

In terms of the challenges faced vis-à-vis pollutant removal, a few studies have investigated the removal of nonconventional pollutants in eMBRs. However, as seen in Table 6.1, there is still a need to improve the removal efficiencies of some contaminants, notably of commonly detected pharmaceutical products in wastewater such as diclofenac and carbamazepine. Fate of the nonconventional pollutants in the eMBR is also to be explored, to determine whether these contaminants were fully degraded, were transformed to other by-products, or were adsorbed to sludge in the eMBRs.

As discussed in Section 6.6, the reduction in energy consumption in eMBRs may be geared towards the reduction of energy used for aeration. Future research may explore the intermittent aeration eMBRs, as what has been applied in MBRs in some previous studies [79].

Another aspect that needs investigation in further studies is the lifespan of electrodes, particularly considering the commonly used sacrificial electrodes. Only a few studies have measured the amount of electrode consumed for a certain amount of treated wastewater. Kurtoğlu Akkaya and Bilgili have measured 0.0572–0.0792 g of aluminum per liter of treated wastewater in an eMBR. The values were shown to have higher values than theoretical values obtained from the equation following Faraday's law [11]. Hasan et al. measured a loss of aluminum by 23 g/day [30]. This corresponded to an estimated lifespan of the electrode of 5 months. On the other hand, Mendes Predolin et al. have estimated the lifetime of an aluminum anode of a pilot-scale eMBR to be 4 months [18]. The lifetime of the anodes depends on the material, current density, and duration of exposure [18]. On the other hand, cathodes also undergo deposition of foulants and other substances and need cleaning after some time of operation. Mendes Predolin et al. have noted

This book belongs to Badji Mokhtar Annaba University Central Library Copyright Elsevier 2025

that a stainless steel cathode in a pilot-scale eMBR needed cleaning after 4 months [18]. This may be delayed by the application of strategies such as diffusers near the cathodes to scour deposits on the surface [30]. There is a need for further studies evaluating the lifetime of electrodes since it affects the operation and the cost. In addition, the release of excessive ions may affect the sludge and effluent toxicity. Hasan et al. measured an aluminum concentration of 8 mg/L in the waste sludge generated after operation of an eMBR, while 0.4 mg/L was obtained in the effluent [30]. Borea et al. obtained a concentration of 0.21 ± 0.02 mg Al^{3+}/L in the effluent of eMBRs [21]. Further studies on measuring and evaluating the concentrations of aluminum in the sludge and in the effluent are also needed [21].

6.8 Conclusions

The eMBRs have been shown to enhance conventional and nonconventional pollutant removal and to reduce membrane fouling rates through different additional mechanisms brought by the application of an electric field. Determining the optimum strength, and mode and duration of application of the electric field is important for better performance of the eMBR.

Recent studies have shown the potential of eMBRs in the treatment not only of low and medium-strength wastewaters but also of high-strength wastewaters, such as landfill leachates and industrial wastewater. Recent studies on eMBRs have also focused on the mechanism of electrooxidation for pollutant and fouling substances removal/ degradation.

There is still a need for further studies on eMBRs, particularly in pilot-scale applications to provide a better picture of their performances in terms of pollutant removal and membrane fouling mitigation, and to give better estimates regarding energy consumption.

References

[1] S. Judd, The status of membrane bioreactor technology, Trends Biotechnol. 26 (2008) 109–116.
[2] P. Krzeminski, L. Leverette, S. Malamis, E. Katsou, Membrane bioreactors—a review on recent developments in energy reduction, fouling control, novel configurations, LCA and market prospects, J. Membr. Sci. 527 (2017) 207–227.
[3] K. Bani-Melhem, M. Elektorowicz, Development of a novel submerged membrane electro-bioreactor (SMEBR): performance for fouling reduction, Environ. Sci. Technol. 44 (2010) 3298–3304.
[4] L. Borea, V. Naddeo, V. Belgiorno, K.-H. Choo, Control of quorum sensing signals and emerging contaminants in electrochemical membrane bioreactors, Bioresour. Technol. 269 (2018) 89–95.

This book belongs to Badji Mokhtar Annaba University Central Library Copyright Elsevier 2025

[5] B.M.B. Ensano, L. Borea, V. Naddeo, M.D.G. de Luna, V. Belgiorno, Control of emerging contaminants by the combination of electrochemical processes and membrane bioreactors, Environ. Sci. Pollut. Res. 26 (2019) 1103–1112.
[6] B.M.B. Ensano, L. Borea, V. Naddeo, V. Belgiorno, M.D.G. de Luna, F.C. Ballesteros, Combination of electrochemical processes with membrane bioreactors for wastewater treatment and fouling control: a review, Front. Environ. Sci. 4 (2016).
[7] S. Ibeid, M. Elektorowicz, J.A. Oleszkiewicz, Novel electrokinetic approach reduces membrane fouling, Water Res. 47 (2013) 6358–6366.
[8] L. Karimi, H. Hazrati, S. Gharibian, H. Shokrkar, Investigation of various anode and cathode materials in electrochemical membrane bioreactors for mitigation of membrane fouling, J. Environ. Chem. Eng. 9 (2021) 104857.
[9] B. Hou, Y. Kuang, H. Han, Y. Liu, B. Ren, R. Deng, et al., Enhanced performance and hindered membrane fouling for the treatment of coal chemical industry wastewater using a novel membrane electro-bioreactor with intermittent direct current, Bioresour. Technol. 271 (2019) 332–339.
[10] T. Wang, H. Zhao, H. Wang, B. Liu, C. Li, Research on degradation product and reaction kinetics of membrane electro-bioreactor (MEBR) with catalytic electrodes for high concentration phenol wastewater treatment, Chemosphere 155 (2016) 94–99.
[11] G. Kurtoğlu Akkaya, M.S. Bilgili, Evaluating the performance of an electro-membrane bioreactor in treatment of young leachate, J. Environ. Chem. Eng. 8 (2020) 104017.
[12] T.J. Belli, A.A. Battistelli, R.E. Costa, C.M.S. Vidal, A.E. Schlegel, F.R. Lapolli, Evaluating the performance and membrane fouling of an electro-membrane bioreactor treating textile industrial wastewater, Int. J. Environ. Sci. Technol. 16 (2019) 6817–6826.
[13] D. Roy, P. Drogui, M. Rahni, J.-F. Lemay, D. Landry, R.D. Tyagi, Effect of cathode material and charge loading on the nitrification performance and bacterial community in leachate treating Electro-MBRs, Water Res. 182 (2020) 115990.
[14] B. Jiang, C. Du, S. Shi, L. Tan, M. Li, J. Liu, et al., Enhanced treatment performance of coking wastewater and reduced membrane fouling using a novel EMBR, Bioresour. Technol. 229 (2017) 39–45.
[15] M.H. Al-Malack, W.K. Al-Nowaiser, Treatment of synthetic hypersaline produced water employing electrocoagulation-membrane bioreactor (EC-MBR) process and halophilic bacteria, J. Environ. Chem. Eng. 6 (2018) 2442–2453.
[16] G. Qian, L. Ye, L. Li, X. Hu, Impact of electrocoagulation on membrane filtration resistance under different proportions of industrial wastewater, J. Chem. Technol. Biotechnol. 93 (2018) 3160–3170.
[17] E. Souza, H.V.D.M. Follmann, L. Dalri-Cecato, A.A. Battistelli, M.A. Lobo-Recio, T.J. Belli, et al., Membrane fouling suppression using intermittent electric current with low exposure time in a sequencing batch membrane bioreactor, J. Environ. Chem. Eng. 8 (2020) 104018.
[18] L. Mendes Predolin, M.J. Moya-Llamas, E.D. Vásquez-Rodríguez, A. Trapote Jaume, D. Prats Rico, Effect of current density on the efficiency of a membrane electro-bioreactor for removal of micropollutants and phosphorus, and reduction of fouling: a pilot plant case study, J. Environ. Chem. Eng. 9 (2021) 104874.
[19] F. Su, Y. Liang, G. Liu, C.R. Mota Filho, C. Hu, J. Qu, Enhancement of anti-fouling and contaminant removal in an electro-membrane bioreactor: significance of electrocoagulation and electric field, Sep. Purif. Technol. 248 (2020) 117077.
[20] A.A. Battistelli, T.J. Belli, R.E. Costa, N.M. Justino, D.D. Silveira, M.A. Lobo-Recio, et al., Application of low-density electric current to performance improvement of membrane bioreactor treating raw municipal wastewater, Int. J. Environ. Sci. Technol. 16 (2019) 3949–3960.
[21] L. Borea, V. Naddeo, V. Belgiorno, Application of electrochemical processes to membrane bioreactors for improving nutrient removal and fouling control, Environ. Sci. Pollut. Res. 24 (2017) 321–333.
[22] L. Borea, B.M.B. Ensano, S.W. Hasan, M. Balakrishnan, V. Belgiorno, M.D.G. de Luna, et al., Are pharmaceuticals removal and membrane fouling in electromembrane bioreactor affected by current density? Sci. Total Environ. 692 (2019) 732–740.

This book belongs to Badji Mokhtar Annaba University Central Library Copyright Elsevier 2025

[23] A.D. Tafti, S.M. Seyyed Mirzaii, M.R. Andalibi, M. Vossoughi, Optimized coupling of an intermittent DC electric field with a membrane bioreactor for enhanced effluent quality and hindered membrane fouling, Sep. Purif. Technol. 152 (2015) 7–13.
[24] M. Chen, L. Ren, K. Qi, Q. Li, M. Lai, Y. Li, et al., Enhanced removal of pharmaceuticals and personal care products from real municipal wastewater using an electrochemical membrane bioreactor, Bioresour. Technol. 311 (2020) 123579.
[25] M. Chen, J. Xu, R. Dai, Z. Wu, M. Liu, Z. Wang, Development of a moving-bed electrochemical membrane bioreactor to enhance removal of low-concentration antibiotic from wastewater, Bioresour. Technol. 293 (2019) 122022.
[26] J. Liu, X. Ju, B. Gao, L. Wang, Effect of electrocoagulation on MBR under different power supply conditions, Biochem. Eng. J. 152 (2019) 107371.
[27] Y. Yang, S. Qiao, R. Jin, J. Zhou, X. Quan, A novel aerobic electrochemical membrane bioreactor with CNTs hollow fiber membrane by electrochemical oxidation to improve water quality and mitigate membrane fouling, Water Res. 151 (2019) 54–63.
[28] Y. Yang, S. Qiao, R. Jin, J. Zhou, X. Quan, Novel anaerobic electrochemical membrane bioreactor with a CNTs hollow fiber membrane cathode to mitigate membrane fouling and enhance energy recovery, Environ. Sci. Technol. 53 (2019) 1014–1021.
[29] X.-B. Ying, J.-J. Huang, D.-S. Shen, H.-J. Feng, Y.-F. Jia, Q.-Q. Guo, Fouling behaviors are different at various negative potentials in electrochemical anaerobic membrane bioreactors with conductive ceramic membranes, Sci. Total Environ. 761 (2021) 143199.
[30] S.W. Hasan, M. Elektorowicz, J.A. Oleszkiewicz, Start-up period investigation of pilot-scale submerged membrane electro-bioreactor (SMEBR) treating raw municipal wastewater, Chemosphere 97 (2014) 71–77.
[31] D.D. Nguyen, H.H. Ngo, W. Guo, T.T. Nguyen, S.W. Chang, A. Jang, et al., Can electrocoagulation process be an appropriate technology for phosphorus removal from municipal wastewater? Sci. Total Environ. 563–564 (2016) 549–556.
[32] K. Bani-Melhem, E. Smith, Grey water treatment by a continuous process of an electrocoagulation unit and a submerged membrane bioreactor system, Chem. Eng. J. 198–199 (2012) 201–210.
[33] Ş. İrdemez, Y.Ş. Yildiz, V. Tosunoğlu, Optimization of phosphate removal from wastewater by electrocoagulation with aluminum plate electrodes, Sep. Purif. Technol. 52 (2006) 394–401.
[34] C.A. Martínez-Huitle, M. Panizza, Electrochemical oxidation of organic pollutants for wastewater treatment, Curr. Opin. Electrochem. 11 (2018) 62–71.
[35] C. García-Gómez, P. Drogui, B. Seyhi, P. Gortáres-Moroyoqui, G. Buelna, M.I. Estrada-Alvgarado, et al., Combined membrane bioreactor and electrochemical oxidation using Ti/PbO_2 anode for the removal of carbamazepine, J. Taiwan Inst. Chem. Eng. 64 (2016) 211–219.
[36] B. Jiang, Q. Zeng, Y. Hou, H. Li, J. Liu, J. Xu, et al., Impacts of long-term electric field applied on the membrane fouling mitigation and shifts of microbial communities in EMBR for treating phenol wastewater, Sci. Total Environ. 716 (2020) 137139.
[37] Y.-K. Wang, W.-W. Li, G.-P. Sheng, B.-J. Shi, H.-Q. Yu, In-situ utilization of generated electricity in an electrochemical membrane bioreactor to mitigate membrane fouling, Water Res. 47 (2013) 5794–5800.
[38] A. Medel, J. Treviño-Reséndez, E. Brillas, Y. Meas, I. Sirés, Contribution of cathodic hydroxyl radical generation to the enhancement of electro-oxidation process for water decontamination, Electrochim. Acta 331 (2020) 135382.
[39] G. Zhu, Y. Peng, B. Li, J. Guo, Q. Yang, S. Wang, Biological removal of nitrogen from wastewater, in: D.M. Whitacre (Ed.), Reviews of Environmental Contamination and Toxicology, Springer, New York, 2008, pp. 159–195.
[40] P.L. McCarty, What is the best biological process for nitrogen removal: when and why? Environ. Sci. Technol. 52 (2018) 3835–3841.
[41] A. Giwa, S. Daer, I. Ahmed, P.R. Marpu, S.W. Hasan, Experimental investigation and artificial neural networks ANNs modeling of electrically-enhanced membrane bioreactor for wastewater treatment, J. Water Process. Eng. 11 (2016) 88–97.

This book belongs to Badji Mokhtar Annaba University Central Library Copyright Elsevier 2025

[42] L. Li, Y. Dong, G. Qian, X. Hu, L. Ye, Performance and microbial community analysis of bio-electrocoagulation on simultaneous nitrification and denitrification in submerged membrane bioreactor at limited dissolved oxygen, Bioresour. Technol. 258 (2018) 168–176.
[43] J. Lakshmi, G. Sozhan, S. Vasudevan, Recovery of hydrogen and removal of nitrate from water by electrocoagulation process, Environ. Sci. Pollut. Res. 20 (2013) 2184–2192.
[44] V. Wei, M. Elektorowicz, J.A. Oleszkiewicz, Electrically enhanced MBR system for total nutrient removal in remote northern applications, Water Sci. Technol. 65 (2012) 737–742.
[45] R.M. Chaudhry, K.L. Nelson, J.E. Drewes, Mechanisms of pathogenic virus removal in a full-scale membrane bioreactor, Environ. Sci. Technol. 49 (2015) 2815–2822.
[46] M. Chen, Q. Lei, L. Ren, J. Li, X. Li, Z. Wang, Efficacy of electrochemical membrane bioreactor for virus removal from wastewater: performance and mechanisms, Bioresour. Technol. 330 (2021) 124946.
[47] Y. Zhu, R. Chen, Y.-Y. Li, D. Sano, Virus removal by membrane bioreactors: a review of mechanism investigation and modeling efforts, Water Res. 188 (2021) 116522.
[48] W. Lv, X. Zheng, M. Yang, Y. Zhang, Y. Liu, J. Liu, Virus removal performance and mechanism of a submerged membrane bioreactor, Process. Biochem. 41 (2006) 299–304.
[49] A.L. Casabuena, H. Shi, Z. Yin, I. Xagoraraki, V.V. Tarabara, Human adenovirus 40 removal in sidestream membrane bioreactor, J. Environ. Eng. 145 (2019) 06019004.
[50] R. Fox, D. Stuckey, MS-2 and T4 phage removal in an anaerobic membrane bioreactor (AnMBR): effect of gas sparging rate, J. Chem. Technol. Biotechnol. 90 (2015) 384–390.
[51] F. Meng, S.-R. Chae, A. Drews, M. Kraume, H.-S. Shin, F. Yang, Recent advances in membrane bioreactors (MBRs): membrane fouling and membrane material, Water Res. 43 (2009) 1489–1512.
[52] Z. Wang, Z. Wu, S. Tang, Extracellular polymeric substances (EPS) properties and their effects on membrane fouling in a submerged membrane bioreactor, Water Res. 43 (2009) 2504–2512.
[53] H. Lin, M. Zhang, F. Wang, F. Meng, B.-Q. Liao, H. Hong, et al., A critical review of extracellular polymeric substances (EPSs) in membrane bioreactors: characteristics, roles in membrane fouling and control strategies, J. Membr. Sci. 460 (2014) 110–125.
[54] M.B. Asif, T. Maqbool, Z. Zhang, Electrochemical membrane bioreactors: state-of-the-art and future prospects, Sci. Total Environ. 741 (2020) 140233.
[55] Y. Yang, S. Qiao, J. Zhou, X. Quan, Mitigating membrane fouling based on in situ •OH generation in a novel electro-fenton membrane bioreactor, Environ. Sci. Technol. 54 (2020) 7669–7676.
[56] A.M. Almusawy, R.H. Al-Anbari, Q.F. Alsalhy, A.E. Al-Najar, E. Drioli, Novel membrane bioreactor system using combination of an intermittent electric field and moving biomedia for treatment of genuine wastewater, Int. J. Environ. Anal. Chem. (2020) 1–23.
[57] M.Y.A. Mollah, R. Schennach, J.R. Parga, D.L. Cocke, Electrocoagulation (EC)—science and applications, J. Hazard. Mater. 84 (2001) 29–41.
[58] S. Ibeid, M. Elektorowicz, J.A. Oleszkiewicz, Electro-conditioning of activated sludge in a membrane electro-bioreactor for improved dewatering and reduced membrane fouling, J. Membr. Sci. 494 (2015) 136–142.
[59] S. Bayar, A. Karagunduz, B. Keskinler, Influences of electroosmosis and electrophoresis on permeate flux and membrane fouling in submerged membrane bioreactors (SMBRs), Water Sci. Technol. 74 (2016) 766–776.
[60] F. Xu, C. Zhao, C.H. Lee, W. Wang, Q. Xu, Anti-biofouling performance of an immobilized indigenous quorum quenching bacterium *Bacillus cereus* HG10 and its influence on the microbial community in a bioreactor, Int. J. Environ. Res. Public Health 16 (2019) 3777.
[61] T. Ergön-Can, B. Köse-Mutlu, İ. Koyuncu, C.-H. Lee, Biofouling control based on bacterial quorum quenching with a new application: rotary microbial carrier frame, J. Membr. Sci. 525 (2017) 116–124.
[62] H.-S. Oh, C.H. Tan, J.H. Low, M. Rzechowicz, M.F. Siddiqui, H. Winters, et al., Quorum quenching bacteria can be used to inhibit the biofouling of reverse osmosis membranes, Water Res. 112 (2017) 29–37.
[63] J. Lee, Y.-J. Won, D.-C. Choi, S. Lee, P.-K. Park, K.-H. Choo, et al., Micro-patterned membranes with enzymatic quorum quenching activity to control biofouling in an MBR for wastewater treatment, J. Membr. Sci. 592 (2019) 117365.

This book belongs to Badji Mokhtar Annaba University Central Library Copyright Elsevier 2025

[64] M. Khan, S.J. Khan, S.W. Hasan, Quorum sensing control and wastewater treatment in quorum quenching/submerged membrane electro-bioreactor (SMEBR(QQ)) hybrid system, Biomass Bioenergy 128 (2019) 105329.
[65] A. Ding, Q. Fan, R. Cheng, G. Sun, M. Zhang, D. Wu, Impacts of applied voltage on microbial electrolysis cell-anaerobic membrane bioreactor (MEC-AnMBR) and its membrane fouling mitigation mechanism, Chem. Eng. J. 333 (2018) 630–635.
[66] S. Meng, X. Meng, W. Fan, D. Liang, L. Wang, W. Zhang, et al., The role of transparent exopolymer particles (TEP) in membrane fouling: a critical review, Water Res. 181 (2020) 115930.
[67] U. Passow, R.F. Shipe, A. Murray, D.K. Pak, M.A. Brzezinski, A.L. Alldredge, The origin of transparent exopolymer particles (TEP) and their role in the sedimentation of particulate matter, Continental Shelf Res. 21 (2001) 327–346.
[68] L.-C. Hua, C. Huang, Y.-C. Su, T.-N.-P. Nguyen, P.-C. Chen, Effects of electro-coagulation on fouling mitigation and sludge characteristics in a coagulation-assisted membrane bioreactor, J. Membr. Sci. 495 (2015) 29–36.
[69] S.L. Sanin, F.D. Sanin, J.D. Bryers, Effect of starvation on the adhesive properties of xenobiotic degrading bacteria, Process. Biochem. 38 (2003) 909–914.
[70] A.A. Battistelli, R.E. da Costa, L. Dalri-Cecato, T.J. Belli, F.R. Lapolli, Effects of electrochemical processes application on the modification of mixed liquor characteristics of an electro-membrane bioreactor (e-MBR), Water Sci. Technol. 78 (2018) 2364–2373.
[71] G. Mouedhen, M. Feki, M.D.P. Wery, H.F. Ayedi, Behavior of aluminum electrodes in electrocoagulation process, J. Hazard. Mater. 150 (2008) 124–135.
[72] B. Ozbey Unal, N. Dizge, A. Karagunduz, B. Keskinler, Combined electrocoagulation and electro-oxidation process in electro membrane bioreactor to improve membrane filtration effectiveness, Bioresour. Technol. Rep. 7 (2019) 100237.
[73] M. Naveed, L. Herath, P. Moldrup, E. Arthur, M. Nicolaisen, T. Norgaard, et al., Spatial variability of microbial richness and diversity and relationships with soil organic carbon, texture and structure across an agricultural field, Appl. Soil Ecol. 103 (2016) 44–55.
[74] W.Z. Huang, J.C. Zhu, J. Ma, X. Zhang, Z. Wu, Identification of microbial communities in open and closed circuit bioelectrochemical MBRs by high-throughput 454 pyrosequencing, PLoS One 9 (2014).
[75] S.-b. He, G. Xue, B.-z. Wang, Factors affecting simultaneous nitrification and de-nitrification (SND) and its kinetics model in membrane bioreactor, J. Hazard. Mater. 168 (2009) 704–710.
[76] M. Jin, X.-W. Wang, T.-S. Gong, C.-Q. Gu, B. Zhang, Z.-Q. Shen, et al., A novel membrane bioreactor enhanced by effective microorganisms for the treatment of domestic wastewater, Appl. Microbiol. Biotechnol. 69 (2005) 229–235.
[77] M. Zeyoudi, E. Altenaiji, L.Y. Ozer, I. Ahmed, A.F. Yousef, S.W. Hasan, Impact of continuous and intermittent supply of electric field on the function and microbial community of wastewater treatment electro-bioreactors, Electrochim. Acta 181 (2015) 271–279.
[78] J. Zhang, A. Satti, X. Chen, K. Xiao, J. Sun, X. Yan, et al., Low-voltage electric field applied into MBR for fouling suppression: performance and mechanisms, Chem. Eng. J. 273 (2015) 223–230.
[79] Y.-K. Wang, X.-R. Pan, Y.-K. Geng, G.-P. Sheng, Simultaneous effective carbon and nitrogen removals and phosphorus recovery in an intermittently aerated membrane bioreactor integrated system, Sci. Rep. 5 (2015) 16281.

This book belongs to Badji Mokhtar Annaba University Central Library Copyright Elsevier 2025

CHAPTER SEVEN

Electrochemical membrane technology for fouling control

Naresh Mameda[1] and Kwang-Ho Choo[1,2,3]

[1]School of Architectural, Civil, Environmental, and Energy Engineering, Kyungpook National University, Daegu, Republic of Korea
[2]Department of Environmental Engineering, Kyungpook National University, Daegu, Republic of Korea
[3]Advanced Institute of Water Industry, Kyungpook National University, Daegu, Republic of Korea

7.1 Introduction

The increasing water scarcity, because of population growth, global warming, and industrial development, is one of the most significant challenges to sustainable development. Seawater and wastewater are used as alternative water resources to satisfy the increasing water demand in water-scarce areas [1]. Significant efforts have been made to develop and utilize membrane separation processes, which have the merits of high treatment efficiency and easy scalability, and thereby, to produce potable water of high quality from those unconventional water sources [2]. Membranes are physical barriers, allowing selective permeation due to the difference in physical or chemical potential gradients [3]. Various types of membranes have been fabricated for different purposes and can be classified as porous membranes, such as microfiltration (MF) and ultrafiltration (UF), and dense membranes, such as reverse osmosis (RO) and nanofiltration (NF) [4]. MF and UF are primarily employed to separate suspended solids, colloid particles, and macromolecules, whereas NF and RO are mainly applied for the separation of low molecular weight compounds and ions [2].

Although the conventional membranes have high separation performance, they are confronted with some difficulties that limit their widespread use. Firstly, membrane treatment is still relatively expensive than other conventional water and wastewater treatment options (e.g., coagulation, adsorption, and biological treatment) [5]. Secondly, membranes, particularly low-pressure membrane processes (MF and UF), are often ineffective at removing dissolved organic contaminants with low molecular weights, requesting further treatments. On the other hand, high-pressure membrane processes (NF and RO) are energy-intensive, and brine management is a secondary issue, resulting in higher operating costs [6]. Thirdly and last, the most critical issue is membrane fouling, which restricts the reliability and the sustainability of membranes for their long-term use. Membrane fouling normally occurs because solutes or particulates clog membrane pores or accumulate on

Electrochemical Membrane Technology for Water and Wastewater Treatment.
DOI: https://doi.org/10.1016/B978-0-12-824470-8.00007-3
© 2022 Elsevier Inc.
All rights reserved.

This book belongs to Badji Mokhtar Annaba University Central Library
Copyright Elsevier 2025

top of the membrane surface leading to a decrease in membrane permeate flux. It is thus necessary to periodically clean the membrane and, so, maintain the initial membrane permeability. Membrane cleaning is costly and labor-intensive, causing secondary problems such as chemical waste and membrane aging. Developing novel electrochemical membrane techniques, which can mitigate membrane fouling, is thus of great interest to both membrane manufacturers and users.

Therefore this chapter covers the recent advances in electrochemical membrane technology, particularly focusing on membrane fouling control. More specifically, this chapter deals with membrane fouling phenomena and mechanisms, electrochemical membrane materials, electrochemical membrane process designs and configurations, electrochemical reactions, and fouling control methods. Finally, we discuss current technical challenges as well as prospects toward fouling management along with future research needs.

7.2 Understanding membrane fouling

7.2.1 Fouling and antifouling strategies

Fouling is defined as the decline of membrane permeability due to the accumulation of substances (foulants) on the membrane surface or inside the membrane matrix. The International Union for Pure and Applied Chemistry defines membrane fouling as: *Fouling is the process resulting in loss of performance of a membrane due to the deposition of suspended or dissolved substances on its external surfaces, at its pore openings, or within its pores* [7]. Regular cleaning and maintenance measures are implemented to ensure maximum permeate flows while keeping the longest membrane lifetime. Fouling can be divided into two parts based on the reversibility of foulants attached to the membrane: the readily removable fraction of the retained stuff is categorized as the reversible fouling layer, whereas the residual part is called the irreversible fouling layer.

According to the types of fouling substances, the fouling phenomena can be broken down into the following: (1) biofouling caused by microbial growth (biofilm); (2) particulate or colloidal fouling caused by the deposition of solids or colloidal materials; (3) organic fouling caused by the sorption of dissolved organic matter; and (4) inorganic fouling caused by mineral precipitation [8,9]. Each of these is associated with feed characteristics, membrane properties, and membrane operations. Biofouling is caused by the activities of microorganisms (e.g., bacteria and algae) that can bind to the membrane and form a biofilm. Microbial adhesion and subsequent colonization are accompanied by extracellular polymeric substance secretions [10,11]. The percentage of organic macromolecules in biofilms is normally in the range of 50%–80% of the total organic matter, including carbohydrates and proteins. Biofouling is the major

This book belongs to Badji Mokhtar Annaba University Central Library Copyright Elsevier 2025

obstacle in RO plants despite significant pretreatments [12]. Chemical cleaning is thus unavoidable to eliminate biofouling, but that is another challenge because the polyamide RO membrane is highly sensitive to oxidizing agents, particularly to chlorine [13]. Intensive aeration and periodic membrane cleaning (e.g., chemically enhanced backwashing) are two of the most effective methods for mitigating biofouling in membrane bioreactors (MBRs). However, these approaches increase energy consumption, reducing the membrane lifetime and hampering membrane durability.

Colloidal fouling frequently occurs when a membrane is used for the treatment of surface water or secondary effluents. Colloidal materials build up on the membrane surface or clog the membrane pore [14]. Aquatic colloids consist of minerals, colloidal silica, manganese oxides, organic colloids, precipitated crystals, or suspended matter.

Organic fouling stems from the adsorption of dissolved organic matter onto the membrane surfaces or pores [15]. Abundant and persistent in aquatic systems (natural water and wastewater), even though its chemical structures vary according to spatio-temporal situations, dissolved organic matter can be classified into various compounds, such as humic acids, fulvic acids, amino acids, proteins, and polysaccharides, which can be considered significant fouling substances in water treatment membranes [16]. Fouling caused by both colloidal and organic matter is typically controlled by air scouring, backwashing, or chemical cleaning [17]. Air scouring and backwashing are employed to remove the deposited cake/gel layer, whereas chemical cleaning eliminates the organic matter tightly bound to the membrane surface.

On the other hand, the fouling by inorganic crystals, also called mineral scaling, occurs at the membrane due to the hydrolysis and/or precipitation of metal ions during membrane filtration [18]. Calcium salts ($CaCO_3$ and $CaSO_4$) with low solubility values are the most common compounds of scaling. This is a significant issue in the membrane desalination process. Scaling is normally controlled by adding antiscalants (e.g., chelating agents) and/or adjusting the solution's pH level (acidic pH conditions).

7.2.2 Classification of fouling according to the resistance-in-series model

Fouling, which causes the membrane flux decline as described above, can be modeled based on a resistance-in-series concept. The model assumes that the total filtration resistance is the sum of all possible fouling factors, such as adsorption, pore clogging, solids accumulation, and concentration polarization, in addition to the intrinsic membrane resistance (Fig. 7.1).

The intrinsic membrane resistance (R_m) is determined based on the membrane (skin layer) thickness, pore size, porosity, and tortuosity. The build-up of solutes nearby the membrane during permeation is the cause of concentration polarization resistance (R_{cp}). The attachment of solutes or particulate solids on top of the membrane results in gel (R_g) or cake (R_c) layers. The particles, whose size is similar to or smaller than the membrane

This book belongs to Badji Mokhtar Annaba University Central Library Copyright Elsevier 2025

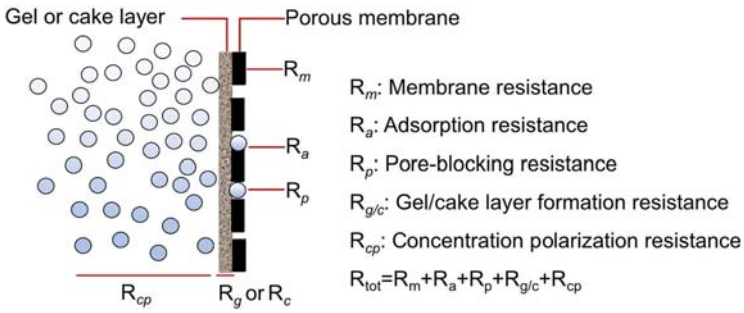

Figure 7.1 Conceptual illustration of the resistance-of-series model for a fouled membrane in a pressure-driven membrane process.

pore size, can either clog the membrane pores (R_p) or sorb on the membrane surface or inside the pores (R_a). With time, the filtration resistance becomes irreversible through the stronger binding of foulants to the membrane surface. Thus minimizing or delaying such transitions reduces irreversible fouling. Electrochemical membrane technology is expected to play a significant role in mitigating both reversible and irreversible fouling behaviors, owing to its electrochemical activities at the membrane surface.

7.2.3 Factors affecting fouling in electrochemical membrane technology

Electrochemical membrane filtration helps mitigate membrane fouling owing to two factors, that is, electric currents (charges) and electrochemical reactions. Electrified membranes have electric charges on their surface, forming an electric double layer [19]. If the electrical double layer thickness is greater than the membrane pore size, the co-ions (i.e., ions with the same charge) cannot penetrate the pores due to electrostatic repulsion (i.e., Donnan exclusion). However, the electrical double layer thickness significantly diminishes in a solution containing ionic substances so that its effect would be minimal in porous membranes. On the other hand, electrochemical reactions take place on the surface of electroconductive membranes, producing reactive species and gases. In aqueous media, reactive chlorine or oxygen species can be produced depending on the applied voltage in addition to hydrogen and oxygen gases. The reactive chemical species can thus degrade organic substances and also clean up the membrane surface.

7.3 Electrochemical membrane materials

Membrane materials play a vital role in developing electrochemical membrane technology because they can influence decontamination and fouling control

This book belongs to Badji Mokhtar Annaba University Central Library Copyright Elsevier 2025

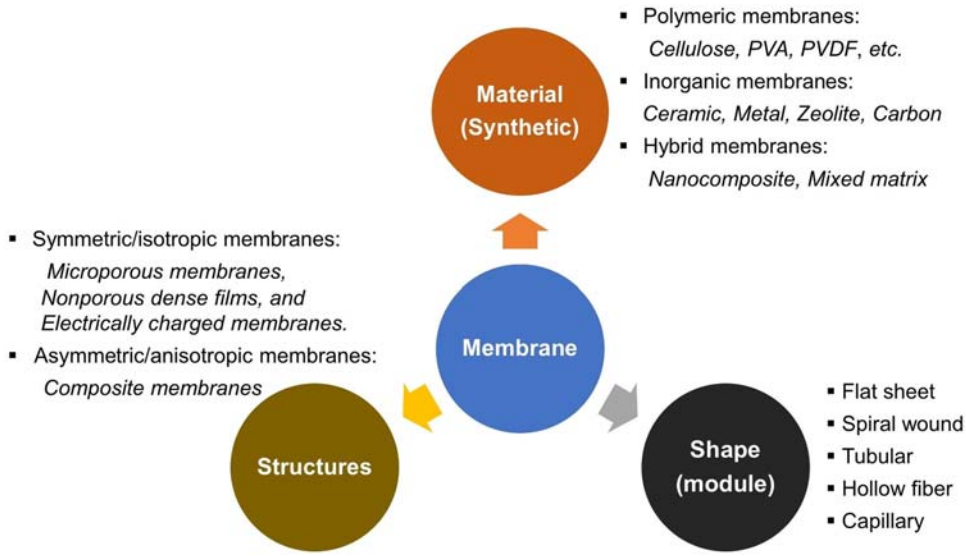

Figure 7.2 Classification of membranes according to their materials, structures, and geometry.

efficiencies. Membrane materials exhibit unique functional properties, morphologies, and transport characteristics as categorized and illustrated in Fig. 7.2. According to membrane material composition, the membrane can be first classified into the following: organic (polymeric) membrane, inorganic membrane, and inorganic-organic hybrid membrane [20]. According to morphological/structural characteristics, the membrane can be classified as symmetric (or isotropic) and asymmetric (anisotropic) ones [21]. The symmetric membrane has a relatively uniform pore size or structural morphology along the membrane's cross-section, whereas the asymmetric membrane has anisotropic structures made from single materials or composites. The membrane geometry is another guideline to classify the membranes into flat sheet, tubular, capillary, and hollow fiber membranes.

The structure and design of electrochemical membranes are greatly influenced by the electrical conductivity of membrane materials, which is also crucial for their treatment and energy efficiency. The characteristics of membranes utilized for electrochemical processes are further described in the following sections.

7.3.1 Nonelectroconductive membranes

Nonconductive regular membranes are employed for electrochemical membrane technology, which combines the membrane and the electrodes. For instance, a two-stage process with an electrochemical unit followed by a membrane unit as a separation medium can be designed. Ceramic [22] and polymeric [23–26] membranes have been used in the combined process for water and wastewater treatments. On the contrary,

This book belongs to Badji Mokhtar Annaba University Central Library Copyright Elsevier 2025

membrane separation and the electrochemical process can be integrated into a single reactor. Both polymeric [27,28] and ceramic [29,30] membranes are also used as separation media in the system, where the electrodes (anode and cathode) are installed beside or above the membranes. The shape and position of electrodes are crucial for their synergistic interactions with the membrane to minimize fouling and energy consumption during membrane filtration [31]. Additionally, nonelectroconductive membranes can be used as substrates to produce hybrid membranes, which serve as both an electrode and a separation medium [32–34]. A porous (mesh) electrode and a membrane are tightly bound together or combined with a certain gap between them ultimately forming a membrane module.

7.3.2 Electroconductive membranes

Electrically conductive membranes, which have the electrical potential or current on the membrane surface, can have more interactions with organic/inorganic substances and microorganisms present in the membrane system [35]. Several types of materials, such as conductive polymers, metal/metal oxides, and carbonaceous structures, are available and used to fabricate electrochemical membranes.

7.3.2.1 Electroconductive polymeric membranes

Over the years, researchers have been investigating various conductive polymers for fouling mitigation in water treatment and desalination [35]. Conductive polymers normally have a conjugated backbone composed of alternating single and double carbon bonds, which allow the electrons to freely move from one atom to another, exhibiting good electrical conductivity [36]. Several conductive polymeric materials, such as polypyrrole, polyaniline, polythiophene, and polyacetylene, have been studied for their unique properties [35,37]. Polypyrrole is one of the most popular conductive polymers due to its high conductivity, stability, and facile synthesis [38]. However, conductive polymers are sparingly soluble in normal solvents, so that membrane fabrication is quite challenging. Conductive polymeric membranes are thus prepared as composites by depositing carbonaceous nanomaterials (e.g., carbon nanotubes and graphene nanoparticles) on a porous support [35,39]. These membranes have relatively low conductivity and electrochemical activity being susceptible to electrochemical oxidation.

7.3.2.2 Electroconductive carbon membranes

Carbonaceous materials (graphene, graphene oxide, and carbon nanotubes) exhibit great potential for the fabrication of conductive membranes in various environmental applications, such as gas separation [40], fuel cells [41], and water treatment [39], because of their high surface areas and electrical conductivity. Carbon-based membranes have merits over other conductive membranes in electrochemical membrane processes, such as larger surface area, high electrical conductivity, inertness, adaptability

This book belongs to Badji Mokhtar Annaba University Central Library Copyright Elsevier 2025

(tunability), and chemical stability [37,39,42]. Carbon-based membranes are also prepared with polymeric binders (e.g., polyvinyl alcohol, polyvinylidene difluoride, and polyvinyl butyral) by phase inversion methods [43,44]. Composite conductive membranes are fabricated either by surface coating or by direct incorporation of a conductive carbon layer into organic and inorganic membranes [39]. Alumina has been employed as a support because of its chemical and thermal stability. The conductive composite membrane with alumina support would be durable for long-term use [45,46]. However, when utilized as an anode, the carbonaceous materials are electrochemically unstable because they are likely to be oxidized.

7.3.2.3 Electroconductive inorganic membranes

Inorganic membranes (metal and metal oxides) appear to be more promising for long-term use because of their excellent chemical, thermal, and mechanical stability. Used in chemical, nuclear, and semiconductor industries for catalyst separation, waste treatment, and gas purification, respectively [47], the porous metal membranes are prepared by compressing metal powders followed by sintering them at high temperatures (at least half their melting point) [48]. A wide range of materials, such as Ni, Pd, Ag, Ti, and their (metal) alloys, bronze, and stainless steel, are used to create the membranes, but stainless steel and porous titanium substrates are the most common to be used. Stainless steel is often used as a support to prepare composite membranes because it has unique advantages, such as high mechanical strength, chemical stability, and electroconductivity [37,49]. Electrofiltration using stainless steel-based membranes is able to control membrane fouling by electrical repulsion; however, they are prone to electrochemical corrosion when a positive potential is applied [50]. In contrast, porous Ti membranes with electrocatalysts are highly attractive for electrocatalytic filtration processes because they are corrosion-resistant [51,52]. Ti mesh is also one of the most successful metal substrates for functionalization using electrocatalysts such as RuO_2, TiO_2-RuO_2, and Sb doped SnO_2 [53–55].

Porous metal oxides (e.g., Al_2O_3, SiO_2, TiO_2, and ZrO_2) have excellent thermal and chemical stability but no electrical conductivity, which is inappropriate as electrode materials. The alteration of titanium oxide (TiO_2) to substoichiometric titanium oxides (Magneli phases; Ti_nO_{2n-1}, $n = 4–10$) by reduction at a high temperature in a hydrogen atmosphere has been applied to create electrically conductive electrodes [56]. Among several titanium oxides ($n = 4$ to 10), the ideal Magneli phase is Ti_4O_7 that has the highest electrical conductivity (1000 S/cm), similar to graphite (727 S/cm). Ti_4O_7-based electrodes are effective for electrochemical reactions because they can serve as both active (i.e., direct electron transfer reactions) and inactive (i.e., producing hydroxy radicals) electrodes [57,58]. Ti_4O_7-based porous membranes have been tested for electrocatalytic membrane reactor treatment of wastewater containing organics (phenols, oil, humic acid) by means of electrochemical oxidation [59–62].

This book belongs to Badji Mokhtar Annaba University Central Library Copyright Elsevier 2025

7.4 Electrochemical membrane process configurations

The combined process of a membrane and an electrode (i.e., electrochemically enhanced membrane filtration) is an emerging technology to control membrane fouling through electrical or electrochemical reactions. The proper designs of process configurations are essential for maximal performance and economic feasibility. Two typical hybrid designs have been introduced: one is a two-stage process and the other is a single-stage all-in-one process (Fig. 7.3). In the two-stage process, the electrochemical process serves as a pretreatment step before membrane separation (Fig. 7.3A). The electrochemical pretreatment, which achieves partial or complete oxidation of organic matter in the feed stream, plays a vital part in controlling membrane fouling [63,64]. For instance, an electrochemical cell using circular boron-doped diamond electrodes was placed before a hollow fiber UF process in two-stage configuration of a membrane filtration design in a wastewater treatment plant [65].

In the single-stage process, membrane separation co-occurs with an electrochemical treatment in a single reactor, yielding a compact design (Fig. 7.3B). The electrical (electrophoretic and electroosmotic forces) and electrochemical reactions are effectively utilized for membrane antifouling. Of the many studies devoted to the single-stage process, one study followed up on applying an electric field to membrane filtration processes, which has been practiced for a long time [66]. Again, an electric field is applied to the membrane with an electrode [67–69]. This arrangement is mainly made for crossflow systems to enhance filtration performance. The enhanced filtration performance apart, electrodes are installed at either side of the nonconductive membranes with a shape of flat sheet, tube,

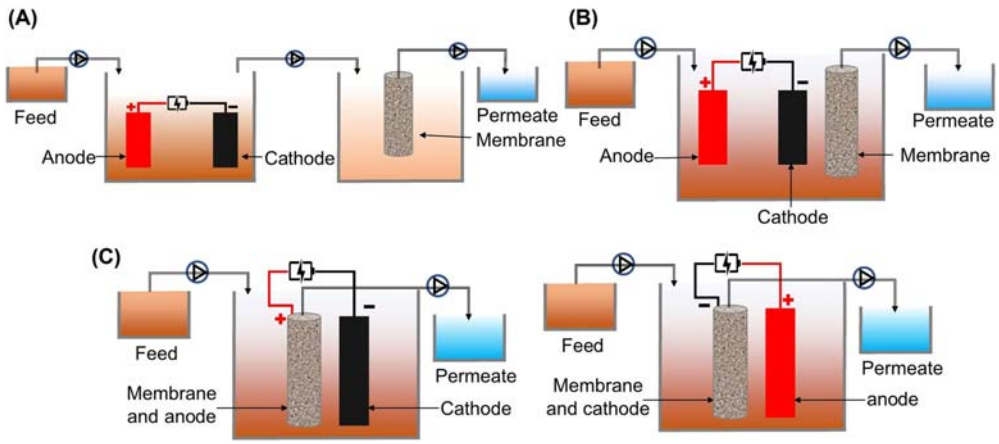

Figure 7.3 Electrochemical membrane process configurations. (A) Two-stage process. (B) Single-stage hybrid process. (C) Bifunctional electroconductive membrane process.

This book belongs to Badji Mokhtar Annaba University Central Library Copyright Elsevier 2025

or spiral in electrofiltration systems [35,70,71], where the design (planar or tubular types) and location of electrodes are essential for the uniform distribution of electric field strengths across the membrane, maximizing the energy efficiency during membrane filtration. On the other hand, tubular electrodes are most effective in electric power usage while preventing membrane fouling [66]. A properly aligned electric field leads to the migration of charged solutes away from the membrane, thus reducing the concentration polarization and increasing the permeate flux. To enhance the energy efficiency, a pulsed electric field is applied instead of a constant electric field [72].

Recently, much attention has been paid to combining electrochemical reactions with membrane filtration process. The hybrid process mitigates membrane fouling by removing organic foulants via electrooxidation or coagulation with electrochemically released metal ions from sacrificing electrodes [27,28,30,73–75]. For instance, an integrated submerged membrane reactor with electrochemical cells was devised to alleviate membrane fouling in which a hollow fiber membrane module was installed between the perforated Ti/IrO_2 anode and Ti/Pt cathode [73]. Another study employed a novel approach by combining a submerged ceramic membrane with stable oxidizing anodes in a single reactor [30]. The electrochemical cell (two IrO_2/Ti anodes and three stainless steel cathodes) was placed beneath the membrane module (flat sheet membranes made of alumina) because the oxidants/gases produced by the electrode could help degrade and/or dislodge the foulants that would otherwise foul the membrane. Another study also reported that a submerged electrobioreactor was able to reduce membrane fouling through a combination of various electrokinetic processes [74]. In this study, a hollow fiber membrane module was placed vertically in the center of the reactor while a cylindrical perforated aluminum anode and a stainless steel cathode encircled the membrane. A new electrocoagulation membrane reactor, which has a UF membrane module between electrodes, was introduced to improve the effluent water quality and also to alleviate membrane fouling [75]. An electrochemical ceramic MBR was employed in another investigation to eliminate pharmaceutical and personal care products from wastewater [34]. In this study, a titanium mesh was mounted vertically in the center of the polyvinyl chloride frame as the cathode, while two Ti/SnO_2-Sb-La anodes were fixed on both sides of the polyvinyl chloride frame. An electrochemical ceramic membrane module was constructed by attaching two pieces of the ceramic membrane to the polyvinyl chloride frame containing the electrodes inside. In another study, another electrochemical ceramic membrane reactor was also developed to alleviate membrane fouling during wastewater treatment [33]. In this study, a titanium mesh was placed into the ceramic membrane's channel to create an electrochemical ceramic membrane. The ceramic membrane with built-in Ti mesh was utilized as the cathode and filter, whereas Ti/SnO_2-Sb-Ce electrodes were employed as the anode being placed adjacent to the ceramic membrane in the reactor. Another study fabricated an electrically conductive feed spacer for a polyvinylidene

This book belongs to Badji Mokhtar Annaba University Central Library Copyright Elsevier 2025

difluoride MF membrane to increase water flux during humic acid solution filtration [32]. In this study, carbon-based ink constituted of graphene nanoplates was coated on the feed spacer, which was placed on top of the MF membrane used as a cathode, and a graphite electrode was employed as an anode in a crossflow cell.

For more compact designs and energy-efficient operations, the synthesis of a membrane, which itself is electroconductive, looks more attractive because it serves as both a membrane and an electrode (Fig. 7.3C). Electric fields are imposed on the membrane surface, resulting in electrochemical reactions [39]. The preparation methods include that of the formation of a membrane using conductive materials (carbon and titanium) or that of the addition of a conductive layer to nonconductive membrane matrices. For example, electroconductive carbon nanotube hollow fiber membranes were tested for filtration of natural organic materials in terms of antifouling and separation performances [43]. In the report, the anode consisted of a cylindrical titanium mesh positioned vertically on the bottom of the reactor, while the cathode consisted of a hollow fiber module with spacing of 2 cm apart from the anode mesh. The reactor was operated in an upflow mode during dead-end filtration applying electric voltages to the membrane. The electric field contributed to a reduction in membrane fouling. In another study, a reactive electrochemical membrane system composed of two Ti_4O_7 ceramic membranes was developed and tested to inactivate bacteria (e.g., *Escherichia coli*) and viruses (e.g., bacteriophage MS2) in a 0.05 M Na_2SO_4 solution [76]. The two Ti_4O_7 ceramic membrane disks served as the anode and the cathode being divided by a rubber ring to create a 5-mm gap between them. Substantive bacterial and virial inactivations (>6 log removals) were achieved with this electrochemical membrane system at a current density of 10 mA/cm^2. In a further study, an electrochemically reactive ceramic membrane made of a suboxide of TiO_2 was evaluated in terms of its filtration and antifouling capabilities during crossflow filtration of algal suspensions under anodic or cathodic polarization [77]. The membrane module consisted of a suboxide of TiO_2 tubular ceramic membrane anode and a stainless steel rod cathode. The cathode was placed through the tubular anode's center, leaving a gap of approximately 4 mm between the cathode and the membrane anode's inner surface. With direct currents (1.25–2.5 mA/cm^2) applied to the membrane module, an isopotential membrane surface was created. The induced electric potential mitigated membrane fouling, resulting in higher critical fluxes up to 526 L/m^2-h. Another study investigated a crossflow carbon composite membrane that was prepared and utilized to examine the effects of an electric field on the filtration flux during oily wastewater treatment [31], in which a composite tubular membrane was used as the cathode, whereas stainless steel was used as the anode. However, there are two critical limitations in electroconductive membranes: electrode corrosion and material costs [78]. Several composite materials have been introduced as they are considered to be more stable. An electroconductive carbon nanotube/Al_2O_3 membrane was fabricated

This book belongs to Badji Mokhtar Annaba University Central Library Copyright Elsevier 2025

through the coating of carbon nanotubes onto a porous Al_2O_3 substrate for the filtration of silica spheres. The carbon nanotube/Al_2O_3 membrane, Ti mesh, and Ag/AgCl were used as the anode, cathode, and reference electrode (positioned inside the membrane module), respectively [45]. In other studies, a TiO_2/carbon membrane anode was used to enhance the flux and permeate quality, whereas a perforated stainless steel tube served as the cathode encircling the tubular membrane anode [79,80].

7.5 Electrochemical reactions

Electric fields or electrochemical reactions combined with membrane filtration can degrade, deactivate, or destabilize dissolved and/or particulate matter in feed streams. The membrane is used with conventional electrodes, or the membrane itself acts as an electrode as described above. In any case, electrochemical reactions take place while controlling membrane fouling with simultaneous degradation of contaminants. Electrochemical reactions include the following: electrophoresis, electrocoagulation, electroflotation, and electrooxidation. Details on the electrochemical reactions are discussed in the following sections.

7.5.1 Electrophoresis

Particles in polar (e.g., aqueous) environments acquire a surface charge owing to dissociation and adsorption reactions at the surface. The surface charge affects the distribution of co- or counter ions nearby in the medium and creates an electrical double layer at the interface. Electrophoresis allows the charged particles to move by the applied voltage, whereas counter ions in the medium migrate to the opposite direction, moving the solvent with them. The motion of charged particles relies on the zeta potential and electric field's strength [81]. The electrophoretic mobility (u_p) has a positive relationship with the zeta potential according to the Helmholz-Smoluchowski equation [Eq. (7.1)], which applies to particles or colloids in aqueous media [82].

$$u_p = \frac{\varepsilon_r \varepsilon_0 \zeta}{\mu} \tag{7.1}$$

where ε_r is the dielectric constant, ε_0 vacuum permittivity (8,854 $\times$ 10^{-12}/CV/m), ζ the zeta potential of particles (V), and μ the dynamic viscosity (Pa-s). The external direct current electric field applied across the membrane has an electrophoresis effect. Electrofiltration (known as forced flow electrophoresis) affects the movement of charged particles, being drawn away from the membrane surface. Thus the permeation flux increases due to the reduced concentration polarization and particle accumulation.

This book belongs to Badji Mokhtar Annaba University Central Library Copyright Elsevier 2025

7.5.2 Electrocoagulation/electroflotation

Electrocoagulation is effective at removing contaminants (e.g., oil, refractory organics, suspended solids, and heavy metals) from water [83]. It has several advantages over the conventional coagulation process, such as process flexibility, reduced sludge production, and relatively low maintenance costs. The electrocoagulation process continuously generates metallic ions (i.e., active coagulants) in aqueous solutions through the electrochemical dissolution of sacrificial anodes. The metallic ions undergo hydrolysis to form polymeric (metallic hydroxides) species at the anode, destabilizing and adsorbing dissolved contaminants [83,84]. Aluminum and iron are commonly utilized for electrocoagulation due to their merits, such as abundance, nontoxicity, and affordability. The electrode has several geometries, such as plate, ball, wire, mesh, rod, and tube.

Electroflotation is a process that makes pollutants float on the water surface via electrochemically formed gas bubbles (molecular hydrogen and oxygen). The reductive production of hydrogen gas at the cathode affects the solution pH. The size of electrochemically generated bubbles is smaller than that of the bubbles produced by gas injection, making electroflotation more effective. The production of gas bubbles proceeds in three steps: nucleation, growth, and separation from the electrode surface. Electroflocculation can be used independently, but it is often combined with electrocoagulation because the integrated system can enhance the separation of fine particles that otherwise neither settle nor float. Electrocoagulation/electroflotation helps mitigate membrane clogging caused by fine particles and organic matter.

7.5.3 Electrochemical oxidation

Electrochemical oxidation can degrade organic compounds present in feed streams (e.g., wastewater). Anodic oxidation plays a major role in electrochemical degradation and can be further divided into two types of reactions: direct oxidation at the anode and indirect oxidation mediated by electrochemically generated oxidants. Direct oxidation means the electron transfer from the substance attached to the anode. Indirect oxidation takes place at either the anode or the cathode. Anodic reactions create physically adsorbed "active oxygen" (adsorbed hydroxyl radicals, $^{\cdot}OH$) or chemisorbed "active oxygen" (oxygen in the lattice of a metal oxide anode, MO_{x+1}) [85]. The physisorbed $^{\cdot}OH$ is one of the most potent oxidants identified after fluorine so that it may guarantee complete oxidation of organics, whereas the chemisorbed "active oxygen" contributes to the formation of selective oxidation products (partial oxidation). The nature of anodic materials impacts the electrochemical oxidation characteristics. For instance, active anodes with low oxygen evolution overpotentials (IrO_2, RuO_2, and Pt) often cause incomplete oxidation of organic contaminants, whereas nonactive anodes with high oxygen evolution overpotentials (SnO_2, PbO_2, and boron-doped diamond) can achieve complete oxidation (i.e., mineralization) [86–88]. Electrolytes

This book belongs to Badji Mokhtar Annaba University Central Library Copyright Elsevier 2025

or anions, which contribute to the generating of oxidants in indirect oxidation, include chloride, sulfate, phosphate, and carbonate.

7.6 Electrical and electrochemical fouling control

Irreversible fouling induced by dissolved organic substances and microbes is the major challenge encountered in the membrane-based treatment system, reducing membrane productivity and increasing the cleaning frequency and membrane replacement costs. The dissolved organic foulants include macromolecular and colloidal organic substances, such as humic acids, fulvic acids, and soluble microbial products. The pretreatment of feed streams is believed to be an appropriate method for removing those foulants, decreasing the membrane cleaning frequency, and enhancing the membrane's lifespan. Pretreatments (e.g., coagulation, adsorption, and oxidation) can modify the physical, chemical, and biological characteristics of feed streams, resulting in improved membrane performance [64,89,90]. Electrochemical techniques have merits over other methods, such as easy instrumentation, versatility, no chemical requirement, compatibility, and operational flexibility [65].

7.6.1 Two-stage serial processes

Serial electrochemical membrane filtration consists of the two-stage unit processes of electrochemical treatment followed by membrane separation (Fig. 7.4). The first-stage electrochemical treatment unit contributes to modifying organic foulants in feed streams, thereby enhancing the membrane flux. Electrooxidation using BiO_x-TiO_2/Ti and boron-doped diamond electrodes was applied for wastewater effluent treatment to mitigate the fouling of MF membranes [65,91]. Significant reductions (36%–67%) in transmembrane pressure occurred when the feed was electrochemically oxidized before membrane filtration, and the degree of reduction increased with an increase in applied current densities [65]. In another study, simulated seawater (which was spiked with 10 mg/L humic acids) was pretreated by electrochemical oxidation using boron-doped diamonds before UF [26]. Electrochemical oxidation should reduce the organic loading to the membrane and increase the repulsion between the membrane surface and organic substances, thereby reducing membrane fouling. Extended electrochemical treatment can further modify the characteristics of foulants so that membrane fouling should be influenced. This study found that long electrochemical treatments switched the fouling mechanism from cake formation to pore blocking. Optimizing electrochemical treatment is needed to minimize membrane fouling along with greater energy efficiency.

This book belongs to Badji Mokhtar Annaba University Central Library Copyright Elsevier 2025

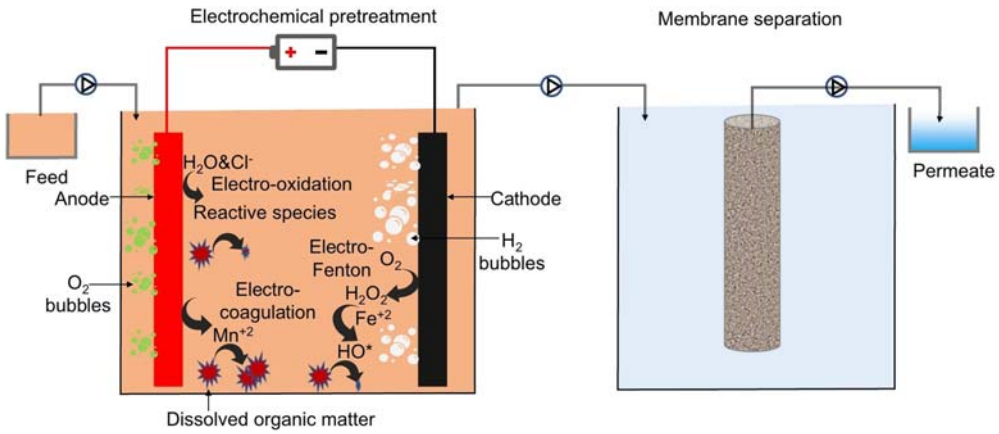

Figure 7.4 Schematic diagram of fouling mitigation by the serial processes comprising electrodes and membranes. Electrochemical treatment precedes membrane separation.

Electrocoagulation creates large flocs and forms loose cake structures while reducing the fouling caused by pore blocking [63,92]. Electrocoagulation using iron controls the fouling of a UF membrane in seawater treatment [93], but not the fouling of an MF membrane during surface water treatment [94]. The characteristics (e.g., floc size) of electrochemically generated flocs and the organic content in the feed may cause the discrepancy because the carbon content in the seawater was smaller than that of surface water. On the other hand, the internal pore blocking and external cake formation were reduced when the anode material was switched from iron to aluminum in the sequential process of electrocoagulation and MF [95]. The aluminum anode removed organics in surface water more substantially than did the iron anode.

Electrochemical oxidation of sacrificial anode (Al/Fe) produces in situ coagulants to form flocs with contaminants (i.e., electrocoagulation), whereas cathodic reduction of water molecules creates hydrogen gas bubbles, promoting the flotation of the flocs (i.e., electroflotation). When the combined process of an electrocoagulation unit and a submerged MBR was applied to treat greywater, membrane fouling was reduced by 13% compared to that of the MBR process alone because of the formation of large flocs [96]. Electroflotation also lowers the degree of pore blocking by forming large aggregates and eliminating the fines from the aqueous phase [97] thereby reducing membrane fouling too.

7.6.2 Single-stage hybrid process

In a single-stage hybrid process, electrochemical reactions and membrane separation occur simultaneously in one reactor, yielding a compact design (Fig. 7.5) [98]. Electrofiltration, which induces an electric field across the membrane and so renders

This book belongs to Badji Mokhtar Annaba University Central Library Copyright Elsevier 2025

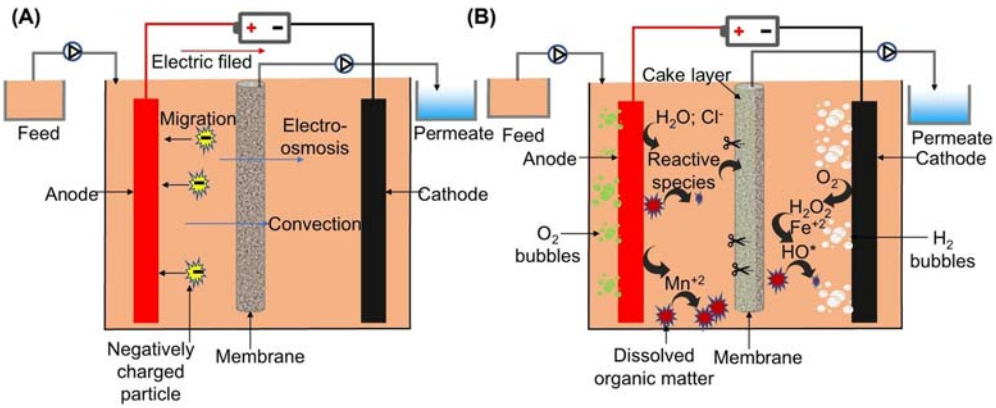

Figure 7.5 Schematic diagram of fouling mitigation by the hybrid process that combines membrane filtration with electrochemical treatment in a single reactor. (A) Electric fields across the membrane create electrophoresis and electroosmosis effects. (B) Electrochemical reactions on the catalytic electrodes decompose dissolved organic matter.

charges on the membrane, has been studied in wastewater treatment (Fig. 7.5A) [78,98,99]. The electrokinetic phenomena, such as electrophoresis and electroosmosis, are the key factors affecting electromicrofiltration with respect to fouling control. Since the membrane surface is nonconductive, electrophoresis governs the migration of charged particles. When direct current electricity was applied either continuously or intermittently to the electrofiltration process for the separation of humic substances, the flux decline was mitigated, increasing the organic rejection [69,100]. This is possible because the electric field induced across the membrane causes electrophoresis, inhibiting the foulants from accumulating at the membrane and eventually enhancing the membrane permeability. An electrically enhanced crossflow MF system was applied to treat oxide-chemical mechanical polishing wastewater, which improved the filtration rate by sixfold compared to the system without the electric field [101]. Applying an electric field coupled with coagulation formed a porous and hydrophilic cake layer, so that membrane fouling was mitigated during the UF of synthetic water containing humic acid [75,102]. The rapid creation of large flocs at high current densities effectively reduced membrane pore blocking. Moreover, the cake layer formed under a strong electric potential is composed of charged particles so that its structure is relatively loose, less influencing the permeability decline.

Electrocatalytic electrodes (anodes) can be mounted on the membrane surface to induce electrophoresis, gas bubble generation, and electrochemical reactions (oxidation and coagulation) simultaneously in a reactor (Fig. 7.5B). Electrophoresis and electrochemical oxidation minimize the concentration polarization and gel layer formation. On the other hand, electroosmosis enhances the permeate flow. Moreover, the electrogenerated gas bubbles (O_2 and H_2) improve the fluid motion at the membrane

This book belongs to Badji Mokhtar Annaba University Central Library Copyright Elsevier 2025

surface. These effects help decrease membrane fouling, improving the membrane flux and lifetime [28,103].

Electrocoagulation and/or electrooxidation can be integrated into membrane filtration in a single reactor as well [30,75,102,104–106]. The electrochemical oxidation process degrades organic molecules, whereas electrocoagulation helps form large and loose flocs. These methods loosen the binding of foulants to the membrane and thereby improve the permeability of cake or gel layers on the membrane. The electrochemical reactions increase the hydrophilicity of foulants through the modification of their surfaces, mitigating membrane fouling. Thus the fouling layers can be readily washed away due to their weaker affinity to the membrane surface.

7.6.3 Electrochemical MBR

An attempt to apply an electric field to an MBR was made to slow down the rate of membrane fouling [107]. An MBR, which has an assembly of the membranes and electrode plates connected inside a bioreactor, was investigated to explore the impact of applied electric fields on the membrane flux of sewage [108]. As the electric field increased, the filtrate flux recovery was improved due to the electrophoretic movement of particulate matter in the sewage. The majority of foulants in water and wastewater streams tend to have negatively charged surfaces so that direct current-mediated electrophoresis can move the foulants away from the membrane surface, which is closer to the cathode [109]. Conversely, the bulk liquid is made to drift to the cathode (known as electroosmosis). Thus the electroosmosis increases the sludge dewaterability on the anode and reduces the hydraulic filtration resistance on the cathode [74].

The applied electric field to an MBR also changes the physical, chemical, and biological properties of biosolids (i.e., their morphology, structure, and composition) via the electrocoagulation process, which may have a positive effect on fouling mitigation in electrochemical MBRs [110–112]. For instance, the neutralization of charged surfaces and the removal of bound water from flocs with electrocoagulation can create larger and more rigid flocs, possibly providing a reduced fouling tendency. A relatively low sludge volume index in the electrochemical MBR, compared to that of the conventional MBR, demonstrates that electrokinetic phenomena enhance the sludge settleability by forming denser flocs. Sacrificial anodes yield metal ions that can coagulate extracellular polymeric substances and soluble microbial products. Coagulated particles form looser fouling layers on the membrane [74,113]. Reactive chlorine species are generated by in situ electrochemical oxidation, which may help mitigate membrane fouling in MBRs [40]. When an electrochemical oxidation system having perforated Ti/IrO_2 anodes and Ti/Pt cathodes was combined with a conventional MBR equipped with an MF module, the electrochemically generated chlorine species

This book belongs to Badji Mokhtar Annaba University Central Library Copyright Elsevier 2025

alleviated the problem of physically irremovable fouling layers by destructing biopolymers, such as proteins and fluorophores [73], thereby mitigating fouling rates.

7.6.4 Bifunctional membrane process

Electroconductive membranes, which can serve as both a membrane and an electrode, are of great interest for fouling control and contaminant decomposition given the bifunctional membranes may exhibit substantial antifouling capability by degrading organic foulants, inactivating microorganisms, and accomplishing membrane self-cleaning. The fouling of an electroconductive membrane can be mitigated by several factors, such as electrostatic repulsion, electrophoretic/electroosmotic forces, electrical inactivation, bubble formation, and electrochemical cleaning that are indicative of bifunctional membranes at work in mitigating fouling rates. The subsequent sections discuss the characteristics of electroconductive membranes.

7.6.4.1 Electrostatic repulsion and electrophoretic effects

The migration of a charged particle relies on electrophoresis so that electric fields can keep foulants away from the membrane if it has the same charge. Electrostatic repulsion exists between a charged particle and the membrane with the same charge (Fig. 7.6). If a direct current electric charge is introduced to an electroconductive membrane, electrostatic repulsion prevents the deposition of particles with the same charge onto the membrane [49,114,115]. The majority of foulants have negative charges and thus the negatively charged membrane (cathode) may repel the foulants well [16]. Pressure-driven membranes are created by using electrically conducting thin films made of cross-linked polyvinyl alcohol and carbon nanotubes on polysulfone support [116]. The effects of applied potentials on the fouling of the composite membrane

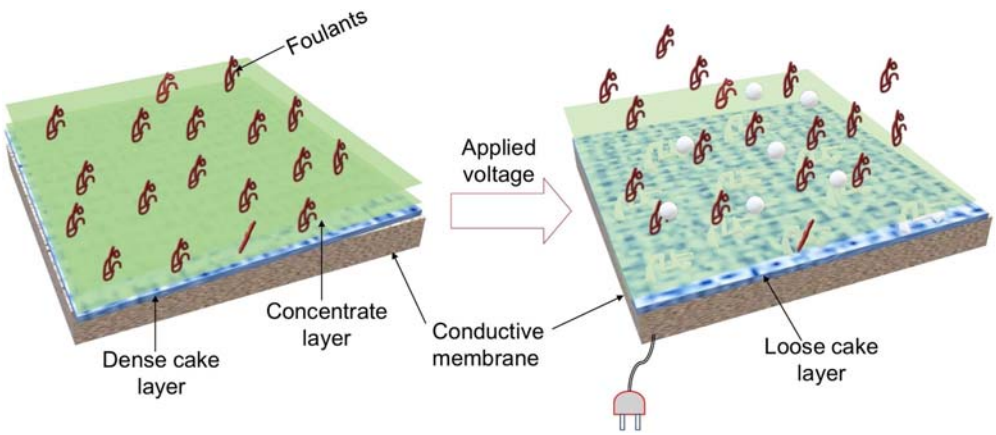

Figure 7.6 Schematic diagram of the electric field applied to a conductive cathodic membrane surface for fouling mitigation.

This book belongs to Badji Mokhtar Annaba University Central Library Copyright Elsevier 2025

were examined by using a solution containing a high concentration (3–5 g/L) of alginic acid in a crossflow filtration cell. The applied electric charge (-3.4 V vs Ag/AgCl) to the composite cathode membrane reduced the operating pressure by 51% compared to the control. The electrostatic repulsive force played a role in minimizing alginate fouling and lowering the transmembrane pressure. In a study, bovine serum albumin was found to fully cover a thin-film composite polyethersulfone membrane when no electric voltage was applied [117]. However, the deposition of bovine serum albumin onto the membrane was substantially suppressed with the presence of a negative electric voltage.

Another electroconductive membrane made from a mixture of carbon nanotubes and polyvinylidene difluoride was able to reduce membrane fouling occurring by natural organic matter, bacteria, humic acids, alginate, and inorganic compounds [44,118,119]. Also, bacterial adhesion to the membrane could be mitigated by electrostatic repulsion as bacterial cell walls are negatively charged. An electroconductive polypyrrole coated filter cloth employed as the cathode also reduced fouling while improving the effluent quality in an MBR [120]. The electrical field (0.2 V/cm) for the polypyrrole modified membrane was effective in fouling control.

7.6.4.2 Electrical/electrochemical inactivation of microorganisms

Membrane biofouling is caused by the growth of bacterial communities on the membrane surface (known as biofilm formation). It is mostly related to bacteria and also caused by yeast and marine organisms in seawater membrane treatment [121,122]. Biofouling control by electrical and electrochemical approaches can be explained in two aspects (Fig. 7.7). One is to inhibit microbial attachment by electrophoresis/electrostatic repulsion. The other is to inactivate microorganisms by electrochemical reactions (i.e., direct oxidation and indirect oxidation).

A polyamide-carbon nanotube composite membrane showed antibiofouling abilities when an alternating electrical potential (1.5 V) was supplied [123]. The membrane flux was fully restored by a quick wash with the feed solution (108 colony-forming units of *Pseudomonas aeruginosa* in 10% Luria-Bertani media) when the electricity was applied to the membrane surface.

An electroconductive composite membrane was fabricated through the deposition of carbon nanotubes on a polyvinylidene difluoride membrane via vacuum filtration and then heat treatment was given for binding [124]. In a dead-end filtration test using a yeast suspension, biofouling prevention was demonstrated. In the study, the membrane was used as the cathode, while a stainless steel plate was used as the anode. The electrogenerated microbubbles (O_2 and H_2) on the membrane surface via water electrolysis contributed to removing particulates from the membrane filter.

The impact of low potentials on bacterial dispersion from electrically conducting carbon nanotube-polyvinyl alcohol cross-linked UF membranes was studied [125]. A

This book belongs to Badji Mokhtar Annaba University Central Library Copyright Elsevier 2025

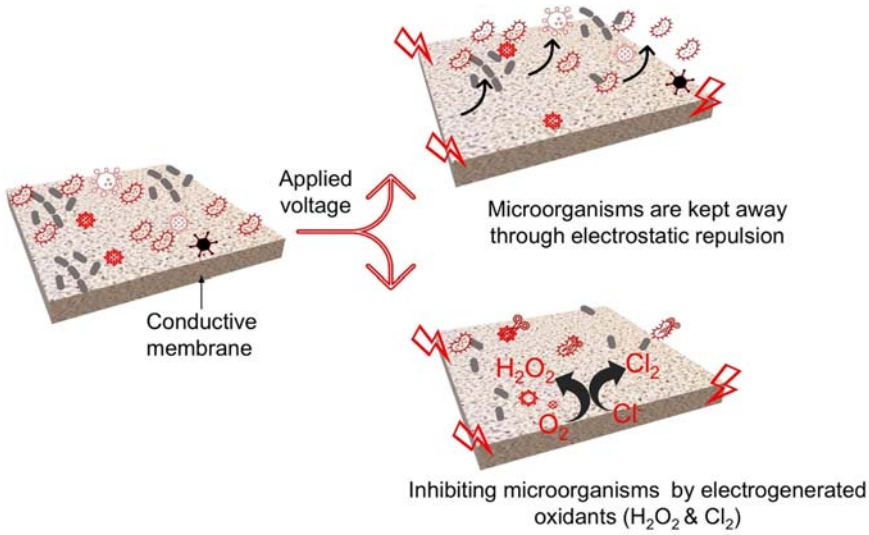

Figure 7.7 Schematic diagram of electrical and electrochemical effects on the inactivation and dispersion of microorganisms during electrofiltration.

direct imaging method connected to a fluorescent microscope was utilized to quantify the deposition and detachment of *E. coli* and microparticle. When an electric potential (1.5 V) was applied to the membrane surface, H_2O_2 was electrochemically generated, resulting in 90% bacterial detachment. The membrane surface was almost biofilm-free during membrane filtration.

The electrochemical reactions, particularly electrooxidation, have been proven to be efficient for the inactivation of microorganisms (virus, bacteria, and fungus) [104,126]. Using electroconductive membranes as the anode has great potential for inactivation of microorganisms because it enables membrane separation with simultaneous oxidative degradation. It is believed that both direct and indirect oxidation processes occur during electrochemical oxidation, contributing to membrane fouling control [127]. Direct oxidation involves the electron transfer from attached microbial cells to the anode membrane [128,129]. Indirect oxidation proceeds in multiple steps. Reactive chlorine or oxygen species are generated from the anode ($Cl_2^{-\cdot}$, Cl_2, $O_2^{-\cdot}$, O_3, H_2O_2, $^{\cdot}OH$) or cathode (e.g., H_2O_2), which can inactivate microbes that possibly adhere to and grow on the membrane surface [125]. In the study, an electrochemical multiwalled carbon nanotube filter was fabricated by depositing multiwalled carbon nanotubes onto a Teflon membrane under a vacuum, which enabled the inactivation of pathogens [130]. The electrochemical carbon nanotube-deposited filter was used as the anode for the inactivation tests of viruses (bacteriophage MS2) and bacteria (*E. coli*) with low potentials (1–3 V) and short electrolysis times (30 s). The filter lowered the number of bacteria and viruses in the effluent to a level below the detection limit in the presence of electric

This book belongs to Badji Mokhtar Annaba University Central Library Copyright Elsevier 2025

potentials (2 and 3 V). Direct and indirect electrochemical reactions prove to be effective for viral and bacterial inactivation.

7.6.4.3 Bubble creation and electrolytic cleaning

Water electrolysis generates O_2 and H_2 gases from the anode and cathode, respectively. It was reported that the gaseous bubbles generated on the electrodes could remove some dirt left on the conductive metals [131]. The creation of gas bubbles from the electroconductive membrane is thus believed to reduce the attachment of foulants to the membrane surface (Fig. 7.8). Electroconductive membranes are also expected to detach fouling layers, such as cakes or biopolymers (e.g., proteins). Indeed, the recovery of electroconductive membrane permeability by bubble generation has been reported [132–134].

When the multiwalled carbon nanotube-loaded polyvinylidene difluoride membrane was used as the cathode, the periodic electrolysis restored the membrane flux to 60%–80% of its initial value during membrane filtration of $CaCO_3$ and yeast suspensions containing 10 g/L NaCl [135]. Membrane cleaning was achieved by the gas bubbles generated by electrolysis, extracting foulants from the membrane. In contrast, when employing a direct/indirect oxidation method, gas bubbles can reduce the reaction area and ion channels, impeding contaminant removal. Thus it is necessary to consider the two competing effects in electroconductive membrane treatment.

The in situ electrochemical reduction of O_2 to H_2O_2 at the cathode is another important reaction with respect to membrane self-cleaning and microbial inactivation [49,119] (Fig. 7.8). A composite electroconductive MF membrane was created by inserting a stainless steel mesh into the polymeric membranes [49]. Applying an external electric field to the stainless steel mesh played a role in fouling control. When an electric field (2 V/cm) was applied to the membrane used as the cathode, the fouling rate for all the model foulants (e.g., bovine serum albumin, sodium alginate, humic acid, and silicon dioxide) tested in batch mode was reduced. The fouling rate in a

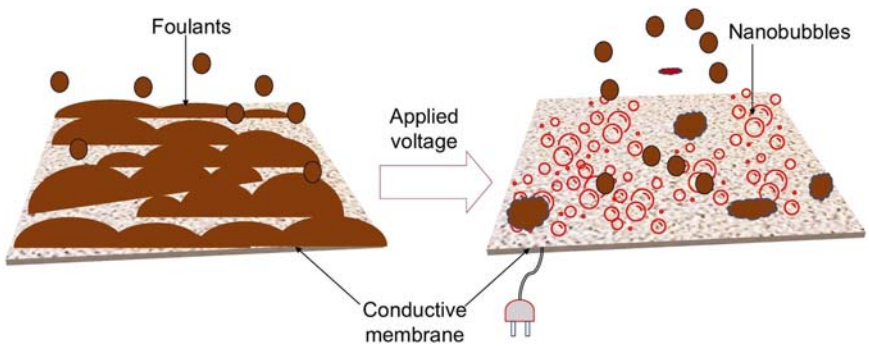

Figure 7.8 Schematic diagram of electrolytic cleaning via gas bubbles and H_2O_2 during electrofiltration.

This book belongs to Badji Mokhtar Annaba University Central Library Copyright Elsevier 2025

continuous flow MBR decreased by ~50% with an electric field (2 V/cm) compared to the control (with no electricity). Electrostatic repulsive force and in situ H_2O_2 production contributed to fouling control. A bioelectrochemical membrane reactor that combines an MBR and a microbial fuel cell was also developed to control membrane fouling by in situ electrogenerated H_2O_2 [136].

7.6.5 Energy consumption for membrane fouling control

Relatively high electrical energy consumption is a significant impediment to electrochemical membrane technology. The specific energy consumption (SEC) to produce the electric field/electrochemical reactions can be estimated as follows [104,137] [Eq. (7.2)]

$$\mathrm{SEC} = \frac{E_{\mathrm{cell}} I t}{V_p} \tag{7.2}$$

where E_{cell} is the cell potential provided by the power source (V), I is the applied current (A), t is the operation time (s), and V_p is the permeated volume (m^3). Data on the energy consumption by various electrochemical membrane processes for fouling alleviation from the literature published in the last decade were compiled and are given in Table 7.1. Considering significant improvements in fouling control by the electric field/electrochemical reactions during membrane filtration, the extra energy consumption seemed to be compensated [147]. Moreover, additional energy requirements for electrochemical MBRs appeared to be minor compared to the overall energy demand for conventional MBRs [149,150]. In some electrochemical membrane systems, the energy consumption was estimated to be very high because electricity was applied not only for fouling control but also for contaminants (e.g., organics) degradation.

7.7 Concluding remarks and future research needs

Membrane fouling is a longstanding issue that reduces membrane productivity and shortens the membrane lifespan. As mentioned throughout this chapter, the integration of membrane filtration and electrochemical processes has significantly improved the membrane's antifouling capacity. We thus come to the following conclusions about electrochemical membrane technology for fouling control:

1. The electrochemical membrane filtration process has several configurations: two-stage serial process, single-stage hybrid process, and bifunctional membrane process. In the two-stage serial process configuration, the electrochemical unit serves as a pretreatment stage before membrane filtration. The single-stage hybrid process contains electrodes and membranes in one reactor. The bifunctional membrane process accomplishes the membrane itself as an electrode and a filter medium.

This book belongs to Badji Mokhtar Annaba University Central Library Copyright Elsevier 2025

This book belongs to Badji Mokhtar Annaba University Central Library

Table 7.1 Summary of the specific energy consumption data obtained from the studies about various electrochemical membrane processes.

Electrochemical membrane process	Treatment method	Membrane type[a]	Applied electrical potential (V)	Specific energy consumption (kWh/m^3)	Reference
Two-stage	Electrocoagulation before membrane distillation	Ethylene chlorotrifluoroethylene copolymer flat sheet microfiltration (MF) (0.1 μm)	3	1.41	[138]
Two-stage	Electrooxidation before MF	Cellulosic flat sheet MF (0.45 μm)	2	0.11	[91]
Two-stage	Electrooxidation before ultrafiltration (UF)	Polyvinylidene difluoride hollow fiber UF (0.04 μm)	6–8.6	4.4–29.8	[65]
Single-stage hybrid	Electrooxidation with MF	Ceramic (alumina) flat sheet MF (0.5 μm)	5.6–10.8	3.11–12.0[b]	[30]
Single-stage hybrid	Electrooxidation with nanofiltration (NF)	Polyamide flat sheet NF (150–300 Da)	5	5.611	[103]
Single-stage hybrid	Electrooxidation with MF	Ceramic (a-Al_2O_3/ZrO_2) flat sheet MF (0.4 μm)	3	3.8×10^{-4}	[139]
Single-stage hybrid	Electrocoagulation with UF	Polyvinylidene difluoride hollow fiber UF (0.03 μm)	1.33–12.84	0.12–8.59	[75]
Single-stage hybrid	Electrolysis with MF	Polyvinylidene difluoride flat sheet MF (0.22 μm)	-0.81 (vs Ag/AgCl)	2.0×10^{-3}	[32]
Single-stage hybrid	Electrocoagulation/oxidation with UF	Polyvinylidene difluoride hollow fiber UF (100 kDa)	7.32	2.73	[140]
Single-stage hybrid	Electrooxidation with MBR	Polyvinylidene difluoride spiral wound MF (0.22 μm)	1.9	0.25	[141]
Single-stage hybrid	Electric field with MBR	Polypropylene melt-blown nonwoven filter (5 μm), terylene filter cloth (22 μm)	0.4	8×10^{-3}	[120]
Single-stage hybrid	Electric field with MBR	Ceramic (alumina) flat sheet MF (0.1 μm)	2.72	5.2×10^{-2}	[142]
Single-stage hybrid	Electrooxidation with MBR	Polyvinylidene difluoride hollow fiber MF (0.4 μm)	2.3	2.9×10^{-2}	[73]
Bifunctional electroconductive membrane	Electrochemical MBR	Polyvinylidene difluoride/ stainless steel mesh MF (0.208 μm)	2	1.2×10^{-5}	[143]
Bifunctional electroconductive membrane	Electrochemical filtration of humic acid	Carbon nanotube/ceramic (Al_2O_3) flat sheet MF (0.12 μm)	2	0.77	[144]

Copyright Elsevier 2025

This book belongs to Badji Mokhtar Annaba University Central Library

Bifunctional electroconductive membrane	Electrochemical cleaning via in situ reactive chlorine species generation	Carbon nanotube/ceramic (ZrO_2) UF (0.054 μm)	3	4.9×10^{-3}	[145]
Bifunctional electroconductive membrane	Electrochemical filtration of oily wastewater, humic acid, and bovine serum albumin	Ti_4O_7/Al_2O_3 ceramic tubular MF (0.2 μm)	30–40	8×10^{-2} (oily wastewater), 6×10^{-2} (humic acid), and 0.17 (bovine serum albumin)	[59]
Bifunctional electroconductive membrane	Electrochemical filtration of polystyrene microspheres	Porous carbon/ceramic (Al_2O_3) plate MF (0.28 μm)	1.5	2.0×10^{-3}	[146]
Bifunctional electroconductive membrane	Electrochemical MF of *Escherichia coli*	Ag-carbon nanotube/ceramic (TiO_2) hollow fiber UF (0.082 μm)	2	2.36×10^{-2}	[114]
Bifunctional electroconductive membrane	Electrochemical UF of *E. coli*	Carbon nanotube-polyvinyl alcohol composite flat sheet UF (0.1–0.5 μm)	1.5	1.44×10^{-3}	[125]
Bifunctional electroconductive membrane	Electropolarization filtration of humic acid and *E. coli*	Carbon nanotube/ceramic (TiO_2) hollow fiber MF (0.129 μm)	± 0.5– ± 1.5 (vs Ag/AgCl)	0.4–1.1	[147]
Bifunctional electroconductive membrane	Electrochemical MBR	Stainless steel mesh into a polyvinylidene difluoride MF (0.062 μm)	2	3.8×10^{-3}	[49]
Bifunctional electroconductive membrane	Electro-Fenton MBR	Porous carbon, carbon nanotube, and Fe^{2+} spun into hollow fiber MF (0.53 μm)	1	8.64×10^{-5}	[148]
Bifunctional electroconductive membrane	Electrochemical filtration of industrial wastewater	Composite metal oxide ($0.8RuO_2$–$0.2TiO_2/TiO_2$) coated Ti mesh filter (3.8 μm)	5	9.39[b]	[53]

[a]Values in the parentheses indicate membrane pore sizes in either micrometer or molecular weight cut-off (Da).
[b]Total specific energy consumption including organics degradation in addition to fouling control.

Copyright Elsevier 2025

2. Electrochemical membrane technology primarily utilizes two types of membrane materials, that is, conductive and nonconductive ones. The major functionality of nonconductive membranes made from polymers and ceramic materials is a separation medium. On the other hand, the conductive membrane has two roles to fulfill as the electrode and the separation medium at the same time.
3. Electrical and electrochemical reactions contribute to fouling control being accompanied by several phenomena, such as electrophoresis, electrocoagulation, electroflotation, and electrooxidation. Electrophoresis helps the foulants to migrate away from the membrane surface. Electrocoagulation (i.e. coagulants) and electroflotation (i.e., gas bubbles) eliminate fine particles from the liquid phase, reducing their contribution to membrane clogging. Direct and indirect electrooxidation degrade or mineralize organic foulants in the feed stream. Electrochemically generated gas bubbles from the bifunctional membrane electrode clean the membrane surface.

There are still several challenges to overcome in electrochemical membrane technology, requiring innovative research and development in this field, mainly:

1. The fabrication of corrosion-resistant and cost-effective electroconductive membranes is needed. Membrane materials should be further improved in terms of electrochemical durability in addition to their activity. Novel membrane materials (e.g., metal-organic framework, MoS_2, MXene, etc.) need to be explored.
2. Synergistic process configurations need to be further investigated considering the electrode's electrochemical reactions, for example, anodically or cathodically generated oxidants, Fenton reactions, photoelectric-Fenton reactions, etc. The coupling of electrochemical membrane filtration with other processes, such as ultrasound and magnetic fields, needs to be considered.
3. The combination of an electrochemical membrane with a bioreactor is an area that has not been well explored. Further research on integrating a microbial electrolysis cell and an MBR would be engaging to explore in the area of renewable energy recovery. The value of hydrogen gases produced during electrochemical treatment is not well investigated yet.
4. The majority of electrochemical membrane filtration research focused on treating synthetic wastewater. Real wastewater streams, which are a lot more complicated, need to be pursued to verify the technological practicality of membrane filtration technology. Besides, long-term operations in the lab and field are also of great interest while evaluating the process sustainability (e.g., membrane lifetime) and its economic feasibility.

Acknowledgment

This research was supported by a grant (no. 2020K1A4A7A02108858) from the National Research Foundation of Korea, funded by the Korean government (Ministry of Science and ICT).

This book belongs to Badji Mokhtar Annaba University Central Library Copyright Elsevier 2025

References

[1] M.A. Shannon, P.W. Bohn, M. Elimelech, J.G. Georgiadis, B.J. Mariñas, A.M. Mayes, Science and technology for water purification in the coming decades, Nature 452 (2008) 301–310.

[2] B. Van Der Bruggen, C. Vandecasteele, T. Van Gestel, W. Doyen, R. Leysen, A review of pressure-driven membrane processes in wastewater treatment and drinking water production, Environ. Prog. 22 (2003) 46–56.

[3] M.G. Buonomenna, Membrane processes for a sustainable industrial growth, RSC Adv. 3 (2013) 5694–5740.

[4] M.D. Kennedy, J. Kamanyi, S.G.S. Rodríguez, N.H. Lee, J.C. Schippers, G. Amy, Water treatment by microfiltration and ultrafiltration, in: Advanced Membrane Technology and Applications, 2008, pp. 131–170.

[5] A.L. Zydney, C.-C. Ho, W. Yuan, Chapter 2 - Fouling phenomena during microfiltration: effects of pore blockage, cake filtration, and membrane morphology, in: D. Bhattacharyya, D.A. Butterfield (Eds.), Membrane Science and Technology, Elsevier, 2003, pp. 27–44.

[6] L.F. Greenlee, D.F. Lawler, B.D. Freeman, B. Marrot, P. Moulin, Reverse osmosis desalination: Water sources, technology, and today's challenges, Water Res. 43 (2009) 2317–2348.

[7] W.J. Koros, Y.H. Ma, T. Shimidzu, Terminology for membranes and membrane processes (IUPAC Recommendations 1996), Pure Appl. Chem. 68 (1996) 1479–1489.

[8] A. Gul, J. Hruza, F. Yalcinkaya, Fouling and chemical cleaning of microfiltration membranes: a mini-review, Polymers 13 (2021) 846.

[9] S. Mikhaylin, L. Bazinet, Fouling on ion-exchange membranes: classification, characterization and strategies of prevention and control, Adv. Colloid Interface Sci. 229 (2016) 34–56.

[10] D. Rana, T. Matsuura, Surface modifications for antifouling membranes, Chem. Rev. 110 (2010) 2448–2471.

[11] S.S.A. Shah, L. De Simone, G. Bruno, H. Park, K. Lee, M. Fabbricino, et al., Quorum quenching, biological characteristics, and microbial community dynamics as key factors for combating fouling of membrane bioreactors, NPJ Clean. Water 4 (2021) 19.

[12] J.S. Baker, L.Y. Dudley, Biofouling in membrane systems—A review, Desalination 118 (1998) 81–89.

[13] H.-C. Flemming, Reverse osmosis membrane biofouling, Exp. Therm. Fluid Sci. 14 (1997) 382–391.

[14] X. Zhu, M. Elimelech, Colloidal fouling of reverse osmosis membranes: measurements and fouling mechanisms, Environ. Sci. Technol. 31 (1997) 3654–3662.

[15] Q. Li, M. Elimelech, Organic fouling and chemical cleaning of nanofiltration membranes: measurements and mechanisms, Environ. Sci. Technol. 38 (2004) 4683–4693.

[16] S. Hong, M. Elimelech, Chemical and physical aspects of natural organic matter (NOM) fouling of nanofiltration membranes, J. Membr. Sci. 132 (1997) 159–181.

[17] N. Hilal, O.O. Ogunbiyi, N.J. Miles, R. Nigmatullin, Methods employed for control of fouling in mf and uf membranes: a comprehensive review, Sep. Sci. Technol. 40 (2005) 1957–2005.

[18] S. Lee, C.-H. Lee, Effect of operating conditions on $CaSO_4$ scale formation mechanism in nanofiltration for water softening, Water Res. 34 (2000) 3854–3866.

[19] C. Cheng, G. Jiang, G.P. Simon, J.Z. Liu, D. Li, Low-voltage electrostatic modulation of ion diffusion through layered graphene-based nanoporous membranes, Nat. Nanotechnol. 13 (2018) 685–690.

[20] P.S. Goh, A.F. Ismail, A review on inorganic membranes for desalination and wastewater treatment, Desalination 434 (2018) 60–80.

[21] A. Lee, J.W. Elam, S.B. Darling, Membrane materials for water purification: design, development, and application, Environ. Sci. Water Res. Technol. 2 (2016) 17–42.

[22] D.J. Son, W.Y. Kim, C.Y. Yun, D. Chang, D.G. Kim, S.O. Chang, et al., Combination of electrolysis technology with membrane for wastewater treatment in rural communities, Int. J. Electrochem. Sci. 9 (2014) 10.

This book belongs to Badji Mokhtar Annaba University Central Library Copyright Elsevier 2025

[23] V. Buscio, M. García-Jiménez, M. Vilaseca, V. López-Grimau, M. Crespi, C. Gutiérrez-Bouzán, Reuse of textile dyeing effluents treated with coupled nanofiltration and electrochemical processes, Materials 9 (2016) 490.
[24] J.C. Diogo, A. Morão, A. Lopes, Persistent aromatic pollutants removal using a combined process of electrochemical treatment and reverse osmosis/nanofiltration, Environ. Prog. Sustain. Energy 30 (2011) 399–408.
[25] T. Xu, L. Cui, H. Li, P. Zou, J. Liang, Effects of electrolytic oxidation for mitigating ultrafiltration membrane fouling caused by different natural organic matter fractions, Environ. Sci. Water Res. Technol. 6 (2020) 645–655.
[26] K. Yang, J. Yin, T. Zhu, B. Liu, G. Li, B. Huang, et al., Effect of boron-doped diamond anode electrode pretreatment on UF membrane fouling mitigation in a cross-flow filtration process, Sep. Purif. Technol. 259 (2021) 118110.
[27] K. Wei, C. Shen, W. Han, J. Li, X. Sun, J. Shen, et al., Advance treatment of chemical industrial tailwater by integrated electrochemical technologies: electrocatalysis, electrodialysis and electro-microfiltration, Chem. Eng. J. 310 (2017) 13–21.
[28] L. Xu, L.-S. Du, C. Wang, W. Xu, Nanofiltration coupled with electrolytic oxidation in treating simulated dye wastewater, J. Membr. Sci. 409–410 (2012) 329–334.
[29] Y. Juang, E. Nurhayati, C. Huang, J.R. Pan, S. Huang, A hybrid electrochemical advanced oxidation/microfiltration system using BDD/Ti anode for acid yellow 36 dye wastewater treatment, Sep. Purif. Technol. 120 (2013) 289–295.
[30] N. Mameda, H.-J. Park, K.-H. Choo, Membrane electro-oxidizer: a new hybrid membrane system with electrochemical oxidation for enhanced organics and fouling control, Water Res. 126 (2017) 40–49.
[31] H.M. Huotari, G. Trägårdh, I.H. Huisman, Crossflow membrane filtration enhanced by an external DC electric field: a review, Chem. Eng. Res. Des. 77 (1999) 461–468.
[32] H.S. Abid, D.J. Johnson, B. Clifford, D.T. Gethin, P. Bertoncello, R. Hashaikeh, et al., Periodic electrolysis technique for in situ fouling control and removal with low-pressure membrane filtration, Desalination 433 (2018) 10–24.
[33] W. Fu, X. Wang, J. Zheng, M. Liu, Z. Wang, Antifouling performance and mechanisms in an electrochemical ceramic membrane reactor for wastewater treatment, J. Membr. Sci. 570–571 (2019) 355–361.
[34] K. Qi, M. Chen, R. Dai, Q. Li, M. Lai, Z. Wang, Development of an electrochemical ceramic membrane bioreactor for the removal of PPCPs from wastewater, Water 12 (2020) 1838.
[35] F. Ahmed, B.S. Lalia, V. Kochkodan, N. Hilal, R. Hashaikeh, Electrically conductive polymeric membranes for fouling prevention and detection: a review, Desalination 391 (2016) 1–15.
[36] G. Wallace, G. Spinks, Conducting polymers – bridging the bionic interface, Soft Matter 3 (2007) 665–671.
[37] Z. Pan, C. Song, L. Li, H. Wang, Y. Pan, C. Wang, et al., Membrane technology coupled with electrochemical advanced oxidation processes for organic wastewater treatment: recent advances and future prospects, Chem. Eng. J. 376 (2019) 120909.
[38] L.-X. Wang, X.-G. Li, Y.-L. Yang, Preparation, properties and applications of polypyrroles, Reactive Funct. Polym. 47 (2001) 125–139.
[39] J.J. Patil, A. Jana, B.A. Getachew, D.S. Bergsman, Z. Gariepy, B.D. Smith, et al., Conductive carbonaceous membranes: recent progress and future opportunities, J. Mater. Chem. A 9 (2021) 3270–3289.
[40] C. Song, T. Wang, H. Jiang, X. Wang, Y. Cao, J. Qiu, Gas separation performance of C/CMS membranes derived from poly(furfuryl alcohol) (PFA) with different chemical structure, J. Membr. Sci. 361 (2010) 22–27.
[41] G. Rambabu, S.D. Bhat, Amino acid functionalized graphene oxide based nanocomposite membrane electrolytes for direct methanol fuel cells, J. Membr. Sci. 551 (2018) 1–11.
[42] F. Perreault, A. Fonseca de Faria, M. Elimelech, Environmental applications of graphene-based nanomaterials, Chem. Soc. Rev. 44 (2015) 5861–5896.

This book belongs to Badji Mokhtar Annaba University Central Library Copyright Elsevier 2025

[43] Y. Yang, S. Qiao, R. Jin, J. Zhou, X. Quan, Fouling control mechanisms in filtrating natural organic matters by electro-enhanced carbon nanotubes hollow fiber membranes, J. Membr. Sci. 553 (2018) 54–62.
[44] Q. Zhang, C.D. Vecitis, Conductive CNT-PVDF membrane for capacitive organic fouling reduction, J. Membr. Sci. 459 (2014) 143–156.
[45] X. Fan, H. Zhao, Y. Liu, X. Quan, H. Yu, S. Chen, Enhanced permeability, selectivity, and antifouling ability of CNTs/Al_2O_3 membrane under electrochemical assistance, Environ. Sci. Technol. 49 (2015) 2293–2300.
[46] H. Mao, M. Qiu, T. Zhang, X. Chen, X. Da, W. Jing, et al., Robust CNT-based conductive ultrafiltration membrane with tunable surface potential for in situ fouling mitigation, Appl. Surf. Sci. 497 (2019) 143786.
[47] M.S.A. Heikkinen, N.H. Harley, Experimental investigation of sintered porous metal filters, J. Aerosol Sci. 31 (2000) 721–738.
[48] B. Zhu, M. Duke, L.F. Dumée, A. Merenda, E. Des Ligneris, L. Kong, et al., Short review on porous metal membranes—fabrication, commercial products, and applications, Membranes 8 (2018) 83.
[49] J. Huang, Z. Wang, J. Zhang, X. Zhang, J. Ma, Z. Wu, A novel composite conductive microfiltration membrane and its anti-fouling performance with an external electric field in membrane bioreactors, Sci. Rep. 5 (2015) 9268.
[50] F.G.F. Qin, J. Mawson, X.A. Zeng, Experimental study of fouling and cleaning of sintered stainless steel membrane in electro-microfiltration of calcium salt particles, Membranes 1 (2011) 119–131.
[51] D. Li, J. Tang, X. Zhou, J. Li, X. Sun, J. Shen, et al., Electrochemical degradation of pyridine by Ti/SnO_2–Sb tubular porous electrode, Chemosphere 149 (2016) 49–56.
[52] X. Li, G. Liu, M. Shi, J. Li, J. Li, C. Guo, et al., Using TiO_2 mesoflower interlayer in tubular porous titanium membranes for enhanced electrocatalytic filtration, Electrochim. Acta 218 (2016) 318–324.
[53] N. Mameda, H. Park, K.-H. Choo, Electrochemical filtration process for simultaneous removal of refractory organic and particulate contaminants from wastewater effluents, Water Res. 144 (2018) 699–708.
[54] Y. Zhang, K. Wei, W. Han, X. Sun, J. Li, J. Shen, et al., Improved electrochemical oxidation of tricyclazole from aqueous solution by enhancing mass transfer in a tubular porous electrode electrocatalytic reactor, Electrochim. Acta 189 (2016) 1–8.
[55] C. Zhou, Y. Wang, J. Chen, J. Niu, Porous Ti/SnO_2-Sb anode as reactive electrochemical membrane for removing trace antiretroviral drug stavudine from wastewater, Environ. Int. 133 (2019) 105157.
[56] J.R. Smith, F.C. Walsh, R.L. Clarke, Electrodes based on Magnéli phase titanium oxides: the properties and applications of Ebonex® materials, J. Appl. Electrochem. 28 (1998) 1021–1033.
[57] P. Geng, J. Su, C. Miles, C. Comninellis, G. Chen, Highly-ordered Magnéli Ti_4O_7 nanotube arrays as effective anodic material for electro-oxidation, Electrochim. Acta 153 (2015) 316–324.
[58] F.C. Walsh, R.G.A. Wills, The continuing development of Magnéli phase titanium sub-oxides and Ebonex® electrodes, Electrochim. Acta 55 (2010) 6342–6351.
[59] P. Geng, G. Chen, Magnéli Ti_4O_7 modified ceramic membrane for electrically-assisted filtration with antifouling property, J. Membr. Sci. 498 (2016) 302–314.
[60] A.M. Zaky, B.P. Chaplin, Porous substoichiometric TiO_2 anodes as reactive electrochemical membranes for water treatment, Environ. Sci. Technol. 47 (2013) 6554–6563.
[61] A.M. Zaky, B.P. Chaplin, Mechanism of p-substituted phenol oxidation at a Ti_4O_7 reactive electrochemical membrane, Environ. Sci. Technol. 48 (2014) 5857–5867.
[62] P. Geng, G. Chen, Antifouling ceramic membrane electrode modified by Magnéli Ti_4O_7 for electro-microfiltration of humic acid, Sep. Purif. Technol. 185 (2017) 61–71.
[63] Z. Al-Qodah, M. Tawalbeh, M. Al-Shannag, Z. Al-Anber, K. Bani-Melhem, Combined electrocoagulation processes as a novel approach for enhanced pollutants removal: a state-of-the-art review, Sci. Total Environ. 744 (2020) 140806.
[64] K. Li, G. Wen, S. Li, H. Chang, S. Shao, T. Huang, et al., Effect of pre-oxidation on low pressure membrane (LPM) for water and wastewater treatment: a review, Chemosphere 231 (2019) 287–300.

This book belongs to Badji Mokhtar Annaba University Central Library Copyright Elsevier 2025

[65] R. Gonzalez-Olmos, A. Penadés, G. Garcia, Electro-oxidation as efficient pretreatment to minimize the membrane fouling in water reuse processes, J. Membr. Sci. 552 (2018) 124–131.
[66] R.J. Wakeman, E.S. Tarleton, Membrane fouling prevention in crossflow microfiltration by the use of electric fields, Chem. Eng. Sci. 42 (1987) 829–842.
[67] G. Brisson, M. Britten, Y. Pouliot, Electrically-enhanced crossflow microfiltration for separation of lactoferrin from whey protein mixtures, J. Membr. Sci. 297 (2007) 206–216.
[68] S. Lentsch, P. Aimar, J.L. Orozco, Enhanced separation of albumin-poly(ethylene glycol) by combination of ultrafiltration and electrophoresis, J. Membr. Sci. 80 (1993) 221–232.
[69] Y.-H. Weng, K.-C. Li, L.H. Chaung-Hsieh, C.P. Huang, Removal of humic substances (HS) from water by electro-microfiltration (EMF), Water Res. 40 (2006) 1783–1794.
[70] T.Y. Chiu, F.J. Garcia Garcia, Critical flux enhancement in electrically assisted microfiltration, Sep. Purif. Technol. 78 (2011) 62–68.
[71] C.-J. Chuang, C.-Y. Wu, C.-C. Wu, Combination of crossflow and electric field for microfiltration of protein/microbial cell suspensions, Desalination 233 (2008) 295–302.
[72] A.L. Ahmad, N. Ibrahim, Automated electrophoretic membrane cleaning for dead-end microfiltration and ultrafiltration, Sep. Purif. Technol. 29 (2002) 105–112.
[73] C.M. Chung, T. Tobino, K. Cho, K. Yamamoto, Alleviation of membrane fouling in a submerged membrane bioreactor with electrochemical oxidation mediated by in-situ free chlorine generation, Water Res. 96 (2016) 52–61.
[74] S. Ibeid, M. Elektorowicz, J.A. Oleszkiewicz, Novel electrokinetic approach reduces membrane fouling, Water Res. 47 (2013) 6358–6366.
[75] J. Sun, C. Hu, T. Tong, K. Zhao, J. Qu, H. Liu, et al., Performance and mechanisms of ultrafiltration membrane fouling mitigation by coupling coagulation and applied electric field in a novel electrocoagulation membrane reactor, Environ. Sci. Technol. 51 (2017) 8544–8551.
[76] S. Liang, H. Lin, M. Habteselassie, Q. Huang, Electrochemical inactivation of bacteria with a titanium sub-oxide reactive membrane, Water Res. 145 (2018) 172–180.
[77] L. Hua, H. Cao, Q. Ma, X. Shi, X. Zhang, W. Zhang, Microalgae filtration using an electrochemically reactive ceramic membrane: filtration performances, fouling kinetics, and foulant layer characteristics, Environ. Sci. Technol. 54 (2020) 2012–2021.
[78] S.N. Jagannadh, H.S. Muralidhara, Electrokinetics methods to control membrane fouling, Ind. Eng. Chem. Res. 35 (1996) 1133–1140.
[79] J. Li, T. Wang, J. Ma, X. Liang, Y. Yang, H. Wang, Anti-pollution electrocatalysis composite membrane and membrane reactor, in, China, 2015.
[80] Y. Yang, J. Li, H. Wang, X. Song, T. Wang, B. He, et al., An electrocatalytic membrane reactor with self-cleaning function for industrial wastewater treatment, Angew. Chem. Int. (Ed.) 50 (2011) 2148–2150.
[81] A.K. Pabby, S.S.H. Rizvi, A.M.S. Requena, Handbook of Membrane Separations: Chemical, Pharmaceutical, Food, and Biotechnological Applications, Second ed., CRC Press, 2015.
[82] J.T.G. Overbeek, Electrokinetic phenomena, Chapter V, in: H.R. Kruyt (Ed.), Colloid Science, Elsevier, Amsterdam, 1952.
[83] M.Y.A. Mollah, R. Schennach, J.R. Parga, D.L. Cocke, Electrocoagulation (EC)—science and applications, J. Hazard. Mater. 84 (2001) 29–41.
[84] P. Cañizares, M. Carmona, J. Lobato, F. Martínez, M.A. Rodrigo, Electrodissolution of aluminum electrodes in electrocoagulation processes, Ind. Eng. Chem. Res. 44 (2005) 4178–4185.
[85] C. Comninellis, Electrocatalysis in the electrochemical conversion/combustion of organic pollutants for waste water treatment, Electrochim. Acta 39 (1994) 1857–1862.
[86] N. Mameda, H. Park, K.-H. Choo, Hybrid electrochemical microfiltration treatment of reverse osmosis concentrate: a mechanistic study on the effects of electrode materials, Desalination 493 (2020) 114617.
[87] N. Mameda, H. Park, S.S.A. Shah, K. Lee, C.-W. Li, V. Naddeo, et al., Highly robust and efficient Ti-based Sb-SnO_2 anode with a mixed carbon and nitrogen interlayer for electrochemical 1,4-dioxane removal from water, Chem. Eng. J. 393 (2020) 124794.

This book belongs to Badji Mokhtar Annaba University Central Library Copyright Elsevier 2025

[88] C.A. Martínez-Huitle, S. Ferro, Electrochemical oxidation of organic pollutants for the wastewater treatment: direct and indirect processes, Chem. Soc. Rev. 35 (2006) 1324–1340.
[89] H. Huang, K. Schwab, J.G. Jacangelo, Pretreatment for low pressure membranes in water treatment: a review, Environ. Sci. Technol. 43 (2009) 3011–3019.
[90] E.-J. Lee, Y.-H. Kim, M.J. Jeon, H.-S. Kim, The effect of aeration types on foulant removal in ex-situ chemical cleaning in place (CIP) with membranes fouled by secondary effluents, Chem. Eng. J. 333 (2018) 730–738.
[91] H. Park, K.-H. Choo, H.-S. Park, J. Choi, M.R. Hoffmann, Electrochemical oxidation and microfiltration of municipal wastewater with simultaneous hydrogen production: Influence of organic and particulate matter, Chem. Eng. J. 215–216 (2013) 802–810.
[92] A. Urtiaga, Electrochemical technologies combined with membrane filtration, Curr. Opin. Electrochem. 27 (2021) 100691.
[93] T.C. Timmes, H.-C. Kim, B.A. Dempsey, Electrocoagulation pretreatment of seawater prior to ultrafiltration: bench-scale applications for military water purification systems, Desalination 249 (2009) 895–901.
[94] A. Bagga, S. Chellam, D.A. Clifford, Evaluation of iron chemical coagulation and electrocoagulation pretreatment for surface water microfiltration, J. Membr. Sci. 309 (2008) 82–93.
[95] N.P. Gamage, S. Chellam, Aluminum electrocoagulation pretreatment reduces fouling during surface water microfiltration, J. Membr. Sci. 379 (2011) 97–105.
[96] K. Bani-Melhem, E. Smith, Grey water treatment by a continuous process of an electrocoagulation unit and a submerged membrane bioreactor system, Chem. Eng. J. 198–199 (2012) 201–210.
[97] N.P. Gamage, S. Chellam, Mechanisms of physically irreversible fouling during surface water microfiltration and mitigation by aluminum electroflotation pretreatment, Environ. Sci. Technol. 48 (2014) 1148–1157.
[98] M.-J. Corbatón-Báguena, S. Álvarez-Blanco, M.-C. Vincent-Vela, E. Ortega-Navarro, V. Pérez-Herranz, Application of electric fields to clean ultrafiltration membranes fouled with whey model solutions, Sep. Purif. Technol. 159 (2016) 92–99.
[99] R.J. Wakeman, C.J. Williams, Additional techniques to improve microfiltration, Sep. Purif. Technol. 26 (2002) 3–18.
[100] C. Hu, M. Li, J. Sun, R. Liu, H. Liu, J. Qu, NOM fouling resistance in response to electric field during electro-ultrafiltration: significance of molecular polarity and weight, J. Colloid Interface Sci. 539 (2019) 11–18.
[101] G.C.C. Yang, T.-Y. Yang, S.-H. Tsai, Crossflow electro-microfiltration of oxide-CMP wastewater, Water Res. 37 (2003) 785–792.
[102] K. Zhao, J. Sun, C. Hu, J. Qu, Membrane fouling reduction through electrochemically regulating flocs aggregation in an electro-coagulation membrane reactor, J. Environ. Sci. 83 (2019) 144–151.
[103] L. Xu, Y. Sun, L. Du, J. Zhang, Removal of tetracycline hydrochloride from wastewater by nanofiltration enhanced by electro-catalytic oxidation, Desalination 352 (2014) 58–65.
[104] M. Sun, X. Wang, L.R. Winter, Y. Zhao, W. Ma, T. Hedtke, et al., Electrified membranes for water treatment applications, ACS ES&T Eng. 1 (2021) 725–752.
[105] W. Yu, N.J.D. Graham, G.D. Fowler, Coagulation and oxidation for controlling ultrafiltration membrane fouling in drinking water treatment: application of ozone at low dose in submerged membrane tank, Water Res. 95 (2016) 1–10.
[106] W. Yu, Y. Yang, N. Graham, Evaluation of ferrate as a coagulant aid/oxidant pretreatment for mitigating submerged ultrafiltration membrane fouling in drinking water treatment, Chem. Eng. J. 298 (2016) 234–242.
[107] B.M.B. Ensano, L. Borea, V. Naddeo, V. Belgiorno, M.D.G. de Luna, F.C. Ballesteros, Combination of electrochemical processes with membrane bioreactors for wastewater treatment and fouling control: a review, Front. Environ. Sci. 4 (2016).
[108] J.-P. Chen, C.-Z. Yang, J.-H. Zhou, X.-Y. Wang, Study of the influence of the electric field on membrane flux of a new type of membrane bioreactor, Chem. Eng. J. 128 (2007) 177–180.
[109] V. Wei, J.A. Oleszkiewicz, M. Elektorowicz, Nutrient removal in an electrically enhanced membrane bioreactor, Water Sci. Technol. 60 (2009) 3159–3163.

This book belongs to Badji Mokhtar Annaba University Central Library Copyright Elsevier 2025

[110] S.W. Hasan, M. Elektorowicz, J.A. Oleszkiewicz, Start-up period investigation of pilot-scale submerged membrane electro-bioreactor (SMEBR) treating raw municipal wastewater, Chemosphere 97 (2014) 71–77.
[111] L.-C. Hua, C. Huang, Y.-C. Su, T.-N.-P. Nguyen, P.-C. Chen, Effects of electro-coagulation on fouling mitigation and sludge characteristics in a coagulation-assisted membrane bioreactor, J. Membr. Sci. 495 (2015) 29–36.
[112] E. Souza, H.V.D.M. Follmann, L. Dalri-Cecato, A.A. Battistelli, M.A. Lobo-Recio, T.J. Belli, et al., Membrane fouling suppression using intermittent electric current with low exposure time in a sequencing batch membrane bioreactor, J. Environ. Chem. Eng. 8 (2020) 104018.
[113] F. Su, Y. Liang, G. Liu, C.R. Mota Filho, C. Hu, J. Qu, Enhancement of anti-fouling and contaminant removal in an electro-membrane bioreactor: significance of electrocoagulation and electric field, Sep. Purif. Technol. 248 (2020) 117077.
[114] X. Fan, Y. Liu, X. Wang, X. Quan, S. Chen, Improvement of antifouling and antimicrobial abilities on silver–carbon nanotube based membranes under electrochemical assistance, Environ. Sci. Technol. 53 (2019) 5292–5300.
[115] K. Wang, L. Xu, K. Li, L. Liu, Y. Zhang, J. Wang, Development of polyaniline conductive membrane for electrically enhanced membrane fouling mitigation, J. Membr. Sci. 570–571 (2019) 371–379.
[116] A.V. Dudchenko, J. Rolf, K. Russell, W. Duan, D. Jassby, Organic fouling inhibition on electrically conducting carbon nanotube–polyvinyl alcohol composite ultrafiltration membranes, J. Membr. Sci. 468 (2014) 1–10.
[117] Q. Liu, G. Qiu, Z. Zhou, J. Li, G.L. Amy, J. Xie, et al., An effective design of electrically conducting thin-film composite (TFC) membranes for bio and organic fouling control in forward osmosis (FO), Environ. Sci. Technol. 50 (2016) 10596–10605.
[118] C. Wang, H. Song, Q. Zhang, B. Wang, A. Li, Parameter optimization based on capacitive deionization for highly efficient desalination of domestic wastewater biotreated effluent and the fouled electrode regeneration, Desalination 365 (2015) 407–415.
[119] S. Wang, S. Liang, P. Liang, X. Zhang, J. Sun, S. Wu, et al., In-situ combined dual-layer CNT/PVDF membrane for electrically-enhanced fouling resistance, J. Membr. Sci. 491 (2015) 37–44.
[120] L. Liu, J. Liu, B. Gao, F. Yang, S. Chellam, Fouling reductions in a membrane bioreactor using an intermittent electric field and cathodic membrane modified by vapor phase polymerized pyrrole, J. Membr. Sci. 394–395 (2012) 202–208.
[121] R. Liébana, L. Arregui, I. Belda, L. Gamella, A. Santos, D. Marquina, et al., Membrane bioreactor wastewater treatment plants reveal diverse yeast and protist communities of potential significance in biofouling, Biofouling 31 (2015) 71–82.
[122] M. Zhang, S. Jiang, D. Tanuwidjaja, N. Voutchkov, E.M.V. Hoek, B. Cai, Composition and variability of biofouling organisms in seawater reverse osmosis desalination plants, Appl. Environ. Microbiol. 77 (2011) 4390–4398.
[123] C.-F. de Lannoy, D. Jassby, K. Gloe, A.D. Gordon, M.R. Wiesner, Aquatic biofouling prevention by electrically charged nanocomposite polymer thin film membranes, Environ. Sci. Technol. 47 (2013) 2760–2768.
[124] B.S. Lalia, F.E. Ahmed, T. Shah, N. Hilal, R. Hashaikeh, Electrically conductive membranes based on carbon nanostructures for self-cleaning of biofouling, Desalination 360 (2015) 8–12.
[125] A. Ronen, W. Duan, I. Wheeldon, S. Walker, D. Jassby, Microbial attachment inhibition through low-voltage electrochemical reactions on electrically conducting membranes, Environ. Sci. Technol. 49 (2015) 12741–12750.
[126] K.P. Drees, M. Abbaszadegan, R.M. Maier, Comparative electrochemical inactivation of bacteria and bacteriophage, Water Res. 37 (2003) 2291–2300.
[127] C.D. Vecitis, G. Gao, H. Liu, Electrochemical carbon nanotube filter for adsorption, desorption, and oxidation of aqueous dyes and anions, J. Phys. Chem. C. 115 (2011) 3621–3629.
[128] H. Liu, X.-Y. Ni, Z.-Y. Huo, L. Peng, G.-Q. Li, C. Wang, et al., Carbon fiber-based flow-through electrode system (FES) for water disinfection via direct oxidation mechanism with a sequential reduction–oxidation process, Environ. Sci. Technol. 53 (2019) 3238–3249.

This book belongs to Badji Mokhtar Annaba University Central Library Copyright Elsevier 2025

[129] A.M. Polcaro, A. Vacca, M. Mascia, S. Palmas, R. Pompei, S. Laconi, Characterization of a stirred tank electrochemical cell for water disinfection processes, Electrochim. Acta 52 (2007) 2595–2602.
[130] C.D. Vecitis, M.H. Schnoor, M.S. Rahaman, J.D. Schiffman, M. Elimelech, Electrochemical multiwalled carbon nanotube filter for viral and bacterial removal and inactivation, Environ. Sci. Technol. 45 (2011) 3672–3679.
[131] V.M.R. Valerij Leontievich Steblianko, Electrolytic Process for Cleaning Electrically Conducting Surfaces in, US, 1996.
[132] D. Bell, R. Sengpiel, M. Wessling, Metallized hollow fiber membranes for electrochemical fouling control, J. Membr. Sci. 594 (2020) 117397.
[133] X. Sun, J. Wu, Z. Chen, X. Su, B.J. Hinds, Fouling characteristics and electrochemical recovery of carbon nanotube membranes, Adv. Funct. Mater. 23 (2013) 1500–1506.
[134] Z. Wu, H. Chen, Y. Dong, H. Mao, J. Sun, S. Chen, et al., Cleaning using nanobubbles: defouling by electrochemical generation of bubbles, J. Colloid Interface Sci. 328 (2008) 10–14.
[135] R. Hashaikeh, B.S. Lalia, V. Kochkodan, N. Hilal, A novel in situ membrane cleaning method using periodic electrolysis, J. Membr. Sci. 471 (2014) 149–154.
[136] Y.-K. Wang, W.-W. Li, G.-P. Sheng, B.-J. Shi, H.-Q. Yu, In-situ utilization of generated electricity in an electrochemical membrane bioreactor to mitigate membrane fouling, Water Res. 47 (2013) 5794–5800.
[137] F.C. Moreira, R.A.R. Boaventura, E. Brillas, V.J.P. Vilar, Electrochemical advanced oxidation processes: a review on their application to synthetic and real wastewaters, Appl. Catal. B Environ. 202 (2017) 217–261.
[138] K. Sardari, P. Fyfe, D. Lincicome, S. Ranil Wickramasinghe, Combined electrocoagulation and membrane distillation for treating high salinity produced waters, J. Membr. Sci. 564 (2018) 82–96.
[139] J. Zheng, Z. Wang, J. Ma, S. Xu, Z. Wu, Development of an electrochemical ceramic membrane filtration system for efficient contaminant removal from waters, Environ. Sci. Technol. 52 (2018) 4117–4126.
[140] J. Sun, C. Hu, K. Zhao, M. Li, J. Qu, H. Liu, Enhanced membrane fouling mitigation by modulating cake layer porosity and hydrophilicity in an electro-coagulation/oxidation membrane reactor (ECOMR), J. Membr. Sci. 550 (2018) 72–79.
[141] K. Vasanthapalaniappan, K. Palani, S.S. Saravanabhavan, N. Jonna, M. Pounsamy, K. Natarajan, et al., A study on novel coupled membrane bioreactor with electro oxidation for biofouling reduction, Environ. Eng. Res. 26 (2021). 200039-200030.
[142] J. Zhang, A. Satti, X. Chen, K. Xiao, J. Sun, X. Yan, et al., Low-voltage electric field applied into MBR for fouling suppression: performance and mechanisms, Chem. Eng. J. 273 (2015) 223–230.
[143] M. Chen, Q. Lei, L. Ren, J. Li, X. Li, Z. Wang, Efficacy of electrochemical membrane bioreactor for virus removal from wastewater: performance and mechanisms, Bioresour. Technol. 330 (2021) 124946.
[144] S. Wei, L. Du, S. Chen, H. Yu, X. Quan, Electro-assisted CNTs/ceramic flat sheet ultrafiltration membrane for enhanced antifouling and separation performance, Front. Environ. Sci. Eng. 15 (2020) 11.
[145] X. Wang, M. Sun, Y. Zhao, C. Wang, W. Ma, M.S. Wong, et al., In situ electrochemical generation of reactive chlorine species for efficient ultrafiltration membrane self-cleaning, Environ. Sci. Technol. 54 (2020) 6997–7007.
[146] S. Chen, G. Wang, S. Li, X. Li, H. Yu, X. Quan, Porous carbon membrane with enhanced selectivity and antifouling capability for water treatment under electrochemical assistance, J. Colloid Interface Sci. 560 (2020) 59–68.
[147] X. Fan, H. Zhao, X. Quan, Y. Liu, S. Chen, Nanocarbon-based membrane filtration integrated with electric field driving for effective membrane fouling mitigation, Water Res. 88 (2016) 285–292.
[148] Y. Yang, S. Qiao, J. Zhou, X. Quan, Mitigating membrane fouling based on in situ •OH generation in a novel electro-fenton membrane bioreactor, Environ. Sci. Technol. 54 (2020) 7669–7676.
[149] J.A. Gil, L. Túa, A. Rueda, B. Montaño, M. Rodríguez, D. Prats, Monitoring and analysis of the energy cost of an MBR, Desalination 250 (2010) 997–1001.
[150] S. Zhang, R. van Houten, D.H. Eikelboom, H. Doddema, Z. Jiang, Y. Fan, et al., Sewage treatment by a low energy membrane bioreactor, Bioresour. Technol. 90 (2003) 185–192.

This book belongs to Badji Mokhtar Annaba University Central Library Copyright Elsevier 2025

This page intentionally left blank

This book belongs to Badji Mokhtar Annaba University Central Library

Copyright Elsevier 2025

CHAPTER EIGHT

Electrochemical membrane technology for environmental remediation

Xiangtong Kong[1], Lihu Liu[2], Changyong Zhang[1], Chia-Hung Hou[3], Zhong Zhang[4] and Jinxing Ma[4]

[1]UNSW Water Research Centre, School of Civil and Environmental Engineering, The University of New South Wales, Sydney, NSW, Australia
[2]College of Resources and Environment, Huazhong Agricultural University, Wuhan, Hubei, P.R. China
[3]Graduate Institute of Environmental Engineering, National Taiwan University, Taipei, Taiwan, ROC
[4]Key Laboratory for City Cluster Environmental Safety and Green Development of the Ministry of Education, School of Ecology, Environment and Resources, Guangdong University of Technology, Guangzhou, Guangdong, P.R. China

8.1 Introduction

The occurrence and the accumulation of micropollutants and heavy metals (e.g., Cu, Cr, and As) in the environment are of increasing concern as a result of our better understanding of the cytotoxicity of these contaminants in an ecological system [1–4]. This concern is also compounded by the lack of viable techniques to remediate complicated matrices such as groundwater, seawater, and soil. Electrochemical membrane technology (e.g., electrodialytic remediation) has been recently developed to remove charged organic pollutants and heavy metals from environmental matrices. This concept is largely based on electrokinetic remediation knowledge, in which an electric current that acts as the "cleaning agent" is applied to the matrix [5–7]. The most important mechanisms involved in an electrochemical (membrane) process with the aim of remediation are summarized as follows (Fig. 8.1) [4]:

In aqueous media/soil,

- Electromigration (or electrophoresis) is the motion of ions (or charged particles) in the aqueous media or water retained in the soil, which is driven by the electrical field applied between the electrodes, that is, anode and cathode. Generally, the cations/positively charged particles move toward the cathode which is negatively polarized during charging; while the anions/negatively charged particles move toward the anode (Fig. 8.1A) [8].
- Electro-osmosis is the motion of water induced by an electric field on net mobile electric charge in a solution [9]. For environmental matrices, the mineral particles are usually negatively charged due to (1) the release of protons, (2) adsorption of anions by the Lewis centers and/or (3) the exchange of aluminum or silicon atoms in the mineral structure for monovalent cations [4]. This results in the water in the electrical

Electrochemical Membrane Technology for Water and Wastewater Treatment.
DOI: https://doi.org/10.1016/B978-0-12-824470-8.00004-8
© 2022 Elsevier Inc.
All rights reserved.

This book belongs to Badji Mokhtar Annaba University Central Library
Copyright Elsevier 2025

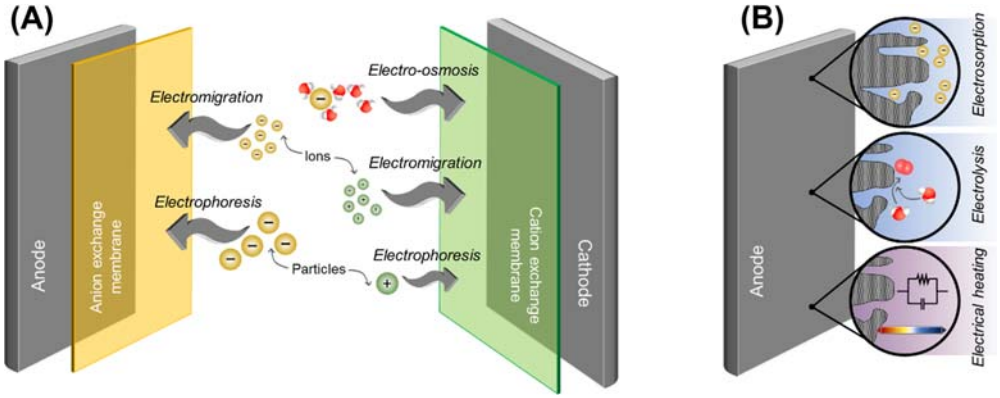

Figure 8.1 Electrochemical (membrane) technology for environmental remediation: (A) Electromigration, electrophoresis, and electro-osmosis processes in aqueous media/soil and (B) electrosorption, electrolysis, and electrical heating processes on the electrode surface (taking anode as an example).

double layer (EDL) (i.e., the Debye layer) being positively charged and the electro-osmotic flux typically flowing from the anode to the cathode. While the velocity of this portion of fluid flow does not depend on the pressure gradient, the magnitude decreases with an increase in the ionic concentration in the solution. Note that the motion of water molecules in electrokinetic remediation can also be given impetus by the concomitant transfer of water in hydrated ions [10].

On the electrode/membrane surface,

- Electrosorption (or capacitive deionization) is the immobilization of counterions in the EDL of a charged porous electrode (Fig. 8.1B) [11,12]. The contribution of electrosorption to the fate of ions depends not only on the electrode potential (because a higher potential over the non-Faradaic reaction window will result in electrolysis), but also on the electrode properties. For a carbonaceous electrode, micropores (with pore size <2 nm) are critical in electrosorption [13].
- Electrolysis involves a number of Faradaic reactions occurring on the anode and cathode surface that are directly in contact with either the solution/soil or the membrane. The Faradaic reactions can contribute to the ion/charge neutralization in the solution/soil by H^+/OH^- production as well as the removal of contaminants (e.g., oxidation of organics at the anode and reduction of heavy metals at the cathode) [14]. The most important reactions are those of water splitting at both the anode and the cathode, and halogen oxidation at the anode and metal electrodeposition at the cathode. While electromigration of produced H^+/OH^- in the media could be a problem because this may influence the ecological habitat, the "acidic front" that forms at the anode and moves toward the cathode which plays an important role in releasing pollutants fixed on mineral particles by dissolution and ion exchange mechanisms [4].

This book belongs to Badji Mokhtar Annaba University Central Library Copyright Elsevier 2025

- Electrical heating is the result of the ohmic heating (or Joule heating) taking effect that forms a temperature gradient between the electrode/solution interface and the media between electrodes (Fig. 8.1B) [15], especially in the vicinity of the electrodes. The working principle of this mechanism is the high ohmic losses that result from the low ionic conductivity of groundwaters/soil. The temperature fluctuation influences the transport of, especially, voltaic organic pollutants [4] and their activities at the electrodes [15].

Based on the aforementioned mechanisms, a number of electrochemical membrane processes (e.g., electrodialytic and electrocatalytic remediation) have been developed and implemented for environmental remediation. This chapter is focused on the discussion of the fundamentals and the setup of these techniques, operating parameters governing the process performance, and the process of contaminant removal under different scenarios. Challenges and perspectives of electrochemical membrane processes for remediation are also reviewed.

8.2 Electrodialytic remediation

8.2.1 Fundamentals

Electrodialytic remediation is a derivative of electrokinetic remediation [16] with the two methods differing in the mode of separation used between the electrodes, on one hand, and the media to remediate, on the other [5] (Fig. 8.2). In contrast

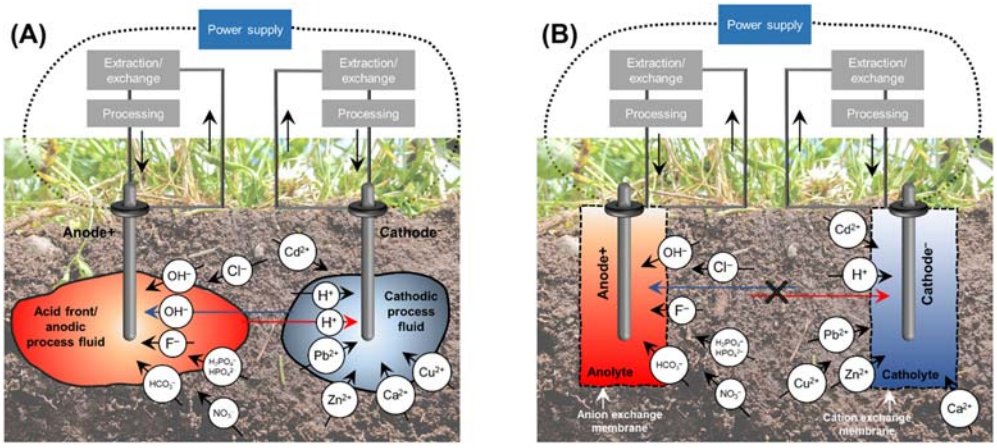

Figure 8.2 Comparison of (A) electrokinetic remediation and (B) electrodialytic remediation. *Adapted from the work by Y.B. Acar, A.N. Alshawabkeh, Principles of electrokinetic remediation, Environ. Sci. Technol. 27 (1993) 2638–2647 [16]. Copyright 1993 American Chemical Society.*

This book belongs to Badji Mokhtar Annaba University Central Library Copyright Elsevier 2025

to the bare electrodes directly touching the media/soil in electrokinetic remediation (Fig. 8.2A), in electrodialytic remediation the ion exchange membranes (IEMs), instead of passive barriers, are used to separate the electrodes from the media/soil (Fig. 8.2B). While the use of IEMs may not rule out the occurrence of side reactions at the electrodes, this can significantly improve the charge/current efficiency of the system: that is, the back-diffusion of co-ions (ions with the same charge of the electrode) from the electrode compartment to the media is largely eliminated [11]. As such, no electron is wasted for ion transfer from one electrode to the other [5]. A research team from the Technical University of Denmark led by Professor Lisbeth M. Ottosen has pioneered the investigation of electrodialytic environment remediation since 1992 [5,6,17–23], with this remediation technique being currently implemented for decontamination of waste from soil, in wastewater treatment plants, of industrial waste from the environment, of fly ash from the air, of harbor sediments from sea and ocean waters, etc. (Table 8.1) [5,17,19–25,27].

Table 8.1 Examples of media to process in electrodialytic remediation.

Categories of media (and electrolyte[a])	Details of contaminants/nutrients	References
Soil		
Danish soil (loamy sand) from a former wood preservation plant (0.01 M $NaNO_3$, pH 3[b])	Heavy metals: Cu (~1400 mg/kg of dry soil), Cr (330 mg/kg), and As. Water content: 17.4% of soil. Initial pH: 5.8.	[5,24]
Sand from a Chlor-alkali plant (0.01 M $NaNO_3$, pH 3)	Heavy metals: Hg (685 mg/kg of dry soil)	[24]
Loamy sand with lime (0.01 M $NaNO_3$, pH 3)	Heavy metals: Cu (2300 mg/kg of dry soil), Pb (830 mg/kg), and Zn (2400 mg/kg)	[24]
Soil from polluted sites involved in wood preservation, cable production, auto lacquer and in the production of electronic devices (0.01 M $NaNO_3$, pH 2)	Heavy metals: Cu (1100–5400 mg/kg of dry soil), Pb (360–940 mg/kg), and Zn (380–1090 mg/kg). Carbonate content (<0.1–12.0). Initial pH: 5.4–7.7	[21]
Waste from WWTPs		
Sludge from the hydro extractor C at WWTP Lynetten, Lynettefællesskabet I/S in Copenhagen, Denmark ($NaNO_3$ solution, pH < 2)	Heavy metals: Cd (2.37 mg/kg dry matter). Organic matter content: 67% of sludge. Initial pH: 5.65	[19]

(*continued*)

This book belongs to Badji Mokhtar Annaba University Central Library Copyright Elsevier 2025

Table 8.1 (Continued)

Categories of media (and electrolyte[a])	Details of contaminants/nutrients	References
Sewage sludge ashes collected at Lynettefællesskabet, Copenhagen, Denmark ($NaNO_3$ solution, pH < 2)	P (~130 g/kg); Heavy metals: Cu (~750 mg/kg), Zn (3100–3300 mg/kg), and Pb (~300 mg/kg)	[17]
Industrial waste		
Sawdust prepared from an 8-year out-of-service *Pinus pinaster Ait*. Pole in Leiria, Portugal (0.01 M $NaNO_3$, pH 2)	Heavy metals: Cu (3149 ± 114 mg/kg), Cr (8281 ± 420 mg/kg), and As (8111 ± 871 mg/kg)	[23]
Mine tailing from Zinkgruvan, Sweden (0.01 M $NaNO_3$, pH < 2)	Heavy metals: Cu (372 mg/kg), Pb (3710 mg/kg), and Zn (7346 mg/kg)	[25]
Fly ash		
Fly ash from an incineration plant in Greenland and the mass-burn facility "Vestforbrænding," Denmark (2.5% NH_3, 0.25 M ammonium citrate/1.25% NH_3, and/or 0.01 M $NaNO_3$, pH < 2)	Heavy metals: Cu (1370–1570 mg/kg dry matter), Pb (4000–8050 mg/kg), Zn (17,150–22,650 mg/kg), Cd (240–280 mg/kg), and Cr (280–3000 mg/kg)	[22]
Harbor sediments		
Sediments from Sisimiut, Greenland, and from Hammerfest, Norway (0.01 M $NaNO_3$, pH 2)	Heavy metals: Cu (77–190 mg/kg), Zn (105–290 mg/kg), Cr (24–28 mg/kg), and Pb (58–66 mg/kg)	[26]
Harbor sediment from Haakonsvern, Bergen, and sediments from Gowanas Canal and Newtown Creek, USA (0.01 M $NaNO_3$, pH < 2)	Heavy metals: Cu (58–634 mg/kg), Zn (153–1192 mg/kg), Pb (62–478 mg/kg), and Cd (4.1–16.6 mg/kg). Initial pH: 6.7–7.5	[20]

[a]Electrolyte stands for the electrolyte in the electrode compartments.
[b]pH was initially adjusted to 3 using HNO_3.

In an electrodialytic remediation system (Fig. 8.2B), the anode and cathode compartments are set at a certain distance to provide an electrical field that drives the directional movement of anions and cations in the media. It can be seen from Table 8.2 that platinized electrodes that are expected to be anti-corrosion are mainly used in electrodialytic remediation. Recent studies have also highlighted the potential of boron-doped diamond and Magnéli phase titanium suboxide (TiO_{1+X}) electrodes in electrochemical advanced oxidation processes as a result of their high activity, conductivity, and chemical stability [28–30], though there is no report available on the use of these materials in electrodialytic remediation process. Commercial IEMs are widely used to separate the electrodes from the media (Table 8.2) [5,17–21,23–25]. In a typical electrodialytic remediation system (i.e., a three-compartment

This book belongs to Badji Mokhtar Annaba University Central Library Copyright Elsevier 2025

Table 8.2 Examples of electrodes and membranes used in electrodialytic remediation.

Electrodes	Materials	Parameters	References
	Platinized electrodes (Bergsøe Anti Corrosion A/S, Denmark)	Diameter: 3 mm and length: 5 cm	[5,21,23,24]
	Platinum coated titanium electrodes (Permascand Co., Sweden)	Diameter: 3 mm	[20,25]
Membranes	**Categories**		**References**
	AEM: 204 SXZL 386, CEM: CR67 HMR 412 (Ionics Inc, USA)		[5]
	SYBRON AEM: MA3470, CEM: MC3475 (Sybron Chemicals Inc, USA)		[24]
	IONICS AEM: 204 SXZR/SXZL 386, CEM: 61 CXL/CZL 386 (Ionics Inc, USA)		[23,24]
	IONICS AEM 204 SZRA B02249C, CEM CR67 HUYN12116B (Ionics Inc, USA)		[17,19–21]
	Membranes International Inc. AEM AMI-7001, CEM CMI-7000 (Membranes International Inc, USA)		[18]

cell shown in Fig. 8.3A), the anolyte is separated from the media by an anion exchange membrane (AEM) and the catholyte, by a cation exchange membrane (CEM) [5,26]. When a voltage is applied between the electrodes, the anions in the pollutant-impaired media can be transported to the anode compartment through the AEM and the cations to the cathode compartment through the CEM. Ideally, no current carries co-ions escaping from the electrode compartments due to the rejection by the IEMs. The use of IEMs also restricts the flushing effect of electro-osmosis, making this mechanism less important in electrodialytic remediation compared to the other aforementioned (Fig. 8.1) mechanism.

The $NaNO_3$ solution at a low pH (2–3) is widely used as the anolyte and the catholyte (Table 8.1) because of the relatively inert nature of nitrate at electrodes and the high solubilities of metal nitrate. In contrast to the electrokinetic remediation in which a basic front is developed from the cathode (due to hydrogen evolution and/or oxygen reduction reactions) and in which heavy metal cations can precipitate in the front (Fig. 8.2A), the electrodialytic remediation can largely avoid this problem with the contaminants accumulated in the electrolytes at much higher concentrations (e.g., Cu, Zn, and Pb in the acidified catholyte [20,23,24] and As, $CuOx_2^{2-}$, and Cr in the anolyte [23]). Nevertheless, pH excursion (i.e., acidification) of the media can also happen to electrodialytic remediation. Because the applied current may exceed the flux of anions moving from the media to the AEM, water dissociation/splitting has been observed on the side of AEM interfacing the media (Fig. 8.3A) [6], resulting in OH^- passing through the AEM to compensate for the deficient anion flux, while resulting in H^+ moving to the opposite direction into the media [5]. In comparison, water dissociation/splitting occurs at the interface between the media and CEM at a

This book belongs to Badji Mokhtar Annaba University Central Library Copyright Elsevier 2025

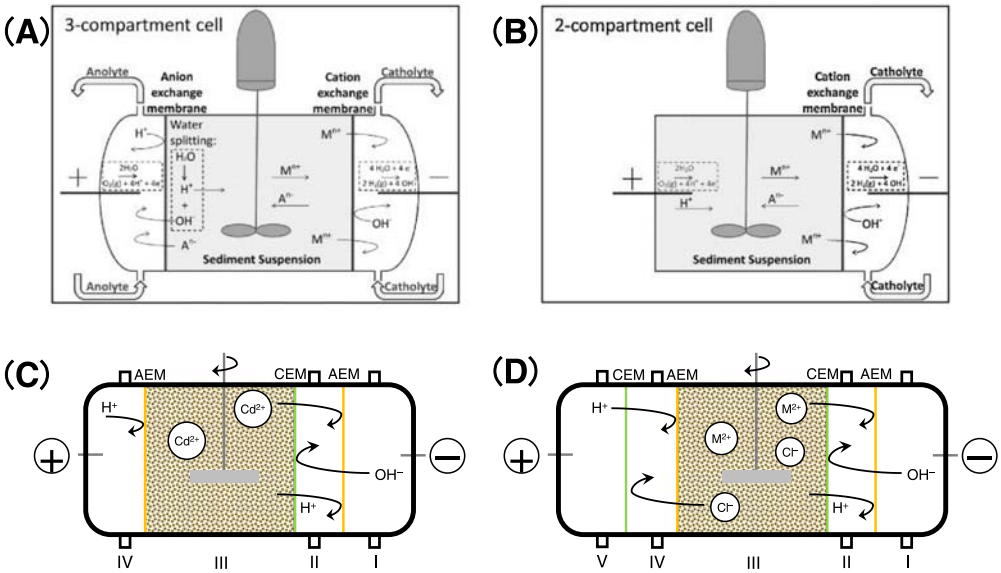

Figure 8.3 (A) Three-compartment and (B) two-compartment electrodialytic remediation cells. (C) Divided cathode compartment and (D) divided anode and cathode compartments in electrodialytic remediation cells. In panels (C) and (D), media to process is placed in the compartment III. Examples of electrolytes used in compartments I, II, IV and V are given in Table 8.1. *(A and B) Reproduced from the work by K.B. Pedersen, L.M. Ottosen, P.E. Jensen, T. Lejon, Comparison of 2-compartment, 3-compartment and stack designs for electrodialytic removal of heavy metals from harbour sediments, Electrochim. Acta 181 (2015) 48–57 [26]. Copyright 2015 Elsevier. (C and D) Adapted from the work by M.R. Jakobsen, J. Fritt-Rasmussen, S. Nielsen, L.M. Ottosen, Electrodialytic removal of cadmium from wastewater sludge, J. Hazard. Mater. 106 (2004) 127–132 [19] and G.M. Nystroem, L.M. Ottosen, A. Villumsen, Electrodialytic removal of Cu, Zn, Pb, and Cd from harbor sediment: influence of changing experimental conditions, Environ. Sci. Technol. 39 (2005) 2906–2911 [20]. Copyright 2004 Elsevier and 2005 American Chemical Society.*

high current density. This is because the cation exchange capacities of most natural matrices are higher than their anion exchange capacities. Cation exchange capacity represents the quantity of negative charge available to attract cations, with the anion exchange capacity related to the positive charge that attracts anions in solution [31,32]. Since the major soil constituents such as clay minerals and soil organic matter possess a net negative charge [33,34], in most soils cation exchange capacities are higher. Note that there are a number of factors that may affect the limiting density, including ion species, their concentrations, and flow rate.

On the condition that acidification that drives the release of metals into the liquid phase is the rating limiting step, the anode can be directly placed in the media because H^+ production by water dissociation at the AEM in a conventional three-compartment cell is less efficient than that directly produced from the anode. The said two-compartment cell has

This book belongs to Badji Mokhtar Annaba University Central Library Copyright Elsevier 2025

been developed and patented at The Technical University of Denmark (Fig. 8.3B) [25,26]. Only a CEM is used to envelop the cathode compartment. This enables the continuous transport of desorbed cations (e.g., Cu^{2+} and Pb^{2+}) into the catholyte while preventing the release of OH^- generated from cathode reactions into the contaminated media. Recent studies have shown that acidification in a two-compartment cell is faster than in a three-compartment cell, resulting in a higher percentage of metals desorbed from the media [25,26,35,36]. While the two-compartment cell can work at a lower voltage drop (e.g., <5 V compared to <30 V of the three-compartment cell [25]) and at a lower energy cost compared to that in its counterpart, this configuration is deemed a better choice only for the applications in which the desorbed contaminants are present as metal ions.

Moreover, the production of OH^- in the cathode compartment is not homogenous with a much higher concentration expected to be observed in the vicinity of the cathode surface. Heterogeneous precipitation can occur at lower metal concentrations compared to homogenous precipitation. These mechanisms are in favor of the precipitation of removed metal cations at the cathode surface and then passivation of the electrode, even though the catholyte is acidified. To solve this problem, a design configuration with a divided cathode compartment has been proposed (Figs. 8.3C and D) [19,20,22]: an AEM is inserted between the CEM and the cathode, which rejects the cations from the media approaching the cathode while allowing OH^- generated at the cathode to pass through; whereas, a divided anode compartment is alternatively used (Fig. 8.3D) when the media contains a high concentration of chloride anions. This is because active chlorine can form ($E^0(Cl_2/Cl^-) = 1.36$ V) via the Volmer-Heyrovsky (V-H) and/or the Volmer-Tafel mechanisms at high voltages (Eqs. 8.1–8.3) [37,38]. While active chlorine is a widely used sanitizer (Eq. 8.4), it can be further converted to a toxic byproduct, chlorate, under anodic polarization (Eq. 8.5). Chlorate poisoning in living beings relates to its attacking sulfhydryl groups, particularly in red blood cells and the kidneys [39]. This likely causes intravascular hemolysis and methemoglobinemia. To overcome this problem, a CEM can be placed in the anode compartment (Fig. 8.3D) with the transport of chloride anions being constrained in the separate chamber (i.e., IV in Fig. 8.3D).

$$\text{Volmer reaction:}\quad M|\text{or } MO_x| + Cl^- \rightarrow M(Cl\bullet)|\text{or } MO_x(Cl\bullet)| + e^- \tag{8.1}$$

$$\text{Heyrovsky reaction :}\quad M(Cl\bullet)|\text{or } MO_x(Cl\bullet)| + Cl^- \rightarrow M|\text{or } MO_x| + Cl_2 + e^- \tag{8.2}$$

$$\text{Tafel reaction:}\quad 2M(Cl\bullet)|\text{or } 2MO_x(Cl\bullet)| \rightarrow 2M|\text{or } 2MO_x| + Cl_2 \tag{8.3}$$

$$\text{Hydrolysis of } Cl_2\text{:}\quad Cl_2 + H_2O \rightarrow HOCl + H^+ + Cl^- \tag{8.4}$$

$$M(2H_2O)|\text{or } MO_x(2H_2O)| + HOCl \rightarrow M|\text{or } MO_x| + ClO_3^- + 5H^+ + 4e^- \tag{8.5}$$

where M stands for a metal electrode and MO_x stands for a metal oxide electrode.

This book belongs to Badji Mokhtar Annaba University Central Library Copyright Elsevier 2025

8.2.2 Critical operating parameters and performance indicators

To date, most electrodialytic remediation cells have been set up at a lab scale with a typical media compartment volume (i.e., compartment III in Fig. 8.3) <1 L. The volume ratio of each electrode compartment (I + II or IV + V in Fig. 8.3) to the media compartment is in a range of 1:2–1:3. The anolyte and catholyte in a volume of 1.5–3 times that of one electrode compartment are individually circulated during the experiment. Operating parameters that have significant impacts on the electrodialytic remediation performance include the current density, remediation time, liquid-solid (L/S) ratio, and stirring of the contaminated media [17,24–26,35]. Correspondingly, voltage drop, current efficiency, change of pH and water content, and contaminant removal (or nutrient recovery) are the most important performance indicators of this technology.

8.2.2.1 Current density and voltage drop

Essentially, ion motivation and removal in electrodialytic remediation are driven by the current (I). This is particularly more efficient in removing contaminants from small pores of the media compared to the conventional extraction methods, because the electric current tends to pass in the area of high conductivity [24]. In comparison, diffusion of the extracting agents and carriers into small pores is always kinetically unfavorable. Current density (i, I/S_{IEM}) in electrodialytic remediation is normalized by the surface area of an IEM because the electrodes are in a shape of wire or rod. A typical current density of 0.1–0.5 mA/cm^2 [5,18,24,40–42] is applicable to most media but a much higher current density (e.g., 1.0–2.0 mA/cm^2) [43–46] is applicable to media with use of a desorbing agent. The electrical cost (E_{m}, kWh/kg) can be estimated according to Eq. (8.6) [41]:

$$E_m = \frac{I \Delta V_{\mathrm{cell}} t}{m} \tag{8.6}$$

where ΔV_{cell}, m and t stand for the voltage drop between electrodes (V), the mass of the media to process (kg), and the remediation duration time (h or days). A higher current for the same material may result in rapid pH change, a higher contaminant removal rate, and/or a shorter remediation time having a trade-off in a higher electrical cost. However, a super high voltage (due to a high current) can cause water-splitting and OH^- production at the CEM [25,43]. As such, a limiting current density of ~0.4 mA/cm^2 is suggested for materials with low conductivity (e.g., soil, mine tailing, and freshwater sediments) and ~1.5 mA/cm^2 for those with high conductivity (e.g., sludge ashes and harbor sediments).

At a constant current, ΔV_{cell} is related to the change of the resistance of the cell (largely the media) with the resistance influenced by (1) the water content in the media, (2) the motivation of the acidic front in the media, and (3) the change

This book belongs to Badji Mokhtar Annaba University Central Library Copyright Elsevier 2025

of the electrode properties [5]. With the remediation process continuing, the media suffers from dewatering that causes an increased ohmic resistance and a higher polarization resistance at the membrane interfaces. This effect is expected to be more significant at the AEM due to water dissociation. However, when the acidic front starts to arrive at the CEM, the overall cell resistance decreases. These mechanisms likely account for the "volcano" shape of ΔV_{cell} observed in electrodialytic remediation (Fig. 8.4A and B). Alternatively, in constant voltage mode, a

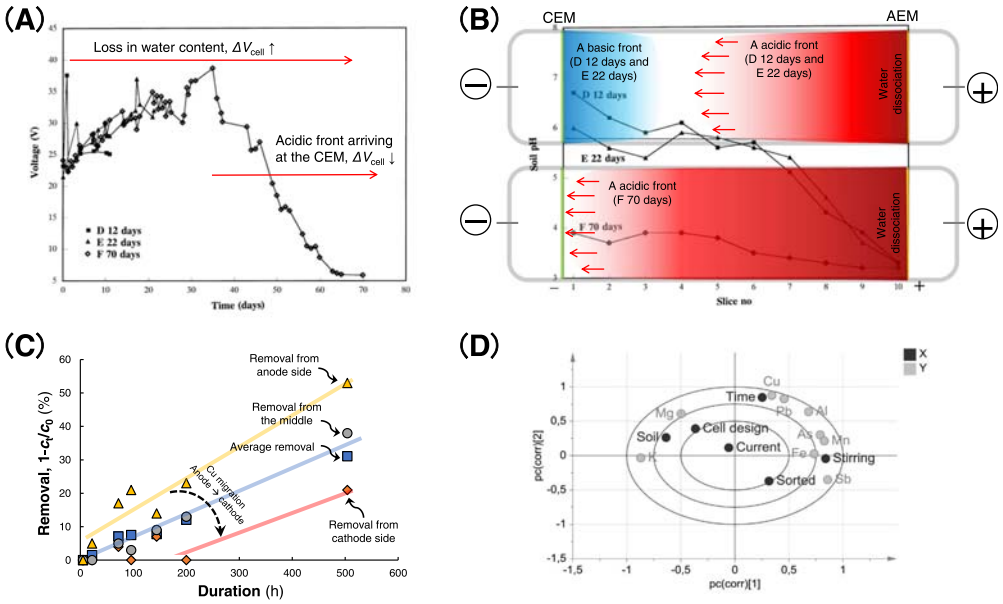

Figure 8.4 Calculations related to electrodialytic remediation: (A) Changes of voltage between working electrodes (ΔV_{cell}) during the experiments when 10 mA was applied to treat polluted soil from wood preservation industry. (B) pH profiles of the media slices and schematic presentation of the acidic front. Experiments were conducted under the same condition of panel (A). The straight line (at pH 5.8) refers to the initial pH value. (C) Cu removal from anode side, middle, and cathode side of the remediation compartment as a function of time (5–504 h) at 20 V. Lines are for visualization purpose only. (D) Weight plot of the projections onto latent structures (PLS) model of all metals. The plot illustrates the independent contribution of matrix variables to the heavy metal removal. Metals and variables located in the same quadrant are positively correlated. *(A) and (B) Adapted from the study by L.M. Ottosen, H.K. Hansen, S. Laursen, A. Villumsen, Electrodialytic remediation of soil polluted with copper from wood preservation industry, Environ. Sci. Technol. 31 (1997) 1711–1715 [5] Copyright 1997 American Chemical Society. (C) Data were retrieved from the study by H.K. Hansen, A. Rojo, L.M. Ottosen, Electrodialytic remediation of copper mine tailings, J. Hazard. Mater. 117 (2005) 179–183 [18]. (D) Reproduced from the work by K.B. Pedersen, P.E. Jensen, L.M. Ottosen, J. Barlindhaug, The relative influence of electrokinetic remediation design on the removal of As, Cu, Pb and Sb from shooting range soils, Eng. Geol. 238 (2018) 52–61 [40] Copyright 2018 Elsevier.*

This book belongs to Badji Mokhtar Annaba University Central Library Copyright Elsevier 2025

potential/voltage gradient of >2 V/cm is suggested [18], which can be lowered by pretreatment (e.g., acidification) of the media to decrease the overall cell resistance.

8.2.2.2 Remediation time

Since metal dissolution and migration to the electrode compartments are rate limiting in electrodialytic remediation, the remediation time has significant influence on the process performance. Fig. 8.4C describes the transfer of Cu in the remediation chamber as a function of time [18] with rapid removal of Cu from the anode side occurring at the beginning of the process. This results in accumulation and phase-lag removal (~200 h) of Cu from the cathode side (Fig. 8.4C). The importance of time on electrodialytic remediation removal efficiencies is applicable to most metals, as for example, there is a positive correlation between time and metal removal for Cu, Pb, Mn, As, Fe, and Al in two weighted components (Fig. 8.4D) [40], which indicates that time is a critical variable for designing the electrodialytic system to remove target contaminants (e.g., heavy metals) from the media. A duration ranging from 5 h to 77 days has been reported in electrodialytic remediation studies with a median value being 14–28 days. In addition, it is indicated that time after acidification rather than the total remediation duration should be a more reliable parameter to describe the process performance. For example, time after acidification to pH 4 (i.e., the time of the experiment running after reaching pH 4) has been used to study the importance of time [26].

8.2.2.3 Liquid-solid ratio of the contaminated media and stirring

The addition of external electrolyte to the contaminated media and/or use of stirring aim at facilitating the mass transfer of contaminants from the media surface into the liquid phase and then transport in the remediation compartment (Fig. 8.3). An L/S ratio ranging from 1.4 to 12 (with a mode of ~4) is widely used [19,20,47] with the species of the electrolyte including water [43,47], inorganic acid solutions (e.g., 0.01–1.0 M HCl) [20], organic acid solutions (e.g., citrate acid, 0.25 M ammonium citrate/1.25% NH_3, and 0.25 M Na-citrate/2.5% NH_3) [48], and ethylenediaminetetraacetic acid/artificial surfactants [49]. The use of assisting agents is to increase (1) the exchangeability of heavy metals from the surface bound form and (2) their mobilities in the electrolyte. Formation of stable tetrammine Cd complexes was observed in a 2.5% NH_3 solution, and higher Pb removal in a 0.25 M Na-citrate solution because Pb forms very stable chelates with citrate [48]. Note that the selection of an appropriate agent depends on the metal species and their association with the contaminated media. A better understanding of the exchangeable, reducible, and oxidizable fractions would significantly improve the efficiency (see Section 8.2.2.5 for details). Moreover, it is intuitively deducible that the remediation efficiency generally increases when the L/S ratio increases [20]; however; a high L/S ratio may result in the water splitting at

This book belongs to Badji Mokhtar Annaba University Central Library Copyright Elsevier 2025

the CEM that increases the local pH [43], which deteriorates the remediation efficiency. A high L/S ratio, on the other hand, poses difficulties in separating the decontaminated media from the electrolyte of a larger volume. In addition, stirring can be directly applied in the remediation compartment (Fig. 8.3). Although results of the projections onto latent structures (PLS) model have shown that stirring has significant positive effects on the metals removal (e.g., Mn, As, and Sb) (Fig. 8.4D) [40], there is limited investigation on an optimal stirring speed with a relatively high speed (1300 rpm) being widely used [47].

8.2.2.4 pH and water content

For performance evaluation, pH is a critical indicator as it determines the dissociation of contaminants (e.g., heavy metals) from the media. Typically, pH measurement of the media is carried out according to the following routines:

- By mixing 10 g of dry media (e.g., soil) and 25 mL deionized (DI) water. After 1 h of agitation, the aqueous pH is measured to report the media pH [5]; or
- By mixing the media in 1 M KCl at a liquid-to-solid ratio (L/S) of 5. After 1 h of agitation, the aqueous pH is measured to report the media pH [25].

During the electrodialytic remediation (without pre-adjustment of pH), an acidic front is initially developed at the AEM with a basic front at the CEM. For example, Fig. 8.4B shows that pH increases in the media slice next to CEM after 12-days operation [5]. While the pH of the same slice on Day 22 is still higher than the initial value, it is significantly lower than that on Day 12 (Fig. 8.4B). This phenomenon indicates that the acidic front forming at the AEM is gradually approaching the CEM during the remediation process. After a longer reaction time, the basic front is equalized and that pH constantly decreases (Fig. 8.4B) [5]. Theoretically, a longer remediation time and a higher current (but below the limiting current) will result in significantly more pH to decrease. However, an overhigh current can cause water dissociation at the CEM, leading to pH to increase in the adjacent area. $pH \leq 4$ is commonly suggested as a threshold for heavy metals (e.g., Cu) release from the solid phase to the solution. As such, adjusting the initial pH to 4 and/or regarding the time after acidification to pH 4 as a more important parameter have been implemented in previous studies [18,26].

Water content change is an important parameter for unadjusted media (i.e., L/S ratio = 0). This occurs due to water dissociation at the AEM and electro-osmosis in the media. As such, the volume of the catholyte increases and the volume of the anolyte decreases during the experiment. While a lower water content results in a higher internal resistance (and increase in ΔV_{cell}), this parameter is less important compared to pH that dominates the contaminant dissociation and mobility in the media during remediation (Fig. 8.4A).

This book belongs to Badji Mokhtar Annaba University Central Library Copyright Elsevier 2025

8.2.2.5 Contaminant speciation and removal

Aforementioned, the dissociation of adsorbed contaminants from the media surface into the electrolyte is the first step of the electrodialytic remediation, which depends not only on the operating parameter but also on the physicochemical properties of the contaminants. For heavy metals, a sequential extraction method can be first applied to evaluate the affinity of metals with the media surface [19,47,50,51]:

I. Acid-soluble fraction (f_{ex}, including water and acid soluble species). Acetic acid extraction: 0.5 g of dry sample was mixed with 20 mL of 0.11 M CH_3COOH (pH 3) for 16 h [19]. The mechanism relates to the release of positively charged ions by replacing with H^+.

II. Reducible fraction (f_{red}, including reducible species and bound to Fe/Mn oxides). Hydroxylammonium chloride extraction: said sediments from (I) were mixed with 20 mL of 0.1 M $NH_2OH-HCl$ (pH 2) for 16 h to create a weak reducing condition [19].

III. Oxidizable fraction (f_{ox}, including oxidizable species and bound to organic matter and sulfides). Hydrogen peroxide attack/ammonium acetate extraction: said sediments from (II) were treated with 5 mL 8.8 M H_2O_2 (premixing for 1 h, extraction at 85°C for 1 h and then evaporation of liquid at 85°C) followed by 25 mL of 1 M NH_4OOCCH_3 (pH 2) for 16 h to obtain an oxidizing phase [19,51]. In steps (I)−(III), a shaker that operated at 250 rpm can be used to keep the sediment in suspension during the extraction. Note that the supernatants from the sequential extractions (I)−(III) contain organic matter and therefore should be preserved by adding concentrated HNO_3 (in a ratio 1:4) and heated at 200 kPa (120°C) for 30 min prior to the measurement of metal contents [47].

IV. Residual fraction (f_r). This fraction can be calculated by either mass balance (i.e., $f_r = 1 - f_{ex} - f_{red} - f_{ox}$) or the same method for quantifying the total metal content. That is, ~0.5 g material and 10 mL of 7.3 M HNO_3 were heated at 200 kPa (120°C) for 30 min [51]. For the latter method, the recovery ($R = f_{ex} + f_{red} + f_{ox} + f_r$) is suggested to determine for the quality control.

Note that the abovementioned three-stage Community Bureau of Reference sequential extraction procedure is widely used for the acidic media because the carbonate concentration in the acidic media is minimal. In comparison, the Tessier sequential extraction procedure is appropriate for the speciation of the trace metals (including exchangeable, carbonate-bound, Fe/Mn oxide-bound, organic matter-bound, and residual fractions) in the neutral and basic media [52]. It is reported that, in electrodialytic remediation, the percentages of heavy metals removed from sediments (termed RE, $RE_i = (c_{0,i} - c_{t,i})/c_{0,i}$ where $c_{0,i}$ and $c_{t,i}$ stand for the initial concentration of metal i and that after remediation) were comparable with the sum of f_{ex} and f_{red} in the sediments before remediation [47]. Metals found in these electromigration

This book belongs to Badji Mokhtar Annaba University Central Library Copyright Elsevier 2025

accessible phases are expected to be mainly adsorbed on the solid phases (such as clay), bound to Fe and Mn hydrated oxides and/or bound (or coprecipitated) with carbonates [52]. In contrast to the other widely reported heavy metals (e.g., Zn and Pb), Cu forms stable organic complexes and sulfides (in the oxidizable phase) [20]. Therefore, a desorption order of Cd > Zn ~ Pb > Cu has been widely reported [20,27,45,47]. While the dissolution of carbonates and oxidation of organic matter that facilitate the desorption of metals in the exchangeable and oxidizable phases may occur during the electrodialytic remediation [40,47], low organic matter and carbonate contents are deemed the important properties of sediments for high-efficient metal extraction and removal from the contaminated media [20].

Similar to the removal of heavy metals, electrodialytic remediation is capable of extracting various cationic and anionic organic contaminants from the media [4,53]. A recent study demonstrates that per- and polyfluoroalkyl substances (PFASs) can also be efficiently removed from the contaminated soil [54] because the pK_a values perfluoroalkyl carboxylates (PFCAs) and perfluoroalkane sulfonates (PFSAs) are less than 2 [55], making the anionic PFASs suitable for electromigration. Results show that, in a three-compartment reactor (Fig. 8.3A), the negatively charged species including C3-C7 PFCAs and C4, C6, and C8 PFSAs migrate to the anode in an electrical field [54]. In comparison, the removal of uncharged PFASs (such as *N*-methyl perfluorooctane sulfonamide (MeFOSA)), perfluorooctane sulfonamidoacetic acid (FOSAA), and ethyl FOSAA (EtFOSAA) occurs as a result of the electro-osmotic flow from the anode to the cathode [54].

The calculations of the contaminant percentage removal (%) and the contaminant removal rate (e.g., %/min) are straightforward with the latter integrated with the influence of the remediation time. Under constrained conditions (e.g., for the same contaminated media), the removal rate has a positive relationship with the current (or voltage) applied to the system, and the ratio, current efficiency (Λ), can be evaluated in regard to the metal removal and the total charge input according to Faraday's law (Eq. 8.7) [12,56].

$$\Lambda = \frac{N_A \sum e_i \frac{(c_{0,i} - c_{t,i})m}{M_i}}{\int I dt} \times 100\% \tag{8.7}$$

where N_A is Avogadro's number, and e_i and M_i are the electron charge and the molar mass of metal *i*. The detailed speciation of the contaminants (e.g., $Cu^{2+}/Cu(OH)^+$, $Pb^{2+}/PbCl^+$) by using Visual MINTEQ simulations can provide a more accurate estimation of e_i for different metals [36,44]. Because the contaminants are always present at much lower concentrations compared to the major components (e.g., H^+, K^+, Cl^- and SO_4^{2-}), the current efficiency (typically <0.3%) [43] is inferior than those obtained in other deionization techniques [14,56]. As such, this results in a relatively high electrical cost ($E_m = 0.4-2.5$ kWh/kg-soil [41,46]). Take Cu as an example, where the

This book belongs to Badji Mokhtar Annaba University Central Library Copyright Elsevier 2025

electrical cost normalized to element removal is in a range of 20–120 kWh/g-Cu [57], which is around 1–2 orders of magnitude higher than that of electrochemical techniques for wastewater treatment [58]. However, the current efficiency in electrodialytic remediation can be further improved by optimization of the system design. The study by Rojo and Cubillos shows that the current efficiency reaches a maximum value of 1.3% by using three bipolar plates in the remediation compartment [42].

8.2.3 Mathematical simulation/modeling methods for electrodialytic remediation

The Section 8.2.2 discusses the critical parameters that may influence the electrodialytic remediation performance, but a (semi)quantitative understanding of the intrinsic relationship between these two parts is still missing. To solve this problem, multivariate methods have been recently introduced in electrodialytic remediation studies [25–27,40,41,45]. This chapter will therefore be focused on a review of these mathematical simulation/modeling methods that play an important role in not only process optimization in different media contamination scenarios but also prediction of single variable and multi-variable response to changes in media properties.

8.2.3.1 Univariate linear regressions

Essentially, data sets collected from electrodialytic remediation studies can be divided into two matrices, $\mathbf{X}$ and $\mathbf{Y}$. $\mathbf{X}$ contains the variables of media properties (e.g., mineral species and Ca^{2+}/HCO_3^- concentrations), design parameters (e.g., two-/three-compartment), and operating conditions (e.g., current, time, and L/S ratio). $\mathbf{X}$ is an $N \times K$ matrix with N and K presenting the numbers of variables and samples/experiments, respectively. In comparison $\mathbf{Y}$ is a matrix ($N \times M$) of variables in response, such as removal efficiencies and energy cost. A preliminary way to visualizing the relationship between $\mathbf{X}$ and $\mathbf{Y}$ data sets is to use scatterplots in a $K \times M$ arrangement. Fig. 8.5 shows an example of scatterplots describing the relationship between variables from 7×3 (current, L/S ratio, and water content) and 7×4 (Cu, Zn, Pb, and Cd removal rates) [20]. Data visualization is straightforward: that is, current and L/S ratio have more significant impacts on metals removal rates compared to water content (i.e., wet or air-dried). Nevertheless, univariate linear regressions only demonstrate the level of correlation between two independent variables. In most cases, we would like to simultaneously understand and predict $\mathbf{Y}$ based on multi-variables. Therefore, multiple linear regression (MLR) or principal component regression (PCR) for single variable in response, $N \times 1$ for $\mathbf{y}$, on one hand, and projection to latent structures (PLS) for multi-variables in response, $N \times M$ for $\mathbf{Y}$ models, on the other, have been introduced and developed for electrodialytic remediation.

This book belongs to Badji Mokhtar Annaba University Central Library Copyright Elsevier 2025

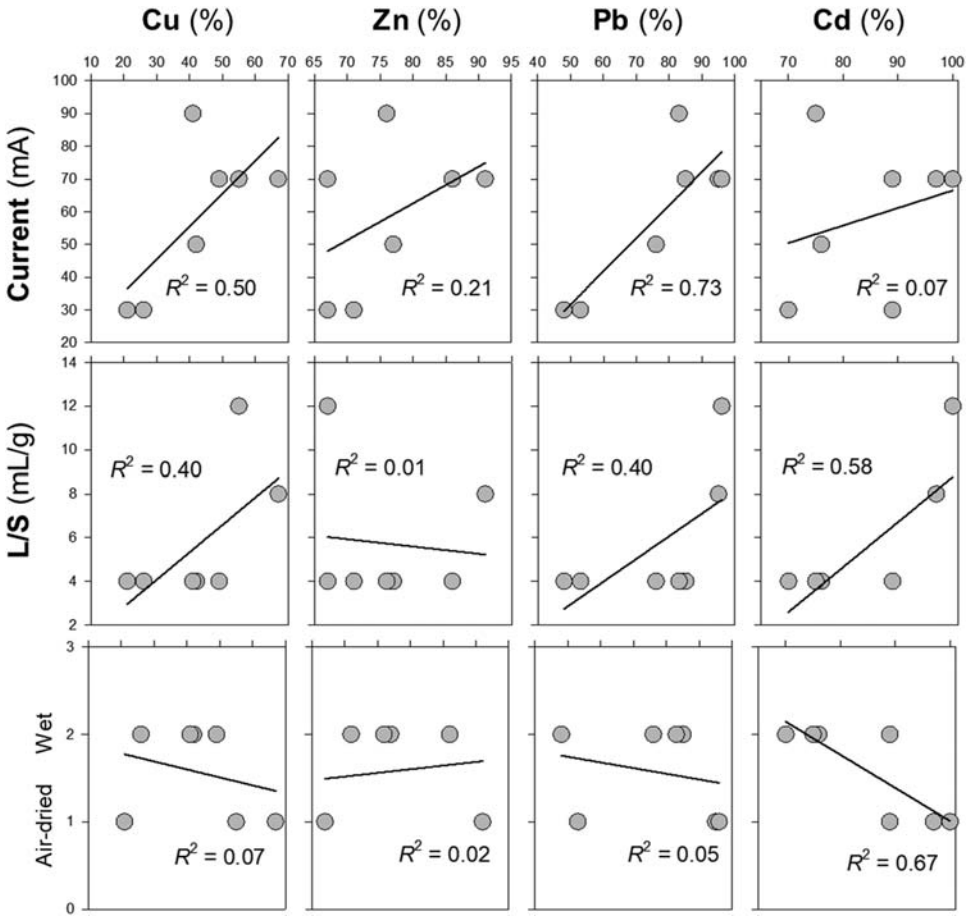

Figure 8.5 Scatterplots with univariate linear regressions describing the level of correlation between two independent variables from X and Y. X describes the parameter matrix with $K = 3$ (current, L/S ratio, and water content) and Y the removal rate in response with $M = 4$ (Cu, Zn, Pb, and Cd). *Data were retrieved from the study by G.M. Nystroem, L.M. Ottosen, A. Villumsen, Electrodialytic removal of Cu, Zn, Pb, and Cd from harbor sediment: influence of changing experimental conditions, Environ. Sci. Technol. 39 (2005) 2906–2911 [20] Copyright 2005 American Chemical Society.*

8.2.3.2 Multiple linear regression and principal component regression

The correlation between $\mathbf{X}$ and a single vector $\mathbf{y}$ (an $N \times 1$ vector) can be evaluated by MLR, that is, $\mathbf{y} = \mathbf{Xb}$. The solution vector $\mathbf{b}$ is obtained from $\mathbf{b} = (\mathbf{X}'\mathbf{X})^{-1}\mathbf{X}'\mathbf{y}$ with the variance of the solution estimated to be $\nu(\mathbf{b}) = (\mathbf{X}'\mathbf{X})^{-1}\ S_E{}^2$ [59]. A classical solution to $\mathbf{Y}$ (an $N \times M$ matrix) is to build M different least squares models. Taking data from Fig. 8.5 as an example, MLR can be established between $\mathbf{X}$ and individual $\mathbf{y}$, that is, Cu, Zn, Pb, or Cd removal rates (Cu removal rates in Fig. 8.6A). While the

This book belongs to Badji Mokhtar Annaba University Central Library Copyright Elsevier 2025

(A) Summary of MLR output

Regression Statistics	
Multiple R	0.83
R Square	0.69
Adjusted R Square	0.38
Standard Error	12.64
Observations	7

ANOVA

	df	SS	MS	F	Significance F
Regression	3	1055	351.67	2.20	0.27
Residual	3	479	159.67		
Total	6	1534			

	Coefficients	Standard Error	t Stat	P-value
Intercept	7.50	31.22	0.24	0.83
X Variable 1	0.40	0.27	1.51	0.23
X Variable 2	2.25	2.60	0.87	0.45
X Variable 3	-0.50	14.54	-0.03	0.97

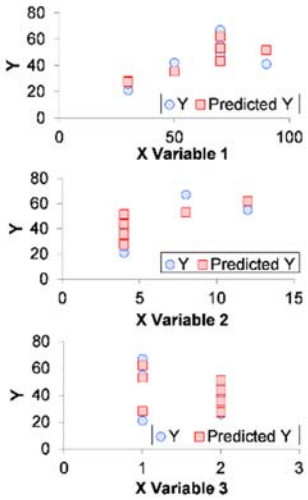

(B)

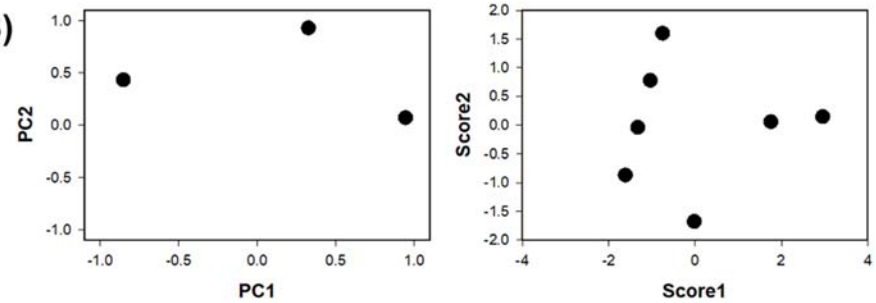

(C) Summary of PCR output

Regression Statistics	
Multiple R	0.83
R Square	0.69
Adjusted R Square	0.53
Standard Error	10.98
Observations	7

ANOVA

	df	SS	MS	F	Significance F
Regression	2	1051.72	525.86	4.36	0.10
Residual	4	482.28	120.57		
Total	6	1534			

	Coefficients	Standard Error	t Stat	P-value
Intercept	43.00	4.15	10.36	0.00
X Variable 1	5.73	2.60	2.20	0.09
X Variable 2	8.32	4.23	1.97	0.12

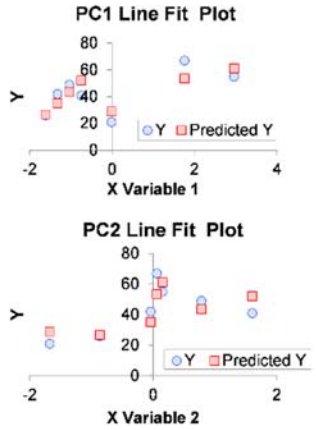

Figure 8.6 (A) Example of MLR established between X ($N = 7$, $K =$ current, L/S ratio, and water content) and y (Cu removal). Variables 1, 2, and 3 stand for current, L/S ratio, and water content, respectively. For variable 3 (water content), assume that air-dried = "1" and wet = "2." (B) Principal components (PC) of variables (1, 2, and 3) and PC scores of all samples ($N = 7$). (C) Principal component regression (PCR). *Data were retrieved from the study by G.M. Nystroem, L.M. Ottosen, A. Villumsen, Electrodialytic removal of Cu, Zn, Pb, and Cd from harbor sediment: influence of changing experimental conditions, Environ. Sci. Technol. 39 (2005) 2906–2911 [20] Copyright 2005 American Chemical Society.*

This book belongs to Badji Mokhtar Annaba University Central Library
Copyright Elsevier 2025

case study in Fig. 8.6A shows that the regression model passes ANOVA test ($F >$ Significance F) with reasonably good prediction, none of the individual variables is significant at $\alpha = 0.05$. Although the MLR model may be improved via quality control (e.g., abatement of the least relevant variable, i.e., "water content" and outliers), its defects including assumption of $\mathbf{X}$ to be noise-free and incapability of handling strongly correlated columns in $\mathbf{X}$ and/or missing values in $\mathbf{X}$ remain [59].

In comparison, PCR replaces the columns in $\mathbf{X}$ with their uncorrelated score vectors from principal component analysis (PCA). Mathematically, PCR is processed by the generation of $\mathbf{T}$ score matrix ($\mathbf{T} = \mathbf{XP}$, $\mathbf{P}$ is a $K \times A$ loading matrix) followed by obtaining the solution vector $\mathbf{b} = (\mathbf{T}'\mathbf{T})^{-1}\mathbf{T}'\mathbf{y}$ from $\mathbf{y} = \mathbf{Tb}$. The advantages of PCR over MLR are as follows: (1) the columns in $\mathbf{T}$ are orthogonal to each other, ensuring the independence for the least-squares calculations; (2) $\mathbf{X}$ is not required to be noise-free/complete because PCA has separated the noise from $\mathbf{X}$; and (3) for PCR, there is no need for consistency check and even less need for quality control [59]. Principal component (PC) loadings and scores in quadrants can be used to evaluate the consistency of initial variables and samples respectively (Fig. 8.6B). Always abnormal operation/settings appear as outliers in the score plots and the squared prediction error plots. In Fig. 8.6B, current has a significantly positive relationship with PC2 while L/S ratio is closely correlated with PC1. In contrast, water content is negatively related to PC1 but positively to PC2. Provided that there is an internal relationship among the N samples/tests, the score matrix can be used to evaluate the design of the electrodialytic remediation experiment. Results in Fig. 8.6C show that PCR can build a better correlation between $\mathbf{X}$ and $\mathbf{y}$ regarding higher R_{adj}^2, higher F, and variable coefficients at more significant levels. Nevertheless, PCR focuses on a single variable in response. In the next section, we will review the projection to latent structures (PLS) that can build a single regression model for multiple variables in $\mathbf{X}$ and $\mathbf{Y}$.

8.2.3.3 Projection to latent structures

The PLS (also known as partial least squares regression procedure) has been applied as a reliable tool for assessment of the comparative experimental variable importance as well as the prediction of treatment performance and specific operating conditions in the electrodialytic remediation process [26]. In PLS, the latent variables should best explain $\mathbf{X}$ and $\mathbf{Y}$, so that these latent variables have the strongest possible relationship between $\mathbf{X}$ and $\mathbf{Y}$ [59]. R^2 values ($R^2 = 1 - \text{Var}(\mathbf{E}_a)/\text{Var}(\mathbf{X}_{a=1})$, where $\mathbf{E}_a$ represents the residuals) can be calculated to assess the variability explained with each latent variable. Note that the scores of PLS are likely to be different from those of PCA because the PCA scores only explain the variance in $\mathbf{X}$ while the PLS scores can also explain $\mathbf{Y}$ at a maximum relationship between $\mathbf{X}$ and $\mathbf{Y}$.

PLS regression can be performed by nonlinear iterative partial least squares algorithm on commercial software such as SIMCA and SPSS Statistics (which also requires

This book belongs to Badji Mokhtar Annaba University Central Library Copyright Elsevier 2025

NumPy and SciPy Python libraries). The proportion of variance explained (by the latent factor) can be calculated to determine the number of the latent variables to choose. To assess the reliability and stability of the calculated PLS models, the correlation factor (R2Y) that is a measure of the fraction of **Y** explained by the model and predictive power (Q2) that is an estimate of the reliability of the model can be calculated [26,40].

Fig. 8.7 shows an example of a PLS model to evaluate the influence of multivariables on energy consumption in both the stirred and the stationary setup [41]. The variable importance in the projection (VIP) values describe the absolute importance of an individual variable in the model under its correlation to both **X** and **Y** [27,51]. VIP values >1 indicate the parameters have a high influence on the response, with VIP values of $0.5-1$ or <0.5, respectively, presenting a moderate and low influence [25,40,41]. In the stirred setup (Fig. 8.7A), all the operating parameters (current: $4-10$ mA, sorted (<2 mm)/nonsorted (<4 mm) and time: $7-35$ days) are significant, and remediation operation at a higher current and/or a longer time results in an increase in E_m (Fig. 8.7B) [41]. Sorted media with a smaller particle size (<2 mm) require a lower energy cost for remediation, which is likely as a result of the higher surface charge density of smaller-size particles that demonstrate a lower resistance for charge and ion transfer between the electrodes [46,60]. In comparison, Fig. 8.7A shows that the media properties (i.e., element composition and organic matter content) play a more important role in determining the energy cost for remediation in the stationary setup [41]. The metal element contents (Al, K, Fe, Mg, Mn, and Cu) have the highest VIP values, and their higher concentrations will likely result in a lower transfer resistance and lower energy input (Fig. 8.7B). Although higher surface charge density is expected for finer particles with bound organic matter, results of PLS model suggest that the packing of the media under the stationary setup elevates the resistance (Fig. 8.7B) [41]. Using the developed multivariate model can provide an insight to the process design and performance prediction for in situ and ex situ remediation.

8.2.4 Emerging applications of electrodialytic remediation

8.2.4.1 Use of flow electrodes in electrodialytic remediation

To date, most studies in electrodialytic remediation use static electrodes (Table 8.2). While these electrodes have been shown viable in removing various contaminants from different media, concerns on the limited surface area in contact with the media and then low removal rate remain. To address this issue, a soil flow-electrode capacitive deionization (Fig. 8.8) has been developed by Xu et al. [61] with the use of a flow electrode [12,56,62,63] not only enabling a decrease in the charge transfer resistance by forming carbon aggregates but also providing a large number of surface sites for heavy metal adsorption. The results show that the electrode content (i.e., the carbon content) has a significant influence on the extraction of Cd from the media at an L/S ratio

This book belongs to Badji Mokhtar Annaba University Central Library Copyright Elsevier 2025

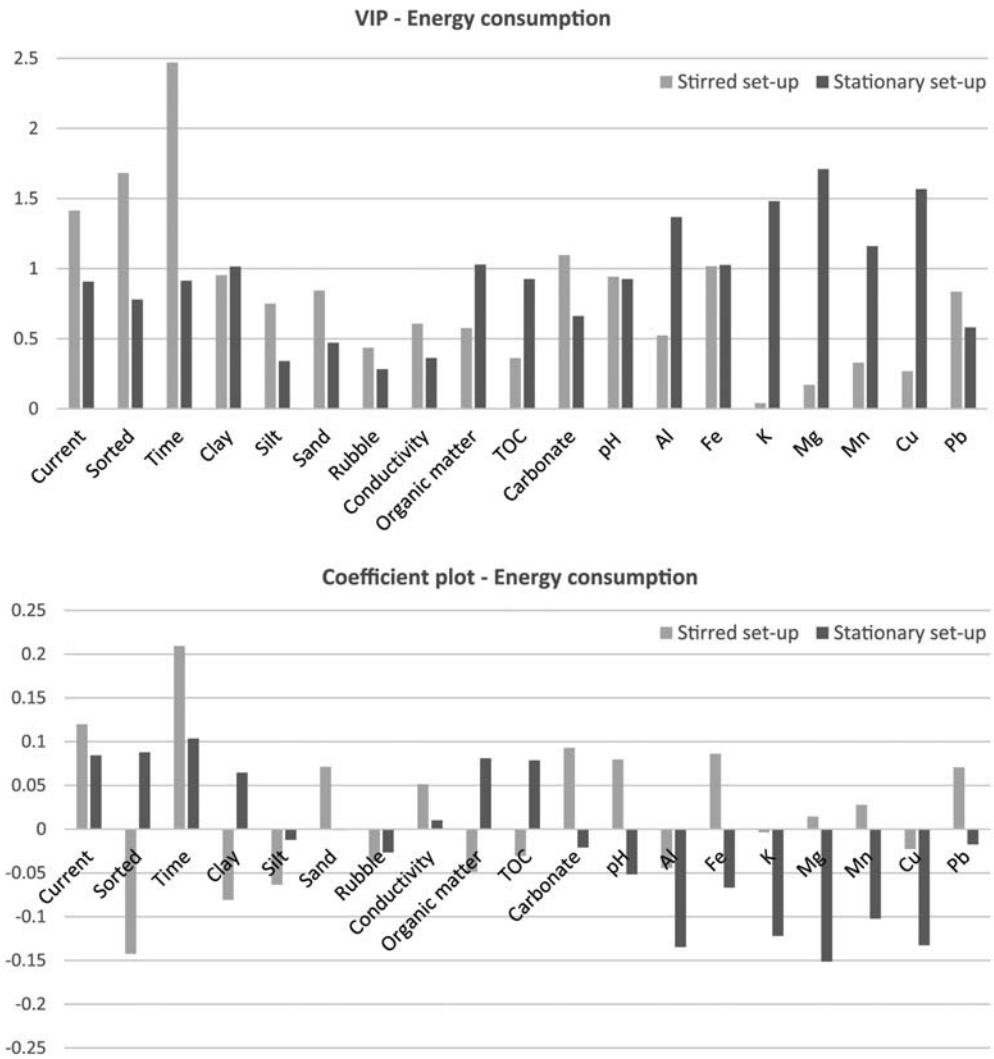

Figure 8.7 VIP plot and coefficient plot of PLS model for multivariate analysis of E_m in electrodialytic remediation of soils. Clay, silt, sand and rubble stand for the fraction with a size of "<2 μm," "2–63 μm," "63 μm–1 mm" and ">1 mm" respectively. "Sorted" is a discrete variable for stirred and stationary setup. In the coefficient plot, values of >0 indicate a positive relationship vis-à-vis E_m while <0, a negative relationship. *Reproduced from the work by K.B. Pedersen, P.E. Jensen, L.M. Ottosen, J. Barlindhaug, Applying multivariate analysis for optimising the electrodialytic removal of Cu and Pb from shooting range soils, J. Hazard. Mater. 368 (2019) 869–876 [41] Copyright 2019 Elsevier.*

This book belongs to Badji Mokhtar Annaba University Central Library Copyright Elsevier 2025

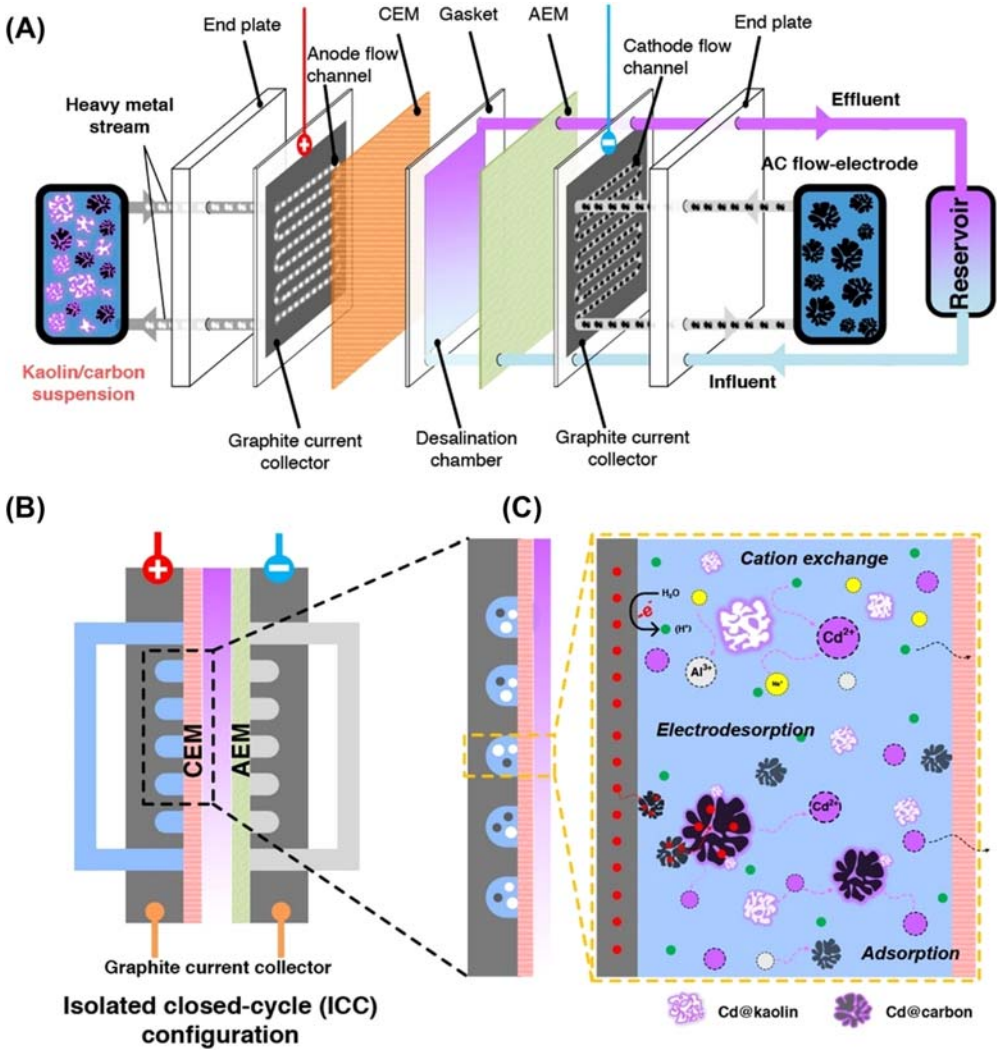

Figure 8.8 Schematic representation of (A) a soil flow-electrode capacitive deionization (S-FCDI) system. (B) A cross-sectional view of the S-FCDI system. (C) Occurrence, transformation and fate of Cd in the anode chamber. *Reproduced from the work by L. Xu, C. Yu, Y. Mao, Y. Zong, B. Zhang, H. Chu, et al., Can flow-electrode capacitive deionization become a new in-situ soil remediation technology for heavy metal removal? J. Hazard. Mater. 402 (2021) 123568 [61] Copyright 2021 Elsevier.*

of 4 [61]. Under acidification, the higher affinity of Cd with the negatively charged carbon surface results in the transfer of Cd from the media (kaolin) to the flow electrode (Fig. 8.8). Once the adsorption capacity is exhausted, the adsorbed Cd can be released via reversal of the polarity and then to migrate across a CEM to the brine [61]. Under the optimized condition (with carbon content = 50 g/L, $i = 0.35$ mA/cm^2, initial pH = 3.2 and initial

This book belongs to Badji Mokhtar Annaba University Central Library Copyright Elsevier 2025

electrolyte concentration = 8.6 mM), >80% Cd can be removed from the media at a relatively low E_m (22.7 kWh/kg-Cd removed) and a minimum loss of Al [61]. These findings indicate that the use of flow electrodes in electrodialytic remediation process can be a promising, cost-effective method for practical applications though further studies on (1) the influence of the residual electrode materials in the remediated media and (2) the stability of the flow electrode in the continuous operation are required.

8.2.4.2 Electrodialytic processes for resource recovery and reactant delivery

In addition to the applications in remediation, the electrodialytic process can be used for resource recovery from the waste. Phosphorous (P) is an essential nutrient without a substitute. With regard to the high P concentrations in municipal wastes (e.g., >10 wt.% in incinerated sewage sludge ashes), there is a recent interest in P recovery by using an electrodialytic process. The study by Guedes et al. shows that with the addition of sulfuric acid, P in sewage sludge ashes can be efficiently transferred to the anolyte while the motion of heavy metals to the other electrode compartment avoids the second contamination with which the conventional treatment techniques may encounter [17]. In total, 60%–70% of P from the ashes can be recovered in a dominant form of orthophosphate in the anolyte [17]. Compared to the remediation studies, the resource recovery process needs more attention as to the fate of nutrients and the recovery rate rather than the removal rate. H_3PO_4 is a major P species at a lower pH ($<pK_{a1} = 2.1$) and this may result in the migration of P to the cathode [64] probably due to the electro-osmosis effect. The coexistence of P and heavy metals in the catholyte requires an extra separation step for P recovery. Moreover, the electrodialytic process can be applied for the recovery of rare earth elements (REE) [65]. By using the similar steps to those of remediation (i.e., solubilization, mobilization, and removal/recovery in the catholyte), the study by Couto et al. shows that around 70% of REE can be extracted from the coal ash under an optimal condition [65]. The recovery was in a range of 55%–62% for Tb and Dy, and 74% for Nd [65]. While further optimization of the operating parameters and an improvement of the element selectivity are essential to make the electrodialytic process more competitive with other widely used recovery methods, these studies open up perspectives on how the best resource can be recovered from the waste via electrochemical technologies.

Electrodialytic (or electrokinetic) delivery of reactants is a reversal of the conventional remediation process with the electrokinetic process distributing reactants (from the electrode compartment) to the low-permeability porous media [66]. Decontamination occurs where the in situ reaction between the reactants and the contaminants takes place. Fig. 8.9A gives a schematic setup of an electrodialytic delivery system [66]. The delivery of a colored charged tracer, MnO_4^-, and its spatial distribution and mixing behavior with the surrounding pore water depend on the background electrolyte concentrations (Fig. 8.9B) [66]. Moreover, a combination of the transport experiments and process-based modeling reveals that the

This book belongs to Badji Mokhtar Annaba University Central Library Copyright Elsevier 2025

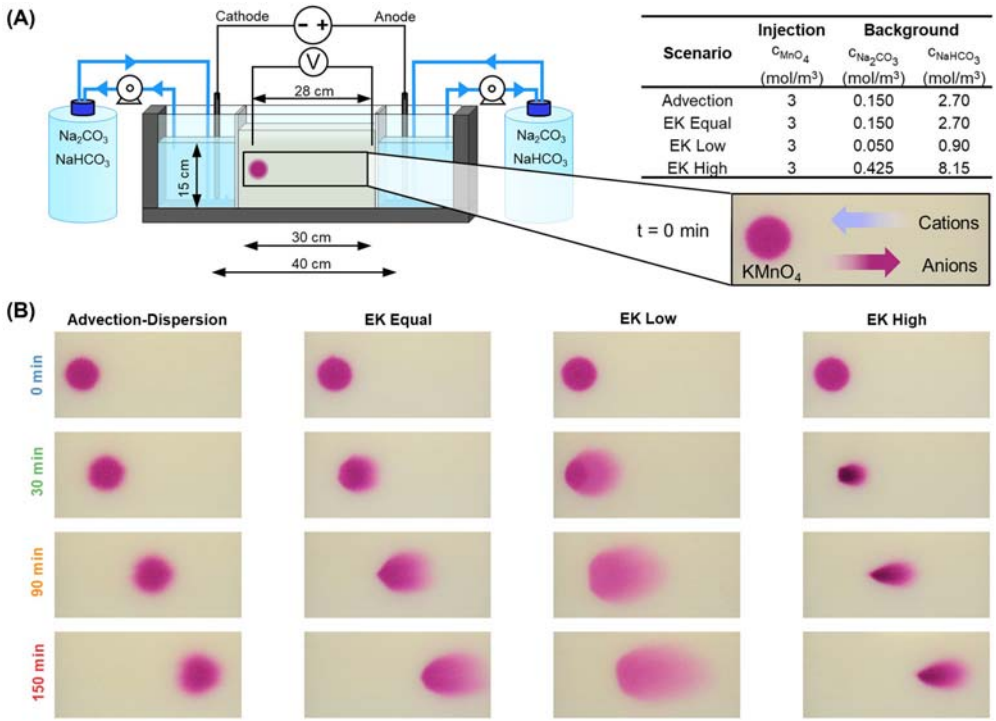

Scenario	Injection c_{MnO_4} (mol/m³)	Background $c_{Na_2CO_3}$ (mol/m³)	Background c_{NaHCO_3} (mol/m³)
Advection	3	0.150	2.70
EK Equal	3	0.150	2.70
EK Low	3	0.050	0.90
EK High	3	0.425	8.15

Figure 8.9 (A) A schematic setup of the electrokinetic delivery system and a summary of background electrolyte concentrations used in the transport experiments. (B) Images depicting the migration of the MnO_4^- plume in said transport experiments. *EK*, Electrokinetic. *Reproduced with permission from R. Sprocati, A. Gallo, R. Sethi, M. Rolle, Electrokinetic delivery of reactants: pore water chemistry controls transport, mixing, and degradation, Environ. Sci. Technol. 55 (2021) 719–729 [66] Copyright 2021 American Chemical Society.*

microscopic charge interactions in the pore water are crucial to the transport of the injected plumes and the reactions with the noncharged organic matter initially present in the porous domain [66]. This novel delivery strategy provides insight to the application of the electrodialytic processes for in situ remediation of contaminated soil and groundwater.

8.3 Electrocatalytic remediation

8.3.1 Fundamentals

In contrast to the electrodialytic remediation that mainly relies on the electrodialysis and non-Faradaic reactions to remove the contaminant, the electrocatalytic membrane

This book belongs to Badji Mokhtar Annaba University Central Library Copyright Elsevier 2025

technology involves either electrocatalytic oxidation treating water contaminated by industrial compounds (such as phenol) [67,68] or reduction of aqueous oxyanions (such as nitrate) from fertilizer runoff [69]. The electrochemical membrane (e.g., an IEM or a proton conducting ceramic membrane [7]) acts as a separator to avoid the short-circuiting of the anode and cathode as well as acting as a proton bridge to facilitate the charge transfer especially in a diluted condition. Fig. 8.10A shows an ideal flow diagram that couples the oxidation of organic compounds with the reduction of other pollutants (e.g., nitrate and perchlorate) [70]. Mechanisms involved in the redox reactions will not be discussed in detail in this section because they are expected to have been well reviewed in previous chapters (e.g., Chapter 2: Fundamentals of Electrochemical Membrane Technology). With regards to the ease of maintenance and the low-cost requirements, the flow-through configuration is rarely used, and the feed solutions always pass through the system in a flow-by mode (Fig. 8.10A). In addition, attention should be paid to the activity, selectivity, and stability of the electrode catalysts in a dilute (typically ionic strength $<10-20$ mM), but complicated matrix (containing competitive ions at relatively higher concentrations).

8.3.2 3D electrochemical system treating low ionic-strength water

For anodic oxidation, the main target for the indirect oxidation reactions is to generate more hydroxyl radicals (•OH) at a low energy cost. Theoretically, increasing the ionic strength can reduce the internal resistance of a conventional electrocatalytic reactor in which the electrodes and the feed solution are arranged in a flow-between configuration (Fig. 8.10B). This can facilitate the flow of ions to the oppositely charged electrodes. However, this method has low operability when dealing with real surface/ground water. More importantly, the introduction of excessive salts elevates the oxidation of chlorides (from NaCl) and the resultant oxidants including hypochlorous acid and chlorate may contribute to the formation of toxic disinfection byproducts [37,72]. Alternatively, one may decrease the space between the electrodes to decrease the internal resistance and then the energy input [71,73]. However, this method will result in a significant increase in the hydraulic loss when the feed solution passes through the ultra-thin spacer between the electrodes, which leads to a higher pumping energy cost and risks of blocking/fouling.

To solve this problem, the group led by Professor John Crittenden developed a three-dimensional (3D) electrochemical system (Fig. 8.10B) that is capable of degrading organic pollutants in low-ionic-strength streams at a reduced energy cost [71]. A widely used proton exchange membrane (PEM), Nafion N-117, served as a substitute to the electrolyte media and was placed between the porous anode and the cathode. This design allowed the protons generated on the anode (via water oxidation) in efficiently passing through the PEM to the cathode on which the hydrogen evolution reaction and/or oxygen

This book belongs to Badji Mokhtar Annaba University Central Library Copyright Elsevier 2025

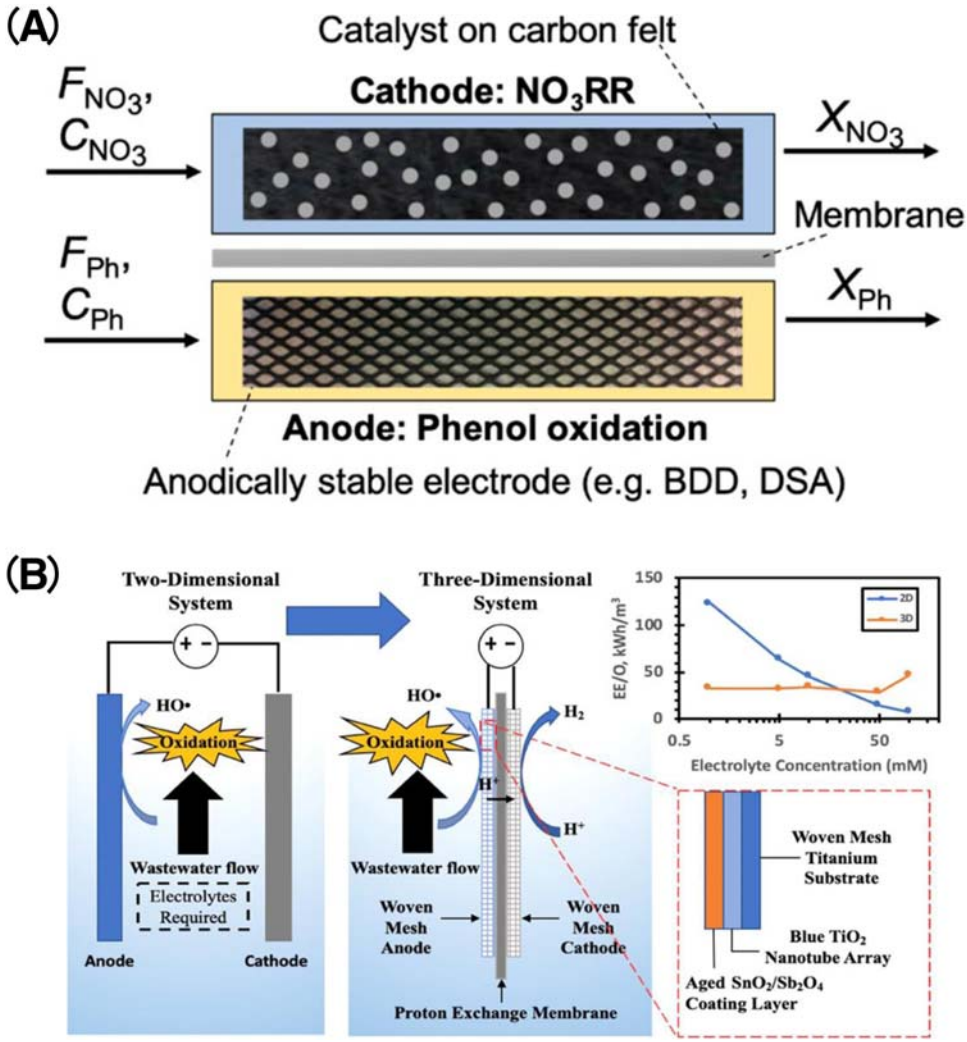

Figure 8.10 Decontamination/remediation mechanisms and parameters of electrocatalytic remediation process (A) A flow diagram describing oxidation (of phenol) and reduction (of nitrate) occurring in an electrocatalytic membrane system for remediation. F_i, C_i, and X_i stand for the flow rate, influent concentration, and conversion of species *i*. *BDD*, Boron-doped diamond; *DSA*, dimensionally stable anodes. (B) Comparison of two-dimensional and three-dimensional electrochemical reactors: configuration and energy costs under various electrolyte concentrations. *Reproduced from the work by (A) N. Singh, B.R. Goldsmith, Role of electrocatalysis in the remediation of water pollutants, ACS Catal. 10 (2020) 3365–3371 [70]. Copyright 2020 American Chemical Society. (B) Reproduced from the work by X. Meng, Z. Chen, C. Wang, W. Zhang, K. Zhang, S. Zhou, et al., Development of a three-dimensional electrochemical system using a blue TiO_2/SnO_2–Sb_2O_3 anode for treating low-ionic-strength wastewater, Environ. Sci. Technol. 53 (2019) 13784–13793 [71] Copyright 2019 American Chemical Society.*

This book belongs to Badji Mokhtar Annaba University Central Library Copyright Elsevier 2025

reduction reaction occur (Fig. 8.10B). In a 3D electrochemical reactor, the protons generated on the anode facing the electrolyte need to penetrate the anode. Since most semiconductors are not proton conductible, this requires both electrodes to be porous. Therefore, Meng et al. used a nanocomposite anode that was prepared from a titanium woven wire mesh [71]. Blue-black TiO_2 nanotubes that have a high band gap ($\Delta E = 3.3$ eV) [74] were formed on the titanium mesh, with an aged $SnO_2-Sb_2O_3$ layer covering the base material. The high band gap of the nanocomposite renders the one-electron transfer reaction ($H_2O \rightarrow \bullet OH$, $\Delta G_{OH} = 2.38$ eV vs reversible hydrogen electrode) more thermodynamically favorable, that is, once OH* is formed as a result of the cleavage of the HO−H bond on the anode [75], it is readily desorbed and transforms to the solvated hydroxyl radical, $\bullet OH_{(aq)}$ [76,77]. Likewise, a stainless-steel wire mesh was used by Meng et al. as a starting cathode [71].

Table 8.3 compares the cell voltage of a 2D and of a 3D system at an applied current density of 30 mA/cm^2. While the voltages of both systems are influenced by the conductivity of the electrolyte, the 3D system has a significantly better performance under various concentrations. Especially, the current flow of the 2D system in DI water is not detectable from that in the surface water decreased from the set value (30 mA/cm^2) to 20 mA/cm^2 due to the cell voltage exceeding the maximum output of the power supply (60 ± 1 V) [71]. In comparison, the applied current density is achievable in the 3D electrochemical system even in a DI stream (with a low conductivity of μS/cm) (Table 8.3). The cell voltage of the 3D system is 23.8%−75.7% lower than that of the 2D system in an electrolyte concentration ranging from 10 to 1 mM Na_2SO_4. The decontamination performances of the 2D and the 3D system were evaluated by the

Table 8.3 Comparison of the cell voltages of the 2D and 3D systems in the electrolyte media of various concentrations.[a]

Electrolyte (Na_2SO_4, mM)	Conductivity (μS/cm)	Voltage (V)		3D voltage reduction (%)
		2D	3D	
DI water	4	ND	27.3	ND
Surface water	112.5	>60.4	15.83	N/A
1	260	38.49	9.35	75.71
5	1074	13.89	7.47	46.22
10	1964	9.65	7.35	23.83
50	8740	5.58	5.42	2.87
100	16,210	5.32	5.26	1.13

[a]*ND*, Not detectable. For the 2D system in DI water, the current in the circuit was negligible and the cell voltage was not detectable. For the 2D system in the surface water, the applied current density was decreased to 20 mA/cm^2 because the voltage exceeded the maximum output of the power supply.
Source: Reproduced from the work by X. Meng, Z. Chen, C. Wang, W. Zhang, K. Zhang, S. Zhou, et al., Development of a three-dimensional electrochemical system using a blue $TiO_2/SnO_2-Sb_2O_3$ anode for treating low-ionic-strength wastewater, Environ. Sci. Technol. 53 (2019) 13784−13793 [71] Copyright 2019 American Chemical Society.

This book belongs to Badji Mokhtar Annaba University Central Library Copyright Elsevier 2025

degradation of an aromatic model compound, benzoic acid [71]. Electrical efficiency per log order reduction (EE/O) is an important parameter that considers the influence of the concentration difference (Eq. 8.8) compared to Eq. (8.6) [78,79]:

$$EE/O = \frac{I\Delta U_{\text{cell}} t}{V_R \log\left(\frac{c_0}{c_f}\right)} \tag{8.8}$$

where ΔU_{cell} (i.e., ΔV_{cell} in Eq. 8.6) is the voltage drop between electrodes (V). V_R is the volume of the anode tank (m^3). Fig. 8.10B shows that the 3D system has a lower EE/O at lower electrolyte concentrations (<20 mM) than the 2D system. For instance, the energy cost of the 3D system is only 27.2% that of the 2D system in 10 mM Na_2SO_4 solution. However, when the stream has a high ionic concentration (≥50 mM) and the ion transfer in the electrolyte media is not rate limiting, the 3D system is less energy efficient compared to the 2D system (Fig. 8.10B), probably because the diffusion coefficient of ions in the PEM is smaller than that in the bulk solution. Overall, the 3D electrochemical system is a promising alternative to environmental remediation under low-ionic-strength conditions.

8.3.3 Proton-conducting membrane cell for H_2S-H_2O coelectrolysis

The electrocatalytic membrane technology can be alternatively used for toxic dissolved gas removal from an ecological system. An example is the proton-conducting membrane cell for H_2S-H_2O coelectrolysis that has been developed to covert H_2S to H_2SO_4 in sea water [7,80]. H_2S occurs in great quantities in natural sources, and its production in sea water is as a result of a complex microbial carbon-sulfur cycle [81]. Under an ideal condition, H_2S is generated in the anoxic region of the seas (e.g., 9.5 mg/L at around 1500 m depth of the Black Sea [82]) with any H_2S overflow being converted to sulfate by dissolved oxygen in the interface layer that exists between the oxygenated top layer and the anoxic region. However, unexpected depletion of the dissolved oxygen in the top layer would decrease the depth of the interface layer, resulting in the risk of destroying the oxygenated environment in the top layer. H_2S-rich waters forcing their way to the surface has been observed in the Marmara Sea and the Mediterranean Sea [83], which poses great threats to the aqueous habitants.

In addition to the widely used adsorption and stripping processes to extract H_2S from the sea water [84], Ipsakis et al. [7,80] proposed a proton-conducting membrane cell for H_2S-H_2O coelectrolysis (Fig. 8.11) based on the concept of sulfur fuel cell. Fig. 8.11 shows that the reactor comprised a proton-conducting solid electrolyte membrane ① sandwiched between the porous electrodes at both sides. Y-doped barium zirconate ($BaZr_{0.85}Y_{0.15}O_{3-\delta}$, BZY) prepared by using a solid state reaction method [85] was used as a starting proton-conducting solid electrolyte [80]. Transition metal mono- and bi-metallic (Co, Ni, Fe, Cu)

This book belongs to Badji Mokhtar Annaba University Central Library Copyright Elsevier 2025

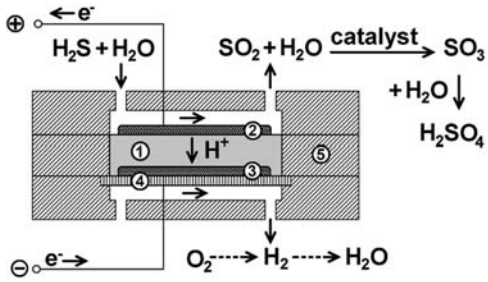

Figure 8.11 Schematic representation of the proton-conducting membrane cell for H_2S-H_2O coelectrolysis. ① Proton-conducting membrane, ② anode, ③ cathode, ④ porous support plate, and ⑤ the metallic case that forms two gas flow channels above the electrodes. *Reproduced from the work by D. Ipsakis, T. Kraia, G.E. Marnellos, M. Ouzounidou, S. Voutetakis, R. Dittmeyer, et al., An electrocatalytic membrane-assisted process for hydrogen production from H_2S in Black Sea: preliminary results, Int. J. Hydrog. Energy 40 (2015) 7530–7538 [80] Copyright 2015 Elsevier.*

catalysts, supported on CeO_2, were synthesized and used as the anode material (②in Fig. 8.11). For the cathode (③ in Fig. 8.11), $La_{0.6}Sr_{0.4}Co_{0.2}Fe_{0.8}O_{3-\delta}$ (LSCF) was used as the active component loaded on a porous Pt film [80]. A porous Al_2O_3 plate (④ in Fig. 8.11) was placed to support the cathode. The channel structure in the metallic case ⑤ enables the uniform gas flows in front of both electrodes.

Fig. 8.12 shows the process flow diagrams of the operation of the proton-conducting membrane cells for H_2S-H_2O coelectrolysis. Essentially, three steps (i.e., seawater pumping and preparation of concentrated H_2S mixtures, H_2S-H_2O coelectrolysis in the proton conducting membrane reactor, and H_2SO_4 production) are required to complete the reactions [7,80]. Another two steps, that is, the purification of the electrolyzer effluent, and heat and energy management, can be added to improve the efficiency [7]:

- *Step 1: Pumping and preparation of concentrated H_2S mixtures.* Seawater with H_2S concentration of 14 ppm is delivered to the system, and a series of heat exchangers (HXs) and turbine (TUR) are used to produce concentrated H_2S/H_2O mixtures [7,80]. In a simplified mode (Fig. 8.12A), the waste heat from the return flow is recovered by a heat exchanger (E1, or HX1 in Fig. 8.13) and delivered to the influent seawater. In a more complete system [7], further heating of the inlet (Fig. 8.13) is performed at HX-2. In the scale-up system (Fig. 8.13), the flue gases pass through HX-2 and HX-3 and, finally, end up in a gas turbine (TUR-1) for power generation [7]. Lastly, the heated water containing a mixture of vapor-liquid is separated in the equilibrium tank (Fig. 8.12) with the gas stream being concentrated up to a 1.0 v/v% H_2S/H_2O and the hot liquid waste returned to E1 or HX1. In the more complete system (Fig. 8.13), the two-stage heat exchangers including HX-3 and ELEC-HX-1 are implemented to further heat the gas stream to 850°C temperature.

This book belongs to Badji Mokhtar Annaba University Central Library Copyright Elsevier 2025

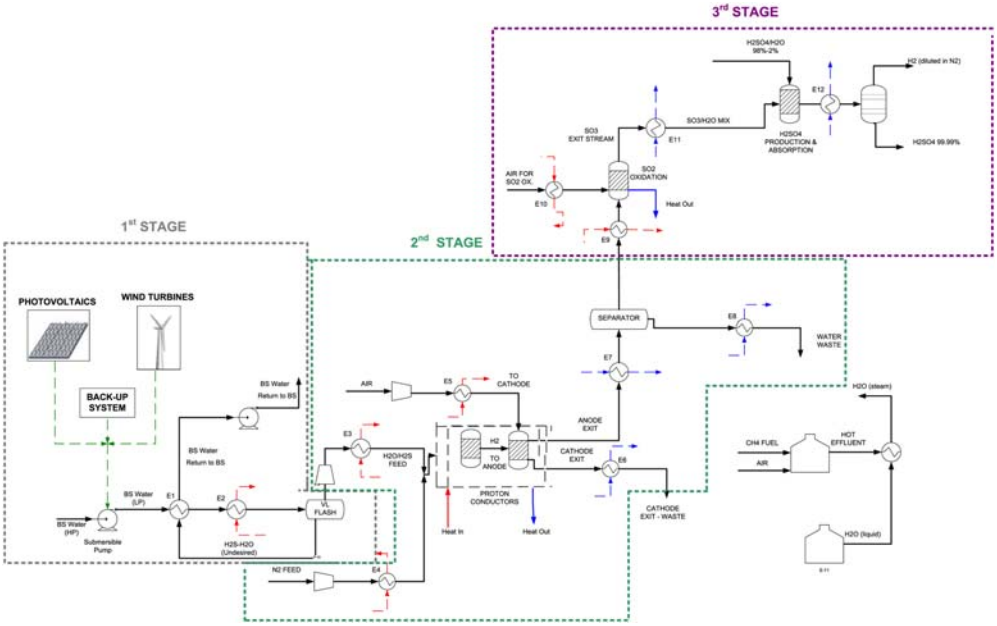

Figure 8.12 An integrated system diagram describing three-stage processes for H_2S-H_2O coelectrolysis. First stage: pumping and preparation of concentrated H_2S mixtures; second stage: proton conducting membrane reactor for H_2S-H_2O coelectrolysis; third stage: H_2SO_4 production and waste management (dash lines connected to E2, E3, E4, E5, E9 and E10: heat supply; dash lines connected to E6, E7, E8, E11 and E12: heat recovery). E (i.e., E1) stands for heat exchanger. *Reproduced from the work by D. Ipsakis, T. Kraia, G.E. Marnellos, M. Ouzounidou, S. Voutetakis, R. Dittmeyer, et al., An electrocatalytic membrane-assisted process for hydrogen production from H_2S in Black Sea: preliminary results, Int. J. Hydrog. Energy 40 (2015) 7530–7538 [80] Copyright 2015 Elsevier.*

- *Step 2: H_2S-H_2O coelectrolysis.* The proton-conducting membrane cell is operated at 850°C temperature under galvanostatic mode (Fig. 8.12). The electrochemical decomposition of inlet H_2S and H_2O (i.e., $H_2S \rightarrow H_2 + S$; $H_2O \rightarrow H_2 + 0.5O_2$) as well as resultant H_2 (i.e., $H_2 \rightarrow 2\,H^+ + 2e^-$) occurs in the electrolyzer. Formation of the SO_2 is also expected via either direction conversion ($H_2S + 2H_2O \rightarrow 3H_2 + SO_2$) or sulfur oxidation ($S + O_2 \rightarrow SO_2$) [7]. For the cathode outlet, it is discharged after heat exchange (Fig. 8.12) in a simplified system. Multiple-stage heat exchangers (HX-4: an air cooler and HX-5: a water cooler) are used in the more complete system (Fig. 8.13), which allows ~800°C temperature reduction and recovery of H_2 in gas cylinders.
- *Step 3: H_2SO_4 production and waste management.*

The anode outlet gas is delivered to a heat exchanger (E9 in Fig. 8.12 and HX-6 in Fig. 8.13) to maintain the gas temperature at 450°C before entering the SO_2 oxidizer ($SO_2 + 0.5O_2 \rightarrow SO_3$). In a simplified system, the SO_3 stream is cooled from the reaction temperature (450°C) to ~200°C in a heat exchanger (E11 in

This book belongs to Badji Mokhtar Annaba University Central Library Copyright Elsevier 2025

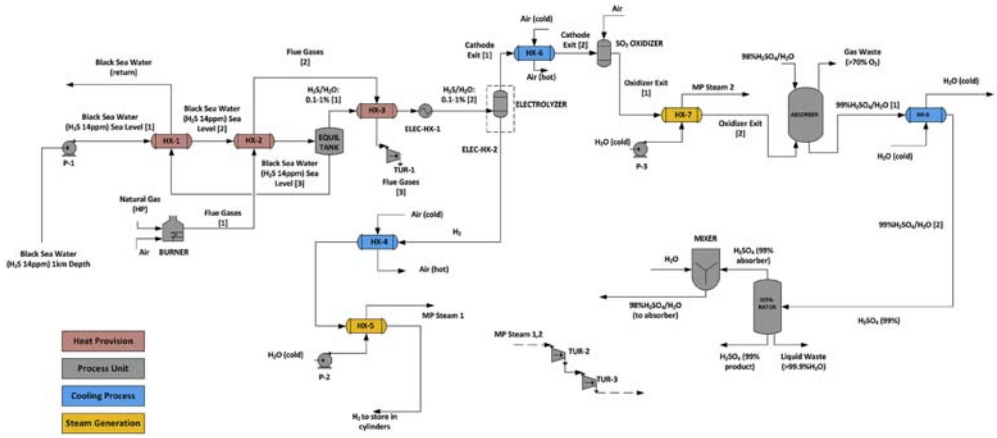

Figure 8.13 A more complete system for H_2S remediation of Black Sea water. HX (i.e., HX-1) stands for heat exchanger. Note that the cathode exit and anode exit were end-for-end labeled. *Reproduced with permission from D. Ipsakis, T. Kraia, M. Konsolakis, G. Marnellos, Remediation of Black Sea ecosystem and pure H_2 generation via H_2S-H_2O co-electrolysis in a proton-conducting membrane cell stack reactor: a feasibility study of the integrated and autonomous approach, Renew. Energy 125 (2018) 806–818 [7]. Copyright 2018 Elsevier.*

Fig. 8.12) before entering the absorber. In the more complete system (Fig. 8.13), the SO_3 stream is water cooled to a much lower temperature (~70°C). To suppress the undesired temperature excursion due to the highly exothermic nature of SO_3 absorption in free water and H_2SO_4 formation [86], 98% H_2SO_4 in trace water is provided to the absorber. A highly pure H_2SO_4 (>99%) mainly constitutes of the liquid outlet, which is then cooled by water (E12 or HX-8). The side products include liquid waste (mainly H_2O), a recycled stream, and, possibly, trace H_2 (Figs. 8.12 and 8.13) [7,80].

In a more complete system, heat and energy management are implemented (Fig. 8.13).

In contrast to the other technologies mentioned in this chapter (mainly focused on lab-scale studies), there has been a pilot-scale/full-scale design (with a capacity of 2000–13,000 t/h) of the proton-conducting membrane for H_2S remediation [7,80]. Take the more complete system shown in Fig. 8.13 as an example, where the major contributor (~45%) to the equipment cost is the fraction made up of compressors and turbines when treating 1950 t/h Black Sea water with 1 v/v% H_2S in the feed [7], followed by the heat exchangers (~35%) and proton-conducting membrane reactor (11.3%). By implementation of heat and energy management facilities, ~28 MWp surplus of power can be generated along with a H_2SO_4 production of 0.5 t/day [7]. Under this operating condition, H_2 production can achieve 0.9 t/day, which can support a 10,000 km travel distance by fuel cell

This book belongs to Badji Mokhtar Annaba University Central Library Copyright Elsevier 2025

electric buses [87]. It was noted that the integrated proton-conducting membrane reactor aiming at the effective remediation of the ecosystem can not achieve a profitable operation under the current market values (i.e., 9.85 €/kg for H_2 and 0.277 €/kWh for the generated electricity) [7]. Alternatively, the proposed process (Fig. 8.13) can become more economically attractive if part of the total fixed capital investment can be subsidized. This hypothesis is plausible in some areas where the local governments may implement regulations against the environmental degradation [7].

8.4 Conclusions and perspectives

Electrochemical membrane technology for environmental remediation involves the use of the ion exchange membrane to improve the ion transport efficiency while achieving reasonable phase separation performance. Further understanding of the material selection, system design, and process optimization is vital to enable wider employment of this technology. The first part of this chapter reviews the general processes occurring in an electrochemical remediation system. The second part summarizes the fundamentals, critical operating parameters, and mathematical optimization approaches for the electrodialytic remediation of contaminated media. In the following part, the use of membrane technologies for electrocatalytic remediation of contaminated media is discussed. It's the purpose of the content of this chapter to clearly show the great potential of the electrochemical membrane technology for environmental remediation.

IEMs play a critical role in the success of a wide spectrum of these technologies in heavy metal removal from the contaminated soil/water, micropollutant removal from surface water, and H_2S removal from seawater. For electrodialytic remediation of contaminated media, water splitting at AEMs renders the formation of an acidic front ($pH < 4$) and subsequent dissolution of heavy metals from the contaminated media. The presence of CEMs enables the separation of extraction electrolyte from the media. The charge density of a membrane is important for the determination of the limiting current, which then influences the remediation time and capital/electrical cost. For electrocatalytic remediation, IEMs serve as a separator as well as a salt bridge. In a dilute environment, an IEM should facilitate the proton transfer from the anode to the cathode to complete the redox reactions. In addition, since direct oxidation and radicals induced oxidation occur on the anode, IEMs used in electrocatalytic remediation should have reasonable chemical stability. While the academia has witnessed significant achievements in electrode and membrane preparation, reactor design, and process optimization in the last decade, a number of critical challenges remain that

This book belongs to Badji Mokhtar Annaba University Central Library Copyright Elsevier 2025

may hinder the wider applications of electrochemical membrane technology for environmental remediation, mainly:

1. *Selectivity and stability of the electrochemical membranes*. Regarding the nature of the environmental matrices, the charged contaminants (e.g., heavy metals, micropollutants, and H_2S) are always present at much lower concentrations compared to the major components (e.g., Na^+ and Cl^-/HCO_3^-), resulting in the dominant transport of the competitive ions and then low Coulombic efficiency for remediation. For example, a generalized selectivity order for common cation transport through CEMs (with sulfonic acid groups) follows: $Ca^{2+} > Mg^{2+} > H^+ > (Cu^{2+} \sim Zn^{2+} \sim Ni^{2+}) > K^+ > Na^+ > Li^+ > Fe^{3+}$ [88]. As abovementioned, Ca^{2+} migration surpasses Cu^{2+} migration in the electrodialytic remediation process. Essentially, there are four possible mechanisms accounting for the ion transport in IEMs, that is, diffusion, electromigration, convection, and surface sit "hopping," with the construction of a thin active layer and manipulation of the interactions between target ions and the membrane to increase the selectivity gaining its popularity [88,89]. Sheng et al. coated thin films with abundant Cu^{2+} binding sites on porous alumina by alternating layer-by-layer adsorption of poly [(*N*,*N*′-dicarboxymethyl) allylamine] (PDCMAA) and protonated poly(allylamine) (PAH) at low pH [90]. Results showed that the $(PDCMAA/PAH)_3PDCMAA$ or $(PDCMAA/PAH)_4$ films had average Cu^{2+}/Mg^{2+} diffusion dialysis selectivities around 50 [90], with the potential mechanisms related to the strong binding of Cu^{2+} to PDCMAA that may (1) create free amine groups for favorable Cu^{2+} transport and (2) suppress Mg^{2+} transport [90]. Additionally, there has been limited investigation on the durability of the membranes in long-term remediation. Ongoing attention to how this may influence the effectiveness of the membranes (e.g., electrical resistance and selectivity) is required.
2. *Electrode innovation and performance enhancement*. Electrode materials are a primary contributor to the capital costs of electrochemical membrane systems for environmental remediation. As such, it is of great significance to develop high-efficiency, low-cost, and long-lifespan electrodes [91–93]. In a symmetric system, the operation of reverse polarity can be applied to remove mineral scale (e.g., calcium precipitates) from the cathode [28,29] and/or regenerate the capacitive capacities [12,56,94], requiring a high stability under both cathodic and anodic polarization. To date, platinized electrodes are widely used in this field, and there is limited investigation on use of more innovative electrodes such as boron-doped diamond and Magnéli phase titanium suboxide electrodes (e.g., Ti_4O_7) that have high activity, conductivity, and chemical stability. In addition, the traditional electrochemical systems utilize static plate/rod electrodes with the flow-by operation of the electrolyte resulting in the formation of a thick diffusion boundary layer ($\sim 100\ \mu m$). Recent studies show that the use of flow electrodes can significantly enhance the electrochemical process performance [95,96]. The number of active surface sites in flow electrodes can be as high as the Brunauer–Emmett–Teller surface site level

This book belongs to Badji Mokhtar Annaba University Central Library Copyright Elsevier 2025

compared to that at a geometric level for a plate electrode [96], which would lead to faster kinetics in the electrode compartment. The mass transfer in the flow electrode system can also be enhanced. It is reported that the mass transfer rate constant increased to $4.48 \times 10 - 5$ m/s compared to the control (0.62×10^{-5} m/s) [96].

3. *Field trials and economic analysis*. Almost 30 years have passed since the electrochemical membrane technology was proposed for environmental remediation; however, there has been limited on-site investigation of these techniques at a pilot/full-scale. A more realistic study by Ipsakis et al. including the flow diagram development, simulation, and overall evaluation was performed on the Aspen Plus Software [7]. Attention should be paid to how the remediation process may influence the micro-environment (e.g., microbiological functions). In addition, the lack of data collected from pilot/full-scale studies hinders a fair economic comparison of the electrochemical membrane technologies with other alternatives for environmental remediation. The life cycle assessment can be applied as a tool for evaluating the sustainability of the contaminated sites remediation though papers looking at the sustainability of the environmental, social, and economic impacts of remediation technologies which are far from sufficient. Future studies with such a holistic focus would facilitate the extension of electrochemical membrane technology into arenas congenial for the development of the knowledge of environmental remediation.

References

[1] M.O. Barbosa, N.F. Moreira, A.R. Ribeiro, M.F. Pereira, A.M. Silva, Occurrence and removal of organic micropollutants: an overview of the watch list of EU Decision 2015/495, Water Res. 94 (2016) 257–279.
[2] P.A. Neale, S. Ait-Aissa, W. Brack, N. Creusot, M.S. Denison, B.R. Deutschmann, et al., Linking in vitro effects and detected organic micropollutants in surface water using mixture-toxicity modeling, Environ. Sci. Technol. 49 (2015) 14614–14624.
[3] L.J. Stephens, S. Munuganti, R.N. Duffin, M.V. Werrett, P.C. Andrews, Is bismuth really the "green" metal? Exploring the antimicrobial activity and cytotoxicity of organobismuth thiolate complexes, Inorg. Chem. 59 (2020) 3494–3508.
[4] M. Rodrigo, N. Oturan, M.A. Oturan, Electrochemically assisted remediation of pesticides in soils and water: a review, Chem. Rev. 114 (2014) 8720–8745.
[5] L.M. Ottosen, H.K. Hansen, S. Laursen, A. Villumsen, Electrodialytic remediation of soil polluted with copper from wood preservation industry, Environ. Sci. Technol. 31 (1997) 1711–1715.
[6] L. Ottosen, H. Hansen, C. Hansen, Water splitting at ion-exchange membranes and potential differences in soil during electrodialytic soil remediation, J. Appl. Electrochem. 30 (2000) 1199–1207.
[7] D. Ipsakis, T. Kraia, M. Konsolakis, G. Marnellos, Remediation of Black Sea ecosystem and pure H2 generation via H2S-H2O co-electrolysis in a proton-conducting membrane cell stack reactor: a feasibility study of the integrated and autonomous approach, Renew. Energy 125 (2018) 806–818.
[8] K.J. Vetter, Electrochemical Kinetics: Theoretical Aspects, Elsevier, 2013.
[9] J.W. Jorgenson, K.D. Lukacs, High-resolution separations based on electrophoresis and electroosmosis, J. Chromatogr. A 218 (1981) 209–216.
[10] J. Ma, J. Ma, C. Zhang, J. Song, R.N. Collins, T.D. Waite, Water recovery rate in short-circuited closed-cycle operation of flow-electrode capacitive deionization (FCDI), Environ. Sci. Technol. 53 (2019) 13859–13867.

This book belongs to Badji Mokhtar Annaba University Central Library Copyright Elsevier 2025

[11] S. Porada, R. Zhao, A. Van Der Wal, V. Presser, P. Biesheuvel, Review on the science and technology of water desalination by capacitive deionization, Prog. Mater. Sci. 58 (2013) 1388–1442.
[12] J. Ma, C. He, D. He, C. Zhang, T.D. Waite, Analysis of capacitive and electrodialytic contributions to water desalination by flow-electrode CDI, Water Res. 144 (2018) 296–303.
[13] R. Zhao, P. Biesheuvel, H. Miedema, H. Bruning, A. Van der Wal, Charge efficiency: a functional tool to probe the double-layer structure inside of porous electrodes and application in the modeling of capacitive deionization, J. Phys. Chem. Lett. 1 (2010) 205–210.
[14] C. Zhang, D. He, J. Ma, W. Tang, T.D. Waite, Faradaic reactions in capacitive deionization (CDI) - problems and possibilities: a review, Water Res. 128 (2018) 314–330.
[15] S. Pei, J. Teng, N. Ren, S. You, Low-temperature removal of refractory organic pollutants by electrochemical oxidation: role of interfacial joule heating effect, Environ. Sci. Technol. 54 (2020) 4573–4582.
[16] Y.B. Acar, A.N. Alshawabkeh, Principles of electrokinetic remediation, Environ. Sci. Technol. 27 (1993) 2638–2647.
[17] P. Guedes, N. Couto, L.M. Ottosen, A.B. Ribeiro, Phosphorus recovery from sewage sludge ash through an electrodialytic process, Waste Manage. 34 (2014) 886–892.
[18] H.K. Hansen, A. Rojo, L.M. Ottosen, Electrodialytic remediation of copper mine tailings, J. Hazard. Mater. 117 (2005) 179–183.
[19] M.R. Jakobsen, J. Fritt-Rasmussen, S. Nielsen, L.M. Ottosen, Electrodialytic removal of cadmium from wastewater sludge, J. Hazard. Mater. 106 (2004) 127–132.
[20] G.M. Nystroem, L.M. Ottosen, A. Villumsen, Electrodialytic removal of Cu, Zn, Pb, and Cd from harbor sediment: influence of changing experimental conditions, Environ. Sci. Technol. 39 (2005) 2906–2911.
[21] L.M. Ottosen, H.K. Hansen, A.B. Ribeiro, A. Villumsen, Removal of Cu, Pb and Zn in an applied electric field in calcareous and non-calcareous soils, J. Hazard. Mater. 85 (2001) 291–299.
[22] A.J. Pedersen, L.M. Ottosen, A. Villumsen, Electrodialytic removal of heavy metals from different fly ashes: influence of heavy metal speciation in the ashes, J. Hazard. Mater. 100 (2003) 65–78.
[23] A.B. Ribeiro, E.P. Mateus, L.M. Ottosen, G. Bech-Nielsen, Electrodialytic removal of Cu, Cr, and As from chromated copper arsenate-treated timber waste, Environ. Sci. Technol. 34 (2000) 784–788.
[24] H.K. Hansen, L.M. Ottosen, B.K. Kliem, A. Villumsen, Electrodialytic remediation of soils polluted with Cu, Cr, Hg, Pb and Zn, J. Chem. Technol. Biotechnol. Int. Res. Process Environ. Clean. Technol. 70 (1997) 67–73.
[25] G.M. Kirkelund, P.E. Jensen, L.M. Ottosen, K.B. Pedersen, Comparison of two- and three-compartment cells for electrodialytic removal of heavy metals from contaminated material suspensions, J. Hazard. Mater. 367 (2019) 68–76.
[26] K.B. Pedersen, L.M. Ottosen, P.E. Jensen, T. Lejon, Comparison of 2-compartment, 3-compartment and stack designs for electrodialytic removal of heavy metals from harbour sediments, Electrochim. Acta 181 (2015) 48–57.
[27] K.B. Pedersen, G.M. Kirkelund, L.M. Ottosen, P.E. Jensen, T. Lejon, Multivariate methods for evaluating the efficiency of electrodialytic removal of heavy metals from polluted harbour sediments, J. Hazard. Mater. 283 (2015) 712–720.
[28] B.P. Chaplin, The prospect of electrochemical technologies advancing worldwide water treatment, Acc. Chem. Res. 52 (2019) 596–604.
[29] S. Garcia-Segura, X. Qu, P.J. Alvarez, B.P. Chaplin, W. Chen, J.C. Crittenden, et al., Opportunities for nanotechnology to enhance electrochemical treatment of pollutants in potable water and industrial wastewater—a perspective, Environ. Sci. Nano 7 (2020) 2178–2194.
[30] J. Xie, J. Ma, C. Zhang, X. Kong, Z. Wang, T.D. Waite, Effect of the presence of carbon in Ti4O7 electrodes on anodic oxidation of contaminants, Environ. Sci. Technol. 54 (2020) 5227–5236.
[31] J.L. Havlin, Fertility☆, Reference Module in Earth Systems and Environmental Sciences, Elsevier, 2013.
[32] E.A. Paul, 1 - Soil microbiology, ecology, and biochemistry in perspective, in: E.A. Paul (Ed.), Soil Microbiology, Ecology and Biochemistry, third ed., Academic Press, San Diego, CA, 2007, pp. 3–24.
[33] H.W. Lee, H. Lee, Y.-M. Kim, R.-S. Park, Y.-K. Park, Recent application of biochar on the catalytic biorefinery and environmental processes, Chin. Chem. Lett. 30 (2019) 2147–2150.

This book belongs to Badji Mokhtar Annaba University Central Library Copyright Elsevier 2025

[34] A. Zhu, Y. Guo, G. Liu, M. Song, Y. Liang, Y. Cai, et al., Hydroxyl radical formation upon dark oxidation of reduced iron minerals: effects of iron species and environmental factors, Chin. Chem. Lett. 30 (2019) 2241–2244.
[35] G.M. Kirkelund, C. Magro, P. Guedes, P.E. Jensen, A.B. Ribeiro, L.M. Ottosen, Electrodialytic removal of heavy metals and chloride from municipal solid waste incineration fly ash and air pollution control residue in suspension – test of a new two compartment experimental cell, Electrochim. Acta 181 (2015) 73–81.
[36] J. Almeida, C. Magro, A.R. Rosário, E.P. Mateus, A.B. Ribeiro, Electrodialytic treatment of secondary mining resources for raw materials extraction: reactor design assessment, Sci. Total Environ. 752 (2021) 141822.
[37] C. Zhang, D. He, J. Ma, T.D. Waite, Active chlorine mediated ammonia oxidation revisited: reaction mechanism, kinetic modelling and implications, Water Res. 145 (2018) 220–230.
[38] A. Frumkin, G. Tadoradze, The mechanism of ionization of molecular chlorine at a platinum electrode, Z. Elektrochem. 62 (1958) 251.
[39] K.R. Olson, I.B. Anderson, N.L. Benowitz, P.D. Blanc, R.F. Clark, T.E. Kearney, et al., Poisoning & Drug Overdose, Lange Medical Books, McGraw-Hill, 2007.
[40] K.B. Pedersen, P.E. Jensen, L.M. Ottosen, J. Barlindhaug, The relative influence of electrokinetic remediation design on the removal of As, Cu, Pb and Sb from shooting range soils, Eng. Geol. 238 (2018) 52–61.
[41] K.B. Pedersen, P.E. Jensen, L.M. Ottosen, J. Barlindhaug, Applying multivariate analysis for optimising the electrodialytic removal of Cu and Pb from shooting range soils, J. Hazard. Mater. 368 (2019) 869–876.
[42] A. Rojo, L. Cubillos, Electrodialytic remediation of copper mine tailings using bipolar electrodes, J. Hazard. Mater. 168 (2009) 1177–1183.
[43] P.E. Jensen, L.M. Ottosen, C. Ferreira, Electrodialytic remediation of soil fines (<63 μm) in suspension—influence of current strength and L/S, Electrochim. Acta 52 (2007) 3412–3419.
[44] G.M. Nystroem, A.J. Pedersen, L.M. Ottosen, A. Villumsen, The use of desorbing agents in electrodialytic remediation of harbour sediment, Sci. Total Environ. 357 (2006) 25–37.
[45] K.B. Pedersen, T. Lejon, P.E. Jensen, L.M. Ottosen, The influence of sediment properties and experimental variables on the efficiency of electrodialytic removal of metals from sediment, J. Environ. Chem. Eng. 5 (2017) 5312–5321.
[46] T.R. Sun, L.M. Ottosen, P.E. Jensen, G.M. Kirkelund, Electrodialytic remediation of suspended soil – comparison of two different soil fractions, J. Hazard. Mater. 203–204 (2012) 229–235.
[47] G.M. Kirkelund, L.M. Ottosen, A. Villumsen, Investigations of Cu, Pb and Zn partitioning by sequential extraction in harbour sediments after electrodialytic remediation, Chemosphere 79 (2010) 997–1002.
[48] A.J. Pedersen, Evaluation of assisting agents for electrodialytic removal of Cd, Pb, Zn, Cu and Cr from MSWI fly ash, J. Hazard. Mater. 95 (2002) 185–198.
[49] X. Yang, L. Liu, W. Tan, C. Liu, Z. Dang, G. Qiu, Remediation of heavy metal contaminated soils by organic acid extraction and electrochemical adsorption, Environ. Pollut. 264 (2020) 114745.
[50] P. Quevauviller, G. Rauret, H. Muntau, A.M. Ure, R. Rubio, J.F. López-Sánchez, et al., Evaluation of a sequential extraction procedure for the determination of extractable trace metal contents in sediments, Fresenius' J. Anal. Chem. 349 (1994) 808–814.
[51] K.B. Pedersen, T. Lejon, P.E. Jensen, L.M. Ottosen, Applying multivariate analysis as decision tool for evaluating sediment-specific remediation strategies, Chemosphere 151 (2016) 59–67.
[52] A. Tessier, P.G.C. Campbell, M. Bisson, Sequential extraction procedure for the speciation of particulate trace metals, Anal. Chem. 51 (1979) 844–851.
[53] P. Guedes, E.P. Mateus, N. Couto, Y. Rodríguez, A.B. Ribeiro, Electrokinetic remediation of six emerging organic contaminants from soil, Chemosphere 117 (2014) 124–131.
[54] M. Sörengård, G. Niarchos, P.E. Jensen, L. Ahrens, Electrodialytic per- and polyfluoroalkyl substances (PFASs) removal mechanism for contaminated soil, Chemosphere 232 (2019) 224–231.
[55] Z. Du, S. Deng, Y. Bei, Q. Huang, B. Wang, J. Huang, et al., Adsorption behavior and mechanism of perfluorinated compounds on various adsorbents—a review, J. Hazard. Mater. 274 (2014) 443–454.
[56] J. Ma, J. Ma, C. Zhang, J. Song, W. Dong, T.D. Waite, Flow-electrode capacitive deionization (FCDI) scale-up using a membrane stack configuration, Water Res. 168 (2020) 115186.

This book belongs to Badji Mokhtar Annaba University Central Library Copyright Elsevier 2025

[57] T.R. Sun, L.M. Ottosen, P.E. Jensen, Pulse current enhanced electrodialytic soil remediation—comparison of different pulse frequencies, J. Hazard. Mater 237–238 (2012) 299–306.
[58] J. Li, J. Ma, R. Dai, X. Wang, M. Chen, T.D. Waite, et al., Self-enhanced decomplexation of Cu-organic complexes and Cu recovery from wastewaters using an electrochemical membrane filtration system, Environ. Sci. Technol. 55 (2021) 655–664.
[59] K. Dunn, Process Improvement Using Data, 2020.
[60] Y.B. Acar, R.J. Gale, A.N. Alshawabkeh, R.E. Marks, S. Puppala, M. Bricka, et al., Electrokinetic remediation: basics and technology status, J. Hazard. Mater. 40 (1995) 117–137.
[61] L. Xu, C. Yu, Y. Mao, Y. Zong, B. Zhang, H. Chu, et al., Can flow-electrode capacitive deionization become a new in-situ soil remediation technology for heavy metal removal? J. Hazard. Mater. 402 (2021) 123568.
[62] J. Ma, D. He, W. Tang, P. Kovalsky, C. He, C. Zhang, et al., Development of redox-active flow electrodes for high-performance capacitive deionization, Environ. Sci. Technol. 50 (2016) 13495–13501.
[63] A. Rommerskirchen, C.J. Linnartz, F. Egidi, S. Kendir, M. Wessling, Flow-electrode capacitive deionization enables continuous and energy-efficient brine concentration, Desalination 490 (2020) 114453.
[64] M. Villen-Guzman, P. Guedes, N. Couto, L.M. Ottosen, A.B. Ribeiro, J.M. Rodriguez-Maroto, Electrodialytic phosphorus recovery from sewage sludge ash under kinetic control, Electrochim. Acta 287 (2018) 49–59.
[65] N. Couto, A.R. Ferreira, V. Lopes, S.C. Peters, E.P. Mateus, A.B. Ribeiro, et al., Electrodialytic recovery of rare earth elements from coal ashes, Electrochim. Acta 359 (2020) 136934.
[66] R. Sprocati, A. Gallo, R. Sethi, M. Rolle, Electrokinetic delivery of reactants: pore water chemistry controls transport, mixing, and degradation, Environ. Sci. Technol. 55 (2021) 719–729.
[67] C.A. Martínez-Huitle, M.A. Rodrigo, I. Sirés, O. Scialdone, Single and coupled electrochemical processes and reactors for the abatement of organic water pollutants: a critical review, Chem. Rev. 115 (2015) 13362–13407.
[68] C.A. Martínez-Huitle, M. Panizza, Electrochemical oxidation of organic pollutants for wastewater treatment, Curr. Opin. Electrochem. 11 (2018) 62–71.
[69] J.-X. Liu, D. Richards, N. Singh, B.R. Goldsmith, Activity and selectivity trends in electrocatalytic nitrate reduction on transition metals, ACS Catal. 9 (2019) 7052–7064.
[70] N. Singh, B.R. Goldsmith, Role of electrocatalysis in the remediation of water pollutants, ACS Catal. 10 (2020) 3365–3371.
[71] X. Meng, Z. Chen, C. Wang, W. Zhang, K. Zhang, S. Zhou, et al., Development of a three-dimensional electrochemical system using a blue $TiO_2/SnO_2–Sb_2O_3$ anode for treating low-ionic-strength wastewater, Environ. Sci. Technol. 53 (2019) 13784–13793.
[72] J.T. Jasper, Y. Yang, M.R. Hoffmann, Toxic byproduct formation during electrochemical treatment of latrine wastewater, Environ. Sci. Technol. 51 (2017) 7111–7119.
[73] P. Ma, H. Ma, S. Sabatino, A. Galia, O. Scialdone, Electrochemical treatment of real wastewater. Part 1: Effluents with low conductivity, Chem. Eng. J. 336 (2018) 133–140.
[74] Y. Yang, M.R. Hoffmann, Synthesis and stabilization of blue-black TiO_2 nanotube arrays for electrochemical oxidant generation and wastewater treatment, Environ. Sci. Technol. 50 (2016) 11888–11894.
[75] V. Viswanathan, H.A. Hansen, J.K. Nørskov, Selective electrochemical generation of hydrogen peroxide from water oxidation, J. Phys. Chem. Lett. 6 (2015) 4224–4228.
[76] S. Siahrostami, S. Jimenez Villegas, A.H. Bagherzadeh Mostaghimi, S. Back, A. Barati Farimani, H. Wang, et al., In atomic scale design of catalysts for electrochemical synthesis of hydrogen peroxide, ACS Catal. (2020).
[77] S. Siahrostami, G.-L. Li, V. Viswanathan, J.K. Nørskov, One-or two-electron water oxidation, hydroxyl radical, or H_2O_2 evolution, J. Phys. Chem. Lett. 8 (2017) 1157–1160.
[78] Z. Song, S. Garg, J. Ma, T.D. Waite, Modified double potential step chronoamperometry (DPSC) method for As(III) electro-oxidation and concomitant As(V) adsorption from groundwaters, Environ. Sci. Technol. 53 (2019) 9715–9724.
[79] Z. Song, S. Garg, J. Ma, T.D. Waite, Selective arsenic removal from groundwaters using redox-active polyvinylferrocene-functionalized electrodes: role of oxygen, Environ. Sci. Technol. 54 (2020) 12081–12091.

This book belongs to Badji Mokhtar Annaba University Central Library Copyright Elsevier 2025

[80] D. Ipsakis, T. Kraia, G.E. Marnellos, M. Ouzounidou, S. Voutetakis, R. Dittmeyer, et al., An electrocatalytic membrane-assisted process for hydrogen production from H2S in Black Sea: preliminary results, Int. J. Hydrog. Energy 40 (2015) 7530–7538.
[81] J.W. Murray, H.W. Jannasch, S. Honjo, R.F. Anderson, W.S. Reeburgh, Z. Top, et al., Unexpected changes in the oxic/anoxic interface in the Black Sea, Nature 338 (1989) 411–413.
[82] L.N. Neretin, I.I. Volkov, M.E. Böttcher, V.A. Grinenko, A sulfur budget for the Black Sea anoxic zone, Deep Sea Research Part I: Oceanographic Research Papers 48 (2001) 2569–2593.
[83] A.Y. Lein, M. Ivanov, On the sulfur and carbon balances in the Black Sea, Black Sea Oceanography, Springer, 1991, pp. 307–318.
[84] S. Naman, I.E. Ture, T.N. Veziroglu, Industrial extraction pilot plant for stripping H_2S gas from Black Sea water, Int. J. Hydrog. Energy 33 (2008) 6577–6585.
[85] K.-D. Kreuer, Proton-conducting oxides, Annu. Rev. Mater. Res. 33 (2003) 333–359.
[86] M. King, M. Moats, W.G. Davenport, Sulfuric Acid Manufacture: Analysis, Control and Optimization, Newnes, 2013.
[87] B. Ale, S.B. Shrestha, Introduction of hydrogen vehicles in Kathmandu Valley: Aa clean and sustainable way of transportation, Renew. Energy 34 (2009) 1432–1437.
[88] T. Luo, S. Abdu, M. Wessling, Selectivity of ion exchange membranes: a review, J. Membr. Sci. 555 (2018) 429–454.
[89] H.B. Park, J. Kamcev, L.M. Robeson, M. Elimelech, B.D. Freeman, Maximizing the right stuff: the trade-off between membrane permeability and selectivity, Science 356 (2017). eaab0530.
[90] C. Sheng, S. Wijeratne, C. Cheng, G.L. Baker, M.L. Bruening, Facilitated ion transport through polyelectrolyte multilayer films containing metal-binding ligands, J. Membr. Sci. 459 (2014) 169–176.
[91] Q. Bao, G. Li, Z. Yang, P. Pan, J. Liu, J. Chang, et al., Electrochemical performance of a three-layer electrode based on Bi nanoparticles, multi-walled carbon nanotube composites for simultaneous Hg(II) and Cu(II) detection, Chin. Chem. Lett. 31 (2020) 2752–2756.
[92] J. Li, Y. Li, Z. Xiong, G. Yao, B. Lai, The electrochemical advanced oxidation processes coupling of oxidants for organic pollutants degradation: a mini-review, Chin. Chem. Lett. 30 (2019) 2139–2146.
[93] Y. Wang, C. Zhou, J. Wu, J. Niu, Insights into the electrochemical degradation of sulfamethoxazole and its metabolite by Ti/SnO_2-Sb/Er-PbO_2 anode, Chin. Chem. Lett. 31 (2020) 2673–2677.
[94] C. He, J. Ma, C. Zhang, J. Song, T.D. Waite, Short-circuited closed-cycle operation of flow-electrode CDI for brackish water softening, Environ. Sci. Technol. 52 (2018) 9350–9360.
[95] C. Zhang, J. Ma, L. Wu, J. Sun, L. Wang, T. Li, et al., Flow electrode capacitive deionization (FCDI): recent developments, environmental applications, and future perspectives, Environ. Sci. Technol. 55 (2021) 4243–4267.
[96] J. Xie, J. Ma, S. Zhao, T.D. Waite, Flow anodic oxidation: towards high-efficiency removal of aqueous contaminants by adsorbed hydroxyl radicals at 1.5 V vs SHE, Water Res. 200 (2021) 117259.

This book belongs to Badji Mokhtar Annaba University Central Library Copyright Elsevier 2025

This page intentionally left blank

This book belongs to Badji Mokhtar Annaba University Central Library

Copyright Elsevier 2025

CHAPTER NINE

Electrodialysis membrane technology for industrial wastewater treatment: recent advances

Ying Mei[1,2], Chenxiao Jiang[2,3], Yang Liu[4], Yang Zhang[4], Lei Wang[5] and Chuyang Y. Tang[2]

[1]Research and Development Center for Watershed Environmental Eco-Engineering, Advanced Institute of Natural Sciences, Beijing Normal University, Zhuhai, Guangdong, P.R. China
[2]Department of Civil Engineering, The University of Hong Kong, Pokfulam, Hong Kong, P.R. China
[3]CAS Key Laboratory of Soft Matter Chemistry, Collaborative Innovation Centre of Chemistry for Energy Materials, School of Chemistry and Materials Science, University of Science and Technology of China, Hefei, Anhui, P.R. China
[4]College of Environment and Safety Engineering, Qingdao University of Science and Technology, Qingdao, Shandong, P.R. China
[5]Shenzhen Key Laboratory of Polymer Science and Technology, College of Materials Science and Engineering, Shenzhen University, Shenzhen, Guangdong, P.R. China

9.1 Introduction to electrodialysis technology

Industrial plants often consume large quantities of water, while generating substantial volumes of wastewater and spent streams that contain various valuable components. The generated industrial wastewater is typically challenging to treat and dispose off due to the complex nature of its composition. For example, some industrial wastewaters may contain high concentrations of heavy metals and toxic organic matter, which renders traditional biological wastewater treatment unfeasible. Therefore, more efficient treatment technologies are needed to remove contaminants from industrial wastewater; thus, helping avoid poisonous industrial wastewater with its adverse impacts to contaminate the environment and bedevil the ecology. In the recent decades, the depletion of some nonrenewable resources and the shortage of freshwater have also been an increasingly stimulating resource recovery from some spent industrial waste streams. Accordingly, it is highly attractive to industries to find an effective way to fractionate their wastewaters into various valuable resources with high efficiency and desirable purity.

Electrodialysis (ED) has been widely applied to separate target ionic constituents of waste streams into different fractions. It shows merit over other separation methods owing to its high selectivity and ability of refinery to products. For instance, ED has been applied for treating waste streams of the electroplating industry that contain various heavy metals, with valuable metals (e.g., Zn, Cu, and Ni) recovered and

Electrochemical Membrane Technology for Water and Wastewater Treatment.
DOI: https://doi.org/10.1016/B978-0-12-824470-8.00005-X
© 2022 Elsevier Inc.
All rights reserved.

This book belongs to Badji Mokhtar Annaba University Central Library
Copyright Elsevier 2025

concentrated while other toxic ones (e.g., Cr and As) removed [1–5]. In addition, ED has great potential for nutrient recovery from wastewater. For example, ED enables the simultaneous concentration of nutrients, on one hand, and removal of toxic heavy metals and organic micropollutants, on the other, which results in a substantially improved nutrient precipitation efficiency and product purity [6,7]. Recently, the incorporation of bipolar ion exchange membranes (IEMs) into ED stack has been demonstrated to regenerate organic/inorganic acid by in situ H^+ and OH^- production from water splitting in bipolar IEMs [8–10]. In these various examples, the ED technology closes the operation loop to enable more efficient recovery and recycling of various resources; thus, helping ED provide a technically and economically feasible way for sustainable development of the industrial wastewater.

This chapter summarizes the advances in the development and innovation of novel IEM membranes and ED processes. Their applications in various fields are discussed, such as water purification, resource recovery, and chemicals production from industrial wastewater. It provides a good basis for the future development of the technology.

9.2 Basic configuration of electrodialysis and brief historical development

A typical ED stack generally comprises the cation exchange membranes (CEMs) and the anion exchange membranes (AEMs) that are alternately arranged between two electrodes (the anode and the cathode), forming a series of diluting compartments and concentrating compartments (Fig. 9.1). During operation, an external voltage is applied to the electrodes to drive cations and anions to migrate towards the cathode and the anode, respectively. The selectivity performance of ED stack is determined by the characteristics of IEMs, with the CEMs and AEMs ideally only permitting cations and anions to pass through, respectively. As a result, target ions are removed from waste streams and fractionated into concentrated product streams. ED can be classified into three different types based on the IEMs applied: (1) selective ED with monovalent IEMs, (2) ED with bipolar IEMs, and (3) ED with liquid IEMs. For example, a liquid membrane containing a layer of organic solvent with ionic extractants can be used as an IEM to accelerate ion transport through the membrane due to carrier-mediated transport. It has been reported that liquid membranes with high permeability and selectivity had resulted in near-complete removal (99.5%) of hexavalent chromium in an ED process [12].

The working principle of ED was first demonstrated by Maigrot and Sabates in 1889 when a combination of the electrolysis and the dialysis processes was proposed for sugar syrup purification. However, the term "Electrodialysis" was only officially reported in Schollmeyer's patent in 1900. It should be noted that ion selective

This book belongs to Badji Mokhtar Annaba University Central Library Copyright Elsevier 2025

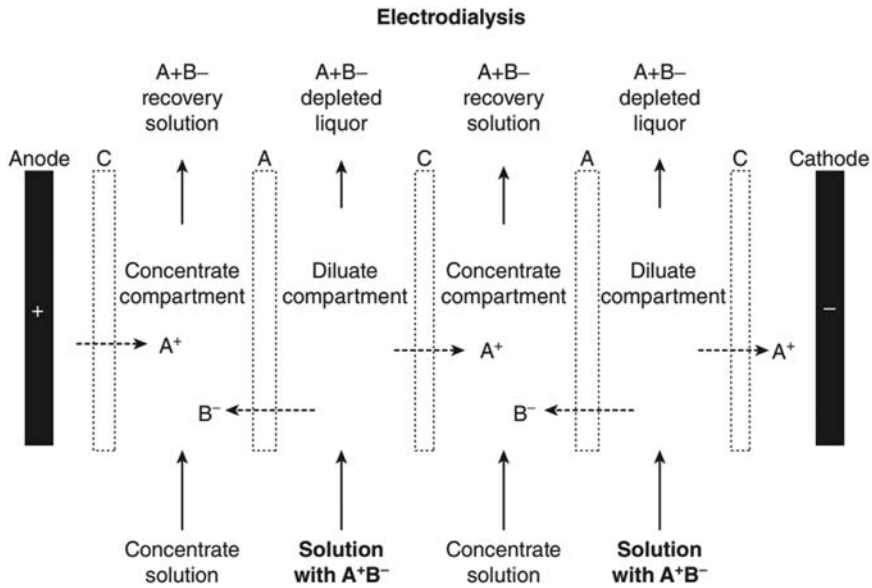

Figure 9.1 Working principle of a typical electrodialysis (ED) stack: Ions with different charges transport from the diluate chamber to the concentrate chamber in opposite directions, being driven by an electric field applied to the electrodes. *Taken from S. Datta, Y.J. Lin, S.W. Snyder, Current and emerging separations technologies in biorefining, in: Advancess in Biorefineries, Elsevier 2014, pp. 112–151 [11] with copyright permission from Elsevier.*

membranes were not used in ED processes until forty years later when Manegold and Kalauch used it in their research on a 3-compartment ED stack [13]. Early researches on IEMs and their structure-to-properties relationship began in 1925. Unfortunately, the poor performance of IEMs at that time prohibited their practical use in industrial applications of ED [14]. With the further development of ion selective membrane materials in the years to come, industrial scale applications of ED processes started in 1950 and were employed for concentration and/or demineralization of electrolyte solutions [15,16]. Aside from applications of ED for producing potable water from brackish water sources, its implementation in wastewater treatment also emerged [14,17].

In 1969, Mihara introduced the concept of electrodialysis reversal (EDR) that can effectively avoid salt precipitation on IEMs during their long-term operation by periodically reversing the ionic transport direction [18]. Combining ED and ion exchange technique as electrodeionization (EDI) was first reported by Matejka in 1970 [19,20] and has been successfully employed for producing high quality ultra-pure water or desalination of media with low conductivity. The ion exchange resin-filled diluate compartments could substantially stimulate the ionic migration towards the concentrate compartments, resulting in highly deionized water. The applications of EDI for environmental wastewater

This book belongs to Badji Mokhtar Annaba University Central Library Copyright Elsevier 2025

treatment was initially explored for removing heavy metals (e.g., Cr^{6+}) from synthetic solution by Alvarado et al., in addition to its application for producing pure water from the diluted stream [21,22]. With the development of the chemically stable, highly ionic selective, and highly electrically conductive membrane materials, ED has been increasingly applied for large scale industrial wastewater treatment.

9.3 Development of ion exchange membranes for industrial wastewater treatment

The performance of the ED process is greatly influenced by the properties of the IEMs. An IEM with simultaneously low electrical resistance and good selectivity is critical to achieve fast transport of ions and efficient separation with low energy consumption [23]. In addition, IEMs should exhibit good mechanical and chemical stability at a reasonable cost.

According to the interaction between functional groups and membrane matrix, IEMs are commonly classified into heterogeneous or homogeneous membranes, which are produced by different manufacturing methods [24]. First usable heterogeneous IEMs, reported by Wyllie in 1948 and Juda in 1950, are prepared by mixing ion exchange resin powders and polymer matrix materials, followed by hot-pressing the product into a film [25,26]. Since charged groups in heterogeneous IEMs are physically mixed with the polymer matrix, these membranes tend to have high electrical resistance and poor permselectivity, resulting in inefficient separation and high energy consumption of ED processes. However, the successful manufacture of homogeneous IEMs and their implementation in ED substantially enhanced the energy efficiency of ED and extended its applications to various industries. There are three general schemes for preparing homogeneous IEMs: (1) polymerization/polycondensation of monomers containing functional sites, (2) introduction of functional groups into a preformed polymeric film, and/or (3) casting a polymer (containing functional moieties) solution into a film [27]. As charged functional groups are chemically attached to the polymer backbone, homogeneous IEMs have a more uniform distribution of charges such that the electrical resistance is relatively low and the membrane permselectivity is better. It should also be noted that, in some specific harsh environments, heterogeneous IEMs may perform better due to their good mechanical and chemical stability [28].

Further development of membrane materials since 1970s facilitated researches on various novel applications of ED processes. For instance, monovalent ion exchange membrane (MIEM) can distinguish between monovalent and multivalent ions of the same charge in a mixture [29,30]. ED with MIEMs was first successfully applied for table salt production from sea water by Asahi Company [14]. Another interesting

This book belongs to Badji Mokhtar Annaba University Central Library Copyright Elsevier 2025

invention in IEM is the bipolar membrane (BM) [14]. A typical BM comprises three functional layers, a cation exchange layer and an anion exchange layer arranged in parallel, with an intermediate layer containing catalysts for water dissociation (Fig. 9.2A and B). Again, by integrating BMs with conventional IEMs within a stack to form BM-based ED process (BMED), an acid/base can be produced from their corresponding salts by electrodialytic water dissociation without adding other chemicals, which

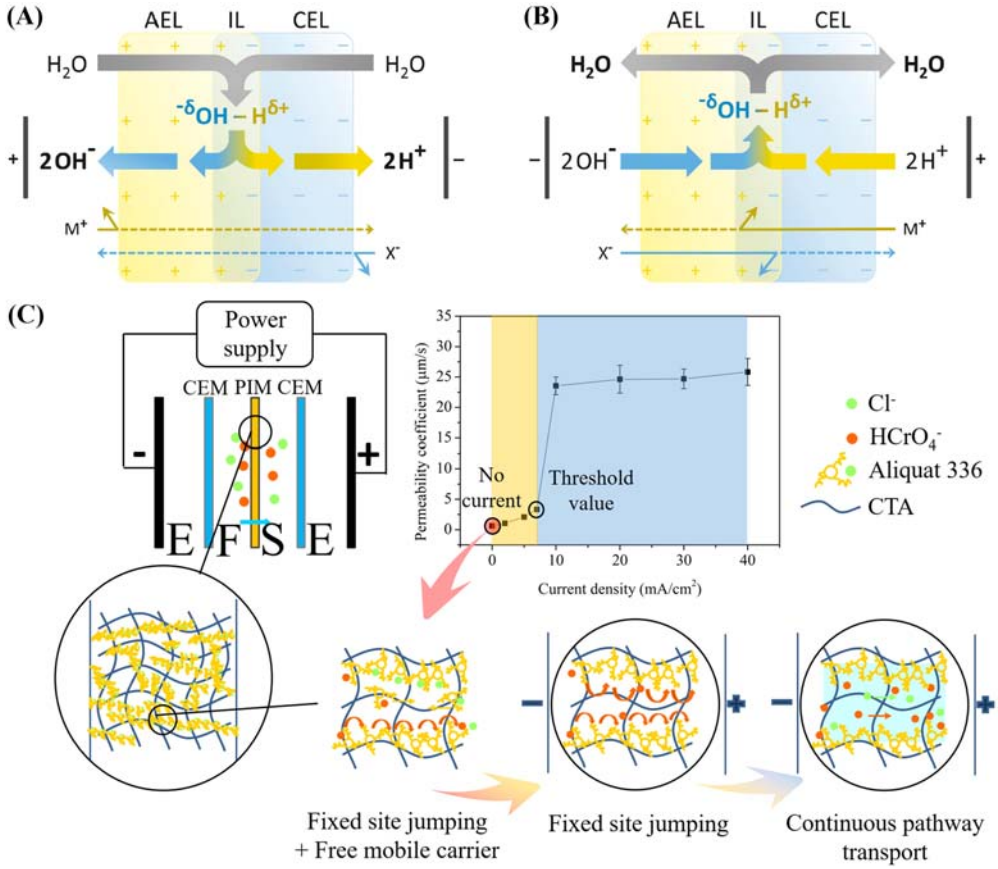

Figure 9.2 The working principle of BMs: (A) BM under reverse bias, where the bipolar junction is firstly depleted of ions and then water dissociates into H^+ and OH^- ions; (B) BM under forward bias, where ions are transported into the membrane and water is formed at the junction; and (C) The mechanism for continuous pathway transport and the current intensity threshold in PIMED transport process. *BMs*, bipolar membranes. *(A) and (B) Reproduced from R. Pärnamäe, S. Mareev, V. Nikonenko, S. Melnikov, N. Sheldeshov, V. Zabolotskii, et al., Bipolar membranes: a review on principles, latest developments, and applications, J. Membr. Sci. 617 (2021) 118538 [31] and (C) Obtained from Z. Li, Y. Liu, B. Wang, Q. Lang, M. Tan, M. Lee, et al., Insights into the facilitated transport mechanisms of Cr(VI) in ionic liquid-based polymer inclusion membrane—electrodialysis (PIM-ED) process, Chem. Eng. J. 397 (2020) 125324 [32] with copyright permission from Elsevier.*

This book belongs to Badji Mokhtar Annaba University Central Library Copyright Elsevier 2025

greatly improves the recyclability and reusability of industrial wastes [33]. The voltage required for water dissociation in BMED is approximately 0.83 V, which is apparently lower than that for conventional water electrolysis (1.23 V). This low voltage requirement makes BMED a good avenue for greener and more sustainable development of industrial activities. For example, BMED was initially applied for HF and HNO_3 harvesting from a pickling bath containing KF and KNO_3 of a steel plant, a process successfully adopted by Washington Steel in 1987 [34]. Another interesting application of bipolar ED was organic acid recovery from fermentation broth [35].

Recently, polymer inclusion membrane (PIM) has rapidly become an attractive topic in the membrane field due to its high ionic transport efficiency and chemical stability [36]. It mainly comprises a liquid phase carrier (extractant), which works as an ion-exchanger and plasticizer to transport specific species across the membrane [37,38]. The composite film of PIM shows better structural stability thanks to the secondary bonds, such as van der Waals forces and hydrogen bonds, between carriers and base polymer [39]. Replacing conventional IEMs with PIMs in an ED stack can simultaneously improve ionic conductivity and enhance selectivity of specific ions (Fig. 9.2C) [32,40]. In addition, PIM demonstrates an overwhelming advantage by blocking hydrogen when selectively transporting anions [40]. Latest researches on ED-PIM used ionic liquids as extractant to purify volatile fatty acids (VFAs), acetic, and hexanoic acids [41] while removing Cr (VI) as $HCrO_4^-$ [42]. There are thresholds for carrier content and current density. Specifically, the transport of Cr(VI) is realized by a fixed-site jumping mechanism in an electric field for carrier content below the threshold value, while the transport in a continuous pathway manner is hypothesized for carrier content above the threshold value [32].

9.4 Electrodialysis for industrial wastewater treatment

ED is a well-known technology for industrial wastewater treatment with its high-quality products, high energy efficiency, autonomous operation, and chemical-free and environmentally friendly process. Numerous cases have been presented for using ED to remove unwanted ions and recover resources from industrial wastewater. As the composition of industrial wastewater strongly depends on the nature of the industry and the characteristics of the site configuration, the specific design of an ED system varies with the waste effluent composition. The ED processes for industrial wastewater treatment can be typically categorized into four types based on its main application aim: (1) ED for water reclamation from dilute streams; (2) ED for nutrient recovery from nutrient wastewater as fertilizer; (3) ED for metal recovery from electroplating industry; and (4) ED for chemical production from waste. Sections 9.4.1–9.4.3 summarize the applications of ED for water reclamation, nutrient recovery, and metal recovery, respectively.

This book belongs to Badji Mokhtar Annaba University Central Library Copyright Elsevier 2025

Due to its increasing popularity and great application potential, the production of valuable chemicals with the assistance of BMED is discussed in detail in Section 9.5. Additional niche applications are also presented in Section 9.6.

9.4.1 Electrodialysis for wastewater reclamation

Some industrial activities produce large quantities of wastewater which need to be treated before their discharge and reuse. Examples include drainage wastewater of petroleum refinery, power plant, oil/gas extraction, and coal mining. The cooling needs of the former two processes consume the majority (~ 90%) of water volume during operation [43]. ED has been adopted as a promising technology for industrial waste water reclamation (Table 9.1). For example, applying ED for desalinating cooling tower blowdown (at a total dissolved solids (TDS) range of 1000–2000 ppm) can achieve a closed-loop operation. Several ED reversal (EDR) systems in the pilot scale have demonstrated substantial removal efficiency (up to 90%) of unwanted impurities in industrial waste with high water recovery efficiency (e.g., 75%) [51,52]. While relative high salt content (higher than 2000 ppm TDS) is generally found in coal mine waste effluents, water recovery of ~90% and salts removal of ~70% were achieved from a coal mine effluent at a concentration of ~2100 ppm TDS by an EDR test. Acid mine drainage containing high concentration of sulfide, iron, and other metals can also be desalinated by ED, obtaining a high removal efficiency of 97%~99% [53]. As a result, drainage wastewater reuse for irrigation has been realized through the removal of salt content (e.g., Na^+) for agricultural application in areas facing water scarcity [53]. Another sweet spot is the treatment of wastewater produced from oil/gas extraction. Approximately 250×10^6 barrels of waste effluents are generated as a byproduct of oil/gas extraction per day, and these waste effluents contain high salt concentration, suspended solids, organic matter, and heavy metals. ED can be adopted to treat the water fall from gas extraction and polymer flooding in the gas extraction industry. A TDS removal efficiency of ~89% was reported for a conventional well effluent (with a TDS of 9100 ppm) after organics removal, while for coalbed methane produced water (with a TDS up to 27,000 ppm), an 80%~90% TDS removal efficiency was achieved [43]. ED has also been applied for recycling polymer flooding water at a TDS range of 500~1000 ppm, obtaining a removal efficiency of 85%~99% at an energy consumption of 0.5–6 kWh/m^3 [44].

9.4.2 Electrodialysis for nutrient recovery from wastewater as fertilizer

In the last several decades, with the explosive growth of economy and population, a large and abundant repository of nutrient-rich waste streams has been generated. Consequently, the management of irrigation tail water, fermentation waste, livestock

This book belongs to Badji Mokhtar Annaba University Central Library Copyright Elsevier 2025

This book belongs to Badji Mokhtar Annaba University Central Library

Table 9.1 Previous researches on ED for wastewater reclamation.

Feed TDS (mg/L)	Electrolyte type	Operating conditions	Energy consumption[a]	Removal efficiency (%)	Water recovery efficiency (%)	References
5000/32,000	Sea/brackish water with residual polymer	24 A/m^2	3–4 kWh/m^3	>97	81.3–96.6	[44]
25,100	Mixed salt	60–100 A, 60 h	10–17 kWh/m^3	90	77	[45]
70,000	Mixed salt and organic matter	0–350 A/m^2, 50 min	7–14 kWh/m^3	91	85	[46]
50,000	NaCl	0.2 A, 48 h	2–7 kWh/kg	N.A.	N.A.	[47]
95,000	Na_2SO_4	2 A, 5 h	7.4 kWh/lb. of TDS removed	35–90	N.A.	[48]
65,000/100,000	Na_2SO_4	0.5–2 A, 1–7 h	8.93–30 kWh/lb. of TDS removed	27	N.A.	[49]
195,000	NaCl	50% of limiting current	N.A.	99	72.5	[50]

N.A., not available.
[a]The energy consumption of ED process is given in the unit of kWh/kg of water produced or kWh/lb. of TDS removed.

Copyright Elsevier 2025

manure, and human-derived waste (urine) has attracted increasing attention in recent years. The presence of high concentrations of nutrients (e.g., nitrogen and phosphorus) would be threatening to the ecosystem if the nutrient-rich wastewater is directly discharged into the aquatic system, leading to environmental problems such as eutrophication. On the other hand, prices of fertilizer raw materials (especially phosphorus) have increased dramatically due to their limited reserve (about $1.2 \sim 5 \times 10^{10}$ t worldwide [54]) and rapid consumption worldwide. Some nutrient wastes contain considerably high concentrations of nitrogen and phosphorus (e.g., up to 4000 and 300 ppm in pig manure, respectively) [10]. Accordingly, nutrient recovery from nutrient-rich wastewater and the simultaneous water reclamation can potentially offer triple-benefits: (1) minimizing the ecological risk of its direct disposal; (2) reusing valuable resources as fertilizer; and, (3) addressing the water scarcity in the rural areas [54]. It will likely be the future trend for sustainable treatment of wastewater, provided nutrients can be recovered in a cost-effective manner. Various studies have been conducted on the use of ED for nutrient recovery (and water reclamation) from agricultural waste.

Struvite ($MgNH_4PO_4.6H_2O$) is a slow-release fertilizer formed by phosphorus and nitrogen precipitating with divalent cation (e.g., magnesium) at high pH [55]. Struvite precipitation has been widely accepted as a promising technology for waste nutrient recovery. However, its formation efficiency is often limited by low actual phosphorous concentration; ideally, a phosphorous concentration of greater than 100 ppm is preferred [6]. The challenge of phosphorous enrichment before struvite precipitation can be addressed by the ED process, which increases the technical and economic feasibility of struvite precipitation [56]. For example, an integrated system of ED and struvite precipitation reactor (Fig. 9.3) showed high phosphate recovery efficiency (93%) from a potato processing effluent [7]. ED, as a pretreatment step to the struvite precipitation reactor, concentrated phosphate (to a satisfying concentration of 9 mM) and removed excess salts in the processing effluent, with both effects promoting higher phosphate recovery. ED was used as a posttreatment step to recover phosphate from the effluent of the struvite precipitation reactor (at a phosphate flux of 16 $mM/m^2/h$), which further improved the phosphate recovery and reduced the phosphate discharge into the environment [7]. Apart from phosphorous enrichment, the requirement of magnesium salt dosage in struvite precipitation could also be eliminated by ED equipped with monovalent IEMs, making phosphorous recovery more cost-effective. Specifically, various ions in the nutrient wastewater were fractionated into three different groups: (1) nutrient components into the anionic product, (2) bivalent cations into the cationic product, and (3) monovalent cations into the brine [57]. Accordingly, the phosphate precipitation can be achieved by pairing recovered nutrient product and bivalent cationic product. In addition, Tran et al. also explored the usage of ED as a preconcentration step of crystallization to enhance the overall

This book belongs to Badji Mokhtar Annaba University Central Library Copyright Elsevier 2025

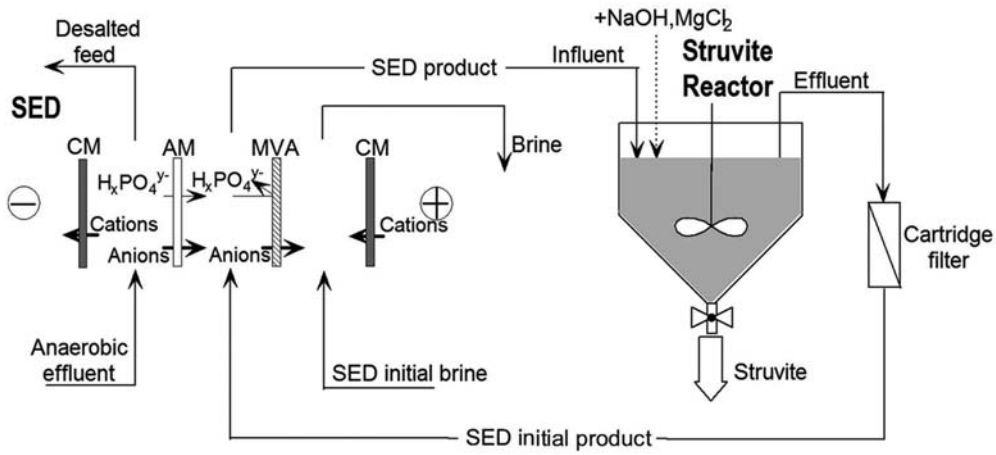

Figure 9.3 Schematic diagram of the hybrid system of selectrodialysis-struvite reactor for phosphate separation and recovery from waste effluent. *Obtained from Y. Zhang, E. Desmidt, A. Van Looveren, L. Pinoy, B. Meesschaert, B. Van der Bruggen, Phosphate separation and recovery from wastewater by novel electrodialysis, Environ. Sci. Technol. 47 (2013) 5888–5895 [7] with copyright permission from ACS.*

recovery efficiency of phosphate. The phosphate concentration reached 16 mM and was followed by precipitation efficiency for calcium phosphate, which was an 82.7% of the processing effluent [58]. Aside from the nitrogen and the phosphorus, harvesting high concentration VFA can be achieved from the liquid fraction of swine hydrolysate. Shi et al. investigated the simultaneous recovery of NH_4^+-N, P, and VFA using two-stages BM ED, achieving a NH_4^+-N recovery efficiency of 78%, PO_4^{3-} of 75%, and VFAs of 87% [10] of the processing effluent.

It should also be noted that there are generally various kinds of other pollutants in nutrient-rich wastewater, such as trace organic contaminants (e.g., antibiotics, pharmaceutical, pesticides, and endocrine disrupting chemicals etc.), dissolved salts, and heavy metals [59]. In ED processes, ionized contaminants and salts can both be driven by the application of an electric field and transport through IEM, accumulating the nutrient in the concentrate. For instance, two representative antibiotics, sulfadiazine and tetracycline, had been revealed to accumulate in the product solution either by electromigration or by membrane sorption in ED [59]. The concentration of the salt and organic micropollutants should be strictly regulated to avoid environmental risks and potential effects on human health, particularly if the recovered nutrient product is intended for reuse as fertilizer [59,60]. Recently, a novel ED system (Fig. 9.4) was proposed to make use of anodic oxidation, in situ removing antibiotics electrochemically within 60 min of nutrient recovery [61]. Meanwhile ED has also been revealed to partition salts from other organics and nutrient ions successfully [62]. ED has been

This book belongs to Badji Mokhtar Annaba University Central Library Copyright Elsevier 2025

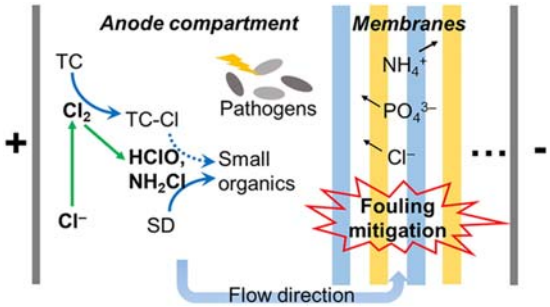

Figure 9.4 Schematic configuration of the single-compartment anode-electrodialysis for in situ electrochemical oxidation of antibiotics in pig manure digestate. *Obtained from L. Shi, Z. Hu, Y. Wang, E. Bei, P.N.L. Lens, O. Thomas, et al., In situ electrochemical oxidation in electrodialysis for antibiotics removal during nutrient recovery from pig manure digestate, Chem. Eng. J. (2020) [61] with copyright permission from Elsevier.*

considered an ideal technology for selectively recovering nutrient ions from waste stream even with low nutrient concentration (below 2000 ppm) while retaining micropollutants [60].

The application of ED for source-separated nutrient waste treatment has been well studied, but it is still challenged by the relatively high energy consumption. Coupling an electrochemical membrane bioreactor to the ED process may provide a way to address the problem. In such a hybrid system, energy (e.g., electricity) along with nutrient was simultaneously harvested in an environmentally friendly manner. For instance, the electricity (with a power density of 23.4 W/m^3) generated in the membrane bioreactor (Fig. 9.5) was in situ utilized by ED for selective phosphate recovery with an efficiency of 54.9% [63]. It makes ED potentially a technically and economically feasible technology for waste nutrient recovery. Aside from the high energy consumption, the fouling problem of ED process caused by di/multivalent ions (e.g., Ca^{2+}, Mg^{2+}) and organic fractions presents another challenge to the product purity and process stability during long-term operation of ED treating real wastewater such as human urine and animal manure. To address this problem, Paepe et al. employed precipitation and an aerobic bioreactor pretreatment to remove hardness ions and oxidize organics, respectively, leading to a more stable long-term continuous operation of the system with minimal maintenance for ~7 months [64]. Meanwhile, the concentration factors of nitrate and phosphate reached 4.3 and 2.6, respectively. EDR also provides a way to relieve membrane fouling caused by organic fraction in nutrient wastewater by frequently reversing the polarities of electrodes, leading to the mitigation of organic matter deposited on membrane surfaces. As a result, complete removal of NH_4^+ from processing wastewater was possible and up to 84% removal efficiency of phosphate was obtained [56].

This book belongs to Badji Mokhtar Annaba University Central Library Copyright Elsevier 2025

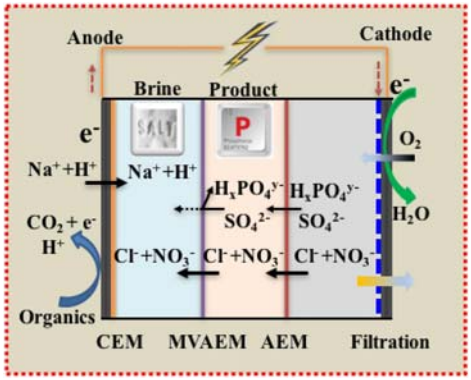

Figure 9.5 Schematic configuration of the selective electrodialysis membrane bioreactor where electricity generated by selective electrodialysis is in situ utilized for nutrient recovery from urine. MVAEM represents monovalent selective anion exchange membrane. *Obtained from Y.-K. Wang, Y.-K. Geng, X.-R. Pan, G.-P. Sheng, In situ utilization of generated electricity for nutrient recovery in urine treatment using a selective electrodialysis membrane bioreactor, Chem. Eng. Sci. 171 (2017) 451–458 [63] with copyright permission from Elsevier.*

9.4.3 Electrodialysis for metals recovery from electroplating industry

Heavy metal pollution has been widely recognized as a serious environmental problem. Its direct emission will not only threaten the environment due to its toxicity, non-biodegradability, and bio-accumulation, but also waste the raw materials. Heavy metal rich waste streams can originate from various anthropogenic activities. Particularly, the wastewater from plating/mining industries is generally acidic/basic and contains high concentration of heavy metals (e.g., Ni, Cu, Zn, Cr, Cd, etc.). Previous researches have extensively studied the use of ED for recovering valuable heavy metals from these waste streams (Table 9.2) while simultaneously realizing water reclamation [71]. The accumulated heavy metal concentrate can be reinjected into the plating bath, while the purified water can be reused as rinse water in the plating processes [72,73]. Accordingly, the life span of bath water in plating/finishing industries can be extended [74].

ED can be directly used for heavy metal removal. Factors impacting the process performance, such as applied voltage, solution pH, ionic species, and formation of metal complexes, have been comprehensively investigated [75]. The removal efficiency of heavy metals generally increases with a higher applied voltage. Heavy metals could exist in solutions in various species, such as the cationic species of nickel and the anionic species of chromium (e.g., CrO_4^{2-}, $HCrO_4^{-}$). The speciation of some heavy metals is strongly dependent on the solution pH. For example, chromium is present in the form of monovalent anion $HCrO_4^{-}$ at low pH and in the form of divalent anion CrO_4^{2-}. For the electroplating wastewater in low pH (pH 2.2), a two-stage ED with

This book belongs to Badji Mokhtar Annaba University Central Library Copyright Elsevier 2025

Table 9.2 Previous researches on ED for heavy metal recovery.

Heavy metal ions	Process design	Removal efficiency (%)	Current efficiency (%)	References
Chromium	ED	98.69–100	N.A.	[65]
Chromium	ED-liquid membrane	99.5	17	[12]
Copper	EDI	31–41	25–47	[66]
Copper	EDI	91.4–94.2	8–40	[1]
Zinc	ED	>80	4.8–8.0	[2]
Arsenic	Precipitation/ED	72–85	N.A.	[67]
Nickel	Two-stage EDI	99.8	77.5 for stage-1; 3.95 for stage-2	[5]
Lithium	Precipitation/ED	82–99	≤ 90	[68–70]

monovalent IEMs was investigated for concentrating chromium in the first stage, and separating chromium from other monovalent impurity ions in the second stage after adjusting the pH to 8.5 [3].

In addition to the recovery of valuable metals, there are generally various toxic impurities (e.g., As, Cr, Se) present in the waste solution which need to be separated from the recovered products. For instance, the World Health Organization (WHO) recommends a limit of arsenic in drinking water at 10 ppb [76]. However, conventional ED processes can hardly realize selective recovery of ions and ionic separation in solutions with multiple similarly-charged ions due to the limited selectivity of conventional IEMs [77]. Researchers have designed a novel ED configuration (selectrodialysis, SED) with monovalent and divalent ions selectivity by introducing the monovalent selective membrane to the ED process. Zhang et al. reported an energy-efficient separation of sulfate ions from chloride ions for synthetic wastewater [78]. SED has also been performed for fractionating arsenic (As(V)) from positive charged copper and zinc ions (Fig. 9.6) for a metallurgical process effluent, obtaining a high arsenic purity (95%) [79].

To tune membrane ion selectivity, many studies have been performed on surface modification of IEMs, including (1) surface layer with a high degree of cross-linking, (2) oppositely charged surface layer, (3) polyelectrolyte multilayers prepared by layer-by-layer deposition, and (4) dense surface layers formed from neutral polymers [80,81]. Xu et al. reported a selectivity value of 354 for H^+/Zn^{2+} and 7 for Na^+/Mg^{2+} using a nanofiltration (NF) membrane in an ED stack [82]. They demonstrated that the involvement of an NF increased the limited current density in (ED). By applying layer-by-layer method, the selectivity value for Cl^-/SO_4^{2-} of over 10 was obtained [83]. Zhao et al. modified AEM by using electric-pulse deposition and the selectivity value reached 47.04 for Cl^-/SO_4^{2-} [84]. On the other hand, White et al. modified Nafion 115 membranes with a multilayer poly (4-styrenesulfonate) (PSS)/protonated poly(allylamine) (PAH) coating method (Fig. 9.7), and the selectivity value for K^+/Mg^{2+} reached more than

This book belongs to Badji Mokhtar Annaba University Central Library Copyright Elsevier 2025

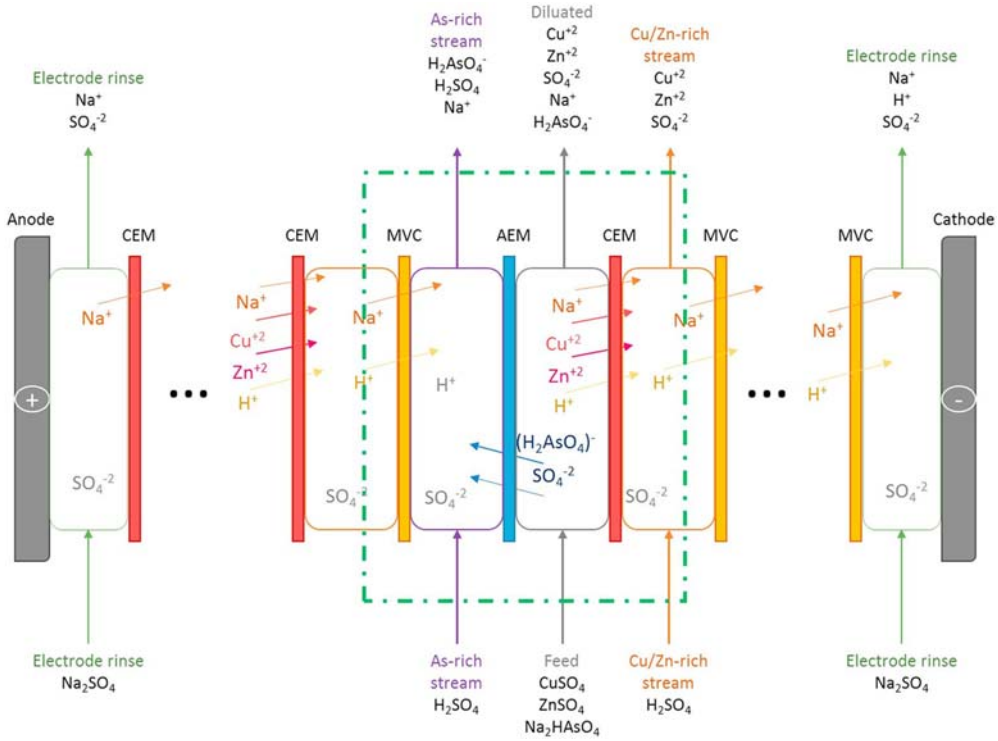

Figure 9.6 Schematic configuration of the selective electrodialysis for the separation and recovery of Cu (II) and Zn (II) from metallurgical process waters containing As (V). *Obtained from M. Reig, X. Vecino, C. Valderrama, O. Gibert, J.L. Cortina, Application of selectrodialysis for the removal of As from metallurgical process waters: recovery of Cu and Zn, Sep. Purif. Technol. 195 (2018) 404–412 [79] with copyright permission from Elsevier.*

1000 [85]. Again, Abdu et al. prepared a CEM with hyperbranched poly(ethyleneimine)/poly(sodium 4-styrene sulfonate) (PEI/PSS) multilayers on the surface, and the selectivity of Na^{+}/Ca^{2+} increased with an increase in PEI/PSS bilayer number [86]. Furthermore, Wang et al. developed a monovalent cation perm-selective exchange membrane (MVC) by interfacial polymerization of a thin-film composite (TFC) on a commercial CEM to better tailor the selectivity of selectrodialysis (SED) process [87]. However, the stability of such TFC-modified IEMs, as well as the full understanding of the permselectivity mechanism induced by the fouling layer or TFC layer, requires further study [88].

The overall efficiency of the ED process can be enhanced by hybridizing ED with other related processes. For industrial metal washing effluents with complex composition of ions mixture, using fluidized pellet reactor as a pretreatment step of ED can effectively crystallize the scale-forming ions (e.g., calcium and nickel ions) and avoid

This book belongs to Badji Mokhtar Annaba University Central Library Copyright Elsevier 2025

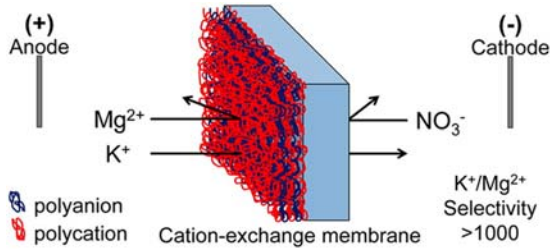

Figure 9.7 Tailored cation exchange membrane with dramatically enhanced selectivity between monovalent and divalent cations through coating Nafion 115 membrane with multilayer poly(4-styrene-sulfonate) (PSS)/protonated poly(allylamine) (PAH) films. *Obtained from N. White, M. Misovich, A. Yaroshchuk, M.L. Bruening, Coating of nafion membranes with polyelectrolyte multilayers to achieve high monovalent/divalent cation electrodialysis selectivities, ACS Appl. Mat. Interfaces 7 (2015) 6620–6628 [85] with copyright permission from ACS.*

membrane scaling in the subsequent ED process [9]. In the following ED with BMs, the conventional inorganic acid/base was regenerated from its corresponding salts [9]. In addition, researchers successfully further enhanced the removal/recovery efficiency of toxic heavy metal ions through hybridizing ion exchange and ED processes (also known as electrodeionization, EDI). The ion exchange resin was assembled in the dilute water compartment. Thanks to the enhanced ion transfer in the dilute compartment, the ionic concentration can be reduced to a very low level [1,66,89–92]. Meanwhile, the energy consumption can be simultaneously reduced owing to the lower internal resistance. In addition, the resin regeneration can be realized by water dissociation which generates H^+ and OH^- [93]. This application scheme is also applicable for treating dilute wastewater (e.g., rinse water in electroplating industry) [66,94]. Ortega et al. reported that the final concentration of arsenic can be lower than the WHO limit with resin electro-regeneration in the hybrid system [95]. The removal efficiency of Cr^{6+} can be higher than 99% with low energy consumption in an EDI system [91]. A two-stage EDI system was performed for a nickel removal efficiency of more than 99.8% from electroplating rinse wastewater that the dilute stream from the first stage was further purified in the second stage [5]. For metallic ions of similar valences, previous researches demonstrated that integrating ED with complex formation reaction can substantially enhance the selectivity of ED by converting target metal ions into oppositely charged complexes. For example, chelating agents (e.g., ethylenediaminetetraacetic acid (EDTA), citric acid, and glycine) have been introduced into ED to form highly stable complexes with the target ions (e.g., nickel, iron, silver, copper etc.). The resulting complexes are negatively charged (e.g., Ni-$(EDTA)^{2-}$) and can preferentially pass through AEM to the product solution [4,77,96]. Removal efficiencies of greater than 95% have been reported for this type of hybrid system [4].

This book belongs to Badji Mokhtar Annaba University Central Library Copyright Elsevier 2025

Lithium recovery—realized by combining the precipitation and ED processes—from waste lithium ion batteries has drawn people's attention due to the dramatic growth in the demand of lithium for battery applications. Lithium can firstly be purified and precipitated by the phosphate. The resulting lithium phosphate can be dissolved in an acid and applied as an anolyte of an ED stack in which lithium is transported through the CEM to the catholyte and converted to lithium carbonate (Fig. 9.8) [68]. However, there is generally cobalt coexisting with lithium in the leach solution of the spent lithium ion battery cathodes. Lizuka et al. fractionated lithium and cobalt by integrating ED with a metal-ion chelation process in which EDTA was introduced to selectively chelate with cobalt ions, and the ED process then selectively removed the resulting negatively charged cobalt-EDTA complex from the positively charged lithium [70]. Lithium can also be separated from cobalt ions by a SED, which allows lithium ions to pass through monovalent ion selective IEM but retains the multivalent cobalt ions [69]. The concentrated effluent of heavy metal can be further electrolyzed to yield metal deposit for usage in the hybrid system of ED and electrolysis [97].

In addition to bench scale tests, Benvenuti et al. performed a full-scale test of nickel recycling with ED in a metallurgical plant in southern Brazil. Near zero emission of pollutants was realized, with the waste effluent reduced by about 90% and the chemical consumption for the nickel plating process saved by 20% [72]. Onorato et al. conducted an ED research of treating a real ground water in central Australia which contained various species of inorganic trace contaminants (i.e., arsenic (V), boron, lithium, selenium (VI), and uranium). They concluded that the removal efficiency of heavy metals is generally dependent on solution pH. The precipitation of heavy metals at

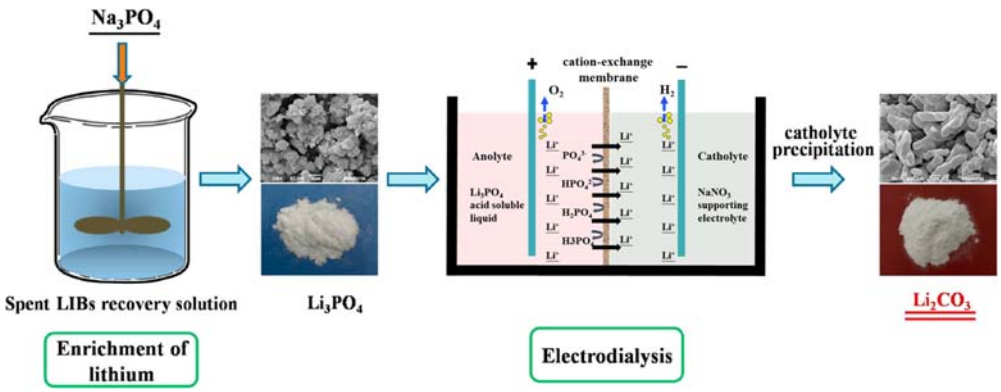

Figure 9.8 Schematic diagram of electrodialysis device with precipitation process for lithium recovery from spent lithium-ion batteries. *Obtained from Y. Song, Z. Zhao, Recovery of lithium from spent lithium-ion batteries using precipitation and electrodialysis techniques, Sep. Purif. Technol. 206 (2018) 335–342 [68] with copyright permission from Elsevier.*

This book belongs to Badji Mokhtar Annaba University Central Library Copyright Elsevier 2025

high pH led to membrane scaling, resulting in higher internal resistance and decreased removal efficiency [98].

9.5 BMED for chemical production from industrial wastewater

BMs are critical components of BMED which determines the electrical performance and energy efficiency of BMED (Table 9.3). The commercially available BMs mainly include Neosepta BP-1/BP-1E from ASTOM, Fumasp FBM from GmbH, and PCCell BP from GmbH. These membranes represent high water dissociation

Table 9.3 The main commercial BM and their applications.

Type	Efficiency	Thickness (μm)	Voltage drop (V)	Applications
ASTOM Neosepta BP-1/BP-1E*	>98%	220	1.2–2.2	• Green production: Methionine [99–101], glycine, phenylalanine, serine, valine [102]; • Inorganic salt transformation: SWRO brine [103–105]; Li_2CO_3 [106], NH_4^+-N [107,108], Boron & Lithium [109]; • Wastes reclamation: acetic acid [110,111], Formic acid [112], l-malic acid [113]; Municipal wastewater [114];
GmbH Fumasp FBM*	98%	180–200	<1.8	• Green production: [EMIM]OH [115], salicylic acid [116], Tetramethyl Ammonium Hydroxide [117]; • Inorganic salt transformation: Sodium Chloride [118,119], $(NH_4)_2SO_4$ [120], Brine [121]; • Wastes reclamation: Acetic acid [110], Inorganic acid/base [9], Glyphosate [122];
GmbH PCCell PC BP*	>98%	220	1.2–2.2	• Green production: Fumaric acid [123–125], Pellet reactor [126], Acetic acid [127], Succinic acid [128]; Alpha-ketoglutaric [129,130]; • Inorganic salt transformation: SWRO brine [131–133], Industrial saline water [134], NH_4^+-N [135,136], KCl [137], borax [138], NaF [139]; Boron & Lithium [140]; • Waste reclamation: Tartaric Acid [8], Phosphoric acid [141], Mixed acid/base [142,143].

BMs, bipolar membranes.
*The properties of the BM were collected from the following references: [123–125,144–151].

This book belongs to Badji Mokhtar Annaba University Central Library Copyright Elsevier 2025

efficiency (> 98%) and low voltage drops, which can be used for green production in the chemical industry, inorganic salt transformation in environmental/chemical engineering processes, and waste reclamation applications. For instance, Neosepta BP-1/1E were used in the pre-/posttreatment of fermentation broth to simultaneously isolate organic salt, on one hand, and the acidification, on the other. It also performs faithfully with high inorganic salt transforming efficiency and the reconcentration of acid and base solution (> 5 mol/L). Meanwhile, Fumasep FBM and PCCell BP from GmbH are widely used in the food industry and in waste reclamation. Benefiting from the development of monopolar IEMs, many commercial BMs were released in the past decades, for example, ChemJOY from China developed CJBPM-1 with above 98% water dissociation efficiency and lower water dissociation voltage (<1.2 V). The developed membranes were successfully used for the reclamation of flue gas desulfurization brine [144]. Also, MemBrain from the Czech Republic developed MEGA BMI-9000 BM by hot pressing the heterogeneous cation and AEMs into a three-layered composite membrane. They have been effectively used in the pH correction of milk whey [152], nutrients and VFAs recovery [10], and Na_2SO_4 transformation [153].

There are three different scenarios for integrating BMED in industrial processes: (1) BMED as a posttreatment process for acid/base recovery from saline wastewater, (2) BMED as a pretreatment process for valuable chemicals generation to improve the overall products generation efficiency and decrease waste discharge, and (3) BMED as both a pre- and posttreatment process to simultaneously realize production efficiency enhancement and chemical recovery from wastewater. The scheme for these scenarios of BMED application is illustrated in Fig. 9.9.

9.5.1 BMED as a posttreatment process for inorganic acid/base generation from wastewater

With the growing population and the changing climate, desalination has been recognized as an effective way to meet the growing demands for freshwater. Thermal desalination and pressure driven membrane desalination (i.e., by reverse osmosis (RO)) are two representative techniques for desalination, by either removing salt from water or recovering water from the salt. However, the increasing implementation of desalination processes raises a critical concern over the disposal of large quantities of concentrated waste (i.e., the desalination brine). Accompanied with the production of freshwater, desalination brines have been recognized as a daunting environmental challenge. The TDS of these concentrated brines is typical 1–3 times higher than seawater, and can cause severe threats to the marine ecology if discharged untreated in the environment. ED has been introduced to the membrane operation system to minimize the waste brine fraction (Fig. 9.10), either through concentrating the brine to a higher mass concentration or through desalinating the brine to the TDS below the seawater. Specifically, the concentration of the treated brine rises to the highest value of 27.13%

This book belongs to Badji Mokhtar Annaba University Central Library Copyright Elsevier 2025

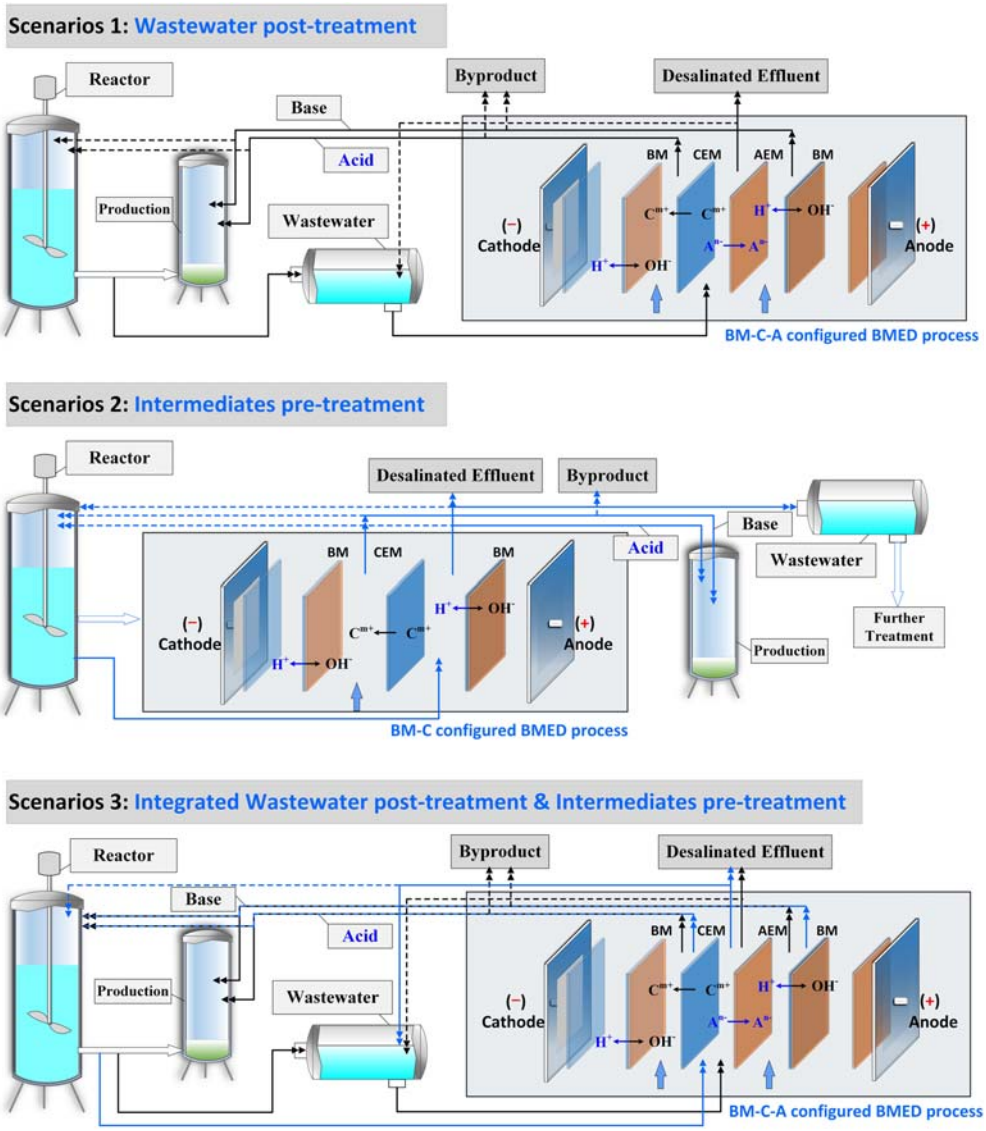

Figure 9.9 The scheme of BMED application in different procedures.

(m/v) with a water recovery ratio of 67.78% and desalination ratio of 72.47%. Such high TDS brine can be further concentrated to produce coarse salt and table salt [154–156]. The ED posttreatment of waste brine can improve the overall water recovery to a higher level (e.g., 97%–98%) [156–158]. Zero liquid discharge can also be realized at a pilot scale by integrating ED and pressure driven membrane processes with high water recovery and mineral byproducts generation [159]. As a result, the

This book belongs to Badji Mokhtar Annaba University Central Library Copyright Elsevier 2025

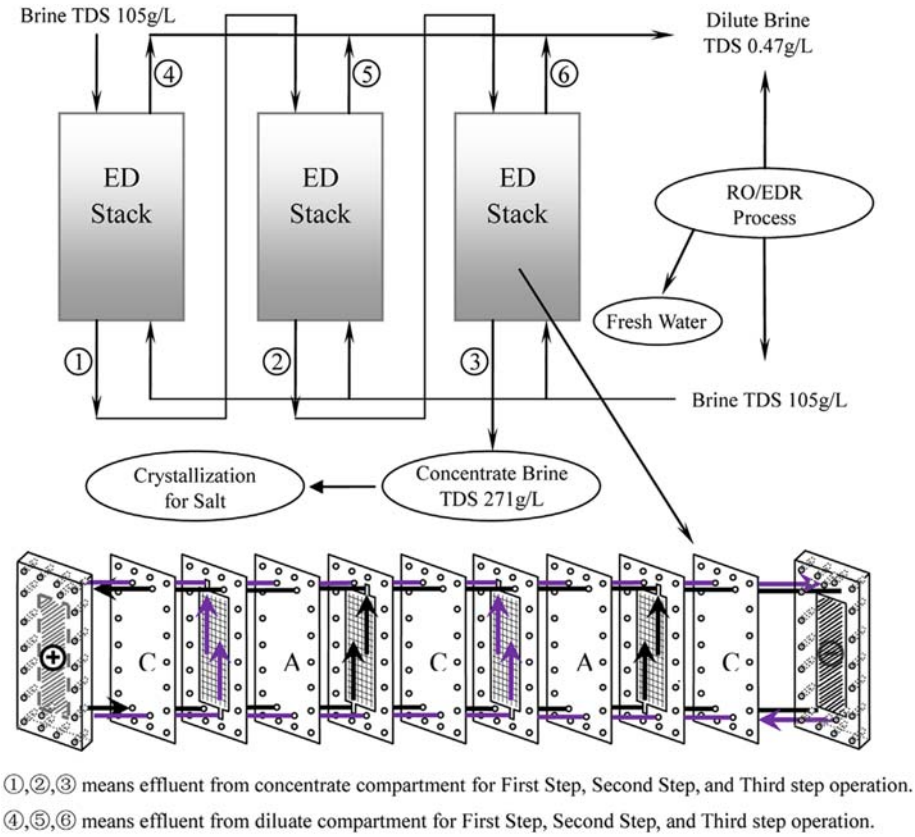

Figure 9.10 The schematic diagram of a flow-sheet concept ED stack with multi-step operation mode used for the treatment of RO concentrated brine. *Reproduced from C.X. Jiang, Y.M. Wang, Z.H. Zhang, T.W. Xu, Electrodialysis of concentrated brine from RO plant to produce coarse salt and freshwater, J. Membr. Sci. 450 (2014) 323–330 [154] with copyright permission from Elsevier.*

potential ecological threat of concentrated brine discharge can be minimized. To remove the contaminant in the concentrated brine, the conventional chemical precipitation approach can be utilized as the pretreatment before using the BMED process for the conversion of RO concentrate into mixed acid and mixed base streams or for electrochlorination for onsite chlorine generation. The bench-scale BMED demonstrated that an RO concentrate could be desalted while producing mixed acids and mixed bases with concentrations as high as 0.2 mol/L. The capital costs required for the train with the BMED is only \$0.43/m^3. The annual operation and maintenance costs of the BMED train (\$0.26/m^3) are lower than both of evaporation pond (\$0.41/m^3) and zero liquid discharge (\$0.81/m^3). If the added-value of the acid and base products and the cost of recovered water are considered, then an additional \$0.1/m^3 could be recovered by using this BMED treatment train.

This book belongs to Badji Mokhtar Annaba University Central Library Copyright Elsevier 2025

The concentrating of multivalent ions may cause membrane scaling, while resulting in decreased process efficiency and shortened lifespan of the membrane stack. To reduce the scaling potential of Ca^{2+}/Mg^{2+}, the pretreatment of the concentrated brine, that is, the softening of brine to remove Ca^{2+} and Mg^{2+}, is generally required before inputting it to the BMED unit [160]. NF and SED are two possible pretreatment approaches to remove these divalent ions from the concentrated brine, before its further processing for the production of base/base using BMED. By externally-coupling the SED and the BMED processes [103], wastewater with mixed ions of Na^{+}, Cl^{-}, and SO_4^{2-} can be fractionized into NaCl and Na_2SO_4 using SED, then the pure NaOH, HCl, and H_2SO_4 can be produced through BMED without evident fouling or degradation on IEMs. Fig. 9.11 illustrates a representative SED and BMED external-coupled treatment. By using this scenario, the purity of the salt streams obtained in the SED unit was higher than 90% for sulfate and 90% for chloride, as a percentage of the processing salt streams fed into SED. The two BMED stages produced pure NaOH solutions, along with HCl-rich (87%) and H_2SO_4-rich (93%) acid streams, respectively, with acceptable energy consumptions. Reig et al. combined SED and BMED such that chloride ions were separated from sulfate ions in the first step, and base (NaOH)/acid (HCl and H_2SO_4) generated from the respective salts of NaCl and Na_2SO_4 in the second step [103].

From the viewpoint of process economy and continuity, SED and BMED are internally integrated by replacing the conventional cation/anion exchange membranes with the monovalent cation/anion perm-selective exchange membranes (MVCs/MVAs), while

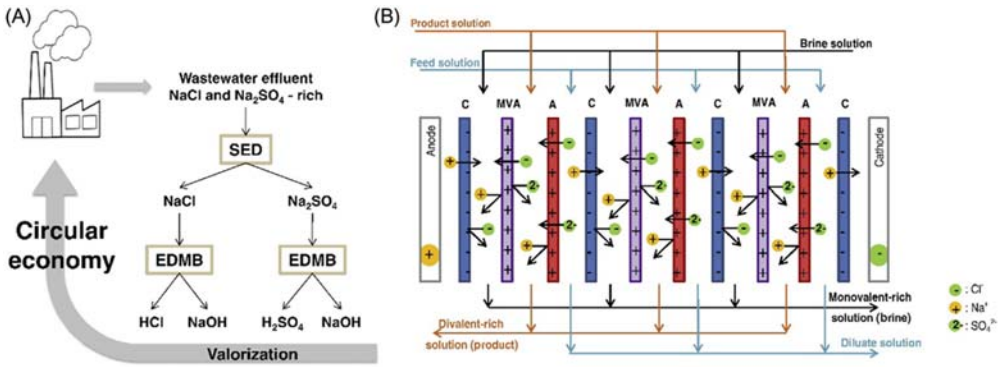

Figure 9.11 Schematic illustrations of (A) the wastewater effluent valorization by ED processes. (B) selectrodialysis (SED) stack including membranes arrangement and definition of stacks streams. *Taken from M. Reig, C. Valderrama, O. Gibert, J.L. Cortina, Selectrodialysis and bipolar membrane electrodialysis combination for industrial process brines treatment: monovalent-divalent ions separation and acid and base production, Desalination 399 (2016) 88–95 [103] with copyright permission from Elsevier.*

This book belongs to Badji Mokhtar Annaba University Central Library Copyright Elsevier 2025

a combine of the independent SED and BMED can be achieved with one BMSED process [104,105]. A lab-scale BMSED assembly with ASTOM ASV/CSO and Selemion ACS/CIMS monovalent selective membranes was studied by changing the operation conditions, such as the power supply mode, current density, and initial brine concentration (Fig. 9.12). The brine desalination efficiency, production efficiency of acid/base, and production quality were investigated to evaluate the feasibility of the designed process. The results indicate that the process worked well when treating the concentrated brine (70–105 g/L). The permselectivity of ions, that is, Na^+/Ca^{2+} and Cl^-/SO_4^{2-} ranged from 5 to 10, and, 50 to 60, respectively. During long-term operation, the brine (105 g/L) was desalinated and transformed into base and acid byproducts under a single continuous mode. The concentrations of NaOH and HCl increased to 2.2 and 1.9 mol/L, respectively. The purities of the NaOH and HCl byproducts both exceeded 99.9%. As such, the process has immense potential for industrialization with a series of advantages: (1) appropriate treatment of brine for disposal or reutilization by using a single step, and (2) reclamation of brine waste into their acid/base byproducts. Thus, BMSED is a potential alternative for "RO concentrated brine management."

NF is another alternative that would separate monovalent ions from brine to assist in value-added byproduct reclamation. By externally integrating the NF and a BMED process (Fig. 9.13), the brine can be effectively desalinated, while fractionating the mixed salts [131].

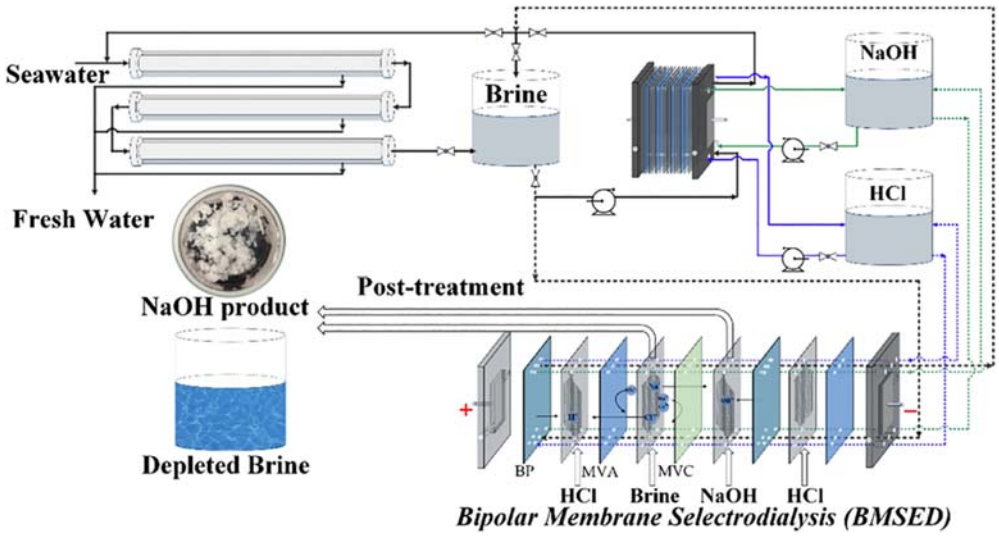

Figure 9.12 The flow scheme of internal integrated SED and BMED process (BMSED). *Obtained from B. Chen, C. Jiang, Y. Wang, R. Fu, Z. Liu, T. Xu, Selectrodialysis with bipolar membrane for the reclamation of concentrated brine from RO plant, Desalination 442 (2018) 8–15 [104] with copyright permission from Elsevier.*

This book belongs to Badji Mokhtar Annaba University Central Library Copyright Elsevier 2025

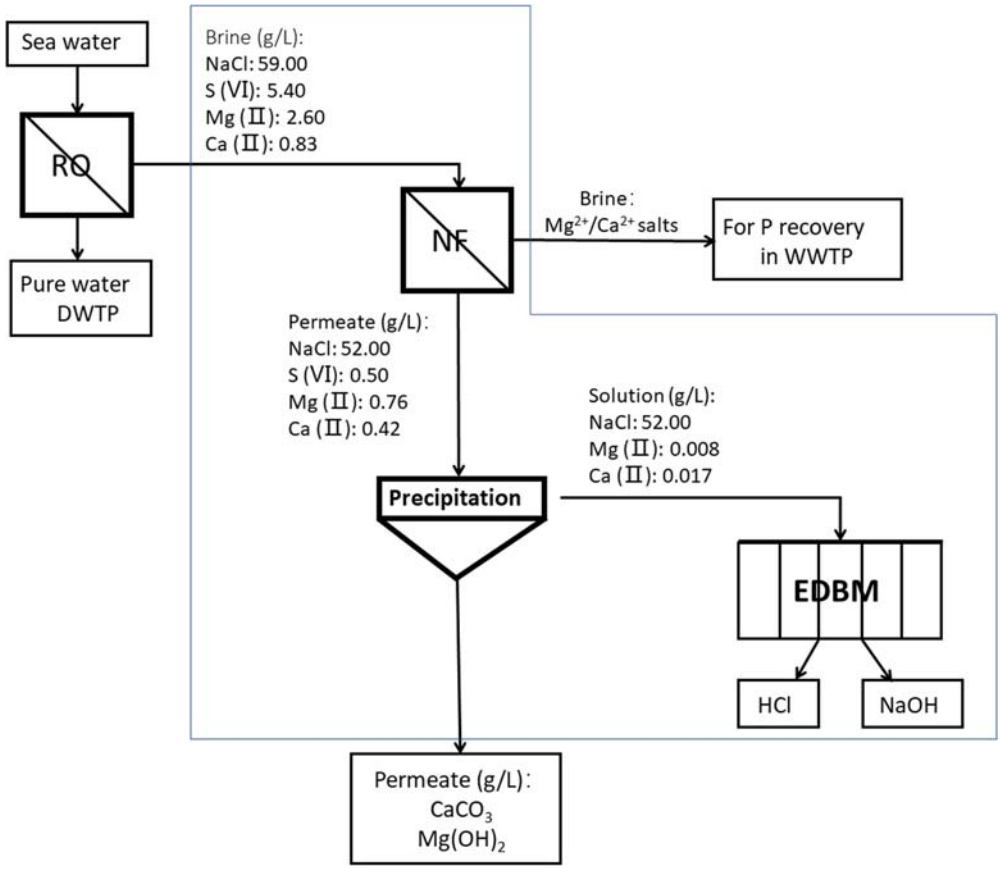

Figure 9.13 The flow scheme of external integrated NF and BMED process for converting SWRO brine into base and acid products. *Reproduced from M. Reig, S. Casas, O. Gibert, C. Valderrama, J.L. Cortina, Integration of nanofiltration and bipolar electrodialysis for valorization of seawater desalination brines: production of drinking and waste water treatment chemicals, Desalination 382 (2016) 13–20 [131] with copyright permission from Elsevier.*

By using a semi-aromatic polyamide NF membrane (NF270) for the softening of SWRO brine, polyvalent ions (Ca^{2+}, Mg^{2+}, Sr^{2+}, Cu^{2+}, Ni^{2+}, and Al^{3+}) were rejected (e.g., enrichment factors of 3.2 for Mg^{2+} and 2.5 for Ca^{2+} when working at 20 bar). The rejection values for Na^{+}, Cl^{+}, and K^{+} were lower, which is mainly dependent on the hydrated ionic radii and speciation. Rejection of polyvalent ions increased with the pressure, but NaCl rejection increased a maximum to 12%. For further purification of the permeate to remove Ca^{2+} and Mg^{2+} and thus meet the BMED requirements, the precipitation treatment by Na_2CO_3 (pH 10.6) and NaOH (pH 11.6) was introduced, and approximately 95% of Ca^{2+} and Mg^{2+}, each, were removed. The resulting brine, containing 50 g/L

This book belongs to Badji Mokhtar Annaba University Central Library Copyright Elsevier 2025

NaCl and a negligible amount of Ca^{2+} and Mg^{2+}, was then input into the BMED stack to produce NaOH and HCl under recirculation configuration. According to the results, conversion percentages of HCl and NaOH were higher than 70% of the produced NaCl brine. The production of NaOH and HCl concentrations was linearly dependent on the applied voltage, though the initial acid and base concentrations had no major effect on the overall performance. The energy consumption and current efficiency was around 2.6 kWh/kg-NaOH and 77%, respectively.

During the waste acid recovery process, the leakage of protons through conventional AEMs is a major challenge encountered. It is necessary to develop AEMs that minimize the leakage of H^+. The special transport mechanisms of proton, that is, Grotthuss and Vehicle mechanisms [161,162], show that water plays an important role in proton conduction. Several strategies have been used to enhance the acid-blocking ability of AEMs, including the introduction of hydrophobic groups, construction of a dense membrane structure, and adoption of the relevant weak base groups [163,164]. However, the above-mentioned endowments of acid-blocking performance result in a higher membrane resistance since the conductivity of anions in AEMs is also reduced. Therefore, the trade-off effect between the AEM conductivity and its corresponding acid-blocking performance should be further investigated. Bai et al. [165] designed a series of weak base AEMs with ion-nanochannels by introducing weak base groups of different carbon chain lengths and grafting densities, and linked these onto the polysulfone skeleton as side chains. The confinement effect in the formed ion-nanochannels contributed to the reduction of membrane water uptake, enhancement of the Donnan exclusion for co-ions, and the facilitating of the transport for counterions simultaneously.

9.5.2 BMED as a posttreatment process for organic acid/base generation from wastewater

About 50%–70% of the cost of the production of organic acid is generated by the recovery of the fermentation product [166–168]. Various technologies including precipitation, extraction, adsorption, ion-exchange system etc., have been proposed for the efficient recovery of organic acids. However, some of these conventional technologies either require further concentration steps and hazardous solvents, and then produce dangerous waste and the concomitant of environmental pollution, or consume high energy and increase the process cost. Electromembrane processes, for example, BMED, have been recognized as an effective alternative for the cleaner production of organic acids from the fermentation broth. The possibility of treating wastewater to recover organic acids has been demonstrated by using BMED, including its hybrid processes integrated with biotechnologies. The feed in the fermentation broth generally contains bivalent ions (Ca^{2+}, Mg^{2+}), monovalent ions (Na^+, K^+, NH_4^+), dissolved organic matter (sugar), and suspended solids/colloidal matter. Prefiltration and

This book belongs to Badji Mokhtar Annaba University Central Library Copyright Elsevier 2025

desalination are generally the preliminaries before the BMED process to obtain pure organic acid product. The pretreatment of solution in the fermentation broth prior to the BMED process is as shown in Fig. 9.14 below. Ion substitution ED is also proposed as a posttreatment in the reclamation of industrial waste acid from metal finishing in order to produce organic acid (e.g., acetic acid) from the corresponding salt. The concentration of metal ions in the produced organic acid can be reduced using monovalent ion permselective exchange membranes; thus, IEMs help obtain a high-purity organic acid product through a simple posttreatment.

Three common configurations have been used for the separation of organic acid from mixtures using BMED, that is, BM−AEM, BM−CEM, BM−AEM−CEM [169]. The BM−CEM−AEM arrangement consists of a BM, an AEM, and an CEM, typically arranged in the sequence shown in Fig. 9.15A. Three compartments, that is, acid, base, and feed compartments (in addition to the two-electrode compartments), are separated by the membranes. Initially, the feed compartment is filled with organic salt from the clarified fermentation broth or the disposed effluent. Low concentrations of supporting electrolyte are added in the base and acid compartments to decrease the stack resistance. Under the applied electrical field, cations migrate through the CEM to the base compartment and combine with hydroxyl ions dissociated from BM to generate the base. Organic anions transport across the AEM to the acid compartment and combine with protons dissociated from BM to generate the acid. Consequently, organic anions are converted into organic acid, and the organic salt in the feed compartment is gradually desalinated and converted into the corresponding products until the depletion of organic salt.

The BM−AEM and BM−CEM configurations are shown in Fig. 9.15B and C, respectively. Each of these configurations consist of two compartments, that is, acid and feed compartments for BM−AEM, and base and feed compartments for

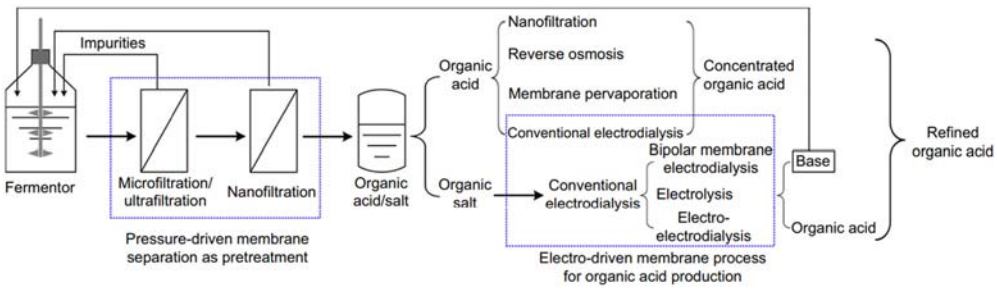

Figure 9.14 BMED for fermentation broth application with pretreatment process. *Obtained from C. Jiang, Y. Wang, T. Xu, 6 - Membranes for the recovery of organic acids from fermentation broths, in: Membrane Technologies for Biorefining, Woodhead Publishing, 2016, pp. 135−161 [169] with copyright permission from Elsevier.*

This book belongs to Badji Mokhtar Annaba University Central Library Copyright Elsevier 2025

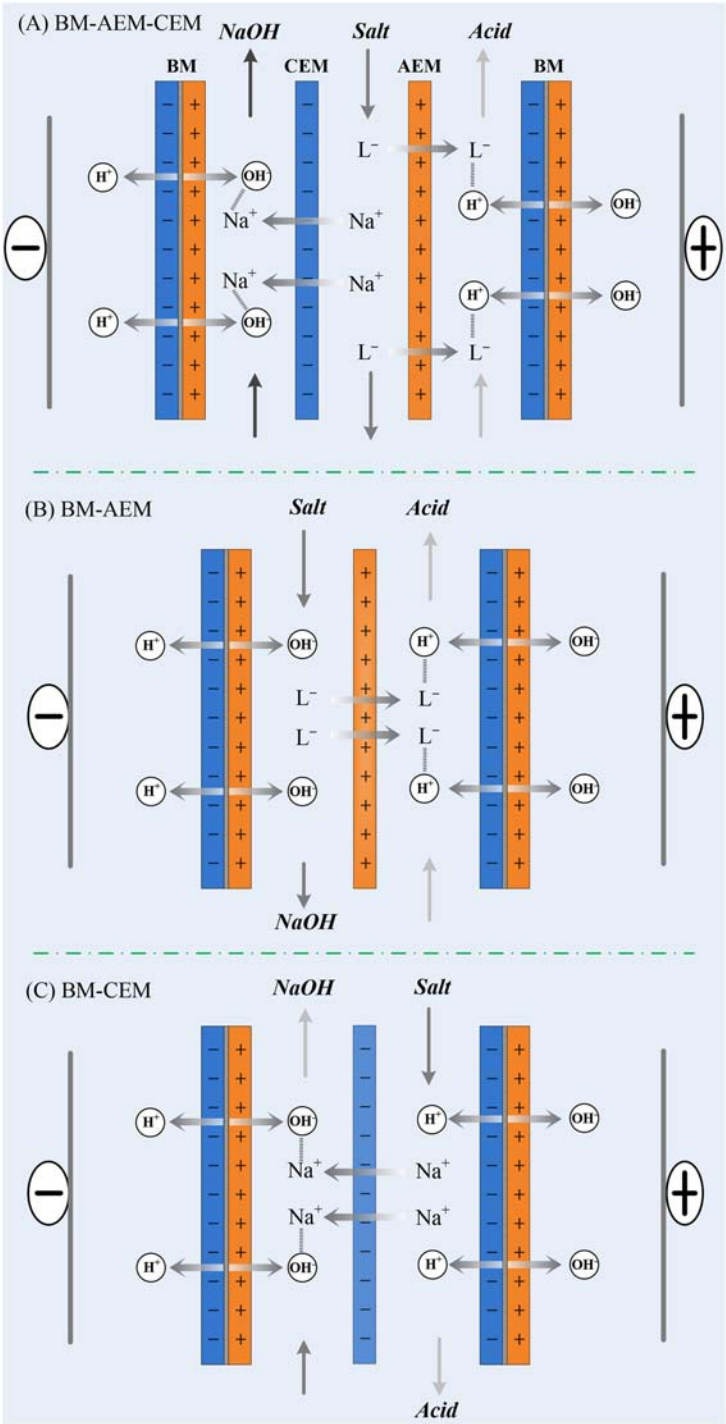

(*Continued*)

This book belongs to Badji Mokhtar Annaba University Central Library

Copyright Elsevier 2025

BM−CEM. For the BM−AEM configuration, organic anions in the feed solution migrate through the AEM into the acid compartment under an electrical potential difference, and are substituted by the OH^- ions that are released from the BM. As a result, organic acid is produced by anions combining with the protons that dissociated from BM on the other side. Cations retained in the feed compartment are converted into base byproducts. In the case of the BM−CEM, cations in the feed solution migrate through the CEM into the base compartment, and are substituted by the protons that are dissociated from the BM. Therefore, pure base is produced by the combination of cations and OH^- provided by the BM on the other side, while organic acid is produced by the substitution of protons in the feed solution.

Among the three configurations, the BM−CEM−AEM configuration provides the higher purity for the produced NaOH and organic acid. However, its energy consumption is also increased owing to higher stack resistance in comparison to BM−AEM and BM−CEM arrangements. BM−AEM can also offer high purity of organic acid products, although the current efficiency of this configuration is reduced due to the diffusion of protons between the adjacent base and feed compartments. Membrane scaling and/or fouling is another important concern for the BM−CEM−AEM and BM−AEM configurations, since foulants are often negatively charged and show greater propensity to foul the positively charged AEM. For BM−CEM, organic salt in the fermentation broth can be efficiently converted into the products with insignificant membrane fouling/scaling due to the absence of AEM. The fouling on a CEM is mainly ascribed to the precipitation of metal ions that can be removed by appropriate pretreatment such as with an NF. Alternatively, postcleaning by inverting the electrode polarity and rinsing by chemicals or gas-liquid mixtures can be effective in rejuvenating the IEMs. Therefore, BM−CEM is the preferable configuration for organic acid conversion. Acetic acid, formic acid, and L-malic acid are the three classical organic acids, whose production using BMED is discussed in what follows next.

Given acetic acid is a common organic acid that is widely used in food, pharmaceutical, and chemical industries; it thus follows that a large number of wastewater sources containing acetic acid of different concentrations have been generated from these industries. It is necessary to consider environment and process cost issues for the recovery of the acetic acid and BMED has been proved an effective approach for the desalination of the wastewater while recovering valuable organic acid product. It has been proposed that BMED

Figure 9.15 Three representative configuration, that is, BM−CEM−AEM, BM−AEM, and BM−CEM for the separation of organic ions from the mixed solution. (A) BM−AEM−CEM; (B) BM−AEM; (C) BM−CEM. *Taken from C. Jiang, Y. Wang, T. Xu, 6 - Membranes for the recovery of organic acids from fermentation broths, in: Membrane Technologies for Biorefining, Woodhead Publishing, 2016, pp. 135−161 [169] with copyright permission from Elsevier.*

This book belongs to Badji Mokhtar Annaba University Central Library Copyright Elsevier 2025

be used for the recovery of acetic acid from acetaldehyde wastewaters [110,111,170], where the membrane configuration and the ion exchange property are critical issues that determine process efficiency (Fig. 9.16). Ion exchange resin, which may facilitate the transport of ions, was filled in the BMED stack to decrease the BMED stack electrical resistance, which decreased the overall process energy consumption. Under the optimized operating conditions, a relatively high current efficiency of 56.72% and low energy consumption of 0.61 kWh/kg were achieved.

The recovery of formic acid was also proposed using the integrated "electro-membrane" process, in which the BMED plays a critical role [112]. The treatment method follows three steps: (1) wastewater neutralization; (2) sodium formate concentration by conventional electrodialysis (CED); and (3) BMED to convert sodium formate into formic acid and sodium hydroxide. The coupling of these processes was performed (Fig. 9.17) with the results that formic acid at about 7 mol/L concentration was produced, with relatively high current efficiency of ~80% under a current density of 50 mA/cm^2. The electrochemical energy consumption was about 2.6 kWh/kg-formic acid.

L-malic acid from a beverage industry wastewater was recovered following a similar method, that is, the combination of CED and BMED [113]. The procedure and the main composition of wastewater are shown in Fig. 9.18. A two-stage ED process coupling CED and BMED was adopted in which BMED was investigated by its having a two-compartment cell (BM/CEM) on a model potassium malate solution over the concentration range 0.4−1.2 equiv./L. The process resulted in a current efficiency of 87%−97%, L-malic acid recovery efficiency of 93%−97%, and specific energy consumption of 1.15−1.27 kWh/kg-malic acid. These results were confirmed by additional runs on real concentrate obtained from the previous CED stage. However,

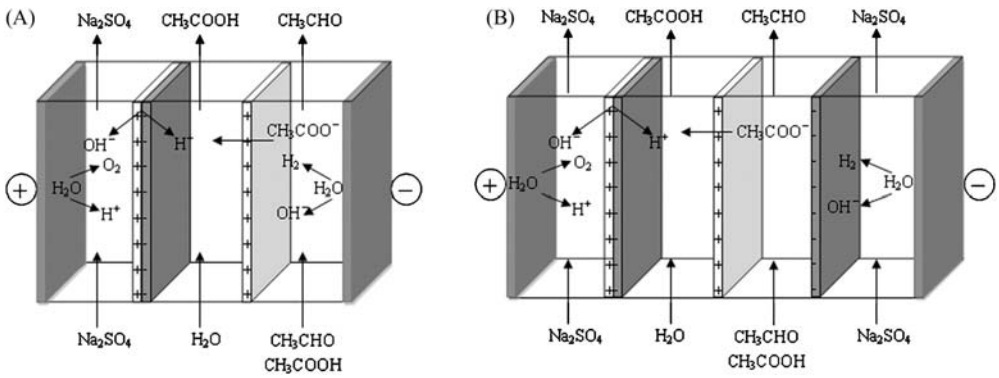

Figure 9.16 The membrane configuration for the recovery of acetic acid from the simulated acetaldehyde wastewaters. *Obtained from X. Zhang, C. Li, Y. Wang, J. Luo, T. Xu, Recovery of acetic acid from simulated acetaldehyde wastewaters: bipolar membrane electrodialysis processes and membrane selection, J. Membr. Sci. 379 (2011) 184−190 [110] with copyright permission from Elsevier.*

This book belongs to Badji Mokhtar Annaba University Central Library Copyright Elsevier 2025

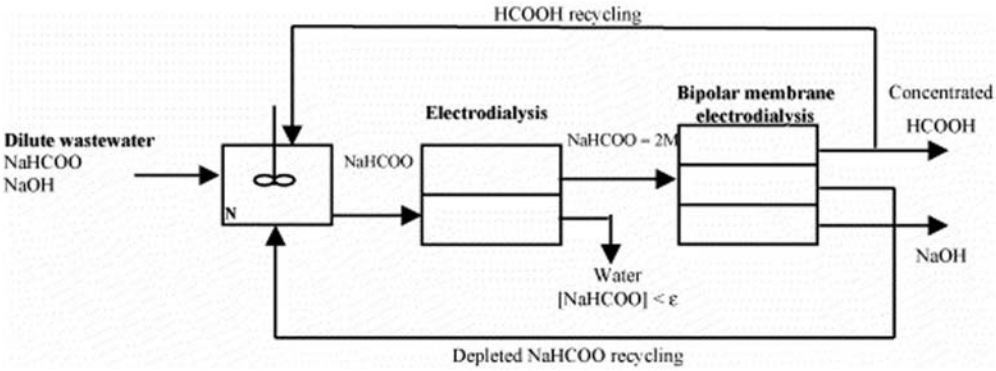

Figure 9.17 The whole process for the treatment of wastewater containing sodium formate and sodium hydroxide: (1) wastewaters neutralization; (2) sodium formate concentration by conventional electrodialysis (CED); and (3) BMED to convert sodium formate into formic acid and sodium hydroxide. *Reproduced from J.S.J. Ferrer, S. Laborie, G. Durand, M. Rakib, Formic acid regeneration by electromembrane processes, J. Membr. Sci. 280 (2006) 509–516 [112] with copyright permission from Elsevier.*

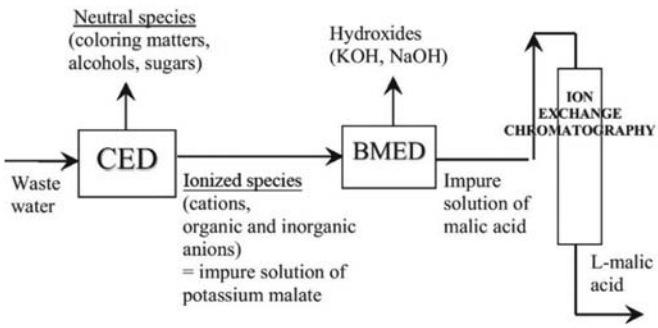

Figure 9.18 The integrated process, that is, CED + BMED + IEX for the recovery of L-malic acid from a beverage industry wastewater. *Obtained from M.-L. Lameloise, R. Lewandowski, Recovering l-malic acid from a beverage industry waste water: experimental study of the conversion stage using bipolar membrane electrodialysis, J. Membr. Sci. 403–404 (2012) 196–202 [113] with copyright permission from Elsevier.*

specific energy consumption was significantly increased (50%) due to the presence of anionic impurities, stressing the importance of a very efficient preliminary purification step. Last, the two-stage ED process allowed malate purity to be raised from 9% in the initial effluent to more than 70%.

In addition to the above common applications of BMED process in the extraction of organic acid from the chemical reaction intermediate, there are additional sweet spots for the cleaner production of the organic acid from the fermentation broth. Amino acid production presents an interesting case, in which BMED can be

This book belongs to Badji Mokhtar Annaba University Central Library Copyright Elsevier 2025

introduced as an alternative to overcome the severe environment pollution and/or process inefficiency of traditional methods. Unlike common carboxylic organic acids, amino acids are a special class of organic acids that also contain an amine group in addition to a carboxyl group. This results in amphiprotic properties in the amino acids, as shown in Scheme 9.1. This makes the recovery of amino acids different from that of common carboxylic organic acid because the charge properties of amino acids are strongly dependent on the solution pH. Amino acids are zwitterionic molecules at their respective isoelectric point (pI) (Table 9.4). Based on this property, amino acid can be fractionated from the fermentation broth by incorporating CED and BMED.

The acid and base generated in the BMED can be used to manipulate the pH of the fermentation broth, thereby achieving the separation of amino acid from the

$$^{+}H_3N{-}RCH{-}COOH \longleftrightarrow H_2N{-}RCH{-}COOH + H^+ \quad (1)$$

$$H_2N{-}RCH{-}COOH \longleftrightarrow H_2N{-}RCH{-}COO^- + H^+ \quad (2)$$

Scheme 9.1 The deprotonation scheme of amino acid.

Table 9.4 The physical-chemistry properties of some amino acids [171].

Amino acid	Structure formula	pI ($pK_1/pK_2/pK_3$)	Side chain charge (pH = 7)
Arginine	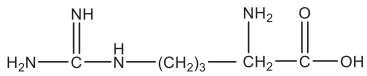	10.76 1.82/8.99/12.48	Positive
Lysine	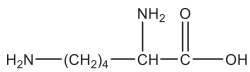	9.60 2.16/9.06/10.54	Positive
Aspartic acid	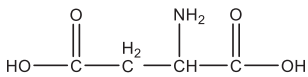	2.85 1.99/3.90/9.90	Negative
Glutamic acid	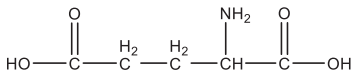	3.15 2.13/4.31	Negative
Alanine	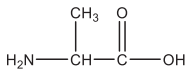	6.01 2.34/9.87	Neutral
Glycine	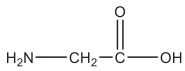	6.06 2.35/9.78	Neutral
Tryptophan	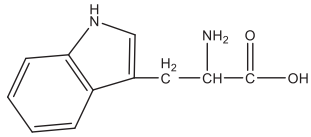	5.89 2.46/9.41	Neutral

This book belongs to Badji Mokhtar Annaba University Central Library Copyright Elsevier 2025

fermentation broth. A two-compartment BMED stack including BM-AEM and BM-CEM cells is commonly used for amino acid production (Fig. 9.19). Take BM-AEM as an example: this cell configuration has been used to produce methionine, alanine, glycine, phenylalanine, serine, valine, lysine, and histidine [99,100,102,172]. In this case, the clarified fermentation broth is circulated in the base chamber and the neutral amino acid will combine with hydroxyl ions and convert into anionic forms. Thereafter, the anionic form can transport across the AEM and combine with protons to generate the neutral amino acid in the acid chamber. The BM-CEM configuration is operated in a similar fashion to BM-AEM, but the feed solution is circulated in the acid compartment and the neutral amino acid is converted into positively charged cations that will migrate through the CEM. The amino acid will be generated in the base compartment correspondingly.

9.5.3 BMED as a pretreatment process

By using BMED for the cleaner production of organic acid from a chemical reactor or fermentation broth, one increases the recovery efficiency of the final product, recovers valuable byproducts (e.g., production of base), and decreases the amount of contaminant in the disposals. For example, methionine is an essential amino acid that is often produced using the so-called hydration method [100,101], in which the synthetic route of hydration approach (a ring-closure reaction and ring-opening reaction) is applied to produce methionine from the fine chemicals (Scheme 9.2). However, enormous quantities of NaOH is consumed to promote ring-opening reaction, while large quantities of sulfuric acid is required to acidify the sodium methionine into methionine acid at the isoelectric point in order to crystalize methionine from its salt mixture. This conventional acidification approach requires the disposal of enormous amounts of acidified wastewater and enriched sodium sulfate salt. To avoid the above issue, BMED can be introduced as an alternative to the acidification procedure (Fig. 9.20). The feasibility of BMED for separating methionine anions from its mixture with sodium carbonate was evaluated using a series of lab-scale tests that were implemented with different membranes and cell-configurations, and with performance indicators with respect to membrane fouling, product recovery efficiency, and the desalination efficiency which were systematically studied. The results indicate that the BM-CEM configuration was the most suitable arrangement and that ChemJOY membranes were suitable for methionine separation with excellent antifouling characteristics. An additional pilot-scale system was implemented, revealing that BMED could produce methionine efficiently at recovery ratio of c. 83.23% and desalination ratio of c. 95.18%.

However, due to the migration of organic anions through the IEM, the recovery ratio for organic acid is limited on condition that there is the adjusting of solution pH to the corresponding isoelectric point, which is generally required [173]. Moreover,

This book belongs to Badji Mokhtar Annaba University Central Library Copyright Elsevier 2025

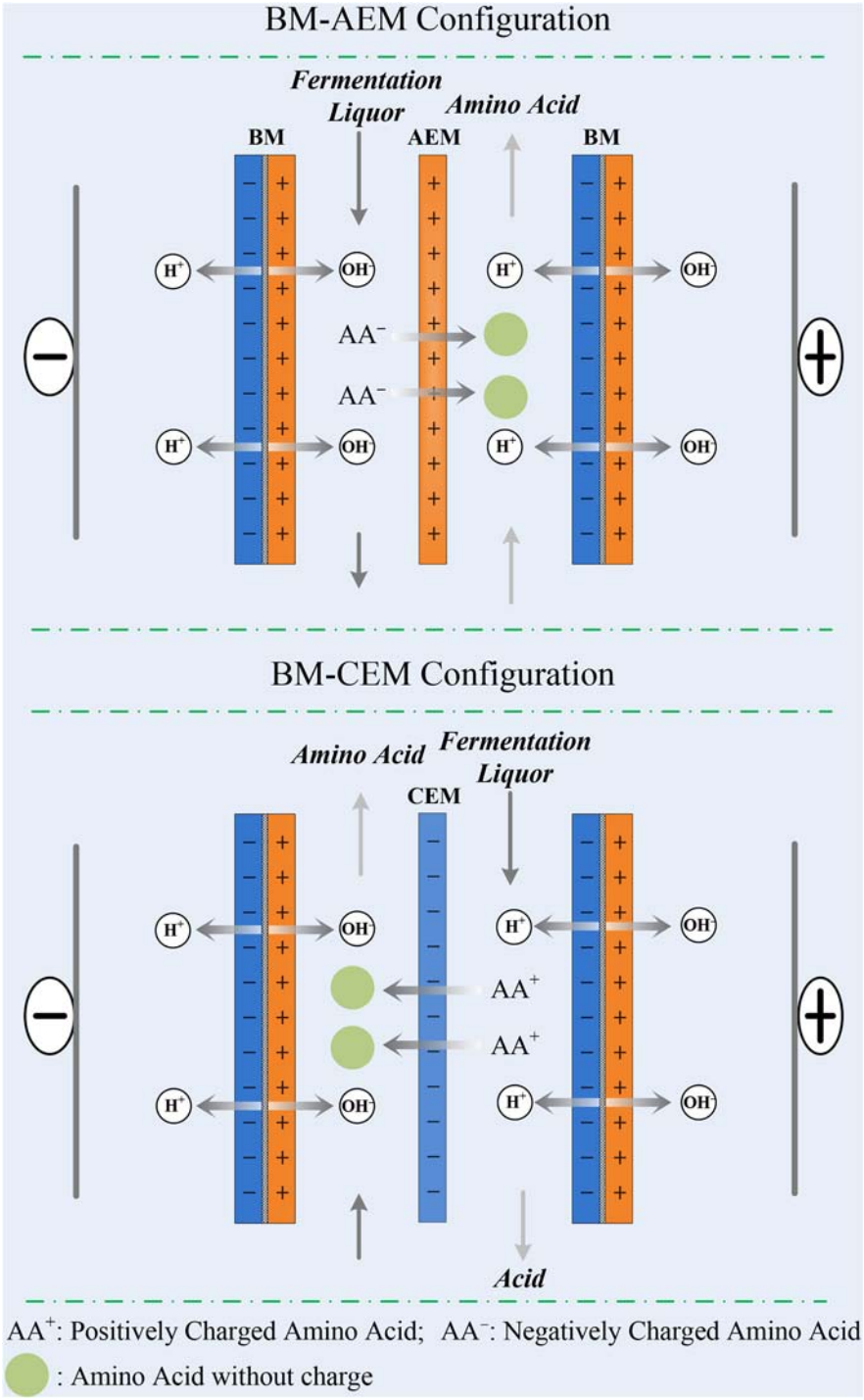

(*Continued*)

This book belongs to Badji Mokhtar Annaba University Central Library Copyright Elsevier 2025

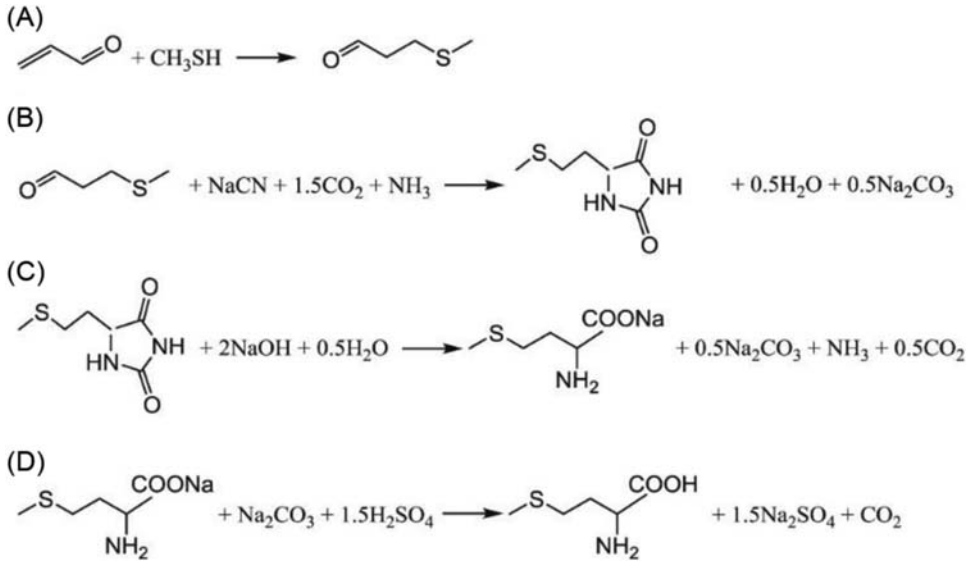

Scheme 9.2 The reaction scheme for preparation of methionine. *Obtained from C. Jiang, Q. Wang, Y. Zhang, Y. Li, Y. Wang, T. Xu, Separation of methionine from the mixture with sodium carbonate using bipolar membrane electrodialysis, J. Membr. Sci. 498 (2016) 48–56 [99] with copyright permission from Elsevier.*

membrane fouling/scaling induced by methionine absorption also decreases performance and the lifespan of IEMs. Inspired by studies on CO_2 capture by amino acid salts, CO_2 enriched gas was used for adjusting pH of the amino acid salt solution to promote the conversion of methionine anions into the neutral molecular form ($MetH^{\pm}$). This neutral form is unresponsive to the electrical field and does not move through the IEM, which minimizes the leakage of amino acid. The zwitterion reaction between methionine anions and CO_2, and the working procedure of CO_2 assisted BMED process are illustrated in Scheme 9.3 and Fig. 9.21. The final pH at equilibrium state was largely determined on the CO_2 partial pressure of CO_2 enriched gas (i.e., fuel gas), with higher CO_2 partial pressure correlated with lower pH. After loading with CO_2, the methionine salt mixture was treated with BMED at different current intensities, where the results indicate the process as robust with both high methionine recovery efficiency and desalination rate. The current efficiency was as high as 87% and the energy consumption was approximately 7.0 kWh/kg-CO_2, given the energy consumption will be further

Figure 9.19 BM-AEM and BM-CEM arrangement for the treatment of amino acid/salt from the fermentation broth. *Obtained from C. Jiang, Y. Wang, T. Xu, 6 - Membranes for the recovery of organic acids from fermentation broths, in: Membrane Technologies for Biorefining, Woodhead Publishing, 2016, pp. 135–161 [169] with copyright permission from Elsevier.*

This book belongs to Badji Mokhtar Annaba University Central Library Copyright Elsevier 2025

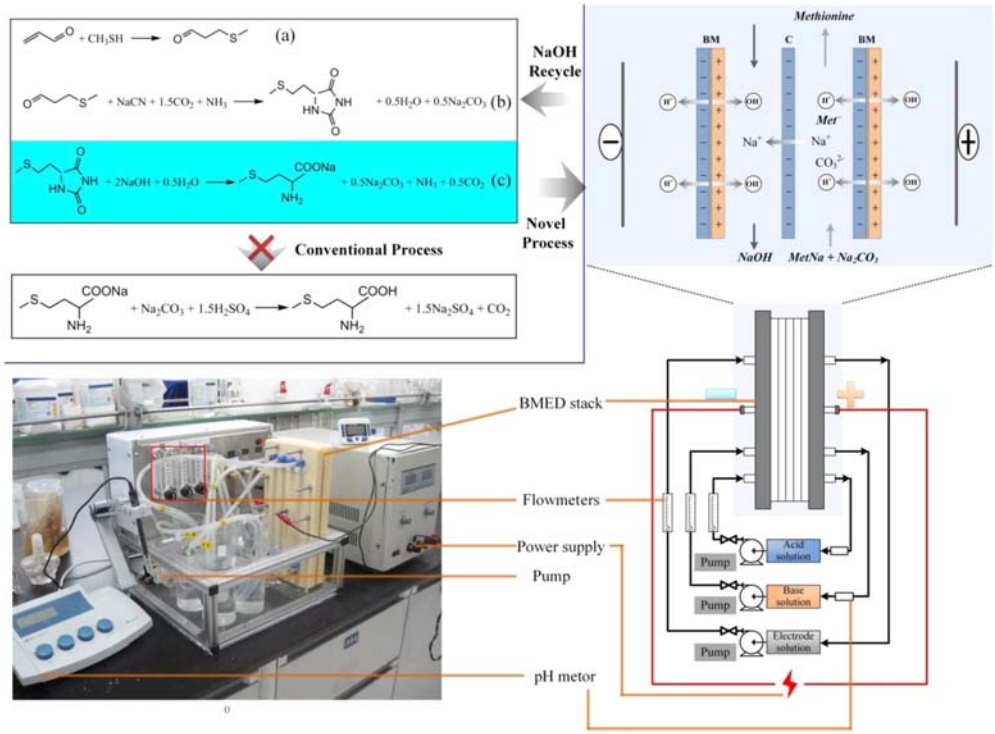

Figure 9.20 BMED as an alternative of conventional acidification approach for the cleaner production methionine from the reactor. *Obtained from C. Jiang, Q. Wang, Y. Zhang, Y. Li, Y. Wang, T. Xu, Separation of methionine from the mixture with sodium carbonate using bipolar membrane electrodialysis, J. Membr. Sci. 498 (2016) 48–56 [99] with copyright permission from Elsevier.*

decreased when considering the additional benefits of the byproduct. The methionine produced had a high purity level that was comparable to the AR grade products. In addition, NaOH and CO_2 were obtained in acid and base compartments, respectively. These byproducts could be recycled to the methionine production, where CO_2 was used as a raw material for methionine synthesis and NaOH was used to catalyze the open-ring reaction. Compared to the conventional process, the BMED-based technology not only avoids the use of copious quantities of acids and bases, but also makes full use of CO_2 from fuel gas.

As aforementioned, the feed in the fermentation broth generally contains inorganic and organic contaminants such as Ca^{2+}, Mg^{2+}, dissolved organic matter (sugar), and suspended solids/colloidal matter. While most organic impurities being bacterial cells, pigments, and other high-molecular-weight residues are removed in downstream fermentation clarified by pressure-driven membrane processes, such as RO, NF, or microfiltration (MF), nevertheless, a small fraction of sugar and low-molecular-weight

This book belongs to Badji Mokhtar Annaba University Central Library Copyright Elsevier 2025

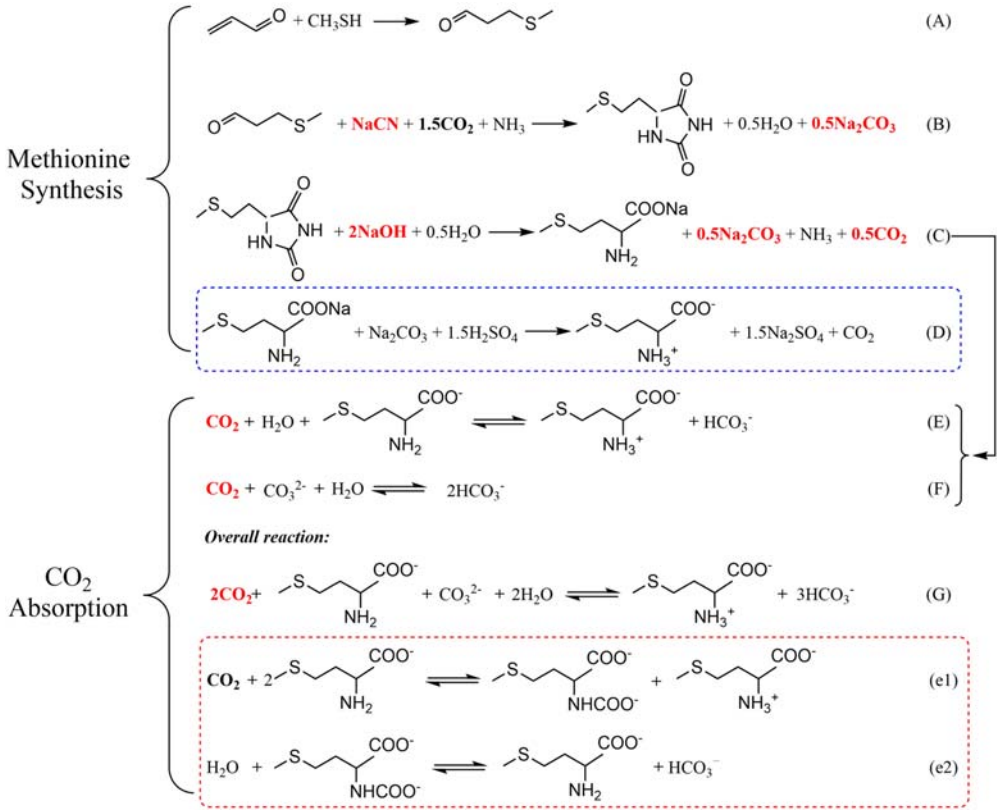

Scheme 9.3 The recycling scheme of CO_2 for the cleaner production of methionine acid. *Obtained from C. Jiang, Y. Zhang, H. Feng, Q. Wang, Y. Wang, T. Xu, Simultaneous CO_2 capture and amino acid production using bipolar membrane electrodialysis (BMED), J. Membr. Sci. 542 (2017) 264–271 [100] with copyright permission from Elsevier.*

natural products can remain in the clarified fermentation broth. In this case, a CED can be introduced afterwards for further treatment and the concentrating of organic acid salt as well. This is conducive to the following BMED process for lactic acid production (Fig. 9.22) from the aspect of energy consumption because the concentration of organic acid in the fermentation liquor is low given product inhibition. If the fermentation broths clarified by the pressure-driven membranes are introduced directly into the BMED stack, the depletion of salts in the feed compartment and the diffusion of organic acids are undesirable for BMED performance [174]. Therefore, CED is often used together with the BMED process for organic acid recovery and production in a two-stage ED process [113,175–184].

The concentration of lactic acid or lactate salt from the effluent of the fermentation broth is as low as 1%–2% [178]. Such a low feed concentration is not cost-effective for

This book belongs to Badji Mokhtar Annaba University Central Library Copyright Elsevier 2025

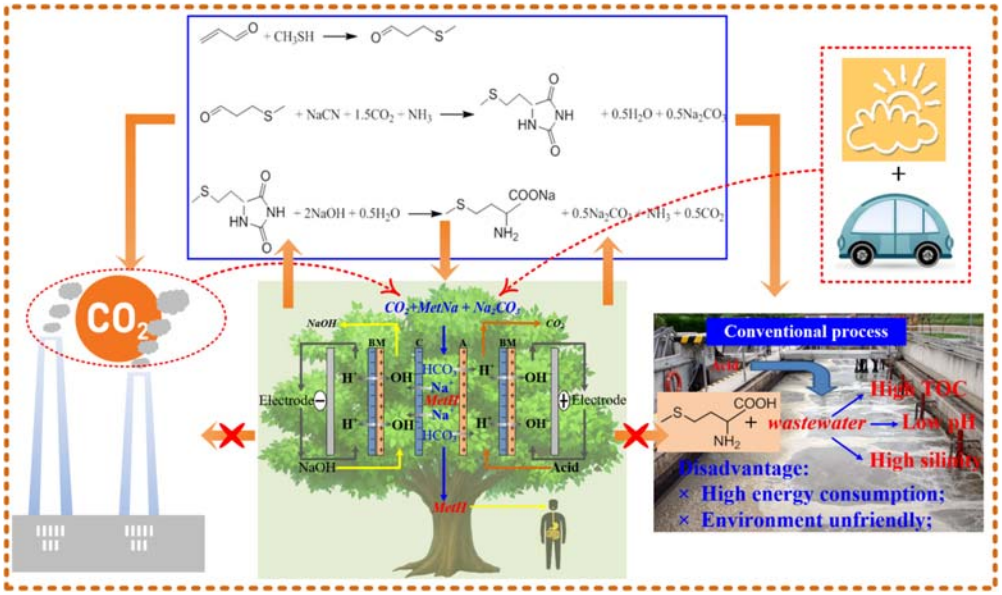

Figure 9.21 The cleaner production route of BMED-integrated CO_2 capture procedure. *Obtained from C. Jiang, Y. Zhang, H. Feng, Q. Wang, Y. Wang, T. Xu, Simultaneous CO2 capture and amino acid production using bipolar membrane electrodialysis (BMED), J. Membr. Sci. 542 (2017) 264–271 [100] with copyright permission from Elsevier.*

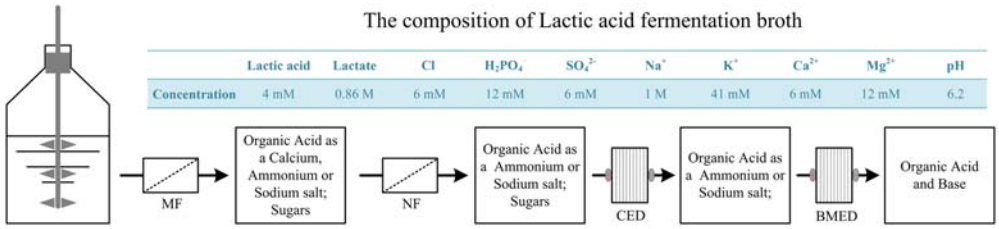

Figure 9.22 Integrated membrane process using MF, NF, CED, and BMED for lactic acid recovery from fermentation broth. *Obtained from C. Jiang, Y. Wang, T. Xu, 6 - Membranes for the recovery of organic acids from fermentation broths, in: Membrane Technologies for Biorefining, Woodhead Publishing, 2016, pp. 135–161 [169] with copyright permission from Elsevier.*

the operation of CED or BMED. In this case, combined CED and BMED, also called two-stage ED, is a rational choice for process intensification. In particular, CED can be used to concentrate the organic acid salt and achieve the purification of organic acid salt from non-migrated impurities such as residual sugar. BMED can be used to acidify the salt to generate the target organic acid, though a base is also produced which can be reused for pH adjustment during the fermentation process. Two-stage ED is not only environmentally friendly but also cost-effective for organic acid production given energy

This book belongs to Badji Mokhtar Annaba University Central Library Copyright Elsevier 2025

consumption is much lower than the conventional process, and since the byproduct of the base can be recycled into the fermentation broth for pH control, which will also decrease the operational cost. Additionally, the whole membrane process, that is, MF-NF-CED-BMED, UF-NF/RO-FO, UF/NF/RO/FO-Electromembrane Filtration (EMF), will provide an effective answer to the question of the cleaner production of organic acids/bases and efficient treatment of wastewater, and finally achieves "zero discharge."

9.6 Electrodialysis for other special/emerging applications

In addition to its applications in resources recovery from industrial wastewater, ED has also been employed for purifying raw materials used in industrial processes and for removing emerging contaminants from the wastewater. It can simultaneously improve the operational efficiency of industrial plants and reduce the amount of toxic pollutants in the waste effluents. Furthermore, recent developments on ED has extended its applications for energy harvesting from waste brine (e.g., by using its reverse ED process—RED). Meanwhile, valuable resources recycling and green production from industrial wastewater can be realized by incorporating ED technology in industrial production processes. In this section, implementation of ED for special applications, including specific chemicals purification, trace contaminants removal, and clean energy generation will be discussed.

9.6.1 Electrodialysis for waste ionic liquid recovery

Ionic liquids, a kind of organic salts, are widely used as an alternative to conventional organic solvent for separation processes in industrial fields. A large quantity of waste ionic liquids is generated annually [185] and due to its high cost, toxicity, and chemical stability in the environment, recovering and recycling of ionic liquids are required instead of their direct disposal. In order to realize ionic liquids reuse, the impurities in the mixture (e.g., solids, solvent water, and hydrolysate) need to be removed [186]. Recently, ED has been proposed for the concentration and recycling of the ionic liquids from dilute aqueous solutions, obtaining a recovery ratio of 85.2% with an overall current efficiency of 80.9% [187]. Trinh et al. reported an ionic liquid recovery ratio of 64% with a current efficiency of 63.5% from the cellulose hydrolyzed products by an ED process [188]. The recovery ratio of ionic liquids from waste effluent and its current efficiency can be further improved by optimizing the operation conditions, such as increasing the employed voltage or the initial ionic liquids concentration [189]. However, membrane fouling by hydrolyzed products in waste effluent pulls back the real world performance of ED processes for recovering ionic liquids.

This book belongs to Badji Mokhtar Annaba University Central Library Copyright Elsevier 2025

To address the membrane fouling issue, UF is applied as a pretreatment step of the ED process to retain hydrolyzed contaminants [190]. A recent study evaluated the feasibility and performance of employing a hybrid system of UF and BMED for protic ionic liquid (triethylammonium hydrogen sulfate, [TEA][HSO_4]) regeneration, resulting in the highest recovery ratio of 93.7% for TEA^+ and 96.4% for SO_4^{2-} [191].

9.6.2 Electrodialysis for trace contaminants removal

ED has been widely applied for wastewater treatment and valuable resource recovery from waste effluent. In addition to the resources to be harvested, there are also toxic organic micropollutants (e.g., antibiotics, pharmaceuticals, endocrine disrupting compounds, and personal care products [59,192]) in waste effluents that are harmful to human health and to the ecological environment. Some of these trace organic contaminants can transport through IEMs and therefore be removed by ED. On the other hand, the contaminants accumulated in the concentrate stream and/or their sorption by the IEMs can be a potential concern that requires further attention [59,192]. For example, a recent study shows that some IEMs had a high sorption value of pesticide (550 $\mu g/cm^3$) at pH 7 [192]. Apart from wastewater containing relatively low concentration of contaminants, antibiotic wastewater comprising high concentration of antibiotics and salts can be treated by a UF membrane modified ED stack where 20.3% of antibiotics is recovered in the product solution [193]. It has also been reported that inorganic trace contaminants, such as fluoride (F^-), nitrate (NO_3^-), and boron can be effectively removed from synthetic wastewater using ED even in the presence of natural organic matter [194]. The removal efficiency of boron is highly pH dependent due to its pH dependent speciation.

9.6.3 Modified electrodialysis for energy recovery

During the last few decades, reverse electrodialysis (RED) technology has gained rapid development for its ability at harvesting salinity gradient energy (SGE) from salt solutions of different concentrations. RED operates in a reversed manner to ED so that usable electricity is generated with the ionic transport through IEMs driven by concentration differences between the two sides of the membrane surface (Fig. 9.23) [195]. Pilot studies on RED have been performed in Netherlands, Italy, and Japan, illustrating power densities to the order of 1 W/m^2. Further, additional studies on RED have demonstrated a power density as high as 1.34 W/m^2 using tailored IEMs with high electrical performance (e.g., area resistance of 0.86 Ωcm^2 and permselectivity of 96.2%) [196]. RED may have potential applications in recovering energy from concentrated waste brine generated in industrial processes and during seawater desalination, leading to energy self-sufficient desalination [197–200]. For example, Li et. al. first proposed a hybrid process of RED and RO for synergistic brine management

This book belongs to Badji Mokhtar Annaba University Central Library Copyright Elsevier 2025

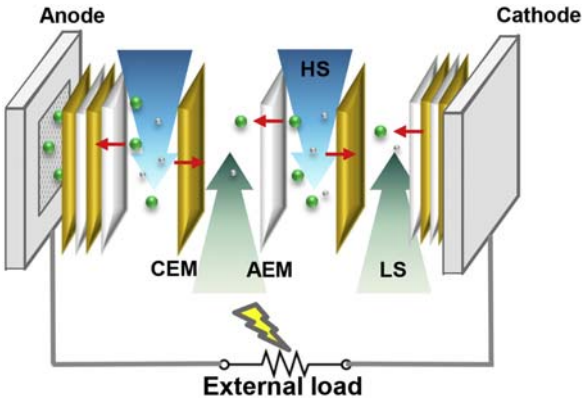

Figure 9.23 Working principle of the reverse electrodialysis stack. *Obtained from Y. Mei, C.Y. Tang, Co-locating reverse electrodialysis with reverse osmosis desalination: synergies and implications, J. Membr. Sci. 539 (2017) 305–312 [195] with copyright permission from Elsevier.*

and energy efficient seawater desalination [201]. Various other studies have also evaluated the feasibility of RED for energy recovery and brine dilution towards enhanced energy efficiency of the whole system [195,202–206].

Inspired by the bioelectrochemical system where electricity is generated by waste organic matter oxidation, novel hybrid systems have been proposed as combining bioelectrochemical system and RED for resources and energy recovery. In such hybrid systems, the highest power densities of 3.44 W/m^2 are generated from both exoelectrogenic bacteria oxidation of organic matter and salinity gradient energy of seawater and river water [207]. By applying a small RED stack with only several (1 ~ 5) cell pair IEMs, various valuable chemicals can be generated in the hybrid systems, such as chemical energy production (e.g., hydrogen and methane) [208–213] and chemicals generation (e.g., hydrogen peroxide, acid/base) [214,215]. Furthermore, it has been reported that pollutant removal (e.g., azo dye, Cr^{6+}) can be realized in one process using direct cathodic reduction and Fenton reaction [216,217].

9.7 Conclusion and future perspectives

ED technology has shown interesting possibilities in the potential applications in valuable resource recovery and production from industrial wastewater. Besides, it can also minimize the ecological risk of the direct disposal of industrial wastewater. However, the process is currently challenged by its relatively high energy footprint due to the poor electrical conductivity of IEMs, apart from the limited selectivity of conventional IEMs that has prohibited its wide application owing to its low energy

This book belongs to Badji Mokhtar Annaba University Central Library Copyright Elsevier 2025

efficiency. Therefore, further developments are required for innovation of IEMs with high electric conductivity, high perm-selectivity of target ions, and low cost.

Previous researches have comprehensively investigated the feasibility for practical applications and the effects on performance of various membrane fabrication methods and membrane designs. Membranes comprising multiple polymer matrices having different cross-linking degree, and the ones with various functional groups, additives, and surface modifications have been explored and tested in ED stack to break through the trade-off between conductivity and permselectivity. In addition, novel IEMs with special designs and applications have been reported, including the monovalent selective membrane, the proton blocking membrane, the mixed matrix membrane, the TFC membrane, the PIM, and the BM. Nevertheless, the membrane microstructure-to-property relationships need to be further understood, as well as the membrane transport and selectivity mechanisms.

Besides, BMED is capable of generating acid and base from its salt counterparts with relatively low energy consumption and, as a result, the cost for waste disposal can be minimized. It has been recognized as a suitable candidate for sustainable chemical processes, with its being applied in conventional waste valorization, mineral extraction, and cleaner production. Enormous innovative applications have been proposed recently, for example, carbon capture and conversion, water electrolysis for hydrogen, coagulation, and novel flow batteries. However, developing BMs with desired co-ion leakage, water dissociation efficiency/rate, resistance, and long-term stability has challenged its practical application. Particularly, designing monopolar layer with appropriate characteristics (i.e., ion exchange capacity, swelling degree, water uptake, and area resistance) is critical to the advanced BM. Meanwhile, the complex interactions between different characters of BM should be considered. For instance, dense and robust BM would narrow ionic channels and suppress co-ion leakage, while increasing the area resistance. Improving the trans-across ionic conductivity will reduce the area resistance, while reducing the voltage losses during water dissociation. Furthermore, tailoring water electrolysis catalysts of BM interlayer can substantially improve BM performance. Functionalizing the bipolar junction with strong ionic groups (e.g., organic catalysts and functionalized inorganics) can accelerate water electrolysis in the interlayer. There is a new class of organic catalysts, including dendrimer (e.g., PAMAM and Boltorn H20), and inorganic catalysts, including oxides/hydroxides metals, complexes, and metal-organic frameworks, in which graphene/carbon materials, such as graphene oxide deposited with phophonic/quaternary group, provide sufficient sites for water electrolysis and for decreasing its overpotential. Further developments on BM materials are expected to improve electromembrane processes and for it to become comparable to the present monopolar membrane based techniques.

Membrane fouling and scaling caused by hardness ions and organic matters have given rise to increasing concerns on the implementation of ED processes, especially for

This book belongs to Badji Mokhtar Annaba University Central Library Copyright Elsevier 2025

ED with long-term operation. To address these problems, the pretreatment steps, such as precipitation, UF, and bioreactor, are required to soften feed streams and remove the organic contaminants from waste streams before being fed into the ED stack. Besides, hybridizing ED with other related processes, such as RO and biotechnologies, can substantially enhance the overall efficiencies of the integrated systems and convert the concentrate effluents directly to usable resources within the one step. It is also worthwhile to further explore ED-based hybrid processes for various waste streams with complex compositions. In addition to the products purification by IEMs in the ED process, ED electrode reactions show an interesting possibility for application in wastewater treatment. Given the processes can be categorized into electrochemical coagulation and electroreduction, it follows that developing sustainable energy resources for the ED process can make the technology more technically and economically attractive in industrial wastewater treatment. For instance, bioelectrochemical technologies (e.g., microbial fuel cell) and salinity gradient energy have both been demonstrated to provide in situ energy for ED processes. Future research will hasten developments that are still needed for the design of the integrated processes to optimize the energy efficiency and innovation of novel application of the system. For instance, internal integration would be generally favored where the reduced electrode reaction results in decreased energy consumption compared to that in external integration.

References

[1] Ö. Arar, Ü. Yüksel, N. Kabay, M. Yüksel, Removal of Cu^{2+} ions by a micro-flow electrodeionization (EDI) system, Desalination 277 (2011) 296–300.

[2] S. Caprarescu, A.-L. Radu, V. Purcar, R. Ianchis, A. Sarbu, M. Ghiurea, et al., Adsorbents/ion exchangers-PVA blend membranes: preparation, characterization and performance for the removal of Zn2 + by electrodialysis, Appl. Surf. Sci. 329 (2015) 65–75.

[3] S.S. Chen, C.W. Li, H.D. Hsu, P.C. Lee, Y.M. Chang, C.H. Yang, Concentration and purification of chromate from electroplating wastewater by two-stage electrodialysis processes, J. Hazard. Mater. 161 (2009) 1075–1080.

[4] S. Frioui, R. Oumeddour, S. Lacour, Highly selective extraction of metal ions from dilute solutions by hybrid electrodialysis technology, Sep. Purif. Technol. 174 (2017) 264–274.

[5] H. Lu, Y. Wang, J. Wang, Recovery of Ni^{2+} and pure water from electroplating rinse wastewater by an integrated two-stage electrodeionization process, J. Clean. Prod. 92 (2015) 257–266.

[6] M. Xie, H.K. Shon, S.R. Gray, M. Elimelech, Membrane-based processes for wastewater nutrient recovery: technology, challenges, and future direction, Water Res. 89 (2016) 210–221.

[7] Y. Zhang, E. Desmidt, A. Van Looveren, L. Pinoy, B. Meesschaert, B. Van der Bruggen, Phosphate separation and recovery from wastewater by novel electrodialysis, Environ. Sci. Technol. 47 (2013) 5888–5895.

[8] X. Vecino, M. Reig, O. Gibert, C. Valderrama, J.L. Cortina, Integration of monopolar and bipolar electrodialysis processes for tartaric acid recovery from residues of the winery industry, ACS Sustain. Chem. Eng. 8 (2020) 13387–13399.

[9] A.T.K. Tran, P. Mondal, J. Lin, B. Meesschaert, L. Pinoy, B. Van der Bruggen, Simultaneous regeneration of inorganic acid and base from a metal washing step wastewater by bipolar membrane electrodialysis after pretreatment by crystallization in a fluidized pellet reactor, J. Membr. Sci. 473 (2015) 118–127.

This book belongs to Badji Mokhtar Annaba University Central Library Copyright Elsevier 2025

[10] L. Shi, Y. Hu, S. Xie, G. Wu, Z. Hu, X. Zhan, Recovery of nutrients and volatile fatty acids from pig manure hydrolysate using two-stage bipolar membrane electrodialysis, Chem. Eng. J. 334 (2018) 134–142.
[11] S. Datta, Y.J. Lin, S.W. Snyder, Current and emerging separations technologies in biorefining, Advancess in Biorefineries, Elsevier, 2014, pp. 112–151.
[12] T.Z. Sadyrbaeva, Removal of chromium(VI) from aqueous solutions using a novel hybrid liquid membrane—electrodialysis process, Chem. Eng. Process. Process. Intensif. 99 (2016) 183–191.
[13] M. Paidar, V. Fateev, K. Bouzek, Membrane electrolysis—history, current status and perspective, Electrochim. Acta 209 (2016) 737–756.
[14] T. Xu, Ion exchange membranes: state of their development and perspective, J. Membr. Sci. 263 (2005) 1–29.
[15] W. Juda, W.A. McRae, Coherent ion-exchange gels and membranes, J. Am. Chem. Soc. 72 (1950) 1044.
[16] A.G. Winger, G.W. Bodamer, R. Kunin, Some electrochemical properties of new synthetic ion exchange membranes, J. Electrochem. Soc. 100 (1953) 178.
[17] G. Saracco, Ionic membrane technologies for the recovery of valuable chemicals from waste waters, Annali di Chim. 93 (2003) 817–826.
[18] M.K.K. Mihara, Polarity reversing electrode units and electrical switching means therefore, U.S., 1969.
[19] Z. MatEjka, Continuous production of high-purity water by electro-deionisation, 1970.
[20] E. Korngold, Electrodialysis processes using ion exchange resins between membranes, 1975.
[21] C. Goffin, J.C. Calay, Use of continuous electrodeionization to reduce ammonia concentration in steam generators blow-down of PWR nuclear power plants, Desalination 132 (2000) 249–253.
[22] L. Alvarado, A. Ramírez, I. Rodríguez-Torres, Cr(VI) removal by continuous electrodeionization: study of its basic technologies, Desalination 249 (2009) 423–428.
[23] M.C. Martí-Calatayud, D.C. Buzzi, M. García-Gabaldón, A.M. Bernardes, J.A.S. Tenório, V. Pérez-Herranz, Ion transport through homogeneous and heterogeneous ion-exchange membranes in single salt and multicomponent electrolyte solutions, J. Membr. Sci. 466 (2014) 45–57.
[24] S. Lee, W. Meng, Y. Wang, D. Wang, M. Zhang, G. Wang, et al., Comparison of the property of homogeneous and heterogeneous ion exchange membranes during electrodialysis process, Ain Shams Eng. J. 12 (2021) 159–166.
[25] G.E. Molau, Heterogeneous ion-exchange membranes, J. Membr. Sci. 8 (1981) 309–330.
[26] S.M. Hosseini, H. Alibakhshi, E. Jashni, F. Parvizian, J.N. Shen, M. Taheri, et al., A novel layer-by-layer heterogeneous cation exchange membrane for heavy metal ions removal from water, J. Hazard. Mater. 381 (2020) 120884.
[27] M. Ahmad, A.A. Qaiser, N.U. Huda, A. Saeed, Heterogeneous ion exchange membranes based on thermoplastic polyurethane (TPU): effect of PSS/DVB resin on morphology and electrodialysis, RSC Adv. 10 (2020) 3029–3039.
[28] X.Y. Nie, S.Y. Sun, Z. Sun, X.F. Song, J.G. Yu, Ion-fractionation of lithium ions from magnesium ions by electrodialysis using monovalent selective ion-exchange membranes, Desalination 403 (2017) 128–135.
[29] Y. Yang, W. Xin, N. Busschaert, H. Furuta, P.A. Gale, Dissecting the chloride–nitrate anion transport assay, Chem. Commun. 53 (2017) 9230–9233.
[30] X.-Y. Nie, S.-Y. Sun, X. Song, J.-G. Yu, Further investigation into lithium recovery from salt lake brines with different feed characteristics by electrodialysis, J. Membr. Sci. 530 (2017) 185–191.
[31] R. Pärnamäe, S. Mareev, V. Nikonenko, S. Melnikov, N. Sheldeshov, V. Zabolotskii, et al., Bipolar membranes: a review on principles, latest developments, and applications, J. Membr. Sci. 617 (2021) 118538.
[32] Z. Li, Y. Liu, B. Wang, Q. Lang, M. Tan, M. Lee, et al., Insights into the facilitated transport mechanisms of Cr(VI) in ionic liquid-based polymer inclusion membrane—electrodialysis (PIM-ED) process, Chem. Eng. J. 397 (2020) 125324.
[33] H.C.V. Mavrov, B. Heitele, F. Rogener, Desalination of surface water to industrial water with lower impact on the environment, 1999.

This book belongs to Badji Mokhtar Annaba University Central Library Copyright Elsevier 2025

[34] G. Pourcelly, Electrodialysis water splitting-application of electrodialysis with bipolar membranes, 2000.
[35] Y.H. Kim, S.H. Moon, Lactic acid recovery from fermentation broth using one-stage electrodialysis, J. Chem. Technol. Biot. 76 (2001) 169–178.
[36] M.R. Yaftian, M.I.G.S. Almeida, R.W. Cattrall, S.D. Kolev, Selective extraction of vanadium(V) from sulfate solutions into a polymer inclusion membrane composed of poly(vinylidenefluoride-co-hexafluoropropylene) and Cyphos (R) IL 101, J. Membr. Sci. 545 (2018) 57–65.
[37] M.I.G.S. Almeida, R.W. Cattrall, S.D. Kolev, Recent trends in extraction and transport of metal ions using polymer inclusion membranes (PIMs), J. Membr. Sci. 415–416 (2012) 9–23.
[38] L. Nghiem, P. Mornane, I. Potter, J. Perera, R. Cattrall, S. Kolev, Extraction and transport of metal ions and small organic compounds using polymer inclusion membranes (PIMs), J. Membr. Sci. 281 (2006) 7–41.
[39] W. Yoshida, Y. Baba, F. Kubota, S.D. Kolev, M. Goto, Selective transport of scandium(III) across polymer inclusion membranes with improved stability which contain an amic acid carrier, J. Membr. Sci. 572 (2019) 291–299.
[40] N. Zhang, Y. Liu, R. Liu, Z. She, M. Tan, D. Mao, et al., Polymer inclusion membrane (PIM) containing ionic liquid as a proton blocker to improve waste acid recovery efficiency in electrodialysis process, J. Membr. Sci. 581 (2019) 18–27.
[41] B.-Y. Wang, N. Zhang, Z.-Y. Li, Q.-L. Lang, B.-H. Yan, Y. Liu, et al., Selective separation of acetic and hexanoic acids across polymer inclusion membrane with ionic liquids as carrier, Int. J. Mol. Sci. 20 (2019) 3915–3933.
[42] B. Wang, Z. Li, Q. Lang, M. Tan, C. Ratanatamskul, M. Lee, et al., A comprehensive investigation on the components in ionic liquid-based polymer inclusion membrane for Cr(VI) transport during electrodialysis, J. Membr. Sci. 604 (2020) 118016.
[43] L. Gurreri, A. Tamburini, A. Cipollina, G. Micale, Electrodialysis applications in wastewater treatment for environmental protection and resources recovery: a systematic review on progress and perspectives, Membranes 10 (2020).
[44] P.A. Sosa-Fernandez, J.W. Post, H. Bruning, F.A.M. Leermakers, H.H.M. Rijnaarts, Electrodialysis-based desalination and reuse of sea and brackish polymer-flooding produced water, Desalination 447 (2018) 120–132.
[45] K. Loganathan, P. Chelme-Ayala, M. Gamal El-Din, Treatment of basal water using a hybrid electrodialysis reversal–reverse osmosis system combined with a low-temperature crystallizer for near-zero liquid discharge, Desalination 363 (2015) 92–98.
[46] H. Hao, X. Huang, C. Gao, X. Gao, Application of an integrated system of coagulation and electrodialysis for treatment of wastewater produced by fracturing, Desalin. Water Treat. 55 (2014) 2034–2043.
[47] B. Rodgers, Electrodeionization versus Electrodialysis: A Clean Up of Produced Water in Hydraulic Fracturing, University of Arkansas, Fayetteville, AR, 2016.
[48] E.G.M. Peraki, Alternative method of flow-back water treatment in shale gas development for environmental protection, in: IFCEE, 2015, pp. 1816–1825.
[49] M. Peraki, E. Ghazanfari, G.F. Pinder, T.L. Harrington, Electrodialysis: an application for the environmental protection in shale-gas extraction, Sep. Purif. Technol. 161 (2016) 96–103.
[50] R.K. McGovern, A.M. Weiner, L.G. Sun, C.G. Chambers, S.M. Zubair, J.H. Lienhard, On the cost of electrodialysis for the desalination of high salinity feeds, Appl. Energy 136 (2014) 649–661.
[51] C.D. Venzke, A. Giacobbo, C.R. Klauck, Cheila Viegas, M. de Aquim, M.A.S. Rodrigues, et al., Integrated membrane processes (EDR-RO) for water reuse in the petrochemical industry, J. Membr. Sci. Res. 4 (2018) 218–226.
[52] R. Bisselink, W. de Schepper, J. Trampé, W. van den Broek, I. Pinel, A. Krutko, et al., Mild desalination demo pilot: new normalization approach to effectively evaluate electrodialysis reversal technology, Water Resour. Ind. 14 (2016) 18–25.
[53] D.C. Buzzi, L.S. Viegas, M.A.S. Rodrigues, A.M. Bernardes, J.A.S. Tenório, Water recovery from acid mine drainage by electrodialysis, Miner. Eng. 40 (2013) 82–89.
[54] M. Maurer, W. Pronk, T.A. Larsen, Treatment processes for source-separated urine, Water Res. 40 (2006) 3151–3166.

This book belongs to Badji Mokhtar Annaba University Central Library Copyright Elsevier 2025

[55] X. Wang, X. Zhang, Y. Wang, Y. Du, H. Feng, T. Xu, Simultaneous recovery of ammonium and phosphorus via the integration of electrodialysis with struvite reactor, J. Membr. Sci. 490 (2015) 65–71.
[56] L. Shi, S. Xie, Z. Hu, G. Wu, L. Morrison, P. Croot, et al., Nutrient recovery from pig manure digestate using electrodialysis reversal: membrane fouling and feasibility of long-term operation, J. Membr. Sci. 573 (2019) 560–569.
[57] Z.L. Ye, K. Ghyselbrecht, A. Monballiu, L. Pinoy, B. Meesschaert, Fractionating various nutrient ions for resource recovery from swine wastewater using simultaneous anionic and cationic selective-electrodialysis, Water Res. 160 (2019) 424–434.
[58] A.T.K. Tran, Y. Zhang, D. De Corte, J.-B. Hannes, W. Ye, P. Mondal, et al., P-recovery as calcium phosphate from wastewater using an integrated selectrodialysis/crystallization process, J. Clean. Prod. 77 (2014) 140–151.
[59] L. Shi, Z. Hu, W.S. Simplicio, S. Qiu, L. Xiao, B. Harhen, et al., Antibiotics in nutrient recovery from pig manure via electrodialysis reversal: sorption and migration associated with membrane fouling, J. Membr. Sci. 597 (2020).
[60] C.M. Mehta, W.O. Khunjar, V. Nguyen, S. Tait, D.J. Batstone, Technologies to recover nutrients from waste streams: a critical review, Crit. Rev. Environ. Sci. Technol. 45 (2014) 385–427.
[61] L. Shi, Z. Hu, Y. Wang, E. Bei, P.N.L. Lens, O. Thomas, et al., In situ electrochemical oxidation in electrodialysis for antibiotics removal during nutrient recovery from pig manure digestate, Chem. Eng. J. (2020).
[62] Y. Zhang, B. Van der Bruggen, L. Pinoy, B. Meesschaert, Separation of nutrient ions and organic compounds from salts in RO concentrates by standard and monovalent selective ion-exchange membranes used in electrodialysis, J. Membr. Sci. 332 (2009) 104–112.
[63] Y.-K. Wang, Y.-K. Geng, X.-R. Pan, G.-P. Sheng, In situ utilization of generated electricity for nutrient recovery in urine treatment using a selective electrodialysis membrane bioreactor, Chem. Eng. Sci. 171 (2017) 451–458.
[64] J. De Paepe, R.E.F. Lindeboom, M. Vanoppen, K. De Paepe, D. Demey, W. Coessens, et al., Refinery and concentration of nutrients from urine with electrodialysis enabled by upstream precipitation and nitrification, Water Res. 144 (2018) 76–86.
[65] R. Gayathri, P.S. Kumar, Recovery and reuse of hexavalent chromium from aqueous solutions by a hybrid technique of electrodialysis and ion exchange, Braz. J. Chem. Eng. 27 (2010) 71–78.
[66] A. Mahmoud, A.F. Hoadley, An evaluation of a hybrid ion exchange electrodialysis process in the recovery of heavy metals from simulated dilute industrial wastewater, Water Res. 46 (2012) 3364–3376.
[67] M. Aliaskari, A.I. Schafer, Nitrate, arsenic and fluoride removal by electrodialysis from brackish groundwater, Water Res. 190 (2021) 116683.
[68] Y. Song, Z. Zhao, Recovery of lithium from spent lithium-ion batteries using precipitation and electrodialysis techniques, Sep. Purif. Technol. 206 (2018) 335–342.
[69] D.N. Afifah, T. Ariyanto, S. Supranto, I. Prasetyo, Separation of lithium ion from lithium-cobalt mixture using electrodialysis monovalent membrane, Eng. J. 22 (2018) 165–179.
[70] A. Iizuka, Y. Yamashita, H. Nagasawa, A. Yamasaki, Y. Yanagisawa, Separation of lithium and cobalt from waste lithium-ion batteries via bipolar membrane electrodialysis coupled with chelation, Sep. Purif. Technol. 113 (2013) 33–41.
[71] F. Fu, Q. Wang, Removal of heavy metal ions from wastewaters: a review, J. Environ. Manage. 92 (2011) 407–418.
[72] T. Benvenuti, M.A. Siqueira Rodrigues, A.M. Bernardes, J. Zoppas-Ferreira, Closing the loop in the electroplating industry by electrodialysis, J. Clean. Prod. 155 (2017) 130–138.
[73] T. Benvenuti, R.S. Krapf, M.A.S. Rodrigues, A.M. Bernardes, J. Zoppas-Ferreira, Recovery of nickel and water from nickel electroplating wastewater by electrodialysis, Sep. Purif. Technol. 129 (2014) 106–112.
[74] T. Scarazzato, Z. Panossian, J.A.S. Tenório, V. Pérez-Herranz, D.C.R. Espinosa, Water reclamation and chemicals recovery from a novel cyanide-free copper plating bath using electrodialysis membrane process, Desalination 436 (2018) 114–124.
[75] C.-V. Gherasim, J. Křivčík, P. Mikulášek, Investigation of batch electrodialysis process for removal of lead ions from aqueous solutions, Chem. Eng. J. 256 (2014) 324–334.

This book belongs to Badji Mokhtar Annaba University Central Library Copyright Elsevier 2025

[76] I. Ali, T.A. Khan, M. Asim, Removal of arsenic from water by electrocoagulation and electrodialysis techniques, Sep. Purif. Rev. 40 (2011) 25–42.
[77] D. Babilas, P. Dydo, Selective zinc recovery from electroplating wastewaters by electrodialysis enhanced with complex formation, Sep. Purif. Technol. 192 (2018) 419–428.
[78] Y. Zhang, S. Paepen, L. Pinoy, B. Meesschaert, B. Van der Bruggen, Selectrodialysis: fractionation of divalent ions from monovalent ions in a novel electrodialysis stack, Sep. Purif. Technol. 88 (2012) 191–201.
[79] M. Reig, X. Vecino, C. Valderrama, O. Gibert, J.L. Cortina, Application of selectrodialysis for the removal of As from metallurgical process waters: recovery of Cu and Zn, Sep. Purif. Technol. 195 (2018) 404–412.
[80] J. Liao, Q. Chen, N. Pan, X. Yu, X. Gao, J. Shen, et al., Amphoteric blend ion-exchange membranes for separating monovalent and bivalent anions in electrodialysis, Sep. Purif. Technol. 242 (2020).
[81] T. Luo, S. Abdu, M. Wessling, Selectivity of ion exchange membranes—a review, J. Membr. Sci. 555 (2018) 429–454.
[82] L. Ge, B. Wu, Q. Li, Y. Wang, D. Yu, L. Wu, et al., Electrodialysis with nanofiltration membrane (EDNF) for high-efficiency cations fractionation, J. Membr. Sci. 498 (2016) 192–200.
[83] Y. Zhang, R. Liu, Q. Lang, M. Tan, Y. Zhang, Composite anion exchange membrane made by layer-by-layer method for selective ion separation and water migration control, Sep. Purif. Technol. 192 (2018) 278–286.
[84] Y. Zhao, J. Zhu, J. Ding, V. Bart, J. Shen, C. Gao, Electric-pulse layer-by-layer assembled of anion exchange membrane with enhanced monovalent selectivity, J. Membr. Sci. 548 (2017) 81–90.
[85] N. White, M. Misovich, A. Yaroshchuk, M.L. Bruening, Coating of nafion membranes with polyelectrolyte multilayers to achieve high monovalent/divalent cation electrodialysis selectivities, ACS Appl. Mat. Interfaces 7 (2015) 6620–6628.
[86] S. Abdu, M. Martí-Calatayud, J.E. Wong, M. García-Gabaldón, M. Wessling, Layer-by-layer modification of cation exchange membranes controls ion selectivity and water splitting, ACS Appl. Mat. Interfaces 6 (2014) 1843–1854.
[87] W. Wang, R. Liu, M. Tan, H. Sun, Q.J. Niu, T. Xu, et al., Evaluation of the ideal selectivity and the performance of selectrodialysis by using TFC ion exchange membranes, J. Membr. Sci. 582 (2019) 236–245.
[88] L. Bazinet, T.R. Geoffroy, Electrodialytic processes: market overview, membrane phenomena, recent developments and sustainable strategies, Membrane (Basel) 10 (2020).
[89] D. Lee, J.-Y. Lee, Y. Kim, S.-H. Moon, Investigation of the performance determinants in the treatment of arsenic-contaminated water by continuous electrodeionization, Sep. Purif. Technol. 179 (2017) 381–392.
[90] C. Peng, R. Jin, G. Li, F. Li, Q. Gu, Recovery of nickel and water from wastewater with electrochemical combination process, Sep. Purif. Technol. 136 (2014) 42–49.
[91] Z. Zhang, D. Liba, L. Alvarado, A. Chen, Separation and recovery of Cr(III) and Cr(VI) using electrodeionization as an efficient approach, Sep. Purif. Technol. 137 (2014) 86–93.
[92] Z. Zhang, A. Chen, Simultaneous removal of nitrate and hardness ions from groundwater using electrodeionization, Sep. Purif. Technol. 164 (2016) 107–113.
[93] L. Alvarado, A. Chen, Electrodeionization: principles, strategies and applications, Electrochim. Acta 132 (2014) 583–597.
[94] T. Scarazzato, Z. Panossian, J.A.S. Tenório, V. Pérez-Herranz, D.C.R. Espinosa, A review of cleaner production in electroplating industries using electrodialysis, J. Clean. Prod. 168 (2017) 1590–1602.
[95] A. Ortega, I. Oliva, K.E. Contreras, I. González, M.R. Cruz-Díaz, E.P. Rivero, Arsenic removal from water by hybrid electro-regenerated anion exchange resin/electrodialysis process, Sep. Purif. Technol. 184 (2017) 319–326.
[96] A.J. Chaudhary, J.D. Donaldson, S.M. Grimes, N.G. Yasri, Separation of nickel from cobalt using electrodialysis in the presence of EDTA, J. Appl. Electrochem. 30 (2000) 439–445.
[97] A. Abou-Shady, C. Peng, J. Bi, H. Xu, J. Almeria O, Recovery of Pb (II) and removal of NO^{3-} from aqueous solutions using integrated electrodialysis, electrolysis, and adsorption process, Desalination 286 (2012) 304–315.

This book belongs to Badji Mokhtar Annaba University Central Library Copyright Elsevier 2025

[98] C. Onorato, L.J. Banasiak, A.I. Schäfer, Inorganic trace contaminant removal from real brackish groundwater using electrodialysis, Sep. Purif. Technol. 187 (2017) 426–435.
[99] C. Jiang, Q. Wang, Y. Zhang, Y. Li, Y. Wang, T. Xu, Separation of methionine from the mixture with sodium carbonate using bipolar membrane electrodialysis, J. Membr. Sci. 498 (2016) 48–56.
[100] C. Jiang, Y. Zhang, H. Feng, Q. Wang, Y. Wang, T. Xu, Simultaneous CO_2 capture and amino acid production using bipolar membrane electrodialysis (BMED), J. Membr. Sci. 542 (2017) 264–271.
[101] X. Lin, J. Pan, M. Zhou, Y. Xu, J. Lin, J. Shen, et al., Extraction of Amphoteric amino acid by bipolar membrane electrodialysis: methionine acid as a case study, Ind. Eng. Chem. Res. 55 (2016) 2813–2820.
[102] H. Grib, L. Bonnal, J. Sandeaux, R. Sandeaux, C. Gavach, N. Mameri, Extraction of amphoteric amino acids by an electromembrane process. pH and electrical state control by electrodialysis with bipolar membranes, J. Chem. Technol. Biotechnol. 73 (1998) 64–70.
[103] M. Reig, C. Valderrama, O. Gibert, J.L. Cortina, Selectrodialysis and bipolar membrane electrodialysis combination for industrial process brines treatment: monovalent-divalent ions separation and acid and base production, Desalination 399 (2016) 88–95.
[104] B. Chen, C. Jiang, Y. Wang, R. Fu, Z. Liu, T. Xu, Selectrodialysis with bipolar membrane for the reclamation of concentrated brine from RO plant, Desalination 442 (2018) 8–15.
[105] H. Yan, W. Li, Y. Zhou, M. Irfan, Y. Wang, C. Jiang, et al., In-situ combination of bipolar membrane electrodialysis with monovalent selective anion-exchange membrane for the valorization of mixed salts into relatively high-purity monoprotic and diprotic acids, Membranes 10 (2020) 135.
[106] C. Chen, C. Meurk, J. Chen, M. Lv, Z. Wen, Y. Jiang, et al., Restoration design for Three Gorges Reservoir shorelands, combining Chinese traditional agro-ecological knowledge with landscape ecological analysis, Ecol. Eng. 71 (2014) 584–597.
[107] X. Zhang, W. Lu, H. Ren, W. Cong, Sulfuric acid and ammonia generation by bipolar membranes electrodialysis: transport rate model for ion and water through anion exchange membrane, Chem. Biochem. Eng. Q. 22 (2008) 1–8.
[108] H. Yan, L. Wu, Y. Wang, M. Irfan, C. Jiang, T. Xu, Ammonia capture from wastewater with a high ammonia nitrogen concentration by water splitting and hollow fiber extraction, Chem. Eng. Sci. 227 (2020).
[109] S. Bunani, K. Yoshizuka, S. Nishihama, M. Arda, N. Kabay, Application of bipolar membrane electrodialysis (BMED) for simultaneous separation and recovery of boron and lithium from aqueous solutions, Desalination 424 (2017) 37–44.
[110] X. Zhang, C. Li, Y. Wang, J. Luo, T. Xu, Recovery of acetic acid from simulated acetaldehyde wastewaters: bipolar membrane electrodialysis processes and membrane selection, J. Membr. Sci. 379 (2011) 184–190.
[111] L. Yu, Q. Guo, J. Hao, W. Jiang, Recovery of acetic acid from dilute wastewater by means of bipolar membrane electrodialysis, Desalination 129 (2000) 283–288.
[112] J.S.J. Ferrer, S. Laborie, G. Durand, M. Rakib, Formic acid regeneration by electromembrane processes, J. Membr. Sci. 280 (2006) 509–516.
[113] M.-L. Lameloise, R. Lewandowski, Recovering l-malic acid from a beverage industry waste water: experimental study of the conversion stage using bipolar membrane electrodialysis, J. Membr. Sci. 403–404 (2012) 196–202.
[114] M. AzadiAghdam, A. Achilli, S.A. Snyder, J. Farrell, Increasing water recovery during reclamation of treated municipal wastewater using bipolar membrane electrodialysis and fluidized bed crystallization, J. Water Process. Eng. 38 (2020) 101555.
[115] S. Himmler, A. König, P. Wasserscheid, Synthesis of [EMIM] OH via bipolar membrane electrodialysis–precursor production for the combinatorial synthesis of [EMIM]-based ionic liquids, Green Chem. 9 (2007) 935–942.
[116] T. Rottiers, B. Van der B, L. Pinoy, Production of salicylic acid in a three compartment bipolar membrane electrodialysis configuration, J. Ind. Eng. Chem. 54 (2017) 190–199.
[117] H. Feng, C. Huang, T. Xu, Production of tetramethyl ammonium hydroxide using bipolar membrane electrodialysis, Ind. Eng. Chem. Res. 47 (2008) 7552–7557.

This book belongs to Badji Mokhtar Annaba University Central Library Copyright Elsevier 2025

[118] W. Ye, J. Huang, J. Lin, X. Zhang, J. Shen, P. Luis, et al., Environmental evaluation of bipolar membrane electrodialysis for NaOH production from wastewater: conditioning NaOH as a CO_2 absorbent, Sep. Purif. Technol. 144 (2015) 206–214.
[119] M. Herrero-Gonzalez, P. Diaz-Guridi, A. Dominguez-Ramos, A. Irabien, R. Ibañez, Highly concentrated HCl and NaOH from brines using electrodialysis with bipolar membranes, Sep. Purif. Technol. 242 (2020) 116785.
[120] Y. Zhang, I. Angelidaki, Recovery of ammonia and sulfate from waste streams and bioenergy production via bipolar bioelectrodialysis, Water Res. 85 (2015) 177–184.
[121] C. Fernandez-Gonzalez, A. Dominguez-Ramos, R. Ibañez, Y. Chen, A. Irabien, Valorization of desalination brines by electrodialysis with bipolar membranes using nanocomposite anion exchange membranes, Desalination 406 (2017) 16–24.
[122] X.-X. Wang, M. Wang, Y.-X. Jia, T.-T. Yao, The feasible study on the reclamation of the glyphosate neutralization liquor by bipolar membrane electrodialysis, Desalination 300 (2012) 58–63.
[123] K. Prochaska, K. Staszak, M.J. Wozniak-Budych, M. Regel-Rosocka, M. Adamczak, M. Wisniewski, et al., Nanofiltration, bipolar electrodialysis and reactive extraction hybrid system for separation of fumaric acid from fermentation broth, Bioresour. Technol. 167 (2014) 219–225.
[124] M.J. Wozniak, K. Prochaska, Fumaric acid separation from fermentation broth using nanofiltration (NF) and bipolar electrodialysis (EDBM), Sep. Purif. Technol. 125 (2014) 179–186.
[125] K. Prochaska, M.J. Wozniak-Budych, Recovery of fumaric acid from fermentation broth using bipolar electrodialysis, J. Membr. Sci. 469 (2014) 428–435.
[126] A.T. Tran, N. Jullok, B. Meesschaert, L. Pinoy, B. Van der Bruggen, Pellet reactor pretreatment: a feasible method to reduce scaling in bipolar membrane electrodialysis, J. Colloid Interface Sci. 401 (2013) 107–115.
[127] R. Patil, J. Genco, H. Pendse, A. van Heiningen, Treating kraft mill extract using bipolar membrane electrodialysis for the production of acetic acid, Tappi J. 15 (2016) 215–226.
[128] M. Szczygiełda, J. Antczak, K. Prochaska, Separation and concentration of succinic acid from post-fermentation broth by bipolar membrane electrodialysis (EDBM), Sep. Purif. Technol. 181 (2017) 53–59.
[129] M. Szczygiełda, K. Prochaska, Alpha-ketoglutaric acid production using electrodialysis with bipolar membrane, J. Membr. Sci. 536 (2017) 37–43.
[130] M. Szczygiełda, K. Prochaska, Effective separation of bio-based alpha-ketoglutaric acid from post-fermentation broth using bipolar membrane electrodialysis (EDBM) and fouling analysis, Biochem. Eng. J. 166 (2021) 107883.
[131] M. Reig, S. Casas, O. Gibert, C. Valderrama, J.L. Cortina, Integration of nanofiltration and bipolar electrodialysis for valorization of seawater desalination brines: production of drinking and waste water treatment chemicals, Desalination 382 (2016) 13–20.
[132] M. Reig, S. Casas, C. Valderrama, O. Gibert, J.L. Cortina, Integration of monopolar and bipolar electrodialysis for valorization of seawater reverse osmosis desalination brines: production of strong acid and base, Desalination 398 (2016) 87–97.
[133] M. Badruzzaman, J. Oppenheimer, S. Adham, M. Kumar, Innovative beneficial reuse of reverse osmosis concentrate using bipolar membrane electrodialysis and electrochlorination processes, J. Membr. Sci. 326 (2009) 392–399.
[134] K. Ghyselbrecht, M. Huygebaert, B. Van der Bruggen, R. Ballet, B. Meesschaert, L. Pinoy, Desalination of an industrial saline water with conventional and bipolar membrane electrodialysis, Desalination 318 (2013) 9–18.
[135] N. van Linden, G.L. Bandinu, D.A. Vermaas, H. Spanjers, J.B. van Lier, Bipolar membrane electrodialysis for energetically competitive ammonium removal and dissolved ammonia production, J. Clean. Prod. 259 (2020) 120788.
[136] L. Dursun, O.N. Ata, A. Kanca, Bipolar membrane electrodialysis for binary salt water treatment: valorization of type and concentration of electrolytes, Ind. Eng. Chem. Res. 60 (2021) 2003–2010.

This book belongs to Badji Mokhtar Annaba University Central Library Copyright Elsevier 2025

[137] S.R. Abdullahi, M.R. Öner, O.N. Ata, Fractional factorial design application for the determination of affecting parameters on the generation of KOH and HCl from simulated wastewater solution by bipolar membrane electrodialysis abstract, Avrupa Bilim ve Teknoloji Dergisi (2019) 866–873.
[138] J. Erkmen, S. Yapici, A environmentally friendly process for boric acid and sodium hydroxide production from borax; bipolar membrane electrodialysis, Desalin. Water Treat. 57 (2016) 20261–20269.
[139] J. Erkmen, S. Yapıcı, M. Arzutuğ, Ö. Aydın, O. Ata, M. Öner, Hydrofluoric acid and sodium hydroxide production by bipolar membrane electrodialysis, Desalin. Water Treat. 57 (2016) 20254–20260.
[140] S. Bunani, M. Arda, N. Kabay, K. Yoshizuka, S. Nishihama, Effect of process conditions on recovery of lithium and boron from water using bipolar membrane electrodialysis (BMED), Desalination 416 (2017) 10–15.
[141] L. Monat, S. Chaudhury, O. Nir, Enhancing the sustainability of phosphogypsum recycling by integrating electrodialysis with bipolar membranes, ACS Sustain. Chem. Eng. 8 (2020) 2490–2497.
[142] F. Ilhan, H.A. Kabuk, U. Kurt, Y. Avsar, M.T. Gonullu, Recovery of mixed acid and base from wastewater with bipolar membrane electrodialysis—a case study, Desalin. Water Treat. 57 (2016) 5165–5173.
[143] F. Ilhan, H.A. Kabuk, U. Kurt, Y. Avsar, H. Sari, M.T. Gonullu, Evaluation of treatment and recovery of leachate by bipolar membrane electrodialysis process, Chem. Eng. Process. Process. Intensif. 75 (2014) 67–74.
[144] M. Xia, C. Ye, R. Cao, H. Huang, J. Huang, An innovative beneficial reclamation of flue gas desulfurization brine using bipolar membrane electrodialysis technique, Int. J. Electrochem. Sci. 13 (2018) 5382–5395.
[145] V. Zabolotskii, N. Sheldeshov, S. Melnikov, Heterogeneous bipolar membranes and their application in electrodialysis, Desalination 342 (2014) 183–203.
[146] X. Liu, Q. Li, C. Jiang, X. Lin, T. Xu, Bipolar membrane electrodialysis in aqua–ethanol medium: production of salicylic acid, J. Membr. Sci. 482 (2015) 76–82.
[147] F. Hanada, K. Hirayama, N. Ohmura, S. Tanaka, Bipolar membrane and method for its production, Google Patents, 1993.
[148] C. Huang, T. Xu, Electrodialysis with bipolar membranes for sustainable development, Environ. Sci. Technol. 40 (2006) 5233–5243.
[149] H. Strathmann, H.J. Rapp, B. Bauer, C.M. Bell, Theoretical and practical aspects of preparing bipolar membranes, Desalination 90 (1993) 303–323.
[150] J. Ran, L. Wu, Y. He, Z. Yang, Y. Wang, C. Jiang, et al., Ion exchange membranes: new developments and applications, J. Membr. Sci. 522 (2017) 267–291.
[151] K. Yan, X. Hang, J. Liu, J. Luo, Y. Wan, Preparation of hypophosphorous acid by bipolar membrane electrodialysis: process optimization and phosphorous acid minimization, Ind. Eng. Chem. Res. 58 (2019) 21855–21863.
[152] A. Merkel, A.M. Ashrafi, J. Ečer, Bipolar membrane electrodialysis assisted pH correction of milk whey, J. Membr. Sci. 555 (2018) 185–196.
[153] J. Kroupa, J. Kinčl, J. Cakl, Recovery of H_2SO_4 and NaOH from Na_2SO_4 by electrodialysis with heterogeneous bipolar membrane, Desalin. Water Treat. 56 (2015) 3238–3246.
[154] C.X. Jiang, Y.M. Wang, Z.H. Zhang, T.W. Xu, Electrodialysis of concentrated brine from RO plant to produce coarse salt and freshwater, J. Membr. Sci. 450 (2014) 323–330.
[155] Y. Zhang, K. Ghyselbrecht, R. Vanherpe, B. Meesschaert, L. Pinoy, B. Van der Bruggen, RO concentrate minimization by electrodialysis: techno-economic analysis and environmental concerns, J. Environ. Manage. 107 (2012) 28–36.
[156] Y. Zhang, K. Ghyselbrecht, B. Meesschaert, L. Pinoy, B. Van der Bruggen, Electrodialysis on RO concentrate to improve water recovery in wastewater reclamation, J. Membr. Sci. 378 (2011) 101–110.
[157] M. Turek, J. Was, P. Dydo, Brackish water desalination in RO–single pass EDR system, Desalin. Water Treat. 7 (2012) 263–266.

This book belongs to Badji Mokhtar Annaba University Central Library Copyright Elsevier 2025

[158] E. Korngold, L. Aronov, N. Daltrophe, Electrodialysis of brine solutions discharged from an RO plant, Desalination 242 (2009) 215–227.
[159] Y. Oren, E. Korngold, N. Daltrophe, R. Messalem, Y. Volkman, L. Aronov, et al., Pilot studies on high recovery BWRO-EDR for near zero liquid discharge approach, Desalination 261 (2010) 321–330.
[160] R. Ibáñez, A. Pérez-González, P. Gómez, A.M. Urtiaga, I. Ortiz, Acid and base recovery from softened reverse osmosis (RO) brines. Experimental assessment using model concentrates, Desalination 309 (2013) 165–170.
[161] N. Agmon, The Grotthuss mechanism, Chem. Phys. Lett. (1995) 456–462.
[162] K. Kreuer, A. Rabenau, W. Weppner, Vehicle mechanism, a new model for the interpretation of the conductivity of fast proton conductors, Angew. Chem. Int. (Ed.) Engl. 21 (1982) 208–209.
[163] L. Wang, Z. Li, Z. Xu, F. Zhang, J.E. Efome, N. Li, Proton blockage membrane with tertiary amine groups for concentration of sulfonic acid in electrodialysis, J. Membr. Sci. 555 (2018) 78–87.
[164] Y. Qian, L. Huang, Y. Pan, X. Quan, H. Lian, J. Yang, Dependency of migration and reduction of mixed $Cr_2O_7^{2-}$, Cu^{2+} and Cd^{2+} on electric field, ion exchange membrane and metal concentration in microbial fuel cells, Sep. Purif. Technol. 192 (2018) 78–87.
[165] T. Bai, M. Wang, B. Zhang, Y. Jia, Y. Chen, Anion-exchange membrane with ion-nanochannels to beat trade-off between membrane conductivity and acid blocking performance for waste acid reclamation, J. Membr. Sci. 573 (2019) 657–667.
[166] I. Bechthold, K. Bretz, S. Kabasci, R. Kopitzky, A. Springer, Succinic acid: a new platform chemical for biobased polymers from renewable resources, Chem. Eng. Technol. 31 (2008) 647–654.
[167] L. Handojo, A.K. Wardani, D. Regina, C. Bella, M.T.A.P. Kresnowati, I.G. Wenten, Electromembrane processes for organic acid recovery, RSC Adv. 9 (2019) 7854–7869.
[168] C. Huang, T. Xu, Y. Zhang, Y. Xue, G. Chen, Application of electrodialysis to the production of organic acids: state-of-the-art and recent developments, J. Membr. Sci. 288 (2007) 1–12.
[169] C. Jiang, Y. Wang, T. Xu, 6 - Membranes for the recovery of organic acids from fermentation broths, Membrane Technologies for Biorefining, Woodhead Publishing, 2016, pp. 135–161.
[170] L. Yu, T. Lin, Q. Guo, J. Hao, Relation between mass transfer and operation parameters in the electrodialysis recovery of acetic acid, Desalination 154 (2003) 147–152.
[171] O.M.K. Readi, H.J. Mengers, W. Wiratha, M. Wessling, K. Nijmeijer, On the isolation of single acidic amino acids for biorefinery applications using electrodialysis, J. Membr. Sci. 384 (2011) 166–175.
[172] T.V. Eliseeva, A.Y. Tekuchev, V.A. Shaposhnik, I.G. Lushchik, Electrodialysis of amino acid solutions with bipolar ion-exchange membranes, Russ. J. Electrochem. 37 (2001) 423–426.
[173] S. Toyoshi, T. Yoshizumi, M. Saeki, T. Kawakita, Method for preventing fouling of electrodialysis membrane, Google Patents, 1987.
[174] Y. Wang, X. Wang, R. Tang, S. Yu, B. Zheng, Y. Feng, A novel thermostable cellulase from Fervidobacterium nodosum, J. Mol. Catal. B: Enzym. 66 (2010) 294–301.
[175] E. Gyo Lee, S.H. Moon, Y. Keun Chang, I.K. Yoo, H. Nam Chang, Lactic acid recovery using two-stage electrodialysis and its modelling, J. Membr. Sci. 145 (1998) 53–66.
[176] A. Bouchoux, H. Roux-de Balmann, F. Lutin, Investigation of nanofiltration as a purification step for lactic acid production processes based on conventional and bipolar electrodialysis operations, Sep. Purif. Technol. 52 (2006) 266–273.
[177] V. Hábová, K. Melzoch, M. Rychtera, B. Sekavová, Electrodialysis as a useful technique for lactic acid separation from a model solution and a fermentation broth, Desalination 162 (2004) 361–372.
[178] E.G. Lee, S.H. Kang, H.H. Kim, Y.K. Chang, Recovery of lactic acid from fermentation broth by the two-stage process of nanofiltration and water-splitting electrodialysis, Biotechnol. Bioprocess. Eng. 11 (2006) 313–318.
[179] H. Habe, Y. Shimada, T. Fukuoka, D. Kitamoto, M. Itagaki, K. Watanabe, et al., Two-stage electrodialytic concentration of glyceric acid from fermentation broth, J. Biosci. Bioeng. 110 (2010) 690–695.
[180] J.H. Kim, J.G. Na, J.W. Yang, Y.K. Chang, Separation of galactose, 5-hydroxymethylfurfural and levulinic acid in acid hydrolysate of agarose by nanofiltration and electrodialysis, Bioresour. Technol. 140 (2013) 64–72.

This book belongs to Badji Mokhtar Annaba University Central Library Copyright Elsevier 2025

[181] B. Kamm, M. Kamm, K. Richter, Formation of aminium lactates in lactic acid fermentation preparation and characterization of 1,4,-piperazinium-(L,L)-dilactate obtained from L(+)-lactic acid (Part I), Acta Biotechnol. 17 (1997) 3–18.
[182] J.H. Choi, S.H. Kim, S.H. Moon, Recovery of lactic acid from sodium lactate by ion substitution using ion-exchange membrane, Sep. Purif. Technol. 28 (2002) 69–79.
[183] V.H. Thang, W. Koschuh, K.D. Kulbe, S. Novalin, Detailed investigation of an electrodialytic process during the separation of lactic acid from a complex mixture, J. Membr. Sci. 249 (2005) 173–182.
[184] M. Hongo, Y. Nomura, M. Iwahara, Novel method of lactic acid production by electrodialysis fermentation, Appl. Environ. Microbiol. 52 (1986) 314–319.
[185] H. Yan, C. Xu, W. Li, Y. Wang, T. Xu, Electrodialysis to concentrate waste ionic liquids: optimization of operating parameters, Ind. Eng. Chem. Res. 55 (2016) 2144–2152.
[186] W. Li, J. Wang, Y. Nie, D. Wang, H. Xu, S. Zhang, Separation of soluble saccharides from the aqueous solution containing ionic liquids by electrodialysis, Sep. Purif. Technol. 251 (2020).
[187] X. Wang, Y. Nie, X. Zhang, S. Zhang, J. Li, Recovery of ionic liquids from dilute aqueous solutions by electrodialysis, Desalination 285 (2012) 205–212.
[188] L.T.P. Trinh, Y.J. Lee, J.-W. Lee, H.-J. Bae, H.-J. Lee, Recovery of an ionic liquid [BMIM]Cl from a hydrolysate of lignocellulosic biomass using electrodialysis, Sep. Purif. Technol. 120 (2013) 86–91.
[189] L. Bai, X. Wang, Y. Nie, H. Dong, X. Zhang, S. Zhang, Study on the recovery of ionic liquids from dilute effluent by electrodialysis method and the fouling of cation-exchange membrane, Sci. China Chem. 56 (2013) 1811–1816.
[190] X. Liang, Y. Fu, J. Chang, Recovery of ionic liquid via a hybrid methodology of electrodialysis with ultrafiltration after biomass pretreatment, Bioresour. Technol. 220 (2016) 289–296.
[191] X. Liang, J. Wang, H. Bao, H. Liu, Accurately-controlled recovery and regeneration of protic ionic liquid after Ionosolv pretreatment via bipolar membrane electrodialysis with ultrafiltration, Bioresour. Technol. 318 (2020) 124255.
[192] L.J. Banasiak, B. Van der Bruggen, A.I. Schäfer, Sorption of pesticide endosulfan by electrodialysis membranes, Chem. Eng. J. 166 (2011) 233–239.
[193] H. Lu, W. Zou, P. Chai, J. Wang, L. Bazinet, Feasibility of antibiotic and sulfate ions separation from wastewater using electrodialysis with ultrafiltration membrane, J. Clean. Prod. 112 (2016) 3097–3105.
[194] L.J. Banasiak, A.I. Schäfer, Removal of boron, fluoride and nitrate by electrodialysis in the presence of organic matter, J. Membr. Sci. 334 (2009) 101–109.
[195] Y. Mei, C.Y. Tang, Co-locating reverse electrodialysis with reverse osmosis desalination: synergies and implications, J. Membr. Sci. 539 (2017) 305–312.
[196] J.Y. Lee, J.H. Kim, J.H. Lee, S. Kim, S.H. Moon, Morphologically aligned cation-exchange membranes by a pulsed electric field for reverse electrodialysis, Environ. Sci. Technol. (2015).
[197] Q. Chen, Y.-Y. Liu, C. Xue, Y.-L. Yang, W.-M. Zhang, Energy self-sufficient desalination stack as a potential fresh water supply on small islands, Desalination 359 (2015) 52–58.
[198] R.A. Tufa, E. Curcio, E. Brauns, W. van Baak, E. Fontananova, G. Di Profio, Membrane distillation and reverse electrodialysis for near-zero liquid discharge and low energy seawater desalination, J. Membr. Sci. 496 (2015) 325–333.
[199] F. Luo, Y. Wang, C. Jiang, B. Wu, H. Feng, T. Xu, A power free electrodialysis (PFED) for desalination, Desalination 404 (2017) 138–146.
[200] Y. Mei, X. Li, Z. Yao, W. Qing, A.G. Fane, C.Y. Tang, Simulation of a novel reverse electrodialysis desalination stack for salt removal efficiency and fresh water recovery, J. Membr. Sci. (2019).
[201] W. Li, W.B. Krantz, E.R. Cornelissen, J.W. Post, A.R.D. Verliefde, C.Y. Tang, A novel hybrid process of reverse electrodialysis and reverse osmosis for low energy seawater desalination and brine management, Appl. Energy 104 (2013) 592–602.
[202] Q. Wang, X. Gao, Y. Zhang, Z. He, Z. Ji, X. Wang, et al., Hybrid RED/ED system: simultaneous osmotic energy recovery and desalination of high-salinity wastewater, Desalination 405 (2017) 59–67.

This book belongs to Badji Mokhtar Annaba University Central Library Copyright Elsevier 2025

[203] A. Ali, R.A. Tufa, F. Macedonio, E. Curcio, E. Drioli, Membrane technology in renewable-energy-driven desalination, Renew. Sust. Energy Rev. 81 (2018) 1–21.
[204] J. Hu, S. Xu, X. Wu, D. Wu, D. Jin, P. Wang, et al., Theoretical simulation and evaluation for the performance of the hybrid multi-effect distillation—reverse electrodialysis power generation system, Desalination 443 (2018) 172–183.
[205] M. Chen, Y. Mei, Y. Yu, R.J. Zeng, F. Zhang, S. Zhou, et al., An internal-integrated RED/ED system for energy-saving seawater desalination: a model study, Energy 170 (2019) 139–148.
[206] Y. Mei, C.Y. Tang, Recent developments and future perspectives of reverse electrodialysis technology: a review, Desalination 425 (2018) 156–174.
[207] J. Liu, G.M. Geise, X. Luo, H. Hou, F. Zhang, Y. Feng, et al., Patterned ion exchange membranes for improved power production in microbial reverse-electrodialysis cells, J. Power Sources 271 (2014) 437–443.
[208] Y. Kim, B.E. Logan, Hydrogen production from inexhaustible supplies of fresh and salt water using microbial reverse-electrodialysis electrolysis cells, Proc. Natl. Acad. Sci. U. S. A. 108 (2011) 16176–16181.
[209] J.Y. Nam, R.D. Cusick, Y. Kim, B.E. Logan, Hydrogen generation in microbial reverse-electrodialysis electrolysis cells using a heat-regenerated salt solution, Environ. Sci. Technol. 46 (2012) 5240–5246.
[210] X. Luo, J.Y. Nam, F. Zhang, X. Zhang, P. Liang, X. Huang, et al., Optimization of membrane stack configuration for efficient hydrogen production in microbial reverse-electrodialysis electrolysis cells coupled with thermolytic solutions, Bioresour. Technol. 140 (2013) 399–405.
[211] X. Luo, F. Zhang, J. Liu, X. Zhang, X. Huang, B.E. Logan, Methane production in microbial reverse-electrodialysis methanogenesis cells (MRMCs) using thermolytic solutions, Environ. Sci. Technol. 48 (2014) 8911–8918.
[212] X. Zhu, M.C. Hatzell, B.E. Logan, Microbial Reverse-electrodialysis electrolysis and chemical-production cell for H production and CO sequestration, Environ Sci. Technol. Lett. 1 (2014) 231–235.
[213] X. Li, I. Angelidaki, Y. Zhang, Salinity-gradient energy driven microbial electrosynthesis of value-added chemicals from CO_2 reduction, Water Res. 142 (2018) 396–404.
[214] X. Zhu, M.C. Hatzell, R.D. Cusick, B.E. Logan, Microbial reverse-electrodialysis chemical-production cell for acid and alkali production, Electrochem. Commun. 31 (2013) 52–55.
[215] X. Li, I. Angelidaki, Y. Zhang, Salinity-gradient energy driven microbial electrosynthesis of hydrogen peroxide, J. Power Sources 341 (2017) 357–365.
[216] X. Li, X. Jin, N. Zhao, I. Angelidaki, Y. Zhang, Novel bio-electro-Fenton technology for azo dye wastewater treatment using microbial reverse-electrodialysis electrolysis cell, Bioresour. Technol. 228 (2017) 322–329.
[217] A. D'Angelo, A. Galia, O. Scialdone, Cathodic abatement of Cr(VI) in water by microbial reverse-electrodialysis cells, J. Electroanal. Chem. 748 (2015) 40–46.

This book belongs to Badji Mokhtar Annaba University Central Library Copyright Elsevier 2025

This page intentionally left blank

This book belongs to Badji Mokhtar Annaba University Central Library

Copyright Elsevier 2025

CHAPTER TEN

Membrane-based electrochemical technologies: I. Membrane capacitive deionization and flow-electrode capacitive deionization

Clare Bales[1], Changyong Zhang[1] and T. David Waite[1,2]
[1]School of Civil and Environmental Engineering, University of New South Wales, Sydney, NSW, Australia
[2]UNSW Centre for Transformational Environmental Technologies (CTET), Yixing, Jiangsu, P.R. China

10.1 Introduction

Capacitive deionization (CDI) is an electrochemical desalination process that involves the removal of ions from water by the application of an electrical potential across the electrodes [1]. The technology was first described by Blair and Murphy in 1960 [2]; however, it was not until the early 2000s that CDI attracted more attention [3,4]. The electrodes can be configured either (in CDI) as a number of static electrode pairs or (in flow-electrode CDI [FCDI]) as a number of flow electrode pairs (refer Fig. 10.1) in which the slurries of conducting particles are transported across the anodic and cathodic current collectors [5]. CDI can be run in either a constant voltage (CV) or a constant current (CC) mode, but the static electrode configuration can be run in either flow-by or flow-through operation and is a batch process: that is, once the electrodes reach capacity, which being a set time for CV mode or a set electrode voltage for CC mode, the applied electrical potential or current is removed or reversed and the ions are released creating a brine stream. FCDI is typically a continuous process with both fresh product and brine being continuously produced and the electrodes continuously regenerated.

The addition of ion exchange membranes (IEMs) on static electrodes, in a technology that has become known as membrane capacitive deionization (MCDI), was first demonstrated by Lee et al. [6]. Typically, standalone cation exchange membranes (CEMs) are placed at the cathode surface and anion exchange membranes (AEMs) at the anode surface [4], although there have been

Electrochemical Membrane Technology for Water and Wastewater Treatment.
DOI: https://doi.org/10.1016/B978-0-12-824470-8.00002-4
© 2022 Elsevier Inc.
All rights reserved.

This book belongs to Badji Mokhtar Annaba University Central Library
Copyright Elsevier 2025

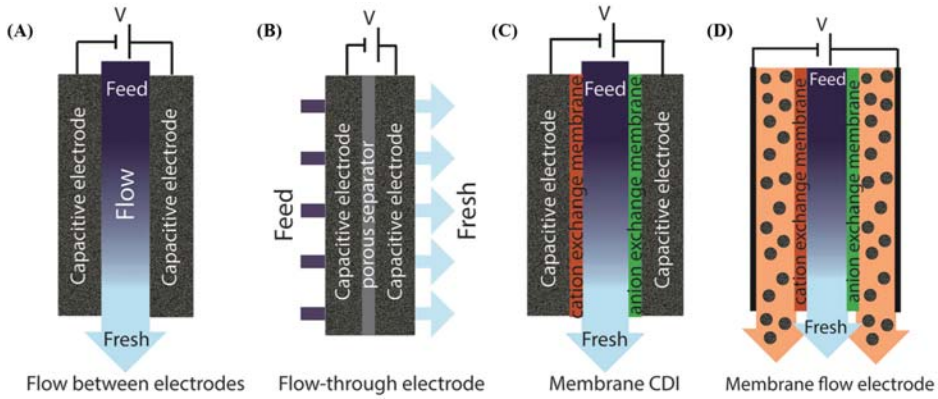

Figure 10.1 Selected CDI cell architectures including (A) static flow between CDI; (B) static flow through CDI; (C) static membrane CDI; and (D) membrane flow CDI. *Adapted with permission from M. Suss, S. Porada, X. Sun, P. Biesheuvel, J. Yoon, V. Presser, Water desalination via capacitive deionization: what is it and what can we expect from it?, Energy Environ. Sci. 8 (2015) 2296–2319 [4], copyright 2015 The Royal Society of Chemistry.*

several reported studies involving the coating of the IEM directly onto the electrode [7]. The use of IEMs with CDI improves the charge efficiency of the system with a lower energy consumption [8] and with demonstrated benefits for electrode longevity [9].

MCDI desalination is currently used in several pilot scale and field scale applications, in particular for desalination of brackish groundwater for potable use [10,11], water softening [12], industrial wastewater treatment [6], and treated domestic wastewater reuse applications [7,13,14].

IEMs are used in FCDI to separate the water stream from the flow-electrode slurry [5]. FCDI can be used for higher salinity feeds than conventional CDI as the regenerated uncharged carbon particles are continuously fed into the stream, which means the system has a much higher salt adsorption capacity [4]. FCDI can have higher charge efficiency than CDI and an associated reduction in energy consumption [15–18].

FCDI desalination is currently still at laboratory scale, but the system shows much promise for low-energy, higher-salinity desalination [5,18–23], resource or nutrient recovery [24–27], and removal of species of interest such as hardness ions [28], copper [29], and uranium [30].

In this chapter, we introduce the MCDI theory; then provide an outline of MCDI performance variations with changes in performance parameters; and end the discussion on MCDI with a brief overview of current MCDI applications. The FCDI section starts with an introduction to FCDI theory; then continues with a description of

This book belongs to Badji Mokhtar Annaba University Central Library Copyright Elsevier 2025

the design and operation of FCDI systems; and ends with an overview of FCDI applications. Finally, a brief summary of the challenges and the future research perspectives of MCDI and FCDI technology are presented.

10.2 Electrode materials and ion exchange membranes

10.2.1 Electrode materials

Carbon-based capacitive materials such as activated carbon (AC) [16,22,31–34], porous [8,35–37] or mesoporous carbon (MC) [38], AC fiber [39,40], carbon nanotubes (CNTs) [41–45], and graphene (GN) [43,46] and graphene xerogels [47] are the most commonly used materials in electrodes for CDI.

Electrodes can also be modified directly to create a similar effect to that of an IEM by the addition of sulfonic and amine groups [46], by oxidation/reduction [40,48], or by the addition of ion exchange polymers during electrode construction [45].

10.2.2 Ion exchange membranes

IEMs are used in both MCDI and FCDI to enhance desalination performance. Ion exchange polymers are directly applied to the electrodes and can be alternatively used in MCDI [37,39]; or directly applied to the spacer [49] or current collector [50,51] as in FCDI.

Commercial IEMs which are typically used in MCDI or FCDI include Tokuyama Neosepta AM-1 and CM-1 [6,35], AMX and CMX [8,10,31–34,36,48], while other products include Tianmei Company AEM-DF-120 and CEM-DF-120 [39], or Beijing Jie Rui Environmental Science and Technology Corporation JAM-II-05 and JCM-II-05 [14]. The thickness of the commercial IEMs used is in the order of 110–170 μm. IEMs can be made specifically for CDI with the CEM usually containing sulfonated groups and the AEM containing aminated groups [52,53].

IEMs can be used to select ions with a preference for particular ions. Shen et al. [14], in a trial on MCDI for treated domestic wastewater, found the use of an AEM with a fixed quaternary ammonium group (JAM-II-05, Beijing Jie Rui Environmental Science and Technology Corporation, China) as having resulted in anion selectivity order of $NO_3^- > Cl^- > SO_4^{2-} > P$. They noted that the selectivity of Cl^- over P is pH dependent: Cl^- is preferentially removed at pH ≤ 7; and P preferentially removed at pH ≥ 8. The AEM Neosepta AMX (selectivity coefficient $(k_{NO_3^-/Cl^-}) = 4.37$) was found to preferentially select NO_3^- over Cl^- [32].

This book belongs to Badji Mokhtar Annaba University Central Library
Copyright Elsevier 2025

10.3 Membrane capacitive deionization

10.3.1 Theory of membrane capacitive deionization

The essential theory of MCDI is similar to the standard static CDI with the application of an electric field applied to remove ions from water. In CDI, the counterions (ions with the opposite charge to that of the local electrode) are adsorbed into the pores of a porous electrode [4], where an ion is stored within the interparticle pore space (macropores) or within the electrical double layers (EDLs) inside the micropores of the porous electrode (refer Fig. 10.2) [1]. Coions (ions with the same charge as the local electrode), on the other hand, migrate from the EDLs to the macropores and, in CDI, to the spacer channel and then to the oppositely charged electrode. In MCDI, with the addition of IEMs to CDI, the coions instead of moving away are kept within the macropores and, given the charge-balancing nature of the macropores, it follows that there is an additional accumulation of counterions within the macropores compared to what is observed in CDI and so a higher desalination performance in MCDI [1] is noticeable. The IEMs also prevent counterions from entering the electrode during reverse current desorb, enabling better electrode desorbing which results in higher desalination performance for the following cycle.

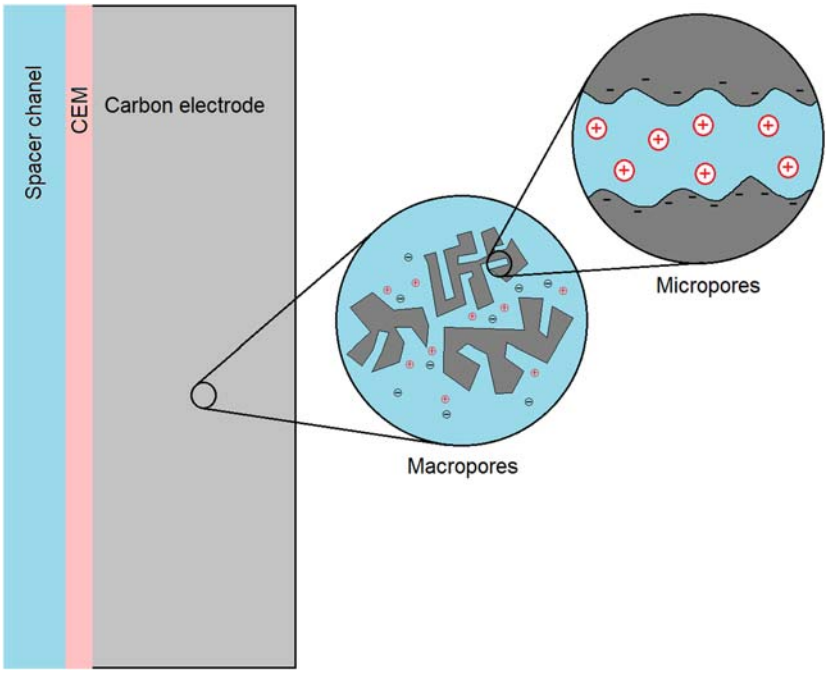

Figure 10.2 Macropores and micropores of the electrode.

This book belongs to Badji Mokhtar Annaba University Central Library Copyright Elsevier 2025

Ion transport through the system can be separated into several components:

- Transport through the spacer channel,
- Transport through the IEM, and
- Transport into the electrodes and EDLs.

The rate limiting step for MCDI is the transport of ions through the IEM. In some cases, higher valency ions can be temporarily stored in the IEM and not adsorbed onto the electrode [54].

Biesheuvel et al. [1] describe a modified Donnan model for ion transport in the micropores and EDLs. The modified Donnan model includes ion absorption by the carbon particles prior to the application of an electrical potential and so better characterizes the desalination performance of both the CDI and MCDI systems. These systems demonstrate, both in theory and via experiments, a 20% performance improvement for zero-potential desorption by MCDI over CDI, and a further 20% improvement for reverse potential desorption by MCDI [1].

MCDI can be operated in either CV or CC mode (Fig. 10.3) [3,4]. CV mode is widely used as the mode of operation for electrode performance studies testing system behaviour as the electrical potential can be applied until the electrode reaches capacity. CC mode, on the other hand, is used in the pilot trials and the field trials when a stable effluent conductivity is desired (refer Fig. 10.3). The desorb mode can be zero volt desorption (ZVD) or reverse voltage desorption (RVD) when operated in the CV mode, or reverse current desorption (RCD) when operated in the CC mode.

The following performance metrics are commonly used when comparing between the different CDI systems in dynamic steady state [55].

Water recovery, WR, is defined as:

$$\mathrm{WR} = \frac{V_d}{V_d + V_c} \tag{10.1}$$

where V_d is the volume of desalinated water and V_c is the volume of brine or concentrate.

The average salt concentration reduction, Δc (mM), is defined as:

$$\Delta c = \frac{\Delta N_d}{V_d} \tag{10.2}$$

where, ΔN_d is the salt removed over one cycle (moles) and defined as:

$$\Delta N_d = \int_{\Delta t_d} Q\,(c_{\mathrm{feed}} - c_{\mathrm{out}})dt \tag{10.3}$$

where, Q is the volumetric flowrate through the cell, c_{feed} is the feed salt concentration (mM), c_{out} is the effluent salt concentration (mM) and Δt_d is the time over which the desalinated water is collected.

This book belongs to Badji Mokhtar Annaba University Central Library Copyright Elsevier 2025

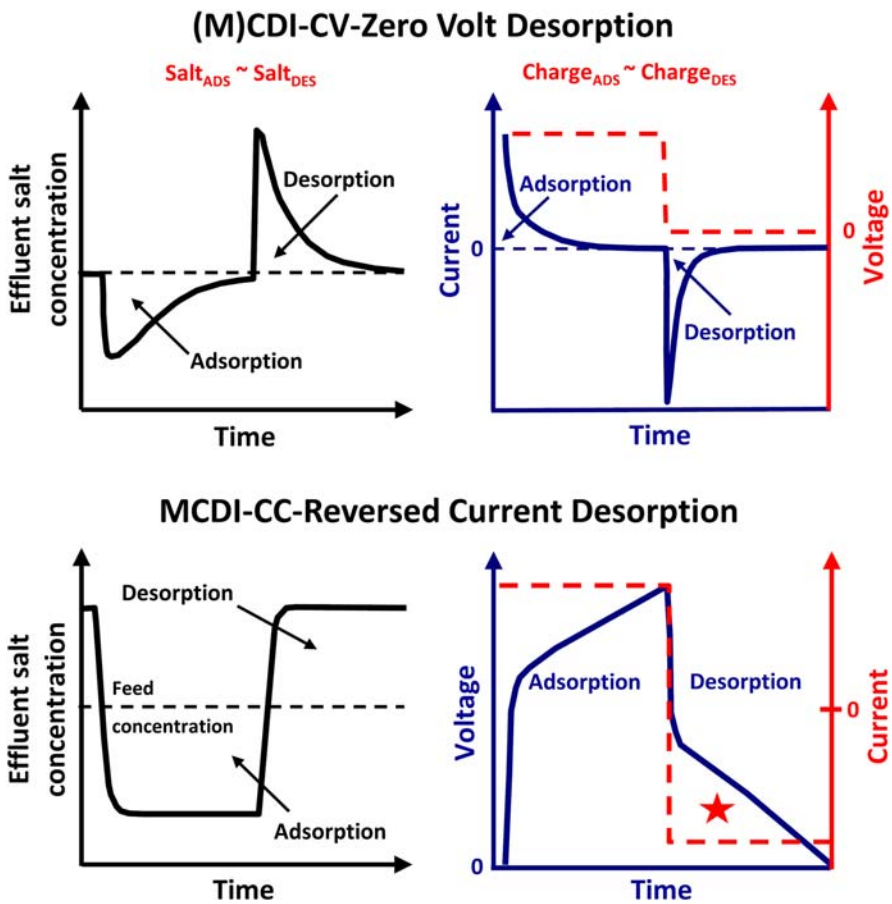

Figure 10.3 MCDI adsorption and desorption cycle analysis for constant voltage (CV) and constant current (CC). *Reproduced with permission from S. Porada, R. Zhao, A. van der Wal, V. Presser, P. Biesheuvel, Review on the science and technology of water desalination by capacitive deionization, Prog. Mater. Sci. 58 (2013) 1388–1442 [3], copyright 2013 Elsevier Ltd.*

The volumetric energy consumption, E_v (kWh/m^3), is defined as:

$$E_v = \frac{E_{\text{in}} - \eta E_{\text{out}}}{V_d} \tag{10.4}$$

where, E_{in} is the total energy input (J) and defined as:

$$E_{\text{in}} = \int_{\Delta t_{\text{cycle}}} \text{IV} dt \text{ where IV} > 0 \tag{10.5}$$

where, IV is the current-voltage product for a single electrode pair (W) and Δt_{cycle} is the total cycle time (min).

This book belongs to Badji Mokhtar Annaba University Central Library Copyright Elsevier 2025

E_{out} is the total recoverable energy from the cell (J) and defined as:

$$E_{out} = \int_{\Delta t_{cycle}} IV dt \text{ where } IV < 0 \tag{10.6}$$

and η is the fraction of E_{out} actually recovered and reused to power another charging phase.

The productivity, P (L/h/m^2), is defined as:

$$P = \frac{V_d}{nA\Delta t_{cycle}} \tag{10.7}$$

where, n is the number of cells (electrode pairs) in the CDI stack (series and parallel) and A is the projected face area (m^2) of one cell.

The average salt adsorption rate, ASAR, (mol/min/cm^2) is defined as:

$$\text{ASAR} = \frac{\Delta N_d}{nA\Delta t_{cycle}} \tag{10.8}$$

The energy normalized adsorbed salt, ENAS (μmol/J) is defined as:

$$\text{ENAS} = \frac{\Delta N_d}{E_{in} - \eta E_{out}} \tag{10.9}$$

The salt adsorption capacity, SAR (mg/g) is defined as:

$$\text{SAR} = \frac{M}{m}\Delta N_d \tag{10.10}$$

where, M (g/mol) is the molar mass of the salt and m (g) is the total mass of the electrodes in the cell.

Finally, charge efficiency, Λ_{cycle}, is defined as [4,55,56]:

$$\Lambda_{cycle} = \frac{zF\Delta N_d}{q_{in}} \tag{10.11}$$

where, z is the charge of the ion or salt mixture ($z = 1$ for monovalent salts), F is Faraday's constant (96,485 C/mol) and q_{in} is the charge transferred at positive current (C) and defined as:

$$q_{in} = \int_{\Delta t_{cycle}} I dt \text{ where } I > 0 \tag{10.12}$$

For batch mode operation, where the effluent from the CDI is recycled back into a small feed water tank with the system charging until the salinity levels taper off at a low value [3], Δt_{cycle} is taken as the time to desalinate and the time to regenerate the electrodes and fill the waste tank [55]. The input and output energy is integrated over

This book belongs to Badji Mokhtar Annaba University Central Library Copyright Elsevier 2025

this experiment time and V_d, V_c, and c_{out} can be measured from the final state of the treated and waste tanks [55]. The performance metrics can be used for FCDI by setting Δt_{cycle} as the total experiment time [55].

10.3.2 Performance of membrane capacitive deionization

10.3.2.1 Desalination performance

MCDI desalination works best for brackish waters with salinities <10 g/L [3]. As the salinity crosses much beyond this, a multi-pass system may be required for low product conductivity requirements, and the energy consumption becomes too high, thereby rendering other desalination technologies more viable [10].

Several parameters can be modified to improve desalination performance with the two critical parameters being the flowrate between electrodes and the applied electrical potential. Studies from our group demonstrate that the slower the flowrate, the longer the hydraulic retention time (HRT) and so the more time for ions to adsorb onto the electrodes thereby improving desalination performance when assessing average effluent concentration (Fig. 10.4). However, as the electrode reaches capacity faster, this leads to a shorter cycle time with the result that the total salt adsorbed, and therefore ASAR, is reduced (Fig. 10.5) [36]. Applying higher adsorption currents in CC mode or higher voltages in CV mode has a similar effect.

For each flowrate, there is an optimal adsorption current (CC mode, refer Fig. 10.5C II); if the current shoots higher than this, the ion transport becomes too fast and the electrodes reach capacity very quickly, the cycle time reduces, and almost no product water is produced (Fig. 10.4). For each influent salinity and flowrate between electrodes, there is an optimal applied current for maximum ion removal (in CC mode). However, this applied current will not yield the optimal water recovery or production volume (Fig. 10.5 II) [36].

There is a tradeoff between the ASAR and the specific energy consumption (SEC) for an MCDI system design [34], where SEC (J/mg), for a CC mode cycle with brackish water, is defined as [34]:

$$\mathrm{SEC} = \frac{E_{in} - \eta E_{out}}{M \Delta N_d} \tag{10.13}$$

For a given system, maximum ASAR is desired whilst consuming minimal energy (note in Fig. 10.6 the inverse of SEC is shown). The desired effluent conductivity and electrode material have a large impact on the relationship between ASAR and SEC (Fig. 10.6); whereas, the influent salinity and required product volume have a smaller impact [34]. Across a wider range of studied areas, further relationships may be elucidated.

This book belongs to Badji Mokhtar Annaba University Central Library Copyright Elsevier 2025

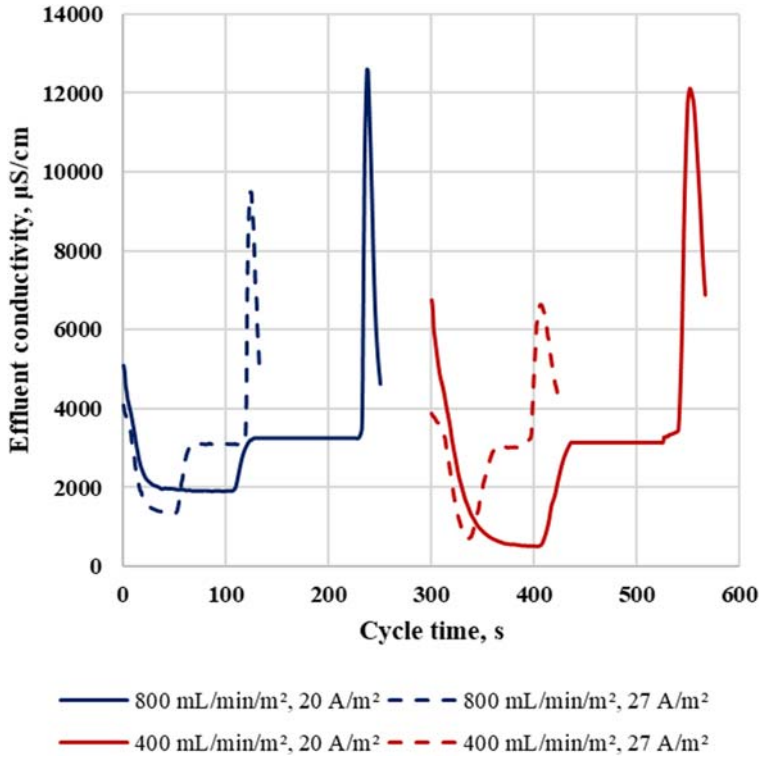

Figure 10.4 Trace conductivity (μS/cm) for flowrate of 400 and 800 mL/min/m^2 at current density of 20 and 27 A/m^2. This experiment was run on a Voltea IS electrode with high hardness influent (Na^+ = 426 mg/L, Ca^{2+} = 298 mg/L, Mg^{2+} = 107 mg/L, Cl^- = 665 mg/L, SO_4^{2-} = 522 mg/L, and HCO_3 = 776 mg/L, conductivity = 3200 μS/cm). The electrode was operated in CC-RCD mode until cell voltage reaches V_{cell} = 1.3 V and a minimum voltage in desorb, V_{min} = 0.4 V with stopped flow during the desorb phase.

When designing an MCDI system, in order to optimize a system for SEC and productivity (or desalinated volume per area of electrode), Wang and Lin [57] proposed a framework that requires only three parameters to be varied for CC mode operation, namely: (1) charging current density, I; (2) water recovery, WR; and (3) number of modules, n. For a given influent conductivity and product conductivity, there exists an optimal tradeoff curve between productivity and SEC with this framework facilitating the correct selection of the number of modules required for a given application.

10.3.2.2 Energy consumption

The energy consumption of the MCDI system is dependent on the salinity removal required [10]. Reported energy consumption for MCDI ranges from 0.1 kWh/m^3 for

This book belongs to Badji Mokhtar Annaba University Central Library Copyright Elsevier 2025

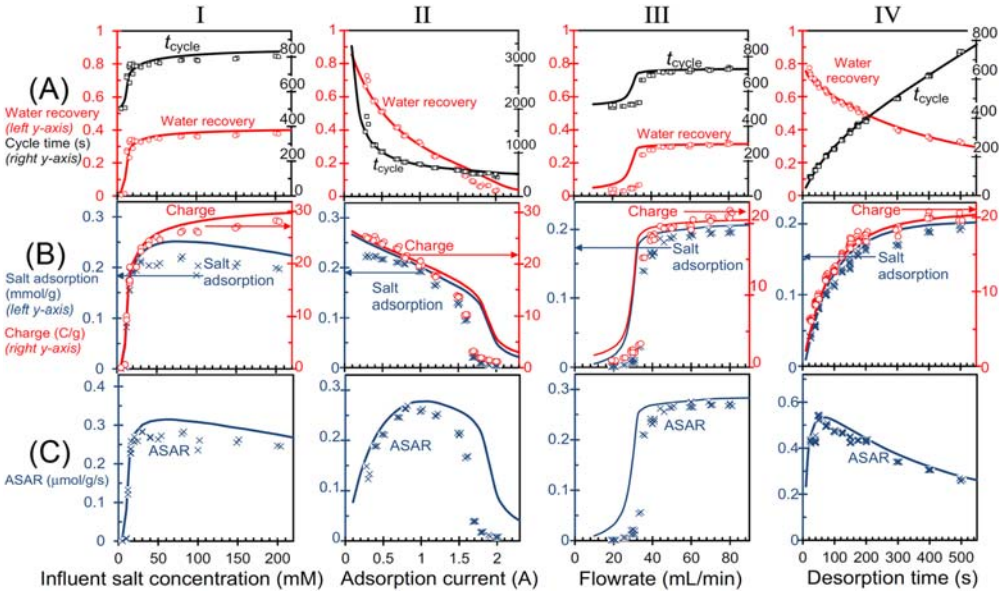

Figure 10.5 Experimental and theoretical results of operation for MCDI in CC-ZVD mode. Water recovery and total cycle time (t_{cycle}) (row A), salt adsorption, and charge per cycle, per gram of total electrode mass (row B), and average salt adsorption rate (ASAR) (row C). Column I is for increasing influent salt concentration, column II for increasing adsorption current, column III for increasing flowrate, and column IV for increasing desorption time. Reference settings are influent salt concentration (NaCl) = 20 mM, adsorption current (applied until the cell voltage reaches V_{cell} = 1.6 V) = 1 A (~37 A/m^2), water flowrate (stack) = 60 mL/min and desorption time = 500 s. *Reproduced with permission from R. Zhao, O. Satpradit, H. Rijnaarts, P. Biesheuvel, A. van der Wal, Optimization of salt adsorption rate in membrane capacitive deionization, Water Res. 47 (2013) 1941–1952 [36]. Copyright 2013 Elsevier Ltd.*

minimal Δc requirements up to 3 kWh/m^3 for higher removal requirements (Table 10.1). MCDI has been shown to have lower energy consumption than CDI due to the increased charge efficiency in the system [8].

When using CC mode with reverse current desorb, energy can be recovered from the electrodes [60]. This has been demonstrated at laboratory scale by recovery back to a super capacitor [61] and, more recently, at pilot scale by Tan, He, Fletcher, and Waite [58] who included a battery system to power the charging cycle and recovered the energy during desorb. The system included a DC-DC bidirectional (buck-boost) convertor for the voltage difference between the MCDI system (typically <1.5 V) and the 12 V battery. Tan et al. [58] were able to recover almost 40% of the energy used in the charging phase. There was not only the ohmic resistance loss within the MCDI unit but also the cable and convertor losses, which contributed to the irrecoverable portion of the energy. This demonstrates that for

This book belongs to Badji Mokhtar Annaba University Central Library Copyright Elsevier 2025

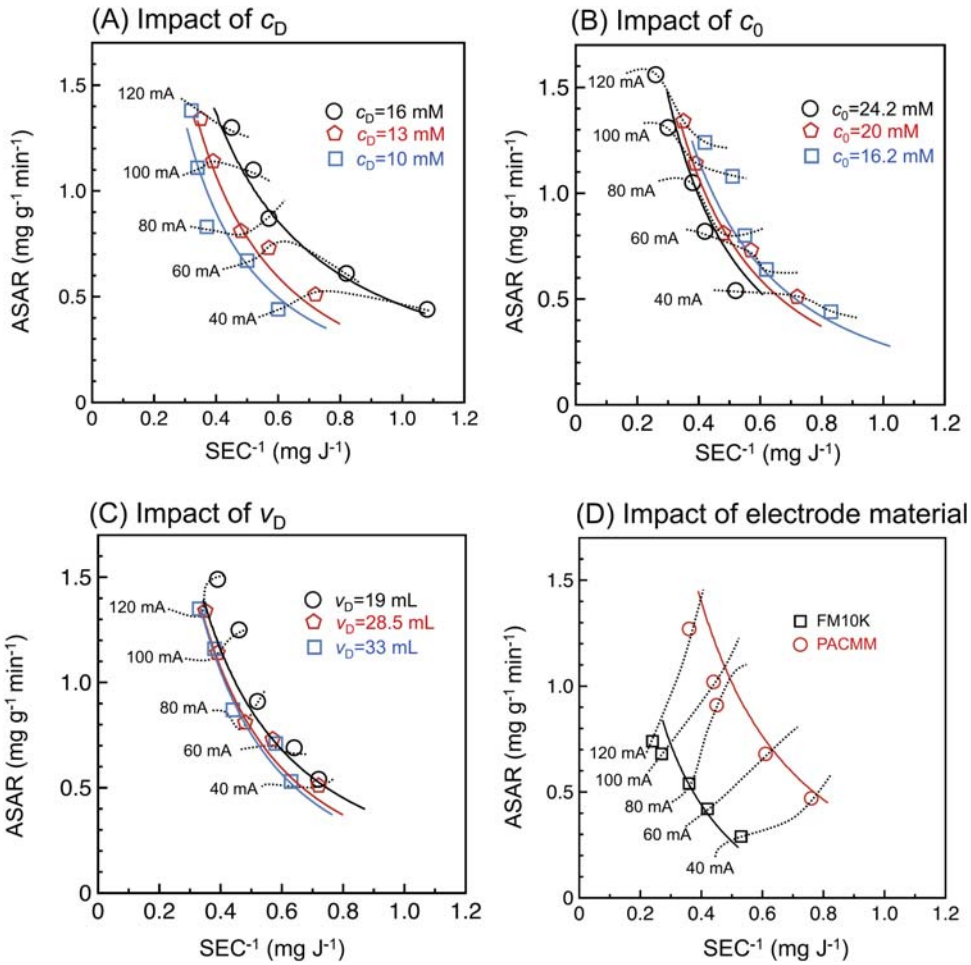

Figure 10.6 Experimental and theoretical results for ASAR versus SEC^{-1} curves for (A) different average product salinities, c_D, (B) different influent salinities, C_0, (C) different product volumes, v_D and (D) different electrode materials. The open symbols are experimental data and the solid curves are simulated results. The dotted curves connect the experimental results that were obtained using the same current. The electrodes were operated in CC-ZVD mode with reference settings c_0, NaCl = 20 mM, c_D = 13 mM for (B) and (C); and 16 mM for (D); v_D = 28.5 mL for (A) and (B); and 33 mL for (D), and electrode material used was PACMM and FM10K. Note for this study ASAR was calculated using grams of carbon rather than electrode area. *Reproduced with permission from L. Wang, S. Lin, Intrinsic tradeoff between kinetic and energetic efficiencies in membrane capacitive deionization, Water Res. 129 (2018) 394–401 [34], copyright 2017 Elsevier Ltd.*

minimal energy consumption of a system optimizing ancillary equipment such as cabling is also important. Higher feed concentrations were found to produce a higher portion of recoverable energy [61].

This book belongs to Badji Mokhtar Annaba University Central Library Copyright Elsevier 2025

This book belongs to Badji Mokhtar Annaba University Central Library

Table 10.1 Specific energy consumption (kWh/m^3) for various MCDI regimes.

CDI type	Electrolyte/influent	Salinity removal (mg/L)	Specific energy consumption (kWh/m^3)	References
MCDI (CC, Tokuyama AM-1 & CM-1)	Power plant wastewater, ~4050 mg/L (5400 μS/cm)[a]	~3862.5 mg/L (5150 μS/cm)[a]	1.96 kWh/m^3	[6]
MCDI (PC, Neosepta AMX, and CMX)	NaCl, 1000–5500 mg/L	750–4500 mg/L	0.25–3 kWh/m^3	[10]
MCDI (PC)	Cooling tower effluent, ~265 and 470 mg/L	186 and 329 mg/L	0.105 and 0.234 kWh/m^3 (2.2 and 2.6 J/mg)	[12]
MCDI (Voltea electrode module)	NaCl, 1900 mg/L	560–780 mg/L	0.28–0.42 kWh/m^3 (includes energy recovery) (1.79–2.11 J/mg)	[58]
MCDI (PC, Neosepta AMX & CMX)	NaCl, 2000 mg/L	1600 mg/L	0.4 kWh/m^3	[59]
MCDI (PC, Neosepta AMX & CMX)	NaCl, 2337.6 mg/L	2185.6 mg/L	0.35 kWh/m^3 (optimized design)	[59]
MCDI (AC, JAM-II-05 & JCM-II-05)	NaCl, 584.4 mg/L	169.5 mg/L (10 electrode pairs) – 298 mg/L (40 electrode pairs)	0.096–0.172 kWh/m^3	[14]

AC, Activated carbon; *CC*, carbon cloth; *PC*, porous carbon.
[a]Assuming that TDS (mg/*L*) = 0.75 × EC (μ*S*/cm) for powerplant wastewater.

Copyright Elsevier 2025

There has been much recent debate regarding the energy consumption of MCDI compared to reverse osmosis (RO) and electrodialysis reversal (EDR) [59,62–64]. MCDI is only suitable for influent concentrations <4 g/L above which the energy consumption becomes extremely high [10,65]. When considering the inclusion of renewable energy, due to the low voltage requirements, MCDI can be easily coupled to a photovoltaic array [66,67] and so the cost of water production for a PV-MCDI system (\$0.8–\$4 m^{-3}) [68] is lower than that reported for similar small sized RO (\$6.5–\$9 m^{-3}) [69] and EDR systems(\$5.8–\$16 m^{-3}) [69,70].

10.3.2.3 Water recovery

Typical reported water recovery for MCDI is 50%, with this relatively low percentage attributed to the operation of continuous flow mode in experimental work [57]. Ramachandran et al. [71] demonstrated the use of low flow during the desorb phase as a means for increasing water recovery in CDI. By using low flow during the desorb, water recoveries of up to 90% can be achieved depending on the scenario used as well as an improvement in thermodynamic efficiency of up to 2–3 times.

The use of stopped flow during the desorb phase, or intermittent flow, has been shown to achieve water recoveries of up to 87% [58]. The achievable water recovery in stopped flow desorb is dependent on the ion removal that is to be achieved. For increased ion removal, either the flowrate can be reduced or the applied potential increased, with the result that the electrodes reach capacity faster and, consequently, a reduced cycle time (Figs. 10.4 and 10.7) is achieved. Studies by our group also demonstrated that shorter cycle times ($V_{min} = 0.6$ V compared to $V_{min} = 0.4$ V) typically result in lower water recoveries (Fig. 10.7).

10.3.2.4 Ion selectivity

Due to the electrochemical nature of the desalination, CDI and MCDI show much promise for the selective removal of ions. For a standard MCDI system, higher valence ions will be favored because of the greater charge attraction [7,12,14,54]. Further, the IEMs play a significant role in the selectivity of ions [52,72], in addition to the permissiveness of selectivity to being altered operationally by increasing or decreasing the charging time [7,73,74] or the HRT (i.e., flowrate) [72], and by increasing or decreasing the applied electrical potential [72,74]. Manipulations of the electrode material such as micropore size selectivity and surface alteration for porous carbon or for alternative materials have been studied with CDI [75]. Typically, increasing the concentration ratio of the ion of interest will improve selectivity of that ion [6,72,74,76,77]. Depending on the application, different selectivity may be targeted; for example, for water softening applications Ca^{2+} and Mg^{2+} will be targeted over Na^{+}, while for agricultural applications Na^{+} and/or Cl^{-} will be targeted, and for potable water applications NO_3^{-} will be targeted over Cl^{-}.

This book belongs to Badji Mokhtar Annaba University Central Library Copyright Elsevier 2025

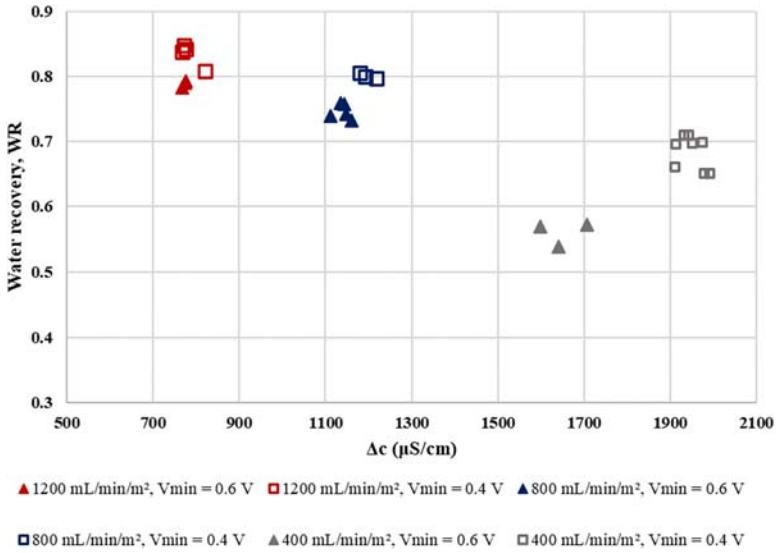

Figure 10.7 Water recovery versus salinity removal, Δc (μS/cm) for decreasing flowrate at minimum desorb voltage, $V_{min} = 0.6$ V (solid points) and $V_{min} = 0.4$ V (hollow points). The cycle time is decreased with decreasing flowrate and increasing minimal voltage. This experiment was run on a Voltea IS electrode with NaCl = 1800 mg/L. The electrode was operated in CC-RCD mode until cell voltage reaches $V_{cell} = 1.3$ V with stopped flow during the desorb phase.

The removal efficiency, RE, of a particular ion, i, is defined as:

$$\mathrm{RE}_i = \frac{C_{i,0} - C_{i,\mathrm{eff}}}{C_{i,0}} \times 100 \tag{10.14}$$

where $C_{i,0}$ is the initial concentration of ion i in the feed and $C_{i,\mathrm{eff}}$ is the average effluent concentration of ion i.

The selectivity of ion i over ion j can be expressed as the ratio of their removal efficiencies:

$$\eta_j^i = \frac{\mathrm{RE}_i}{\mathrm{RE}_j} \tag{10.15}$$

Shorter cycle times lead to higher selectivity of the monovalent cations Na^+ and K^+ as they are able to diffuse faster. As the cycle time increases, divalent ions replace the monovalent ions in the EDLs which means a greater selectivity for Ca^{2+} and Mg^{2+} (Fig. 10.8) [7,78].

Increasing the adsorption current reduces the selectivity of Ca^{2+} over Na^+ (CC-ZVD at a ratio of $[Ca^{2+}]_0 = 10$ mM:$[Na^+]_0 = 20$ mM) [72]. With high HRTs (i.e., low flowrate which leads to shorter cycle times), the selectivity of Ca^{2+} over Na^+ has

This book belongs to Badji Mokhtar Annaba University Central Library Copyright Elsevier 2025

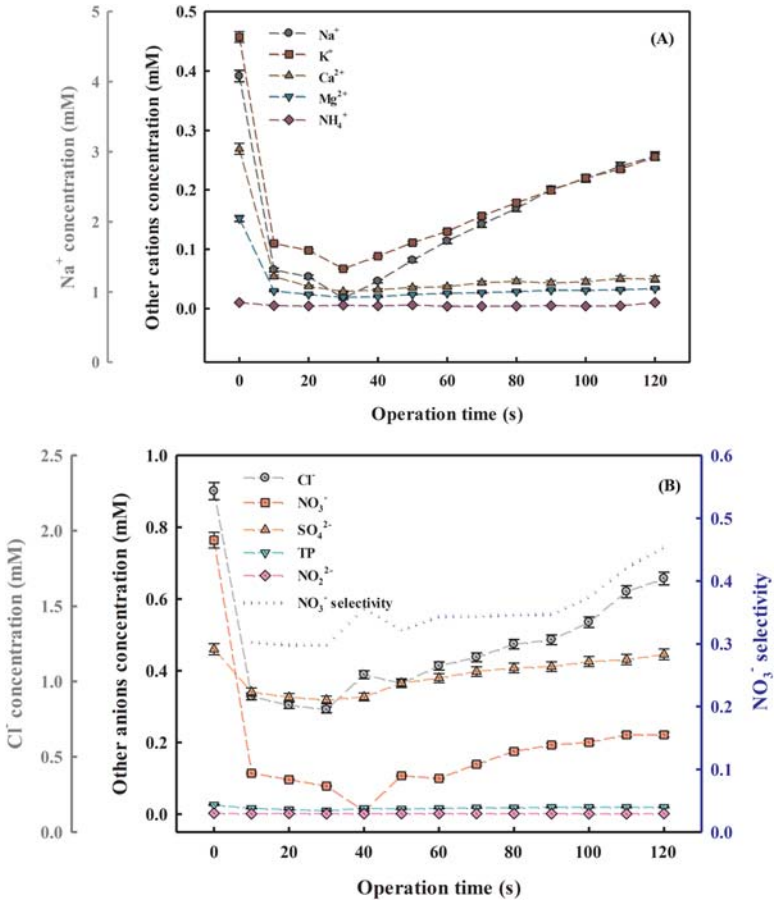

Figure 10.8 Changes in permeate (A) cation and (B) anion concentrations obtained from ion-selective MCDI cells during the treatment of wastewater. The MCDI system was operated in CV mode with an applied voltage between 1.2 and 1.5 V. *Reproduced with permission from D.I. Kim, P. Dorji, G. Gwak, S. Phuntsho, S. Hong, H. Shon, Reuse of municipal wastewater via membrane capacitive deionization using ion-selective polymer-coated carbon electrodes in pilot-scale, Chem. Eng. J. 372 (2019) 241–250 [7], copyright 2019 Elsevier B.V.*

been shown to be reduced [72]. The addition of a CEM (Neosepta, Tokuyama Co.) enabled divalent cation selectivity with the CEM transport selectivity factor facilitating faster transport of Ca^{2+} through the CEM than it did for Na^{+} [72].

For both CDI and MCDI, selectivity of NO_3^- over Cl^- has been shown to increase with an increase in cycle time (CV-ZVD mode at equal concentrations 5 mM:5 mM); however, the increase was more dramatic with CDI having a selectivity of 3.88 at the longest cycle time tested (120 min) compared to 1.65 for MCDI [74]. In longer cycle times, NO_3^- replaces Cl^- and SO_4^- due to its hydrophobicity and

This book belongs to Badji Mokhtar Annaba University Central Library Copyright Elsevier 2025

high affinity to the carbon electrode (Fig. 10.8) [7]. The reduced selectivity of MCDI compared to CDI is attributed to the fact that ion transport through the IEM is the rate limiting step with the removal of NO_3^- and Cl^- relatively similar as they have the same ionic charge and similar diffusion coefficients. In comparison, in CDI, the higher electrostatic attraction of NO_3^- to the AC electrode resulting from the smaller hydration ratio can be utilized to promote selectivity [74]. As the ratio of NO_3^- to Cl^- increases, selectivity of NO_3^- also increases, though again with a lower enhancement for MCDI compared to CDI. In addition, as the applied voltage is increased, the selectivity of NO_3^- is reduced [74].

At high concentrations of phosphorus ($[P]_0 = 4$ and 16 mM) in feed solutions containing only phosphorus, a reduced pH (~ 6) leads to improved phosphorus removal in both CC and CV modes [77,79]. As $H_2PO_4^-$ dominates over HPO_4^{2-} at low pH, a larger number of the monovalent phosphate ions are required for charge neutralization, resulting in an increased adsorption capacity (Fig. 10.9). This difference, however, is not noted at lower concentrations, $[P]_0 = 0.4$ mM [79] or with mixed solutions of P and Cl^- [77,79]. At pH < 7 where $H_2PO_4^-$ dominates, there is preferential removal of Cl^- due to its smaller hydraulic radius and increased ability to move into the micropores; while at pH > 7 where HPO_4^{2-} starts to dominate, there is preferential removal of P due to the divalent ion's transporting faster through the membrane and/or its increased ease of accumulation within the EDLs (Fig. 10.9) [77].

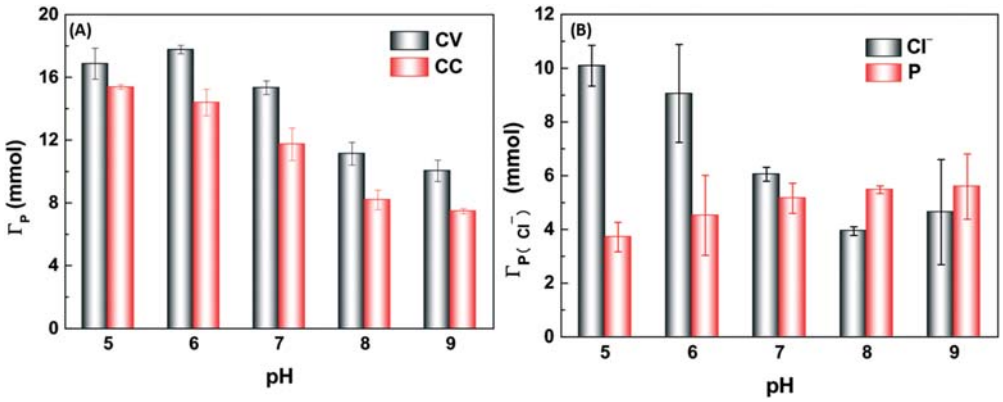

Figure 10.9 Effect of initial pH on the (A) P electrosorption capacity for CC and CV modes. $[P]_0 = 16.1$ Mm; and (B) electrosorption capacities of P and Cl^- in CC mode. $[P]_0 = [Cl^-]_0 = 16.1$ mM. Error bars are the standard deviation of the samples from triplicate measurements. *Adapted with permission from X. Huang, D. He, W. Tang, P. Kovalsky, T.D. Waite, Investigation of pH-dependent phosphate removal from wastewaters by membrane capacitive deionization (MCDI), Environ. Sci. Water Res. Technol. 3 (2017) 875–882 [77], copyright 2017 the Royal Society of Chemistry.*

This book belongs to Badji Mokhtar Annaba University Central Library Copyright Elsevier 2025

Increasing the applied voltage and flowrate resulted in improved removal efficiency of phosphorus, although the overall ionic removal decreased with higher flowrate [79].

Operational changes to optimize for selectivity need to be undertaken with other parameters also in mind. For example, in CC-RVD mode, the minimal applied current that can reasonably achieve the required desalination performance should be chosen to maximize water recovery and minimize energy consumption [76].

10.3.3 Applications of membrane capacitive deionization

10.3.3.1 Potable applications

MCDI is well suited to the treatment of brackish groundwater for potable water applications [3,4] with many investigations having focused on this application [10,80]. In a field trial of CDI treatment of groundwaters, it was found that moderate levels of Ca^{2+} (106 mg/L) and of Mg^{2+} (96.8 mg/L) and high levels of silica (88 mg/L) did not have a major impact on total dissolved solid (TDS) removal efficiency, while reducing TDS removal efficiency from 82% to 75% over 15 days of operation. Removal efficiency was restored to original levels after rinsing the electrodes with a 0.01 M citric acid cleaning solution [11]. Total organic carbon (TOC) levels of 2 mg/L did, however, result in a TDS removal efficiency reduction from 86% to 55% after 15 days; though, system performance was restored after cleaning the electrodes with 0.01 M citric acid followed by 0.01 M NaOH [11]. MCDI is better suited to the treatment of source waters with high TOC compared to CDI as organics can be prevented from entering the electrode by the addition of an AEM [9] before the electrode. This is particularly the case when the addition of an AEM is coupled with a reverse potential desorb which prevents the accumulation of organics on the AEM and limits biofilm growth [9]. Upstream filters are also recommended for high TOC applications.

10.3.3.2 Treated domestic wastewater reuse

Recently, several studies have focused on applications for treated domestic wastewater reuse [7,13,14], with particular attention given to the examination of fouling impacts on the high organic loads present in these feed streams [9,81].

Studies on the effect of the presence of humic acid and sodium alginate on NaCl and $CaCl_2$ removal by MCDI using CV-RVD mode found a decline in desalination performance over a 15 day period (Fig. 10.10) [81]. For humic acid, it was suspected that there was competition between the H^+ derived from the humic acid and Na^+, and the formation of complexes between Ca^{2+} and the humic acid likely rendered Ca^{2+} less available for removal by electrosorption. For sodium alginate, the accumulation of fouling on the IEM, in particular, the build up of complexes with Ca^{2+}, leads to a decline in desalination performance. Two types of fouling mechanisms were observed: with humic acid, the pores became blocked and resisted being recovered by

This book belongs to Badji Mokhtar Annaba University Central Library Copyright Elsevier 2025

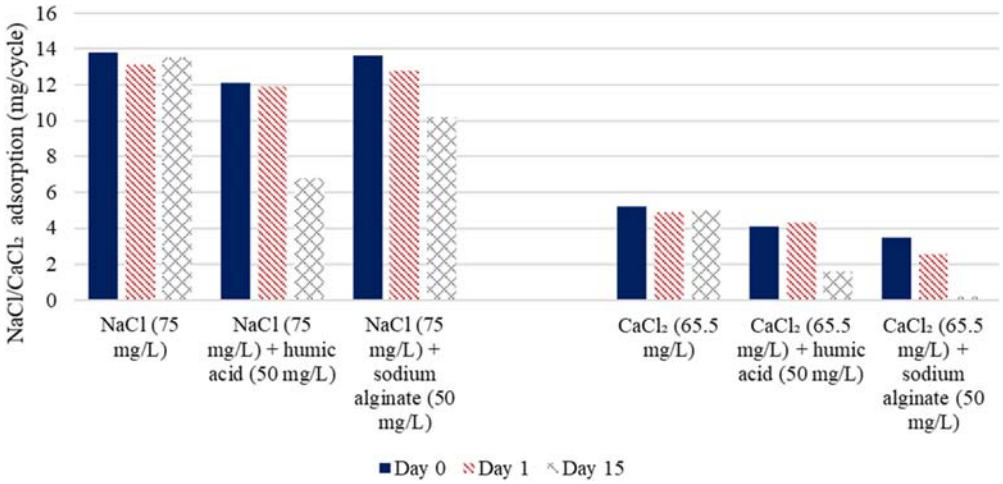

Figure 10.10 NaCl and $CaCl_2$ adsorption at days 0, 1 and 15 for influent with pure NaCl and pure $CaCl_2$, and the influent dosed with humic acid and sodium alginate. The MCDI configuration was CV-RVD mode with an applied voltage of 1.2 V and a flowrate of 20 mL/min (1000 mL/min/m^2) with AC fiber felts and cation and anion exchange membranes (Hangzhou Greenhe Environment Co., Ltd, China). *Data retrieved from L. Chen, C. Wang, S. Liu, Q. Hu, L. Zhu, C. Cao, Investigation of the long-term desalination performance of membrane capacitive deionization at the presence of organic foulants, Chemosphere 193 (2018) 989–997 [81], copyright 2017 Elsevier Ltd.*

cleaning; whereas, with sodium alginate, cake development took place that was recovered with cleaning. Pretreatment to minimize the presence of dissolved organic matter in the MCDI feed is recommended.

In a similar study, Hassanvand et al. [9] compared the performance of CDI (CV-ZVD) with MCDI (CV-RVD) with influent waters high in organics. A higher salt concentration was used (NaCl, 584 mg/L and NaCl, 496.7 mg/L + $CaCl_2$, 55.5 mg/L) [9] more in line with treated domestic wastewaters [13] with 60 mg/L of humic acid added to the NaCl and 60 mg/L of sodium alginate added to the NaCl + $CaCl_2$ solution. They found a significant reduction in salt adsorption and charge efficiency for CDI over 18 cycles and, only, a minimal reduction in salt adsorption and no reduction in charge efficiency for MCDI. Chen et al. [81] also observed limited performance decline after 1 day with the NaCl + humic acid and NaCl + sodium alginate solutions (Fig. 10.10).

Hassanvand et al. [9] suggest that the limited extent of fouling observed with MCDI is likely related to the reverse potential applied during the desorb phase. The negatively charged organics that accumulate on the AEM during charging are repelled during desorption and, to some extent, are also likely to be removed by the sheer force resulting from flow through the spacer channel [9]. These foulants have a high molecular weight, so are less likely to penetrate the membrane compared to other

This book belongs to Badji Mokhtar Annaba University Central Library Copyright Elsevier 2025

studied organics such as octane. After a cleaning regime of 0.01 M NaOH for 120 min followed by 0.1 M NaOH for 60–120 min, the salt adsorption (for the CDI case) was restored. An accumulation of carbon in the cleaning solution was found, and they speculated that the NaOH was degrading the polyvinylidene fluoride electrode binder. Cleaning with an acid solution for both CDI and MCDI rather than alkali to limit the detrimental effects on the electrode and membranes was recommended [9].

In a five month study with a 40 electrode pair stack, the production of high quality water for reuse applications was demonstrated [14]. Using a CV-ZVD mode, they found an 82% decrease in charging time in studies where the charging time was stopped once the effluent conductivity reached 250 μS/cm. This resulted in a decrease in charge efficiency from 95% to 75% and a reduction in productivity from 1.36 to 0.96 L/h/m^2. After the system's five months of operation, Shen et al. [14] found organic fouling on the AEM and the anode and inorganic scaling on the CEM and cathode. They did not include any cleaning regime in the study, and recommended cleaning with freshwater, chemical, acid, or alkali solution and reversing the voltage during discharge in order to prevent biofouling and scaling [14].

10.3.3.3 Industrial applications

One of the first demonstrations of the use of MCDI in an industrial application was for desalination of power plant wastewater [6]. The MCDI system used exhibited a 19% higher salt removal than CDI. In a stream predominately made up of Na^+ and Cl^-, no performance decline over 500 cycles was observed.

MCDI has been shown to be effective in a variety of deionization and softening applications. Over a one year trial period on desalination of water for cooling towers, van Limpt and van der Wal [12] showed that total water savings of up to 28% and wastewater savings of up to 48% could be achieved by the use of MCDI. In addition, chemical savings of up to 78% and 85% at the two study sites examined were demonstrated. This is not only of financial benefit but also of importance when considering site safety implications.

Recent investigations by our group with high hardness water (1180 mg/L as $CaCO_3$ with TDS of 2800 mg/L) found no decrease in desalination performance or increase in energy consumption over the 1 month of operation. The study was conducted using a Voltea IS activated carbon MCDI module.

10.3.3.4 Agricultural applications

For MCDI, the higher the desalination requirement the larger the number of electrode cells needed and therefore the higher the costs. By coupling a performance and costing model to an agricultural model, Bales et al. [82] demonstrated the profitability of MCDI in detailed studies at two locations [68]. They demonstrated that, due to the decline of crop yield with increasing irrigation salinity, there is a window of bore salinities at which

This book belongs to Badji Mokhtar Annaba University Central Library Copyright Elsevier 2025

installation of an MCDI system is more profitable than irrigation with brackish groundwater. Greenhouse applications were found to be well suited to MCDI desalination with a profit increase of up to AU$40,000/ha/year for greenhouse strawberries where the local groundwater has a conductivity of approximately 3000 μS/cm [68].

10.3.3.5 Cost of membrane capacitive deionization desalinated water

The cost of MCDI desalinated water is highly dependent on the cost of IEMs with the cost of water increasing from ~$0.25 m^{-3} to ~$0.8 m^{-3} for a low versus high cost IEM with a 5-year life time system with influent salinity of 50 mequiv/L and product of 8.5 mequiv/L and production rate of 158 m^3/h (Fig. 10.11) [80]. Capital costs outweigh operating costs significantly, and so further work to improve system lifecycles is recommended [68,80].

As the influent salinity increases and the desalination requirements increase, the water price increases as the number of modules required to meet the specific production rate increases [68,80]. The water price determined for desalination of brackish groundwater for agricultural applications (Fig. 10.12) would be marginally lower than that for potable water applications, as there was no disinfection requirement included.

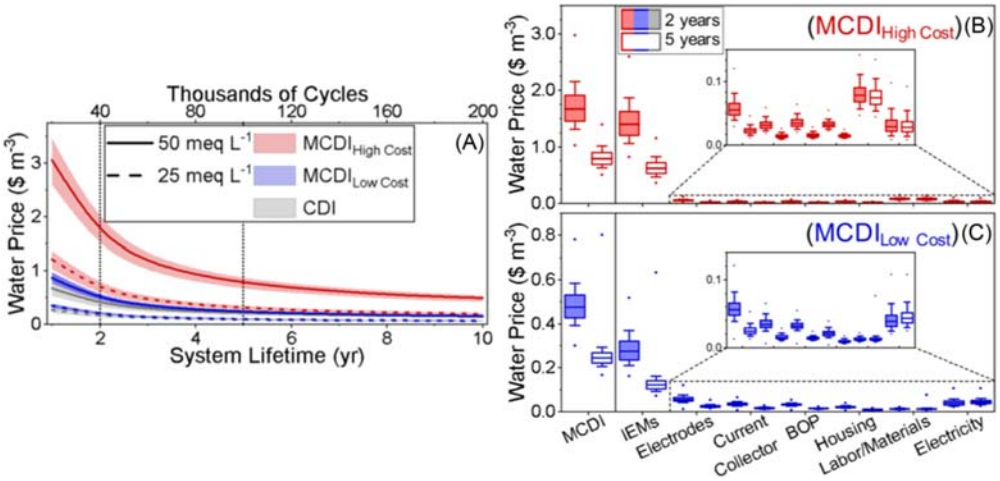

Figure 10.11 (A) Median water price ranges for CDI (gray, lower bands) and MCDI with $100 m^{-2} (red, upper bands) and $20 m^{-2} (blue, middle bands) IEMs at influent concentrations of 25 and 50 mequiv/L as a function of system lifetime/median total cycles. Shaded boundaries indicate the 25–75th percentiles. (B and C) The relative contribution of each constituent cost for MCDI at 2 (shaded) and 5 year (open) lifetimes at 50 mequiv/L. Boxes represent 25th, 50th, and 75th quartiles, whiskers represent 10th and 90th deciles, and dots represent min/max. For average product water concentration of 8.5 mequiv/L and a production rate of 158 m^3/h. *Reproduced with permission from S. Hand, J.S. Guest, R.D. Cusick, Technoeconomic analysis of brackish water capacitive deionization: navigating tradeoffs between performance, lifetime, and material costs, Environ. Sci. Technol. 53 (2019) 13353–13363 [80], copyright 2019 American Chemical Society.*

This book belongs to Badji Mokhtar Annaba University Central Library Copyright Elsevier 2025

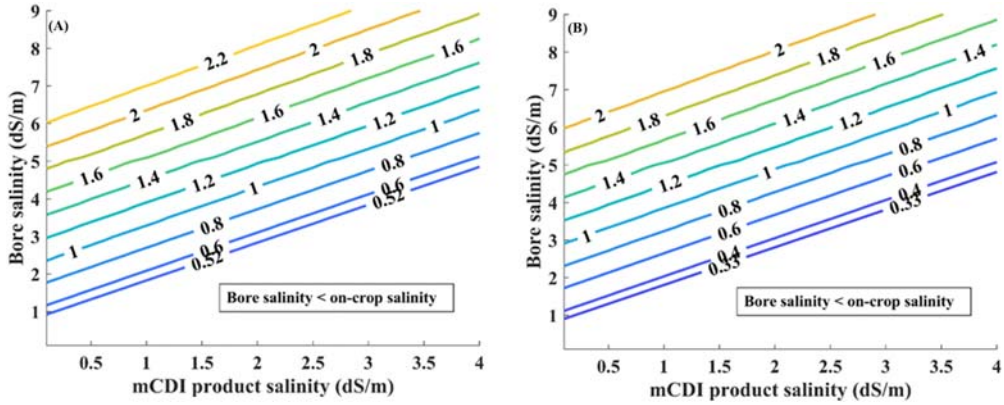

Figure 10.12 Water price, AU\$ m^{-3}, for a production rate of 33 m^3/h for (A) full installation and operating costs including bore, storage, MCDI desalination and brine disposal; and (B) MCDI desalination and storage installation and operating costs only. Electrode lifetime assumed to be 5 years. Note, prices presented here are in AU\$ m^{-3} (US\$1 = AU\$1.27). *Reproduced with permission from C. Bales, B. Lian, J. Fletcher, Y. Wang, T.D. Waite, Site specific assessment of the viability of membrane Capacitive Deionization (mCDI) in desalination of brackish groundwaters for selected crop watering, Desalination 502 (2021) 114913 [68], copyright 2020 Elsevier B.V.*

There are many scenarios where the water price is less than \$1 m^{-3} making MCDI a cost effective desalination method, particularly for inland remote or regional locations.

10.4 Flow capacitive deionization

10.4.1 Theory and development of flow capacitive deionization

Of the many existing CDI variants, FCDI is attracting particular interest. FCDI involves the use of flowable carbon particles as the electrodes and, by continuously replenishing the electrode chambers with fresh or regenerated slurry electrodes, this membrane-based electrochemical technology not only is expected to achieve high desalting efficiency but also has the potential to be operated continuously [15–18]. Although underpinning mechanisms relating to ion removal in an FCDI system can be partially attributed to capacitive ion removal processes (i.e., ion migration in an electrical field followed by adsorption in counter electrodes), electrodialytic contributions also play a significant role (i.e., ion migration into the electrode chamber but remain in the electrolyte) [83,84]. One paramount advantage of FCDI is the flexible management of flowable electrodes outside of the apparatus, enabling rapid separation of brine or resources [24,27,85]. In addition, like other electrochemical systems, FCDI can be potentially integrated with renewable energy sources (e.g., solar and wind energy) and used in rural off-grid power regions.

This book belongs to Badji Mokhtar Annaba University Central Library Copyright Elsevier 2025

The past seven years has witnessed a dramatic increase in the number of academic publications in the FCDI area with the majority of efforts (45%) concentrated on process developments (e.g., application broadening and operation optimization) and system designs, with some attention also paid to cell architecture, fundamental mechanisms, and system characterization (Fig. 10.13). While desalination is still the dominant application area for FCDI, new applications such as resource recovery and contaminant abatement have become popular in recent years [26,29,86,87].

10.4.2 Flow capacitive deionization design and operation

A typical FCDI cell generally consists of current collectors, separators, and spacers which are held together by a pair of perspex endplates. The schematic representation and photos of the major components of a small-scale FCDI system are provided in Fig. 10.14 [88]. In this section, we will provide a comprehensive review of these components as well as various FCDI cell configurations and operational modes.

10.4.2.1 Flow-electrodes

The properties of the flow-electrodes play an important role in ion removal from the feed stream. Flow-electrodes can be readily prepared by mixing active materials, conductive additives, and supporting electrolyte in an appropriate ratio. The solid weight percentage (wt.%) of electrodes can be calculated as:

$$\text{Solid content (wt.\%)} = \frac{\text{Active materials} + \text{Solid conductive Additives}}{\text{Active materials} + \text{Conductive Additives} + \text{Electrolyte}} \tag{10.16}$$

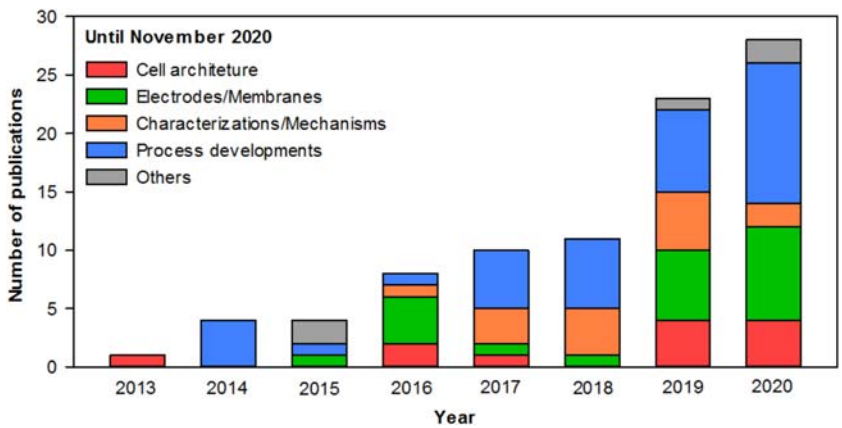

Figure 10.13 Number of academic publications in FCDI field since 2013. *Data were collected from Scopus and Google scholar databases up to November 2020.*

This book belongs to Badji Mokhtar Annaba University Central Library Copyright Elsevier 2025

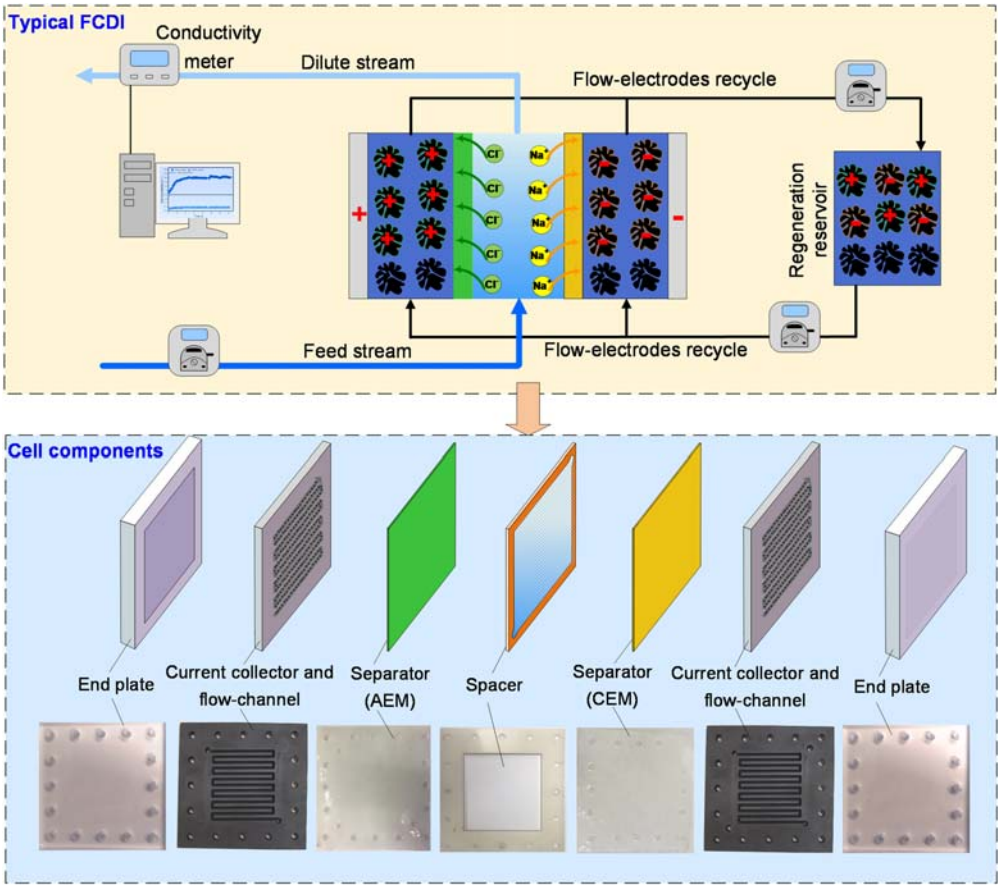

Figure 10.14 Schematic representation of a typical bench-scale FCDI cell and its major components. Photos of the major components are also provided. *Adapted with permission from C. Zhang, L. Wu, J. Ma, M. Wang, J. Sun, T.D. Waite, Evaluation of long-term performance of a continuously operated flow-electrode CDI system for salt removal from brackish waters, Water Res. 173 (2020) 115580 [88], copyright 2021 American Chemical Society.*

Extensive research has been undertaken with the goal of developing high-performance flow-electrodes for FCDI systems. In this section, we provide an overview of the existing flow-electrode materials and designs.

10.4.2.1.1 Active materials

Based on the ion adsorption mechanisms, active materials can be classified into two categories: capacitive materials and charge-transfer materials.

Similar to MCDI electrodes, carbon-based capacitive materials (e.g., AC [16,22], MC [38], CNTs [41–44], and GN [43]) are commonly used active materials for flow-electrodes

This book belongs to Badji Mokhtar Annaba University Central Library Copyright Elsevier 2025

(Table 10.2) as they have excellent conductivity and high specific surface area. By the introduction of functional groups/atoms and coating with additional components (e.g., transitional metal oxides (such as MnO_2), ion selective polymers, and electron mediators), the performances of the traditional carbon materials may be greatly enhanced with better wettability, larger capacitance, higher ion selectivity, and better suspension flowability/stability [42,90,91,104,105]. For instance, the introduction of oxygen containing functional groups such COOH, C = O, and C − OH through chemical oxidation of AC electrodes has been shown to significantly improve ion adsorption capacity and flowability of the suspension electrodes [91]. Furthermore, it has also been documented that sulfonation of CNT-based flow electrodes alleviates inter-tube aggregation and promotes electron transfer between current collector and flowable particles [42]. Charge-transfer materials (e.g., $NaMnO_2$, $Na_2Fe_2P_2O_7$, $Na_2NiFe(CN)_6$, $NaTi_2(PO_4)_3$, $Na_3V_2(PO_4)_3$, MoS_2, CuHCF, and BiOCl) are regarded as promising active material alternatives due to their larger ion storage capacity and higher flexibility for ion selective removal [106−110]. While limited studies have been conducted on the use of these materials in the FCDI field (except for sporadic cases in flow supercapacitor/battery systems [111]), it is expected that increasing number of applications of these promising materials will be realized in the following years.

Slurry electrodes with a solid mass loading of 5 − 20 wt.% (Table 10.2) are typically employed in order to strike a balance between slurry conductivity and viscosity. However, the conductivity (0.1 − 1 mS/cm) of slurry electrodes is intrinsically lower than that of static electrodes [112], mainly as a result of the discontinuous nature of the slurry electrode electrical network. While an increase in the loading of active materials can enhance the conductivity and performance of the slurry electrodes, so also reduced flowability will result in elevated pumping energy and a high risk of cell blockage [101]. Therefore, it is important to select appropriate conductive additives and supporting electrolyte as well as to balance their ratio in order to enhance the overall performance of the slurry electrodes.

10.4.2.1.2 Conductive additives

In slurry electrodes, two types of conductive additives are typically used: (1) solid particles with high conductivity, and (2) aqueous electron-mediators.

Typical solid conductive substances are carbon black (CB), CNTs, GN/reduced graphene oxide (rGO), and molybdenum carbide (MXene). CB is a collection of dense carbon particles which have superior electrical conductivity but relatively low surface area (<120 m^2/g) [113]. A previous study revealed that adding 1.5 wt.% CB into slurry electrodes resulted in a remarkable improvement of ion removal efficiency and charge efficiency, which can be attributed to the enhanced electron transfer within the slurry electrodes (Fig. 10.15A) [92]. Graphite powder has also been employed as a conductive additive with its properties such as powder size, powder shape, conductivity, and pore structure playing an important role in determining the system performance [93]. Other studies found that CNTs can serve as a bridge between AC

This book belongs to Badji Mokhtar Annaba University Central Library Copyright Elsevier 2025

This book belongs to Badji Mokhtar Annaba University Central Library

Table 10.2 Summary of the flow-electrode composition for various applications.

Active materials	Conductive additives	Electrolyte	Applications	References
1 wt.% AC	14 mM H_2Q[c]	n/a	Brackish water desalination	[89]
3.5 wt.% AC at cathode, 4.13 wt.% AC/MnO_2 at anode	1.5 wt.% CB	5.85 g/L NaCl	Brackish water desalination	[90]
5 wt.% AC	n/a	5.85 g/L NaCl	Brackish water and seawater desalination	[5]
5 wt.% AC	0.25 wt. FCNT[i]	2.7 g/L NaCl	Brackish water and seawater desalination	[41]
3.01 wt.% MC	n/a	11.7 g/L NaCl	Brackish water desalination	
3.01 wt.% CNTs	n/a	11.7 g/L NaCl	Brackish water desalination	[44]
6.48 wt.% AC	1 wt.% CNTs	11.7 g/L NaCl	Brackish water desalination	
13 wt.% oxidized AC	n/a	10 g/L NaCl	Brackish water desalination	[91]
20 wt.% AC	1 wt.% CB	0.65 g/L Na_2SO_4	Brackish water desalination	[92]
8.33 wt.% AC	6.25 wt.% SGP-5[d]	25 g/L NaCl	Seawater desalination	
8.33 wt.% AC	6.25 wt.% ICB0520[e]	25 g/L NaCl	Seawater desalination	
8.33 wt.% AC	6.25 wt.% LNC 3 − 10 G[f]	25 g/L NaCl	Seawater desalination	[93]
8.33 wt.% AC	6.25 wt.% PC0520[g]	25 g/L NaCl	Seawater desalination	
8.33 wt.% AC	6.25 wt.% EXO 5[h]	25 g/L NaCl	Seawater desalination	
8.5 wt.% AC	n/a	75 g/L NaCl	Seawater desalination	[94]
25.45 wt.% (AC − N[a]) at anodes, 25.45 wt.% (AC − S[b]) at cathodes	n/a	25 g/L NaCl	Seawater desalination	[22]
5 wt.% AC	n/a	n/a	Double displacement reactions	[87]
9 wt.% AC	1 wt.% CB	1 g/L NaCl	Ammonia recovery	[95]
9 wt.% AC	1 wt.% CB	2 g/L NaCl	Brackish water softening	[28]
10 wt.% AC	n/a	3.5 g/L Na_2SO_4	Concurrent nitrogen and phosphorus recovery	[85]
9 wt.% Activated charcoal	1 wt.% CB	n/a	Uncharged Ca-UO_2-CO_3 ternary complex removal	[96]

(*continued*)

Copyright Elsevier 2025

This book belongs to Badji Mokhtar Annaba University Central Library

Table 10.2 (Continued)

Active materials	Conductive additives	Electrolyte	Applications	References
16 wt.% MnO_2	4 wt.% CB	142 g/L Na_2SO_4	Electrochemical flow capacitor	[97]
18 wt.% carbon bead	2 wt.% CB	142 g/L Na_2SO_4	Electrochemical flow capacitor	[98]
20.7 wt.% carbon beads	2.3 wt.% CB, 0.139 M PPD[j]	112 g/L NaOH	Electrochemical flow capacitor	[99]
15 wt.% AC	n/a	n/a	Capacitive mixing	[100]
10 wt% AC	n/a	35.1 g/L NaCl	Capacitive mixing	
10 wt.% AC	n/a	0.25 M MEA[k]	Capacitive mixing	[101]
10 wt.% AC	n/a	n/a	Capacitive mixing	
10 wt.% AC	n/a	29.2 g/L NaCl	Flow electrode reverse electrodialysis	[102]

[a]AC-N: activated carbon contains ion-selective functional group of trimethylammonium.
[b]AC-S: activated carbon contains ion-selective functional group of sulfonate.
[c]H_2Q: aqueous hydroquinone.
[d]SGP-5: artificial graphite.
[e]ICB0520: bead-shaped material produced by carbonizing thermosetting resin.
[f]LNC 3 − 10 G: natural graphite.
[g]PC0520: pitch-based graphite coating, ICB grade.
[h]EXO 5: expanded graphite.
[i]FCNT: functionalized carbon nanotubes.
[j]PPD: p-phenylenediamine.
[k]MEA: monoethanolamine.
Source: Reproduced with permission C. Zhang, J. Ma, L. Wu, J. Sun, L. Wang, T. Li, et al., Flow electrode capacitive deionization (FCDI): recent developments, environmental applications, and future perspectives, Environ. Sci. Technol. 55 (2021) 4243−4267 [103], copyright 2021 American Chemical Society.

Copyright Elsevier 2025

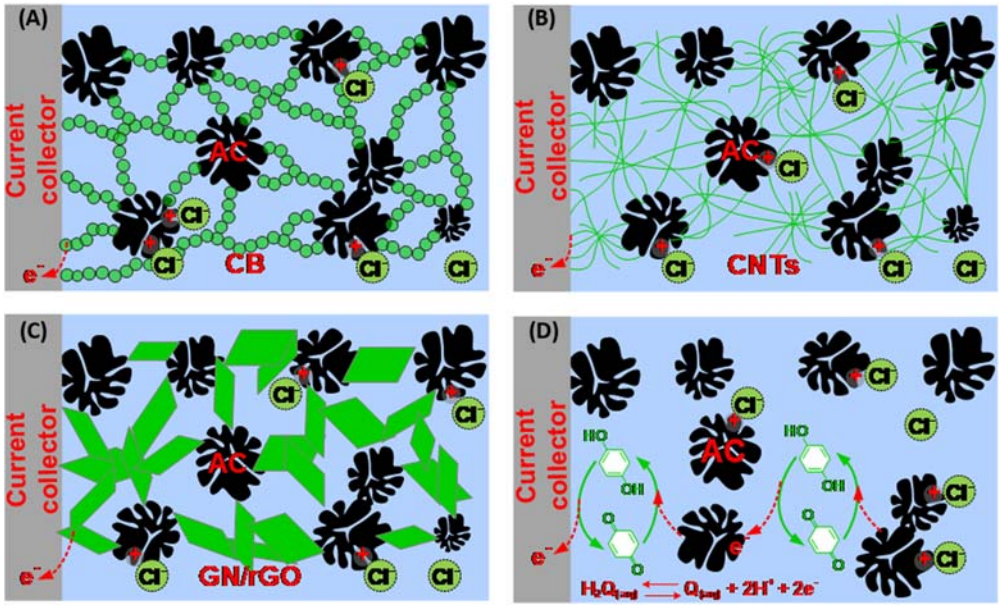

Figure 10.15 Schematic representation of the role of conductive additives in flow-electrode systems. Representative conductive additives are (A) carbon black (CB), (B) carbon nanotubes (CNTs), (C) graphene or reduced grapheme oxide (GN/rGO), and (D) hydroquinone and benzoquinone (H2Q/Q). *Adapted with permission from B. Akuzum, P. Singh, D.A. Eichfeld, L. Agartan, S. Uzun, Y. Gogotsi, et al., Percolation characteristics of conductive additives for capacitive flowable (semi-solid) electrodes, ACS Appl. Mater. Interfaces 12 (2020) 5866–5875 [114], copyright 2021 American Chemical Society.*

particles to enhance connectivity and conductivity of the suspension electrodes (Fig. 10.15B) [41]. Addition of even a small amount of CNTs (e.g., 0.25 wt.%) will lead to at least a doubling in ion removal rate. rGO has also been shown to be an effective conductive additive and can substantially accelerate the electron transfer within the suspension network (Fig. 10.15C) [89]. Note that the addition of these solid conductive additives will also improve the slurry viscosity with the selection of the appropriate amount of the additives being of great importance in avoiding particle aggregation and cell clogging [115].

Aqueous electron-mediators (e.g., hydroquinone (H_2Q), indigo carmine, p-phenylenediamine (PPD) and m-phenylenediamine (MPD)) are another type of conductive additives and take advantage of the fast and reversible redox reactions that take place at the particle electrode/electrolyte or current collector/electrolyte interfaces, thereby, facilitating electron transfer within the suspension electrodes.

Note that these mediators generally have proton-coupled multielectron exchange ability with some of them (PPD and MPD) prefering basic conditions, whereas others (H_2Q) are more suitable for use under acidic conditions [116–120]. Previous studies

This book belongs to Badji Mokhtar Annaba University Central Library Copyright Elsevier 2025

from our group indicated that the facile redox transformation between hydroquinone (H_2Q)/benzoquinone (Q) (Eq. 10.17) in the flowable electrode matrix facilitated both electron and ion transfer (Fig. 10.15D) resulting in a significantly enhanced salt removal rate (by approximately 130%). In addition, the H_2Q/Q cycle was found to be highly reversible, indicating the feasibility of use of H_2Q/Q as a conductive additive.

$$H_2Q_{(aq)} \rightarrow Q_{(aq)} + 2H^+ + 2e^- \tag{10.17}$$

10.4.2.1.3 Electrolyte

Electrolyte, as the major component of flow-electrodes (accounting for more than 80 wt.%), is used to disperse the solid particles and forms a homogeneous slurry. It is generally believed that adding an appropriate amount of varied salts (e.g., NaCl) into the electrolyte can greatly reduce the ohmic resistance of the flow-electrodes and enhance the FCDI system's ion removal performance [92,94]. For example, when the electrolyte salt concentration was increased from 0.5 to 1.25 M, the electronic conductivity of the flow-electrode was enhanced by 25% [121]. However, excessive addition of salt might result in negative influences such as particle aggregation and high slurry viscosity, as well as undesired counter-ion back diffusion and co-ion leakage during the desalination process [101,122].

10.4.2.2 Separator and spacer

The separator is a critical component of an FCDI cell, and not only serving as a physical barrier between the electrode chamber and spacer chamber but also acting as the ion pathway between the two chambers. Numerous separators such as free-standing IEMs (Fig. 10.16A) and nanofiltration membranes (NF) have been extensively explored in FCDI processes. Spacers are also commonly employed in FCDI devices to support separators (e.g., IEMs), provide a flow path for feedwater, and enhance mixing [123]. Both non-conductive porous materials (e.g., nylon and polyester sheet) and conductive materials (e.g., carbon cloth and ion-exchange resin) can be used as FCDI spacers. As most of FCDI separator and spacer materials are similar to those in MCDI systems, no further description will be provided here.

Note that the use of commercial flat-sheet membranes or spacer will increase the contact resistance within the system, while leading to a deterioration in performance and elevated energy consumption. More importantly, the scale-up of the FCDI device will be a great challenge considering the complexity of the system (e.g., usage of various components). As such, efforts have been made to combine different components together, such as by coating the ion exchange polymer (e.g., phenylene oxide in dimethylacetamide or *N*-methyl-2-pyrrolidone) onto the spacer or current collector to form a membrane-spacer-assembly (MSA) (Fig. 10.16B) [49] or

This book belongs to Badji Mokhtar Annaba University Central Library Copyright Elsevier 2025

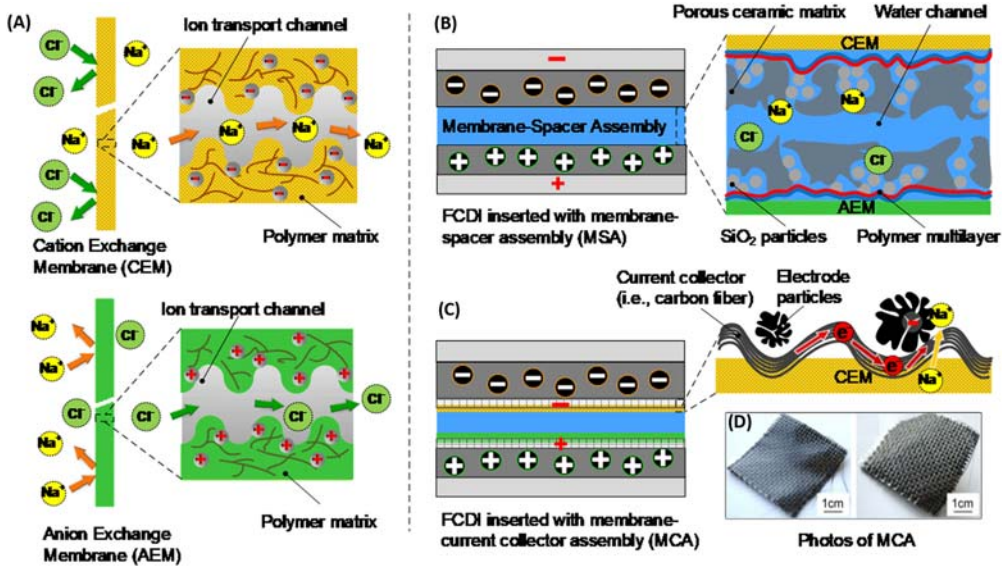

Figure 10.16 Schematic drawings of (A) cation exchange membrane (CEM) and anion exchange membrane (AEM), (B) FCDI with a membrane-spacer assembly (MSA), (C) FCDI with a membrane-current collector assembly (MCA) and (D) photos of the MCA. *Adapted with permission from K.S. Lee, Y. Cho, K.Y. Choo, S. Yang, M.H. Han, D.K. Kim, Membrane-spacer assembly for flow-electrode capacitive deionization, Appl. Surf. Sci. 433 (2018) 437–442 [49] and C.J. Linnartz, A. Rommerskirchen, J. Walker, J. Plankermann-Hajduk, N. Köller, M. Wessling, Membrane-electrode assemblies for flow-electrode capacitive deionization, J. Membr. Sci. 605 (2020) 118095 [50], copyright 2021 Elsevier.*

membrane-current collector-assembly (MCA) (Fig. 10.16C and D) [50,51]. Given the use of MSA and MCA has been shown to result in a drastic increase in the rate of charge transport and enhanced ion removal rate, it thus follows that the use of MSA or MCA is likely to simplify FCDI scale-up with lower costs and less laborious processes required.

10.4.2.3 Cell configurations

The first generation of FCDI, invented by Jeon et al. [5] in 2013, was a three-chamber 2D cell (Fig. 10.17A) that has been widely used in laboratory scale studies. To improve the treatment capacity and broaden the application of FCDI, modifications of the traditional 2D configuration have been carried out. Yang et al. [124] introduced a 2D FCDI system, which had a stack of five-unit cells and consisted of six graphite current collectors, IEMs, spacers, and gaskets (Fig. 10.17B). The 2D stack FCDI exhibited similar ion removal performance, but five times higher treatment capacity compared to a single unit cell. It has also been demonstrated that by inserting multiple pairs of IEMs in the FCDI system and creating alternate feed and brine chambers

This book belongs to Badji Mokhtar Annaba University Central Library Copyright Elsevier 2025

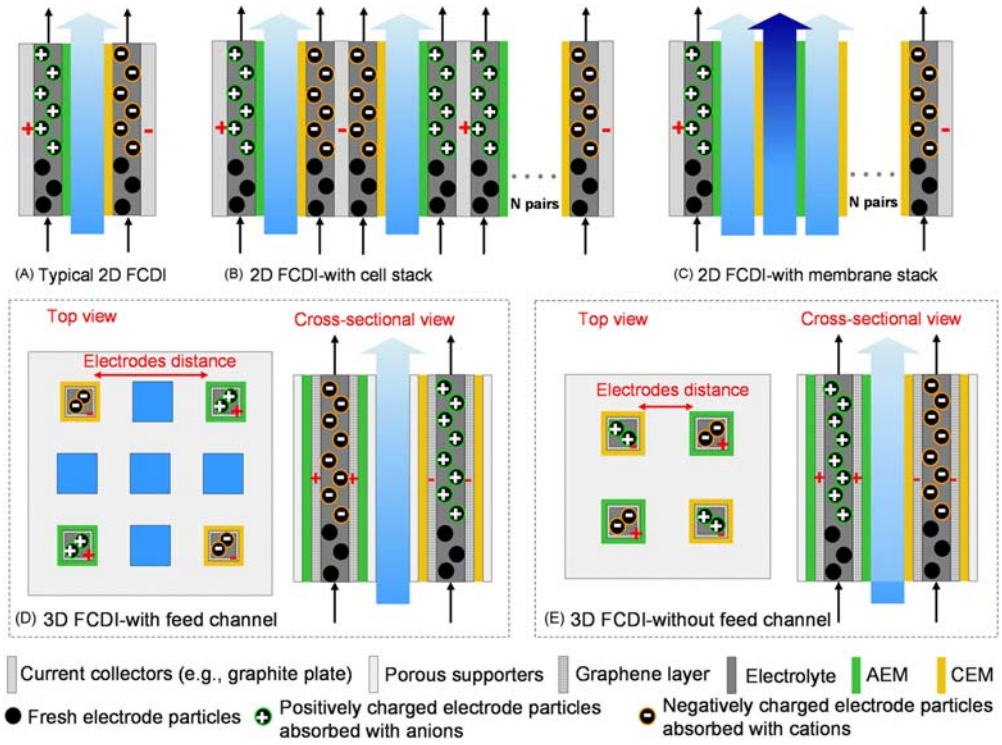

Figure 10.17 Schematic representation of various FCDI configurations: (A) typical 2D FCDI, (B) 2D FCDI with cell stack, (C) 2D FCDI with membrane stack, (D) 3D FCDI with additional feed channels, and (E) 3D FCDI without feed channels. *Reproduced with permission C. Zhang, J. Ma, L. Wu, J. Sun, L. Wang, T. Li, et al., Flow electrode capacitive deionization (FCDI): recent developments, environmental applications, and future perspectives, Environ. Sci. Technol. 55 (2021) 4243–4267 [103], copyright 2021 American Chemical Society.*

between the two current collectors, FCDI can be shown to achieve excellent water desalination performance at a reasonable energy consumption (Fig. 10.17C) [125].

Scaling-up of the 2D FCDI system, however, still represents a major challenge. To simplify the cell fabrication, Cho et al. [19] developed a 3D lattice structured FCDI device with low-cost porous cordierite with numerous hollow lattices used as the supporting substrate. The cordierite lattices were successively coated with ion exchange polymers and graphene layers with the coated lattices acting as the electrode chamber while the uncoated lattices served as the feed chamber (Fig. 10.17D). The 3D FCDI system has various advantages such as doing without expensive free-standing IEMs and current collectors, flexibility for cell design, and ease of scale-up.

One shortcoming of the 3D FCDI is the large distance between the anode and cathode chambers resulting in low ion removal efficiency. Therefore, a modified 3D FCDI configuration was developed by directly adopting the porous ceramic walls between the lattice as

This book belongs to Badji Mokhtar Annaba University Central Library Copyright Elsevier 2025

the spacers through which water flows (Fig. 10.17E) [126]. In this modified configuration, properly adjusting the permeability of the porous ceramic material will be of vital importance for ion migration and thus ion removal performance.

10.4.2.4 Operation modes

Although considerable attention has been given to the choice of FCDI components and configuration designs, selecting the appropriate operation mode is also critical for system performance [127]. A number of unique operation modes for flow-electrode management have been developed since 2013 with these classified as isolated closed-cycle (ICC), short-circuited closed-cycle (SCC), and single cycle (SC) modes (Fig. 10.18).

In the classical ICC operation, two individual slurry streams are recirculated separately in their own electrode channels and reservoirs (Fig. 10.18A) [5]. By periodically charging and discharging the cell, ion electro-adsorption and electro-desorption can be achieved, similar to the classical CDI system [28]. When introducing a secondary channel/module and manipulating the external electric circuit, the particle electrodes can be continuously regenerated enabling brine separation (Fig. 10.18B and C) [109,110,128,129], and energy recovery (Fig. 10.18D) [130].

Since electrode regeneration is complex in the ICC mode, another operation strategy termed SCC has been proposed. As illustrated in Fig. 10.18E, in the SCC mode, both anodic and cathodic particle electrodes are mixed in a shared reservoir after leaving their electrode channels, resulting in spontaneous electrode regeneration and ion desorption into the electrolyte [21,23].

The invention of the SC mode further simplified the system [131]. In this operation mode, a single closed-flow loop with slurry electrode is directly recycled from one chamber to another (Fig. 10.18F) [131]. During the operation, both adsorption and desorption occur simultaneously within the electrode chamber, leading to an efficient usage of the slurry electrodes. By introducing two water chambers (e.g., one dilute and one brine water chamber) separated by an IEM [18], the continuous operation of the FCDI system can be realized with the electrodes successfully regenerated and the removed ions accumulated in the brine chamber. By immersing a microfiltration module within the SCC/SC FCDI electrode reservoir, brine can be effectively separated from the flow-electrode, while leading to the continuous and stable running of the system [15,88].

10.4.3 Applications of flow capacitive deionization

FCDI can be applied in various areas including (1) water desalination, (2) selective resource recovery, and (3) contaminant abatement. In addition, other emerging applications (e.g., CO_2 capture and RO brine concentration) are being developed.

This book belongs to Badji Mokhtar Annaba University Central Library Copyright Elsevier 2025

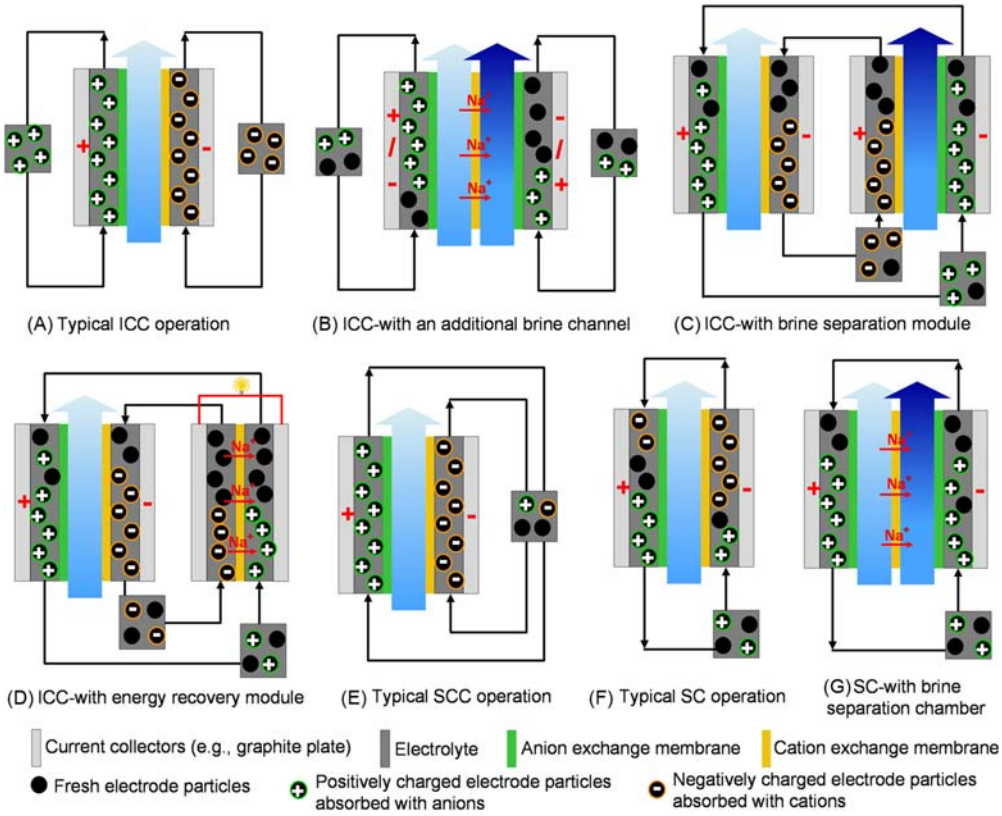

Figure 10.18 Schematic representation of (A) typical ICC FCDI, (B) symmetric ICC FCDI with an additional brine separation channel in which the two electrodes serve alternatively as anode and cathode, (C) ICC FCDI with an additional brine separation module, (D) ICC FCDI with an additional energy recovery module, (E) typical SCC FCDI, (F) typical SC FCDI, and (G) SC FCDI with an additional brine separation channel. *Reproduced with permission C. Zhang, J. Ma, L. Wu, J. Sun, L. Wang, T. Li, et al., Flow electrode capacitive deionization (FCDI): recent developments, environmental applications, and future perspectives, Environ. Sci. Technol. 55 (2021) 4243–4267 [103], copyright 2021 American Chemical Society.*

10.4.3.1 Water desalination

For FCDI, the electrodes can be easily regenerated outside the system, while enabling the desalination of higher salinity feeds [5,18–22]. It has been documented that FCDI will remove ions from high strength streams with the salt concentration close to seawater [23]. Most studies of FCDI performance, however, have been undertaken with the simple (synthetic) feed streams with most attention given to the choice of the electrode, the separator, and the spacer materials as well as the cell configuration. As such, there is a need to explore the application of FCDI for treatment of more complex real waters such as river, lakes, and ground waters.

This book belongs to Badji Mokhtar Annaba University Central Library Copyright Elsevier 2025

10.4.3.2 Resource recovery

Another important application field for FCDI is to selectively recover resources (e.g., phosphorus, ammonia, and valuable heavy metals) from waters and wastewaters. Taking advantage of the easy management of the slurry electrode, the target ions can be selectively accumulated and then separated from the electrode chamber in a continuous manner.

Nutrients such as phosphate and ammonia are present in municipal and agricultural wastewaters, and cause serious environmental problems (e.g., eutrophication) if discharged to natural water bodies. Conversely, phosphate and ammonia are valuable nutrients in relation to agricultural activities [110,129,132–134] and, therefore, nutrient recovery is of paramount importance in view of the potential environmental and economic benefits. Motivated by this idea, Fang et al. [24], on one hand, and Zhang et al. [25], on the other, employed FCDI to extract and concentrate ammonia and phosphate from synthetic wastewaters. The results revealed that ~80% of nutrient ions can be removed and accumulated in the electrode chamber. However, separation of these nutrient ions from the electrolyte remains a challenge. By integrating a gas permeable membrane (flat-sheet or hollow-fiber) with an FCDI device (Fig. 10.19A), the NH_4^+ ions transported to the cathode chamber can be converted to dissolved ammonia (due to the high local pH). In view of the volatility of ammonia, it is readily transported through the gas permeable membrane and may be captured in an acid

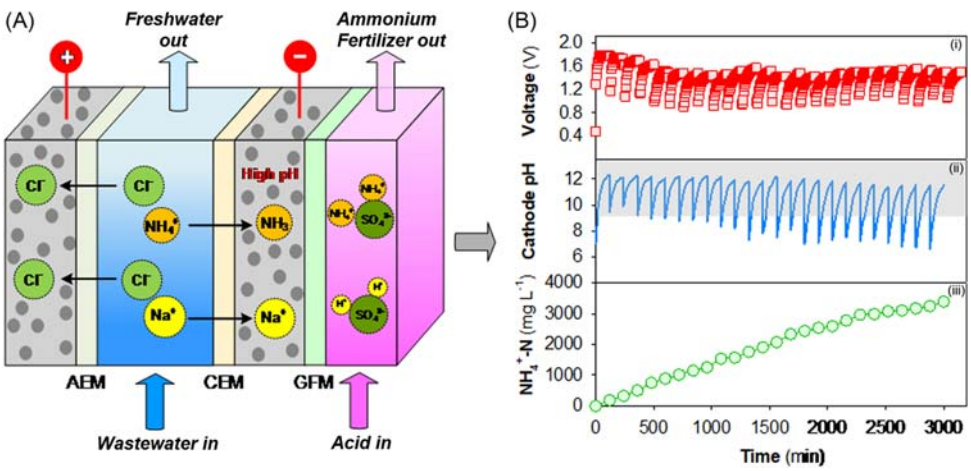

Figure 10.19 (A) Schematic representation of a four chamber ammonia recovery FCDI reactor and (B) the variations of (1) cell voltage, (2) cathode pH, and (3) ammonium concentration in the recovery chamber. *Reproduced with permission C. Zhang, J. Ma, J. Song, C. He, T.D. Waite, Continuous ammonia recovery from wastewaters using an integrated capacitive flow electrode membrane stripping system, Environ. Sci. Technol. 52 (2018) 14275–14285 [26], copyright 2018 American Chemical Society.*

This book belongs to Badji Mokhtar Annaba University Central Library Copyright Elsevier 2025

solution as ammonium salt (e.g., $(NH_4)_2SO_4$) [95,135]. Nearly 80% of NH_4^+ can be effectively recovered using the FCDI system, with the NH_4^+ being concentrated by 78-fold after 48 h continuous running (Fig. 10.19B) [26]. Phosphate (P) is another important nutrient ion that can be potentially recovered and reused as fertilizers in agricultural activities. By employing magnetic iron oxide impregnated carbon flow-electrode, P can be selectively extracted from the wastewater in a cost-effective manner. In fact, a P-rich stream was obtained on regeneration of the exhausted magnetic electrodes using an alkali solution [134].

Apart from the nutrient ions, FCDI also shows great potential in removal and recovery of other valuable resources including metals such as lithium. As one of the crucial elements for rechargeable batteries, many studies have investigated the possibility of extracting lithium from seawater or salty lakes. It has been reported that more than 85% of the lithium existing in the wastewater can be continuously recovered using FCDI, even in the presence of a wide range of background salt concentrations [27].

10.4.3.3 Contaminant abatements

Technologies capable of targeted contaminant removal from water/wastewater are desirable in achieving "fit-for-purpose" treatment. Electrochemical technologies are generally believed to be competitive, especially for selective removal of various contaminants such as heavy metals, toxic oxyanion, and organic ionic species. Provided the scale-up issue can be resolved, FCDI is expected to be superior to conventional MCDI for the removal of various target contaminants in an energy-efficient and continuous manner.

The excessive presence of hardness ions such as calcium and magnesium in water will result in severe scaling/fouling problems during water/wastewater treatment and transport [136]. It has been shown that SC FCDI could be an effective method for brackish water softening [28]. As discussed earlier, a high selectivity of divalent Ca^{2+} over monovalent Na^+ has been observed, with the selectivity factor largely dependent on the system operating parameters (e.g., current density and HRT). By using SCC operation, a stable electrolyte pH around 7 can be sustained during the continuous mixing of the anodic/cathodic particle electrodes in the shared reservoir, greatly alleviating the possibility of calcium scaling within the system. Note that CEMs play an important role for Ca^{2+} transport in the electric field, and coating particular calcium-selective layers (e.g., hydrophilic polymer film or Ca-alginate) on the electrode surface has been demonstrated to be an effective approach to facilitate the preferential removal of Ca^{2+} [52,137,138]. In recent studies, the use of FCDI in the treatment of synthetic wastewater containing high concentrations of Cu^{2+} ions had been examined, with results showing that Cu^{2+} could be selectively removed compared to Na^+, with a high Cu^{2+}/Na^+ selectivity factor of 2.8 obtained under a cell voltage of 1.2 V [29]. However, more investigations are required to verify the effectiveness and robustness of FCDI for the treatment of complex real wastewaters containing various contaminants.

This book belongs to Badji Mokhtar Annaba University Central Library Copyright Elsevier 2025

10.4.3.4 Emerging applications

With an eye to the future, we believe that there will be more innovative applications for FCDI. Some potential areas include:

1. Desalination of high-strength feed streams: This involves the integration of FCDI with traditional technologies such as RO, electrodialysis (ED), or ion exchange systems to generate high-quality ultrapure water from high salinity feed streams at lower energy consumption [20,139,140].
2. CO_2 capture: While MCDI has been demonstrated to have the potential to capture CO_2 gas without additional chemical consumption, FCDI could be even more effective given the ease of management of the slurry electrodes [141–143].
3. Dairy and beverage processing: FCDI could potentially be used in the dairy industry for applications such as milk demineralization and lactic acid separation, as well as beverage processing including vinasse demineralization and tartrate stabilization [144,145].
4. Brine concentration: Similar to ED, FCDI has also been explored for efficient brine concentration and facilitating the subsequent crystallization of minerals (e.g., P crystallization from the brine solution as vivianite) [146]. This could be a promising approach to achieving the ultimate goal of zero liquid discharge [147,148].

10.5 Challenges and perspectives

MCDI and FCDI are membrane-based electrochemical technologies that can be used for a wide range of applications. Involving the removal of ions from water by the application of an electrical potential across two static electrodes with IEMs in front of them, MCDI is a batch mode process by first creating a product stream and then creating a brine stream. The system works well for water desalination of brackish waters, treated domestic wastewaters, and industrial wastewaters. While the system can be modified to enable ion selectivity through operational adjustments or IEM selection, still the fact remains that the overall cost of water production is similar to other desalination technologies for treatment of brackish water ($< \sim 4$ g/L), especially when considering the use of renewable energy to power the system. Due to the low voltage requirements, MCDI can be easily coupled to photovoltaics.

Challenges for MCDI include:

- Operational longevity: There are only a few published studies in which results of long term trials are presented. In most cases, however, it has been reported that electrode fouling and scaling are minor issues and, if problematic, can be reversed with an appropriate cleaning solution.
- Energy consumption with high influent salinity: The energy consumption of MCDI becomes higher than other desalination technologies when the influent salinity is higher than ~ 4 g/L.

This book belongs to Badji Mokhtar Annaba University Central Library Copyright Elsevier 2025

- Scalability to large applications: While the results of relatively small sized field trials are typically reported in the literature, a number of companies (including Voltea and EST Water and Technologies Company) have successfully commercialized MCDI with many reports of large scale industrial applications [4,149].
- Monovalent ion selectivity: Typically, MCDI will select for divalent ions; whereas, for many applications such as agriculture, monovalent ions are required to be removed preferentially.
- Resource recovery: Whilst many nutrients are separated during the MCDI process, there is still considerable work to be done on the recovery of nutrients so that they are available for reuse.
- Limited salt removal capacity: For scenarios with a high salt removal requirement a multi-pass system of MCDI would be required. This significantly increases both the operational and capital expenditure.

FCDI involves the removal of ions from water by the application of an electrical potential across a large number of flowing electrodes, typically AC. It is a continuous process with the electrodes being constantly regenerated, and a product and brine stream constantly being generated. With much recent work having been focused on optimizing the design and operation of the system, FCDI is well suited to desalination of higher salinity influent, resource recovery, and contaminant abatement. Due to the constant regeneration process, FCDI is a more efficient process that CDI.

Challenges for FCDI include:

- Non-synthetic test waters: Typically, trials are run in the laboratory with model feed streams rather than actual groundwater or wastewater. Gaining a better understanding of the influence of mixed solutions on FCDI performance is essential.
- Operational longevity: Current trials have typically been limited to short duration laboratory studies.
- Scalability: Current trials have been limited to small scale laboratory units with some work being done on scale up.
- Resource recovery: Much like MCDI, in FCDI, there is still considerable work to be done on the recovery of nutrients such that the products are available for reuse.

Despite there being several challenges for MCDI and FCDI desalination, the technologies, both, hold promise as viable water treatment technologies of the future. The relatively low energy requirements of both technologies and the ability to being easily coupled to photovoltaics suggest their suitability for inland and remote applications. The ability for ion selectivity make the technologies very useful for a range of applications. There have been many field trials of small to medium sized pilot scale MCDI units, though challenges in scale-up of FCDI to comparable size represents a major limitation to proper assessment of the viability of this interesting technology.

This book belongs to Badji Mokhtar Annaba University Central Library Copyright Elsevier 2025

References

[1] P.M. Biesheuvel, R. Zhao, S. Porada, A. van der Wal, Theory of membrane capacitive deionization including the effect of the electrode pore space, J. Colloid Interface Sci. 360 (2011) 239–248.

[2] J.W. Blair, G.W. Murphy, Electrochemical Demineralization of Water With Porous Electrodes of Large Surface Area, ACS Publications, 1960.

[3] S. Porada, R. Zhao, A. van der Wal, V. Presser, P. Biesheuvel, Review on the science and technology of water desalination by capacitive deionization, Prog. Mater. Sci. 58 (2013) 1388–1442.

[4] M. Suss, S. Porada, X. Sun, P. Biesheuvel, J. Yoon, V. Presser, Water desalination via capacitive deionization: what is it and what can we expect from it? Energy Environ. Sci. 8 (2015) 2296–2319.

[5] S.-i. Jeon, H.-r. Park, J.-g. Yeo, S. Yang, C.H. Cho, M.H. Han, et al., Desalination via a new membrane capacitive deionization process utilizing flow-electrodes, Energy Environ. Sci. 6 (2013) 1471–1475.

[6] J.-B. Lee, K.-K. Park, H.-M. Eum, C.-W. Lee, Desalination of a thermal power plant wastewater by membrane capacitive deionization, Desalination 196 (2006) 125–134.

[7] D.I. Kim, P. Dorji, G. Gwak, S. Phuntsho, S. Hong, H. Shon, Reuse of municipal wastewater via membrane capacitive deionization using ion-selective polymer-coated carbon electrodes in pilot-scale, Chem. Eng. J. 372 (2019) 241–250.

[8] R. Zhao, P. Biesheuvel, A. van der Wal, Energy consumption and constant current operation in membrane capacitive deionization, Energy Environ. Sci. 5 (2012) 9520–9527.

[9] A. Hassanvand, G. Chen, P. Webley, S. Kentish, An investigation of the impact of fouling agents in capacitive and membrane capacitive deionisation, Desalination 457 (2019) 96–102.

[10] R. Zhao, S. Porada, P. Biesheuvel, A. van der Wal, Energy consumption in membrane capacitive deionization for different water recoveries and flow rates, and comparison with reverse osmosis, Desalination 330 (2013) 35–41.

[11] W. Zhang, M. Mossad, L. Zou, A study of the long-term operation of capacitive deionisation in inland brackish water desalination, Desalination 320 (2013) 80–85.

[12] B. van Limpt, A. van der Wal, Water and chemical savings in cooling towers by using membrane capacitive deionization, Desalination 342 (2014) 148–155.

[13] M. Lee, C.-S. Fan, Y.-W. Chen, K.-C. Chang, P.-T. Chiueh, C.-H. Hou, Membrane capacitive deionization for low-salinity desalination in the reclamation of domestic wastewater effluents, Chemosphere 235 (2019) 413–422.

[14] Y.-Y. Shen, S.-H. Sun, S.-W. Tsai, T.-H. Chen, C.-H. Hou, Development of a membrane capacitive deionization stack for domestic wastewater reclamation: a pilot-scale feasibility study, Desalination 500 (2021) 114851.

[15] C. Zhang, L. Wu, J. Ma, A.N. Pham, M. Wang, T.D. Waite, Integrated flow-electrode capacitive deionization and microfiltration system for continuous and energy-efficient brackish water desalination, Environ. Sci. Technol. 53 (2019) 13364–13373.

[16] G.J. Doornbusch, J.E. Dykstra, P.M. Biesheuvel, M.E. Suss, Fluidized bed electrodes with high carbon loading for water desalination by capacitive deionization, J. Mater. Chem. A 4 (2016) 3642–3647.

[17] Y. Gendel, A.K.E. Rommerskirchen, O. David, M. Wessling, Batch mode and continuous desalination of water using flowing carbon deionization (FCDI) technology, Electrochem. Commun. 46 (2014) 152–156.

[18] A. Rommerskirchen, Y. Gendel, M. Wessling, Single module flow-electrode capacitive deionization for continuous water desalination, Electrochem. Commun. 60 (2015) 34–37.

[19] Y. Cho, K.S. Lee, S. Yang, J. Choi, H.-r Park, D.K. Kim, A novel three-dimensional desalination system utilizing honeycomb-shaped lattice structures for flow-electrode capacitive deionization, Energy Environ. Sci. 10 (2017) 1746–1750.

[20] H.J. Chung, J. Kim, D.I. Kim, G. Gwak, S. Hong, Feasibility study of reverse osmosis–flow capacitive deionization (RO-FCDI) for energy-efficient desalination using seawater as the flow-electrode aqueous electrolyte, Desalination 479 (2020) 114326.

[21] S. Yang, H. Kim, S.-i Jeon, J. Choi, J.-g Yeo, H.-r Park, et al., Analysis of the desalting performance of flow-electrode capacitive deionization under short-circuited closed cycle operation, Desalination 424 (2017) 110–121.

This book belongs to Badji Mokhtar Annaba University Central Library

Copyright Elsevier 2025

[22] H.-r Park, J. Choi, S. Yang, S.J. Kwak, S.-i Jeon, M.H. Han, et al., Surface-modified spherical activated carbon for high carbon loading and its desalting performance in flow-electrode capacitive deionization, RSC Adv. 6 (2016) 69720–69727.
[23] S.-i Jeon, J.-g Yeo, S. Yang, J. Choi, D.K. Kim, Ion storage and energy recovery of a flow-electrode capacitive deionization process, J. Mater. Chem. A 2 (2014) 6378.
[24] K. Fang, H. Gong, W. He, F. Peng, C. He, K. Wang, Recovering ammonia from municipal wastewater by flow-electrode capacitive deionization, Chem. Eng. J. 348 (2018) 301–309.
[25] J. Zhang, L. Tang, W. Tang, Y. Zhong, K. Luo, M. Duan, et al., Removal and recovery of phosphorus from low-strength wastewaters by flow-electrode capacitive deionization, Sep. Purif. Technol. 237 (2020) 116322.
[26] C. Zhang, J. Ma, J. Song, C. He, T.D. Waite, Continuous ammonia recovery from wastewaters using an integrated capacitive flow electrode membrane stripping system, Environ. Sci. Technol. 52 (2018) 14275–14285.
[27] Y. Ha, H.B. Jung, H. Lim, P.S. Jo, H. Yoon, C.-Y. Yoo, et al., Continuous lithium extraction from aqueous solution using flow-electrode capacitive deionization, Energies 12 (2019) 2913.
[28] C. He, J. Ma, C. Zhang, J. Song, T.D. Waite, Short-circuited closed-cycle operation of flow-electrode CDI for brackish water softening, Environ. Sci. Technol. 52 (2018) 9350–9360.
[29] X. Zhang, F. Yang, J. Ma, P. Liang, Effective removal and selective capture of copper from salty solution in flow electrode capacitive deionization, Environ. Sci. Water Res. Technol. 6 (2020) 341–350.
[30] J. Ma, Y. Zhang, R.N. Collins, S. Tsarev, N. Aoyagi, A.S. Kinsela, et al., Flow-electrode CDI removes the uncharged Ca–UO2–CO3 ternary complex from brackish potable groundwater: complex dissociation, transport, and sorption, Environ. Sci. Technol. 53 (2019) 2739–2747.
[31] Y.-J. Kim, J.-H. Choi, Enhanced desalination efficiency in capacitive deionization with an ion-selective membrane, Sep. Purif. Technol. 71 (2010) 70–75.
[32] Y.-J. Kim, J.-H. Kim, J.-H. Choi, Selective removal of nitrate ions by controlling the applied current in membrane capacitive deionization (MCDI), J. Membr. Sci. 429 (2013) 52–57.
[33] J.-H. Lee, J.-H. Choi, The production of ultrapure water by membrane capacitive deionization (MCDI) technology, J. Membr. Sci. 409 (2012) 251–256.
[34] L. Wang, S. Lin, Intrinsic tradeoff between kinetic and energetic efficiencies in membrane capacitive deionization, Water Res. 129 (2018) 394–401.
[35] P. Biesheuvel, A. van der Wal, Membrane capacitive deionization, J. Membr. Sci. 346 (2010) 256–262.
[36] R. Zhao, O. Satpradit, H. Rijnaarts, P. Biesheuvel, A. van der Wal, Optimization of salt adsorption rate in membrane capacitive deionization, Water Res. 47 (2013) 1941–1952.
[37] J.-Y. Lee, S.-J. Seo, S.-H. Yun, S.-H. Moon, Preparation of ion exchanger layered electrodes for advanced membrane capacitive deionization (MCDI), Water Res. 45 (2011) 5375–5380.
[38] M. Tian, Y. Sun, C. Zhang, J. Wang, W. Qiao, L. Ling, et al., Enabling high-rate electrochemical flow capacitors based on mesoporous carbon microspheres suspension electrodes, J. Power Sources 364 (2017) 182–190.
[39] P. Liang, L. Yuan, X. Yang, S. Zhou, X. Huang, Coupling ion-exchangers with inexpensive activated carbon fiber electrodes to enhance the performance of capacitive deionization cells for domestic wastewater desalination, Water Res. 47 (2013) 2523–2530.
[40] I. Cohen, E. Avraham, M. Noked, A. Soffer, D. Aurbach, Enhanced charge efficiency in capacitive deionization achieved by surface-treated electrodes and by means of a third electrode, J. Phys. Chem. C 115 (2011) 19856–19863.
[41] Y. Cho, C.Y. Yoo, S.W. Lee, H. Yoon, K.S. Lee, S. Yang, et al., Flow-electrode capacitive deionization with highly enhanced salt removal performance utilizing high-aspect ratio functionalized carbon nanotubes, Water Res. 151 (2019) 252–259.
[42] Y. Cai, X. Zhao, Y. Wang, D. Ma, S. Xu, Enhanced desalination performance utilizing sulfonated carbon nanotube in the flow-electrode capacitive deionization process, Sep. Purif. Technol. 237 (2020) 116381.
[43] S. Sasi, A. Murali, S.V. Nair, A.S. Nair, K.R.V. Subramanian, The effect of graphene on the performance of an electrochemical flow capacitor, J. Mater. Chem. A 3 (2015) 2717–2725.

This book belongs to Badji Mokhtar Annaba University Central Library Copyright Elsevier 2025

[44] K. Tang, S. Yiacoumi, Y. Li, C. Tsouris, Enhanced water desalination by increasing the electroconductivity of carbon powders for high-performance flow-electrode capacitive deionization, ACS Sustain. Chem. Eng. 7 (2018) 1085–1094.
[45] Y. Liu, L. Pan, X. Xu, T. Lu, Z. Sun, D.H. Chua, Enhanced desalination efficiency in modified membrane capacitive deionization by introducing ion-exchange polymers in carbon nanotubes electrodes, Electrochim. Acta 130 (2014) 619–624.
[46] P. Liu, H. Wang, T. Yan, J. Zhang, L. Shi, D. Zhang, Grafting sulfonic and amine functional groups on 3D graphene for improved capacitive deionization, J. Mater. Chem. A 4 (2016) 5303–5313.
[47] X. Gu, Y. Yang, Y. Hu, M. Hu, C. Wang, Fabrication of graphene-based xerogels for removal of heavy metal ions and capacitive deionization, ACS Sustain. Chem. Eng. 3 (2015) 1056–1065.
[48] A. Omosebi, X. Gao, J. Rentschler, J. Landon, K. Liu, Continuous operation of membrane capacitive deionization cells assembled with dissimilar potential of zero charge electrode pairs, J. Colloid Interface Sci. 446 (2015) 345–351.
[49] K.S. Lee, Y. Cho, K.Y. Choo, S. Yang, M.H. Han, D.K. Kim, Membrane-spacer assembly for flow-electrode capacitive deionization, Appl. Surf. Sci. 433 (2018) 437–442.
[50] C.J. Linnartz, A. Rommerskirchen, J. Walker, J. Plankermann-Hajduk, N. Köller, M. Wessling, Membrane-electrode assemblies for flow-electrode capacitive deionization, J. Membr. Sci. 605 (2020) 118095.
[51] F. Yang, J. Ma, X. Zhang, X. Huang, P. Liang, Decreased charge transport distance by titanium mesh-membrane assembly for flow-electrode capacitive deionization with high desalination performance, Water Res. 164 (2019) 114904.
[52] T. Luo, S. Abdu, M. Wessling, Selectivity of ion exchange membranes: a review, J. Membr. Sci. 555 (2018) 429–454.
[53] A. Hassanvand, K. Wei, S. Talebi, G.Q. Chen, S.E. Kentish, The role of ion exchange membranes in membrane capacitive deionisation, Membranes 7 (2017) 54.
[54] A. Hassanvand, G.Q. Chen, P.A. Webley, S.E. Kentish, A comparison of multicomponent electrosorption in capacitive deionization and membrane capacitive deionization, Water Res. 131 (2018) 100–109.
[55] S.A. Hawks, A. Ramachandran, S. Porada, P.G. Campbell, M.E. Suss, P. Biesheuvel, et al., Performance metrics for the objective assessment of capacitive deionization systems, Water Res. 152 (2019) 126–137.
[56] M.A. Anderson, A.L. Cudero, J. Palma, Capacitive deionization as an electrochemical means of saving energy and delivering clean water. Comparison to present desalination practices: will it compete? Electrochim. Acta 55 (2010) 3845–3856.
[57] L. Wang, S. Lin, Theoretical framework for designing a desalination plant based on membrane capacitive deionization, Water Res. 158 (2019) 359–369.
[58] C. Tan, C. He, J. Fletcher, T.D. Waite, Energy recovery in pilot scale membrane CDI treatment of brackish waters, Water Res. 168 (2020) 115146.
[59] S. Porada, L. Zhang, J. Dykstra, Energy consumption in membrane capacitive deionization and comparison with reverse osmosis, Desalination 488 (2020) 114383.
[60] P. Długołęcki, A. van der Wal, Energy recovery in membrane capacitive deionization, Environ. Sci. Technol. 47 (2013) 4904–4910.
[61] J. Kang, T. Kim, H. Shin, J. Lee, J.-I. Ha, J. Yoon, Direct energy recovery system for membrane capacitive deionization, Desalination 398 (2016) 144–150.
[62] M. Qin, A. Deshmukh, R. Epsztein, S.K. Patel, O.M. Owoseni, W.S. Walker, et al., Comparison of energy consumption in desalination by capacitive deionization and reverse osmosis, Desalination 455 (2019) 100–114.
[63] S.K. Patel, M. Qin, W.S. Walker, M. Elimelech, Energy efficiency of electro-driven brackish water desalination: electrodialysis significantly outperforms membrane capacitive deionization, Environ. Sci. Technol. 54 (2020) 3663–3677.
[64] S.-Y. Pan, A.Z. Haddad, A. Kumar, S.-W. Wang, Brackish water desalination using reverse osmosis and capacitive deionization at the water-energy nexus, Water Res. (2020) 116064.
[65] P. Sharan, T.J. Yoon, S.M. Jaffe, T. Ju, R.P. Currier, A.T. Findikoglu, Can capacitive deionization outperform reverse osmosis for brackish water desalination? Clean. Eng. Technol. (2021) 100102.

This book belongs to Badji Mokhtar Annaba University Central Library Copyright Elsevier 2025

[66] W. Zhang, M. Mossad, J.S. Yazdi, L. Zou, A statistical experimental investigation on arsenic removal using capacitive deionization, Desalin. Water Treat. 57 (2016) 3254–3260.
[67] C. Tan, C. He, W. Tang, P. Kovalsky, J. Fletcher, T.D. Waite, Integration of photovoltaic energy supply with membrane capacitive deionization (MCDI) for salt removal from brackish waters, Water Res. 147 (2018) 276–286.
[68] C. Bales, B. Lian, J. Fletcher, Y. Wang, T.D. Waite, Site specific assessment of the viability of membrane Capacitive Deionization (mCDI) in desalination of brackish groundwaters for selected crop watering, Desalination 502 (2021) 114913.
[69] A. Al-Karaghouli, L.L. Kazmerski, Energy consumption and water production cost of conventional and renewable-energy-powered desalination processes, Renew. Sustain. Energy Rev. 24 (2013) 343–356.
[70] C. Fernandez-Gonzalez, A. Dominguez-Ramos, R. Ibañez, A. Irabien, Sustainability assessment of electrodialysis powered by photovoltaic solar energy for freshwater production, Renew. Sustain. Energy Rev. 47 (2015) 604–615.
[71] A. Ramachandran, D.I. Oyarzun, S.A. Hawks, M. Stadermann, J.G. Santiago, High water recovery and improved thermodynamic efficiency for capacitive deionization using variable flowrate operation, Water Res. 155 (2019) 76–85.
[72] L. Wang, S. Lin, Mechanism of selective ion removal in membrane capacitive deionization for water softening, Environ. Sci. Technol. 53 (2019) 5797–5804.
[73] R. Zhao, M. van Soestbergen, H. Rijnaarts, A. van der Wal, M. Bazant, P. Biesheuvel, Time-dependent ion selectivity in capacitive charging of porous electrodes, J. Colloid Interface Sci. 384 (2012) 38–44.
[74] S.-W. Tsai, L. Hackl, A. Kumar, C.-H. Hou, Exploring the electrosorption selectivity of nitrate over chloride in capacitive deionization (CDI) and membrane capacitive deionization (MCDI), Desalination 497 (2021) 114764.
[75] X. Zhang, K. Zuo, X. Zhang, C. Zhang, P. Liang, Selective ion separation by capacitive deionization (CDI) based technologies: a state-of-the-art review, Environ. Sci. Water Res. Technol. 6 (2020) 243–257.
[76] W. Tang, D. He, C. Zhang, T.D. Waite, Optimization of sulfate removal from brackish water by membrane capacitive deionization (MCDI), Water Res. 121 (2017) 302–310.
[77] X. Huang, D. He, W. Tang, P. Kovalsky, T.D. Waite, Investigation of pH-dependent phosphate removal from wastewaters by membrane capacitive deionization (MCDI), Environ. Sci. Water Res. Technol. 3 (2017) 875–882.
[78] E.N. Guyes, A.N. Shocron, Y. Chen, C.E. Diesendruck, M.E. Suss, Long-lasting, monovalent-selective capacitive deionization electrodes, npj Clean Water 4 (2021) 1–11.
[79] J. Jiang, D.I. Kim, P. Dorji, S. Phuntsho, S. Hong, H.K. Shon, Phosphorus removal mechanisms from domestic wastewater by membrane capacitive deionization and system optimization for enhanced phosphate removal, Process. Saf. Environ. Prot. 126 (2019) 44–52.
[80] S. Hand, J.S. Guest, R.D. Cusick, Technoeconomic analysis of brackish water capacitive deionization: navigating tradeoffs between performance, lifetime, and material costs, Environ. Sci. Technol. 53 (2019) 13353–13363.
[81] L. Chen, C. Wang, S. Liu, Q. Hu, L. Zhu, C. Cao, Investigation of the long-term desalination performance of membrane capacitive deionization at the presence of organic foulants, Chemosphere 193 (2018) 989–997.
[82] C. Bales, P. Kovalsky, J. Fletcher, T.D. Waite, Low cost desalination of brackish groundwaters by capacitive deionization (CDI)–implications for irrigated agriculture, Desalination 453 (2019) 37–53.
[83] J. Ma, C. He, D. He, C. Zhang, T.D. Waite, Analysis of capacitive and electrodialytic contributions to water desalination by flow-electrode CDI, Water Res. 144 (2018) 296–303.
[84] P. Nativ, Y. Badash, Y. Gendel, New insights into the mechanism of flow-electrode capacitive deionization, Electrochem. Commun. (2017).
[85] Y. Bian, X. Chen, L. Lu, P. Liang, Z.J. Ren, Concurrent nitrogen and phosphorus recovery using flow-electrode capacitive deionization, ACS Sustain. Chem. Eng. 7 (2019) 7844–7850.

This book belongs to Badji Mokhtar Annaba University Central Library Copyright Elsevier 2025

[86] J. Song, J. Ma, C. Zhang, C. He, T.D. Waite, Implication of non-electrostatic contribution to deionization in flow-electrode CDI: case study of nitrate removal from contaminated source waters, Front. Chem. 7 (2019).
[87] C.J. Linnartz, A. Rommerskirchen, M. Wessling, Y. Gendel, Flow-electrode capacitive deionization for double displacement reactions, ACS Sustain. Chem. Eng. 5 (2017) 3906−3912.
[88] C. Zhang, L. Wu, J. Ma, M. Wang, J. Sun, T.D. Waite, Evaluation of long-term performance of a continuously operated flow-electrode CDI system for salt removal from brackish waters, Water Res. 173 (2020) 115580.
[89] J. Ma, D. He, W. Tang, P. Kovalsky, C. He, C. Zhang, et al., Development of redox-active flow electrodes for high-performance capacitive deionization, Environ. Sci. Technol. 50 (2016) 13495−13501.
[90] X. Xu, M. Wang, Y. Liu, T. Lu, L. Pan, Ultrahigh desalinization performance of asymmetric flow-electrode capacitive deionization device with an improved operation voltage of 1.8 V, ACS Sustain. Chem. Eng. 5 (2016) 189−195.
[91] K.B. Hatzell, M.C. Hatzell, K.M. Cook, M. Boota, G.M. Housel, A. McBride, et al., Effect of oxidation of carbon material on suspension electrodes for flow electrode capacitive deionization, Environ. Sci. Technol. 49 (2015) 3040−3047.
[92] P. Liang, X. Sun, Y. Bian, H. Zhang, X. Yang, Y. Jiang, et al., Optimized desalination performance of high voltage flow-electrode capacitive deionization by adding carbon black in flow-electrode, Desalination 420 (2017) 63−69.
[93] S. Yang, H.-r Park, J. Yoo, H. Kim, J. Choi, M.H. Han, et al., Plate-shaped graphite for improved performance of flow-electrode capacitive deionization, J. Electrochem. Soc. 164 (2017) E480−E488.
[94] S. Yang, J. Choi, J.G. Yeo, S.I. Jeon, H.R. Park, D.K. Kim, Flow-electrode capacitive deionization using an aqueous electrolyte with a high salt concentration, Environ. Sci. Technol. 50 (2016) 5892−5899.
[95] C. Zhang, J. Ma, D. He, T.D. Waite, Capacitive membrane stripping for ammonia recovery (CapAmm) from dilute wastewaters, Environ. Sci. Technol. Lett. 5 (2017) 43−49.
[96] J. Ma, Y. Zhang, R.N. Collins, et al., CDI removes the uncharged Ca-UO_2-CO_3 ternary complex from brackish potable groundwater: complex dissociation, transport, and sorption, Environ. Sci. Technol. 53 (2019) 2739−2747.
[97] K.B. Hatzell, L. Fan, M. Beidaghi, M. Boota, E. Pomerantseva, E.C. Kumbur, et al., Composite manganese oxide percolating networks as a suspension electrode for an asymmetric flow capacitor, ACS Appl. Mater. Interfaces 6 (2014) 8886−8893.
[98] J.W. Campos, M. Beidaghi, K.B. Hatzell, C.R. Dennison, B. Musci, V. Presser, et al., Investigation of carbon materials for use as a flowable electrode in electrochemical flow capacitors, Electrochim. Acta 98 (2013) 123−130.
[99] K.B. Hatzell, M. Beidaghi, J.W. Campos, C.R. Dennison, E.C. Kumbur, Y. Gogotsi, A high performance pseudocapacitive suspension electrode for the electrochemical flow capacitor, Electrochim. Acta 111 (2013) 888−897.
[100] M.C. Hatzell, K.B. Hatzell, B.E. Logan, Using flow electrodes in multiple reactors in series for continuous energy generation from capacitive mixing, Environ. Sci. Technol. Lett. 1 (2014) 474−478.
[101] S. Porada, D. Weingarth, H.V.M. Hamelers, M. Bryjak, V. Presser, P.M. Biesheuvel, Carbon flow electrodes for continuous operation of capacitive deionization and capacitive mixing energy generation, J. Mater. Chem. A 2 (2014) 9313.
[102] F. Liu, O. Coronell, D.F. Call, Electricity generation using continuously recirculated flow electrodes in reverse electrodialysis, J. Power Sources 355 (2017) 206−210.
[103] C. Zhang, J. Ma, L. Wu, J. Sun, L. Wang, T. Li, et al., Flow electrode capacitive deionization (FCDI): recent developments, environmental applications, and future perspectives, Environ. Sci. Technol. 55 (2021) 4243−4267.
[104] M. Seredych, D. Hulicova-Jurcakova, G.Q. Lu, T.J. Bandosz, Surface functional groups of carbons and the effects of their chemical character, density and accessibility to ions on electrochemical performance, Carbon 46 (2008) 1475−1488.

This book belongs to Badji Mokhtar Annaba University Central Library Copyright Elsevier 2025

[105] D. Li, X.-A. Ning, C. Yang, X. Chen, Y. Wang, Rich heteroatom doping magnetic carbon electrode for flow-capacitive deionization with enhanced salt removal ability, Desalination 482 (2020) 114374.
[106] K. Singh, S. Porada, H.D. de Gier, P.M. Biesheuvel, L.C.P.M. de Smet, Timeline on the application of intercalation materials in capacitive deionization, Desalination 455 (2019) 115–134.
[107] P. Srimuk, X. Su, J. Yoon, D. Aurbach, V. Presser, Charge-transfer materials for electrochemical water desalination, ion separation and the recovery of elements, Nat. Rev. Mater. (2020).
[108] M. Metzger, M.M. Besli, S. Kuppan, S. Hellstrom, S. Kim, E. Sebti, et al., Techno-economic analysis of capacitive and intercalative water deionization, Energy Environ. Sci. (2020).
[109] T. Kim, C.A. Gorski, B.E. Logan, Low energy desalination using battery electrode deionization, Environ. Sci. Technol. Lett. 4 (2017) 444–449.
[110] M. Son, B.L. Aronson, W. Yang, C.A. Gorski, B.E. Logan, Recovery of ammonium and phosphate using battery deionization in a background electrolyte, Environ. Sci. Water Res. Technol. (2020).
[111] H. Liu, K. Zhao, Asymmetric flow electrochemical capacitor with high energy densities based on birnessite-type manganese oxide nanosheets and activated carbon slurries, J. Mater. Sci. 51 (2016) 9306–9313.
[112] B. Kastening, W. Schiel, M. Henschel, Electrochemical polarization of activated carbon and graphite powder suspensions: Part I. Capacity of suspensions and polarization dynamics, J. Electroanal. Chem. Interfacial Electrochem. 191 (1985) 311–328.
[113] B. Marinho, M. Ghislandi, E. Tkalya, C.E. Koning, G. de With, Electrical conductivity of compacts of graphene, multi-wall carbon nanotubes, carbon black, and graphite powder, Powder Technol. 221 (2012) 351–358.
[114] B. Akuzum, P. Singh, D.A. Eichfeld, L. Agartan, S. Uzun, Y. Gogotsi, et al., Percolation characteristics of conductive additives for capacitive flowable (semi-solid) electrodes, ACS Appl. Mater. Interfaces 12 (2020) 5866–5875.
[115] G. Hwang, A. Gomez-Flores, S.A. Bradford, S. Choi, E. Jo, S.B. Kim, et al., Analysis of stability behavior of carbon black nanoparticles in ecotoxicological media: hydrophobic and steric effects, Colloids Surf. A: Physicochem. Eng. Asp. 554 (2018) 306–316.
[116] N.J. Ke, S.-S. Lu, S.-H. Cheng, A strategy for the determination of dopamine at a bare glassy carbon electrode: p-phenylenediamine as a nucleophile, Electrochem. Commun. 8 (2006) 1514–1520.
[117] Y. Chung, K.H. Hyun, Y. Kwon, Fabrication of a biofuel cell improved by the π-conjugated electron pathway effect induced from a new enzyme catalyst employing terephthalaldehyde, Nanoscale 8 (2016) 1161–1168.
[118] N. Song, C.J. Gagliardi, R.A. Binstead, M.-T. Zhang, H. Thorp, T.J. Meyer, Role of proton-coupled electron transfer in the redox interconversion between benzoquinone and hydroquinone, J. Am. Chem. Soc. 134 (2012) 18538–18541.
[119] Q. Wei, Y. Hu, J. Wang, Q. Ru, X. Hou, L. Zhao, et al., Low energy consumption flow capacitive deionization with a combination of redox couples and carbon slurry, Carbon 170 (2020) 487–492.
[120] N.A. Thu Tran, N.M. Phuoc, H. Yoon, E. Jung, Y.-W. Lee, B.-G. Kang, et al., Improved desalination performance of flow- and fixed-capacitive deionization using redox-active quinone, ACS Sustain. Chem. Eng. 8 (2020) 16701–16710.
[121] C.R. Dennison, M. Beidaghi, K.B. Hatzell, J.W. Campos, Y. Gogotsi, E.C. Kumbur, Effects of flow cell design on charge percolation and storage in the carbon slurry electrodes of electrochemical flow capacitors, J. Power Sources 247 (2014) 489–496.
[122] D. Moreno, M.C. Hatzell, Influence of feed-electrode concentration differences in flow-electrode systems for capacitive deionization, Ind. Eng. Chem. Res. 57 (2018) 8802–8809.
[123] D.A. Vermaas, M. Saakes, K. Nijmeijer, Enhanced mixing in the diffusive boundary layer for energy generation in reverse electrodialysis, J. Membr. Sci. 453 (2014) 312–319.
[124] S. Yang, S.-i Jeon, H. Kim, J. Choi, J.-g Yeo, H.-r Park, et al., Stack design and operation for scaling up the capacity of flow-electrode capacitive deionization technology, ACS Sustain. Chem. Eng. 4 (2016) 4174–4180.
[125] J. Ma, J. Ma, C. Zhang, J. Song, W. Dong, T.D. Waite, Flow-electrode capacitive deionization (FCDI) scale-up using a membrane stack configuration, Water Res. 168 (2020) 115186.

This book belongs to Badji Mokhtar Annaba University Central Library Copyright Elsevier 2025

[126] K.Y. Choo, K.S. Lee, M.H. Han, D.K. Kim, Study on the electrochemical characteristics of porous ceramic spacers in a capacitive deionization cell using slurry electrodes, J. Electroanal. Chem. 835 (2019) 262–272.
[127] K. Luo, Q. Niu, Y. Zhu, B. Song, G. Zeng, W. Tang, et al., Desalination behavior and performance of flow-electrode capacitive deionization under various operational modes, Chem. Eng. J. 389 (2020) 124051.
[128] A. Rommerskirchen, C.J. Linnartz, D. Müller, L.K. Willenberg, M. Wessling, Energy recovery and process design in continuous flow–electrode capacitive deionization processes, ACS Sustain. Chem. Eng. 6 (2018) 13007–13015.
[129] T. Kim, C.A. Gorski, B.E. Logan, Ammonium removal from domestic wastewater using selective battery electrodes, Environ. Sci. Technol. Lett. 5 (2018) 578–583.
[130] J. Ma, P. Liang, X. Sun, H. Zhang, Y. Bian, F. Yang, et al., Energy recovery from the flow-electrode capacitive deionization, J. Power Sources 421 (2019) 50–55.
[131] J. Ma, C. Zhang, F. Yang, X. Zhang, M.E. Suss, X. Huang, et al., Carbon black flow electrode enhanced electrochemical desalination using single-cycle operation, Environ. Sci. Technol. 54 (2020) 1177–1185.
[132] R. Broséus, J. Cigana, B. Barbeau, C. Daines-Martinez, H. Suty, Removal of total dissolved solids, nitrates and ammonium ions from drinking water using charge-barrier capacitive deionisation, Desalination 249 (2009) 217–223.
[133] A. Epshtein, O. Nir, L. Monat, Y. Gendel, Treatment of acidic wastewater via fluoride ions removal by SiO_2 particles followed by phosphate ions recovery using flow-electrode capacitive deionization, Chem. Eng. J. (2020) 125892.
[134] C. Zhang, M. Wang, W. Xiao, J. Ma, J. Sun, H. Mo, et al., Phosphate selective recovery by magnetic iron oxide impregnated carbon flow-electrode capacitive deionization (FCDI), Water Res. 189 (2021) 116653.
[135] C. Zhang, J. Ma, T.D. Waite, The impact of absorbents on ammonia recovery in a capacitive membrane stripping system, Chem. Eng. J. 382 (2020) 122851.
[136] M. Ahn, R. Chilakala, C. Han, T. Thenepalli, Removal of hardness from water samples by a carbonation process with a closed pressure reactor, Water 10 (2018) 54.
[137] H. Yoon, J. Lee, S.-R. Kim, J. Kang, S. Kim, C. Kim, et al., Capacitive deionization with Ca-alginate coated-carbon electrode for hardness control, Desalination 392 (2016) 46–53.
[138] J. Kim, A. Jain, K. Zuo, R. Verduzco, S. Walker, M. Elimelech, et al., Removal of calcium ions from water by selective electrosorption using target-ion specific nanocomposite electrode, Water Res. 160 (2019) 445–453.
[139] D.A. Vermaas, S. Bajracharya, B.B. Sales, M. Saakes, B. Hamelers, K. Nijmeijer, Clean energy generation using capacitive electrodes in reverse electrodialysis, Energy Environ. Sci. 6 (2013) 643–651.
[140] P. Dorji, J. Choi, D.I. Kim, S. Phuntsho, S. Hong, H.K. Shon, Membrane capacitive deionisation as an alternative to the 2nd pass for seawater reverse osmosis desalination plant for bromide removal, Desalination 433 (2018) 113–119.
[141] L. Legrand, Q. Shu, M. Tedesco, J.E. Dykstra, H.V.M. Hamelers, Role of ion exchange membranes and capacitive electrodes in membrane capacitive deionization (MCDI) for CO_2 capture, J. Colloid Interface Sci. 564 (2020) 478–490.
[142] L. Legrand, O. Schaetzle, M. Tedesco, H.V.M. Hamelers, Electrical energy from CO_2 emissions by direct gas feeding in capacitive cells, Electrochim. Acta 319 (2019) 264–276.
[143] L. Legrand, O. Schaetzle, R. De Kler, H. Hamelers, Solvent-free CO_2 capture using membrane capacitive deionization, Environ. Sci. Technol. 52 (2018) 9478–9485.
[144] G.Q. Chen, S.L. Gras, S.E. Kentish, Separation technologies for salty wastewater reduction in the dairy industry, Sep. Purif. Rev. 48 (2018) 325–353.
[145] L. Paltrinieri, E. Huerta, T. Puts, W. van Baak, A.B. Verver, E.J.R. Sudholter, et al., Functionalized anion-exchange membranes facilitate electrodialysis of citrate and phosphate from model dairy wastewater, Environ. Sci. Technol. 53 (2019) 2396–2404.
[146] C. Zhang, X. Cheng, M. Wang, J. Ma, R. Collins, A. Kinsela, et al., Phosphate recovery as vivianite using a flow-electrode capacitive desalination (FCDI) and fluidized bed crystallization (FBC) coupled system, Water Res. 194 (2021) 116939.

This book belongs to Badji Mokhtar Annaba University Central Library Copyright Elsevier 2025

[147] L. Lee, H. Ng, S. Ong, J. Hu, G. Tao, K. Kekre, et al., Capacitive deionization for RO brine recovery in NEWater production, Water Pract. Technol. 3 (2008).
[148] A. Rommerskirchen, C.J. Linnartz, F. Egidi, S. Kendir, M. Wessling, Flow-electrode capacitive deionization enables continuous and energy-efficient brine concentration, Desalination 490 (2020) 114453.
[149] Voltea Ltd, Voltea CapDI, 2020.

This book belongs to Badji Mokhtar Annaba University Central Library Copyright Elsevier 2025

CHAPTER ELEVEN

Membrane-based electrochemical technologies: II. Microbial desalination cell

Kuichang Zuo[1], Shuai Luo[2] and Xia Huang[2]
[1]The Key Laboratory of Water and Sediment Sciences, Ministry of Education, College of Environment Sciences and Engineering, Peking University, Beijing, P.R. China
[2]School of Environment, Tsinghua University, Beijing, P.R. China

11.1 Introduction

The world is increasingly focused on water and energy conservation. It is estimated that the energy consumption for municipal wastewater treatment utilizing traditional activated sludge processes is 0.2–0.4 kWh/m^3 [1], which accounts for 1%–3% of the total electricity consumption in the United States and other developed countries combined [2,3]. While the chemical energy contained in the organic fraction of domestic wastewater is estimated to be nearly 1.93 kWh/m^3 [3], which is 5–10 times the energy required for wastewater treatment. Still the fact remains that the energy contained in the wastewater is often wasted in activated sludge processes, during which the organic species face two outcomes: to be oxidized into CO_2 with the energy released in the form of heat or be transformed into excess sludges that are disposed off in the posttreatment process such as landfilling. Microbial fuel cells (MFCs) can recover the chemical energy from the wastewater in the form of electricity and realize simultaneous wastewater treatment by the oxidation of bioelectrochemical-active bacteria [4]. During the past decade, the configuration and performance of MFCs have improved significantly with fuel cell volume increasing from a few microliters [4] to over 250 L [5,6], and maximum power density increasing from 0.01 mW/m^2 [7] to 3.3 W/m^2 [8]. Nevertheless, the power production and energy efficiency of existing MFCs are still relatively low, and the produced low-grade electricity with low voltage, current, and stability can hardly be directly recovered in practical applications.

Microbial desalination cells (MDCs) take off as an MFC-derived technology that offers simultaneous wastewater treatment, power generation, and desalination, realizing in situ utilization of the produced electricity for saltwater desalination without requiring extra energy input (excepting energy for pumping) [9]. Since its invention which

Electrochemical Membrane Technology for Water and Wastewater Treatment.
DOI: https://doi.org/10.1016/B978-0-12-824470-8.00008-5
© 2022 Elsevier Inc.
All rights reserved.

This book belongs to Badji Mokhtar Annaba University Central Library
Copyright Elsevier 2025

is 10 years now, MDCs have drawn the attention of the research community and undergone significant development. In stacked MDCs, which invention led to an improved desalination rate and a better current efficiency [10,11], ion exchange resins are packed in the desalination chamber to decrease internal resistance [12–15]. Some extended functions such as MDC for nutrients recovery [16,17], heavy metal removal [18], integration with reverse osmosis [19–21], forward osmosis (FO) [22,23], microfiltration process [24–26], and conventional anaerobic/aerobic process [27–29] for water desalination and advanced wastewater treatment have also been reported. The size of MDC reactors has been improved from several millimeters to 10 L [13] and even those over 100 L [30] are known to exist. These developments have greatly improved the performance of an MDC in terms of desalination efficiency, energy production, and wastewater treatment and have led many to explore its potential in functioning as an independent or integrated unit for advanced wastewater treatment and saltwater desalination.

In this chapter, we discuss the MDC's fundamental principle, reactor configurations, key influential factors, and applications in different integrated processes, as well as the challenges of and the difficulties in their future development. The MDC principle and related electrochemically active bacteria and electrode materials that fundamentally determine the power generation of MDCs are highlighted. We further summarize the configuration of the MDC reactors and identify the key influential factors that affect MDC performance. Finally, we discuss the application of MDC as an independent technology or integrated unit with other processes for water treatment in different scenarios.

11.2 Microbial desalination cell principle

11.2.1 Microbial fuel cell and electricity generation

MDC shares the same fundamental principle with MFC on generating electricity—bioelectricity generation using bacteria. While it was in 1911 that Potter—who is generally credited as the first one to have done so—observed electrical current generated by bacteria [31], it's only in the early 1990s that MFCs gained the interest of the research community and in the early 21st century that work on MFCs increased significantly.

A typical MFC is made of four parts: an anaerobic bioanode, a cathode, a membrane between the two electrodes, and an external electric circuit (Fig. 11.1A) [9]. During operation, microorganisms on the bioanode degrade (oxidize) organic matters to produce electrons and H^+. The electrons travel through a series of respiratory

This book belongs to Badji Mokhtar Annaba University Central Library Copyright Elsevier 2025

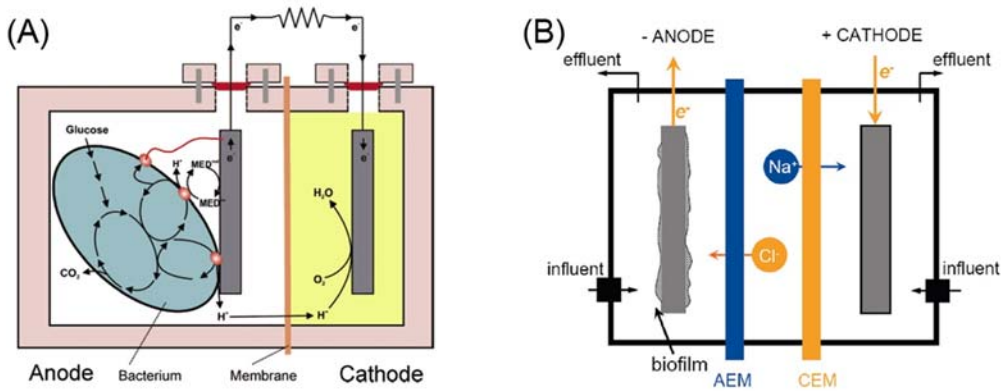

Figure 11.1 Schematic diagram of (A) MFC; and (B) MDC. Panel A illustrates the operating principles of an MFC. A bacterium in the anode compartment transfers electrons obtained from an electron donor (glucose) to the anode electrode. This occurs either through direct contact, nanowires, or mobile electron shuttles (small spheres represent the final membrane associated shuttle). During electron production, protons are also produced in excess. These protons migrate through the cation exchange membrane into the cathode chamber. The electrons flow from the anode through an external resistance (or load) to the cathode where they react with the final electron acceptor (oxygen) and protons. *Adapted and reproduced from B.E. Logan, B. Hamelers, R.A. Rozendal, U. Schrorder, J. Keller, S. Freguia, et al., Microbial fuel cells: methodology and technology. Environ. Sci. Technol. 40 (2006) 5181–5192, copyright © 2006 American Chemical Society. Panel B illustrates the principle of MDC. Adapted and reproduced from X.X. Cao, X. Huang, P. Liang, K. Xiao, Y.J. Zhou, X.Y. Zhang, et al., A new method for water desalination using microbial desalination cells. Environ. Sci. Technol. 43 (2009) 7148–7152, copyright © 2009 American Chemical Society.*

enzymes in the bacterial cell and are released to the anode material. They then flow through the external electrical load (e.g., resistor) to the cathode, realizing the reduction of terminal electron acceptor (TEA, e.g., O_2). At the same time, the microorganism-produced H^+ travels across the ion exchange membrane to the cathode chamber and, here, reacts with the TEAs and electrons that flowed from the anode through the external electric circuit.

The voltage generated by the MFC is difficult to predict because of the complicated biochemical reaction and electron transfer process in the bacterial cell [32,33]. However, there are limits to the maximum voltages that can be generated based on the thermodynamic relationship between the electron donners (substrates) and acceptors (oxidizers). The maximum electromotive force (E) is given by Eq. 11.1 and Eq. 11.2 [32,33]

$$E = E^0 - \frac{RT}{nF}\ln(\prod) \tag{11.1}$$

$$\prod = \frac{[\text{products}]^p}{[\text{reactants}]^r} \tag{11.2}$$

This book belongs to Badji Mokhtar Annaba University Central Library Copyright Elsevier 2025

where E^0 is the standard cell electromotive force, $R = 8.31447$ J/mol is the gas constant, T is the absolute temperature (K), n is the number of electrons transferred, and $F = 96{,}485$ C/mol is Faraday's constant. The reaction quotient is the ratio of the activities of the products divided by the reactants raised to their respective stoichiometric coefficients. By IUPAC (International Union of Pure and Applied Chemistry) convention, all reactions are written in the direction of chemical reduction, that is, r [oxidized species] $+ne^- \rightarrow p$ [reduced species]. The products are always the reduced species, and the reactants are the oxidized species. r and p are the number of reactants and products in the reactions. The E^0 of hydrogen is 0 V under standard conditions: temperature of 298K, and chemical concentrations of 1M for liquids and 1 bar for gases. E^0 values of other species are calculated vis-à-vis this E^0 of hydrogen.

MFCs utilize organic substrates to produce electricity, and the most commonly utilized organic is acetate. The (Eq. 11.3) is the reduction reaction equation of HCO_3^-/acetate couple, and (Eq. 11.4) is its potential (E) at pH of 7, acetate of 1 g/L (16.9 mM), and HCO_3^- concentration of 5 mM that is expressed as:

$$2HCO_{3^-} + 9\,H^+ + 8e^- \rightarrow CH_3COO^- + 4H_2O \quad E^0 = 0.187\ \text{V} \tag{11.3}$$

$$E = E^0 - \frac{RT}{8F}\ln\left(\frac{[CH_3COO^-]}{[HCO_3^-]^2[H^+]^9}\right) = -0.300\text{V} \tag{11.4}$$

With the potential of different species, it is possible to calculate the total cell potential (Eq. 11.5), which equals the difference between the potential of the two species.

$$E_{\text{total}} = E_{\text{cathode}} - E_{\text{anode}} \tag{11.5}$$

For example, when acetate and oxygen are utilized in the anode and cathode, respectively, in an MFC with the above conditions, the total voltage $E_{\text{total}} = 0.805 - (-0.300) = 1.115$ V.

11.2.2 Microbial desalination cell

MDCs are derived from MFCs, and they offer simultaneous wastewater treatment, electricity generation, and desalination without requiring extra energy input. The first MDC—invented in 2009—was derived from a cubic-shaped MFC [9] and consisted of an additional middle desalination chamber formed by inserting an anion exchange membrane (AEM) and a cation exchange membrane (CEM) between the anode and the cathode of an MFC (Fig. 11.1B). During operation, saltwater would be introduced in the middle chamber. When the external electric circuit was connected between the two electrodes, the formed electric field would drive the migration of cations and anions from the middle chamber to the cathode and anode chambers, respectively, realizing desalination of saltwater. The desalination mechanism of MDC is similar to

This book belongs to Badji Mokhtar Annaba University Central Library Copyright Elsevier 2025

electrodialysis [13], but the driving electric force is the energy extracted from organics contained in wastewater. Therefore, an MDC requires no external energy input for desalination, representing an energy-saving technology for the needs of wastewater treatment and desalination.

11.2.3 Electroactive microorganism

Electroactive microorganisms are essential for the anode of an MDC, for they are the biological catalysts that transform the chemical energy in wastewater organics into electricity for driving water desalination. Currently, several electroactive bacterial strains have been identified in bioelectrochemical systems, including *Geobacter sulfurreducens*, *Rhodoferax ferrireducens*, *Shewanella* sp., etc. [33–35] The growth of these electroactive microorganisms can form a biofilm on the anode material, and then they can exchange electrons with the solid electrode [33,34,36,37].

The electron transfer between the electroactive microorganism and the solid anode can be realized through a direct or an indirect mechanism (Fig. 11.1A) [33]. The direct electron transfer occurs due to the direct contact between the surface of the anode material and the cell membrane of the electroactive bacterial. While for some bacteria such as *G. sulfurreducens* the cytochrome c proteins in the cell membrane can directly transfer intracellular electrons to the anode surface [38], still there are studies that have reported that the direct electron transfer also took place via extracellular conductive pili or bacterial nanowires [39]. In comparison, indirect electron transfer is better understood and has been confirmed in many bacteria such as *Shewanella oneidensis, Pseudomonas alcaliphila*, and *Pseudomonas aeruginosa* [33]. Indirect electron transfer is often realized by the circulating transport and redox reaction of mediators taking place between the electroactive bacteria and the anode surface: the mediators are oxidized by the electroactive bacteria and reduced by the anode, realizing the transfer of electrons from the electroactive bacteria to the anode surface. Mediators can be produced by the electroactive bacteria or through external addition, and common mediators include pigments [40] and quinone substances [41].

Since the electroactive microorganism is the anodic catalyst, its availability along the anodic chamber determines the current production and the desalination performance of the MDC. In an MDC, the growth of biofilms is a slow process and consists of four stages: cell-anode attachment, cell-cell adhesion, maturation, and detachment [42]. While many factors can affect the growth and electroactivity of the anodic bacteria, including the type and concentration of organic substrate, the concentration and pH of electrolyte, the resistance of an external electric load, the fluid condition, and the anode materials, etc., still it's the combination of these factors that affects the amount, age, and electroactivity of the microorganisms.

This book belongs to Badji Mokhtar Annaba University Central Library Copyright Elsevier 2025

11.2.4 Electrode materials

Given an anode material functions not only as an electron conductor but also as the carrier of the electroactive bacteria, therefore, it follows that an electrode material must have several characteristics to suit its dual purpose, such as high biocompatibility, high surface area, electrically conductive, resistant to corrosion, mechanically robust, and low cost, etc. [43–46] Common electrode materials in laboratory MDCs include a large variety of carbon materials and several metal materials (Fig. 11.2), which vary greatly in structure and surface area.

Carbon-based materials are the most widely used materials for MDC anodes because of their good biocompatibility, chemical stability, conductivity, and relatively low cost. In terms of configuration, carbon-based electrodes can be divided into (1) plane structures, (2) foam structures, (3) packed structures, and (4) brush structures, and each of these has different properties and performance graphs to follow. Typical plane structural carbon-based materials include carbon paper, graphite plate or sheet, and carbon cloth. Given carbon paper and graphite plate or sheet have compact structures and relatively smooth surfaces, therefore, it follows these are good anode materials to quantitatively measure the biomass of the grown electroactive bacteria per unit surface area in small-scale MDCs. However, these two materials are brittle and possess low surface area. In comparison, carbon cloth is porous and flexible, and it possesses higher surface area for the attachment and growth of electroactive bacteria. Nevertheless, similar with carbon paper and graphite sheet, the advantages of carbon cloth comes at the relatively high cost, which inhibits their application in large-scale MDCs.

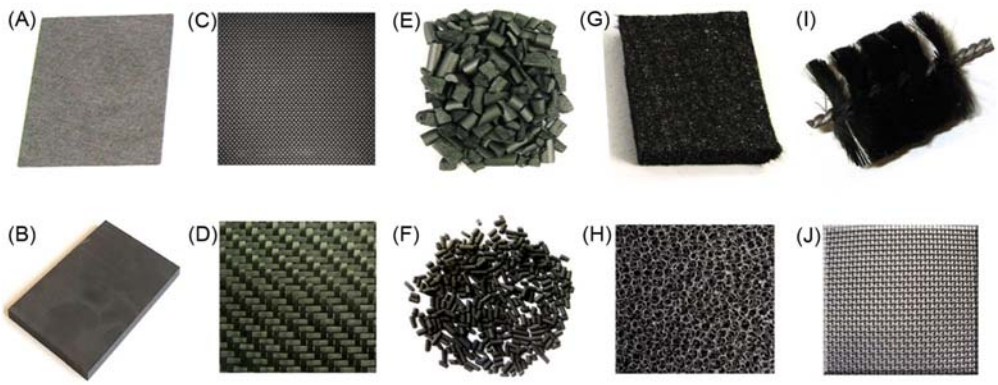

Figure 11.2 Photographs of electrode materials used for MDC. (A) carbon paper; (B) graphite plate; (C) carbon cloth; (D) carbon mesh; (E) granular graphite; (F) granular activated carbon; (G) carbon felt; (H) reticulated vitrified carbon; (I) carbon brush; (J) stainless steel mesh. *Adapted and reproduced from J. Wei, P. Liang, X. Huang, Recent progress in electrodes for microbial fuel cells. Bioresour. Technol. 102 (2011) 9335–9344, copyright © 2011, Elsevier Ltd.*

This book belongs to Badji Mokhtar Annaba University Central Library Copyright Elsevier 2025

Graphite or carbon felt is a three-dimensional carbon fabric material. Its loose texture confers high porosity for bacterial growth than the texture of carbon cloth or graphite sheets confer, but the growth of bacteria is more likely restricted by the mass transfer of substrate and products due to the small-sized pores. Therefore, the felt has been cut into cubes and placed into anode chambers to improve the mass transfer and increase the available surface area for bacterial growth [14]. Due to the much larger surface area than plane electrodes, carbon felt often provides a higher number of bacteria per unit volume of anode chamber and produces higher power. Therefore, carbon felt is suitable for large-scale MDC application.

Besides carbon felt, the MDC anode chamber can be filled with carbon-based granular materials [15], with these being cheap, simple, and more practical for large-scale MDCs. To conduct the produced electrons from the grown electroactive biofilm, current collectors such as graphite rods or metal meshes are needed to connect the packed bed with the external circuit. The granules also need to be packed tightly to decrease the contact resistance and improve electron conduction. Since the size of granular carbon materials is often at a millimeter or even a centimeter scale, the formed interstitial pores in the packed bed are also at a millimeter scale, which is good for water flow and mass transfer. However, the porosities of the packed electrode are relatively low (only ranging from 30% to 50% for granular media), thus potential clogging during long-term operation might be a problem. In addition, the packing bed anode only makes use of the outer surface of granular carbon for electroactive bacteria growth, while a large amount of the inner electrode materials is not utilized. As a result, the packing bed anode requires a large mass of the electrode material, and thus it often possesses high weight and is not conducive to transport.

Carbon brush is an ideal electrode material because it is often made of carbon fibers that are wound into a twisted core consisting of two titanium wires [47], where the carbon fibers provide the high surface area needed for electroactive bacteria attachment and growth and the conductive titanium core is conductive and highly efficient for electron collection. In addition, the carbon brush possesses high porosity and low weight, which is conducive to mass transfer and transport; while the size (brush diameter and length) of the carbon brush is easily tuneable, giving versatility in the application of carbon brush in either small-scale or large-scale MDCs.

Apart from carbon-based materials, metal materials are much more conductive than carbon materials. Therefore, metal materials such as gold, stainless steel mesh, and titanium have been utilized in bioelectrochemical systems for fundamental or practical study. However, metal materials are not widely applicable as the carbon material in MDCs because of the former's low biocompatibility and corrosion resistivity. So far, only titanium has qualified as the common base material for anodes. But its low surface area inhibits bacterial growth, resulting in a power generation that is one to two magnitudes lower than that by carbon-based materials [48,49].

This book belongs to Badji Mokhtar Annaba University Central Library Copyright Elsevier 2025

11.2.5 Membrane materials

Given the function of the MFC membrane is to separate the anode and cathode reactions and prevent the transport of oxygen into the anode chamber while permitting selective transport of ions, it follows, therefore, the materials that can prevent diffusion of oxygen and microorganisms will be utilized as the separator in an MFC, including CEM, AEM, j-cloth, glass fibers, ceramics, photocopy paper and, even, nonmembrane (single-chamber MFC) [37]. However, the membranes in MDC function for ion exchange to realize water desalination or ion extraction, and each membrane should have selectivity that allows the transfer of either anions or cations to the adjacent chambers. Therefore, commercial ion exchange membranes that can be utilized in electrodialysis systems can also be utilized in MDCs. Though electrodialysis is a mature technology and the ion exchange membranes have also experienced significant development and wide industrial application in the past century, still there are very few studies focusing on membrane materials in MDCs. One of the few interests to fuel the research on MDC membrane material is to increase its conductivity to improve desalination rate, which could be realized by increasing the hydrophilicity and ion exchange capability by producing Polysulfone with sulfonated poly-ether-ether ketone membranes [50] or producing sulfonated sodium polyether ketone CEMs with quaternary ammonium chloride and poly(2,6-dimethyl 1,4-phenylene oxide) AEM [51]. Another issue to stimulate interest in membrane studies in MDC is biofouling, where people have also infused silver nanoparticles into carbon nanotube membranes in MDCs to prevent bacteria from migrating through the membranes [52]. Nevertheless, compared to these improvements on membrane property, a more important challenge for membrane use is its high cost. Since large amounts of ion exchange membranes are needed to improve the desalination rate in MDC, their cost can account for over 50% of the total capital cost of the whole MDC reactor (when cheap electrode materials are utilized). In addition, apart from the properties of the membrane materials, it's their relative position in the MDC reactor that plays a more important role in affecting desalination performance. Some membranes have been used instead of ion exchange membranes, such as forward osmosis membranes (FOMs), bipolar membranes (BPMs), etc., in MDCs for high water recovery or chemical production. These applications will be discussed in the following sections.

11.3 Microbial desalination cell configurations

The basic MDC is mainly made up of the anode, the cathode, and the desalination chambers, which can meet the purpose of wastewater treatment and desalination. However, the basic type of MDC proved ineffective in satisfying the various demands

This book belongs to Badji Mokhtar Annaba University Central Library Copyright Elsevier 2025

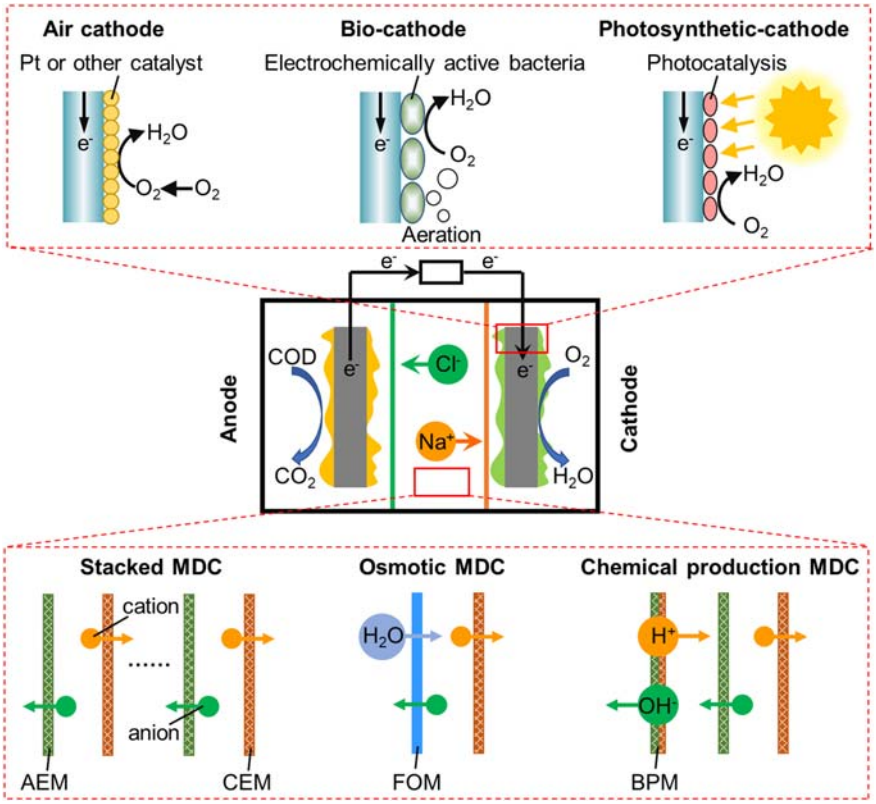

Figure 11.3 Modification of cathode and membrane stack to fabricate various MDC configurations. *AEM*, anion exchange membrane; *CEM*, cation exchange membrane; *FOM*, forward osmosis membrane; *BPM*, bipolar membrane.

for sustainable wastewater treatment and desalination. Therefore, the basic MDC to be improved—as far as efficiency and functions are concerned—by optimizing MDC cathode, middle membrane, and other configurations (Fig. 11.3) [13,53–55] became a need and led to the invention of new types of MDCs.

11.3.1 Optimizing microbial desalination cell cathode

11.3.1.1 Air-cathode microbial desalination cell

The first MDC was invented by utilizing ferricyanide solution as the cathode electron acceptor [9], which is toxic and needs frequent refilling. Fortunately, an aerated cathode was applied to alternate the traditional MDC to reduce the chemical cost, where oxygen was found a favorable terminal electron acceptor due to its high cost-effectiveness and availability. The aerated MDC was first applied by Mehanna et al. [21], and it achieved a

This book belongs to Badji Mokhtar Annaba University Central Library Copyright Elsevier 2025

desalination efficiency of 43% with coulombic efficiency of 68%. Subsequently, air cathodes with a passive oxygen transfer process have also been developed (Fig. 11.3) [56,57] which need no aeration and possess the advantage of low energy consumption. However, redox kinetics for the oxygen reduction reaction on the air cathode is often slow at ambient conditions. Expensive noble metals such as Pt is often utilized as cathode catalyst to improve reaction rate [56,58,59]. In addition, these catalysts are vulnerable to organic or bacterial contamination during long-term operation [60,61], and they need frequent activation or even replacement.

11.3.1.2 Biocathode microbial desalination cell

In addition to growing on noble metals, electrochemically active bacteria on the biocathode are also good catalysts to initiate the reduction of oxygen to produce electricity (Fig. 11.3) [62]. Compared to the conventional air-cathode, biocathode has the advantage of a high potential to reduce construction cost, with the bacterial catalyst being much cheaper to grow than on noble metals. The self-regeneration of electrochemically active bacterial cells also guarantees long-term operation stability, avoiding organic- or biofouling. In addition, the aerobic metabolism of microorganisms on the biocathode also oxidizes organic pollutants, enabling an "anaerobic-aerobic" treatment process for wastewater when hydraulically connecting the anode and biocathode chambers. With these advantages, the biocathode MDC (with power densities of 268.1 mW/m^2) [25,63] can reach comparable or even higher power generation capability than do noble metal-based air cathode MDCs (112.6 mW/m^2) [24] with similar size. As a result, the low-cost, efficient, and stable biocathode MDC is easy to scale up. The biggest volume of single unit MDC reached 10 L [13], which utilized a pack-bed biocathode utilizing granular activated carbon as microorganism carriers and realized a power density of 33.1 W/m^3.

Nevertheless, despite these advantages, the biocathode MDC also faces several drawbacks. Compared with the conventional air-cathode, the starting-up process of the biocathode is much slower and may take several days, or even months. The aerobic biocathode also requires oxygen, where the input of oxygen utilizing aeration can also cause high energy consumption, which is not conducive to its scaling up. To solve these problems, the addition of organic compounds can be applied to promote microorganisms to grow and metabolize and, thereby, to reduce the start-up time [64]. Nonoxygen electron acceptors such as sulfate, nitrate, iron, fumarate, and other ions have also been utilized in the anaerobic biocathode [65], which avoids aeration and can decrease operational cost. In addition, the anaerobic biocathode also causes denitrification and phosphorus uptake and, consequently, realizes the removal of nutrients from wastewater. The biocathode also enables the production of valuable chemicals (e.g., hydrogen and valuable organic compounds) [66].

This book belongs to Badji Mokhtar Annaba University Central Library Copyright Elsevier 2025

11.3.1.3 Photosynthetic microbial desalination cell

Biocathode MDC is introduced with bacterial inoculation and acclimation in the cathode. However, the aerated biocathodes consume massive energy during operation, diminishing the energy recovery efficiency. Avoidance of external aeration is a method available to solve the problem, where algae inoculation into the cathode can take advantage of sunlight to directly produce oxygen for the cathode as the terminal electron acceptor (Fig. 11.3). The attached algae on the cathode directly supply the oxygen onto the cathode surface to improve its local concentration and enhance power output [67]. To investigate the feasibility of photosynthetic MDC, the batch and continuous operation modes have been applied to test the desalination efficiency and power output [68]. It was found that salt removal efficiencies in batch and continuous flow photosynthetic MDC were 27.7% and 22.7%, respectively [68]. The most important advantage of the photosynthetic MDC is in its having no need to input external energy to drive the system. The growth of algae on the cathode could also help improve the oxidation of organic compounds in the wastewater. In addition, the grown algae could be harvested to produce chemical products (e.g., oil), realizing wastewater treatment, saltwater desalination, solar energy harvest, and chemicals production.

11.3.1.4 Microbial capacitive desalination cell

Besides the development of cathode catalysts, other electrode materials have also been investigated. One problem of MDC operation is that under the desalination process, the cations and anions migrate to the anode and cathode, respectively, to cause ionic accumulation. The excessive ionic accumulation will lead to the imbalance of anolyte and catholyte pH, inhibiting microbial growth and metabolism. Thus, one disadvantage of MDC operation is the need for frequent infusion of anolyte and catholyte to regulate the ionic concentration and pH [69]. To solve this problem, a new MDC system has been developed by combining the technology of electrochemical desalination and capacitive deionization (CDI). The modified MDC is good to enable ions to be adsorbed onto the capacitive electrodes instead of freely flowing inside the anode or cathode chambers and causing side effects on anode microorganisms or cathode catalysts. The integrated capacitive MDC was proved to be feasible for the low-concentration saline water with a desalination rate of 200.6 mg/(L.h) [70]. Wen et al. further found that a capacitive MDC could achieve a higher desalination rate than the traditional MDCs, and the high desalination efficiency could be maintained for the long-term due to consistent ionic refreshing by the capacitive electrodes [71]. In addition, due to the production of electricity, the capacitive MDC was also reported to realize 7–25 times higher desalination efficiency than the traditional CDI, greatly benefiting the deionization process in the saltwater treatment process.

This book belongs to Badji Mokhtar Annaba University Central Library Copyright Elsevier 2025

11.3.2 Optimizing membrane stack

In addition to optimizing the cathode catalysts and electrode materials, the membrane stack between the anode and cathode has also been optimized to improve the desalination efficiency, water recovery, and even production of valuable chemicals. The optimization of the membrane stack mainly focuses on utilizing novel membranes, for example, CEM, AEM, FOM, and BPM, or optimizing their numbers and configurations (Fig. 11.3).

11.3.2.1 Multistage microbial desalination cell

Single-stage MDC has the configuration of an anode and a cathode sandwiching one pair of AEM and CEM to form a desalination chamber in the middle, utilizing electricity to drive the ion (e.g., Na^+, Cl^-) to migrate to realize the desalination process [72]. However, the transfer of every single electron from the anode to the cathode can only drive one pair of ions (cation and anion) to be separated from the desalination chamber in the single-stage MDC, causing limited charge transfer efficiency and salt removal rate [73]. Therefore, configuration modification can be performed by increasing AEM and CEM pairs to improve charge transfer efficiency and increase the salt removal rate (Fig. 11.3) [74]. The prototype stacked MDC was constructed by forming two desalination chambers and one concentrated chamber in the middle of the MDC using two pairs of CEM and AEM [10]. The assembled multistage MDC realized improved total desalination rates vis-à-vis the desalination rates of the original single-chamber MDC by a 40% jump [10]. Subsequently, the AEM and CEM pairs in the MDC stack were optimized in terms of desalination rate and charge efficiency, and it was found that 10 desalination cells could achieve the highest charge efficiency (836%) compared to that achieved by various numbers of desalination cells (6−14 cells) [75]. This is because although the increase of AEM and CEM pairs could improve the desalination rate, the increased desalination chambers could also cause an increase of internal resistance and concentration overpotential, which is not conducive to current production and the improvement of desalination rate.

11.3.2.2 Osmotic microbial desalination cell

In the conventional MDC, wastewater is utilized in the anode to provide electron donors for the electrochemically active bacteria and saltwater is introduced in the middle membrane stack for purification. Since typical saltwater such as seawater and brackish water has a much higher ionic concentration than wastewater in the anode chamber, salt ions can be easily migrated from the middle desalination chamber to the anode chamber to realize desalination of saltwater. To further improve the water recovery of desalinated water in the effluent of the middle desalination chamber, a promising approach is to take advantage of the osmotic pressure between the saltwater

This book belongs to Badji Mokhtar Annaba University Central Library Copyright Elsevier 2025

and wastewater by utilizing an FOM to extract water from the anodic wastewater (Fig. 11.3) [76]. The substitution of the AEM by the FOM has the potential not only to improve the recovery of desalinated water but also to decrease the production of wastewater in the anode chamber. In addition, it was reported that the application of FO to substitute CEM could also reduce the internal resistance and increase the current generation [77]. The diluted seawater from osmotic MDC could also be applied as catholyte to reduce water consumption [78]. Further, the replacement of the AEM by the FOM could also decrease construction cost, which is also conducive to the application and scale-up of MDC technology.

11.3.2.3 Microbial chemical production cell

Suitable transformation of an MDC cannot only solve the problem of ionic accumulation in the electrode chamber but also give the MDC the new function of chemical production. The new function can be achieved by the chamber addition and new membrane integration. Previous studies have proved that the combination of a microbial electrodialysis desalination cell and a chemical production cell, together, could simultaneously achieve the functions of wastewater treatment, desalination, and chemical production [79]. The basic structure was to create a desalination chamber and an acid production chamber by utilizing a CEM, an AEM, and a BPM, where the membrane arrangement strategy was that of a CEM placed between the desalination and the cathode chamber, and an AEM placed between the desalination and the acid-production chambers, and a BPM inserted between the anode and the acid-production chambers (Fig. 11.3) [79]. During operation, the BPM decomposes water to produce the hydrogen ion and hydroxide, and the adjacent AEM allows the migration of Cl^- under an electric field, realizing accumulation of HCl in the acid production chamber. The modified chemical production MDC was proved to generate the malic acid at the concentration of 0.236 M [80]. Besides the acid, the bases are also produced from the chemical production chamber utilizing a similar strategy, such as the production of tetramethylammonium hydroxide [81]. By utilizing the electricity produced from the wastewater, this approach could increase the chemical production rate with less energy consumption, which could add value and increase the economic benefit to the MDC system.

11.3.3 Other configurations

Different from the traditional MDC constructed as cubic or flat shape, the tubular MDC is also constructed with a coaxial cylindrical AEM and a CEM separating the central anode, middle desalination, and the outer cathode chambers [22]. An up-flow operation mode and an air cathode are often utilized for tubular MDCs, and the flow path of the desalinated water could be optimized by flowing partial of desalinated water to the cathode surface as catholyte to improve oxygen reduction reaction. This

This book belongs to Badji Mokhtar Annaba University Central Library Copyright Elsevier 2025

strategy not only reduces the energy consumption for cathode aeration but also improves the NH_4^+ removal efficiency when the excessive NH_4^+ in the desalinated effluent is completely oxidized to NO_3^- [22,82]. The advantage of the tubular MDC is the ease with which it scales up to fetch high treatment capacity because the tubular MDC could easily enlarge the reactor volume, and the tubular MDC units could also be easily integrated for improved desalination efficiency, controllability, and compactness [83,84]. For example, a large-scale MDC system with a volume of 105 L was constructed by integrating 30 tubular MDC units, and the system achieved a current generating capacity of nearly 2000 mA and a salt removal rate of 9.2 kg/m^3/day [30]. The easy combination process of multiple tubular up-flow MDCs could also enable integrating MDC units into a small box [30]. With more development on MDC configuration, the performance of the MDC would be improved, and the MDC technology promoted closer to its practical application.

11.4 Optimization of microbial desalination cell devices and operational conditions

Configuration optimization can address the intrinsic limitation of the MDC like low charge transfer efficiency and salt removal rate and, thereby, improve its wastewater treatment performance, yielding better desalination efficiency, electricity production, and charge transfer efficiency, while broadening the scope of its applications such as for chemical production and water extraction, etc. To further improve the performance of an MDC, the operational parameters can also be optimized to maintain its stable operation. Based on the working principle of an MDC, the desalination efficiency and related chemical production rate are mainly determined by the current generation. Therefore, operation conditions should be optimized to improve the electron production by the electrochemically active microorganisms and ionic transportation (e.g., Na^+, Cl^-) across the membranes. In this section, multiple strategies are discussed to optimize these factors and improve MDC performance.

11.4.1 External resistance

External resistance is the leading direct factor affecting the current generation and can be easily adjusted during an MDC operation. Due to the instability of power production ability at different MDC operational stages, the external resistance should be adjusted accordingly. For example, it is generally believed that high external resistance should be utilized to improve the inoculation of electrochemically active microorganisms during the starting-up period but, with the growth of anodic bacteria, the

This book belongs to Badji Mokhtar Annaba University Central Library Copyright Elsevier 2025

external resistance should be decreased to stimulate the current production capability and improve bacterial activity. Thus, upon the accomplishment of the starting up stage, the current generation capability can become improved for high-rate desalination with low external resistance. For instance, it was reported that when the external resistance decreased from 1000 to 10 Ω, the maximum current density increased by 680% from its initial starting up magnitude, with columbic efficiency increasing by 275% [85]. In another 1 L up-flow MDC, the total desalination increased from 42.3% to 60.1% with the external resistance decreasing from 6 to 0.1 Ω [86]. Since the external resistance can be automatically and easily controlled by utilizing electronic components and programming, it is probably the most important operating factor during practical application, especially for the integrated system with multiple MDC units.

11.4.2 Internal resistance

Although changing external resistance is convenient to control the current generation capability, current production capability is also limited by the MDC internal resistance. The internal resistance increases with the MDC desalination efficiency, which causes decreased conductivity of the saltwater and increases resistance. Though several approaches have been utilized to decrease the internal resistance of MDC without changing its configuration, still the main approach is to decrease the intermembrane distances between CEMs and AEMs. For example, it was reported that the internal resistance decreased from 449 to 25 Ω when the intermembrane distance decreased from 20 to 3 mm [9,21]. As a result, the desalination rate was improved with the decreased internal resistance. The desalination efficiency increased 7–12 times with the intermembrane distance decreasing from 2.5 to 0.3 cm [87]. A multistacked MDC with confined intermembrane spaces less than 0.5 mm also realized charge transfer efficiency of 836% [75] vis-a-vis starting up stage. Theoretically, the smaller the intermembrane distance is, the lower the internal resistance. In a practical electrodialysis reactor that has a similar stacked membrane structure with MDC, the intermembrane distance is generally lower than 1 mm, which may instruct the construction of MDC reactors.

Despite that decreasing intermembrane distance has effectively reduced internal resistance, a small intermembrane distance would cause increased hydraulic resistance and decreased hydraulic retention time (HRT). As a result, the intermembrane distances can hardly be further reduced below 0.5 mm level, which limits the MDC ability for advanced desalination to produce ultra-pure water, because the internal resistance increases exponentially with the decrease of salinity at low concentrations. To further decrease internal resistance and enlarge intermembrane distance, there is another approach, that is, to fill the ion-exchange resins into the desalination chamber to increase the ionic conductivities. For example, it was reported that the desalination

This book belongs to Badji Mokhtar Annaba University Central Library Copyright Elsevier 2025

rate of the MDC after filling the ion-exchange resins was 1.5−8 times higher than the traditional MDC without resin filling (Fig. 11.4A) [12]. The packing of ion exchange resins enables advanced desalination of wastewater at a high rate, with the conductivity of desalinated effluent reaching several tens of μS/cm, which is comparable with the concentration of effluent produced by first stage reverse osmosis and has great potential

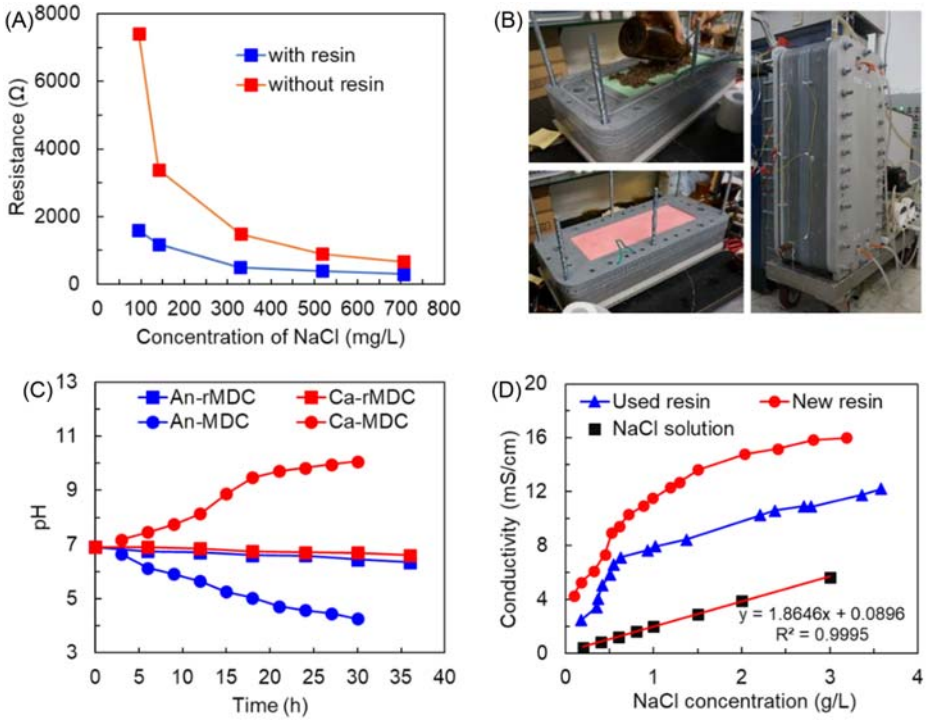

Figure 11.4 Operational optimization to enhance MDC performance. (A) Packing ion exchange resin in the MDC decreased the MDC internal resistance. (B) Image of the packing of ion exchange resins in a large scale MDC reactor. (C) Recirculating anolyte and catholyte stabilized the pH in anode and cathode chambers. *An*, anode; *Ca*, cathode; *rMDC*, recirculated MDC; *MDC*, normal MDC. (D) Conductivity of salt solution and ion-exchange-resin-packed salt solution indicated that the conductivity of used ion exchange resin decreased during long-term operation due to inorganic scaling. *For (A) Reproduced with permission from F. Zhang, M. Chen, Y. Zhang, R. J. Zeng, Microbial desalination cells with ion exchange resin packed to enhance desalination at low salt concentration. J. Membr. Sci. 417 (2012) 28−33, copyright © 2012 Elsevier B.V; (B) Reproduced with permission from K. Zuo, J. Cai, S. Liang, S. Wu, C. Zhang, P. Liang, et al., A ten liter stacked microbial desalination cell packed with mixed ion-exchange resins for secondary effluent desalination. Environ. Sci. Technol. 48 (2014) 9917−9924, copyright © 2014 American Chemical Society; (C) Reproduced with permission from Y. Qu, Y. Feng, W. Xin, L. Jia, J. Lv, W. He, et al., Simultaneous water desalination and electricity generation in a microbial desalination cell with electrolyte recirculation for pH control. Bioresour. Technol. 106 (2012) 89−94 [88], copyright © 2011 Elsevier Ltd; (D) Reproduced with permission from K C. Zuo, L. L. Yuan, J. C. Wei, P. Liang, X. Huang, Competitive migration behaviors of multiple ions and their impacts on ion-exchange resin packed microbial desalination cell. Bioresour. Technol. 146 (2013) 637−642, copyright © 2013 Elsevier Ltd.*

This book belongs to Badji Mokhtar Annaba University Central Library Copyright Elsevier 2025

to be utilized in large MDC reactor (Fig. 11.4B) [13]. However, the packing of ion exchange resin also causes increased cost and potentially other instability risks (e.g., fouling, scaling, blocking), which means pretreatment may be necessary to guarantee its stable operation.

11.4.3 pH control

During the operation of an MDC, the pH in the anode chamber decreases due to proton production from the microbial organic degradation, while the cathodic pH would increase due to the production of hydroxide during oxygen reduction reaction. The pH imbalance will inhibit the anodic microbial activity and cathodic reduction reaction. It was reported that one unit of pH difference could result in a voltage decrease of 95 mV [88], inhibiting current production and desalination rate. The pH increase in the cathode could also cause precipitation of scale-forming ions, such as Ca^{2+}, Mg^{2+}, etc., leading to scaling and blocking of the cathode chamber. In addition, the pH imbalance could also result in the back diffusion of proton and hydroxide through CEM and AEM to desalination chambers, causing pH change of the produced desalinated water and brine [89]. Therefore, pH control is important to guarantee the stable operation of MDC systems.

To address the pH imbalance problem, a solution could be to add a phosphorous buffer solution (PBS) to maintain stable pH in the anode and cathode chambers [90]. However, the massive amounts of PBS required were not feasibly available for practical long-term operation due to the high cost [15,63,91]. Another method of recirculating the solution between the anode and cathode chambers has been proposed to solve the pH imbalance problem [88]. This approach could eliminate pH imbalance and improve power generation and desalination efficiency (Fig. 11.4C) [88]. However, the recirculation of the electrolyte could also bring the anodic remaining organic matters and microbes to the cathode chamber, which may cause fouling of the air-cathode catalyst or result in activity decrease of the autotrophic bacteria on the biocathode [88]. In addition, the recirculation of the oxygen-rich catholyte to the anaerobic anode chamber may also cause performance decline of the anode electrochemically active bacteria, inhibiting electricity production and desalination rate.

To prevent the contamination of the cathode surface from organic and microorganism fouling, a glass fiber separator was added to the water-facing side of the air cathode, and the activity of the cathodic catalyst was thus maintained [92]. The modified MDC system could operate stably with a desalination efficiency of $>40\%$ for over 60 days, much better than the recirculated MDC without a separator. Another similar structured MDC also indicated that the addition of a separator on the cathode could extend the operation and increase the recovery efficiency of nitrogen and phosphorus [16]. In addition to adding separators to protect the cathode, improving proton

This book belongs to Badji Mokhtar Annaba University Central Library Copyright Elsevier 2025

transfer efficiency in the anode chamber by utilizing a modified ion exchange membrane could mitigate the accumulation of protons and stabilize pH in the anode. It was proved that pH variation could be reduced by 54% utilizing this approach [16]. Nevertheless, the pH variation is a complicated problem in practical scenarios, and it may be solved with comprehensive management of MDC in terms of different operation parameters, such as flow rate, external resistance, etc.

11.4.4 Operational conditions

11.4.4.1 Anodic substrate concentration

Substrate concentration is an important factor affecting the power production and desalination efficiency of MDC, which provides the carbon source needed for the anodic microorganism metabolism to generate electricity. A proper concentration of substrate is important for the stable operation of the MDC. Domestic wastewater typically has a chemical oxygen demand (COD) of several hundreds of mg/L, which is reported to contain chemical energy of $\sim 2.0\ \mathrm{kWh/m^3}$ [3] and could realize self-desalination with desalination efficiency of $>90\%$ [24]. Nevertheless, excessive carbon supply would negatively affect microbial activity because the growth of thick biofilm inhibits the mass transfer and electron production efficiency [42,93]. For example, COD concentration at 1000−1500 mg/L was reported to be a suitable concentration range for MDC operation, and the desalination rate could reach 0.3−0.4 g/(L.h) [94]. Excessive or limited substrate supply would limit the desalination rate. Furthermore, substrate type is another factor to affect desalination efficiency. Easily degradable compounds such as glucose and acetate are suitable carbon sources for the electrogenic bacteria utilization for power generation [95], while refractory organics can hardly be utilized for electricity production.

11.4.4.2 Catholyte solution

Since air-cathode and autotrophic-bacteria-based biocathode have no requirement on the input of chemicals (e.g., carbon sources), therefore the catholyte has no need to be replaced frequently during operation. As a result, saline buffer solutions are often utilized in the cathode chamber to stabilize pH and provide the conductivity needed to improve current generation. Conventionally, ferricyanide and PBS are utilized as the catholyte for MDC operation [96]. However, the expensive PBS and unrecoverable ferricyanide increase the operational cost, which is not conducive to the scaling up of the MDC system. Therefore, substitutive catholyte has been utilized to reduce the operational cost of the MDC. The partially desalinated water (effluent from the desalination chamber) with a certain concentration of remaining ions such as Na^+ or Mg^{2+} to provide the necessary conductivity (e.g., 10−30 mS/cm) could be applied as catholyte to enable current production and effectuate the desalination rate [94]. The treated wastewater (anode effluent) could also be utilized as a catholyte. Despite the residual

This book belongs to Badji Mokhtar Annaba University Central Library Copyright Elsevier 2025

organics in anode effluent having the risk to pollute the cathode catalyst, the increased conductivity (anolyte receives ions from the middle desalination chamber during desalination process) is conducive to decreasing internal resistance. In addition, the relatively low pH of anode effluent is also conducive to neutralizing the pH in cathode chambers, which is beneficial to current production and desalination.

11.4.4.3 Temperature

Temperature is another important factor that could strongly influence the performance of the MDC system through affecting the activity of the electrogenic bacteria and the competitive microorganism species, such as methanogenic bacteria [97]. Low temperature ($<5°C$) in winter is not conducive to the growth of all anodic bacterial species, for it not only decreases current production and desalination efficiency but also inhibits the organics removal performance for wastewater treatment. At psychrophilic temperatures ($10°C-20°C$), the electrogenic bacteria illustrate high activity for current generation while the methanogenic bacterial activity is still inhibited, which is conducive to current production and for improving the columbic efficiency [98]. While a further increase in the temperature could theoretically improve the activity of electrogenic bacteria for current production, nevertheless, high temperature is also favorable to the growth of methanogenic bacteria, which competes with electrogenic bacteria for anodic carbon sources to produce methane and decreases columbic efficiency.

In addition, high temperature is also beneficial for the permeability of ion exchange membranes to decrease internal resistance [99]. Therefore, a suitable temperature needs to be utilized to balance the competition between electrogenic bacteria and methanogens. It was reported that $25°C-30°C$ was suitable for achieving simultaneously high current generation and desalination performance [90,99].

11.4.5 Operation mode

Operational mode can also affect MDC performance and stability. It was reported that batch mode did not perform as well as the continuous mode in the electrode chambers because of the great internal resistance caused by the high pH imbalance and low electrolyte conductivity inside the MDC chambers [100]. Reinfusion of the anolyte and catholyte was required to maintain the stable operation of the MDC [101], yet the laborious manipulation of manual reinfusion is difficult for the scale-up of the MDC system. On the contrary, the continuous mode can be easily realized in practical scenarios compared to the complicated batch operation mode. In addition, the continuous mode provides better mixing in the electrode chambers to distribute organic carbon sources and stabilize pH, because both—organic carbon sources and a stable pH—are critical for improving power production and desalination efficiency [102]. Similarly, the continuous mode is also superior to the batch mode for the middle desalination chamber, which provides a stable salinity and internal resistance during operation and is easier to scale up.

This book belongs to Badji Mokhtar Annaba University Central Library Copyright Elsevier 2025

HRT is an important parameter in the continuous operation mode by affecting desalination rate and desalination efficiency. While lengthy HRT could improve the desalination percentage of the saltwater effluent due to slow salt loading rate. While a short HRT could increase the total desalination rate with a low salt removal percentage in the desalination effluent due to the lack of an adequate HRT for desalination. For example, a previous study showed that HRT of 20 h could realize a desalination percentage of 35%, while a decline of HRT to 6 h decreased the desalination percentage to only 12% [87]. A proper HRT needs to be designed for the MDC operation in terms of its comprehensive performance, such as organics removal, current production, and desalination.

11.4.6 Fouling and scaling

The CEM and AEM are the main components in the MDC to enable the separation of ions, and their entity and functions should be maintained to guarantee high desalination performance. However, the membranes are vulnerable to biofouling and scaling due to the existence of microbes and the transfer of organics under the electric field. The membrane scaling would gradually block ion transport channels and finally inhibit mass transport of the ions, posing a threat to the desalination efficiency and current generation. The main scale-forming ionic species are Ca^{2+} and Mg^{2+}. It was reported that only 0.4% and 0.1% of Ca^{2+} and Mg^{2+}, respectively, were transported through the CEM under the electric driving force, while the majority of these ions were precipitated on the membrane surface causing pH imbalance, internal resistance increase (from 37 to 140 Ω), and desalination efficiency decline (from 29% to 13%) [103]. Other studies also proved that Ca^{2+} and Mg^{2+} could cause severe precipitation on the membrane surface or in the packed resin and increase the internal resistance during long-term operation (Fig. 11.4D) [15,53,100,104]. Besides inorganic scaling, membrane fouling caused by organics and microorganisms could also decrease membrane permeability. The growth of bacteria on the membrane could also cause membrane degradation. It was reported that certain bacteria such as *Pseudomonas* and *Desulfovibrio* could produce toxic and corrosive substances, which could cause damage to the ultrafiltration membrane materials [105].

To solve these problems, certain approaches have been developed to alleviate membrane fouling and scaling. For example, membranes have been modified to prevent the attachment and growth of microorganisms utilizing antitoxic barrier substances [52,106]. Silver nanoparticle was reported an effective material in membrane contamination reduction [106], which is beneficial for increasing the membrane permeability and lifetime during long-term operation. In addition, increasing membrane hydrophilicity and ionic exchange capabilities could greatly increase the desalination efficiency and alleviate inorganic scaling. For example, mixing the polysulfone with a sulfonated poly-ether-ether ketone to fabricate a hybrid membrane could increase the membrane hydrophilicity and ionic transfer efficiency to increase

This book belongs to Badji Mokhtar Annaba University Central Library Copyright Elsevier 2025

the desalination efficiency [50]. Similar studies have also been extensively carried out to investigate the effect of membrane modification on scaling mitigation [51,107].

11.4.7 Mathematical modeling for operation optimization

Mathematical modeling that can simulate the process of organics degradation, current generation, and ion migration is a convenient approach to help understand the MDC working process and instruct operational optimization. Most of the models are constructed based on Nernst–Monod equation [108], and the main parameters are obtained from published information or calibration and validation utilizing experimental data [109]. By experimentally varying operational factors such as flow rate, concentration, pH, etc., of anolyte, catholyte, and saltwater, and external resistance, the obtained performance results (current, effluent concentration, etc.) can be utilized for the model calibration and validation [72,108,109]. The validated model cannot only predict the MDC performance but also help design the MDC systems and instruct their operation. For example, Ping et al. [72] developed a mathematical model to simulate the dynamic behavior of MDCs in terms of organic supply, salt loading, and current generation. After validation by experimental data from both a bench- and a large-scale MDC system, it could fit the current generation well and simulate the change of salt concentration under various operating conditions. In an improved model, the effluent conductivity with the concentration of different ionic species such as Na^+, K^+, Mg^{2+}, Ca^{2+}, Cl^-, NO_3^-, and SO_4^{2-} could be predicted at different HRT and even with a different integration of multiple MDC units [108]. However, current models face some drawbacks. The main challenge is inaccuracy. Due to the complicated bioelectrochemical process including anodic bacteria metabolism, cathodic catalysis, and ionic migration, an accurate MDC model can be hardly established because it not only needs a large number of mathematical formulas to describe the complex relationship between different processes, but also generates massive unknown parameters that can be hardly experimentally obtained or queried from published sources. Most models used the ordinary differential equation to perceive the anode, cathode, and desalination chamber as one entity, while the distribution of the organic or ionic species inside each chamber is often neglected. Useful models need to be developed to help design high-performance MDC systems.

11.5 Microbial desalination cell application

11.5.1 Wastewater treatment

11.5.1.1 Domestic wastewater

Domestic wastewater has a relatively low organic concentration with COD of 100–1000 mg/L. With an HRT of several hours and days in the anode chamber, the

This book belongs to Badji Mokhtar Annaba University Central Library Copyright Elsevier 2025

COD loading is about 1–2 kg COD/(day · m^3-anode volume) [110] (energy contained in COD of about 14.7 kJ/g [111,112]), which indicates that chemical energy of 4-8 kWh is input to the anode (per 1 m^3) per day and could be utilized for energy extraction during its treatment [2]. Since the domestic wastewater contains no refractory species and its organic species can be easily biologically degraded, the treatment of domestic wastewater is efficient in MDC. The removal efficiency of organic species can typically reach >60% under anaerobic biological metabolism in the anode chamber [30,91,96]. However, due to the substantial decline in electricity production and desalination performance with the increase of organics removal, the organics removal efficiency in MDC anode can hardly reach >90%. In addition, the anaerobic biological reaction in the anode chamber cannot remove nutrients, resulting in unqualified effluent quality for direct discharge or reuse. To address these problems, continuously flowing wastewater from the anaerobic anode to the aerobic cathode has been developed [25,26,28,29]. This approach could easily improve the removal of organic to over 90% due to the sequential anaerobic and aerobic biodegradation process [25,26,28,29]. With proper placement of the ion exchange membranes between the anode and cathode, this approach could also extract cationic (NH_4^+) and anionic (NO_3^-, $H_xPO_4^{x-3}$) nutrients from anode and cathode chambers respectively to the middle membrane stack, realizing nutrients removal efficiency of over 90% [25,26,28,29]. This hydraulic connection between the anode and the cathode could greatly improve the treatment efficiency of domestic wastewater and enable its post-discharge or reuse.

11.5.1.2 Industrial wastewater

The sources of the industrial wastewater are extensively variable, including pesticide application, food and chemical product preservatives, incineration of municipal waste, leather and circuit industry, and other manufacturing-related industrial processes [113]. Compared with domestic wastewater, these industrial sources can produce wastewater with massive quantities of refractory organics and high salinity, combined with multiple heavy metals [113]. Traditional MDC could be utilized for biodegradation of refractory organics. For example, industrial dyes such as Malachite Green and Sunset Yellow can be effectively degraded with two bacterial strains, *Bacillus subtilis moh3* and MTCC (Microbial Type Culture Collection Centre, Chandigarh, India) strain *Aeromonas hydrophila* subsp. *hydrophila 8049*, with maximum removal efficiency reaching over 90% in the anode chamber. However, since industrial wastewater often possesses high-strength organics, a single unit of MDC anode cannot completely remove the organic species in the industrial wastewater. Therefore, multistage MDCs containing an alternative anaerobic anode and aerobic cathode chambers have been constructed to address this problem. For example, a 2.8 L multistage MDC was applied to treat the diluted industrial wastewater (COD = 8723 mg/L, conductivity of 24,612 μS/cm) (Fig. 11.5A) [27]. With the wastewater flowing serially from anode-1

This book belongs to Badji Mokhtar Annaba University Central Library Copyright Elsevier 2025

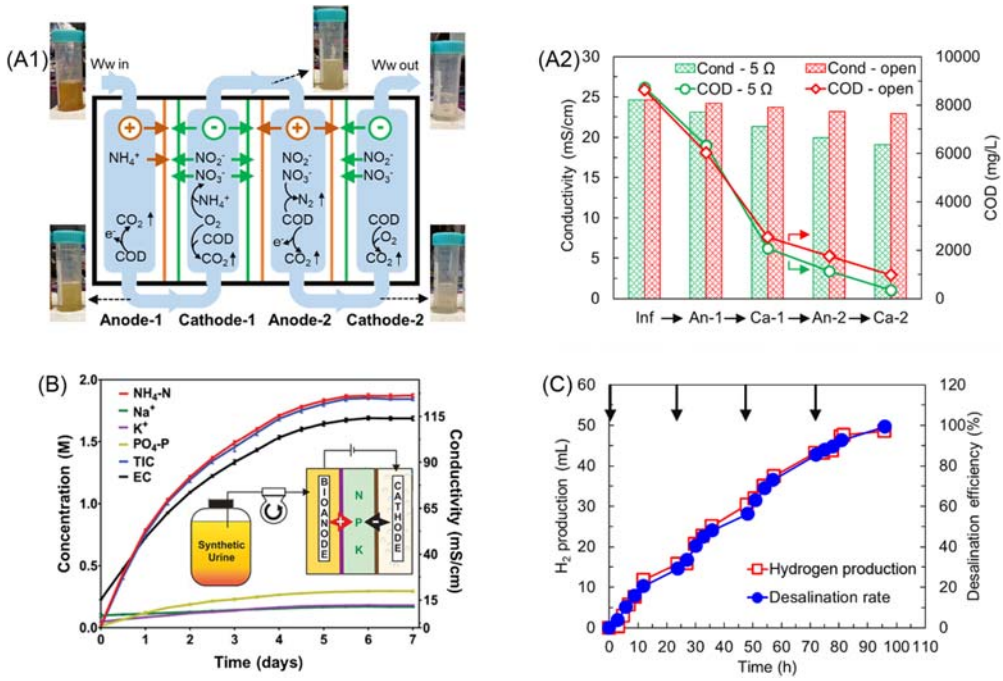

Figure 11.5 The functions MDC technology. (A) Construction of a multistage MDC for advanced treatment of high-strength industrial wastewater, with (A1) showing the configuration and mechanism and (A2) illustrating the removal of organics and salinity in different chambers. *Ww*, wastewater; *Cond*, conductivity; *Inf*, influent; *An*, anode chamber; *Ca*, cathode chamber. (B) Midcompartment up-concentration of key species NH_4-N, Na^+, K^+, PO_4^-P, and total inorganic carbon (TIC) and electric conductivity (EC) versus time at an average current density of 29.3 A/m^2. Insert shows the schematic. (C) Accumulated H_2 production and desalination efficiency in MEDC during batch operation with an applied voltage of 0.8 V. Arrows indicate electrolytes replacement. *For (A) Reproduced with permission from K. Zuo, J. Chang, F. Liu, X. Zhang, P. Liang, X. Huang, Enhanced organics removal and partial desalination of high strength industrial wastewater with a multi-stage microbial desalination cell. Desalination 423 (2017) 104–110, copyright © 2017 Elsevier B. V.; (B) Reproduced with permission from P. Ledezma, J. Jermakka, J. Keller, S. Freguia, Recovering nitrogen as a solid without chemical dosing: bio-electroconcentration for recovery of nutrients from urine. Environ. Sci. Tech. Lett. 4 (2017) 119–124, copyright © 2017 American Chemical Society; (C) Reproduced with permission from H. Luo, P.E. Jenkins, Z. Ren, Concurrent desalination and hydrogen generation using microbial electrolysis and desalination cells. Environ. Sci. Technol. 45 (2010) 340–344, copyright © 2011 American Chemical Society.*

to cathode-1, anode-2, and cathode-2, the COD removal efficiencies were 27.5%, 48.7%, 10.7%, and 9.0%, respectively, in each chamber. The removal efficiencies of COD, nitrogen, and salinity reached 95.9%, 89.2%, and 22.3%, respectively, in the final effluent, indicating superior removal of the high-strength organic species. To further improve the removal of salinity in industrial wastewater, an external voltage can be added to drive the migration of ions. By adding an external voltage of 1 V, the

This book belongs to Badji Mokhtar Annaba University Central Library Copyright Elsevier 2025

salinity removal efficiency could be further increased to 31.6%, realizing enhanced desalination efficiency of the high salinity industrial wastewater. However, the applied external voltage cannot exceed 1.2 V because the produced oxygen—due to water decomposition on anode at high external voltage—would be harmful to the anaerobic biological metabolism to produce electricity [114].

Besides organics, the high concentration of heavy metals in industrial wastewater is another perplexing problem to solve, and the multistage MDC could become an effective solution due to its high-cost efficiency. The electric driving force provided by MDC could migrate metal ions from the original wastewater into the concentration chamber [115]. For example, a four-chambered MDC was constructed to treat wastewater containing Cu(II) at an initial concentration of 800 mg/L, the removal efficiency of Cu(II) reached 94.1% [116]. Several other heavy metals (e.g., Hg, Ni) could also be removed from the collected wastewater [53].

11.5.2 Water desalination

11.5.2.1 Seawater desalination

One of the main functions of MDC is water desalination. Compared with conventional energy-intensive technologies such as RO, ED, and thermal processes (multieffect distillation, etc.), MDC possesses the advantage of low energy consumption [117,118]. Seawater desalination is a major interest for MDC research, and experiments have been intensively performed using synthetic and real seawater. It was reported that the desalination efficiency of synthetic saltwater could reach >90% with sufficient HRTs [9,54]. The main reason for efficient seawater desalination is due to the concentration gradient, which is conducive to the ion migration from the high-strength seawater in the middle chamber to the low concentration of domestic wastewater in the anode chamber. In addition, the main species in seawater is NaCl, where the Na^+ and Cl^- possess smaller charge and size compared to other divalent cationic and anionic species (Ca^{2+}, Mg^{2+}, SO_4^{2-}, etc.), and is easier to be electrically removed [86]. Nevertheless, the desalination efficiency of real seawater is lower than synthetic seawater, mainly due to the complicated species (organics, scale-forming ions, bacteria, etc.) causing bad effects (organic/biofouling, scaling, etc.) on MDC membranes. It was reported that with the presence of Ca^{2+} or Mg^{2+}, the desalination efficiency would gradually decrease due to ionic scaling on the ionic exchange [103,119], which reduces ion transfer rate and decreases the MDC desalination performance. Therefore, certain measurements such as pretreatment should be taken into consideration to address this problem for the real application of MDC in seawater desalination.

11.5.2.2 Brackish water desalination

Besides the seawater, MDCs could also achieve a high desalination rate of the brackish water, which typically possesses a salinity of 1—5 g/L [91,120]. Since brackish water has lower salinity than seawater, the MDCs could realize higher desalination efficiency with a

This book belongs to Badji Mokhtar Annaba University Central Library Copyright Elsevier 2025

shorter operation time (or HRT) and a smaller MDC volume. However, the low salinity in brackish water also causes reduced conductivity and an increase in the internal resistance of the MDC system, which in turn impedes the desalination efficiency of the MDC. To address this problem, resin-packed MDC could be utilized. It was reported that the addition of ion exchange resins could increase the desalination rate by 1.5−8 times with a decrease of internal resistance by 55%−272% [12]. The addition of ion exchange resins could treat the brackish water with low salinity (0.70 g/L) and high removal efficiency (greater than 90%) [12]. Another study indicated that a scale-up resin-packed stacked MDC with a volume of 10 L could reach the desalination efficiency of 95.80% for brackish water [13], with effluent conductivity comparable to the effluent from one stage RO. Furthermore, other configurations of MDCs such as microbial capacitive desalination cells have been proved efficient in achieving high desalination efficiency for water with low salinity [121,122].

11.5.2.3 Water softening

Traditional water softening methods include lime soda addition, ion exchange resin, nanofiltration, RO, ED, etc. [54] for reducing the hardness (Ca^{2+}, Mg^{2+}) in water. However, these traditional methods often produce large quantities of sludge [104], require posttreatment, for example, regeneration utilizing harsh chemicals, or are energy intensive. Therefore, MDCs could be utilized for water softening with low energy consumption and no need for posttreatment. For example, a bench-scale MDC was utilized in a previous study to soften the hard water collected from several places, and it was reported that more than 90% of the hardness could be removed [104]. Nevertheless, the risk of membrane scaling induced by these inorganic species cannot be ignored in water softening, operation conditions should be optimized to alleviate this problem.

11.5.3 Resource recovery

11.5.3.1 Nitrogen and phosphorus recovery

Given MDCs migrate the ions from the wastewater or seawater into the concentration chambers to produce brine and enrich ions [123], MDCs have a high potential to recover and collect the valuable ions from wastewater. Nutrients including nitrogen (NH_4^+, NO_3^-, etc.) and phosphorus are the most common wastes and valuable species in domestic wastewater [124]. Efforts have been made in traditional methods to remove nitrogen and phosphorus utilizing alternating anaerobic and aerobic conditions to realize nitrification, denitrification, phosphorus adsorption/release, and even anammox processes [124]. However, these processes are complicated and slow, and they remove these valuable species without recovery.

Fortunately, MDCs extract the chemical energy from the wastewater to drive the recovery of valuable species by utilizing suitable configuration and operational strategies. In one study, the ammonium-containing wastewater is treated as saline water and

This book belongs to Badji Mokhtar Annaba University Central Library Copyright Elsevier 2025

desalinated in the middle desalination chamber, while the ammonium is transferred and accumulated into the cathode and could be recovered by aeration stripping [125], with recovery efficiency reaching 80 g-N/($m^2 \cdot$ day). In another study, the CEM is placed facing the anode and the AEM facing the cathode (Fig. 11.5B), an MDC design that allows the transportation of cations and anions from the anode and cathode, respectively, into the middle chamber under the influence of an electrochemical current. The benefit of this design lies in the MDC simultaneously recovering multiple cations (e.g., NH_4^+ and K^+) from the anode chamber and anions (NO_3^- etc.) from the cathode chambers. For example, it was previously reported that the recovery rates of N, P, and K could reach 7.18, 0.52, and 1.62 kg/($m^3 \cdot$ day), respectively for the treatment of urine [126]. Other studies have also been reported using MDC to recover nutrients, even volatiles fatty acids, from different types of wastewaters (e.g., effluent from anaerobic digestion) [123,127,128]. The recovered solution could be applied as farmland fertilizer substitutes to achieve waste reuse.

However, it should be noted that nutrient recovery in MDC might encounter certain problems. For example, back diffusion of the accumulated nutrient species due to concentration gradient could decrease the recovery efficiency. Continuous reinfusion of the corresponding solution to reduce the concentration gradient is a good strategy to maintain the ionic migration rate [129,130]. Other strategies such as aeration stripping for ammonia and precipitation for phosphorus could also address the nutrient accumulation problem. In addition, ionic competition between background ions (e.g., Na^+ Cl^-) and target nutrients is another problem to inhibit nutrients migration rate [131]. Developing nutrients-selective ion exchange membranes may improve the transfer of nutrients and mitigate competitive ion migration, realizing selective recovery of target valuable species.

11.5.3.2 Chemical and gas production

Besides nutrient recovery, the production of valuable chemicals as another approach for resource recovery can also be realized in the MDC system. For example, applying an additional voltage to enable the hydrogen evolution reaction can be realized in the MDC cathode to achieve simultaneous desalination and hydrogen production. This system was called microbial electrolysis and desalination cell (MEDC) [132,133]. It was previously reported that the MEDC system could achieve a maximum H_2 production rate of 1.5 $m^3/(m^3 \cdot$ day) from the cathode chamber (Fig. 11.5C) [133]. Instead of using external voltage, utilizing chemical energy contained in the concentration difference between different saltwater streams can also drive the production of hydrogen in the cathode, which is the microbial reverse-electrodialysis electrolysis cell (MREDC) [134–137]. Besides hydrogen gas, other chemicals could also be produced in the electrode chambers or the middle membrane stack in MDC. For example, by utilizing BPMs, acid and alkali can be produced in the membrane stack [138]. While in the cathode, alkali can also be accumulated and recovered. In addition, other species

This book belongs to Badji Mokhtar Annaba University Central Library Copyright Elsevier 2025

such as methane [137] and H_2O_2 [139], can also be produced with the addition of chemical energy from the concentration gradient between saltwater and fresh water. However, the common problems in MDC could also affect the performance of MDC for chemical production, including pH change in the cathode, fouling of ion exchange membranes, an increase of internal resistance, etc. Optimization of operational mode and parameters may resolve these problems.

11.5.3.3 Heavy metal recovery

While many conventional methods have been applied to remove the heavy metals from the wastewater, such as chemical precipitation, ion-exchange, adsorption, membrane filtration, and electrodialysis [140], still the fact remains that these methods—though they are efficient in removing metals—demand high energy and strict operating conditions to perform. MDCs can avoid the above drawbacks and, simultaneously, achieve the organic and heavy metal removal. The currently popular strategy to recover the heavy metals is to use stacked MDCs to drive the targeted heavy metal ions to the collection chamber and, then, perform electrochemical reactions to collect metal precipitate or compounds on the electrode surface. For example, An et al. constructed a four-chamber MDC system to separate Cu^{2+} from the wastewater and reduced Cu^{2+} to Cu_2O and Cu deposits on the cathode [116]. Using similar strategies, other heavy metals could also be recovered. For example, Cr^{6+} could be reduced to Cr_2O_3 and deposited on the cathode surface [141]. Heavy metals could also be transformed into stable sludge form for the following recovery process [142]. Furthermore, multistage MDC could also be utilized to enrich heavy metals. The concentrated metal solution could be applied for the postphysiochemical processes (e.g., precipitation) for recovery.

11.6 Integrating microbial desalination cells with existing technologies

Besides the application of a single MDC for water treatment, the desalination performance can be enhanced by combining MDC with different desalination technologies. Researchers have investigated the feasibility of utilizing MDCs as a pretreatment or posttreatment process for reverse osmosis [20], forward osmosis, and electrodialysis [54].

11.6.1 Integration of microbial desalination cell with RO

Nowadays, RO stands as a dominant option for harnessing freshwater from brackish water and seawater, where approximately 69% of global desalination capacity is dominated by RO plants [143]. However, the downside of the RO technology is in its

This book belongs to Badji Mokhtar Annaba University Central Library Copyright Elsevier 2025

being energy-intensive and, hence, a costly process. Thermodynamically, the required energy to retrieve 50% of freshwater from a 35 g/L TDS simulated seawater solution by RO is 1.06 kWh/m^3 [144]. However, this value increases to 3–4 kWh/m^3 when the entire system including the pretreatment of feed solution and pumping is considered [144]. In a conventional RO technology, the energy required to desalinate water is proportional to the influent water salinity. Therefore, coupling MDC technology as a predesalination system could reduce the water salinity before it is further desalinated within RO, thus decreasing the energy consumption by the downstream RO device. In addition, since MDC is a zero-energy consuming technology that drives the desalination process by extracting energy from organics contained in wastewater, this type of integration would decrease the total energy consumption for water desalination. For example, if an RO is coupled with an upflow MDC as the preceding process that can remove 30% of TDS in saline water for the downstream RO, then the energy requirement for the downstream RO could decrease from 3.7 to 3.5 kWh/m^3 [86]. Under this condition, if considering the bioelectricity generated by the upflow MDC, then the energy needed for the integrated system can be further decreased to 2.9 kWh/m^3, thereby decreasing about 21% of the overall energy cost of an RO system without the upflow MDC.

Besides the energy-saving aspect, other aspects such as operation stability and system compatibility also need to be considered in the MDC-RO integrated system. In the MDC, ions are driven by an electric field to permeate the ion exchange membranes (IEMs). As a result, MDCs are resistant to suspended solids and scalant ions [145]. As a comparison, water molecules are driven by pressure to permeate through the RO membranes, while almost all ions are rejected by RO membranes. The accumulation of ions (especially scalant ions such as Ca^{2+}, Mg^{2+}, SO_4^{2-}, and CO_3^{2-}, etc.) on the feed side of the RO membrane can cause serious scaling, resulting in a decline of water production and membrane lifetime. Therefore, coupling MDC, which is more resistant to both organic and inorganic fouling/scaling, as the pretreatment process could not only help improve desalination performance but also mitigate the scaling of the downstream RO membrane. In addition, despite both IEMs and RO membranes being susceptible to fouling/scaling by organic and inorganic substances in the feed solution, IEMs could be easily cleaned compared to RO membranes [146]. Besides the application of MDC as a pretreatment process, MDC can also work as a posttreatment unit for an RO system to enhance the removal of pollutants that can be hardly removed by the RO membrane. For example, boron is a challenging pollutant for the RO membrane, especially at neutral pH, but its removal may be improved in an MDC process under an electric field. In addition to boron, an MDC could also be applied to selectively eliminate several heavy metals, such as arsenic, chromate, etc. after the RO process [20].

In addition, the desalination capacity of MDC and RO should also be taken into consideration during the integration of the two systems. In the MDC process, despite the

This book belongs to Badji Mokhtar Annaba University Central Library Copyright Elsevier 2025

desalination efficiency of >90% for seawater-level saline water, which has been reported in many studies [147], still MDC needs large volumes of freshwater (low salinity wastewater) working as an anolyte and catholyte to receive the salt. The ratio of the consumed anolyte to the resulting desalinated water can range from ten to over one hundred [74,148,149]. This requirement not only brings difficulty in the acquisition of large volumes of wastewater but also increases the pumping cost and system complexity. Both factors could affect the cost efficiency of the MDC-RO integrated system.

11.6.2 Integration of microbial desalination cell with FO

Unlike an RO system that recovers pure water from saline feed solution driven by high pressure, an FO reactor extracts water from low concentration feed solution to the high concentration draw solution driven by the osmotic pressure caused by concentration difference [150]. In an MDC, low-salinity solutions are used as anodic and cathodic electrolytes, and high-salinity water is desalinated in the middle chamber. Therefore, the MDC and FO can be integrated into three modes (Fig. 11.6):

1. FO-MDC system: the wastewater and seawater are used as the feed and draw solution, respectively, of an FO cell, so that their corresponding effluents are then worked as the anolyte and saltwater, respectively, in the MDC. Finally, the anolyte effluent flows to the cathode working as catholyte [82];
2. MDC-FO system: the effluent of the desalination chamber in an MDC is sent as feed to the FO cell, and the FO feed effluent solution is then sent back again toward the desalination compartment in the MDC [151];
3. MDC-FO-MDC system: the anodic wastewater effluent of the MDC flows to the feed of the FO system, where the water in the feed is extracted to the draw solution. The diluted draw solution of the FO cell effluent is finally sent back to the MDC desalination chamber to remove ionic species, realizing the production of high-quality water.

These three coupling modes have different performance indicators and properties.

For the first type of FO-MDC integrated system, the water in the low-salinity wastewater is extracted by the seawater in the FO system, realizing enrichment of the organics in the feed effluent and salinity decline of the draw solution. The enriched COD concentration is conducive to electricity generation in the downstream MDC anode, while the diluted draw solution effluent can also be further desalinated in the MDC desalination chamber. As a result, this type of integrated system has been known to recover five-volume units of clean water (desalination efficiency of 95.7%) with a one-volume unit of seawater [82]. In addition, organics in the wastewater can also be effectively removed (>60.7%) with wastewater flowing serially from the anaerobic anode to the aerobic cathode. Compared with the synergistic integration of MDC and FO in the first mode, the concept of the second integration mode is simple: to extract

This book belongs to Badji Mokhtar Annaba University Central Library Copyright Elsevier 2025

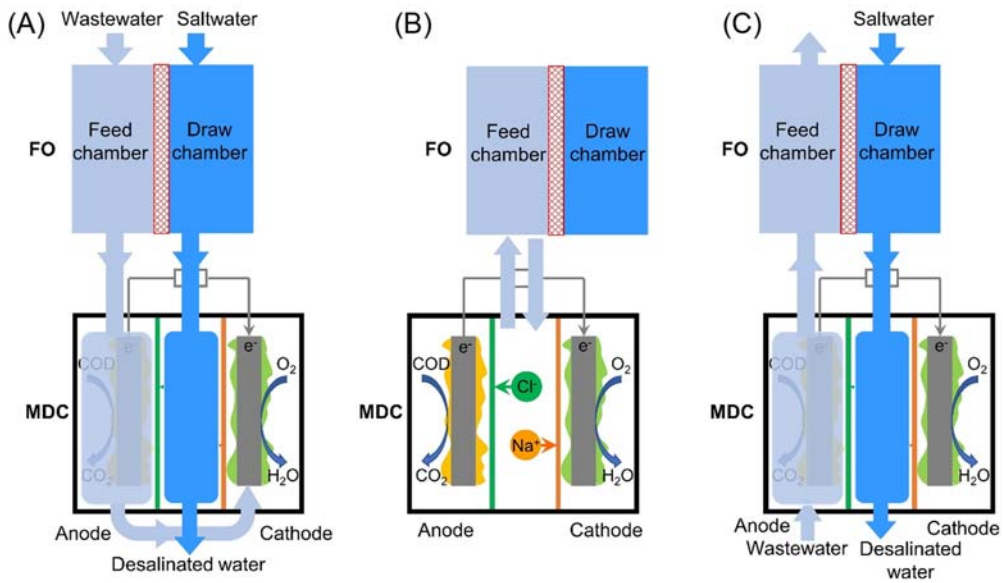

Figure 11.6 Three types of integration mode for MDC-FO system. (A) FO-MDC system; (B) MDC-FO system; and (C) MDC-FO-MDC system.

as much water as possible from the feed solution by the FO system, an MDC is utilized to continuously remove the accumulated salt in the FO feed solution. This coupling mode could realize water recovery as high as 83.5% from landfill leachate [151], which is high and provides a great approach for efficient water recovery from refractory wastewaters. The third integration mode is similar with the first integration mode except that the flow direction of wastewater is opposite. It also shares similar benefits: (1) the FO process in the MDC-FO system could reduce the volume of wastewater and recover high-quality water, thereby improving wastewater reuse; (2) the decreased volume of wastewater is also conducive to its posttreatment; (3) compared with the integration mode, the pretreatment of organics in MDC anode is conducive to the mitigation of membrane fouling of the downstream FO system.

In addition to the improved performance of the integrated system, some challenges remain to be addressed. First, the treatment capacity between FO and MDCs must be well-coordinated, given the fact that FO treatment is usually fast while MDCs are always slow due to their biological processes. Such differences suggest that to guarantee adequate MDC HRT, the volume of the MDC should be significantly larger than that of the FO [151]. Second, reverse salt flux, which is a serious problem in the FO process, also needs to be carefully addressed in the integrated system to ensure desalination performance. In addition, the energy consumption of the integrated system should be properly evaluated. In the MDC and FO integrated system, electricity can be produced in the MDC, while the FO unit extracts water driven by the concentration gradient and requires no energy

This book belongs to Badji Mokhtar Annaba University Central Library Copyright Elsevier 2025

input (pressure, electricity, etc.) Therefore, the integrated system with a specific configuration and wastewater condition needs to be examined for energy input.

11.7 Challenges and perspectives

Compared to other energy-intensive wastewater treatment processes, MDC provides great potential for sustainable desalination and renewable energy production, and it adds value to wastewater. Recent developments in reactor design, materials selection, and operating optimization have significantly improved the cost-efficiency of MDC. However, several challenges remain to be addressed to push MDCs towards practical application.

11.7.1 Relatively low performance

The main limitation of an MDC is its relatively low performance on wastewater treatment and desalination. In an MDC, wastewater treatment is realized in the anode chamber depending on the biological metabolism of electrochemically active bacteria, which occurs in an anaerobic condition so that the biological reactions are typically slow. As a result, prolonged HRT ranging from several hours to days is needed in an MDC for complete degradation of organic pollutants, which is much longer than conventional aerobic treatment processes and membrane bioreactors. The prolonged HRT also results in a large reactor size, resulting in high capital costs and large footprint. Besides the decelerated anodic biological metabolism, the sole anaerobic process in the anode chamber can also hardly remove nutrients that often require alternating anaerobic/aerobic/oxic treatment in conventional activated sludge processes. As a result, the slowly removed nutrients and organic species in the wastewater effluent may need posttreatment before being reused or discharged into natural water bodies.

Besides wastewater treatment, the electricity produced by the MDC also illustrates low voltage and power density. Therefore, it is impossible to desalinate saltwater at high salt removal speeds or to an extremely high salt removal efficiency (percentage) to produce pure water. An MDC can only partially desalinate saltwater with desalination speed and salt removal percentage lower than other technologies such as RO, membrane distillation [152], and even CDI [153,154], etc. Besides the limited desalination percentage in the saltwater, the low voltage of MDC also limits the salt enrichment efficiency in brine, which results in large volumes of produced brine with relatively low concentration factor especially in stacked MDCs. As a result, MDCs not only produce large quantities of brine that need further treatment but also achieve low

This book belongs to Badji Mokhtar Annaba University Central Library Copyright Elsevier 2025

recovery of desalinated water. In addition, since osmotic water transport from the desalination chamber to the electrode chambers occurs during the operation of an MDC, the long HRT of saltwater in the desalination chamber caused by the low desalination speed further increases the loss of desalinated water, leading to the decrease of water recovery.

To address these limitations, one strategy is incorporating MDCs with existing wastewater treatment technologies to achieve further sustainability. It is proven that MDCs can be used as pretreatment or posttreatment of the RO or FO systems to improve the overall performance on wastewater treatment and saltwater desalination and to reduce the overall cost [90]. Another potential strategy is applying MDC for valuable species recovery during water treatment, such as nutrients, noble metals, etc., instead of just for water desalination [123]. This application could add value to the MDC technology and enhance its cost-efficiency.

11.7.2 Instability

Most of the previous MDCs are operated in batch mode, which causes unstable performance during the operation. The pH change is the main issue in MDC, it decreases in the anode chamber and increases in the cathode chamber during operation. As a result, the decreased pH in anode chamber not only affects the activity of anodic microorganism but also increases the overpotential, both effects would weaken the power generation and decrease desalination performance. Besides pH change in the electrode chambers, the conductivity in the saltwater decreases while that of the electrolyte increases with operation time. The decrease of conductivity in saltwater increases the ohmic resistance of the MDC, which would cause the decline of current production and inhibit further desalination of the saltwater. Properly increasing the conductivity of the electrolyte could decrease the ohmic resistance of the electrode chamber, but exorbitant salinity could also inhibit the bacteria activity thus reducing power generation.

Not only is the batch operation mode the cause of performance decline but also the continuously operating mode of the MDC could do the same during long-term operation. The main long-term effect in MDC is biofouling of IEM adjacent to the anode chamber and inorganic scaling of the IEM adjacent to the cathode chamber. Biofouling is an important phenomenon that occurs as a result of microbial adhesion or absorption on the surface of the membrane, developing a gluey polymeric layer of a biofilm [103]. The biofouling process not only decreases the ion permeability of IEM but may also cause degradation of the IEM, decreasing its ion separation efficiency. Inorganic scaling often occurs on the cathode IEM due to the accumulation of scaling ions (Ca^{2+}, Mg^{2+}, SO_4^{2-}, CO_3^{2-}, etc.) and increase of pH [15], even as it can also affect IEM property and desalination performance. Besides membrane fouling and scaling, the activity of anodic microorganisms and cathodic catalysts may also

This book belongs to Badji Mokhtar Annaba University Central Library Copyright Elsevier 2025

decrease during long-term operation. The deterioration of anode microorganisms is often caused by the growth, aging, or other impacts (blocking, toxicity, etc.) of the biofilm. On the other hand, the decreased activity of the cathode catalyst is often caused by fouling, scaling, and/or poisoning by reaction with other substances. In addition, the carbon-based electrode materials in the anode are also reported degradable during long-term operation, which would also cause the decreased performance of the MDC.

11.7.3 Scale-up and high cost

Since its invention, the MDC has been developed for over 10 years now and has gone through a series of development cycles, with the largest size being reported as 105 L [30] which realizes 2A of bioelectricity generation and 9.2 kg/($m^3 \cdot$ day) of salt removal. Several unpublished studies (Xia Huang et al. in Tsinghua University, China) have increased the volume of an MDC unit to over 200 L and used it in the wastewater treatment plant for real wastewater treatment and desalination. Nevertheless, even this MDC volume is too small to meet today's clean water needs, where the liquid volume in the real, practical applications can range from hundreds to thousands of cubic meters per hour. Since the difficulty increases exponentially with the increase of reactor size, a potential strategy for MDC scale-up is coupling multiple MDC units into arrays. Mathematical modeling can be utilized as a powerful tool to guide the design and management of the multiple MDC units, in terms of hydraulic connection, electric connection, and operation such as water flow rate and electricity management. Besides multiple MDCs integration, incorporating MDCs with other water treatment processes such as RO and FO could also have benefits in its performance improvement. A life cycle assessment on the cost efficiency of the incorporated systems should be performed to move MDCs towards practical application.

11.8 Conclusion

In this chapter, a comprehensive review of the MDC has been presented while attempting to highlight the fundamental principle, configuration development, possible applications, and advances in the field of saltwater desalination and wastewater treatment. MDCs are derived from MFCs, and they are still at a very early stage of research. The recent development has greatly improved the MDC configuration, including stacked MDC, resin-packed MDC, photoactive MDC, capacitive MDC, and multistage MDC. The performance of MDC has also been improved by optimizing key influential factors such as internal resistance, solution pH, and operational conditions. As a result, MDCs can

This book belongs to Badji Mokhtar Annaba University Central Library Copyright Elsevier 2025

be utilized in various applications including water softening, heavy metals removal, chemical production, and resources recovery. However, many obstacles including relative low performance, instability, difficulty in scale-up, and high cost hinder the application of MDC for wastewater treatment and saltwater desalination. Therefore, we should understand the unique requirements of MDCs in different application scenarios to realize their cost-effective application.

Integrating multiple MDCs or incorporating MDCs with existing water treatment processes is a good strategy to scale up the MDC technology and enable their function for practical wastewater treatment and saltwater desalination. Mathematical modeling can be a powerful tool to guide the design and management of the integrated MDC system in terms of hydraulic connection and electricity management. Besides water treatment and desalination, recovering value-added resources from wastewater can be another attractive application for MDCs, in which attempt the requirement on MDC size and cost is relatively not strict, and the advantage of low energy consumption in MDC can be fully highlighted. However, meticulous future investigations concerning long-term effects of MDC operation such as membrane scaling/fouling, electrodes stability, microbial growth, and catalyst durability are needed to improve the feasibility of the MDC for practical applications.

References

[1] K. Xiao, Y. Xu, S. Liang, T. Lei, J. Sun, X. Wen, et al., Engineering application of membrane bioreactor for wastewater treatment in China: current state and future prospect, Front. Environ. Sci. Eng. 8 (2014) 805–819.
[2] E.S. Heidrich, T.P. Curtis, J. Dolfing, Determination of the internal chemical energy of wastewater, Environ. Sci. Technol. 45 (2011) 827–832.
[3] P.L. McCarty, J. Bae, J. Kim, Domestic wastewater treatment as a net energy producer-can this be achieved? Environ. Sci. Technol. 45 (2011) 7100–7106.
[4] K.C. Zuo, H. Liu, Q.Y. Zhang, P. Liang, X. Huang, C.D. Vecitis, A single-use paper-shaped microbial fuel cell for rapid aqueous biosensing, ChemSusChem 8 (2015) 2035–2040.
[5] Y. Feng, W. He, J. Liu, X. Wang, Y. Qu, N. Ren, A horizontal plug flow and stackable pilot microbial fuel cell for municipal wastewater treatment, Bioresour. Technol. 156 (2014) 132–138.
[6] R.D. Cusick, B. Bryan, D.S. Parker, M.D. Merrill, M. Mehanna, P.D. Kiely, et al., Performance of a pilot-scale continuous flow microbial electrolysis cell fed winery wastewater, Appl. Microbiol. Biotechnol. 89 (2011) 2053–2063.
[7] B.H. Kim, H.J. Kim, M.S. Hyun, D.H. Park, Direct electrode reaction of Fe(III)-reducing bacterium, *Shewanella putrefaciens*, J. Microbiol. Biotechnol. 9 (1999) 127–131.
[8] G.G. Kumar, Z. Awan, K.S. Nahm, J.S. Xavier, Nanotubular MnO_2/graphene oxide composites for the application of open air-breathing cathode microbial fuel cells, Biosens. Bioelectron. 53 (2014) 528–534.
[9] X.X. Cao, X. Huang, P. Liang, K. Xiao, Y.J. Zhou, X.Y. Zhang, et al., A new method for water desalination using microbial desalination cells, Environ. Sci. Technol. 43 (2009) 7148–7152.
[10] X. Chen, X. Xia, P. Liang, X. Cao, H. Sun, X. Huang, Stacked microbial desalination cells to enhance water desalination efficiency, Environ. Sci. Technol. 45 (2011) 2465–2470.
[11] N.A. Shehab, G.L. Amy, B.E. Logan, P.E. Saikaly, Enhanced water desalination efficiency in an air-cathode stacked microbial electrodeionization cell (SMEDIC), J. Membr. Sci. 469 (2014) 364–370.

This book belongs to Badji Mokhtar Annaba University Central Library Copyright Elsevier 2025

[12] F. Zhang, M. Chen, Y. Zhang, R.J. Zeng, Microbial desalination cells with ion exchange resin packed to enhance desalination at low salt concentration, J. Membr. Sci. 417 (2012) 28–33.
[13] K. Zuo, J. Cai, S. Liang, S. Wu, C. Zhang, P. Liang, et al., A ten liter stacked microbial desalination cell packed with mixed ion-exchange resins for secondary effluent desalination, Environ. Sci. Technol. 48 (2014) 9917–9924.
[14] A. Morel, K.C. Zuo, X. Xia, J.C. Wei, X. Luo, P. Liang, et al., Microbial desalination cells packed with ion-exchange resin to enhance water desalination rate, Bioresour. Technol. 118 (2012) 43–48.
[15] K.C. Zuo, L.L. Yuan, J.C. Wei, P. Liang, X. Huang, Competitive migration behaviors of multiple ions and their impacts on ion-exchange resin packed microbial desalination cell, Bioresour. Technol. 146 (2013) 637–642.
[16] X. Chen, D.Y. Sun, X.Y. Zhang, P. Liang, X. Huang, Novel self-driven microbial nutrient recovery cell with simultaneous wastewater purification, Sci. Rep. 5 (2015).
[17] S.T. Ren, M.C. Li, J.Y. Sun, Y.H. Bian, K.C. Zuo, X.Y. Zhang, et al., A novel electrochemical reactor for nitrogen and phosphorus recovery from domestic wastewater, Front. Environ. Sci. Eng. 11 (2017).
[18] Q.Y. Ping, I.M. Abu-Reesh, Z. He, Boron removal from saline water by a microbial desalination cell integrated with donnan dialysis, Desalination 376 (2015) 55–61.
[19] H.P. Luo, H. Li, Y.B. Lu, G.L. Liu, R.D. Zhang, Treatment of reverse osmosis concentrate using microbial electrolysis desalination and chemical production cell, Desalination 408 (2017) 52–59.
[20] A. ElMekawy, H.M. Hegab, D. Pant, The near-future integration of microbial desalination cells with reverse osmosis technology, Energy Environ. Sci. 7 (2014) 3921–3933.
[21] M. Mehanna, T. Saito, J.L. Yan, M. Hickner, X.X. Cao, X. Huang, et al., Using microbial desalination cells to reduce water salinity prior to reverse osmosis, Energy Environ. Sci. 3 (2010) 1114–1120.
[22] H.Y. Yuan, I.M. Abu-Reesh, Z. He, Enhancing desalination and wastewater treatment by coupling microbial desalination cells with forward osmosis, Chem. Eng. J. 270 (2015) 437–443.
[23] Y.B. Lu, Z. He, Mitigation of salinity buildup and recovery of wasted salts in a hybrid osmotic membrane bioreactor-electrodialysis system, Environ. Sci. Technol. 49 (2015) 10529–10535.
[24] K. Zuo, Z. Wang, X. Chen, X. Zhang, J. Zuo, P. Liang, et al., Self-driven desalination and advanced treatment of wastewater in a modularized filtration air cathode microbial desalination cell, Environ. Sci. Technol. 50 (2016) 7254–7262.
[25] K. Zuo, M. Chen, F. Liu, K. Xiao, J. Zuo, X. Cao, et al., Coupling microfiltration membrane with biocathode microbial desalination cell enhances advanced purification and long-term stability for treatment of domestic wastewater, J. Membr. Sci. 547 (2018) 34–42.
[26] F.B. Liu, L.S. Wang, K.C. Zuo, S. Luo, X.Y. Zhang, P. Liang, et al., A novel operational strategy to enhance wastewater treatment with dual-anode assembled microbial desalination cell, Bioelectrochemistry 126 (2019) 99–104.
[27] K. Zuo, J. Chang, F. Liu, X. Zhang, P. Liang, X. Huang, Enhanced organics removal and partial desalination of high strength industrial wastewater with a multi-stage microbial desalination cell, Desalination 423 (2017) 104–110.
[28] K.C. Zuo, F.B. Liu, S.T. Ren, X.Y. Zhang, P. Liang, X. Huang, A novel multi-stage microbial desalination cell for simultaneous desalination and enhanced organics and nitrogen removal from domestic wastewater, Environ. Sci. Wat. Res. 2 (2016) 832–837.
[29] F.B. Liu, S. Luo, H. Wang, K.C. Zuo, L.S. Wang, X.Y. Zhang, et al., Improving wastewater treatment capacity by optimizing hydraulic retention time of dual-anode assembled microbial desalination cell system, Sep. Purif. Technol. 226 (2019) 39–47.
[30] F. Zhang, Z. He, Scaling up microbial desalination cell system with a post-aerobic process for simultaneous wastewater treatment and seawater desalination, Desalination 360 (2015) 28–34.
[31] M.C. Potter, A.D. Waller, Electrical effects accompanying the decomposition of organic compounds, Proc. R. Soc. London. Ser. B Contain. Pap. Biol. Character 84 (1911) 260–276.
[32] B.E. Logan, B. Hamelers, R.A. Rozendal, U. Schrorder, J. Keller, S. Freguia, et al., Microbial fuel cells: methodology and technology, Environ. Sci. Technol. 40 (2006) 5181–5192.
[33] B.E. Logan, Microbial Fuel Cell, Wiley-Interscience, Hoboken, 2008.

This book belongs to Badji Mokhtar Annaba University Central Library Copyright Elsevier 2025

[34] B.E. Logan, Exoelectrogenic bacteria that power microbial fuel cells, Nat. Rev. Microbiol. 7 (2009) 375–381.
[35] B.E. Logan, J.M. Regan, Electricity-producing bacterial communities in microbial fuel cells, Trends Microbiol. 14 (2006) 512–518.
[36] A.P. Borole, G. Reguera, B. Ringeisen, Z.-W. Wang, Y. Feng, B.H. Kim, Electroactive biofilms: current status and future research needs, Energy Environ. Sci. 4 (2011) 4813–4834.
[37] C. Santoro, C. Arbizzani, B. Erable, I. Ieropoulos, Microbial fuel cells: from fundamentals to applications. A review, J. Power Sour. 356 (2017) 225–244.
[38] D.R. Lovley, Bug juice: harvesting electricity with microorganisms, Nat. Rev. Microbiol. 4 (2006) 497–508.
[39] G. Reguera, K.D. McCarthy, T. Mehta, J.S. Nicoll, M.T. Tuominen, D.R. Lovley, Extracellular electron transfer via microbial nanowires, Nature 435 (2005) 1098–1101.
[40] K. Rabaey, N. Boon, S.D. Siciliano, M. Verhaege, W. Verstraete, Biofuel cells select for microbial consortia that self-mediate electron transfer, Appl. Environ. Microbiol. 70 (2004) 5373–5382.
[41] S. Freguia, S. Tsujimura, K. Kano, Electron transfer pathways in microbial oxygen biocathodes, Electrochim. Acta 55 (2010) 813–818.
[42] H.M. Saeed, G.A. Husseini, S. Yousef, J. Saif, S. Al-Asheh, A. Abu Fara, et al., Microbial desalination cell technology: a review and a case study, Desalination 359 (2015) 1–13.
[43] A. Rinaldi, B. Mecheri, V. Garavaglia, S. Licoccia, P. Di Nardo, E. Traversa, Engineering materials and biology to boost performance of microbial fuel cells: a critical review, Energy Environ. Sci. 1 (2008) 417–429.
[44] K. Guo, A. Prévoteau, S.A. Patil, K. Rabaey, Engineering electrodes for microbial electrocatalysis, Curr. Opin. Biotechnol. 33 (2015) 149–156.
[45] Mustakeem Electrode materials for microbial fuel cells: nanomaterial approach. Mater. Renew. Sustain. Energy 4 (2015) 22.
[46] J. Wei, P. Liang, X. Huang, Recent progress in electrodes for microbial fuel cells, Bioresour. Technol. 102 (2011) 9335–9344.
[47] K.C. Zuo, S. Liang, P. Liang, X.C. Zhou, D.Y. Sun, X.Y. Zhang, et al., Carbon filtration cathode in microbial fuel cell to enhance wastewater treatment, Bioresour. Technol. 185 (2015) 426–430.
[48] C. Dumas, A. Mollica, D. Féron, R. Basséguy, L. Etcheverry, A. Bergel, Marine microbial fuel cell: use of stainless steel electrodes as anode and cathode materials, Electrochim. Acta 53 (2007) 468–473.
[49] K.C. Zuo, H. Liu, Q.Y. Zhang, P. Liang, C.D. Vecitis, X. Huang, Enhanced performance of nitrogen-doped carbon nanotube membrane-based filtration cathode microbial fuel cell, Electrochim. Acta 211 (2016) 199–206.
[50] M. Ghasemi, W.R.W. Daud, J. Alam, H. Ilbeygi, M. Sedighi, A.F. Ismail, et al., Treatment of two different water resources in desalination and microbial fuel cell processes by poly sulfone/sulfonated poly ether ether ketone hybrid membrane, Energy 96 (2016) 303–313.
[51] F.L. Moruno, J.E. Rubio, P. Atanassov, J.M. Cerrato, C.G. Arges, C. Santoro, Microbial desalination cell with sulfonated sodium poly(ether ether ketone) as cation exchangemembranes for enhancing power generation and salt reduction, Bioelectrochemistry 121 (2018) 176–184.
[52] C.Y. Ma, C.H. Hou, Enhancing the water desalination and electricity generation of a microbial desalination cell with a three-dimensional macroporous carbon nanotube-chitosan sponge anode, Sci. Total Environ. 675 (2019) 41–50.
[53] A. Al-Mamun, W. Ahmad, M.S. Baawain, M. Khadem, B.R. Dhar, A review of microbial desalination cell technology: configurations, optimization and applications, J. Clean. Prod. 183 (2018) 458–480.
[54] M. Tawalbeh, A. Al-Othman, K. Singh, I. Douba, D. Kabakebji, M. Alkasrawi, Microbial desalination cells for water purification and power generation: a critical review, Energy 209 (2020).
[55] F.A. Alseroury, Microbial desalination cells: progress and impacts, J. Biochem. Technol. 9 (2018) 40–52.
[56] B.E. Logan, Scaling up microbial fuel cells and other bioelectrochemical systems, Appl. Microbiol. Biotechnol. 85 (2010) 1665–1671.
[57] S. Freguia, K. Rabaey, Z. Yuan, J. Keller, Sequential anode–cathode configuration improves cathodic oxygen reduction and effluent quality of microbial fuel cells, Water Res. 42 (2008) 1387–1396.

This book belongs to Badji Mokhtar Annaba University Central Library Copyright Elsevier 2025

[58] O. Lefebvre, T. Ha Nguyen, A. Al-Mamun, I. Chang, H. Ng, T-RFLP reveals high β-proteobacteria diversity in microbial fuel cells enriched with domestic wastewater, J. Appl. Microbiol. 109 (2010) 839–850.
[59] S. Cheng, H. Liu, B.E. Logan, Power densities using different cathode catalysts (Pt and CoTMPP) and polymer binders (Nafion and PTFE) in single chamber microbial fuel cells, Environ. Sci. Technol. 40 (2006) 364–369.
[60] A. Al-Mamun, M.S. Baawain, F. Egger, H.Y. Ng, Optimization of a baffled-reactor microbial fuel cell using autotrophic denitrifying bio-cathode for removing nitrogen and recovering electrical energy, Biochem. Eng. J. 120 (2017) 93–102.
[61] A. Al-Mamun, M.S. Baawain, B.R. Dhar, I.S. Kim, Improved recovery of bioenergy and osmotic water in an osmotic microbial fuel cell using micro-diffuser assisted marine aerobic biofilm on cathode, Biochem. Eng. J. 128 (2017) 235–242.
[62] D.R. Lovley, Powering microbes with electricity: direct electron transfer from electrodes to microbes, Environ. Microbiol. Rep. 3 (2011) 27–35.
[63] Q. Wen, H. Zhang, Z. Chen, Y. Li, J. Nan, Y. Feng, Using bacterial catalyst in the cathode of microbial desalination cell to improve wastewater treatment and desalination, Bioresour. Technol. 125 (2012) 108–113.
[64] A.W. Jeremiasse, H.V. Hamelers, E. Croese, C.J. Buisman, Acetate enhances startup of a H2-producing microbial biocathode, Biotechnol. Bioeng. 109 (2012) 657–664.
[65] A. Cournet, M.-L. Délia, A. Bergel, C. Roques, M. Bergé, Electrochemical reduction of oxygen catalyzed by a wide range of bacteria including Gram-positive, Electrochem. Commun. 12 (2010) 505–508.
[66] R.A. Rozendal, H.V.M. Hamelers, K. Rabaey, J. Keller, C.J.N. Buisman, Towards practical implementation of bioelectrochemical wastewater treatment, Trends Biotechnol. 26 (2008) 450–459.
[67] B. Kokabian, V.G. Gude, Sustainable photosynthetic biocathode in microbial desalination cells, Chem. Eng. J. 262 (2015) 958–965.
[68] B. Kokabian, U. Ghimire, V.G. Gude, Water deionization with renewable energy production in microalgae-microbial desalination process, Renew. Energy 122 (2018) 354–361.
[69] P. Xu, J.E. Drewes, D. Heil, Beneficial use of co-produced water through membrane treatment: technical-economic assessment, Desalination 225 (2008) 139–155.
[70] L. Yuan, X. Yang, P. Liang, L. Wang, Z.-H. Huang, J. Wei, et al., Capacitive deionization coupled with microbial fuel cells to desalinate low-concentration salt water, Bioresour. Technol. 110 (2012) 735–738.
[71] Q. Wen, H. Zhang, H. Yang, Z. Chen, J. Nan, Y. Feng, Improving desalination by coupling membrane capacitive deionization with microbial desalination cell, Desalination 354 (2014) 23–29.
[72] Q. Ping, C. Zhang, X. Chen, B. Zhang, Z. Huang, Z. He, Mathematical model of dynamic behavior of microbial desalination cells for simultaneous wastewater treatment and water desalination, Environ. Sci. Technol. 48 (2014) 13010–13019.
[73] V.G.G. Bahareh Kokabian, Beneficial bioelectrochemical systems for energy, water, and biomass production, J. Microb. Biochem. Technol. (2013).
[74] Y. Kim, B.E. Logan, Microbial desalination cells for energy production and desalination, Desalination 308 (2013) 122–130.
[75] X. Chen, H. Sun, P. Liang, X. Zhang, X. Huang, Optimization of membrane stack configuration in enlarged microbial desalination cells for efficient water desalination, J. Power Sour. 324 (2016) 79–85.
[76] R.L. McGinnis, M. Elimelech, Energy requirements of ammonia–carbon dioxide forward osmosis desalination, Desalination 207 (2007) 370–382.
[77] Y. Zhang, I. Angelidaki, A new method for in situ nitrate removal from groundwater using submerged microbial desalination–denitrification cell (SMDDC), Water Res. 47 (2013) 1827–1836.
[78] F. Zhang, K.S. Brastad, Z. He, Integrating forward osmosis into microbial fuel cells for wastewater treatment, water extraction and bioelectricity generation, Environ. Sci. Technol. 45 (2011) 6690–6696.
[79] G. Liu, Y. Zhou, H. Luo, X. Cheng, R. Zhang, W. Teng, A comparative evaluation of different types of microbial electrolysis desalination cells for malic acid production, Bioresour. Technol. 198 (2015) 87–93.
[80] G. Liu, H. Luo, H. Wang, B. Wang, R. Zhang, S. Chen, Malic acid production using a biological electrodialysis with bipolar membrane, J. Membr. Sci. 471 (2014) 179–184.

This book belongs to Badji Mokhtar Annaba University Central Library Copyright Elsevier 2025

[81] H. Feng, C. Huang, T. Xu, Production of tetramethyl ammonium hydroxide using bipolar membrane electrodialysis, Ind. Eng. Chem. Res. 47 (2008) 7552–7557.
[82] H. Yuan, I.M. Abu-Reesh, Z. He, Mathematical modeling assisted investigation of forward osmosis as pretreatment for microbial desalination cells to achieve continuous water desalination and wastewater treatment, J. Membr. Sci. 502 (2016) 116–123.
[83] Z. Ge, C.G. Dosoretz, Z. He, Effects of number of cell pairs on the performance of microbial desalination cells, Desalination 341 (2014) 101–106.
[84] S. Sevda, I.M. Abu-Reesh, Improved petroleum refinery wastewater treatment and seawater desalination performance by combining osmotic microbial fuel cell and up-flow microbial desalination cell, Environ. Technol. 40 (2019) 888–895.
[85] S. Chen, H. Luo, Y. Hou, G. Liu, R. Zhang, B. Qin, Comparison of the removal of monovalent and divalent cations in the microbial desalination cell, Front. Environ. Sci. Eng. 9 (2015) 317–323.
[86] K.S. Jacobson, D.M. Drew, Z. He, Use of a liter-scale microbial desalination cell as a platform to study bioelectrochemical desalination with salt solution or artificial seawater, Environ. Sci. Technol. 45 (2011) 4652–4657.
[87] Q. Ping, Z. He, Effects of inter-membrane distance and hydraulic retention time on the desalination performance of microbial desalination cells, Desal. Water Treat. 52 (2014) 1324–1331.
[88] Y. Qu, Y. Feng, W. Xin, L. Jia, J. Lv, W. He, et al., Simultaneous water desalination and electricity generation in a microbial desalination cell with electrolyte recirculation for pH control, Bioresour. Technol. 106 (2012) 89–94.
[89] Q. Ping, O. Porat, C.G. Dosoretz, Z. He, Bioelectricity inhibits back diffusion from the anolyte into the desalinated stream in microbial desalination cells, Water Res. 88 (2015) 266–273.
[90] S. Sevda, H. Yuan, Z. He, I.M. Abu-Reesh, Microbial desalination cells as a versatile technology: functions, optimization and prospective, Desalination 371 (2015) 9–17.
[91] H. Luo, P. Xu, Z. Ren, Long-term performance and characterization of microbial desalination cells in treating domestic wastewater, Bioresour. Technol. 120 (2012) 187–193.
[92] X. Chen, P. Liang, Z. Wei, X. Zhang, X. Huang, Sustainable water desalination and electricity generation in a separator coupled stacked microbial desalination cell with buffer free electrolyte circulation, Bioresour. Technol. 119 (2012) 88–93.
[93] M. Ragab, A. Elawwad, H. Abdel-Halim, Simultaneous power generation and pollutant removals using microbial desalination cell at variable operation modes, Renew. Energy 143 (2019) 939–949.
[94] A. Ebrahimi, G.D. Najafpour, D.Y. Kebria, Performance of microbial desalination cell for salt removal and energy generation using different catholyte solutions, Desalination 432 (2018) 1–9.
[95] T. Jafary, A. Al-Mamun, H. Alhimali, M.S. Baawain, M.S. Rahman, S. Rahman, et al., Enhanced power generation and desalination rate in a novel quadruple microbial desalination cell with a single desalination chamber, Renew. Sustain. Energy Rev. 127 (2020) 109855.
[96] H. Luo, P. Xu, T.M. Roane, P.E. Jenkins, Z. Ren, Microbial desalination cells for improved performance in wastewater treatment, electricity production, and desalination, Bioresour. Technol. 105 (2012) 60–66.
[97] A. Larrosa-Guerrero, K. Scott, I. Head, F. Mateo, A. Ginesta, C. Godinez, Effect of temperature on the performance of microbial fuel cells, Fuel 89 (2010) 3985–3994.
[98] G.S. Jadhav, M.M. Ghangrekar, Performance of microbial fuel cell subjected to variation in pH, temperature, external load and substrate concentration, Bioresour. Technol. 100 (2009) 717–723.
[99] M. Ragab, A. Elawwad, H. Abdel-Halim, Evaluating the performance of microbial desalination cells subjected to different operating temperatures, Desalination 462 (2019) 56–66.
[100] Q. Ping, B. Cohen, C. Dosoretz, Z. He, Long-term investigation of fouling of cation and anion exchange membranes in microbial desalination cells, Desalination 325 (2013) 48–55.
[101] C.M. Werner, B.E. Logan, P.E. Saikaly, G.L. Amy, Wastewater treatment, energy recovery and desalination using a forward osmosis membrane in an air-cathode microbial osmotic fuel cell, J. Membr. Sci. 428 (2013) 116–122.
[102] K.S. Jacobson, D.M. Drew, Z. He, Efficient salt removal in a continuously operated upflow microbial desalination cell with an air cathode, Bioresour. Technol. 102 (2011) 376–380.
[103] H. Luo, P. Xu, P.E. Jenkins, Z. Ren, Ionic composition and transport mechanisms in microbial desalination cells, J. Membr. Sci. 409 (2012) 16–23.

This book belongs to Badji Mokhtar Annaba University Central Library Copyright Elsevier 2025

[104] K.S. Brastad, Z. He, Water softening using microbial desalination cell technology, Desalination 309 (2013) 32–37.
[105] P.-Y. Hong, N. Moosa, J. Mink, Dynamics of microbial communities in an integrated ultrafiltration–reverse osmosis desalination pilot plant located at the Arabian Gulf, Desal. Water Treat. 57 (2016) 16310–16323.
[106] T. Laoui, A.M. Al-Amer, A.B. Khalil, A. Abbas, M. Khraisheh, M.A. Atieh, Novel anti-microbial membrane for desalination pretreatment: a silver nanoparticle-doped carbon nanotube membrane, Desalination 376 (2015) 82–93.
[107] F.L. Moruno, J.E. Rubio, C. Santoro, P. Atanassov, J.M. Cerrato, C.G. Arges, Investigation of patterned and non-patterned poly (2, 6-dimethyl 1, 4-phenylene) oxide based anion exchange membranes for enhanced desalination and power generation in a microbial desalination cell, Solid. State Ion. 314 (2018) 141–148.
[108] Q. Ping, Z. Huang, C. Dosoretz, Z. He, Integrated experimental investigation and mathematical modeling of brackish water desalination and wastewater treatment in microbial desalination cells, Water. Res. 77 (2015) 13–23.
[109] S. Luo, H. Sun, Q. Ping, R. Jin, Z. He, A review of modeling bioelectrochemical systems: engineering and statistical aspects, Energies 9 (2016) 111.
[110] O. Lefebvre, A. Uzabiaga, I.S. Chang, B.-H. Kim, H.Y. Ng, Microbial fuel cells for energy self-sufficient domestic wastewater treatment—a review and discussion from energetic consideration, Appl. Microbiol. Biotechnol. 89 (2011) 259–270.
[111] U. Schröder, From wastewater to hydrogen: biorefineries based on microbial fuel-cell technology, ChemSusChem Chem. Sustain. Energy Mater. 1 (2008) 281–282.
[112] J. Wan, J. Gu, Q. Zhao, Y. Liu, COD capture: a feasible option towards energy self-sufficient domestic wastewater treatment, Sci. Rep. 6 (2016) 25054.
[113] K. Hayat, S. Menhas, J. Bundschuh, H.J. Chaudhary, Microbial biotechnology as an emerging industrial wastewater treatment process for arsenic mitigation: a critical review, J. Clean. Prod. 151 (2017) 427–438.
[114] A. Kadier, Y. Simayi, P. Abdeshahian, N.F. Azman, K. Chandrasekhar, M.S. Kalil, A comprehensive review of microbial electrolysis cells (MEC) reactor designs and configurations for sustainable hydrogen gas production, Alex. Eng. J. 55 (2016) 427–443.
[115] E.T. Sayed, N. Shehata, M.A. Abdelkareem, M.A. Atieh, Recent progress in environmentally friendly bio-electrochemical devices for simultaneous water desalination and wastewater treatment, Sci. Total Environ. 748 (2020) 141046.
[116] Z. An, H. Zhang, Q. Wen, Z. Chen, M. Du, Desalination combined with copper (II) removal in a novel microbial desalination cell, Desalination 346 (2014) 115–121.
[117] E. Drioli, A. Ali, F. Macedonio, Membrane distillation: recent developments and perspectives, Desalination 356 (2015) 56–84.
[118] S. Jamaly, N.N. Darwish, I. Ahmed, S.W. Hasan, A short review on reverse osmosis pretreatment technologies, Desalination 354 (2014) 30–38.
[119] B. Zhang, Z. He, Improving water desalination by hydraulically coupling an osmotic microbial fuel cell with a microbial desalination cell, J. Membr. Sci. 441 (2013) 18–24.
[120] C. Shanshan, L. Guangli, Z. Renduo, Q. Bangyu, L. Yong, Development of the microbial electrolysis desalination and chemical-production cell for desalination as well as acid and alkali productions, Environ. Sci. Technol. 46 (2012) 2467–2472.
[121] C. Forrestal, P. Xu, P.E. Jenkins, Z. Ren, Microbial desalination cell with capacitive adsorption for ion migration control, Bioresour. Technol. 120 (2012) 332–336.
[122] C. Forrestal, P. Xu, Z. Ren, Sustainable desalination using a microbial capacitive desalination cell, Energy Environ. Sci. 5 (2012) 7161–7167.
[123] F. Liu, H. Moustafa, M.S.E.-D. Hassouna, Z. He, Resource recovery from wastewater can be an application niche of microbial desalination cells, Environ. Int. 142 (2020) 105855.
[124] S.-P. Sun, C.P.i Nàcher, B. Merkey, Q. Zhou, S.-Q. Xia, D.-H. Yang, et al., Effective biological nitrogen removal treatment processes for domestic wastewaters with low C/N ratios: a review, Environ. Eng. Sci. 27 (2010) 111–126.

This book belongs to Badji Mokhtar Annaba University Central Library Copyright Elsevier 2025

[125] Y. Zhang, I. Angelidaki, Submersible microbial desalination cell for simultaneous ammonia recovery and electricity production from anaerobic reactors containing high levels of ammonia, Bioresour. Technol. 177 (2015) 233–239.
[126] P. Ledezma, J. Jermakka, J. Keller, S. Freguia, Recovering nitrogen as a solid without chemical dosing: bio-electroconcentration for recovery of nutrients from urine, Environ. Sci. Tech. Lett. 4 (2017) 119–124.
[127] Y. Gao, D. Sun, H. Wang, L. Lu, H. Ma, L. Wang, et al., Urine-powered synergy of nutrient recovery and urine purification in a microbial electrochemical system, Environ. Sci. Water Res. Technol. (2018).
[128] D. Sun, Y. Gao, D. Hou, K. Zuo, X. Chen, P. Liang, et al., Energy-neutral sustainable nutrient recovery incorporated with the wastewater purification process in an enlarged microbial nutrient recovery cell, J. Power Sour. 384 (2018) 160–164.
[129] M. Qin, C. White, S. Zou, Z. He, Passive separation of recovered ammonia from catholyte for reduced energy consumption in microbial electrolysis cells, Chem. Eng. J. 334 (2018) 2303–2307.
[130] W.A. Tarpeh, J.M. Barazesh, T.Y. Cath, K.L. Nelson, Electrochemical stripping to recover nitrogen from source-separated urine, Environ. Sci. Technol. 52 (2018) 1453–1460.
[131] Y. Liu, M. Qin, S. Luo, Z. He, R. Qiao, Understanding ammonium transport in bioelectrochemical systems towards its recovery, Sci. Rep. 6 (2016) 22547.
[132] M. Mehanna, P.D. Kiely, D.F. Call, B.E. Logan, Microbial electrodialysis cell for simultaneous water desalination and hydrogen gas production, Environ. Sci. Technol. 44 (2010) 9578–9583.
[133] H. Luo, P.E. Jenkins, Z. Ren, Concurrent desalination and hydrogen generation using microbial electrolysis and desalination cells, Environ. Sci. Technol. 45 (2010) 340–344.
[134] X. Luo, J.Y. Nam, F. Zhang, X.Y. Zhang, P. Liang, X. Huang, et al., Optimization of membrane stack configuration for efficient hydrogen production in microbial reverse-electrodialysis electrolysis cells coupled with thermolytic solutions, Bioresour. Technol. 140 (2013) 399–405.
[135] J.Y. Nam, R.D. Cusick, Y. Kim, B.E. Logan, Hydrogen generation in microbial reverse-electrodialysis electrolysis cells using a heat-regenerated salt solution, Environ. Sci. Technol. 46 (2012) 5240–5246.
[136] X.P. Zhu, M.C. Hatzell, B.E. Logan, Microbial reverse-electrodialysis electrolysis and chemical-production cell for H_2 production and CO_2 sequestration, Environ. Sci. Tech. Lett. 1 (2014) 231–235.
[137] X. Luo, F. Zhang, J. Liu, X.Y. Zhang, X. Huang, B.E. Logan, Methane production in microbial reverse-electrodialysis methanogenesis cells (MRMCs) using thermolytic solutions, Environ. Sci. Technol. 48 (2014) 8911–8918.
[138] S. Chen, G. Liu, R. Zhang, B. Qin, Y. Luo, Y. Hou, Improved performance of the microbial electrolysis desalination and chemical-production cell using the stack structure, Bioresour. Technol. 116 (2012) 507–511.
[139] X. Li, X. Jin, N. Zhao, I. Angelidaki, Y. Zhang, Novel bio-electro-Fenton technology for azo dye wastewater treatment using microbial reverse-electrodialysis electrolysis cell, Bioresour. Technol. 228 (2017) 322–329.
[140] Y. Dong, J. Liu, M. Sui, Y. Qu, J.J. Ambuchi, H. Wang, et al., A combined microbial desalination cell and electrodialysis system for copper-containing wastewater treatment and high-salinity-water desalination, J. Hazard. Mater. 321 (2017) 307–315.
[141] Z. An, H. Zhang, Q. Wen, Z. Chen, M. Du, Desalination combined with hexavalent chromium reduction in a microbial desalination cell, Desalination 354 (2014) 181–188.
[142] F. Meng, Q. Zhao, Z. Zheng, L. Wei, K. Wang, J. Jiang, et al., Simultaneous sludge degradation, desalination and bioelectricity generation in two-phase microbial desalination cells, Chem. Eng. J. 361 (2019) 180–188.
[143] E. Jones, M. Qadir, M.T.H. van Vliet, V. Smakhtin, S.-M. Kang, State desalination brine production: a Glob. outlook, Sci. Total Environ. 657 (2019) 1343–1356.
[144] M. Elimelech, W.A. Phillip, The future of seawater desalination: energy, technology, and the environment, Science 333 (2011) 712–717.
[145] H.A. Abdulgader, V. Kochkodan, N. Hilal, Hybrid ion exchange – pressure driven membrane processes in water treatment: a review, Sep. Purif. Technol. 116 (2013) 253–264.

This book belongs to Badji Mokhtar Annaba University Central Library Copyright Elsevier 2025

[146] D.H. Kim, A review of desalting process techniques and economic analysis of the recovery of salts from retentates, Desalination 270 (2011) 1–8.
[147] V. Gude, B. Kokabian, V. Gadhamshetty, Beneficial bioelectrochemical systems for energy, water, and biomass production, J. Microb. Biochem. Technol. 6 (2013) 2.
[148] H.P. Luo, P.E. Jenkins, Z.Y. Ren, Concurrent desalination and hydrogen generation using microbial electrolysis and desalination cells, Environ. Sci. Technol. 45 (2011) 340–344.
[149] Y. Kim, B.E. Logan, Series assembly of microbial desalination cells containing stacked electrodialysis cells for partial or complete seawater desalination, Environ. Sci. Technol. 45 (2011) 5840–5845.
[150] T.Y. Cath, A.E. Childress, M. Elimelech, Forward osmosis: principles, applications, and recent developments, J. Membr. Sci. 281 (2006) 70–87.
[151] S.M. Iskander, J.T. Novak, Z. He, Enhancing forward osmosis water recovery from landfill leachate by desalinating brine and recovering ammonia in a microbial desalination cell, Bioresour. Technol. 255 (2018) 76–82.
[152] K. Zuo, W. Wang, A. Deshmukh, S. Jia, H. Guo, R. Xin, et al., Multifunctional nanocoated membranes for high-rate electrothermal desalination of hypersaline waters, Nat. Nanotechnol. 15 (2020) 1025–1032.
[153] K. Zuo, X. Huang, X. Liu, E.M. Gil Garcia, J. Kim, A. Jain, et al., A hybrid metal–organic framework–reduced graphene oxide nanomaterial for selective removal of chromate from water in an electrochemical process, Environ. Sci. Technol. 54 (2020) 13322–13332.
[154] J. Kim, A. Jain, K.C. Zuo, R. Verduzco, S. Walker, M. Elimelech, et al., Removal of calcium ions from water by selective electrosorption using target-ion specific nanocomposite electrode, Water Res. 160 (2019) 445–453.

This book belongs to Badji Mokhtar Annaba University Central Library Copyright Elsevier 2025

This page intentionally left blank

This book belongs to Badji Mokhtar Annaba University Central Library

Copyright Elsevier 2025

CHAPTER TWELVE

Membrane-based electrochemical technologies: III. Selective ion removal and recovery

Anaira Román Santiago[1], Jemin Jeon[1], Emmanuel Kayiwa[2], Roland Cusick[2] and Xiao Su[1]
[1]Department of Chemical and Biomolecular Engineering, University of Illinois-Urbana Champaign, Urbana, IL, United States
[2]Department of Civil and Environmental Engineering, University of Illinois-Urbana Champaign, Urbana, IL, United States

12.1 Introduction

Water scarcity and exposure to anthropogenic contaminants are major drivers for the development of more efficient and cost-effective technologies for water remediation [1]. Water treatment technologies remove a variety of contaminants, with applications ranging from drinking water purification [2] and reuse of wastewater for irrigation [3] to industrial metal removal or recovery [4]. Membrane separation is a commonly used method for cleaning water due to its advantages over chemical and biological treatment methods, such as the ability to remove non-biodegradable pollutants, reduced chemical consumption and waste disposal, and the capability to separate suspended particles [5]. Membrane processes include microfiltration (MF), ultrafiltration (UF), nanofiltration (NF), membrane bioreactors (MBR), membrane distillation (MD), reverse osmosis (RO), and forward osmosis (FO), all of which have been used across a range of applications [6].

Traditional membrane separation relies on the rejection of certain contaminant species through size exclusion, hydrophobic effects, and/or electrostatic interactions [7]. However, one of the main drawbacks of membrane technologies is their tendency to foul due to the buildup of pollutants on the membrane surface, which leads to the deterioration of membrane performance [8]. Moreover, emerging pollutants present additional challenges to membrane efficiency. For example, RO membranes are considered to be one of the most effective technologies for the removal of micropollutants to date, yet they exhibit poor rejection towards disinfection byproducts such as *N*-nitrosodimethylamine (NDMA) [9,10], a pollutant of emerging concern classified as a probable human carcinogen [11]. Furthermore, although state-of-the-art membranes for desalination possess high water-solute selectivity, these materials often do not achieve adequate ion rejections for water

Electrochemical Membrane Technology for Water and Wastewater Treatment.
DOI: https://doi.org/10.1016/B978-0-12-824470-8.00012-7
© 2022 Elsevier Inc.
All rights reserved.

This book belongs to Badji Mokhtar Annaba University Central Library
Copyright Elsevier 2025

matrices with low total dissolved solids (TDS) [12]. In many cases—such as heavy metals, metalloids, and organic ions—the contaminants of concern can exist in a charged state. These ionic species pose a great challenge to water treatment not only because they are present in ultradilute concentrations, which makes it difficult to remove these using the conventional physical filtration processes, but also because competing ions are present which often hinders the ability to selectively separate target ions from the aqueous mediums [13]. Thus, there is a need for improving molecular selectivity to achieve energy-efficient separations, provide reusable water, and potentially enable resource recovery.

Electrochemical separation and electrochemical oxidation processes can be promising approaches to water purification due to their modularity, enhanced selectivity, and high efficiency for contaminant removal/degradation [14]. Electrosorption-based separation methods have demonstrated remarkable selectivity towards different pollutants such as heavy metals [15–17], organic anions [13], polyfluoroalkyl substances (PFAS), and halogenated aromatic compounds [18]. Increased selectivity and reversible sorption have also allowed for the recovery of valuable elements such as lithium [4].

At the same time, electrochemical advanced oxidation processes (EAOPs) have shown superior performance for degradation of organic pollutants and their mineralization to innocuous species [19]. However, the efficiency of EAOPs can often be restricted by mass transfer limitations and high energy consumption when treating large volumes of wastewater [6]. Another disadvantage of EAOPs is the potential generation of toxic byproducts, which often need to be removed or posttreated [20]. Hence, implementation of these electrochemical methods without a proper evaluation of their pros and cons can often be inadequate to address the multiple needs of water treatment.

As a result, the coupling of membrane separation and electrochemical technology has become a promising path for water remediation as it exploits the advantages of each method to achieve a more efficient treatment train. In fact, coupling membrane systems with electrochemical technologies is a strategy already being explored in wastewater treatment plants (WWTP) today [21,22]. Advanced treatment procedures in WWTPs involve the use of either MF or UF as pretreatment, followed by RO, and a final posttreatment using an advanced oxidation process to remove remaining contaminants [12]. Nevertheless, the synergistic design of both technologies provides new advantages over their individual use. It has been shown that the combination of EAOPs with membrane separation as a single system (and not separate units) helps mitigate membrane fouling and improve overall efficiency [20,23,24]. Hence, there has been a significant recent focus on developing integrated electrochemical technologies with membranes for water remediation, which we shall refer to as *membrane-based electrochemical systems* for the remainder of the chapter.

For the scope of this chapter, we will focus on three main types of membrane-based electrochemical technologies, classified according to their configurations: Electrodialysis (ED), membrane capacitive deionization (MCDI), and electrochemical filtration systems (EFS). Details about each system and its assemblies will be discussed

This book belongs to Badji Mokhtar Annaba University Central Library Copyright Elsevier 2025

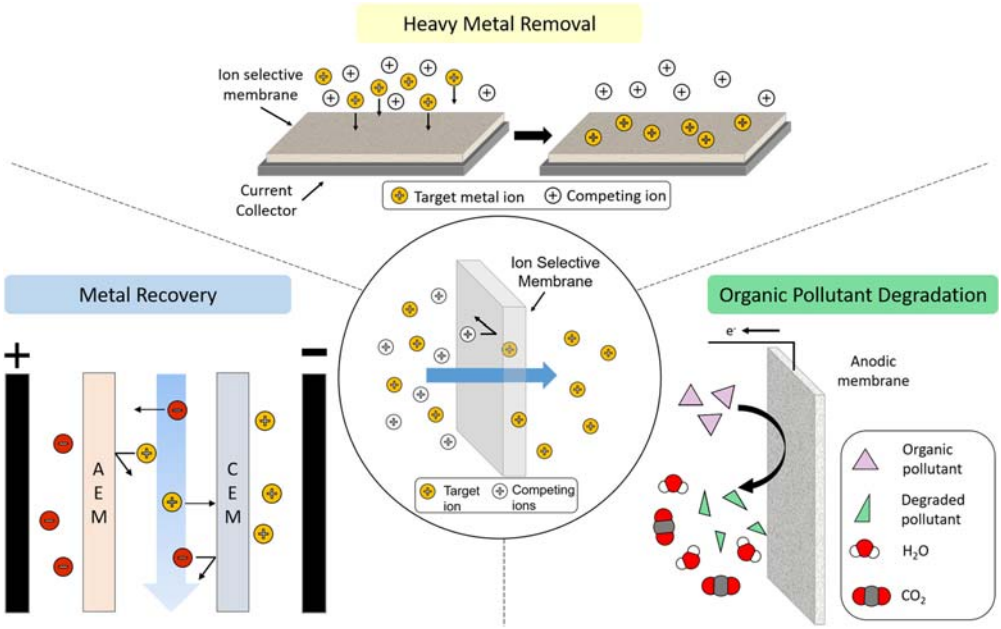

Figure 12.1 Membrane-based electrochemical technologies and their applications for selective ion removal and recovery.

in Section 12.3. Each configuration has its own advantages and is used for a wide variety of applications within the water remediation field as presented in Fig. 12.1.

The aim of this chapter is to provide a review of membrane-based electrochemical technologies for water treatment with a focus on selective ion removal and recovery applications. The chapter covers important concepts and definitions in the field of selective electrochemical separations that are essential to understand the mechanisms of selective ion removal. In addition, the chapter provides an overview of recent literature on the aforementioned systems for applications such as selective metal removal and recovery, as well as the remediation of dilute water contaminants, including organic ions and other nonmetallic contaminants. Lastly, the chapter explores the feasibility of electrochemical treatment technologies for large-scale applications, as well as the challenges that need to be overcome to achieve efficient water purification processes.

12.2 Principles of selective ion removal and recovery

In this section, we introduce the basic concepts and terminology used in the electrochemical separation field. First, we explain the concept of selective ion

This book belongs to Badji Mokhtar Annaba University Central Library Copyright Elsevier 2025

separation and the major components of membrane-based electrochemical technologies which determine their performance. Next, we provide key parameters that have been broadly adopted across the literature to evaluate the performance of these ion-removal processes. Finally, we discuss several separation mechanisms for ion selectivity leveraged by membrane-based electrochemical systems.

12.2.1 Overview

Precipitation, liquid chromatography, and membranes can all be used to achieve ion separation [25–27]. There has been a great deal of attention surrounding the convergence of ion separation methods and electrochemical systems during the last several decades to tackle environmental and industrial issues more sustainably [28,29].

Electrification of ion separation systems can not only reduce chemical input but also often enable process intensification in a compact module, lowering secondary pollution [4,30,31]. For instance, metal electrodeposition and metal electroprecipitation can selectively remove metal ions and have recently been used as a viable technique for metal nanofabrication and metal recovery from industrial wastes, respectively [32,33]. Also, the judicious selection of appropriate ion exchange membranes (IEMs) in ED and electroosmotic filtration can sometimes enable ion selectivity [27,34,35]. Recently, modification of electrodes with selective adsorbent layers has been applied to micropollutant removal and metal ion remediation. Selective materials such as electroactive and redox-active polymers have gained increased interest due to their electrochemically tunable selectivity towards the removal of contaminants, even in dilute feed solutions [17,18,36].

12.2.1.1 Concept of selective ion separation

First, we would like to differentiate our use of terminology between selective ion separation from nonselective ion separation. Nonselective ion separation refers to the separation of cations or anions from a feed phase regardless of physicochemical characteristics other than their charge states. For example, a cation exchange membrane (CEM) whose selectivity between two different cations is negligible will be considered nonselective toward any specific cation. Thus, an ion separation method that uses only the CEM should be also considered nonselective from a cation separation perspective even though one may argue that it separates cations from anions. On the other hand, selective ion separation is capable of separating target ion species among competing positively or negatively charged ions. For instance, the sodium (Na) superionic conductor (NASICON) was adapted to all-solid-state lithium batteries as a solid-state electrolyte [37,38]. It was reported that a lithium-based NASICON-type solid-state electrolyte was used as a lithium-selective membrane in an electrodeposition technique against sodium ion (Na^+), the most abundant cation in seawater [39]. In

This book belongs to Badji Mokhtar Annaba University Central Library Copyright Elsevier 2025

this case, the separation system using the NASICON membrane is considered ion-selective because the system had selectivity towards the lithium ion (Li^+) over Na^+.

Electrochemical ion separation methods encompass additional components to be featured beyond the membrane itself (i.e., electrodes, electrolyte, and external power to apply voltage). Key selective components of an electrochemical system, which present ion selective mechanisms (explained in Section 12.2.2), are usually the electrode and/or membrane material. However, various operating conditions can be optimized to increase the ion selectivity, depending on the process at play. In most of the ion separation methods found in literature, physicochemical ion-selective mechanisms rely on electrodes modified with selective adsorbents, and/or the modification of membranes to increase ion selectivity. Although there are a plethora of ion separation techniques using electrode adsorbents without membranes, we will focus this chapter on electrochemical approaches that utilize a membrane for operation. A few definitions and ion separation performance parameters are explained in the following subsections.

12.2.1.2 Competing ions

A feed solution for selective ion separation usually contains more than one cationic or anionic species. During the feed phase, other ions with the same charge as an ion of interest which compete with an ion of interest to be separated by the system will be referred to as competing ions. Because most of the ion separation mechanisms are dependent on the charge of ions to some extent, the presence of competing ions usually has negative impacts on the separation of a target species [40]. During a selective ion separation process in a mixture of ions, there are always competing species that can decrease the performance of the system. For instance, the relatively high affinity of a competing ion to a selective component could end up reducing the adsorption capacity and rates of the system, thereby lowering the selectivity towards the target ion [41].

In many cases, feed solution matrices such as seawater and wastewater are highly concentrated with competing ions and foulants while the concentration of a target ion species is dilute [42]. The key aspect of a selective component requires a tailored design to enhance the differences between physicochemical characteristics of a target and the competing species. For example, Su et al. reported that a poly(vinylferrocene) (PVF)-carbon nanotube (CNT) anode selectively adsorbed chromium and arsenic oxyanions with an uptake greater than 100 mg Cr/g adsorbent in the presence of over 200-fold excess of competing anions [17]. Investigation of the key selectivity mechanisms indicated that the redox-groups at the anode had a stronger charge transfer to the heavy metal oxyanions than it had for competing anions.

12.2.1.3 Ion removal and recovery

Both ion removal and recovery processes can be considered as separation techniques. Separation of toxic heavy metal ions and ionic organic pollutants from tap water,

This book belongs to Badji Mokhtar Annaba University Central Library Copyright Elsevier 2025

surface water, and/or wastewater is considered as a removal process, while the separation of valuable metal ions from industrial waste and brine can be classified as recovery processes [43]. For a successful recovery operation, it is important to have, not only a high recovery rate, but also a high regeneration efficiency because the adsorbent and recovered ion must be recycled. In many ion-removal-and-recovery applications, the concentration of target ions is typically low (usually in the parts-per-billion (ppb) range), so a number of separation techniques must be used in combination to increase the removal or recovery rate [44].

Owing to intensive research on electrochemically selective materials, electrochemically mediated removal and recovery processes have been converging toward the intensification of separation processes. Chen et al. recently reported an electrochemical system that performs harmful heavy metal remediation and value-added metal recovery from multicomponent metal ion mixtures at once by using potential-dependent selectivity of redox-active metallopolymers, PVF, and poly(ferrocenylsilane) (PFS) [15]. In their study, PVF-CNT showed high selectivity for CrO_4^{2-} over MoO_4^{2-} while PFS-CNT showed selectivity for MoO_4^{2-}over CrO_4^{2-}, implying that a multiple-step electrochemical system can recover valuable metals and remove toxic metals from multicomponent mixtures with fewer steps.

12.2.1.4 Performance metrics of selective ion separation

Membrane-based electrochemical separation methods also share many of the existing performance parameters with conventional ion separation methods to evaluate their separation performance. To name a few, selectivity coefficient, removal efficiency, and adsorption capacity are the most common performance parameters found in the literature. It is noted that the performance parameters and the terminology, especially for selective ion separation, vary by paper because many of the electrochemically assisted ion separation systems are relatively new and have been evolving more or less independently [45]. In this subsection, we introduce the definitions of important parameters for electrochemical ion separation.

To determine membrane selectivity, parameters such as selectivity coefficient, separation factor, adsorption selectivity, selectivity factor, selectivity rate, ion selectivity ratio, and distribution coefficient are used. All of these parameters compare two ions—a target ion A and a competing ion B. First, selectivity coefficient ($\alpha_{A,B}$) is defined as:

$$\alpha_{A,B} = \frac{\left(C_{A,i} - C_{A,f}\right)/C_{A,f}}{\left(C_{B,i} - C_{B,f}\right)/C_{B,f}}$$

where $C_{x,i}$ and $C_{x,f}$ are the initial and final concentrations of x ion, respectively. The expression of the selectivity coefficient is directly obtained from K_{eq}, the

This book belongs to Badji Mokhtar Annaba University Central Library Copyright Elsevier 2025

thermodynamic equilibrium constant of the competitive adsorption/binding reactions of the species A and B, $A + S = A - S$ and $B + S = B - S$, as described below,

$$\alpha_{A,B} = K_{eq} = \frac{K_A}{K_B} = \frac{[A-S]/([A][S])}{[B-S]/([B][S])} = \frac{\left(C_{A,i} - C_{A,f}\right)/C_{A,f}}{\left(C_{B,i} - C_{B,f}\right)/C_{B,f}} = \frac{N_A^{ads}/N_{A,f}^{sol}}{N_B^{ads}/N_{B,f}^{sol}}$$

where K_x is an equilibrium constant for the adsorption/binding reaction between an ion, x, and a sorption site, S and $X - S$ represents the ion bound to the sorption site S. N_x^{ads} and N_x^{sol} represent the number of x ions adsorbed and the number of x ions in the feed solution, respectively. The selectivity coefficient is mainly affected by two factors: physicochemical properties of a binding site and the target ion, and the external energy driving the ion transport. Ion properties that dictate selective binding can include the size, charge state, and hydration number [45,46]. The externally applied electric field facilitates the mass transfer of counter ions to an electrode by electromigration [45,46]. Separation factor [47,48] and adsorption selectivity [49] have the same expression defined as:

$$Separation\ factor = \frac{C_A^{ads}/C_{A,i}^{sol}}{C_B^{ads}/C_{B,i}^{sol}}$$

where C_x^{ads} and $C_{x,i}^{sol}$ represent the adsorbed concentration and the initial concentration of x ion in the feed solution. Selectivity factor [50] and selectivity rates [51] have been used by Guyot et al., with the expression defined as:

$$Selectivity\ factor = \frac{N_A}{N_A + N_B}$$

where N_x represents the number of x ions separated into a recovery compartment. Note that all the parameters except the selectivity factor include the initial feed concentration term in the denominator, thus making these metrics dependent on feed condition.

12.2.2 Mechanisms and key components for ion selectivity in membrane-based electrochemical technologies

An advantage of electrochemical separation methods is that multiple components can be integrated into one system, which can lead to process intensification [31]. Membrane-based electrochemical technologies such as MCDI and ED achieve selective removal of target ions even in a low concentration feed by combining various ion selective mechanisms at different locations along the ionic pathway: bulk solution, membrane matrix, and electrode interface/matrix [52]. Although in some studies, packing ion resins [53] or activated carbon [54] in bulk solution was used to control electromigration of competing ions, ion selectivity in the membrane-based electrochemical methods discussed in this chapter heavily relies on the electrode and membrane. Moreover, packing solid

This book belongs to Badji Mokhtar Annaba University Central Library Copyright Elsevier 2025

conductors or highly concentrated media can often increase the hydraulic pressure affecting the stability of a system [52]. Thus, in this section, our focus will be key selective components driven by the membrane and/or electrode materials, as well as electrochemically enhanced mechanisms.

12.2.2.1 Ion selective mechanisms: ion exchange, size exclusion, and selective immobilization

12.2.2.1.1 Ion exchange

Ion exchange refers to the reversible interchange between ions with a similar charge. Ion exchange occurs at the sites of fixed ions (i.e., functional groups) permanently bound within the matrix of a membrane which act as counterions. Charged species bound on oppositely charged sites are replaced with ions of a similar charge through the introduction of a feed solution until the ionic complexes reach equilibrium [55]. Due to the Donnan exclusion, co-ions with a similar charge of the membrane functional groups are restricted from entering into the membrane matrix and thus do not participate in the ion-exchange process [56]. When external driving forces such as pressure and potential gradient are applied, ions selectively adsorbed within the matrix move from site to site and eventually pass through the membrane. Usually, the greater the size and the valency of an ion, the higher the affinity it has with the membrane functional sites.

Anion exchange membrane (AEM) and CEM are the most commonly used membranes where the selective mechanism of ion exchange is at work in electrochemical ion separation technologies. Based on our definition for selectivity, many conventional AEM and CEM themselves are nonselective towards target ions of a similar charge. However, they play a key role in partitioning ions from counterions and are thus critical components in membrane separation technologies. For example, an IEM can be used to isolate the ions of a redox couple which must stay on one side to prevent contamination of the effluent and, at the same time, to permit the flow-specific counterions across the membrane for the completion of the electric circuit [57]. Also, IEMs can be fabricated to provide permselectivity between competing ions of different or equal charge valences, as well as between counterions. Monovalent ion selective membranes separate monovalent ions from a feed solution containing both monovalent and multivalent ions. To enhance monovalent-ion selectivity, Güler et al. coated both sides of the surface of a conventional AEM with thin cation exchange layers which restricted the passage of divalent anions such as sulfate [58]. This modified AEM itself is capable of selective ion separation just with an additional external field to transport monovalent anions while blocking divalent anions by electrostatic repulsion [58].

12.2.2.1.2 Size exclusion

Size exclusion, one of the physical mechanisms of ion rejection along with dehydration and electrostatic repulsion [59], is also an ion selective mechanism broadly used in

This book belongs to Badji Mokhtar Annaba University Central Library Copyright Elsevier 2025

membrane-based electrochemical ion separation techniques. The pore size of a synthesized membrane or electrode matrix is finely controlled to exclusively transport smaller ions while rejecting larger ones. Therefore, the comparison between the sizes of competing ions is critical to construct proper pore size distribution. Effective ion size highly depends on the solvation characteristics of ions [60]. In aqueous media under an electric field, an ion with higher valence and smaller hydration size usually migrates faster. However, a higher valence ion is likely to have a larger hydrated ion size [61]; thus, tuning membrane pore sizes to be smaller than the hydrated size of competing divalent ions is often used to provide ion selectivity towards monovalent ions. Li et al. fabricated an electrochemically tunable ion-sieve membrane (ETISM) with a Prussian blue (PB) coordination polymer, where the size of pores at the subnanometer scale can be modulated by the applied potential which reduces PB to Prussian white (PW). Based on structural changes between PW and PB, the ETISM platform showed enhanced permeation rates for small hydrated metal ions (i.e., Cs^+ and K^+) while the permeation rates of relatively large hydrated metal ions (Mg^{2+} and La^{3+}) remained unchanged [62].

Though less common, electrode interface and interior structures are also modified to control the pore size distribution in an electrode matrix for size exclusion. Hawks et al. reported that ultramicroporous carbon used as an electrode in capacitive deionization (CDI) can display a strong ion sieving effect. Subnanometer pores formed after moderate activation of the carbon electrode achieved selective adsorption of the planar and weakly hydrated nitrate molecules over other competing anions (i.e., SO_4^{2-} and Cl^-) with larger hydrated sizes and more tightly bound solvation shell [60]. PB and its analogs (PBAs) have also been studied as electrode materials for selective ion intercalation with the size exclusion mechanism at work based on the size and hydration energy of cations [63–65]. It was shown that the ions with smaller hydration energy such as Cs^+ and K^+ are more readily intercalated into the lattice of PBAs under an applied insertion potential [65,66].

12.2.2.1.3 Selective immobilization

Lastly, selective immobilization of target ions on electrode interface/matrix plays a major role in the ion selectivity of many state-of-the-art electrochemical separation methods. Recent interest in the modification and functionalization of electrode materials has paved the way for more efficient approaches to selective ion binding and removal [67]. Selective immobilization of ions can be achieved through various physicochemical mechanisms including intercalation, electrosorption, electrodeposition, electrocoagulation, and conversion [45]. Among these mechanisms, electrosorption is a widely explored mechanism used in CDI, with both Faradaic and non-Faradaic electrochemical systems employing this mechanism. Many of these immobilization mechanisms are based on the physicochemical characteristics of ions (i.e., ion exchange

This book belongs to Badji Mokhtar Annaba University Central Library Copyright Elsevier 2025

and size exclusion). An important advantage of selective immobillization is that both electrochemical potential and surface interactions (through tailored adsorbent sites) can be leveraged to achieve molecularly selective separations.

Recently, an extensive amount of research has been published on ion selective immobilization mechanisms with the techniques of high selectivity and capacity, governed by molecularly designed electrode materials. For an example of selective electrosorption, Kim et al. reported the selective and reversible capture of arsenite anions (As(III)). At optimal oxidation potentials, the anode coated with PVF-CNT showed over 90% of the removal efficiency of the toxic arsenic anions in the presence of 20-fold excess of chloride anions (Cl^-) [16]. Liu et al. conducted selective electrodeposition of uranyl cations (U(IV)) with an exceptionally high capacity [68]. A carbon electrode was functionalized with an amidoxime-based polymer, which is a highly selective material with a uranium uptake of 200 mg/g. In combination with a half-wave rectified alternating current method, this modified electrode repeatedly and selectively adsorbed and electrodeposited uranyl ions up to 1932 mg/g, while other competing cations with weaker binding easily came off the electrode surface due to an alternating current [68].

12.2.2.2 Key selective components

In this subsection, key selective components in membrane-based electrochemical ion separation mechanisms are briefly explained. Although this was partially addressed in the previous section, it is important to understand which variables can be tailored within a membrane-based electrochemical system so as to lead to the aforementioned selective mechanisms. Beginning from the bottom of Fig. 12.2, novel membrane material and their proper fabrication mainly assist selective ion separation through the ion exchange and size exclusion mechanisms by controlling pore size and electrostatic characteristics of the resin. As mentioned for size exclusion, a membrane can sometimes be tuned to function also as an electrode itself, thereby having dual functionality [62]. Next, judicious selection of electrode materials is essential to adjust the physicochemical properties of the electrode interface [69,70]. Modification of the surface of a membrane or electrode with functional groups or redox molecules enables the system to gain selective immobilization mechanisms to control the overpotential of selective electrodeposition or reaction and/or to tune the binding/complexation energy between a target ion and the electrode surface [15]. Apart from adjustment of the physicochemical properties of the electrode surface, a wide range of electrochemical methods applied by a potentiostat allows one to electrochemically control the overall environment of the separation system. To name some, migration of ions, pH of a solution, charge states of redox-switchable molecules, and electrode surface potential can be finely tuned to provide or assist the ion selectivity [70]. Finally, selective metal

This book belongs to Badji Mokhtar Annaba University Central Library Copyright Elsevier 2025

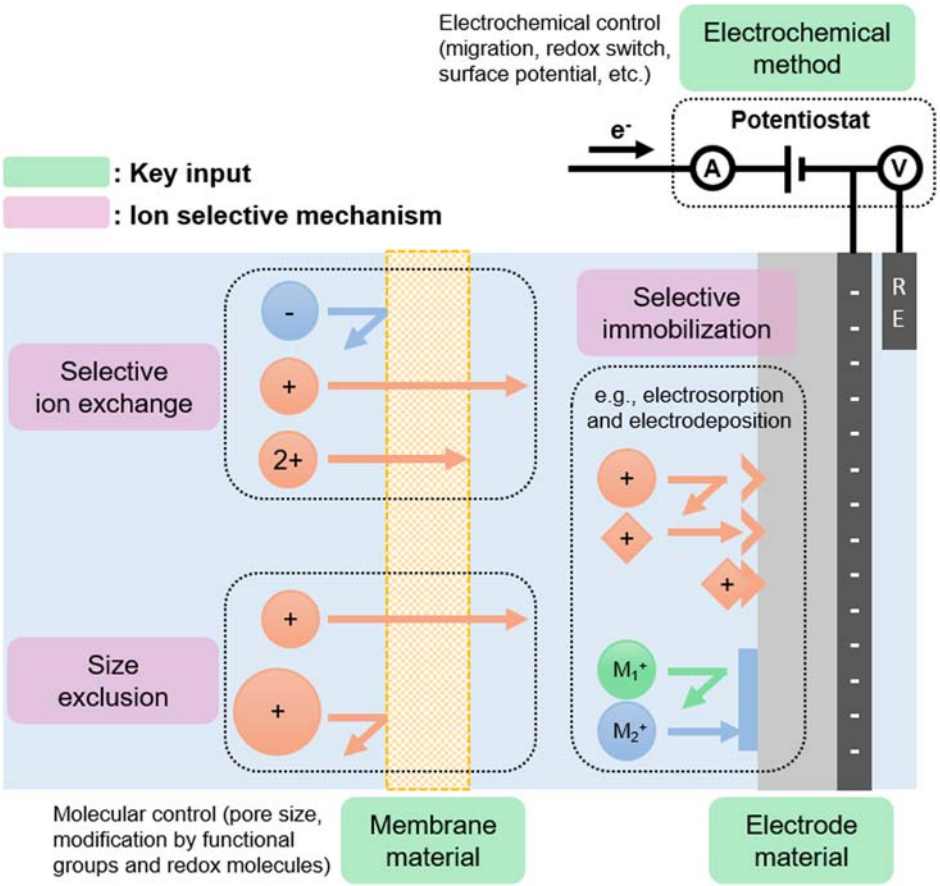

Figure 12.2 Ion selective mechanisms and key selective components in membrane-based electrochemical technologies. Selective immobilization includes various methods such as electrosorption, intercalation, electrodeposition, and electroprecipitation.

electrodeposition can be achieved by applying the optimal reduction potential such that target metal ions are deposited while other metal ions remain in the feed [68,71,72].

12.3 Architectures and fabrication of membrane modules

The practical application of membranes and electrodes used for selective separations or recovery of ions depends upon their performance in continuous flow reactors. The three most ubiquitous types of reactor configurations employed include ED, modifications of CDI systems, and EFS. In the ED configuration, there are no

This book belongs to Badji Mokhtar Annaba University Central Library Copyright Elsevier 2025

electrodes in the repeating unit (denoted as the cell pair) with the membrane serving as the principal component for selective separation [73]. The cell pairs of CDI reactors always utilize electrodes—capacitive or faradaic—and can be modified to include membranes [74]. EFS, in contrast to these two reactor configurations, uses a membrane as an electrode and a filter in a design intended to facilitate degradation of pollutants [75].

12.3.1 Electrodialysis

ED consists of a stack of alternating cation and anion exchange membranes (CEMs and AEMS, respectively) sandwiched between two electrodes that provide an electrochemical driving force for ionic transport. Ions transfer across the membranes via an applied electric potential in a process that yields two streams of varying ionic concentration as shown in Fig. 12.3. In one compartment, the anions and cations become less concentrated, forming a dilute stream, while the solution in the receiving compartment becomes more concentrated [76]. Given the central role of ion-exchange membranes in conventional ED in ionic separation, it follows that the functionalization of the CEMs and AEMs can enable preferential and selective transport of a particular ionic species across each membrane type.

Different fabrication strategies have been employed to enhance the selectivity of IEMs with the most common being layer-by-layer assembly and ion imprinting.

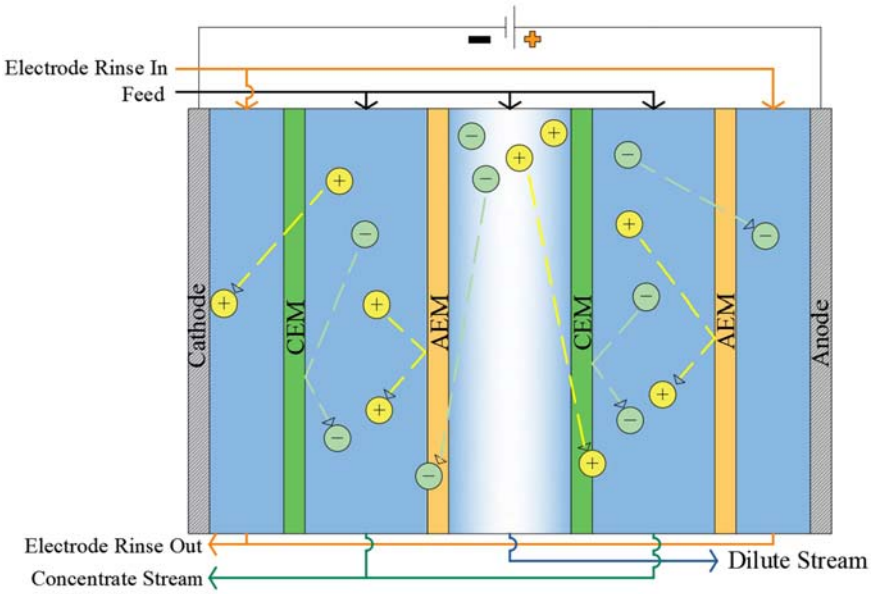

Figure 12.3 Schematic of electrodialysis system.

This book belongs to Badji Mokhtar Annaba University Central Library Copyright Elsevier 2025

Firstly, the layer-by-layer assembly involves the creation of thin-film membranes of a desired thickness from polyelectrolytes by dip-coating, spray coating, or electrodepositing them onto a substrate in a manner that enables tailored composition and tunable properties [78]. The resulting polyelectrolyte multilayer membrane (PEMM) is free of defects, thus avoiding issues that reduce separation efficiency and making it an ideal technique for the fabrication of membranes used in separation-based processes. Secondly, ion imprinted polymers (IIPs) are developed by complexing a polymerizable ligand and metal which are subsequently polymerized with the aid of a crosslinker—at this point, the template ion is then removed which yields a three-dimensional recognition cavity inside the polymer network [79–81]. Both layer-by-layer assembly and ion imprinting were leveraged by Deng et al. (2014) electrodepositing polyethyleneimine (PEI) onto a commercial CEM with copper nitrate serving as the template ion to promote selective transport of copper for water purification [82].

Another important application in ED-based separation is one for the recovery of precious metals such as lithium. Exfoliation of phyllosilicate materials, in particular, has garnered increased attention to surmount the poor monovalent selectivity of conventional IEMs. A two-step process is typically employed to create such membranes which consist of exfoliation of the layered material and reassembly via filtration or casting [83]. Induced stacking of the formed 2D-sheets usually exhibits a lamellar microstructure which have nanochannels that are uniform and highly oriented which can be designed to facilitate the selective transport of ions [83–85]. Razmjou et al. found that exfoliation of vermiculite and its reassembly into a membrane can create lithium selective nanochannels [85]. ED is also capable of separating species based on valency through the use of selective IEMs. For example, Nie et al. employed commercial monovalent selective CEMs such as Selemion CSO, which led to selective lithium recovery over competing Mg^{2+} ions [47]. Other types of membranes and materials found in ED separations are listed in Tables 12.1–12.3.

12.3.2 CDI and CDI-related systems

12.3.2.1 Capacitive deionization

CDI is a process that couples charge storage within electric double layers (EDL) of carbon electrodes to ion removal from water and has been researched extensively for brackish water desalination (Fig. 12.4A). The non-functionalized carbon materials (i.e., carbon cloth, carbon aerogel, activated carbon, etc.) realize selectivity by exploiting ions' physical properties (molecular size, valence, electronegativity, etc.) to selectively store ions since valence and molecular size have been known to significantly affect the diffusion and migration rates of ions under an applied electric potential [52,86]. Carbon-based electrode materials in CDI are prepared in a facile manner—typically by using a

This book belongs to Badji Mokhtar Annaba University Central Library Copyright Elsevier 2025

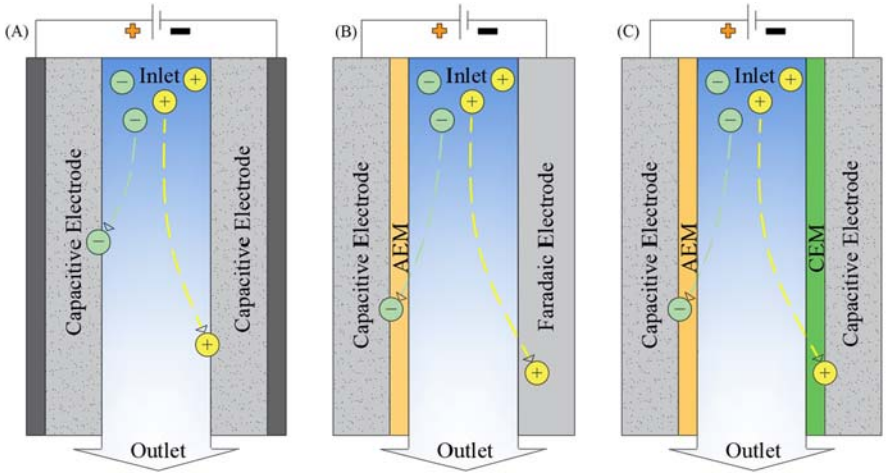

Figure 12.4 CDI and CDI-related systems schematics. (A) CDI, (B) hybrid CDI, and (C) MCDI. *CDI*, capacitive deionization; *MCDI*, membrane capacitive deionization.

conductive agent and binder—to generate a slurry that is cast onto a substrate or be free-standing [87]. The functionalization of carbon materials can increase the selectivity of target ions by introducing functional groups onto the surface that are capable of chemical interactions [52]. A promising method to modify the surface charge of carbon materials is through quaternary amines and cationic or anionic surfactants. Oyarzun et al. used a cetrimonium bromide cationic surfactant to enhance anion adsorption and sodium dodecyl benzene sulfonate to improve cation adsorption capacity to selectively capture nitrate ions [88].

12.3.2.2 Hybrid capacitive deionization

A derivative of CDI, hybrid CDI uses a battery-type electrode (e.g., MnO_2) that can undergo redox reactions, in addition to a capacitive electrode with a free-standing IEM situated in front to prevent readsorption of target ions (see Fig. 12.4B) [89]. Selectivity of hybrid CDI is attributed to the preferential intercalation of ions into the battery electrodes' structure with a multiplicity of materials developed for sodium removal. Other ions have strong affinities to target ions or organics, fast kinetics, modularity, absence of chemical regeneration steps and electronic tunability [17,18,90,91]. Song et al. were able to capture toxic arsenic oxyanion using a hybrid CDI cell composed of PVF-coated graphite paper substrate and a CEM to prevent readsorption of arsenic oxyanion on carbon cloth for the purpose of water remediation [92].

12.3.2.3 Membrane capacitive deionization

MCDI is a modification to CDI cells architecture to include CEMs and AEMs between the deionization channel and capacitive electrodes, which are either

This book belongs to Badji Mokhtar Annaba University Central Library Copyright Elsevier 2025

free-standing or coated directly onto the electrode (see Fig. 12.4C) [74]. The inclusion of IEMs improves removal efficiency by retaining co-ions within the electrode chamber, which drives more ions into the carbon macropore and allows for more thorough ion depletion during desorption [74,93]. Membranes and electrodes used in MCDI are prepared in a similar way to those of ED and CDI, respectively, and can be used for ion selective separation and recovery. Shi et al. extracted lithium in a MCDI cell that housed activated carbon electrodes, a monovalent selective CEM, and a commercial AEM [94]. The electrodes in the CDI and the MCDI cells used for separation and recovery are generally static, and the fluid traverses the cell perpendicular to the electric potential in a flow-by operational mode. However, there is potential for other cell architectures and flow conditions to be used such as flow electrode CDI [95], flow-through electrodes [96,97], and desalination batteries [98,99] with advantages unique to each cell.

12.3.2.4 Electrochemical filtration systems

Removal of recalcitrant contaminants through degradation is possible by employing a type of electrochemical membrane reactor (EMR) known as an EFS. As shown in Fig. 12.5, such reactors use a membrane as an anode and typically a noble metal cathode. Using the membrane as both an electrode and a filter enhances the oxidation efficiency due to improved mass transfer to the cathode surface. An EMR for the degradation of p-chloraniline was constructed by Zheng et al., which comprised a Ti/SnO_2-Sb anode and $\alpha-Al_2O_3$ ceramic membrane [100]. Applications of ED, hybrid CDI, MCDI, and EMR technologies are provided in the Applications Section.

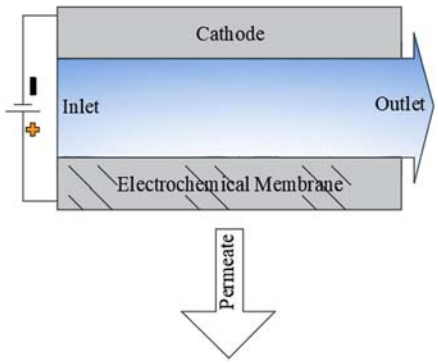

Figure 12.5 Schematic of electrochemical filtration system.

This book belongs to Badji Mokhtar Annaba University Central Library Copyright Elsevier 2025

12.4 Applications

This section reviews recent studies on different applications for selective separations using the introduced membrane-based electrochemical technologies. Specifically, we discuss three main applications for water treatment and purification: metal removal, selective metal recovery, and remediation of dilute contaminants. Each section highlights recent developments in the field and provides a brief overview of how these technologies are implemented for water purification and environmental remediation.

12.4.1 Selective removal of heavy metals and metalloids

Heavy metals are natural inorganic constituents—found in surface and groundwater through the discharge of industrial processes—which have significantly altered the geochemical and biochemical balance of surface and groundwater. Heavy metals of concern include copper (Cu), lead (Pb), mercury (Hg), Cadmium (Cd), Chromium (Cr), Nickel (Ni), and Zinc (Zn) [101], given that these are pollutants are often environmentally persistent and have diverse physicochemical properties not adequately addressed by current treatment technologies. These metals pose a serious threat to human health as they are toxic, carcinogenic, and have a tendency to bioaccumulate in living organisms, with the possibility of attaining levels that disrupt metabolic processes [102]. Excessive heavy metal concentrations can also result in soil quality degradation, crop yield reduction, and poor quality of agricultural products. Heavy metal pollution often originates from anthropogenic sources including dyes, pesticides, fertilizers, bleaching agents, metal plating, and mining [103]. To curb their concentrations in the environment, government agencies like the United States Environmental Protection Agency (USEPA) have set the maximum contaminant levels for heavy metals, such as 1.3, 0.015, 0.002, 0.005, 0.1, and 5 mg/L for Cu, Pb, Hg, Cd, Cr, and Zn respectively [104]. Due to stringent regulation of heavy metals, various treatment methods have been developed for their removal. In this section, we present membrane-based electrochemical technologies for heavy metal removal of As, Cr, Pb, and Cu as representative of the few studies that have investigated heavy metal removal using selective membranes or adsorbents in reactors. A summary of these is presented in Table 12.1.

12.4.1.1 Arsenic

Arsenic (As) occurs in the aqueous environment primarily as arsenite (AsO_3^{3-}) or arsenate (AsO_4^{3-}), with respective oxidation states of As(III) and As(V), the former being more toxic and intractable. Long-term exposure to arsenic oxyanion species can cause a host of illnesses such as cancer of the skin, the lung, the bladder, and/or the kidney, in addition to detrimental effects on the central nervous system [109]. Song et al. demonstrated selective arsenite removal using a PVF/CNT electrode as the electrosorbent, incorporated into a hybrid CDI cell with a carbon cloth cathode [92]. Selectivity coefficients reached 57.6 over

This book belongs to Badji Mokhtar Annaba University Central Library Copyright Elsevier 2025

This book belongs to Badji Mokhtar Annaba University Central Library

Table 12.1 Studies on membrane-based electrochemical systems for metal/metalloid removal [49,82,92,105–108].

Target species	Module	Membrane materials selection	Initial concentration	Water matrix	Performance (SC, RE)	Energy consumption	References
As (III)	Hybrid CDI	CEM:Type II Fuji Film AE: PVF-CNT	150 μg/L	C_0: 150 μg/L As (III), 2 mM $NaHCO_3$, 2.5 mM NaCl, 1 mM $NaNO_3$, 2.5 mM Na_2SO_4 and 10 mg/L humic acid	SC: 57.6 over Cl^-, 18.2 over NO_3^-, 14.2 over SO_4^{2-}, and 2.1 over PO_4^{3-} RE: 51.5% ± 1.3%	0.12 kwh/m^3	[92]
As (V)	Membrane sorption	FeO nanocomposite membrane	18.52 mg/L	C_0: 9.68 mg/L SO_4^{2-}, 15.19 mg/L NO_3^-, 353.43 mg/L Cl^-	SC: 4.60 over SO_4^{2-}, 46.65 over NO_3^-, 4.36 over Cl^-, 0.92 over PO_4^{3-}	—	[49]
Cr (VI)	EFS	CNT/PVDF/Stainless steel mesh membrane	1 mg/L	C_0: 100 mM Na_2SO_4	RE: 95.2%	—	[107]
	EMR	Heterogeneous AEM, homogeneous CEM	300 mM	C_0: 300 mM $NiCl_2$	RE: 92.6%	—	[106]
Pb (II)	Hybrid CDI	AEM FAS-PET 130	1 ppm	C_0: 1 ppm for Pb, Ca, and Mg	SC 3.5 over Ca, 3.3 over Mg	—	[105]
Cu (II)	ED	Cu ion imprinted CEM	0.8 M $Cu(NO_3)_2$	C_0: 0.8 M $Zn(NO_3)_2$	SC: 2.11 over Zn	—	[82]
	MCDI	Commercial AEM and CEM AE: activated carbon fiber	500 mg/L $CuCl_2$	C_0: 500 mg/L $ZnCl_2$	RE: 42.8%	1.24 Wh/g	[108]

AE, Active electrode; C_0, initial concentration of competing species; *PVDF*, polyvinylidene difluoride; *RE*, removal efficiency; *SC*, selectivity coefficient.
[a]In the table

Copyright Elsevier 2025

competing chloride anions with a low energy consumption of 0.12 kWh/m^3, which was attributed to the 0 V potential used to remove 51.5% of arsenite at an initial micropollutant concentration of 150 μg/L. Chaudhury et al. used an unconventional electro-enhanced membrane sorption device, where a ferric oxyhydroxide (FeO) nanocomposite membrane was situated between two platinum electrodes and it selectively adsorbed arsenic and phosphate ions migrating through the membrane [49]. Arsenate adsorption selectivity of 21.79 and 46.65 over nitrate were obtained at 0 and 10 V, respectively.

12.4.1.2 Chromate

The appearance of chromate (Cr) in natural waters is either trivalent Cr(III) or hexavalent Cr(VI) with the latter coming from industrialized processes such as metal plating, textiles, and tanneries. The more toxic hexavalent chromate exists in the forms of $Cr_2O_7^{2-}$, $HCrO_4^-$ at pH <6, and CrO_4^{2-} at pH >6 [17]. Studies on the removal of chromium have centered around Cr(VI) as Cr(III) occurs naturally in the earth's crust and is needed in the human diet. Liu et al. demonstrated the feasibility of an electrochemical filtration system housing a CNT/polyvinylidene difluoride/stainless steel mesh membrane as the cathode and Ti-Ru anode [107]. At a potential of 5 V the removal efficiency of Cr(VI) was found to be 95.2% in the presence of 100 mM Na_2SO_4. Khan et al. used an EMR to separate Cr(VI) and potassium from a solution comprising equimolar concentrations of K_2CrO_4 and $NiCl_2$ of 300 mM [106]. A recovery of 92.6% for Cr(VI) and 63.7% for potassium was exhibited for the ED-like reactor, comprising a heterogenous AEM and homogenous CEM being operated at a potential of 5 V and pH <6.

12.4.1.3 Lead

Lead (Pb^{2+}) may leach into drinking water through metal corrosion of aging pipes, fixtures, or faucets and during the production of paint and pesticides making it an intractable pollutant. As a potent neurotoxin, lead can have severe effects on children and cause developmental delays, fatal infant encephalopathy, and congenital paralysis [110]. Few studies have shown selective lead removal by membrane-based electrochemical technologies. Dong et al. showed the feasibility of a hybrid CDI apparatus with activated carbon electrodes and a commercial AEM FAS-PET 130 used to enhance the discharge efficiency of Pb(II) [105]. The system achieved first cycle removals of 58%, 72%, and 82% in a 2, 4, or 8 electrode design which was attributed to the increase in flow path length. First cycle selectivity coefficients of 3.5 and 3.3 were exhibited over competing Ca^{2+} and Mg^{2+} in a single pass flow-by operational mode in a 2-layer electrode configuration.

12.4.1.4 Copper

When ingested in large amounts, Copper (Cu) can cause detrimental health effects such as cancer, kidney failure, and respiratory problems [111]. Copper is one of the most widely used metals and arises in the environment from industrial effluents from

This book belongs to Badji Mokhtar Annaba University Central Library Copyright Elsevier 2025

sources such as smelting, electroplating, and electric appliances manufacturing processes. To remove copper in aqueous solution, Deng et al. imprinted copper onto a CEM to endow the membrane with copper specificity [82]. Its use in an ED reactor exhibited separation factors of 2.11 over zinc at a potential of −1.2 V for two hours. Wang et al. showed that it is possible to both remove and recover Cu(II) in a MCDI cell comprising activated carbon fiber electrodes, with carboxyl and hydroxyl functional groups serving as electron donors for reduction of Cu(II) to Cu(I)/C(0) [108]. Copper was preferentially adsorbed and electrodeposited over zinc at potentials of 0.8 V, due to the smaller hydrated radius of Cu(II) at a recovery efficiency of electrodeposited Cu of 42.8% relative to the amount removed (52.5 mg/g) at a specific energy consumption of 1.24 Wh/g. However, the electrodeposited electrodes required acid cleansing for regeneration.

12.4.2 Selective recovery of metal ions

The exponentially growing demand for personal electronic devices as well as energy and data storage from a wide array of industries including information technology has put enormous pressure on natural metal resources [112]. Thus, the mining and usage of both major metals and noble/rare-earth metals have been remarkably increasing [113,114], resulting in rising metal pollutants in the environment, and possible depletion of valuable metal resources in the near future. All these concerns, alongside a growing interest in sustainable development, have directed researchers to the recovery and removal of metal ions from the environment. Mining metals from a rich source (i.e., Li^+ from seawater) and recycling valuable metals from secondary resources such as electronic wastes and industrial wastewater are gaining rapid importance [45]. The group of valuable metals, the so-called critical elements, includes the rare-earth elements (REE), and the platinum-group metals (PGM), W, Co, Nb, V, etc. [115]. The concentration of metal ions in these secondary resources is generally low (usually in the parts-per-billion range), so the integration of different separation systems has been studied to improve recovery efficiency. Several methods are well-known for metal ion separation in an aqueous system: extraction, ion exchange, precipitation, adsorption, coagulation, and membrane filtration [116]. However, many of the conventional techniques require complicated steps and are chemically wasteful, thereby making it hard to achieve sustainability. In this section, we introduce applications of membrane-based electrochemical methods for the recovery of valuable metal ions (Table 12.2). It should be noted that the hybridization of electrochemical techniques and membranes for selective ion separation is relatively new, so there are few studies on selective membrane-based electrochemical techniques.

12.4.2.1 Lithium

Since the advent of lithium-ion batteries with countless applications, the availability of lithium, a key element, has now become universal [48]. Brine and seawater are the

This book belongs to Badji Mokhtar Annaba University Central Library Copyright Elsevier 2025

This book belongs to Badji Mokhtar Annaba University Central Library

Table 12.2 Studies on membrane-based electrochemical systems for metal ion recovery [4,39,47,48,50,51,94,117–119].

Target species	Module	Membrane materials selection	Initial concentration	Water matrix	Performance	Energy consumption	References
Li	MCDI	CIMS (monovalent selective CEM) and AEM	0.0058 mol LiCl/L	C_0: 0.0058 mol MgCl/L	Selectivity: 2.95	0.0018 kWh/mol	[94]
	MC-MCDI	CEM and AEM λ-MnO_2 as Li^+ selective adsorbent	216 mM Li^+	C_0: 3306 mM Na^+, 473 mM K^+, 395 mM Mg^{2+}, 8 mM Ca^{2+} in simulated brine.	SC: 804 over Na^+, 387 over Mg^{2+}.	57 kJ/mol	[4]
	ED	Mo_6S_8 and $LiMn_2O_4$ membranes	1 M Li_2SO_4	C_0: 0.1 M $CoSO_4$. 0.1 M N_2SO_4 at the recovery compartment	Selectivity rate: ~100% over Co^{2+}	—	[51]
	ED	PP13-TFSI (N-methyl-N-propylpiperidium bis (trifluoromethane-sulfonyl) imide) impregnated between Nafion 324	170 ppb	C_0: 10,500 ppm Na, 1350 ppm Mg, 400 ppm Ca, 380 ppm K	SC:76.7 over Na. 32.9 over Mg, 8.95 over Ca, and 6.54 over K RE: 22.2%	—	[118]
	Reverse ED	Li ionic superconductor-type crystals	170 ppb	C_0: 10,500 ppm Na, 1350 ppm Mg, 400 ppm Ca, 380 ppm K	Competing ions below the detection limit of ICP-AES RE: 7%	—	[119]
	ED	Monovalent selective CEM and AEM	150 mg/L	C_0: 10–60 g/L Mg^{2+}	Permselectivity: 20.2–33.0 over Mg^{2+} RE: 94.5%	0.0019 kWh/g Li	[47]
	Electrodeposition	NASICON solid-state electrolyte AE: Cu and Ru-containing electrodes	0.1–0.2 ppm	Seawater in anode compartment $LiClO_4$-propylene carbonate in cathode compartment	Na^+ below the detection limit of ICP-Ms Deposition: 57 μg Li/cm^2 Cu electrode	—	[39]
Co	Batch ED	Mo_6S_8 electrochemical transfer junction	0.1 M $CoSO_4$	C_o: 0.1 M $NiSO_4$.	Selectivity factor: ~99%	—	[50]

Copyright Elsevier 2025

This book belongs to Badji Mokhtar Annaba University Central Library

				0.1 M N_2SO_4 at the recovery compartment			
	ED	Liquid membrane (trialkylbenzylammonium chloride + tri-n-octylamine in 1,2-dichloroethane), CEM & AEM	0.01 M Co (II)	C_o: 0.01 M Ni (II) 3−6 M HCl	SF: 145 Co over Ni (1:1 Co:Ni)/400 (10:1 Co:Ni with 0.1 M Co(II))	—	[48]
W	Batch ED	AEM AE: Ti/MMO wire	—	Deep eutectic solvent: Choline chloride and malonic acid (MA) (1:1) Choline chloride and oxalic acid (OA) (1:1)	SF: 3.37 (As over W) RE: 18.2% As and 5.4% W in MA mixture SF: 2.24 (W over As) RE: 5.0% As and 11.2% W in OA mixture	—	[117]

AE, Active electrode; C_0, Initial Concentration of competing species; *RE*, removal efficiency; *SC*, Selectivity coefficient; *SF*, separation factor.
Selectivity: $(C_{Li+,f}/C_{Li+,i})/(C_{Mg2+,f}/C_{Mg2+,i})$.
The ratio of the transported ions over the ratio in the initial solution.

Copyright Elsevier 2025

main sources for lithium ions and, recently, e-waste (electronic waste) and desalination concentrate from seawater have gained a great deal of attention as secondary sources for lithium recovery [120]. A couple of obstacles in lithium mining are the extremely negative reduction potential leading to the difficulty in efficient electroplating and the dilute concentration of Li^+ in the major sources with excess competing ions. Thus, conventional lithium separation methods such as lime soda evaporation, solvent extraction, and adsorption suffer from low energy efficiency, chemically demanding process, and long operation time to recover lithium ions [121–123].

MCDI has been adopted by several studies for lithium selective separation. Shi et al. separated Li^+ from a feed containing Li^+ and Mg^{2+} using a MCDI system equipped with monovalent-ion-selective CEM and AEM [94]. The incorporation of the CEM increased the selectivity of Li^+ over Mg^{2+} up to 2.95 under 1.0 V within 10 min, and the technique achieved a moderate recovery rate of 38.4%. Notably, the specific energy consumption remained low even in their customized large module. Kim et al. used three separate channels in a MCDI system for selective lithium recovery in a simulated brine [4] (Fig. 12.6). Known as multichannel membrane CDI (MC-MCDI), this CDI system employs two channels (i.e., feed channel and side channel for redox couple materials), with an added ion-concentrated channel containing λ-MnO_2, a lithium selective adsorbent for the up-concentration of lithium ions. The reversible redox couple of ferri/ferrocyanide provides an energy-efficient and robust desalination mechanism by enabling continuous operation and lithium enrichment. The electrochemical approach proved that MCDI can be a potential industry-scale

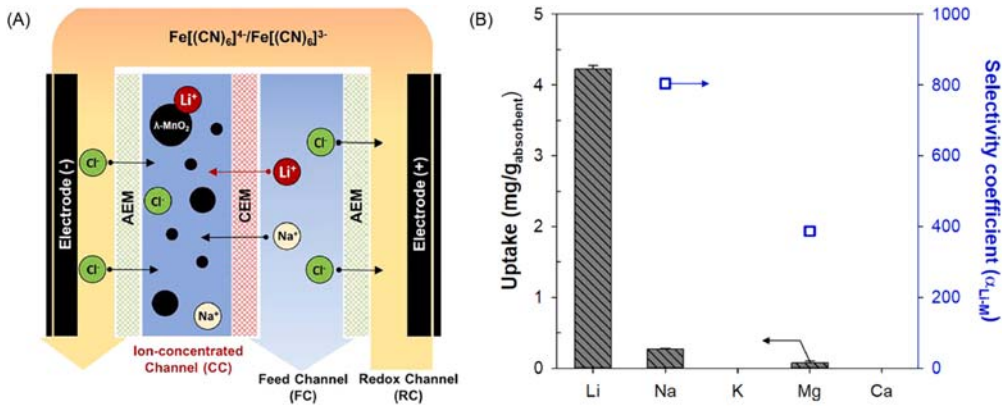

Figure 12.6 Multichannel membrane-modified CDI (MC-MCDI). (A) Schematic of the redox-mediated MC-MCDI for lithium ion recovery. (B) Uptakes of Li^+, Na^+, K^+, Mg^{2+}, and Ca^{2+}, and the selectivity coefficients of Li^+ against the competing ions. *Reprinted from [4] with permission from Elsevier. Credit: N. Kim, X. Su, C. Kim, Electrochemical lithium recovery system through the simultaneous lithium enrichment via sustainable redox reaction, Chem. Eng. J. (2020) 127715.*

This book belongs to Badji Mokhtar Annaba University Central Library Copyright Elsevier 2025

candidate for lithium recovery, showing the selectivity coefficient as high as 804 over Na^+ and 387 over Mg^{2+}.

The development of various lithium selective membranes has allowed ED to be adopted for selective lithium separation. Guyot et al. synthesized Mo_6S_8 and $LiMnO_4$ electrochemical transfer junctions (ETJs) based on oxide layer onto porous ceramics [51]. As Li^+ selectively crossed over $LiMnO_4$ and Co^{2+} over Mo_6S_8, these multiple membrane junctions enabled the simplification of a multiple-step separation between the metal cations often found in leachates in an aqueous medium, thus providing 100% of selectivity rate for Li^+. Hoshino investigated the lithium selectivity performance of an ionic-liquid organic membrane (IL-i-OM) and an ionic semiconductor-type crystal newly introduced to ED for seawater [118,119]. PP13-TFSI (*N*-methyl-*N*-propylpiperidium bis (trifluoromethane-sulfonyl) imide) was impregnated between two Nafion 324 layers to use as an IL-i-OM because the TFSI functional group shows high Li^+ conductivity while the Nafion layers efficiently prevent the outflow of the ionic liquid [118]. Selective Li^+ permeation by the membrane obtained the removal efficiency (or recovery ratio) of 22.2% by blocking the other competing ions (Fig. 12.7). In another study, a lithium ionic superconductor was used as a Li separation membrane [119]. Lithium ions selectively permeated through the membrane, and concentrated in the positive electrode compartment, reaching 7% of removal efficiency after 72 h. This process generated electricity driven by the differential lithium-ion concentration between the two electrodes. Nie et al. placed monovalent selective ion-exchange membranes to separate Li^+ from the binary synthetic brine containing Mg^{2+} ions [47]. After ED for 3 h with a constant current density of 5.9 A/m^2, a removal efficiency of 94.5% and low energy

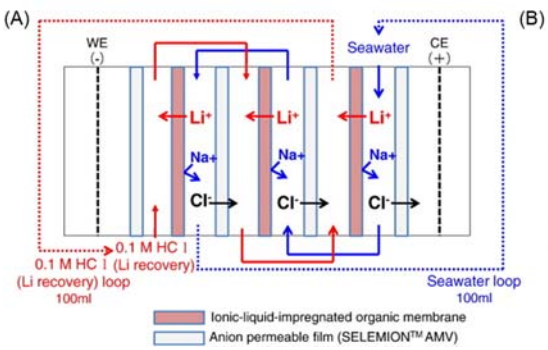

(B)

(a) IL-i-OM

	Na	Mg	Ca	K	Li
Concentration in seawater (Oarai beach, Japan)	10500 ppm	1350 ppm	400 ppm	380 ppm	170 ppb
⇩ Electrodialysis (2 V, 2 h)					
	Na	Mg	Ca	K	Li
Concentration in HCl	1.24 ppm	0.37 ppm	0.05 ppm	0.43 ppm	10.1 ppb
Recovery ratio	0.009%	0.03%	0.01%	0.27%	**5.94%**

(b) High-durability IL-i-OM

	Na	Mg	Ca	K	Li
Concentration in seawater (Oarai beach, Japan)	10500 ppm	1350 ppm	400 ppm	380 ppm	170 ppb
⇩ Electrodialysis (2 V, 2 h)					
	Na	Mg	Ca	K	Li
Concentration in HCl	39.41 ppm	11.6 ppm	12.34 ppm	15.87 ppm	37.7 ppb
Recovery ratio	0.38%	0.86%	3.09%	4.18%	**22.2%**

Figure 12.7 Selective Li^+ permeation by the membrane blocking the other competing ions. (A) Schematic of IL-i-OM-assisted ED system for lithium-ion recovery. (B) The recovery ratio of Li^+ and other competing cations after 2 h at the applied voltage of 2 V. *Reprinted from [118] with permission from Elsevier. Credit: T. Hoshino, Preliminary studies of lithium recovery technology from seawater by electrodialysis using ionic liquid membrane, Desalination 317 (2013) 11–16.*

This book belongs to Badji Mokhtar Annaba University Central Library Copyright Elsevier 2025

consumption were attributed to the high permselectivity up to 33.0 over Mg^{2+}. Besides CDI and ED techniques, Yang et al. conducted a proof-of-concept lithium electrodeposition from seawater by using a solar-power electrolysis and (NASICON)-type solid-state electrolyte as a selective membrane [39]. The NASICON membrane efficiently blocked Na^{+}, the other major cation under the detection limit of ICP-Ms, and the solar-powered cell obtained the electrodeposition rate of 57 μg Li/cm^2.

12.4.2.2 Cobalt

Cobalt (Co) and Nickel (Ni) are easily found in daily life as a form of corrosion and wear-resistant metal alloys, rechargeable batteries, and blue color pigments. Due to the similarity of the physicochemical properties of Co and Ni, the separation of cobalt ions from nickel ions using classical methods such as precipitation and crystallization remains challenging [124]. Their reduction potentials are also close to each other, making selective electrodeposition extremely challenging. Guyot et al. reported selective cobalt extraction in a batch ED system using the same Mo_6S_8 ETJ applied in their lithium selective separation [50]. After the intercalation of cobalt and nickel ions from the feed compartment, the optimal applied potential allowed only Co^{2+} to be deintercalated and cross over the ETJ, achieving the high selectivity factor of 99%. This result was mainly attributed to the facile intercalation kinetics of Co^{2+} and the extraction potential of Co^{2+} lower than that of Ni^{2+} by 0.1 V in the recovery compartment cell. Sadyrbaeva et al. introduced a liquid membrane to an ED system for cobalt-nickel ion separation [48]. The system had not only both AEM and CEM to control the acidic pH and confine metal ions as well as chloride anions in the middle compartment, but also a liquid membrane containing tri-n-octylamine or trialkylbenzylammonium chloride in 1,2-dichloroethane. The selective mechanism of the membrane was based on the different stability of anionic chloride complexes of cobalt and nickel. In other words, cobalt (II) can form anionic complexes $CoCl_4^{2-}$ in a highly acidic HCl solution while nickel (II) complexes still stay cationic. Under the optimal constant current conditions, cobalt (II) anionic complexes were selectively transported through the liquid membrane, achieving the separation factor of 145 toward cobalt (II) in a 1:1 cobalt-nickel mixture and 400 in a 10:1 mixture.

12.4.2.3 Tungsten

Tungsten (W) has a wide range of uses in the production of cemented carbides, mill, alloys, and steels and has been assigned as one of the critical raw materials by the European Union and the United States of America [125,126]. Mining residues from the tungsten ore are considered low-grade secondary resources, but they often contain arsenic from arsenopyrite (FeAsS), which is one of the harmful elements that are of environmental concern [127]. To recover tungsten and remove arsenic from these

This book belongs to Badji Mokhtar Annaba University Central Library Copyright Elsevier 2025

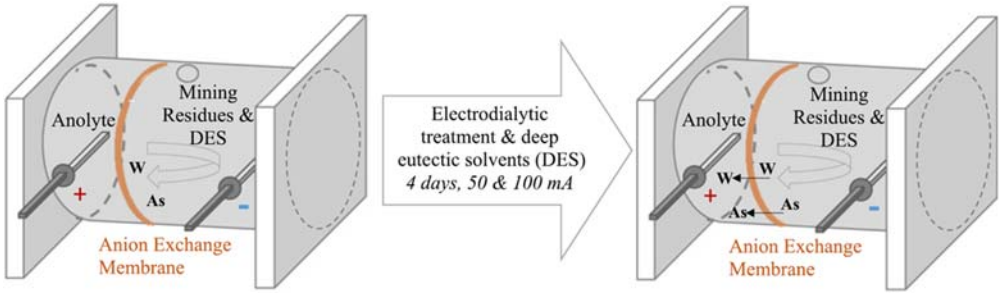

Figure 12.8 Schematic of electrodialytic two-compartment cell with DES for selective ion separation between W and As. *Reprinted from [117] with permission from Elsevier. Credit: J. Almeida, R. Craveiro, P. Faria, A.S. Silva, E.P. Mateus, S. Barreiros, A. Paiva, A.B. Ribeiro, Electrodialytic removal of tungsten and arsenic from secondary mine resources—deep eutectic solvents enhancement, Sci. Total Environ. 710 (2020) 136364.*

mining residues, Almeida et al. coupled ED with deep eutectic solvents (DES) as a proof of concept [117] (Fig. 12.8). DES, a mixture of hydrogen bond donors and acceptors, has been considered promising for the extraction of metals from many sources due to its advantages in terms of costs, toxicity, and biodegradability [128]. The results showed that selective extraction highly relied on various eutectic solvents, thus indicating the importance of electrolyte/solvent/process selection. For instance, the mixture of choline chloride and oxalic acid (1:1) provided a high separation factor of 2.24 for tungsten, while the separation factor of the mixture of choline chloride and malonic acid (1:1) was 3.37 toward arsenic.

12.4.3 Remediation of dilute contaminants

This section highlights the membrane-based electrochemical technologies for the treatment of dilute contaminants other than the metallic ions discussed so far. It is important to note that certain organic contaminants are also ionic species. As such, we discuss current and emerging technologies for the removal of organics, as well as selective separation of other nonmetallic ions of interest.

12.4.3.1 Removal and degradation of organic pollutants

Just like heavy metals and metalloids, organic ions have sparked much attention due to their toxicity and ubiquity in the environment. In particular, organics pose a great challenge because of their biorefractory nature, and propensity to be metabolized to more soluble and, in some cases, even more toxic byproducts [129]. Many of these persistent pollutants show resistance to the conventional processes used in water treatment plants, such as biological treatment, coagulation, chemical oxidation, and adsorption [19]. Other approaches for the removal of organic contaminants include the use of EAOPs such as anodic oxidation (AO), electro-Fenton (EF), photoelectro-Fenton (PEF) and solar

This book belongs to Badji Mokhtar Annaba University Central Library Copyright Elsevier 2025

photoelectro-Fenton (SPEF) to remove pharmaceuticals, dyes, and other organic molecules [130,131]. However, these methods incur high capital costs and operational costs which has hampered their implementation on a larger scale. More recently, the integration of electrochemical systems and membrane technology has shown the way to a promising alternative for the removal of organic pollutants due to the enhanced removal efficiency, ease of application, and improved antifouling ability of membranes [6].

Membrane-based electrochemical systems have been used to target the removal of a number of different organic contaminants from water. For example, Tan et al. used a multi-walled carbon nanotube (MWCNT)-based electrochemical filtration system (EFS) to degrade antibiotics such as sulfamethoxazole, ciprofloxacin, and amoxicillin in water [132]. The conducted studies used binary and ternary mixtures of these antibiotics. Breakthrough curves for each of these mixtures are shown in Fig. 12.9. Results show that

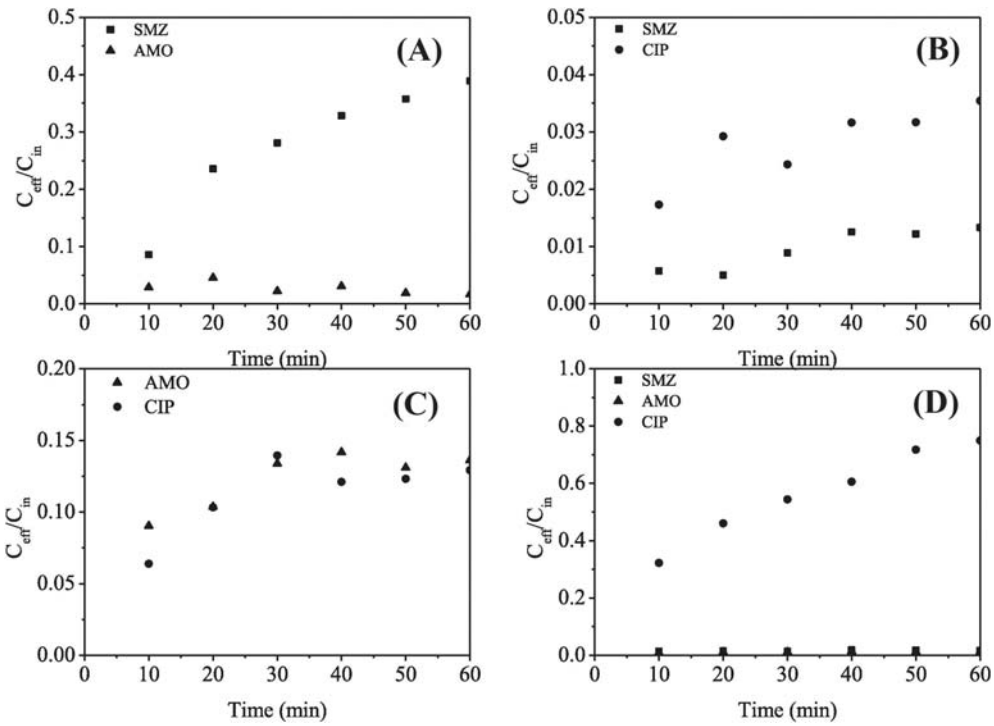

Figure 12.9 Simultaneous removal of different antibiotics using MWCNT-based electrochemical membrane filtration. (A) SMZ and AMO binary mixture; (B) SMZ and CIP binary mixture; (C) AMO and CIP binary mixture; and (D) SMZ, CIP, and AMO ternary mixture. *Reprinted from [132] with permission from Elsevier. Credit: T.Y. Tan, Z.T. Zeng, G.M. Zeng, J.L. Gong, R. Xiao, P. Zhang, B. Song, W.W. Tang, X.Y. Ren, Electrochemically enhanced simultaneous degradation of sulfamethoxazole, ciprofloxacin and amoxicillin from aqueous solution by multi-walled carbon nanotube filter, Sep. Purif. Technol. 235 (2020) 116167–116167.*

This book belongs to Badji Mokhtar Annaba University Central Library Copyright Elsevier 2025

the EFS achieved 98%, 95%, and 20% simultaneous removal and adsorption capacities of 6.47, 5.52, and 1.49 mg/g for amoxicillin, sulfamethoxazole, and ciprofloxacin, respectively. Degradation of another antibiotic, sulfadiazine, was carried out using a polyvinylfluoride/stainless steel mesh EFS [133]. The membrane, which was used as a cathode, was tested using both synthetic and natural water matrices. The removal efficiency in natural water was 79.7%, which was just a 4.4% decrease compared to its performance in synthetic deionized water. P-chloroaniline (PCA), a precursor to antimicrobial products and pesticides, has also been degraded using EFS [100,134]. For example, Zheng et al. used a cathodic MF membrane made out of an epoxy resin and Al_2O_3 on a titanium mesh support and obtained the complete degradation of PCA and a 75.1% mineralization ratio via homogeneous EF reactions [100].

Besides antibiotics, phenols have also been the focus of membrane-based electrochemical systems for water purification. For instance, Yang et al. created a system for the removal of phenol, protein, and glucose using a porous carbon/CNT hollow-fiber cathode [135]. They focused on enhancing the fouling control by coupling an EFS with EF processing and compared their results vis-à-vis the same system without the electron-Fenton assistance. This integrated system removed 89.2%, 65.4%, and 83.5% of protein, glucose, and phenol, respectively; and it was concluded that protein, glucose, and phenol removal performance using the coupled system was 2.7, 6.2, and 9.7 times higher, respectively, than those using the membrane separation alone. Phenolic wastewater treatment was also investigated using a TiO_2 loaded carbon electrochemical membrane [136]. The electrochemical membrane system achieved 86.3% of total organic carbon removal and 99.4% removal of phenol from a 2.0 mM synthetic phenol solution. Zaky and Chaplin also performed an extensive study of p-substituted phenol oxidation mechanisms using a substoichiometric Ti_4O_7 reactive electrochemical membrane and density functional theory (DFT) calculations [137]. A 92.9%–99.9% removal for p-methoxyphenol and 96.9%–98.5% for p-nitrophenol were observed depending on the applied current densities, whereas negligible to no removal was observed at open-circuit conditions. DFT calculations showed that p-benzoquinone was likely removed by its reaction with hydroxide radicals formed during the electrochemical experiments. The same system was also applied for oxidation of perfluoroalkyl substances such as perfluorooctanoic acid and perfluorooctane sulfonic acid, for which they obtained high removal rates and permeate concentrations below detection level [138].

Apart from the capabilities for efficient separation, it is important to consider the extent to which these systems can be applied in practical contexts. Hence, some studies have explored the feasibility for scaling up membrane-based electrochemical systems for organic treatment in real wastewater. For example, Cui et al. investigated the arrangement of electrochemical oxidation, an upflow biological aerated filter, and ED in pilot plant scale to remove N-heterocyclic contaminants and salts from industrial

This book belongs to Badji Mokhtar Annaba University Central Library Copyright Elsevier 2025

discharge water [139]. Their combined process achieved considerably lower operating costs than the industrial water price in the locality, over 90% removal of target species (tricyclazole, 1H-1,2,4-triazole and propiconazole) and over 99% salt removal. MCDI has been evaluated at a pilot scale for wastewater reclamation using 50 pairs of anion/cation exchange electrodes [140]. The results showed high removal of nitrate (over 91%), and negligible deterioration in its performance during a 15-day operation. Mameda et al. studied a hybrid membrane system that employed electrochemical oxidation for secondary treatment of textile industry wastewater effluent [141]. Pilot-scale tests for this study presented substantial removal of turbidity, color and 1,4 dioxane, and displayed relatively low energy consumption when compared to other electrochemical oxidation processes. A more detailed discussion and technoeconomic analyses on electrochemical membrane systems will be presented in the following section (Section 12.5).

12.4.3.2 Selective removal of inorganic ions

Despite recent advances in the field, membrane-based electrochemical technologies often show limited selectivity towards specific organic pollutants. Although current systems display significant performances for pollutant degradation, most of these techniques rely on pathways that are not inherently selective towards the target species, and which at times can form toxic byproducts when reacting with other ions in the solution [100,142,143]. An example of this phenomenon was demonstrated by a study that combined AO using a boron-doped diamond (BDD) anode and a CEM. The system was used to treat secondary effluent from a municipal sewage treatment plant which contained 29 target pharmaceuticals and pesticides [143]. While almost complete mineralization of the majority of the organic matter was achieved in just 2 h of electrolysis, oxidation of chloride ions that were present in the wastewater yielded hypochlorite (ClO^-), chlorate (ClO_3^-), perchlorate (ClO_4^-), chloramines, and organochlorinated byproducts, which are known to be persistent toxic pollutants. Moreover, the production of ions such as ClO_3^- and ClO_4^- during the electrolysis process reached high concentrations of up to 1.5 and 1.0 mM, respectively, which requires the placement of an additional electrochemical reduction process to counteract their formation. Furthermore, there are applications that require selectivity towards certain ions that are desired to be recaptured, like the recovery of valuable nutrients such as ammonium ($NH4^+$), phosphorus, and nitrate (NO_3^-). While relatively few in number, studies that have examined the ability to selectively capture ions in membrane-based electrochemical systems are presented in Table 12.3.

12.4.3.2.1 Nitrate

As can be seen from Table 12.3, research on selectivity using these systems has mainly focused on nitrate removal. Although most research on nitrate removal is designed to

This book belongs to Badji Mokhtar Annaba University Central Library Copyright Elsevier 2025

This book belongs to Badji Mokhtar Annaba University Central Library

Table 12.3 Studies on membrane-based electrochemical systems for selective removal of dilute ions from water. [144–153].

Target species	Module	Membrane materials selection	Initial concentration	Water matrix	Performance	Energy consumption	References.
F^-	ED	PC-MVA & PC-MVK IEMs	5–15 mg F^-/L	C_0:15–45 mg NO_3^-/L, 0.5 g NaCl/L	RE: 80%–90%	32–82 kWh/kg F^-	[147]
	Batch ED	Neosepta AMX & CMX	2 mg F^-/L	C_0: 40 mg Cl^-/L, 50 mg SO_4^{2-}/L	RE: 63%–96%	4–37 kWh/kg F^-	[144]
	ED	Neosepta AMX-SB & CMX-SB	5 mg/L NaF	C_0: 5 g NaCl/L, 100 mg $NaNO_3$/L Simulated brackish water	RE: 65.6%	—	[146]
NO_3^-	MCDI	Neosepta AMX & CMX	2 mM $NaNO_3$	C_0: 5 mM NaCl	SC: 4.37 over Cl^-[a]	—	[149]
	Batch ED	Conductive binder heterogenous AEM	50 mM KNO_3	C_0: 50 mM KCl	SC: ~3 over Cl^- SC[a]: ~5 over Cl^-	—	[151]
	MCDI	Ion exchange polymer coated carbon electrode with A520E resin	0.85 mM NO_3^-	C_0: 2.27 mM Cl^-, 0.43 mM SO_4^{2-} Real municipal wastewater	RE: 81.5%	—	[148]
	ED	PCA-SK & PCA-SA	225 mg/L NO_3^-	C_0: 707 mg SO_4^{2-}/L, 2674 mg Cl^-/L Real brackish water	RE: 88%	13.2 W h/L	[145]
	MCDI	Neosepta AM-1 & CM-1	233 mg/L NO_3^-	C_0: 90 mg Cl^-/L, 40 mg SO_4^{2-}/L Groundwater sample	RE: 98%	0.4 kWh/m^3	[153]
	ED	Neosepta AMX-SB & CMX-SB	100 mg $NaNO_3$/L	C_0: 5 g NaCl/L, 5 mg/L NaF Simulated brackish water	RE: 94.1%	—	[146]
PO_4^{3-}	Dead-end filtration cell	NH_2-MIL-101 mixed matrix UF membrane	0.5 mg/L P of KH_2PO_4	C_0: Cl^-, SO_4^{2-}, and NO_3^- at the same molar level as P	RE: 74.0% q_e: 79.414 mg P/g	0.0678 kJ/L	[150]
	ED	Guanidinium-functionalized AEM	10 mM NaH_2PO_4	C_0: 30 mM NaCl, 1 mM Na_2SO_4 Model dairy wastewater	RE: 72.1%	—	[152]

C_0, Initial concentration of competing species; q_e, uptake capacity; *RE*, removal efficiency; *SC*, selectivity coefficient.
[a]Selectivity at equilibrium (not dynamic).

Copyright Elsevier 2025

eradicate it as a pollutant due to its detrimental effects on aquatic ecosystems and associated risks with cancer [154], nitrate is also an essential nutrient used by plants as a source of nitrogen. Nitrate is used as fertilizers, food preservatives, pharmaceuticals, and in the production of explosives [155]. Thus, improving the selectivity towards nitrate can be useful to recover it as a value-added commodity. However, this task has proven to be a difficult, since selectivity towards nitrate is typically hindered by the presence of chloride ions in water due to their identical ionic charge, and similar diffusion coefficients (1.90×10^{-9} m^2/s for NO_3^- and 2.03×10^{-9} m^2/s for Cl^-) [156]. Although millimolar concentrations of nitrate can be removed at selectivity coefficient values ranging from 6 to 10 (based on state-of-art research), higher selectivity values than reported in the literature are needed to reduce life cycle treatment costs according to Hand and Cusick [157].

There has been significant attention to achieving competitive electrosorption between nitrate and chloride using commercial IEMs in MCDI systems. The use of Neosepta AMX AEMs indicated that nitrate selectivity could be increased with decreasing applied current [149]. The work reported a selectivity coefficient of 4.37 (NO_3^-/Cl^-) at equilibrium in a 5 mM NaCl and 2 mM $NaNO_3$ solution, but the performance drastically decreased when operated dynamically. Another study used a Voltea brand MCDI setup and Neosepta AM-1 AEMs to investigate NO_3^- transport in a 24-cell system [153]. Results showed that 98% of nitrate was removed from a 233 mg/L NO_3^- groundwater sample while achieving a slower Cl^- removal rate. However, the removal rate for sulfate ions was equal to the removal rate of nitrate, suggesting no selectivity toward sulfate.

There have also been significant advances in the development of tailored membranes to achieve nitrate-selective separations. For example, a recent study showed that nitrate selectivity over chloride increases with the increasing number of alkyl groups in heterogenous AEM conductive binders, and compared their performance versus commercialized AEMs [151]. Results show that higher selectivity coefficients were obtained for the conductive binder AEMs in both equilibrium and dynamic conditions (Fig. 12.10). The study

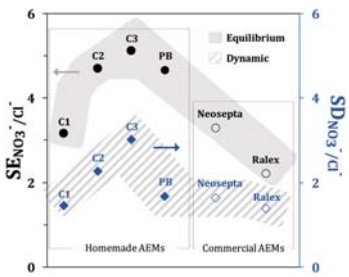

Figure 12.10 Nitrate selectivity using conductive binder anion exchange membranes, polymeric binder (PB), and commercial anion exchange membranes at equilibrium (SE) and under dynamic conditions (SD). *Reprinted from [151] with permission from Elsevier. Credit: T. Mubita, S. Porada, P. Aerts, A. van der Wal, Heterogeneous anion exchange membranes with nitrate selectivity and low electrical resistance, J. Membr. Sci. 607 (2020) 376–7388.*

This book belongs to Badji Mokhtar Annaba University Central Library Copyright Elsevier 2025

also found that it is possible to identify selectivity based on the hydration energy for monovalent ions of similar hydrated sizes. The selectivity was attributed to the lower hydration energy of NO_3^- (314 kJ/mol) than that of Cl^- (381 kJ/mol) [158], which meant NO_3^- has fewer water molecules surrounding it, allowing the formation of stronger electrostatic interactions with the ion-exchange sites in the membranes. Kim et al. created a nitrate selective electrode for desalination of wastewater using a MCDI system [148]. Using a nitrate selective A520E resin within the electrode it was possible to achieve 81.5% removal of NO_3^- from real wastewater effluent samples, with preferential adsorption for NO_3^- versus other competing species such as chloride and sulfate.

12.4.3.2.2 Phosphorus

Phosphorus is an essential nutrient and a vital cell component [159]. Unlike nitrogen fertilizers, which can be produced via the Haber-Bosch process, phosphorus is mainly harvested from phosphate rock (thus being of limited supply) and is often mined from places with both heavy metal and uranium [160]. Although there are ways to recover phosphate from wastewater and sewage sludge, the current cost for recovered phosphorus greatly exceeds that for phosphorus from phosphate rock [161]. Hence, selective phosphate recovery has also been pursued as an application for membrane-based systems, as an avenue for decreasing phosphorus resource recovery from wastewater. For instance, a study investigated the selective rejection of phosphate ions (PO_4^{3-}) using an UF membrane coupled with CDI [150]. The dual-layer mixed matrix membrane, which was created using NH_2-MIL-101 metal organic framework (MOF) in a polyethersulfone (PES) polymer matrix, achieved 74% removal of phosphate from synthetic wastewater containing coexisting ions at the same molar level of P. The performance of their CDI-UF system was not influenced by the incorporation of neither Cl^- nor NO_3^- or SO_4^{2-}, demonstrating selectivity towards phosphate while also exhibiting high permeability. Recovery of phosphate from model dairy wastewater was also explored by using acrylate monomer to create AEMs with guanidinium groups as ion exchange sites [152]. Using ED, the system showed 72.1% of permselectivity towards NaH_2PO_4. The same group also conducted a study using a guanidinium-based polyelectrolyte to prepare a functionalized AEM which displayed increased permeation of phosphate over sulfate during ED [162].

12.4.3.2.3 Fluoride

Other ions, such as fluoride, have also been of great interest in the separation from water using membrane-based electrochemical systems. ED seems to be the most prevalent method for fluoride separation among membrane-based electrochemical approaches, mainly by leveraging commercial IEMs. Arahman et al. examined fluoride separation from groundwater using commercial IEMs and monovalent selective AEMs in a batch ED setup [163]. The study compared the performance of the system using the standard AEM against a monovalent-selective AEM, and found that the selectivity

This book belongs to Badji Mokhtar Annaba University Central Library Copyright Elsevier 2025

did not improve based on the type of membrane employed. Additionally, it was found that the presence of chloride ions hampered the selectivity towards fluoride since chloride could permeate through the membrane more easily, and it thus required less applied voltage to remove the same amount of fluoride ions from water. The separation of fluoride from water containing a ternary mixture of sulfate, chloride, and fluoride ions was also studied using standard IEMs and ED [144]. Using an F^-: Cl^-: SO_4^{2-} ratio of 1:25:25, fluoride was separated with a 96% removal from a 2 mg F^-/L solution. This degree of removal was much higher than using lower F^- to Cl^- or SO_4^{2-} ratios, and was explained by the increased ionic strength of the solution. Banasiak and Schäfer conducted experiments to investigate the effect of organic matter on the selectivity of commercial IEMs towards fluoride [146]. Their results showed that the presence of organic matter enhanced the removal of F^- due to the complexation with organic molecules. They also found that there was competitive permeation between NO_3^- and F^-, since the system was only able to remove about 65.6% of F^-, whereas 94.1% of NO_3^- was removed. A recent study focused on the effect of nitrate on the selectivity of fluoride using commercial monovalent-selective IEMs in an ED system [147]. It was concluded that the nitrate removal efficiency was higher than that for fluoride due to the smaller hydrated radius and higher mobility of NO_3^-. Despite this, an effluent fluoride concentration below the World Health Organization (WHO)'s guidelines for F^- levels in drinking water was obtained.

12.5 Technoeconomic analysis considerations

Technoeconomic analysis (TEA) is an essential tool that is used to establish a development pathway for novel selective separation technologies by evaluating the economic feasibility of a set of design and operating decisions such as material choice, target ions, and relative removal. TEAs yield economic data by using a process or input-output model to size equipment which is then used to estimate capital and operational costs [164], and can be leveraged to highlight key parameters that have the greatest influence on system lifecycle costs. In this section, we present important design considerations for membrane-based separations technologies through insight gained from TEAs of CDI and MCDI as no TEAs have been developed for selective ED processes.

TEAs for CDI and MCDI processes have shown that membrane selectivity, water recovery, influent concentration, cell voltage limit, and system lifetime significantly affect the lifecycle cost of treating water [157]. The total cost of CDI and MCDI systems for brackish water deionization is generally dominated by the capital costs, with the cost of IEMs being the primary contributor to lifecycle water. This enables electrochemical reactors that include IEMs to essentially be costed based on the price per square meter of membrane and system lifetime, as is done for ED reactors.

This book belongs to Badji Mokhtar Annaba University Central Library Copyright Elsevier 2025

While TEAs have yet to be conducted for ion selective redox polymer-based systems, a recent TEA for CDI showed how impactful ion selective removal of ions can be on life-cycle water treatment costs. Hand and Cusick constructed an ion-selective parameterized process model TEA elucidating distinct feedback between target ion concentration, material ion-selectivity, and capital cost. If the target ion influent and effluent concentrations are in the millimolar scale, as is the case for nitrate, then system sizing led to scenarios in which the pump and capacitor energy requirements are more influential than the capital costs leading to lifecycle treatment costs below 0.05 USD/m^3 [157]. However, for target ion influent concentrations in the micromolar scale (e.g., perchlorate), material selectivity must reach values greater than 100 to achieve similar life cycle costs. Regardless of treatment conditions and the selectivity of separation, electrode longevity is the primary driver of system costs, with target electrode lifetimes ranging in the 60,000–120,000 charge/discharge cycles [157]. Therefore, electrode material development should focus on both ion-selectivity and durability to enable full-scale implementation of electrochemical separation technologies.

12.6 Conclusions and perspectives

Membrane-based electrochemical technologies have been shown as promising alternatives to conventional water treatment applications due to the combined advantages that they provide, such as improved antifouling ability, modularity, and increased removal efficiencies. ED and MCDI show promising potential for implementation of these technologies on a larger scale while maintaining efficient removal rates with low energy consumption compared to currently used EAOPs. EFS can exhibit additional improvements to membrane separation processes, such as convection-enhanced mass transport and increased electroactive surface area, which further alleviates diffusion limitations that typical electrochemical processes have. Hence, these technologies have provided new pathways to address multiple applications within the field of water purification such as heavy metal removal, metal and nutrient recovery, and remediation of dilute pollutants.

Despite the rapid increase of studies in the field, the focus on molecular selectivity using electrochemical membranes is a relatively new area of research, and it needs to be further investigated to benchmark performance for various environmental and water purification applications, especially in comparison with more well-established techniques. Moreover, several challenges must be overcome for these systems to be implemented at a larger scale. First, there is a need for a fundamental understanding of the mass transport phenomenon, reaction kinetics, and selectivity mechanisms that occur in membrane-based electrochemical processes to become one able at designing optimized systems durability. Second, life cycle and technoeconomic analyses for these processes are scarce and urgently

This book belongs to Badji Mokhtar Annaba University Central Library Copyright Elsevier 2025

needed to adequately determine their feasibility beyond the lab scale. Finally, many experiments have been conducted using synthetic solutions which do not exactly represent real wastewater or groundwater. Performing feasibility studies using real water samples would also enable the evaluation of system selectivity against environmentally relevant competing ions.

Another challenge to overcome is the formation of toxic byproducts when degrading organic pollutants due to the low catalytic selectivity towards compounds of interest. Since current reactive electrochemical methods do not target specific pollutants, the reaction of compounds of interest with the other ions in the solution can produce perchlorates or halogenated organic compounds with little to no control over the electrochemical reaction pathways. So, it is crucial to monitor and identify products when using EAOPs to degrade contaminants. Furthermore, it is important to develop selective materials for the membrane and the electrode, as well as develop large-scale membrane fabrication methods. In particular for EFS, the development of conductive membranes is an area that needs further exploration since these systems rely mostly on the membrane's performance to achieve efficient separation. Finally, molecular design of membranes can lead to higher conductivity, superior antifouling and corrosion properties, tailored pore sizing, high permeability, and selectivity towards ions of interest. Thus, we expect continued research and a growing interest to persevere in the selective membrane-based electrochemical separation systems, which will help pave a path to a future where more sustainable water purification methods with valuable element recovery in results can be expected.

Acknowledgments

This work was supported by the National Science Foundation (NSF) under CBET Grant# 1942971 to X. S. and J. J., and NSF CBET grant #1931941 to X. S., R. C., and E. K. We would also like to thank the startup funds from the University of Illinois, Urbana-Champaign and the Department of Chemical and Biomolecular Engineering to make this study possible.

References

[1] M.A. Shannon, P.W. Bohn, M. Elimelech, J.G. Georgiadis, B.J. Marías, A.M. Mayes, Science and Technology for Water Purification in the Coming Decades, Nature Publishing Group, 2008, pp. 301–310.

[2] X. Chen, M. Qiu, H. Ding, K. Fu, Y. Fan, A reduced graphene oxide nanofiltration membrane intercalated by well-dispersed carbon nanotubes for drinking water purification, Nanoscale 8 (10) (2016) 5696–5705.

[3] Z. Qian, H. Miedema, L.C.P.M. de Smet, E.J.R. Sudhólter, Modelling the selective removal of sodium ions from greenhouse irrigation water using membrane technology, Chem. Eng. Res. Des. 134 (2018) 154–161.

[4] N. Kim, X. Su, C. Kim, Electrochemical lithium recovery system through the simultaneous lithium enrichment via sustainable redox reaction, Chem. Eng. J. (2020) 127715.

This book belongs to Badji Mokhtar Annaba University Central Library Copyright Elsevier 2025

[5] C. Trellu, B.P. Chaplin, C. Coetsier, R. Esmilaire, S. Cerneaux, C. Causserand, et al., Electro-oxidation of organic pollutants by reactive electrochemical membranes, Chemosphere 208 (2018) 159–175.
[6] Z. Pan, C. Song, L. Li, H. Wang, Y. Pan, C. Wang, et al., Membrane technology coupled with electrochemical advanced oxidation processes for organic wastewater treatment: recent advances and future prospects, Chem. Eng. J. 376 (2019) 120909.
[7] H. Siegrist, A. Joss, Review on the fate of organic micropollutants in wastewater treatment and water reuse with membranes, Water Sci. Technol. 66 (6) (2012) 1369–1376.
[8] A. Lee, J.W. Elam, S.B. Darling, Membrane materials for water purification: design, development, and application, Environ. Sci. Water Res. Technol. 2 (1) (2016) 17–42.
[9] T. Fujioka, L.D. Nghiem, S.J. Khan, J.A. McDonald, Y. Poussade, J.E. Drewes, Effects of feed solution characteristics on the rejection of N-nitrosamines by reverse osmosis membranes, J. Membr. Sci. 409–410 (2012) 66–74.
[10] Y. Miyashita, S.H. Park, H. Hyung, C.H. Huang, J.H. Kim, Removal of n-Nitrosamines and Their Precursors by Nanofiltration and Reverse Osmosis Membranes, American Society of Civil Engineers, 2009.
[11] Environmental Protection Agency Federal Facilities Restoration, U. and R. Office, Technical Fact Sheet – N-Nitroso-dimethylamine (NDMA), 2017.
[12] J.R. Werber, A. Deshmukh, M. Elimelech, The Critical Need for Increased Selectivity, Not Increased Water Permeability, for Desalination Membranes, American Chemical Society, 2016, pp. 112–120.
[13] X. Su, H.J. Kulik, T.F. Jamison, T.A. Hatton, Anion-selective redox electrodes: electrochemically mediated separation with heterogeneous organometallic interfaces, Adv. Funct. Mater. 26 (20) (2016) 3394–3404.
[14] X. Su, Electrochemical Interfaces for Chemical and Biomolecular Separations, Elsevier Ltd., 2020, pp. 77–93.
[15] R. Chen, J. Feng, J. Jeon, T. Sheehan, C. Rüttiger, M. Gallei, et al., Structure and potential-dependent selectivity in redox-metallopolymers: electrochemically mediated multicomponent metal separations, Adv. Funct. Mater. 2009307 (2021) 1–11.
[16] K. Kim, S. Cotty, J. Elbert, R. Chen, C.H. Hou, X. Su, Asymmetric redox-polymer interfaces for electrochemical reactive separations: synergistic capture and conversion of arsenic, Adv. Mater. 32 (6) (2020) 1–8.
[17] X. Su, A. Kushima, C. Halliday, J. Zhou, J. Li, T.A. Hatton, Electrochemically-mediated selective capture of heavy metal chromium and arsenic oxyanions from water, Nat. Commun. 9 (1) (2018) 1–9.
[18] K. Kim, P. Baldaguez Medina, J. Elbert, E. Kayiwa, R.D. Cusick, Y. Men, et al., Molecular tuning of redox-copolymers for selective electrochemical remediation, Adv. Funct. Mater. 30 (52) (2020) 1–10.
[19] F.C. Moreira, R.A.R. Boaventura, E. Brillas, V.J.P. Vilar, Electrochemical Advanced Oxidation Processes: A Review on Their Application to Synthetic and Real Wastewaters, Elsevier B.V, 2017, pp. 217–261.
[20] S.O. Ganiyu, E.D. Van Hullebusch, M. Cretin, G. Esposito, M.A. Oturan, Coupling of membrane filtration and advanced oxidation processes for removal of pharmaceutical residues: a critical review, Sep. Purif. Technol. 156 (2015) 891–914.
[21] S. Miralles-Cuevas, I. Oller, A. Agüera, J.A.S. Pérez, R. Sánchez-Moreno, S. Malato, Is the combination of nanofiltration membranes and AOPs for removing microcontaminants cost effective in real municipal wastewater effluents? Environ. Sci. Water Res. Technol. 2 (3) (2016) 511–520.
[22] S. Miralles-Cuevas, I. Oller, A. Agüera, J.A. Sánchez Pérez, S. Malato, Strategies for reducing cost by using solar photo-Fenton treatment combined with nanofiltration to remove microcontaminants in real municipal effluents: toxicity and economic assessment, Chem. Eng. J. 318 (2017) 161–170.
[23] D.P. Ho, S. Vigneswaran, H.H. Ngo, Photocatalysis-membrane hybrid system for organic removal from biologically treated sewage effluent, Sep. Purif. Technol. 68 (2) (2009) 145–152.

This book belongs to Badji Mokhtar Annaba University Central Library Copyright Elsevier 2025

[24] S. Mozia, A.W. Morawski, Hybridization of photocatalysis and membrane distillation for purification of wastewater, Catal. Today 118 (1–2) (2006) 181–188.
[25] S. Ahuja, Chromatography and Separation Science, Elsevier, 2003.
[26] B.L. Karger, L.R. Snyder, C. Horvath, Introduction to Separation Science, Wiley, 1973.
[27] L.N. Moskvin, A classification of separation methods, Sep. Purif. Rev. 45 (1) (2016) 1–27.
[28] A. Dash, R. Chakravarty, Electrochemical separation: promises, opportunities, and challenges to develop next-generation radionuclide generators to meet clinical demands, Ind. Eng. Chem. Res. 53 (10) (2014) 3766–3777.
[29] S. Kim, H. Yoon, D. Shin, J. Lee, J. Yoon, Electrochemical selective ion separation in capacitive deionization with sodium manganese oxide, J. Colloid Interface Sci. 506 (2017) 644–648.
[30] J.P.H. Perez, K. Folens, K. Leus, F. Vanhaecke, P. Van Der Voort, G. Du Laing, Progress in hydrometallurgical technologies to recover critical raw materials and precious metals from low-concentrated streams, Resour. Conserv. Recycl. 142 (2019) 177–188.
[31] K. Scott, Process intensification: an electrochemical perspective, Renew. Sustain. Energy Rev. 81 (2018) 1406–1426.
[32] L.P. Bicelli, B. Bozzini, C. Mele, L. D'Urzo, A review of nanostructural aspects of metal electrodeposition, Int. J. Electrochem. Sci. 3 (4) (2008) 356–408.
[33] R.F. Marques, C. Garcia, P. Lecante, S.J. Ribeiro, L. Noé, N.J. Silva, et al., Electro-precipitation of Fe_3O_4 nanoparticles in ethanol, J. Magnetism Magnetic Mater. 320 (19) (2008) 2311–2315.
[34] H. Strathmann, Ion-Exchange Membrane Separation Processes, Elsevier, 2004.
[35] M.C. Porter, Handbook of Industrial Membrane Technology, Noyes Publications, 1989.
[36] R. Candeago, K. Kim, H. Vapnik, S. Cotty, M. Aubin, S. Berensmeier, et al., Semiconducting polymer interfaces for electrochemically assisted mercury remediation, ACS Appl. Mater. Interfaces 12 (44) (2020) 49713–49722.
[37] N. Anantharamulu, K. Koteswara Rao, G. Rambabu, B. Vijaya Kumar, V. Radha, M. Vithal, A wide-ranging review on Nasicon type materials, J. Mater. Sci. 46 (9) (2011) 2821–2837.
[38] M. Hou, F. Liang, K. Chen, Y. Dai, D. Xue, Challenges and perspectives of NASICON-type solid electrolytes for all-solid-state lithium batteries, Nanotechnology 31 (13) (2020) 132003.
[39] S. Yang, F. Zhang, H. Ding, P. He, H. Zhou, Lithium metal extraction from seawater, Joule 2 (9) (2018) 1648–1651.
[40] A. Biswas, J.P. Gustafsson, H. Neidhardt, D. Halder, A.K. Kundu, D. Chatterjee, et al., Role of competing ions in the mobilization of arsenic in groundwater of Bengal Basin: insight from surface complexation modeling, Water Res. 55 (2014) 30–39.
[41] T.X. Dang, E.W. McCleskey, Ion channel selectivity through stepwise changes in binding affinity, J. Gen. Physiol. 111 (2) (1998) 185–193.
[42] S. Handley-Sidhu, T.K. Mullan, Q. Grail, M. Albadarneh, T. Ohnuki, L.E. Macaskie, Influence of pH, competing ions and salinity on the sorption of strontium and cobalt onto biogenic hydroxyapatite, Sci. Rep. 6 (1) (2016) 23361.
[43] M. Tian, L. Fang, X. Yan, W. Xiao, K.H. Row, Determination of heavy metal ions and organic pollutants in water samples using ionic liquids and ionic liquid-modified sorbents, J. Anal. Methods Chem. 2019 (2019) 1948965.
[44] F. Edition, Guidelines for drinking-water quality, WHO Chron. 38 (4) (2011) 104–108.
[45] I. Chernyshova, D. Bakuska, S. Ponnurangam, Selective recovery of critical and toxic elements from their low-concentrated solutions using surface-based electrochemical separation methods, Multidisciplinary Advances in Efficient Separation Processes, ACS Publications, 2020, pp. 115–165.
[46] H.I. Maarof, W.M.A.W. Daud, M.K. Aroua, Recent trends in removal and recovery of heavy metals from wastewater by electrochemical technologies, Rev. Chem. Eng. 33 (4) (2017) 359–386.
[47] X.-Y. Nie, S.-Y. Sun, Z. Sun, X. Song, J.-G. Yu, Ion-fractionation of lithium ions from magnesium ions by electrodialysis using monovalent selective ion-exchange membranes, Desalination 403 (2017) 128–135.
[48] T.Z. Sadyrbaeva, Separation of cobalt(II) from nickel(II) by a hybrid liquid membrane–electrodialysis process using anion exchange carriers, Desalination 365 (2015) 167–175.

This book belongs to Badji Mokhtar Annaba University Central Library Copyright Elsevier 2025

[49] S. Chaudhury, O. Nir, Electro-enhanced membrane sorption: a new approach for selective ion separation and its application to phosphate and arsenic removal, Ind. Eng. Chem. Res. 59 (22) (2020) 10595–10605.
[50] E. Guyot, S. Seghir, J. Lecuire, C. Boulanger, M. Levi, Y. Shilina, et al., Mo6S8 electrochemical transfer junction for selective extraction of Co^{2+}-ions from their mixture with Ni^{2+}-ions, J. Electrochem. Soc. 160 (3) (2013) A420.
[51] E. Guyot, S. Seghir, S. Diliberto, J.M. Lecuire, C. Boulanger, Lithium recovery by electrochemical transfer junction based on intercalation host matrix, Electrochem. Commun. 23 (2012) 29–32.
[52] X. Zhang, K. Zuo, X. Zhang, C. Zhang, P. Liang, Selective ion separation by capacitive deionization (CDI) based technologies: a state-of-the-art review, Environ. Sci. Water Res. Technol. 6 (2) (2020) 243–257.
[53] K. Zuo, L. Yuan, J. Wei, P. Liang, X. Huang, Competitive migration behaviors of multiple ions and their impacts on ion-exchange resin packed microbial desalination cell, Bioresour. Technol. 146 (2013) 637–642.
[54] Y. Bian, X. Yang, P. Liang, Y. Jiang, C. Zhang, X. Huang, Enhanced desalination performance of membrane capacitive deionization cells by packing the flow chamber with granular activated carbon, Water Res. 85 (2015) 371–376.
[55] K. Dorfner, Ion Exchangers, Walter de Gruyter, 2011.
[56] S. Kumar, S. Jain, History, introduction, and kinetics of ion exchange materials, J. Chem. 2013 (2013) 957647.
[57] T. Luo, S. Abdu, M. Wessling, Selectivity of ion exchange membranes: a review, J. Membr. Sci. 555 (2018) 429–454.
[58] E. Güler, W. van Baak, M. Saakes, K. Nijmeijer, Monovalent-ion-selective membranes for reverse electrodialysis, J. Membr. Sci. 455 (2014) 254–270.
[59] B. Corry, Mechanisms of selective ion transport and salt rejection in carbon nanostructures, MRS Bull. 42 (2017) 306–310.
[60] S.A. Hawks, M.R. Cerón, D.I. Oyarzun, T.A. Pham, C. Zhan, C.K. Loeb, et al., Using ultramicroporous carbon for the selective removal of nitrate with capacitive deionization, Environ. Sci. Technol. 53 (18) (2019) 10863–10870.
[61] J. Kim, A. Jain, K. Zuo, R. Verduzco, S. Walker, M. Elimelech, et al., Removal of calcium ions from water by selective electrosorption using target-ion specific nanocomposite electrode, Water Res. 160 (2019) 445–453.
[62] Z.-Q. Li, M.-Y. Wu, X.-L. Ding, Z.-Q. Wu, X.-H. Xia, Reversible electrochemical tuning of ion sieving in coordination polymers, Anal. Chem. 92 (13) (2020) 9172–9178.
[63] J.G. Gamaethiralalage, K. Singh, S. Sahin, J. Yoon, M. Elimelech, M.E. Suss, et al., Recent advances in ion selectivity with capacitive deionization, Energy Environ. Sci. 14 (3) (2021) 1095–1120.
[64] M. Giorgetti, E. Scavetta, M. Berrettoni, D. Tonelli, Nickel hexacyanoferrate membrane as a coated wire cation-selective electrode, Analyst 126 (12) (2001) 2168–2171.
[65] T. Ikeshoji, Separation of alkali metal ions by intercalation into a prussian blue electrode, J. Electrochem. Soc. 133 (10) (1986) 2108–2109.
[66] M. Asai, A. Takahashi, K. Tajima, H. Tanaka, M. Ishizaki, M. Kurihara, et al., Effects of the variation of metal substitution and electrolyte on the electrochemical reaction of metal hexacyanoferrates, RSC Adv. 8 (65) (2018) 37356–37364.
[67] R. Chen, T. Sheehan, J.L. Ng, M. Brucks, X. Su, Capacitive deionization and electrosorption for heavy metal removal, Environ. Sci. Water Res. Technol. 6 (2) (2020) 258–282.
[68] C. Liu, P.-C. Hsu, J. Xie, J. Zhao, T. Wu, H. Wang, et al., A half-wave rectified alternating current electrochemical method for uranium extraction from seawater, Nat. Energy 2 (4) (2017) 1–8.
[69] P. Srimuk, X. Su, J. Yoon, D. Aurbach, V. Presser, Charge-transfer materials for electrochemical water desalination, ion separation and the recovery of elements, Nat. Rev. Mater. 5 (7) (2020) 517–538.
[70] P. Hosseinzadeh, Y. Lu, Design and fine-tuning redox potentials of metalloproteins involved in electron transfer in bioenergetics, Biochim. Biophys. Acta 1857 (5) (2016) 557–581.

This book belongs to Badji Mokhtar Annaba University Central Library Copyright Elsevier 2025

[71] R.D. Armstrong, M. Todd, J.W. Atkinson, K. Scott, Selective electrodeposition of metals from simulated waste solutions, J. Appl. Electrochem. 26 (4) (1996) 379–384.
[72] L. Doulakas, K. Novy, S. Stucki, C. Comninellis, Recovery of Cu, Pb, Cd and Zn from synthetic mixture by selective electrodeposition in chloride solution, Electrochim. Acta 46 (2–3) (2000) 349–356.
[73] H. Strathmann, Electrodialysis, a mature technology with a multitude of new applications, Desalination 264 (3) (2010) 268–288.
[74] M.E. Suss, S. Porada, X. Sun, P.M. Biesheuvel, J. Yoon, V. Presser, Water desalination via capacitive deionization: what is it and what can we expect from it? Energy Environ. Sci. 8 (8) (2015) 2296–2319.
[75] J. Zheng, Z. Wang, J. Ma, S. Xu, Z. Wu, Development of an electrochemical ceramic membrane filtration system for efficient contaminant removal from waters, Environ. Sci. Technol. 52 (7) (2018) 4117–4126.
[76] D.D. Ratnayaka, M.J. Brandt, K.M. Johnson, CHAPTER 10 - Specialized and advanced water treatment processes, in: D.D. Ratnayaka, M.J. Brandt, K.M. Johnson (Eds.), Water supply, sixth ed., Butterworth-Heinemann, Boston, 2009, pp. 365–423.
[77] W.A. Tarpeh, J.M. Barazesh, T.Y. Cath, K.L. Nelson, Electrochemical stripping to recover nitrogen from source-separated urine, Environ. Sci. Technol. 52 (3) (2018) 1453–1460.
[78] N. Joseph, P. Ahmadiannamini, R. Hoogenboom, I.F.J. Vankelecom, Layer-by-layer preparation of polyelectrolyte multilayer membranes for separation, Polym. Chem. 5 (6) (2014) 1817–1831.
[79] T.P. Rao, R. Kala, S. Daniel, Metal ion-imprinted polymers–novel materials for selective recognition of inorganics, Anal. Chim. Acta 578 (2) (2006) 105–116.
[80] T.A. Sergeyeva, S.A. Piletsky, E.V. Piletska, O.O. Brovko, L.V. Karabanova, L.M. Sergeeva, et al., In situ formation of porous molecularly imprinted polymer membranes, Macromolecules 36 (19) (2003) 7352–7357.
[81] C. Branger, W. Meouche, A. Margaillan, Recent advances on ion-imprinted polymers, Reactive Funct. Polym. 73 (6) (2013) 859–875.
[82] H. Deng, S. Zhao, Q. Meng, W. Zhang, B. Hu, A novel surface ion-imprinted cation-exchange membrane for selective separation of copper ion, Ind. Eng. Chem. Res. 53 (39) (2014) 15230–15236.
[83] A. Razmjou, M. Asadnia, E. Hosseini, A. Habibnejad Korayem, V. Chen, Design principles of ion selective nanostructured membranes for the extraction of lithium ions, Nat. Commun. 10 (1) (2019) 5793.
[84] J.J. Shao, K. Raidongia, A.R. Koltonow, J. Huang, Self-assembled two-dimensional nanofluidic proton channels with high thermal stability, Nat. Commun. 6 (2015) 7602.
[85] A. Razmjou, G. Eshaghi, Y. Orooji, E. Hosseini, A.H. Korayem, F. Mohagheghian, et al., Lithium ion-selective membrane with 2D subnanometer channels, Water Res. 159 (2019) 313–323.
[86] C. Zhang, J. Ma, J. Song, C. He, T. David Waite, Continuous ammonia recovery from wastewaters using an integrated capacitive flow electrode membrane stripping system, Environ. Sci. Technol. (2018).
[87] Y. Li, N. Chen, Z. Li, H. Shao, L. Qu, Frontiers of carbon materials as capacitive deionization electrodes, Dalton Trans. 49 (16) (2020) 5006–5014.
[88] D.I. Oyarzun, A. Hemmatifar, J.W. Palko, M. Stadermann, J.G. Santiago, Ion selectivity in capacitive deionization with functionalized electrode: theory and experimental validation, Water Res. X 1 (2018) 100008.
[89] J. Lee, S. Kim, C. Kim, J. Yoon, Hybrid capacitive deionization to enhance the desalination performance of capacitive techniques, Energy Environ. Sci. 7 (11) (2014) 3683–3689.
[90] X. Su, K.-J. Tan, J. Elbert, C. Rüttiger, M. Gallei, T.F. Jamison, et al., Asymmetric Faradaic systems for selective electrochemical separations, Energy Environ. Sci. 10 (5) (2017) 1272–1283.
[91] X. Mao, W. Tian, Y. Ren, D. Chen, S.E. Curtis, M.T. Buss, et al., Energetically efficient electrochemically tunable affinity separation using multicomponent polymeric nanostructures for water treatment, Energy Environ. Sci. 11 (10) (2018) 2954–2963.
[92] Z. Song, S. Garg, J. Ma, T.D. Waite, Selective arsenic removal from groundwaters using redox-active polyvinylferrocene-functionalized electrodes: role of oxygen, Environ. Sci. Technol. 54 (19) (2020) 12081–12091.

This book belongs to Badji Mokhtar Annaba University Central Library Copyright Elsevier 2025

[93] P.M. Biesheuvel, A. van der Wal, Membrane capacitive deionization, J. Membr. Sci. 346 (2) (2010) 256–262.
[94] W. Shi, X. Liu, C. Ye, X. Cao, C. Gao, J. Shen, Efficient lithium extraction by membrane capacitive deionization incorporated with monovalent selective cation exchange membrane, Sep. Purif. Technol. 210 (2019) 885–890.
[95] S. Hand, R.D. Cusick, Characterizing the impacts of deposition techniques on the performance of MnO_2 cathodes for sodium electrosorption in hybrid capacitive deionization, Environ. Sci. Technol. 51 (20) (2017) 12027–12034.
[96] M.E. Suss, T.F. Baumann, W.L. Bourcier, C.M. Spadaccini, K.A. Rose, J.G. Santiago, et al., Capacitive desalination with flow-through electrodes, Energy Environ. Sci. 5 (11) (2012) 9511.
[97] L. Guo, M. Ding, D. Yan, M.E. Pam, S. Vafakhah, C. Gu, et al., High speed capacitive deionization system with flow-through electrodes, Desalination 496 (2020) 114750.
[98] D. Xu, W. Wang, M. Zhu, C. Li, Recent advances in desalination battery: an initial review, ACS Appl. Mater. Interfaces 12 (52) (2020) 57671–57685.
[99] M. Pasta, C.D. Wessells, Y. Cui, F. La Mantia, A desalination battery, Nano Lett. 12 (2) (2012) 839–843.
[100] J. Zheng, S. Xu, Z. Wu, Z. Wang, Removal of p-chloroaniline from polluted waters using a cathodic electrochemical ceramic membrane reactor, Sep. Purif. Technol. 211 (2019) 753–763.
[101] M. Yadav, R. Gupta, R.K. Sharma, Chapter 14 - Green and sustainable pathways for wastewater purification, in: S. Ahuja (Ed.), Advances in Water Purification Techniques, Elsevier, 2019, pp. 355–383.
[102] K. Singh, M. Agarwal, Renu, Heavy metal removal from wastewater using various adsorbents: a review, J. Water Reuse Desalin. 7 (4) (2017) 387–419.
[103] M. Renu, Agarwal, K. Singh, Heavy metal removal from wastewater using various adsorbents: a review, J. Water Reuse Desalin. 7 (4) (2016) 387–419.
[104] O.W. Us Epa, National Primary Drinking Water Regulations, US EPA, 2015.
[105] Q. Dong, X. Guo, X. Huang, L. Liu, R. Tallon, B. Taylor, et al., Selective removal of lead ions through capacitive deionization: role of ion-exchange membrane, Chem. Eng. J. 361 (2019) 1535–1542.
[106] J. Khan, B.P. Tripathi, A. Saxena, V.K. Shahi, Electrochemical membrane reactor: in situ separation and recovery of chromic acid and metal ions, Electrochim. Acta 52 (24) (2007) 6719–6727.
[107] L. Liu, Y. Xu, K. Wang, K. Li, L. Xu, J. Wang, et al., Fabrication of a novel conductive ultrafiltration membrane and its application for electrochemical removal of hexavalent chromium, J. Membr. Sci. 584 (2019) 191–201.
[108] C. Wang, L. Chen, S. Liu, Activated carbon fiber for adsorption/electrodeposition of Cu (II) and the recovery of Cu (0) by controlling the applied voltage during membrane capacitive deionization, J. Colloid Interface Sci. 548 (2019) 160–169.
[109] D. Mohan, C.U. Pittman Jr., Arsenic removal from water/wastewater using adsorbents—a critical review, J. Hazard. Mater. 142 (1–2) (2007) 1–53.
[110] A.L. Wani, A. Ara, J.A. Usmani, Lead toxicity: a review, Interdiscip. Toxicol. 8 (2) (2015) 55–64.
[111] A. Royer, T. Sharman, Copper Toxicity, in StatPearls, StatPearls Publishing, Treasure Island, FL, 2021.
[112] S. Chu, Critical Materials Strategy, DIANE publishing, 2011.
[113] T. Watari, K. Nansai, K. Nakajima, Major metals demand, supply, and environmental impacts to 2100: a critical review, Resour. Conserv. Recycl. 164 (2021) 105107.
[114] E.H.M. Size, Share Trends Analysis Report by Product, by Application, by Region, and Segment Forecasts, 2020–2027, GlobeNewswire, 2020.
[115] S.M. Hayes, E.A. McCullough, Critical minerals: a review of elemental trends in comprehensive criticality studies, Resour. Policy 59 (2018) 192–199.
[116] Y. Liao, M. Wang, D. Chen, Electrosorption of uranium(VI) by highly porous phosphate-functionalized graphene hydrogel, Appl. Surf. Sci. 484 (2019) 83–96.
[117] J. Almeida, R. Craveiro, P. Faria, A.S. Silva, E.P. Mateus, S. Barreiros, et al., Electrodialytic removal of tungsten and arsenic from secondary mine resources—deep eutectic solvents enhancement, Sci. Total Environ. 710 (2020) 136364.

This book belongs to Badji Mokhtar Annaba University Central Library Copyright Elsevier 2025

[118] T. Hoshino, Preliminary studies of lithium recovery technology from seawater by electrodialysis using ionic liquid membrane, Desalination 317 (2013) 11–16.
[119] T. Hoshino, Innovative lithium recovery technique from seawater by using world-first dialysis with a lithium ionic superconductor, Desalination 359 (2015) 59–63.
[120] S. Kim, J. Kim, S. Kim, J. Lee, J. Yoon, Electrochemical lithium recovery and organic pollutant removal from industrial wastewater of a battery recycling plant, Environ. Sci. Water Res. Technol. 4 (2) (2018) 175–182.
[121] A. Battistel, M.S. Palagonia, D. Brogioli, F. La Mantia, R. Trócoli, Electrochemical methods for lithium recovery: a comprehensive and critical review, Adv. Mater. 32 (23) (2020) 1905440.
[122] V. Flexer, C.F. Baspineiro, C.I. Galli, Lithium recovery from brines: a vital raw material for green energies with a potential environmental impact in its mining and processing, Sci. Total Environ. 639 (2018) 1188–1204.
[123] S. Nishihama, K. Onishi, K. Yoshizuka, Selective recovery process of lithium from seawater using integrated ion exchange methods, Solvent Extraction Ion. Exch. 29 (3) (2011) 421–431.
[124] R.A. Kumbasar, Selective extraction of cobalt from strong acidic solutions containing cobalt and nickel through emulsion liquid membrane using TIOA as carrier, J. Ind. Eng. Chem. 18 (6) (2012) 2076–2082.
[125] I. Union, Communication from the Commission to the European Parliament, the Council, the European Economic and Social Committee and the Committee of the Regions. A New Skills Agenda for Europe, Brussels, 2014.
[126] U.G. Survey, Mineral commodity summaries, US Geol. Surv. 198 (2019) 2011.
[127] C. Candeias, R. Melo, P.F. Ávila, E.F. da Silva, A.R. Salgueiro, J.P. Teixeira, Heavy metal pollution in mine–soil–plant system in S. Francisco de Assis–Panasqueira mine (Portugal), Appl. Geochem. 44 (2014) 12–26.
[128] F. Pena-Pereira, J. Namieśnik, Ionic liquids and deep eutectic mixtures: sustainable solvents for extraction processes, ChemSusChem 7 (7) (2014) 1784–1800.
[129] A.B.A. Boxall, C.J. Sinclair, K. Fenner, D. Kolpin, S.J. Maund, When Synthetic Chemicals Degrade in the Environment, American Chemical Society, 2004.
[130] E. Brillas, J.A. Garrido, R.M. Rodríguez, C. Arias, P.L. Cabot, F. Centellas, Wastewaters by electrochemical advanced oxidation processes using a BDD anode and electrogenerated H_2O_2 with Fe (II) and UVA light as catalysts, Portugaliae Electrochim. Acta (2008) 15–46.
[131] H. Olvera-Vargas, N. Oturan, D. Buisson, M.A. Oturan, A coupled Bio-EF process for mineralization of the pharmaceuticals furosemide and ranitidine: feasibility assessment, Chemosphere 155 (2016) 606–613.
[132] T.Y. Tan, Z.T. Zeng, G.M. Zeng, J.L. Gong, R. Xiao, P. Zhang, et al., Electrochemically enhanced simultaneous degradation of sulfamethoxazole, ciprofloxacin and amoxicillin from aqueous solution by multi-walled carbon nanotube filter, Sep. Purif. Technol. 235 (2020) 116167.
[133] J. Sun, Q. Wang, J. Zhang, Z. Wang, Z. Wu, Degradation of sulfadiazine in drinking water by a cathodic electrochemical membrane filtration process, Electrochim. Acta 277 (2018) 77–87.
[134] S. Xu, J. Zheng, Z. Wu, M. Liu, Z. Wang, Degradation of p-chloroaniline using an electrochemical ceramic microfiltration membrane with built-in electrodes, Electrochim. Acta 292 (2018) 655–666.
[135] Y. Yang, S. Qiao, J. Zhou, X. Quan, A novel porous-carbon-based hollow fiber membrane with electrochemical reduction mediated by in-situ hydroxyl radical generation for fouling control and water treatment, Appl. Catal. B: Environ. 255 (2019) 117772.
[136] H. Wang, Q. Guan, J. Li, T. Wang, Phenolic wastewater treatment by an electrocatalytic membrane reactor, Catal. Today 236 (Part A) (2014) 121–126.
[137] A.M. Zaky, B.P. Chaplin, Mechanism of p-substituted phenol oxidation at a Ti_4O_7 reactive electrochemical membrane, Environ. Sci. Technol. 48 (10) (2014) 5857–5867.
[138] T.X.H. Le, H. Haflich, A.D. Shah, B.P. Chaplin, Energy-efficient electrochemical oxidation of perfluoroalkyl substances using a Ti_4O_7 reactive electrochemical membrane anode, Environ. Sci. Technol. Lett. 6 (8) (2019) 504–510.

This book belongs to Badji Mokhtar Annaba University Central Library Copyright Elsevier 2025

[139] T. Cui, Y. Zhang, W. Han, J. Li, X. Sun, J. Shen, et al., Advanced treatment of triazole fungicides discharged water in pilot scale by integrated system: enhanced electrochemical oxidation, upflow biological aerated filter and electrodialysis, Chem. Eng. J. 315 (2017) 335–344.
[140] D.I. Kim, P. Dorji, G. Gwak, S. Phuntsho, S. Hong, H. Shon, Reuse of municipal wastewater via membrane capacitive deionization using ion-selective polymer-coated carbon electrodes in pilot-scale, Chem. Eng. J. 372 (2019) 241–250.
[141] N. Mameda, H.J. Park, K.H. Choo, Membrane electro-oxidizer: a new hybrid membrane system with electrochemical oxidation for enhanced organics and fouling control, Water Res. 126 (2017) 40–49.
[142] X. Zhu, D. Jassby, Electroactive membranes for water treatment: enhanced treatment functionalities, energy considerations, and future challenges, Acc. Chem. Res. (2019).
[143] S. Garcia-Segura, J. Keller, E. Brillas, J. Radjenovic, Removal of organic contaminants from secondary effluent by anodic oxidation with a boron-doped diamond anode as tertiary treatment, J. Hazard. Mater. 283 (2015) 551–557.
[144] O. Arar, E. Yavuz, U. Yuksel, N. Kabay, Separation of low concentration of fluoride from water by electrodialysis (ED) in the presence of chloride and sulfate ions, Sep. Sci. Technol. 44 (7) (2009) 1562–1573.
[145] M.B.S. Ali, A. Mnif, B. Hamrouni, M. Dhahbi, Denitrification of brackish water by electrodialysis: effect of process parameters and water characteristics, Surf. Eng. Appl. Electrochem. 46 (3) (2010) 253–262.
[146] L.J. Banasiak, A.I. Schäfer, Removal of boron, fluoride and nitrate by electrodialysis in the presence of organic matter, J. Membr. Sci. 334 (1–2) (2009) 101–109.
[147] M. Grzegorzek, K. Majewska-Nowak, A.E. Ahmed, Removal of fluoride from multicomponent water solutions with the use of monovalent selective ion-exchange membranes, Sci. Total Environ. 722 (2020) 137681.
[148] D.I. Kim, R.R. Gonzales, P. Dorji, G. Gwak, S. Phuntsho, S. Hong, et al., Efficient recovery of nitrate from municipal wastewater via MCDI using anion-exchange polymer coated electrode embedded with nitrate selective resin, Desalination 484 (2020) 114425.
[149] Y.J. Kim, J.H. Kim, J.H. Choi, Selective removal of nitrate ions by controlling the applied current in membrane capacitive deionization (MCDI), J. Membr. Sci. 429 (2013) 52–57.
[150] R. Liu, Y. Sui, X. Wang, Metal–organic framework-based ultrafiltration membrane separation with capacitive-type for enhanced phosphate removal, Chem. Eng. J. 371 (2019) 903–913.
[151] T. Mubita, S. Porada, P. Aerts, A. van der Wal, Heterogeneous anion exchange membranes with nitrate selectivity and low electrical resistance, J. Membr. Sci. 607 (2020) 376–7388.
[152] L. Paltrinieri, E. Huerta, T. Puts, W. Van Baak, A.B. Verver, E.J.R. Sudhölter, et al., Functionalized anion-exchange membranes facilitate electrodialysis of citrate and phosphate from model dairy wastewater, Environ. Sci. Technol. 53 (5) (2019) 2396–2404.
[153] H.I. Uzun, E. Debik, Economical approach to nitrate removal via membrane capacitive deionization, Sep. Purif. Technol. 209 (2019) 776–781.
[154] M. Habermeyer, A. Roth, S. Guth, P. Diel, K.H. Engel, B. Epe, et al., Nitrate and Nitrite in the Diet: How to Assess Their Benefit and Risk for Human Health, Wiley-VCH Verlag, 2015, pp. 106–128.
[155] (USGS), U.S.G.S. Nitrogen and Water, [cited 2021]. Available from: https://www.usgs.gov/special-topic/water-science-school/science/nitrogen-and-water?qt-science_center_objects = 0#qt-science_center_objects.
[156] J.S. Newman, K.E. Thomas-Alyea, Electrochemical Systems, Wiley, Hoboken, NJ, 2004.
[157] S. Hand, R.D. Cusick, Emerging investigator series: capacitive deionization for selective removal of nitrate and perchlorate: impacts of ion selectivity and operating constraints on treatment costs, Environ. Sci. Water Res. Technol. 6 (4) (2020) 925–934.
[158] D.W. Smith, Ionic hydration enthalpies, J. Chem. Educ. 54 (9) (1977) 540–542.
[159] N. Shitan, K. Yazaki, New Insights into the Transport Mechanisms in Plant Vacuoles, Elsevier Inc., 2013, pp. 383–433.

This book belongs to Badji Mokhtar Annaba University Central Library Copyright Elsevier 2025

[160] N. Haneklaus, Y. Sun, R. Bol, B. Lottermoser, E. Schnug, To Extract, or Not to Extract Uranium From Phosphate Rock, That Is the Question, American Chemical Society, 2017, pp. 753–754.
[161] P. Cornel, C. Schaum, Phosphorus recovery from wastewater: needs, technologies and costs, Water Sci. Technol. 59 (6) (2009) 1069–1076.
[162] L. Paltrinieri, L. Poltorak, L. Chu, T. Puts, W. van Baak, E.J.R. Sudhölter, et al., Hybrid polyelectrolyte-anion exchange membrane and its interaction with phosphate, Reactive Funct. Polym. 133 (2018) 126–135.
[163] N. Arahman, S. Mulyati, M.R. Lubis, R. Takagi, H. Matsuyama, The removal of fluoride from water based on applied current and membrane types in electrodialyis, J. Fluor. Chem. 191 (2016) 97–102.
[164] C. Burk, Techno-Economic Modeling for New Technology Development, AIChE, 2018.

This book belongs to Badji Mokhtar Annaba University Central Library Copyright Elsevier 2025

CHAPTER THIRTEEN

Membrane-based electrochemical technologies for simultaneous water treatment and salinity-gradient energy production

Miao Gao and Wen-Wei Li
Department of Environmental Science and Engineering, University of Science and Technology of China, Hefei, P.R. China

13.1 Introduction

Energy shortage, water deficiency, and global climate change are key intertwined challenges faced by the human society [1]. The needs for addressing these challenges have motivated technology innovation in sustainable energy production and water/wastewater treatment. While these individual processes have been intensively investigated in earlier studies, still over the past decade a host of new technologies have arisen that target at simultaneous water purification and energy production. One promising field is the use of membrane-based electrochemical technologies to capture the salinity-gradient energy (SGE) from mixing of different waters in nature [2]. For example, the osmosis pressure difference between seawater and river water is as high as 23 atm, equivalent to the energy generated from water falling over a dam more than 230 m high [3]. In theory, approximately 23.0 kW/h/m^3 electric power can be generated from this salinity gradient. However, although the concept of obtaining energy by mixing fresh water and salt water has been proposed early in 1954 [4], the technology development in this field has been rather slow and the water-embodied SGE has been largely untapped until recently. This chapter introduces several prevailing membrane-based electrochemical SGE-capturing technologies, including pressure-retarded osmosis (PRO), reverse electrodialysis (RED), and capacitive donnan potential (CDP) [5–11]. The fundamentals and recent advances of these technologies are summarized, and the remaining challenges and future prospects of their commercialized applications are highlighted.

Electrochemical Membrane Technology for Water and Wastewater Treatment.
DOI: https://doi.org/10.1016/B978-0-12-824470-8.00011-5
© 2022 Elsevier Inc.
All rights reserved.

This book belongs to Badji Mokhtar Annaba University Central Library
Copyright Elsevier 2025

13.2 Fundamentals of membrane-based electricity generation technologies

13.2.1 Pressure-retarded osmosis

The concept of utilizing PRO for sustainable energy supply was first proposed by Loeb and Norman in 1975 [12]. In a PRO system, water molecules percolate through a semipermeable membrane from a low-salinity solution (e.g., river or wastewater) to a pressurized high-salinity one (such as seawater), and the resulting water flow then turns a turbine to generate electricity [5,13].

PRO systems can be operated in an open-loop or a closed-loop mode. In the open-loop configuration, the fresh water is lost to seawater (draw solution), and the diluted seawater is directly discharged without water reclamation [6]. In contrast, the closed-loop PRO requires draw solution regeneration (i.e., condensation), which offers opportunities for clean water production simultaneously (Fig. 13.1A) [14]. The draw solution regeneration may be realized by applying interfacial evaporation or membrane distillation technologies [15]. However, these technologies require extra energy input and might find profitable applications only when low-grade heat energy is available. Reverse osmosis (RO) may be adopted as an alternative to interfacial evaporation or membrane distillation technologies for combining with. Notably, such a combination not only enables more efficient water reclamation but also favors decreased RO operation cost due to dilution of RO feedwater. As a consequence, the overall energy consumption of RO process can be signifiantly decreased and the ecological risks of RO brine discharge can be alleviated [5].

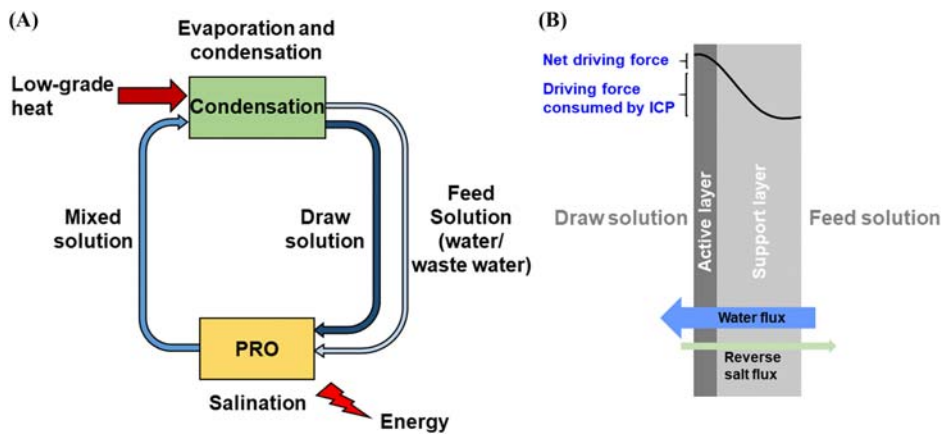

Figure 13.1 Schematic of (A) closed-loop pressure-retarded osmosis (PRO) system with draw solution regeneration and (B) ICP across PRO membrane.

This book belongs to Badji Mokhtar Annaba University Central Library Copyright Elsevier 2025

Osmotic membrane is a critical component of the PRO system. The membrane water flux and salt rejection properties are critically affected by the internal concentration polarization (ICP) (Fig. 13.1B). PRO can be regarded as the opposite process of RO, and therefore in the early stages of this technology the RO membrane was directly used. However, the thick RO membrane (with bulky support layers) suffers from severe ICP and hence low water flux [16,17]. To minimize ICP, surface-modified, thin-film membranes with improved membrane hydrophilicity and internal structure gradually became prevalent [18–22], enabling significantly enhanced power generation (5.7–10 W/m^2) in PRO systems [17,23]. Recently, Lee et al. further optimized the membrane by using an ultra-thin polyethylene support (thinness $<10\ \mu m$) with low pore tortuosity [24], and achieved an unprecedentedly high power density (approximately 35.7 W/m^2) at 20 bar when using 1.0 M NaCl as draw solution. Polymetric membranes such as polysulfone, polyethersulfone, polybenzimidazole, and polyamide-based membranes are commonly applied for PRO systems [18]. However, these membranes for PRO system are prone to fouling when river water or wastewater is adopted as the feedwater. To mitigate membrane fouling, various hydrophilic nanoparticles (e.g., graphene oxides) are usually immobilized on the membrane surface or incorporated into the membrane matrix [18,25,26].

Apart from optimizing the membrane material, effective fouling control also relies on implementation of appropriate pretreatment [27]. For example, forward osmosis can be applied before PRO to reduce the membrane fouling (Fig. 13.2), enabling a stable power output of $>5\ W/m^2$ in the system for treating real wastewater effluent [28]. To maximize the energy production and water reclamation performances of PRO systems, other factors such as the draw solution type and temperature should also be optimized. Generally, monovalent cations with small hydrated ion radius are more favorable draw solution than divalent cations to lower the membrane ICP [15,29]. A draw solution adaptable to thermal regeneration is usually preferred for the closed-loop PRO, because it not only enables utilization of

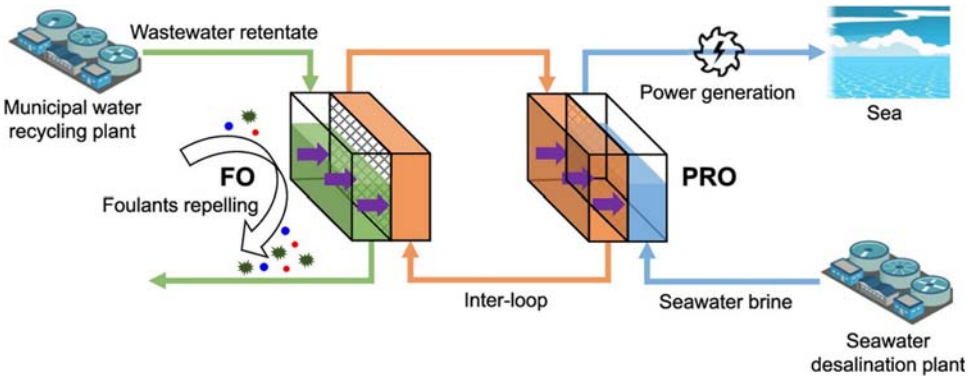

Figure 13.2 Schematic illustration of an forward osmosis-pressure retarded osmosis hybrid system [28].

This book belongs to Badji Mokhtar Annaba University Central Library Copyright Elsevier 2025

low-grade heat [29] but also renders raised osmotic pressure of draw solution and decreased viscosity of feed water to enhance water flux [5,30].

13.2.2 Reverse electrodialysis

The membrane-based RED technology is another attractive option to capture SGE [31]. Compared with PRO that mainly relies on transmembrane water flow, RED functions by leveraging the selective ion movement across membranes. RED is a reversed process of electrodialysis and shares similar reactor configurations to the latter. In brief, the high- and low-salinity solutions are separated by selective ion exchange membranes that are alternately deployed in membrane stacks, and the directional migration of cations and anions across these membranes results in an ionic current (Fig. 13.3) [32]. In this way, chemical potential energy is directly converted into electrical energy. In spite of its simplicity and long history [4], the RED technology has been advancing very slowly until 2007 when the Netherlands started the so-called Blue Energy project, which directly utilizes lake water and seawater for power generation [33,34]. In the first SGE power plant built in 2014, the treatment capacity reached 220 m^3/h for both river water and sea water, although the power generation capacity of the system still needs considerable improvement to become economically profitable.

The RED system can be used as a standalone technology or combined with other processes to form a closed-loop configuration, similar to PRO. For example, it can be combined with RO to regenerate the high-salinity solution and thus to simultaneously

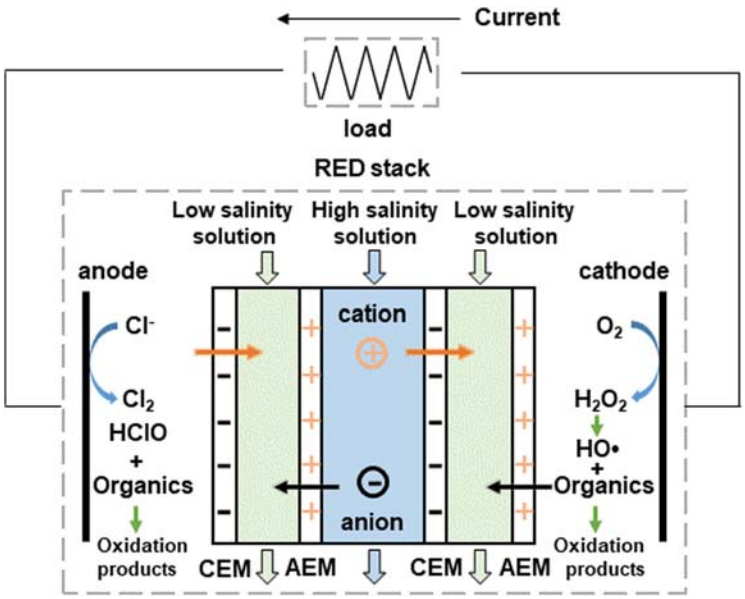

Figure 13.3 The principles of reverse electrodialysis process for electricity generation.

This book belongs to Badji Mokhtar Annaba University Central Library Copyright Elsevier 2025

enhance desalination of seawater or high-salinity industrial wastewater for clean water production [35,36]. Importantly, the generated electricity in this system may be in situ utilized for water decontamination, thereby realizing self-driven water treatment. For example, in a recently reported RED system for treating synthetic wastewater, the generated electricity was in situ utilized to drive electrosynthesis of active chlorine species and hydrogen peroxide (H_2O_2) at the anode and cathode, respectively. These reactive species and their derivatives then efficiently attack water contaminants, thereby realizing efficient water purification without need for external energy input (Fig. 13.3) [37].

Membrane properties critically determine the performance of a RED system. Over the past few years, intensive research efforts have been devoted to optimizing the membrane material, mainly targeting at lowering the internal resistance and ion polarization of the membranes [38]. Two-dimensional materials including boron nitride [39], MoS_2 [40], graphene oxides [41], and transition-metal carbides and/or nitrides (MXenes) [42–44] have gradually stood out from the crowd as a promising candidate for membrane material for RED systems, because they mostly possess abundant surface charge and controllable nanofluidic channels (with nano confinement effect) to favor a selective ion permeation [45–49]. For example, power density of up to 10^6 W/m^2 was generated by a RED with single-layer, nanopore MoS_2 membrane [40]. In addition, 2D $Ti_3C_2T_x$-MXene membrane with surface-charge-controlled nanofluidic ion transport channels (Fig. 13.4) was also applied in a RED for treating mixing artificial seawater (0.5 M NaCl) and river water, achieving a higher power output (up to 4.6 W/m^2) than most reported membrane-based SGE devices. Encouragingly, the overall output voltage of 10 tandem MXene-RED stacks reached 1.66 V, implying a

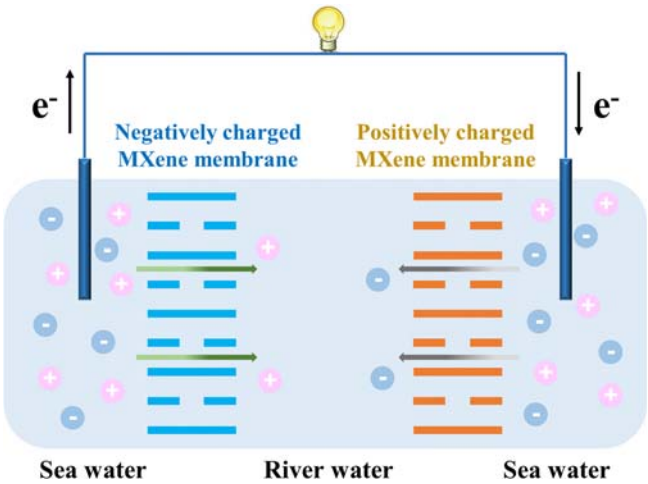

Figure 13.4 Scheme of the MXene membrane-based nanofluidic energy harvesting device [50].

This book belongs to Badji Mokhtar Annaba University Central Library Copyright Elsevier 2025

great potential for directly using such MXene-RED stacks for powering electronic devices [50]. Due to the need for directional ion movement, asymmetric design of membrane that allows for nonlinear ionic transport across the membrane and an inwardly rectifying current was also proposed [51], which has led to the rapid development of biomimetic heterogeneous membranes for high-efficiency SGE capture [52–55]. Hu et al. reported an ionized wood membrane with the aligned nanochannels of the cellulose nanofibers, where the surfaces of the nanochannels were functionalized to positively or negatively charged surfaces. With this membrane, the RED device generated a voltage as high as 9.8 V and power density of 5.14 mW/m^2 [56]. Another important consideration for a RED membrane is the antifouling property, that is, resistance to deposition of various organic matters/ biomolecules and inorganic salt from water onto membrane surface. Several antifouling membranes have been developed by incorporating hydrophilic, conductive nanomaterials into the membrane matrix [57]. For example, the incorporation of Ag nanoparticles into MXene membrane significantly improved its resistance to organic fouling, enabling 98% flux recovery (relative to 87% recovery for the pristine MXene membrane) [42].

To maximize power harvest in RED and avoid unfavorable environmental impacts, the properties of the electrode materials and the selection of an appropriate electrochemical reaction system are also of vital importance. Water splitting is the most common electrochemical reaction in RED, where oxygen and/or chlorine gases (from seawater) are generated at the anode and hydrogen (an important fuel gas) is produced at the cathode. The oxygen-generating anode can also be replaced by a bioanode with enriched microorganisms to degrade organic matters (which reaction is thermodynamically more favorable), thereby realizing simultaneous water purification and efficient H_2 production (1.6 m^3-H_2/m^3-anolyte/day). Thus, by combining the SGE and bioenergy, the RED stack system achieved high electron efficiency of 86% at a salinity ration of 50 [58], resulting in up to 118 Wh/m^3 energy harvest [36]. Considering the relatively high overpotentials of cathodic H_2 production, oxygen reduction reaction has been suggested as an alternative, which has led to the development of microbial RED cell (the combination of RED and microbial fuel cells). For example, a microbial RED cell stack containing five pairs of RED cells was demonstrated to produce a power density of 3.6 W/m^2, with chemical oxygen demand removal of 98% and coulombic efficiency of 64% [58,59]. It should be noted that the electricity generation in wastewater-related RED is usually unstable due to fluctuations in wastewater properties and environmental conditions. Thus, compared to direct harvest of electric energy, a more appealing option would be to utilize the SGE-derived electricity in situ for CO_2 reduction, which not only enables effective energy storage but also contributes to CO_2 capturing [60]. This process can be realized by simply altering the cathode reaction system. Feng et al. developed a novel RED with Bi film cathode, which achieved self-driven CO_2-to-formate conversion (with maximum formate concentration of 185.4 mg/L) by extracting the energy from salinity gradient and wastewater [61,62].

This book belongs to Badji Mokhtar Annaba University Central Library Copyright Elsevier 2025

One important challenge for RED application is scaling up. Metz et al. reported a small-scale RED stack of 50 cells (10×10 cm^2 membrane area), which produced a power density of about 0.93 W/m^2 for treating river water and seawater. However, the high cell resistance due to the shielding effect of the spacers and the large electrode spaces present important limitations for such a stacked system. Tremendous efforts have been devoted to improve the spacer and manifold design [63,64]. For example, the internal resistance of low-salinity feedwater for RED was significantly decreased by applying a small intermembrane distance (approximately 60 μm), endowing the RED system with a high power density of 2.2 W/m^2 [65]. However, the over-compacted membrane array and narrow channels can severely limit the water hydrodynamics and may aggravate membrane fouling and lower ions permeation [66]. Although strategies such as periodical reversal of feed streams can help to mitigate membrane fouling due to changed polarity of the stack that favors efficient release of accumulated multivalent ions and organic foulants from the membrane [67], still it cannot fundamentally address the membrane fouling challenge. Thus, more rational designs of RED is still needed for stable water treatment application.

13.2.3 Capacitive systems

Recently, capacitive mixing (CapMix) systems have emerged as another promising SGE capturing technology. This technology was inspired by conventional supercapacitors and batteries, and was first proposed by Brogioli in 2009 [68,69]. Unlike the PRO and RED processes that are simultaneously fed with high- and low-salinity solutions and create continuous and relatively-stable electric current, the CapMix process is based on sequential exposure of the electrodes to two solutions with different salinity, which leads to alternate charging and discharging of the system. Such processes can be enhanced by adding an ion exchange membrane on the top of the electrode [69] to allow selective passage of counter-ions and retain co-ions, which favors the development of a high electrode potential. In membrane-associated CapMix process, not only the electrodes but also the membranes can be charged in a high-salinity solution due to the Donnan potential development as a result of uneven distribution of ions between the membrane [10,70–76]. Thus, this process is also named CDP process. Subsequently, the membrane and the electrode both can be discharged in a low-salinity solution. Because more energy can be captured than consumed in the charge-discharge cycles, net energy can be harvested in this system (Fig. 13.5).

Electrical energy in a CDP-CapMix process is usually captured via a four-step cycle (Fig. 13.5). Initially, the capacitive electrodes in a high-salinity solution (seawater) are polarized under open circuit condition as a result of a membrane potential development (Step 1). Next, the capacitive electrodes are connected to an external circuit, which gives rise to electrical current and drives the flow of ions in the electrolyte to respective electrode (Step 2, the charging process). Once the capacitive electrodes are

This book belongs to Badji Mokhtar Annaba University Central Library Copyright Elsevier 2025

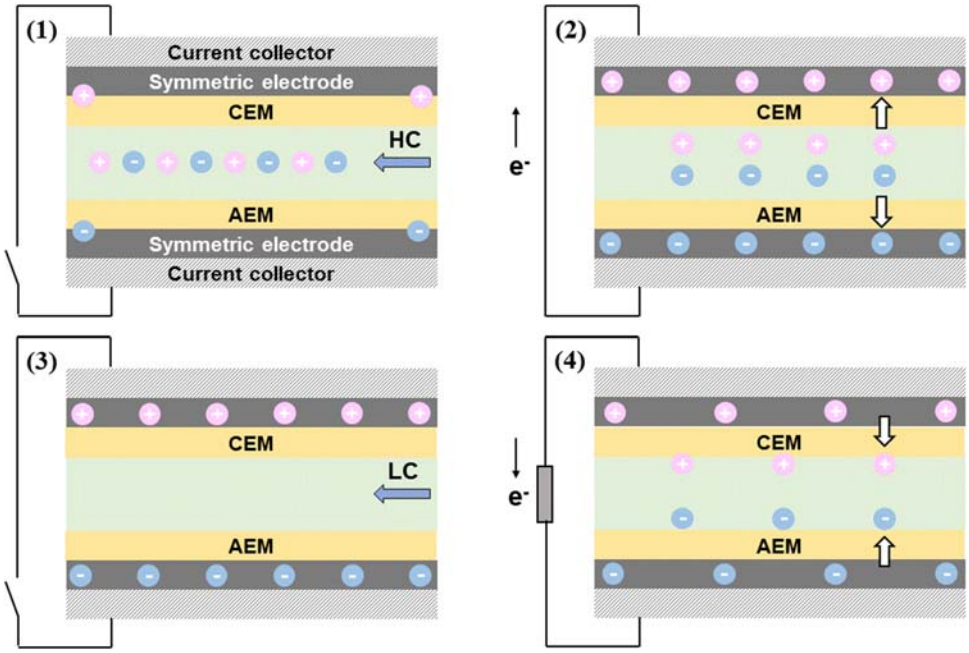

Figure 13.5 Schematic diagram of the four-step cycle of capacitive donnan potential for harvesting energy. LC and HC refer to low and high concentration solutions respectively [77].

fully charged (zero voltage), the circuit is again opened (no current) and a low-salinity solution (river water) is introduced, which reverses the potential polarity of the membranes (Step 3). The electrodes are then connected to an external circuit, creating an electrical current in the opposite direction (Step 4, the discharging process). Thus, in this process, the solution concentration changes results in adsorption/desorption or intercalation/detachment interaction between the electrode/membrane materials and the ions in the solution, which causes electrode potential changes and power generation [78–80].

Similar to PRO and RED processes, the CDP-CapMix process can also be integrated with water/wastewater treatment processes. Notably, the CDP process is simpler and could be more easily scaled up because it does not require a water turbine nor a large number of ion exchange membranes, although the achievable power density is still much lower than those by the PRO and RED processes. The CDP can combine with capacitive deionization (CDI, an electrochemical technology for adsorbing ions from low salt concentration) to realize simultaneous water purification and energy production [81]. This water treatment system is advantageous in that the energy consumption for CDI can be partially covered by CDP process and, in turn, the CDI brine can serve as the high-salinity solution for CDP, thereby addressing the energy and brine disposal issues simultaneously [10,82].

This book belongs to Badji Mokhtar Annaba University Central Library Copyright Elsevier 2025

The membrane and electrode materials significantly affect the performance of the CDP-CapMix systems, similar to PRO and RED systems [83,84]. Thus, similar membrane optimization strategies for lowering ICP, overpotential, and mitigating membrane fouling can be applied to favor practical application of CDP-CapMix systems [71]. Regarding the electrode, one unique property of CapMix systems distinct from other electrochemical systems is capacitive performance. Qiu et al. used a hybrid capacitor that consisted of a $Na_4Mn_9O_{18}$ battery electrode and a porous activated carbon electrode for Na^+ capture and Cl^- adsorption, respectively. Attributed to the opposite salinity-dependencies of two electrodes in their potentials, a voltage difference as high as 110 mV could be developed between the electrodes when fresh water and salt water alternately flowed through the hybrid capacitor, enabling efficient extraction of the SGE [80]. In addition, graphene hydrogel electrodes with macroporous structure and abundant negative charge have also been used in CapMix systems to enable rapid adsorption and desorption of ions, exhibiting a high capacitance and rapid response to ion concentration change (Fig. 13.6). The system achieved unprecedented

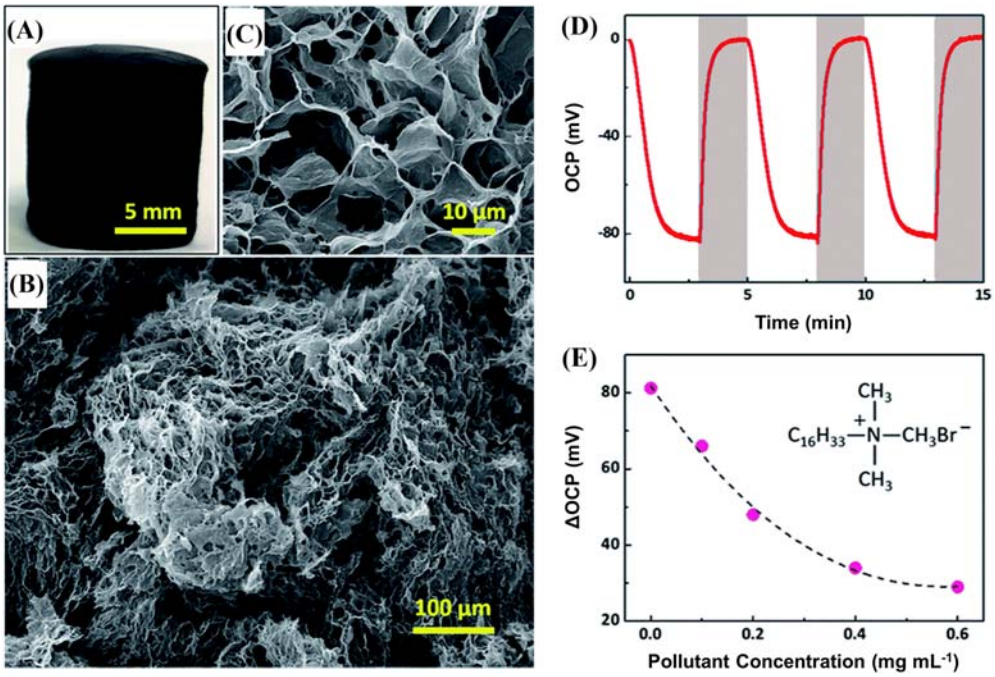

Figure 13.6 (A) Photograph and (B, C) scanning electron microscopy images of a free-standing graphene hydrogel electrode for capacitive mixing systems; (D) open circuit potential (OCP) of the electrode when alternately immersed in the low concentration (white background) and high concentration (dark background) solutions, and (E) the relationship between ion concentration and the OCP change [85].

This book belongs to Badji Mokhtar Annaba University Central Library Copyright Elsevier 2025

maximum voltage and power density output of 288.5 mV and 482.4 mW/m^2, respectively. The outstanding performance was associated with the double-channel construction, superior membrane potential, and the macroporous structure and negatively-charged surface of the graphene hydrogel electrodes [85]. For a scaled-up application, stacks of CapMix may also be applied. Hamelers et al. demonstrated that pairs of CapMix connected in parallel allowed for 18% more energy extraction than that connected in series for multiple wire-shaped electrode, ascribed to the reduced internal resistance by the additional flow ions paths between parallel electrode pairs. This system achieved a highest power density of 2.7 mW/g, far outperforming other configurations such as flat plate CapMix cell (1.26 mW/g) and a wire electrode cell (0.34 mW/g) [86].

The CapMix electrodes can also be combined with a bioelectrochemical system (BES) such as a microbial fuel cell to further improve the energy production and water treatment capability. For example, a hybrid system was constructed by deploying the CDP-CapMix electrodes in a middle chamber located between the BES anode and cathode chambers. Driven by both wastewater-derived bioenergy and SGE, the system exhibited significantly enhanced power density ($\sim$500 mW/m^2) versus the CDP-CapMix solo system ($\sim$10 mW^{-2}) [77].

The performances of some representative PRO, RED, and CDP systems reported so far have been provided in Table 13.1. To sum up, although the membrane-based electrochemical technologies of PRO, RED, and CDP can all be used for SGE capturing and water treatment, their potential application ranges and current development status differ obviously, and their performances are affected drastically by membrane and electrode materials and reactor configurations. PRO is a relatively mature technology with higher achievable power density than the other two, but the used semipermeable membranes in PRO are prone to blocking and fouling in water treatment application. For RED, it is more resistant to membrane fouling, but scaling-up presents a severe barrier to its application [51]. CDP is a relatively new and better-scalable technology, but the low energy efficiency of this system makes it economically unattractive. Thus, considerable research efforts are still needed to further move them from lab study into practical application.

13.3 Future perspectives and outlook

PRO, RED, CapMix, and their hybrid systems offer exciting opportunities to realize SGE capture and water/wastewater treatment simultaneously. However, these technologies are still on the horizon and there are considerable restrictions in performance and cost. Membrane materials with minimal ICP, good trade-off between

This book belongs to Badji Mokhtar Annaba University Central Library Copyright Elsevier 2025

This book belongs to Badji Mokhtar Annaba University Central Library

Table 13.1 Performances of some representative PRO, RED, and CDP systems.

System	Membrane	Electrode	Solution	Brine water (g/L)	Dilute water (g/L)	Power density (W/m^2)	References
PRO	Nanofiber-supported TFC	No	NaCl	29.2	0	8.0	[14]
	Cellulose acetate		$MgCl_2$	63.8	0	4.3	[29]
	TFC			63.8	0	10.2	
	TFC		Ammonium carbamate	45.2	0	13.6	[15]
	Poly(tetrafluoroethylene)/polypropylene		—	Cold liquid	Hot liquid	14.0	[87]
	Polyamide		NaCl	35.1	0	1.4	[88]
	Polyvinyl alcohol-coated polyethylene		NaCl	58.4	0	35.7	[24]
	Sulfonate-functionalized		NaCl	58.4	0	14.6	[89]
	Poly(benzoxazole-co-imide)-TFC-Cl		NaCl	58.4	0	26.6	[90]
	$Ti_3C_2T_x$ MXene/GO		NaCl	116.9	River water	56.4	[91]
RED	Fumasep anion and cation exchange membranes	Ru-Ir oxides@Ti mesh	NaCl	30	1	0.93	[63]
	Neosepta anion and cation exchange membranes	Ru-Ir oxides@Ti mesh	NaCl	30	1	0.6	[64]
	$Ti_3C_2T_x$	Ag/AgCl	NaCl	29.2	0.6	4.6	[50]
	Silk-based	Ag/AgCl	KCl/NaCl	29.2	0.06–6	2.86	[46]
	MoS_2	Ag/AgCl	KCl	74.6	0.07	10^6	[40]
	Ionic diode	Ag/AgCl	NaCl	29.2	0.6	3.46	[55]
	Two block copolymers	ITO	—	Natural seawater	River water	2.04	[54]
	Ionic diode	—	—	Salt lake	River water	5.1	[53]
	Three-dimensional gel	Ag/AgCl	NaCl	29.2	0.6	5.06	[52]

(*continued*)

Copyright Elsevier 2025

This book belongs to Badji Mokhtar Annaba University Central Library

Table 13.1 (Continued)

System	Membrane	Electrode	Solution	Brine water (g/L)	Dilute water (g/L)	Power density (W/m^2)	References
	Sulfonated polyethersulfone	Ag	NaCl	233.8	5.8	3.92	[92]
	Nafion	Ag/AgCl	KCl	298.2	29.8	1.11	[93]
CDP	CEM	Carboniced peat moss	NaCl	30	1	5.33	[84]
	AEM	Graphene hydrogel	NaCl	29.2	1.2	0.5	[85]
	AEM/CEM	Porous carbon	NaCl	0.6	29.8	0.072	[69]
	AEM/CEM	Porous carbon	NaCl	30	1	0.26	[71]
	Without	Porous carbon	NaCl	35.1	0.6	0.06	[94]
	AEM	MoS_2	NaCl	300	1	16	[95]
	Selective	Activated carbon	NaCl	29.2	1.2	1.1	[96]

AEM, anion exchange membrane; *CEM*, cation exchange membrane; *CDP*, Capacitive donnan potential; *PRO*, pressure-retarded osmosis; *RED*, reverse electrodialysis; *TFC*, thin-film composite.

Copyright Elsevier 2025

permeability and selectivity, high antifouling ability, and robustness under varied environmental and temperature conditions are still to be explored. In addition, electrode materials that can be better adapted to water purification applications are also needed. Rigorous techno-economic assessments are needed to identify the prospect of large-scale energy application of these materials. Effective, sustainable technologies for the high-salinity solution regeneration and clean water extraction are also on urgent demand. These would necessitate a better understanding of membrane processes in such systems, a more rational design of materials and reactors based on the specific technology features, and the exploration of sustainable supplement technologies.

In light of the different principles and technology features of PRO, RED, and CapMix, different electrochemical reaction systems may be adopted. For RED, the ferrous-ferric iron redox couple for electrode reaction is promising, but the issue of membrane and electrode fouling caused by iron precipitation is still to be addressed. For CDP, battery-type electrode materials are preferred, but there is difficulty in providing satisfactory electrical conductivity to match with capacitive materials such as activated carbon for high voltage and excellent power generation. Moreover, the utilization of waste heat, and the fates of brines and wastewater in these systems deserve more investigation.

It is noteworthy that there are also many other membrane-based technologies available for combining water treatment with energy recovery, such as capillary-driven [97], moist induction [98], and solar-based technologies [11,99,100]. These new systems may hopefully be developed as standalone technologies or in combination with the existing SGE-capture technologies to render more sustainable water treatment and energy production processes. For example, a novel photoelectrochemical osmotic cell combining sustainable solar energy and membrane-based SGE capture has been developed for sustainable wastewater treatment [7,11]. In all, the merging of electrochemical and membrane processes may create immense opportunities for more sustainable water treatment processes, thereby paving an exciting new pathway to address the multiple challenges of energy shortage, water deficiency, and global warming.

Acknowledgments

The authors thank the National Key Research and Development Program of China (2018YFA0901301), the National Natural Science Foundation of China (51778597 and 51821006), and the Fundamental Research Funds for the Central Universities (WK3530000011) for supporting this work.

References

[1] M. Gao, Z.-Y. Guo, X.-Y. Wang, W.-W. Li, Self-supported, Sulfate-functionalized nickel hydroxide nanoplates with enhanced wettability and conductivity for use in high-performance supercapacitors, ChemSusChem 12 (2019) 5291–5299.

[2] R.R. Gonzales, A. Abdel-Wahab, S. Adham, D.S. Han, S. Phuntsho, W. Suwaileh, et al., Salinity gradient energy generation by pressure retarded osmosis: a review, Desalination 500 (2021).

This book belongs to Badji Mokhtar Annaba University Central Library Copyright Elsevier 2025

[3] Z. Jia, B. Wang, S. Song, Y. Fan, Blue energy: current technologies for sustainable power generation from water salinity gradient, Renew. Sustain. Energy Rev. 31 (2014) 91–100.
[4] R.E. Pattle, Production of electric power by mixing fresh and salt water in the hydroelectric pile, Nature 174 (1954) 660.
[5] M. Tawalbeh, A. Al-Othman, N. Abdelwahab, A.H. Alami, A.G. Olabi, Recent developments in pressure retarded osmosis for desalination and power generation, Renew. Sustain. Energy Rev. 138 (2021).
[6] S. Wang, Q. Zhu, C. He, B. Zhang, Q. Chen, M. Pan, Model-based optimization and comparative analysis of open-loop and closed-loop RO-PRO desalination systems, Desalination 446 (2018) 83–93.
[7] H. Feng, M. Chen, R. Chen, X. Zhu, Q. Liao, D. Ye, et al., Anion-exchange membrane electrode assembled photoelectrochemical cell with a visible light responsive photoanode for simultaneously treating wastewater and generating electricity, Ind. Eng. Chem. Res. 59 (2019) 137–145.
[8] G. Han, J.S. de Wit, T.-S. Chung, Water reclamation from emulsified oily wastewater via effective forward osmosis hollow fiber membranes under the PRO mode, Water Res. 81 (2015) 54–63.
[9] E. Jwa, Y.-M. Yun, H. Kim, N. Jeong, K.S. Hwang, S. Yang, et al., Energy-efficient seawater softening and power generation using a microbial electrolysis cell-reverse electrodialysis hybrid system, Chem. Eng. J. 391 (2020).
[10] M.W. Saleem, Y.A.C. Jande, W.-S. Kim, Pure water and energy production through an integrated electrochemical process, J. Appl. Electrochem. 47 (2017) 315–325.
[11] C. Wang, M. Sun, Y. Zhao, M. Huo, X. Wang, M. Elimelech, Photo-electrochemical osmotic system enables simultaneous metal recovery and electricity generation from wastewater, Environ. Sci. Technol. 55 (2021) 604–613.
[12] S. Loeb, R.S. Norman, Osmotic power plants, Science 189 (1975) 654–655.
[13] S.J. Einarsson, B. Wu, Thermal associated pressure-retarded osmosis processes for energy production: a review, Sci. Total Environ. 757 (2021).
[14] B. Nhu-Ngoc, J.R. McCutcheon, Nanofiber supported thin-film composite membrane for pressure-retarded osmosis, Environ. Sci. Technol. 48 (2014) 4129–4136.
[15] M.S. Islam, S. Sultana, S. Adhikary, M.S. Rahaman, Highly effective organic draw solutions for renewable power generation by closed-loop pressure retarded osmosis, Energy Convers. Manage. 171 (2018) 1226–1236.
[16] K.L. Lee, R.W. Baker, H.K. Lonsdale, Membranes for power-generation by pressure-retarded osmosis, J. Membr. Sci. 8 (1981) 141–171.
[17] N.Y. Yip, A. Tiraferri, W.A. Phillip, J.D. Schiffrnan, L.A. Hoover, Y.C. Kim, et al., Thin-film composite pressure retarded osmosis membranes for sustainable power generation from salinity gradients, Environ. Sci. Technol. 45 (2011) 4360–4369.
[18] I.L. Alsvik, M.-B. Hagg, Pressure retarded osmosis and forward osmosis membranes: materials and methods, Polymers 5 (2013) 303–327.
[19] T.Y. Cath, A.E. Childress, M. Elimelech, Forward osmosis: principles, applications, and recent developments, J. Membr. Sci. 281 (2006) 70–87.
[20] N.Y. Yip, A. Tiraferri, W.A. Phillip, J.D. Schiffman, M. Elimelech, High performance thin-film composite forward osmosis membrane, Environ. Sci. Technol. 44 (2010) 3812–3818.
[21] A. Achilli, T.Y. Cath, A.E. Childress, Power generation with pressure retarded osmosis: an experimental and theoretical investigation, J. Membr. Sci. 343 (2009) 42–52.
[22] S. Zhao, L. Zou, C.Y. Tang, D. Mulcahy, Recent developments in forward osmosis: opportunities and challenges, J. Membr. Sci. 396 (2012) 1–21.
[23] S. Chou, R. Wang, L. Shi, Q. She, C. Tang, A.G. Fane, Thin-film composite hollow fiber membranes for pressure retarded osmosis (PRO) process with high power density, J. Membr. Sci. 389 (2012) 25–33.
[24] S.J. Kwon, K. Park, D.Y. Kim, M. Zhan, S. Hong, J.-H. Lee, High-performance and durable pressure retarded osmosis membranes fabricated using hydrophilized polyethylene separators, J. Membr. Sci. 619 (2021).
[25] S.N.A. Idris, N. Jullok, W.J. Lau, H.L. Ong, C.D. Dong, Graphene oxide incorporated polysulfone substrate for flat sheet thin film nanocomposite pressure retarded osmosis membrane, Membranes 10 (2020) 19.

This book belongs to Badji Mokhtar Annaba University Central Library Copyright Elsevier 2025

[26] D. Rana, T. Matsuura, Surface modifications for antifouling membranes, Chem. Rev. 110 (2010) 2448–2471.
[27] L. Zhang, Q. She, R. Wang, S. Wongchitphimon, Y. Chen, A.G. Fane, Unique roles of aminosilane in developing anti-fouling thin film composite (TFC) membranes for pressure retarded osmosis (PRO), Desalination 389 (2016) 119–128.
[28] Z.L. Cheng, X. Li, T.-S. Chung, The forward osmosis-pressure retarded osmosis (FO-PRO) hybrid system: a new process to mitigate membrane fouling for sustainable osmotic power generation, J. Membr. Sci. 559 (2018) 63–74.
[29] H. Gong, D.D. Anastasio, K. Wang, J.R. McCutcheon, Finding better draw solutes for osmotic heat engines: understanding transport of ions during pressure retarded osmosis, Desalination 421 (2017) 32–39.
[30] S. Adhikary, M.S. Islam, K. Touati, S. Sultana, A.S. Ramamurthy, M.S. Rahaman, Increased power density with low salt flux using organic draw solutions for pressure-retarded osmosis at elevated temperatures, Desalination 484 (2020).
[31] R.A. Tufa, S. Pawlowski, J. Veerman, K. Bouzek, E. Fontananova, G. di Profio, et al., Progress and prospects in reverse electrodialysis for salinity gradient energy conversion and storage, Appl. Energy 225 (2018) 290–331.
[32] J.L. Di Salvo, A. Cosenza, A. Tamburini, G. Micale, A. Cipollina, Long-run operation of a reverse electrodialysis system fed with wastewaters, J. Environ. Manage. 217 (2018) 871–887.
[33] J. Veerman, D.A. Vermaas, Reverse Electrodialysis: Fundamentals (2016) 77–133.
[34] J.W. Post, H.V.M. Hamelers, C.J.N. Buisman, Influence of multivalent ions on power production from mixing salt and fresh water with a reverse electrodialysis system, J. Membr. Sci. 330 (2009) 65–72.
[35] X. Luo, X. Cao, Y. Mo, K. Xiao, X. Zhang, P. Liang, et al., Power generation by coupling reverse electrodialysis and ammonium bicarbonate: implication for recovery of waste heat, Electrochem. Commun. 19 (2012) 25–28.
[36] M.C. Hatzell, I. Ivanov, R.D. Cusick, X. Zhu, B.E. Logan, Comparison of hydrogen production and electrical power generation for energy capture in closed-loop ammonium bicarbonate reverse electrodialysis systems, Phys. Chem. Chem. Phys. 16 (2014) 1632–1638.
[37] P. Ma, X. Hao, A. Galia, O. Scialdone, Development of a process for the treatment of synthetic wastewater without energy inputs using the salinity gradient of wastewaters and a reverse electrodialysis stack, Chemosphere 248 (2020).
[38] Y.D. Raka, R. Bock, H. Karoliussen, O. Wilhelmsen, O.S. Burheim, The influence of concentration and temperature on the membrane resistance of ion exchange membranes and the levelised cost of hydrogen from reverse electrodialysis with ammonium bicarbonate, Membranes 11 (2021).
[39] L. Bocquet, Nanofluidics coming of age, Nat. Mater. 19 (2020) 254–256.
[40] J. Feng, M. Graf, K. Liu, D. Ovchinnikov, D. Dumcenco, M. Heiranian, et al., Single-layer MoS_2 nanopores as nanopower generators, Nature 536 (2016) 197.
[41] P.R. Kidambi, G.D. Nguyen, S. Zhang, Q. Chen, D. Kong, J. Warner, et al., Facile fabrication of large-area atomically thin membranes by direct synthesis of graphene with nanoscale porosity, Adv. Mater. 30 (2018).
[42] R.P. Pandey, K. Rasool, V.E. Madhavan, B. Aissa, Y. Gogotsi, K.A. Mahmoud, Ultrahigh-flux and fouling-resistant membranes based on layered silver/MXene ($Ti_3C_2T_x$) nanosheets, J. Mater. Chem. A 6 (2018) 3522–3533.
[43] J. Wang, P. Chen, B. Shi, W. Guo, M. Jaroniec, S.-Z. Qiao, A regularly channeled lamellar membrane for unparalleled water and organics permeation, Angew. Chem. Int. Ed. 57 (2018) 6814–6818.
[44] Y. Sun, Y. Li, Potential environmental applications of MXenes: a critical review, Chemosphere 271 (2021) 129578.
[45] F.H.J. van der Heyden, D. Stein, C. Dekker, Streaming currents in a single nanofluidic channel, Phys. Rev. Lett. 95 (2005).
[46] W. Xin, Z. Zhang, X. Huang, Y. Hu, T. Zhou, C. Zhu, et al., High-performance silk-based hybrid membranes employed for osmotic energy conversion, Nat. Commun. 10 (2019).
[47] A. Siria, P. Poncharal, A.L. Biance, R. Fulcrand, X. Blase, S.T. Purcell, et al., Giant osmotic energy conversion measured in a single transmembrane boron nitride nanotube, Nature 494 (2013) 455–458.

This book belongs to Badji Mokhtar Annaba University Central Library Copyright Elsevier 2025

[48] M.E. Suk, N.R. Aluru, Water transport through ultrathin graphene, J. Phys. Chem. Lett. 1 (2010) 1590–1594.
[49] M. Heiranian, A.B. Farimani, N.R. Aluru, Water desalination with a single-layer MoS_2 nanopore, Nat. Commun. 6 (2015).
[50] L. Ding, D. Xiao, Z. Lu, J. Deng, Y. Wei, J. Caro, et al., Oppositely charged $Ti_3C_2T_x$ MXene membranes with 2D nanofluidic channels for osmotic energy harvesting, Angew. Chem. Int. (Ed.) 59 (2020) 8720–8726.
[51] Y. Zhou, L. Jiang, Bioinspired nanoporous membrane for salinity gradient energy harvesting, Joule 4 (2020) 2244–2248.
[52] Z. Zhang, L. He, C. Zhu, Y. Qian, L. Wen, L. Jiang, Improved osmotic energy conversion in heterogeneous membrane boosted by three-dimensional hydrogel interface, Nat. Commun. 11 (2020).
[53] X. Zhu, J. Hao, B. Bao, Y. Zhou, H. Zhang, J. Pang, et al., Unique ion rectification in hypersaline environment: a high-performance and sustainable power generator system, Sci. Adv. 4 (2018).
[54] Z. Zhang, X. Sui, P. Li, G. Xie, X.-Y. Kong, K. Xiao, et al., Ultrathin and ion-selective Janus membranes for high-performance osmotic energy conversion, J. Am. Chem. Soc. 139 (2017) 8905–8914.
[55] J. Gao, W. Guo, D. Feng, H. Wang, D. Zhao, L. Jiang, High-performance ionic diode membrane for salinity gradient power generation, J. Am. Chem. Soc. 136 (2014) 12265–12272.
[56] Q.-Y. Wu, C. Wang, R. Wang, C. Chen, J. Gao, J. Dai, et al., Salinity-gradient power generation with ionized wood membranes, Adv. Energy Mater. 10 (2020).
[57] X. Tong, B. Zhang, Y. Chen, Fouling resistant nanocomposite cation exchange membrane with enhanced power generation for reverse electrodialysis, J. Membr. Sci. 516 (2016) 162–171.
[58] Y. Kim, B.E. Logan, Hydrogen production from inexhaustible supplies of fresh and salt water using microbial reverse-electrodialysis electrolysis cells, Proc. Natl. Acad. Sci. U. S. A. 108 (2011) 16176–16181.
[59] Y. Kim, B.E. Logan, Microbial reverse electrodialysis cells for synergistically enhanced power production, Environ. Sci. Technol. 45 (2011) 5834–5839.
[60] P. Ma, X. Hao, F. Proietto, A. Galia, O. Scialdone, Assisted reverse electrodialysis for CO_2 electrochemical conversion and treatment of wastewater: a new approach towards more eco-friendly processes using salinity gradients, Electrochim. Acta 354 (2020).
[61] Y. Tian, D. Li, C. Li, J. Liu, J. Wu, G. Liu, et al., Self-driving CO_2-to-formate electro-conversion on Bi film electrode in novel microbial reverse-electrodialysis CO_2 reduction cell, Chem. Eng. J. 414 (2021).
[62] Y. Tian, D. Li, G. Liu, C. Li, J. Liu, J. Wu, et al., Formate production from CO_2 electroreduction in a salinity-gradient energy intensified microbial electrochemical system, Bioresour. Technol. 320 (2021).
[63] J. Veerman, M. Saakes, S.J. Metz, G.J. Harmsen, Reverse electrodialysis: performance of a stack with 50 cells on the mixing of sea and river water, J. Membr. Sci. 327 (2009) 136–144.
[64] J. Veerman, R.M. de Jong, M. Saakes, S.J. Metz, G.J. Harmsen, Reverse electrodialysis: comparison of six commercial membrane pairs on the thermodynamic efficiency and power density, J. Membr. Sci. 343 (2009) 7–15.
[65] D.A. Vermaas, M. Saakes, K. Nijmeijer, Doubled power density from salinity gradients at reduced intermembrane distance, Environ. Sci. Technol. 45 (2011) 7089–7095.
[66] J. Veerman, M. Saakes, S.J. Metz, G.J. Harmsen, Electrical power from sea and river water by reverse electrodialysis: a first step from the laboratory to a real power plant, Environ. Sci. Technol. 44 (2010) 9207–9212.
[67] D.A. Vermaas, D. Kunteng, J. Veerman, M. Saakes, K. Nijmeijer, Periodic feedwater reversal and air sparging as antifouling strategies in reverse electrodialysis, Environ. Sci. Technol. 48 (2014) 3065–3073.
[68] D. Brogioli, Extracting renewable energy from a salinity difference using a capacitor, Phys. Rev. Lett. 103 (2009).
[69] B.B. Sales, M. Saakes, J.W. Post, C.J.N. Buisman, P.M. Biesheuvel, H.V.M. Hamelers, Direct power production from a water salinity difference in a membrane-modified supercapacitor flow cell, Environ. Sci. Technol. 44 (2010) 5661–5665.

This book belongs to Badji Mokhtar Annaba University Central Library Copyright Elsevier 2025

[70] S. Ahualli, M. Mar Fernandez, G. Iglesias, M.L. Jimenez, F. Liu, M. Wagterveld, et al., Effect of solution composition on the energy production by capacitive mixing in membrane-electrode assembly, J. Phys. Chem. C 118 (2014) 15590–15599.
[71] O. Burheim, B.B. Sales, O. Schaetzle, F. Liu, H.V.M. Hamelers, Auto generative capacitive mixing for power conversion of sea and river water by the use of membranes, ASME J. Energy Resour. Technol. 135 (2013).
[72] F. Liu, O. Schaetzle, B.B. Sales, M. Saakes, C.J.N. Buisman, H.V.M. Hamelers, Effect of additional charging and current density on the performance of capacitive energy extraction based on Donnan Potential, Energy Environ. Sci. 5 (2012) 8642–8650.
[73] M. Marino, L. Misuri, R. Ruffo, D. Brogioli, Electrode kinetics in the "capacitive mixing" and "battery mixing" techniques for energy production from salinity differences, Electrochim. Acta 176 (2015) 1065–1073.
[74] D. Brogioli, R. Ziano, R.A. Rica, D. Salerno, O. Kozynchenko, H.V.M. Hamelers, et al., Exploiting the spontaneous potential of the electrodes used in the capacitive mixing technique for the extraction of energy from salinity difference, Energy Environ. Sci. 5 (2012) 9870–9880.
[75] M. Marino, L. Misuri, M.L. Jimenez, S. Ahualli, O. Kozynchenko, S. Tennison, et al., Modification of the surface of activated carbon electrodes for capacitive mixing energy extraction from salinity differences, J. Colloid Interface Sci. 436 (2014) 146–153.
[76] M.M. Fernandez, R.M. Wagterveld, S. Ahualli, F. Liu, A.V. Delgado, H.V.M. Hamelers, Polyelectrolyte-vs membrane-coated electrodes for energy production by capmix salinity exchange methods, J. Power Sources 302 (2016) 387–393.
[77] M.C. Hatzell, R.D. Cusick, B.E. Logan, Capacitive mixing power production from salinity gradient energy enhanced through exoelectrogen-generated ionic currents, Energy Environ. Sci. 7 (2014) 1159–1165.
[78] J. Lee, H. Yoon, J. Lee, T. Kim, J. Yoon, Extraction of salinity-gradient energy by a hybrid capacitive-mixing system, ChemSusChem 11 (2018) 638.
[79] D. Kang, Q. Liu, J. Gu, Y. Su, W. Zhang, D. Zhang, "Egg-Box"-assisted fabrication of porous carbon with small mesopores for high-rate electric double layer capacitors, ACS Nano 9 (2015) 11225–11233.
[80] F. Zhan, G. Wang, T. Wu, Q. Dong, Y. Meng, J. Wang, et al., Salinity-difference-driven power generation by a hybrid capacitive approach, Energy Technol. 6 (2018) 238–241.
[81] S. Vafakhah, Z. Beiramzadeh, M. Saeedikhani, H.Y. Yang, A review on free-standing electrodes for energy-effective desalination: recent advances and perspectives in capacitive deionization, Desalination 493 (2020).
[82] S. Porada, D. Weingarth, H.V.M. Hamelers, M. Bryjak, V. Presser, P.M. Biesheuvel, Carbon flow electrodes for continuous operation of capacitive deionization and capacitive mixing energy generation, J. Mater. Chem. A 2 (2014) 9313–9321.
[83] A. Siekierka, K. Smolinska-Kempisty, M. Bryjak, Charge-doped electrodes for power production using the salinity gradient in CapMix, Desalination 495 (2020).
[84] H. Zhu, W. Xu, G. Tan, E. Whiddon, Y. Wang, C.G. Arges, et al., Carbonized peat moss electrodes for efficient salinity gradient energy recovery in a capacitive concentration flow cell, Electrochim. Acta 294 (2019) 240–248.
[85] F. Zhan, Z. Wang, T. Wu, Q. Dong, C. Zhao, G. Wang, et al., High performance concentration capacitors with graphene hydrogel electrodes for harvesting salinity gradient energy, J. Mater. Chem. A 6 (2018).
[86] F. Liu, T.F.W. Donkers, R.M. Wagterveld, O. Schaetzle, M. Saakes, C.J.N. Buisman, et al., Parallel up-scaling of Capacitive Mixing (CapMix) system enhances the specific performance, Electrochim. Acta 187 (2016) 104–112.
[87] J. Li, Z. Zhang, R. Zhao, B. Zhang, Y. Liang, R. Long, et al., Stack thermo-osmotic system for low-grade thermal energy conversion, ACS Appl. Mater. Interfaces 13 (2021) 21371–21378.
[88] Y. Kakihana, N. Jullok, M. Shibuya, Y. Ikebe, M. Higa, Comparison of pressure-retarded osmosis performance between pilot-scale cellulose triacetate hollow-fiber and polyamide spiral-wound membrane modules, Membranes 11 (2021).

This book belongs to Badji Mokhtar Annaba University Central Library Copyright Elsevier 2025

[89] R.R. Gonzales, Y. Yang, M.J. Park, T.-H. Bae, A. Abdel-Wahab, S. Phuntsho, et al., Enhanced water permeability and osmotic power generation with sulfonate-functionalized porous polymer-incorporated thin film nanocomposite membranes, Desalination 496 (2020).
[90] S.J. Moon, S.M. Lee, J.H. Kim, S.H. Park, H.H. Wang, J.H. Kim, et al., A highly robust and water permeable thin film composite membranes for pressure retarded osmosis generating 26 $W \cdot m^{-2}$ at 21 bar, Desalination 483 (2020).
[91] H. Gao, W. Chen, C. Xu, S. Liu, X. Tong, Y. Chen, Two-dimensional $Ti_3C_2T_x$ MXene/GO hybrid membranes for highly efficient osmotic power generation, Environ. Sci. Technol. 54 (2020) 2931–2940.
[92] A.H. Avci, T. Rijnaarts, E. Fontananova, G. Di Profio, I.F.V. Vankelecom, W.M. De Vos, et al., Sulfonated polyethersulfone based cation exchange membranes for reverse electrodialysis under high salinity gradients, J. Membr. Sci. 595 (2020).
[93] H. Wang, W. Xie, B. Yu, B. Qi, R. Liu, X. Zhuang, et al., Simultaneous solar steam and electricity generation from synergistic salinity-temperature gradient, Adv. Energy Mater. 11 (2021).
[94] J. Yu, T. Ma, Harvesting blue energy with carbon electrodes of asymmetric nanopore distributions, Nano Energy 82 (2021).
[95] H. Zhu, J. Lai, C.G. Arges, Y. Wang, X. Zhu, Engineering the interlayer spacing of molybdenum disulfide for efficient salinity gradient energy recovery in concentration flow cells, Electrochim. Acta 342 (2020).
[96] F. Zhan, G. Wang, T. Wu, Q. Dong, Y. Meng, J. Wang, et al., High performance asymmetric capacitive mixing with oppositely charged carbon electrodes for energy production from salinity differences, J. Mater. Chem. A 5 (2017) 20374–20380.
[97] C. Li, Z. Tian, L. Liang, S. Yin, P.K. Shen, Electricity generation from capillary-driven ionic solution flow in a three-dimensional graphene membrane, ACS Appl. Mater. Interfaces 11 (2019) 4922–4929.
[98] Q. Lyu, B. Peng, Z. Xie, S. Du, L. Zhang, J. Zhu, Moist-induced electricity generation by electrospun cellulose acetate membranes with optimized porous structures, ACS Appl. Mater. Interfaces 12 (2020) 57373–57381.
[99] E. Cao, Z. Chen, H. Wu, P. Yu, Y. Wang, F. Xiao, et al., Boron-induced electronic-structure reformation of CoP nanoparticles drives enhanced pH-universal hydrogen evolution, Angew. Chem. Int. (Ed.) Engl. 59 (2020) 4154–4160.
[100] P. Yang, K. Liu, Q. Chen, J. Li, J. Duan, G. Xue, et al., Solar-driven simultaneous steam production and electricity generation from salinity, Energy Environ. Sci. 10 (2017) 1923–1927.

This book belongs to Badji Mokhtar Annaba University Central Library Copyright Elsevier 2025

Index

Note: Page numbers followed by "*f*" and "*t*" refer to figures and tables, respectively.

A

Acid-soluble fraction, 239
"Active" anodes, 120–121
Active-chlorine-mediated decontamination, 120–121
Additive, 50
Advanced oxidation process (AOP), 90–91
Aluminum hydroxides, 164–169
Amino acids, 293–294
Anaerobic electrochemical membrane bioreactor (AnEMBR), 95
Anchoring methods, 156–157
Anion exchange membrane (AEM), 10, 17–18, 231–232, 266, 317–318, 364–365
Anodic electrooxidation, 169
Anodic •OH-mediated decontamination, 119–120
Antifouling membrane, 128–130
Antimicrobial nanomaterials, 145–146
Aqueous electron-mediators, 343

B

Bioelectrochemical-active bacteria, 361
Biofilm cathode, 450
Biofouling, 196–197
Biofouling mitigation, 130–131
Bipolar junction, 304
Bipolar membrane (BM), 268–270
Blue-black TiO_2 nanotubes, 250–252
Blue Energy project, 448
BM-based ED process (BMED)
  posttreatment process
    for inorganic acid/base generation, 282–288
    for organic acid/base generation, 288–295
  pretreatment process, 295–301
Boltzmann constant, 60
Boron-doped diamond (BDD) electrodes, 9
Bovine serum albumin (BSA), 95–96

C

Calcium salts, 197
Capacitive deionization (CDI), 2–3, 317
Capacitive donnan potential (CDP), 445
Capacitive mixing (CapMix) systems, 451
CapMix electrodes, 454
Carbon-based antimicrobial nanomaterials, 146
Carbon-based membranes, 200–201
Carbon electrode oxidation, 18–19
Carbon nanotube (CNT), 87
Carbon nanotube-based membranes, 94–95
Carbon nanotubes hollow fiber membranes (CNT-HFMs), 185
Cation exchange membrane (CEM), 10, 97–98, 231–232, 266, 317–318, 364–365, 406–407
CDP-CapMix process, 451–452
Cell configurations, 345–347
Cellular oxidative stress, 144
Chemical vapor deposit (CVD), 13, 96–97
Chlorate poisoning, 234
Chloride oxidation, 18–19
Chlorosulfonic acid (CSA), 84–86
CNT-FeOOH sorption sites, 126–127
Colloidal fouling, 197
Composite conductive membranes, 200–201
Composite membrane, 90–92
Computational fluid dynamics (CFD), 157
Conductive membranes (CMs), 1–2, 81
  CM-based electrochemical technology, 6*t*
  composite membranes, 84–86
  electrochemical membrane oxidation, 22*t*, 25–26
  electrochemical membrane reduction, 26–27
  membrane fouling mitigation, 21–25
  mixed matrix membranes, 86–88
  polymer-based membrane materials, 83–89, 84*f*
Conductive polymeric membranes, 200
Conductive polymers (CPM), 81–82
Constant current (CC), 322*f*
Constant voltage (CV), 322*f*
Convection, 51
Convection flow effects, 4
Conventional disinfection technologies, 141
Conventional electrodialysis (CED), 292
Conventional membranes, 195–196

This book belongs to Badji Mokhtar Annaba University Central Library
Copyright Elsevier 2025

Conventional physical filtration processes, 403–404
Current efficiency (CE), 70

D

3D CNT networks, 114–115
3D electrochemical system, 250–253
Diffusion, 51
3-dimensional (3D) porous electrodes, 153
Direct electrochemical oxidation, 9
Direct oxidation, 143
Disinfection
  antimicrobial nanomaterials, 145–146
  conventional and nonconventional water resources, 141
  direct oxidation, 144
  electroporation, 145
  free radical generation and cell structure decomposition, 141–142
  indirect oxidation, 144–145
  microbial concentration, 142
  operation cost, 142
  performance comparison of, 147–151
  principal mechanisms, 142–143, 143*f*
  reactor configuration
    designs, 142
    development progress of, 151–152
    evaluation and comparison, 154–156
    flow-by reactor, 152–153
    limitations and challenges, 156–157
    stirred reactor, 152
  reactors, 150
Donnan effect, 54–55
Donnan steric pore model (DSPM) theory, 52
Dry-wetting spinning, 12

E

ED reversal (EDR), 17
EF-induced polarization phenomena, 44
Electrical double layer (EDL), 19, 44, 320
  existing forms of ions, 57–59
  formation mechanism and configuration of, 55–57
  Gouy–Chapman model, 60–61
  Gouy–Chapman–Stern model, 61–62
  Helmholtz model, 59–60
  modified Donnan model, 62
  regulation mechanism of, 63
Electrical energy consumption, 147
Electrical heating, 229
Electrically conductive materials, 111–112
Electric field (EF), 43–44, 204–205
Electrified carbon nanotube membrane technology
  electrically conductive materials, 111–112
  electrochemical reaction kinetics, 111–112
  reactor configuration, 115–116
Electrified membranes (EMs), 44
Electroactive membranes
  CNT, 112–113
  MWCNT, 112–113
  oxygen-containing groups, 114–115
  peroxymonosulfate (PMS) activation, 114–115
  SWCNT, 112–113
Electrocatalytic electrodes, 209–210
Electrocatalytic remediation
  3D electrochemical system, 250–253
  fundamentals, 249–250
  proton-conducting membrane cell, 253–257
Electrochemical advanced oxidation processes (EAOPs), 1–2, 404
Electrochemical CNT membranes
  decontamination of toxic inorganic contaminants, 125–128
  direct electro-oxidation of contaminants, 117–119
  electroactive antifouling membranes, 128–131
  energy consumption, 124–125, 125*t*
  indirect electro-oxidation of contaminants, 119–124
  nanoconfinement effects in, 131–132
Electrochemical filtration systems (EFS), 404–405
Electrochemical membrane bioreactor (eMBR), 25–26, 81–82, 163
  challenges and future prospects, 189–190
  energy consumption, 187–189, 188*t*
  membrane fouling mitigation
    mechanisms of, 175–178, 176*f*
    mixed liquor properties, 178–181
  microbiological community, 185–187, 187*t*
  nonconventional pollutant removal
    pathogenic viruses, 174–175
    phenols, 172–173
    trace organic pollutants, 173–174
  operating conditions, materials, and configurations

This book belongs to Badji Mokhtar Annaba University Central Library
Copyright Elsevier 2025

configurations and membrane materials, 183–185, 184*f*
current density and duration of application, 181–182
electrode materials, 182–183
pollutant removal
nitrogen, 170–171
organic pollutants, 164–170
phosphorus, 171–172
Electrochemical membrane modules, 100–102
Electrochemical membrane oxidation, 22*t*, 25–26
Electrochemical membrane process configurations
bifunctional electroconductive membrane process, 202*f*
compact designs and energy-efficient operations, 204–205
single-stage hybrid process, 202*f*
two-stage process, 202*f*
Electrochemical membrane reduction, 26–27
Electrochemical membrane technology
applications, 14*t*
electrodialysis, 13–17
membrane capacitive deionization, 18–19
microbial desalination cell, 21
microbial fuel cell, 19–21
reverse electrodialysis, 17–18
capacitive deionization (CDI), 2–3
classification of, 4–7
CM-based electrochemical process, 1–2
conductive membranes (CMs), 1–2
electrochemical membrane oxidation, 22*t*, 25–26
electrochemical membrane reduction, 26–27
membrane fouling mitigation, 21–25
defined, 4
efficacy/cost-effectiveness, membrane process, 1
electric field (EF), 43–44
electrochemical processes, 3–4
electrodialysis (ED), 2–3
historical development of, 2–3
membrane film, 1
membrane fouling control and long-term operational stability, 43
membrane processes, 4
microbial fuel cell (MFC), 2–3
preparation
of conductive membrane, 12–13
of ion exchange membrane, 11
surface-charged membranes, 1–2
timeline of development, 2*f*
water contamination and climate change, 1
working principles of, 7–11, 8*f*
Electrochemical oxidation, 5*t*, 9, 207, 404
Electrochemical reaction kinetics, 111–112
Electrochemical reactions
electrochemical oxidation, 206–207
electrocoagulation/electroflotation, 206
electrophoresis, 205
fundamentals of, 68–70
membrane electrode process, 72–74
reactive species in, 71–72
Electrochemical separation, 404
Electrocoagulation, 208, 218
Electrocoagulation membrane reactor (ECMR), 66–68
Electroconductive membranes, 214
Electrodeionization (EDI), 267–268
Electrode materials, 319
Electrodeposition, 12
Electrodialysis (ED), 2–3, 13–17, 81–82, 265–266, 404–405
basic configuration and historical development, 266–268
for energy recovery, 302–303
for industrial wastewater treatment
ion exchange membranes, 268–270
metals recovery, 276–281
nutrient recovery, 271–275
wastewater reclamation, 271
nonrenewable resources, 265
for trace contaminants removal, 302
for waste ionic liquid recovery, 301–302
Electrodialysis reversal (EDR), 267–268, 329
Electrodialytic remediation
critical operating parameters and performance indicators
contaminant speciation and removal, 239–241
current density and voltage drop, 235–237, 236*f*
liquid-solid ratio, 237–238
pH and water content, 238
remediation time, 237
fundamentals, 229–234, 229*f*, 230*t*, 233*f*
mathematical simulation/modeling methods
applications of, 245–249

This book belongs to Badji Mokhtar Annaba University Central Library Copyright Elsevier 2025

Electrodialytic remediation (*Continued*)
multiple linear regression and principal component regression, 242–244
projection to latent structures, 244–245
resource recovery and reactant delivery, 248–249
univariate linear regressions, 241
Electro-Fenton (EF), 5*t*
Electro-Fenton driven decontamination, 121–124
Electrofiltration, 201, 208–209
Electroflocculation, 206
Electroflotation, 206, 208
Electrokinetic effect, 45
Electrokinetic ions/colloids
electromigration
electric mobility and migration number of ions, 46–47
electroosmosis, 49–50
electrophoresis, 47–49
ion electromigration, 45–46
Electrolysis, 5*t*, 228
Electrolyte, 344
Electro-membrane process, 288–289
Electromigration, 5*t*, 227
Electroosmosis, 5*t*, 49–50, 177, 227–228
Electrooxidation, 169
Electrophoretic mobility, 48
Electrosorption, 5*t*, 228
Electrosorption-based separation methods, 404
Electrospinning, 11–12
Electrostatic repulsion, 8, 129
Energy consumption, 124–125, 325–329, 361
Energy shortage, 445
Enhanced membrane separation, 81–82
Extracellular polymeric substances (EPS), 74, 175

F

Faradaic reactions, 7, 228
Faraday's law, 8, 70
Field strength and zeta potential, 50
Flat-sheet (FS), 100
Flow capacitive deionization
active materials, 339–340
applications of, 347–351
cell configurations, 345–347
challenges and perspectives, 351–352
conductive additives, 340–344
contaminant abatements, 350
electrolyte, 344
emerging applications, 351
flow-electrodes, 338–344
operation modes, 347
resource recovery, 349–350
separator and spacer, 344–345
theory and development of, 337–338, 338*f*
water desalination, 348
Flow-electrode capacitive deionization (FCDI), 9, 318

G

Global climate change, 445
Gouy–Chapman model, 60–61
Gouy–Chapman–Stern model, 61–62
Graphene (Gr), 87, 146
Graphene-based membranes, 95–96
Graphene oxide (GO), 95
Graphitized carbon fiber membranes, 144

H

Halogenated organic contaminants, 124
Heavy metal pollution, 276
Helmholtz model, 59–60
Heterogeneous precipitation, 234
Highest occupied molecular orbital (HOMO), 83
H_2O_2-concentrated interface, 144
H_2S-H_2O coelectrolysis, 253–257
Humic acid (HA), 95–96
Hydraulic retention time (HRT), 147

I

IEM-based electrochemical technology, 6*t*
Indirect oxidation, 143
Industrial wastewater treatment
for BMED
posttreatment process, for inorganic acid/base generation, 282–288
posttreatment process, for organic acid/base generation, 288–295
pretreatment process, 295–301
ion exchange membranes, 268–270
metals recovery, 276–281
nutrient recovery, 271–275
wastewater reclamation, 271
Inorganic CM, 12–13
Inorganic materials, 81–82
In situ polymerization, 11–12

This book belongs to Badji Mokhtar Annaba University Central Library
Copyright Elsevier 2025

Internal concentration polarization (ICP), 447
Ion diffusion, 53
Ion exchange membranes (IEMs), 81, 229–230, 268–270, 317–319
  heterogenous IEMs, 98–99
  homogeneous IEM, 98
  mixed matrix IEMs, 100
  pseudohomogeneous IEMs, 99–100
Ion transmembrane mass transfer
  Donnan effect, 54–55
  Nernst–Planck equation, 51–54
Irreversible fouling, 207

L

Lactic acid production, 298–299
Landfilling, 361
Layer-by-layer (LBL) modification, 99
Limited salt removal capacity, 352
Lithium recovery, 280
Lowest occupied molecular orbital (LOMO), 83

M

Membrane-based electricity generation technologies
  capacitive systems, 451–454, 452*f*, 453*f*
  future perspectives, 454–457
  pressure-retarded osmosis, 446–448, 446*f*
  reverse electrodialysis, 448–451, 448*f*
Membrane bioreactors (MBRs), 163
Membrane capacitive deionization (MCDI), 2–3, 9, 18–19, 81–82, 317–319
  CC mode, 321
  challenges and perspectives, 351–352
  CV mode, 321
  electrical double layers (EDLs), 320
  modified Donnan model, 321
Membrane-current collector-assembly (MCA), 344–345
Membrane distillation (MD), 81–82
Membrane filtration, 141
Membrane fouling, 10
  bifunctional membrane process, 211–215
  classification of, 197–198, 199*f*
  electrochemical MBR, 210–211
  electroconductive membranes, 200–201
  energy consumption for, 215, 216*t*
  factors, 198
  fouling and antifouling strategies, 196–197
  nonelectroconductive membranes, 199–200
  single-stage hybrid process, 208–210, 209*f*
  two-stage serial processes, 207–208, 208*f*
Membrane fouling and scaling, 304–305
Membrane fouling mitigation, 21–25
Membrane separation, 403
Membrane-spacer-assembly (MSA), 344–345
Mesh-based electrodes, 153
Metal and metal-oxide membrane materials
  carbon-based membrane materials and MXene, 94–97
  carbon nanotube-based membranes, 94–95
  composite membrane, 90–92
  graphene-based membranes, 95–96
  metallic membrane, 89–90
  MXene-based membranes, 96
Metal-based antimicrobial nanomaterials, 146
Metallic membrane, 89–90
Metals recovery, 276–281
Microbial adhesion, 196–197
Microbial desalination cells (MDCs), 21, 81–82
  air-cathode microbial desalination cell, 369–370
  biocathode microbial desalination cell, 370
  challenges and perspectives
    instability, 392–393
    low performance, 391–392
    scale-up and high cost, 393
  configurations, 368–374
  cubic-shaped MFC, 364–365
  desalination mechanism of, 364–365
  electroactive microorganism, 365
  electrode materials, 366–367, 366*f*
  energy-saving technology, 364–365
  external electric circuit, 364–365
  with FO, 389–391, 390*f*
  functions, 361–362, 383*f*
  membrane materials, 368
  microbial capacitive desalination cell, 371
  microbial chemical production cell, 373
  microbial fuel cell and electricity generation, 362–364, 363*f*
  multistage microbial desalination cell, 372
  and operational conditions
    anodic substrate concentration, 378
    catholyte solution, 378–379
    external resistance, 374–375
    fouling and scaling, 380–381
    internal resistance, 375–377

This book belongs to Badji Mokhtar Annaba University Central Library Copyright Elsevier 2025

Microbial desalination cells (MDCs) (*Continued*)
mathematical modeling, 381
operation mode, 379–380
pH control, 377–378
temperature, 379
osmotic microbial desalination cell, 372–373
photosynthetic microbial desalination cell, 371
research community and, 361–362
with RO, 387–389
wastewater treatment
brackish water desalination, 384–385
chemical and gas production, 386–387
domestic wastewater, 381–382
heavy metal recovery, 387
industrial wastewater, 382–384
nitrogen and phosphorus recovery, 385–386
seawater desalination, 384
water softening, 385
Microbial fuel cell (MFC), 2–3, 11, 19–21, 81–82, 361
Microbial inactivation, 152–153
Microbial metabolism, 5*t*
Microfiltration (MF), 195
Migration, 51
Mixed matrix membranes, 86–88
Modified Donnan model, 62
Modified phase inversion, 12
Monovalent ion exchange membrane (MIEM), 268–270
Monovalent ion selectivity, 352
Multiwalled CNT (MWCNT), 112–113, 146
MXene-based membranes, 96

N

Nanoconfinement effects, 131–132
Nanoscale zerovalent iron (NZVI), 147
Nanowire-assisted electroporation, 143, 145
Nernst–Planck equation, 43–44, 51–54
Nitrogen-containing compounds, 170–171
4-nitrophenol, 123–124
Nitrosomonas, 186–187
N-nitrosodimethylamine, 123–124, 403–404
"Nonactive" anodes, 120–121
Non-biodegradable pollutants, 403
Non-Faradaic electrosorption process, 9
Non-Faradaic reaction, 7–9
Nonrenewable resources, 265
Nonsacrificial electrodes, 182–183
Non-synthetic test waters, 352
"No phase transition" process, 10
Nutrient recovery, 271–275

O

Operational longevity, 352
Organic acid production, 299–301
Organic fouling, 196–197
Organic pollutants, 164–169
Oxidizable fraction, 239
Oxygen-containing groups, 114–115

P

Para-toluene sulfonic acid (PTS), 84–86
Particle size distribution (PSD), 179
Perfluorooctane sulfonate, 124
Peroxymonosulfate (PMS) activation, 114–115
Phase inversion, 12
Plasma treatment, 99
PLS regression, 244–245
Poisson–Boltzmann equation, 60
Polarization
deformability and, 64–65
in electrochemical membrane separation, 66–68
polarity and dipole moment of molecules, 63–64
Pollutant filtration process, 44–45
Pollutant removal, in eMBRs
nitrogen, 164–171
organic pollutants, 164–170
phosphorus, 171–172
Polymer-based CM, 12
Polymer-based membrane materials, 82–83
Polymer blending, 11
Polymer inclusion membrane (PIM), 270
Polypyrrole, 200
Polytetrafluoroethylene (PTFE), 112–113
Pore filling, 11
Porous metal oxides, 201
Pressure-driven membranes, 211–212
Pressure-retarded osmosis (PRO), 445–448, 446*f*
Process intensification, 299–301
Pseudo-first-order model, 147
Pulsed electrical field (PEF), 17

R

Rare earth elements (REE), 248
Reactive oxygen species, 173

This book belongs to Badji Mokhtar Annaba University Central Library
Copyright Elsevier 2025

Reactor configuration, 115–116
designs, 142
development progress of, 151–152
evaluation and comparison, 154–156
flow-by reactor, 152–153
limitations and challenges, 156–157
stirred reactor, 152
Reduced chemical consumption, 403
Reduced graphene oxide (rGO), 95–96
Reducible fraction, 239
Residual fraction, 239
Resource recovery, 352
Reverse current desorption (RCD), 321
Reverse electrodialysis (RED), 10, 17–18, 302–303, 445, 448–451, 448*f*
Reverse osmosis (RO), 329, 446

S

Salinity gradient energy (SGE), 302–303, 445
Sandwiched electro-Fenton system, 122*f*
Scalability, 352
Selective ion removal and recovery, 405*f*
CDI and CDI-related systems
capacitive deionization, 415–416, 416*f*
electrochemical filtration systems, 417, 417*f*
hybrid capacitive deionization, 416, 416*f*
membrane capacitive deionization, 416–417
cobalt, 426, 427*f*
dilute contaminants, remediation of
inorganic ions, 430–434
organic pollutants, 427–430
electrochemical ion separation method, 407
electrodialysis, 414–415, 414*f*, 419*t*
heavy metals and metalloids, removal of
arsenic, 418–420
chromate, 420
copper, 420–421
lead, 420
ion exchange, 410
key components for, 409–413
key selective components, 412–413, 413*f*
lithium, 421–426, 425*f*
mechanisms, 409–413
membrane-based electrochemical systems for, 422*t*, 431*t*
nonselective ion separation, 406–407
performance metrics of, 408–409
selective immobilization, 411–412
separation techniques, 407–408
size exclusion, 410–411
sodium (Na) superionic conductor (NASICON), 406–407
technoeconomic analysis considerations, 434–435
tungsten, 426–427
Selectrodialysis, 277
Self-assembly, 13
Separator, 344–345
Silver nanoparticles (AgNPs), 146–147
Single-walled CNT (SWCNT), 112–113, 146
Sintering method, 12
Sodium dodecyl benzene sulfonate (SDBS), 84–86
Sodium formate concentration, 292, 293*f*
Sol-gel method, 12
Solid–liquid interfaces, 44
Solid materials, 50
Spacers, 344–345
Specific energy consumption (SEC), 324
Standard hydrogen electrode (SHE), 69
Sulfomethoxazole (SMX), 174
Surface-charged membranes, 1–2
Synergistic process configurations, 218

T

Temperature, 50
Thomas–Fermi shielding distance, 60
Three-dimensional (3D) graphene-based framework, 73–74
Total Phosphorus (TP) removal, 171
Transparent exopolymeric particles (TEP), 177–178

U

Ultrafiltration (UF), 195

V

Vacuum-assisted filtration (VAF), 96
Vacuum filtration, 112–113
Vapor phase polymerization (VPM), 88
Versatility, 71
Visual MINTEQ simulations, 240–241
Volumetric energy consumption, 322

W

Waste acid recovery process, 288
Waste disposal, 403

This book belongs to Badji Mokhtar Annaba University Central Library Copyright Elsevier 2025

Wastewater neutralization, 292, 293*f*
Wastewater reclamation, 271
Wastewater treatment
  nonconventional pollutant removal, in eMBR
    pathogenic viruses, 174–175
    phenols, 172–173
    trace organic pollutants, 173–174
  pollutant removal, in eMBRs
    nitrogen, 170–171
    organic pollutants, 164–170
    phosphorus, 171–172
  in recent studies, 165*t*
Wastewater treatment plants (WWTP), 404
Water content change, 238
Water deficiency, 445
Water desalination, 348
Water oxidation, 18–19
Water purification, 404
Water recovery, 321
Water scarcity, 403
World Health Organization (WHO), 277

Z

Zero volt desorption (ZVD), 321

This book belongs to Badji Mokhtar Annaba University Central Library
Copyright Elsevier 2025

Electrochemical Membrane Technology for Water and Wastewater Treatment

Edited by
Zhiwei Wang, Kwang-Ho Choo, Chuyang Y. Tang and T. David Waite

Describes the increasingly important role of electrochemical membrane technology, particularly in water/wastewater treatments and environmental sustainability

Edited by

Zhiwei Wang
State Key Laboratory of Pollution Control and Resource Reuse, Shanghai Institute of Pollution Control and Ecological Security, School of Environmental Science and Engineering, Tongji University, Shanghai, P.R. China

Kwang-Ho Choo
Department of Environmental Engineering, Kyungpook National University, Daegu, Republic of Korea

Chuyang Y. Tang
Department of Civil Engineering, The University of Hong Kong, Hong Kong, P.R. China

T. David Waite
School of Civil and Environmental Engineering, The University of New South Wales, Sydney, NSW, Australia

Electrochemical membrane technology has drawn extensive attention worldwide during the past decade in water and wastewater treatment. Coupling electrochemical process with membrane technology not only enables a higher removal or decomposition of pollutants in waters but also ensures a more effective control of membrane fouling as well as a more highly selective separation process. The recent development of electrochemical membrane technology has also extended its applications in desalination, energy harvest, and resource recovery from seawater and wastewaters. *Electrochemical Membrane Technology for Water and Wastewater Treatment* consolidates state-of-the-art research developments in electrochemical membrane technology in water reclamation and sustainability in terms of fundamental theories, membrane and electrode materials, reactor designs, fouling control mechanisms, and applications.

This book also introduces fundamental theories and applications of electrochemical membrane technology. The knowledge gaps and future research perspectives in electrochemical membrane technology are also addressed. This book is an excellent resource for the understanding of fundamental theories, latest developments, and future prospects in electrochemical membrane technology, which can benefit a broad audience of researchers and engineers working in water purification, membrane technology, and electrochemical process.

- Consolidates scattered knowledge of electrochemical membrane technology into a more accessible resource
- Provides a comprehensive review of fundamental theories, membrane materials, and module design as well as the latest devel opments of electrochemical membrane technology
- Provides a state-of-the-art review on the applications of electrochemical membrane technology
- Includes a detailed discussion on the challenges and prospects of electrochemical membrane technology in different applications

ISBN 978-0-12-824470-8

9 780128 244708

ELSEVIER elsevier.com/books-and-journals

This book belongs to Badji Mokhtar Annaba University Central Library

Copyright Elsevier 2025